New dynamics in axions and flavor

Memoria de Tesis Doctoral realizada por

Pablo Quílez Lasanta

presentada ante el Departamento de Física Teórica
de la Universidad Autónoma de Madrid
para la obtención del Título de Doctor en Ciencias.

Tesis Doctoral dirigida por

Prof. **M. Belén Gavela-Legazpi**

Catedrática del Departamento de Física Teórica
de la Universidad Autónoma de Madrid

Madrid, 25 de octubre de 2019

Publications

This thesis is based on the following scientific publications:

Journal articles in this thesis

[1] **Flavor-changing constraints on electroweak ALP couplings**
M. B. Gavela, R. Houtz, P. Quilez, R. del Rey, O. Sumensari
European Physical Journal C, 79, 369 (2019) and *arXiv:1901.02031 [hep-ph]*

[2] **Automatic Peccei-Quinn symmetry.**
M. B. Gavela, M. Ibe, P. Quilez, T. T. Yanagida
European Physical Journal C, 79, 542 (2019) and *arXiv:1812.08174 [hep-ph]*

[3] **Axion couplings to electroweak gauge bosons.**
G. Alonso-Álvarez, M. B. Gavela, P. Quilez
European Physical Journal C, 79, 223 (2019) and *arXiv:1811.05466 [hep-ph]*

[4] **Color Unifed Dynamical Axion.**
M. K. Gaillard, M. B. Gavela, R. Houtz, P. Quilez, R. del Rey
European Physical Journal C, 78, 972 (2018) and *arXiv:1805.06465 [hep-ph]*

[5] **Gauged Lepton Flavour.**
R. Alonso, E. Fernandez Martinez, M. B. Gavela, B. Grinstein, L. Merlo, P. Quilez
Journal of High Energy Physics, 2016, 119 (2016) and *arXiv:1609.05902 [hep-ph]*

Proceedings

[6] **Gauging Lepton Flavour.**
P. Quilez
52st Rencontres de Moriond on Electroweak Interactions and Unified Theories
arXiv:1609.05902 [hep-ph]

Acknowledgements

Parece mentira que ya haya llegado el momento. La tesis está acabada y toca mirar con perspectiva estos bonitos cuatro años y recordar con una sonrisa todos los buenos momentos y a todas las personas sin quiénes esta tesis no hubiese sido posible. O sin quiénes la tesis hubiese sido un camino mucho más aburrido.

En primer lugar, tengo mucho que agradecer a Belén. Nunca podría haber imaginado cuando nos cruzamos por primera vez en el ascensor del IFT la suerte que iba a tener de hacer la tesis contigo. Gracias por dirigirme la tesis y por guiarme en este camino con tu única intuición física. Gracias por contagiarme tu pasión por la física y mostrarme lo apasionante y divertido que puede llegar a ser intentar entender cómo funciona el mundo a nuestro alrededor al nivel más fundamental. Además de aprender mucha física, mediante tu ejemplo y una gran exigencia me has mostrado la importancia del rigor y la honestidad en ciencia. También debo agradecerte las increíbles oportunidades que me has brindado, permitiendome hacer múltiples estancias y presentándome y animándome a interaccionar con la comunidad internacional. Pero sobre todo gracias por preocuparte más allá y por la dedicación y el cariño que he recibido de tu parte durante estos años.

No puedo olvidarme de Igor y Theopisti, que me introdujeron en el mundo de la investigación y de los axiones. Gracias a los dos.

This thesis, like most important things in life, would have not been possible without the collaborative effort of several people. I am indebted to all my collaborators from which I have learned so much: Rachel Houtz, Benjamin Grinstein Enrique Fernandez-Martinez, Gonzalo Alonso, Luca Merlo, Mashahiro Ibe, Mary K. Gaillard, Olcyr Sumensari, Rocío Del Rey, Rodrigo Alonso and Tsutomu T. Yanagida. Thank you all.

I would like to thank the members of the jury: Andreas Ringwald, Margarita García and Javier Redondo for kindly accepting to participate in it.

Durante los primeros meses del doctorado, cuando más perdido estaba, siempre conté con la ayuda de Enrique, Luca y Rodrigo. Gracias Enrique por estar siempre disponible para resolverme hasta la enésima duda. Admiro la forma clara y elegante que tienes de entederlo todo. Por ello, eres sin duda el alma del Pheno-coffee y siempre he salido de tu despacho con un conocimiento más profundo del que tenía al entrar. Pero también gracias por contribuir al buen ambiente de la segunda planta con tu permanente sonrisa. Gracias Luca por sentarte conmigo para entender el último detalle de cada cuenta que se me atascaba y por todo lo que me has enseñado sobre

flavour y el SM. Y por supuesto gracias por protagonizar uno de los momentos más divertidos de la tesis: el video de la Master Formula con aparición estelar de Mary K incluida. Muchas gracias Rodrigo por tu paciencia y por enseñarme tantas cosas cuando tanto me quedaba por aprender. Gracias también a ti y a Verónica por leer la tesis y elaborar el informe para el doctorado internacional.
Siendo colaboradora, pero también mucho más, no puedo olvidarme de mi hermana de doctorado más cercana. ¡Al final no sé cancelaron los infinitos, Rocío! A ti te agradezco la ayuda para capear todo lo que supone hacer el doctorado y todos los buenos momentos, desde la escapada a Bled con los colegas de Invisibles hasta la estancia de Berkeley. Pero sobre todo gracias por mostrarme otra forma de ver la vida. Gracias también mis otras hermanas de doctorado, Ilaria y a Sara, y a mi hermanastra, Raquel, por enseñarme distintos aspectos sobre gravedad y por las risas en Japón y en Nueva York. I am indebted to Rachel for patiently revising this manuscript and improving my English. It has also been a pleasure to work with you and share some unforgettable moments (like when I broke into Belen's place).

El doctorado también me ha brindado la oportunidad de desarrollar mi pasión por la docencia y la divulgación, y eso se lo debo a Carlos Pena, María José, Pepe y Belén por permitirme adentrarme en este mundo. Gracias también a Emilia y a Claudia, compañeras incansables de fatigas docentes.

Gracias a todos los compañeros del IFT por hacer este camino más agradable: Javi Martín, David Gordo, Ezquiaga, Medrano, Edu, José Romero, Claudia, Thomas, Javi Quilis, Jorge y alguno más que seguro que me olvido. Gracias también a todo el equipo de secretaría del IFT y a Javier y Ana en el departamento por facilitarnos los inmundos papeleos y hacerlo siempre de buena gana. En especial, gracias a Isabel por el cariño con el que siempre me has tratado y por la ayuda con las bicis. Los últimos meses no hubiesen sido iguales sin las partidas de ping-pong con Medrano y Nadir y las comidas con los matemáticos. Y muchísimas gracias a Medrano por toda la ayuda con la entrega de la tesis, te has ganado unas cerves.

Desde luego una de las ventajas de trabajar con Belén ha sido formar parte de la red de Invisibles que me ha permitido conocer gente de la que tanto he aprendido. Gracias a Xabi, Josu, Gonzalo, Elena, Rupert, Álvaro, Andrés, Andrew, Olcyr y a todo el resto. But Invisibles has also given me the opportunity to attend amazing lectures by top physicists from whom I have learned so much. I would like to specially thank Andy Cohen for his outstanding lectures that allowed me to gain a deeper understanding of instantons and foster my motivation for physics.
A Invisibles también le debo las increíblemente enriquecedoras estancias que he realizado. During my long research stay in Berkeley I was warmly hosted by Zoltan Ligeti (thanks for the bike, the letters of recommendation and all your help) and Mary K. Gaillard. It has been an authentic priviledge to work with Mary K. from whom I have learned so much. I will always remember how much I enjoyed discussing with you different wild ideas in the blackboard of your office. And some of them finally lead to our published paper and tons of other pending projects. Thank you very much for your inspiration. Thank you also to Erik, Evan and Satyam that enriched my stay in the Bay area with volleyball matches in Ocean beach, the cool road trip

down south for Thanksgiving or the crazy trip to Las Vegas. I would also like to thank the IMPU for the nice stay in Japan where I was kindly hosted by Tsutomu and Mashahiro. Aunque pocos pueden competir con la hospitalidad tica. Ha sido un placer y realmente enriquecedor pasar un mes en Costa Rica. Pepe, Alejandro y Joe han sido unos anfitriones excepcionales y todo lo que ofrece el pais no se ha quedado atrás. Gracias también a Joey y a Fernando con quienes ha sido un placer compartir esta aventura. Gracias por último a Alberto Nicolis por acogerme en Nueva York. Y por supuesto gracias a Belén, Enrique y Raquel por hacer esta estancia y la japonesa especiales.

También debo agradecer el apoyo económico a la fundación de la Caixa y felicitar a la Asociacion de becarios por los geniales eventos que organiza.

Otro aspectos importantes y enriquecedores de mi vida durante los inicios del doctorado ha sido el voluntariado en ESN. Aparte de permitirme conocer a gente maravillosa bailando una bachata, me ha mostrado lo impresionante de los proyectos que se pueden llevar a cabo sólo con la voluntad de hacerlos. Gracias a la ChiniJunta - Carmen, Rocío, Carlos, Blanca, Victor y Jorge - por el gran equipo que se ha convertido en un grupo de buenos amigos. Gracias en especial a Victor por las cervezas, las fiestas, los kapis y los mil viajes con los erasmus. Gracias también a Marta, Vicente y a Mero. Pero ESN también me ha permitido conocer a erasmus especiales como a Manrico y Marine que también se han convertido en amigos. Gracias por esas cenitas de los lunes y por seguir visitándonos ahora en Torrecilla.

Muchas gracias también a todas las personas que me han permitido desconectar de la tesis. Al reducto oldenburger en Madrid - Fer, Cris y Fayu-, muchas gracias por las risas sinceras y las tardes que se pasan volando. También gracias a toda la cuadrilla de Santo por crear esa burbuja en la que todo está como siempre y nos permite disfrutar juntos de los pequeños placeres de la vida. Gracias a Nicoló por los estupendos plannings deportivos semanales de volley y padel. Gracias también en este último año a Bea, Richi y todo el grupo de italianos por las cenitas en el matador, los platos de pasta al pesto y los atardeceres en el parque de las 7 tetas.

Zaragoza, como Santo, también ha sido ese refugio que se busca cuando se necesita un poco de estabilidad y de seguridad. Muchas gracias a los Machadianos que siempre están allí. Sobre todo gracias a Ayala y a Noe, compañeros de innumerables aventuras, que nunca han fallado cuando les he necesitado. Gracias por ser las personas que lo saben todo de mí, y aún así siempre están a mi lado.

Por supuesto, muchas gracias a Zahariano, mi inseparable compañero de estudio y una de las personas que mejor me entiende. Ya sea un error en un código, elegir postdoc, o tomar cualquier decisión siempre he podido pedirte ayuda.

A mi familia le debo la educación que me ha dado. Gracias por ese apoyo incondicional y esa seguridad que te permite salir a luchar por tus objetivos sin miedo. Mamá, gracias por acompañarme día a día, escucharme y respaldarme en mis decisiones. Papá gracias por compartir y fomentar esa curiosidad que me ha llevado a dedicarme a la ciencia. Tata, gracias

por entenderme y desear siempre lo mejor para mi. Gracias también a todos por ayudarme evadirme con nuestros combos que tanto disfrutamos de tenis, comida, mus y gintonic.

Por último, muchas gracias Ila. Muchas gracias por estar siempre ahí, en las idas y venidas y por ser mi compañera de viaje. Por eso muchos de estos agradecimientos tienen que ver contigo. Tu contribución a esta tesis (además del dibujito del instanton) está presente en todos los rincones. Gracias por haberme dado fuerzas cuando lo necesitaba y por apoyarme siempre. Ha marcado la diferencia.

Abstract

Despite the great success of the Standard Model of Particle Physics in describing Nature, it cannot account for some crucial experimental observations and theoretical issues. Therefore, the Standard Model requires to be extended. This thesis is devoted to the study of two of the theoretical issues: the absence of CP violation in the strong interactions, e.g. the strong CP problem, and the tantalizing pattern of masses and mixings of the elementary fermions, that is, the flavor puzzle. For both problems, novel (ultraviolet complete) dynamical solutions are proposed. Complementarily, the model-independent techniques of effective field theories are applied to chart new territory in parameter space.

In the flavor arena, the leptonic flavor symmetry of the Standard Model is gauged, promoting the Yukawa couplings to dynamical fields. The results of this theory are compared with those expected from the effective ansatz of minimal flavour violation.

In the strong CP arena, two composite (dynamical) axion solutions to the strong CP problem are proposed: in a first work the axion mass is raised in a framework with an unified strong sector, while in a second work an invisible axion with an accidental Peccei-Quinn symmetry is constructed.

In addition, new regions in parameter space for the effective couplings of axions and axion-like particles are explored. In particular, this thesis goes beyond the *one-coupling-at-a-time* approach, considering the simultaneous effect of several effective couplings: the axion coupling to electroweak gauge bosons and the gluonic coupling in the first work, and the full bosonic electroweak basis for a generic axion-like particle without gluonic coupling in the second one.

Resumen

A pesar del gran éxito del Modelo Estándar de la física de partículas a la hora de describir la naturaleza, todavía existan ciertas observaciones experimentales y enigmas teóricos que este paradigma no es capaz de acomodar. Por ello el Modelo Estándar debe ser ampliado. Esta tesis se ha centrado en el estudio de dos de estos enigmas teóricos: el problema CP fuerte y la desconcertante estructura de masas y parámetros mezcla de los fermiones elementales, el llamado puzle del sabor. Para ambos problemas, se han propuesto nuevas soluciones dinámicas completas en el ultravioleta. De forma complementaria, se han aplicado las técnicas de teorías efectivas de campos, que permiten no depender del modelo concreto, para explorar nuevo territorio en el espacio de parámetros.

En el campo de la física del sabor, se ha convertido la simetría de sabor del sector leptónico en una simetría gauge. Para ello, los acoplos de Yukawa de los leptones son considerados campos dinámicos. Los resultados de esta teoría han sido comparados con los esperados del tratamiento efectivo basado en la hipótesis de violación mínima del sabor .

En el campo del problema CP fuerte, se han propuesto dos soluciones de tipo axión compuesto (dinámico): en un primer trabajo la masa del axión es aumentada en una teoría con el sector fuerte unificado, mientras que en un segundo trabajo se ha construido una teoría de axión "invisible" en la que la simetría de Peccei-Quinn surge de forma accidental.

Además, se han explorado nuevas regiones del espacio de parámetros de los acoplos efectivos de axiones y partículas de tipo axion. En particular, esta tesis ha ido un paso más allá del tratamiento en el que los efectos de cada acoplo son considerados de forma independiente para estudiar los efectos de la presencia simultánea varios acoplos efectivos: el acoplo del axión a los bosones electrodébiles y el acoplo gluónico en el primer trabajo, y la base bosónica electrodébil completa para partículas de tipo axión genéricas en el segundo.

Contents

Motivation and goals

The Standard Model of particle physics (SM) is one of the greatest achievements of scientific endeavor. This theory brings together special relativity and quantum mechanics, in a consistent theory describing three of the four fundamental forces of the Universe: strong, weak and electromagnetic interactions. It also includes the full set of fundamental particles that compose all the known Universe. This theory has been able to explain essentially all experimental facts of the visible Universe and predict a large variety of phenomena below the TeV scale with an unprecedented accuracy.

The fourth fundamental interaction, gravity, governs the dynamics of large scale structures and it is satisfactory described at the classical level by the theory of General Relativity (GR). Within this framework, and thanks to recent astronomical data, a new era of cosmology has been opened. Fundamental questions related to the origin and evolution of the Universe, that have been historically in the realm of Philosophy, can now be addressed scientifically. Moreover, with the discovery of gravitational waves by the LIGO and Virgo collaborations (a long-time prediction of General Relativity) a new window to explore the Universe has been opened.

Nevertheless, despite the great success of the SM and GR in describing nature, there are still experimental observations that cannot be accounted for:

- **Dark Matter**: Around a 25% of the energy budget of the Universe is most plausibly composed by a new type of matter that the SM does not account for.
- **Dark Energy**: The accelerated expansion of the Universe that has been observed can be included in the GR Einstein's equations via a cosmological constant term. The energy involved in this acceleration amounts to $\sim$70% of the energy of the Universe and its nature remains unknown.
- **Matter-antimatter asymmetry**: The observed Universe is almost entirely made of matter and comparatively not much antimatter. The SM interactions are not completely equivalent for matter and antimatter, but this asymmetry alone does not suffice to explain the observed asymmetry.
- **Neutrino masses**: Within the SM, neutrinos are massless. However, the measurement of neutrino oscillations implies that at least two neutrinos are massive and the SM needs

to be extended to account for this fact. In particular, it also remains unknown whether neutrinos are Majorana or Dirac particles.

Apart from these well-established experimental facts that remain unexplained by the SM, there are also some unsatisfactory issues of our theoretical description of nature that have fostered active research in particle physics. They correspond generically to fine-tunings in the parameters that describe the different SM interactions and represent interesting hints that guide us in the search for new physics. Indeed, the quest to explain small parameters has been shown in the past to be an exceptional tool to gain a deeper understanding of nature. The main such tensions or fine-tunings are:

- **Electroweak hierarchy problem**: The lightness of the Higgs particle is not well understood, since its mass is not protected by any symmetry, and it is expected to be very sensitive to high-energy extensions of the SM. The Higgs mass can still be accommodated within the SM, at the cost of a severe fine tuning in the parameters.
- **Flavor puzzle**: While quark and charged lepton masses present a large hierarchy, neutrinos do not. Furthermore, the mixing is small in the quark sector while large in the leptonic one. This tantalizing pattern of masses and mixings of the elementary fermions composing the visible universe calls for an underlying explanation.
- **Strong CP problem**: The fact that the strong interactions do not seem to violate the CP symmetry is not well understood, since this symmetry is indeed violated in the weak sector. Or in other words, why is the θ-parameter describing the QCD vacuum so small, $\bar{\theta} < 10^{-10}$? Again this fact does not contradict the SM since it can be accommodated but at the cost of a fine tuning.

My research within this thesis has been mainly devoted to these last two issues: new dynamical solutions to the strong CP problem and to the flavor puzzle; and their phenomenological consequences have been examined.

As guiding principles, symmetries and the promotion of couplings of the SM to dynamical fields will play a crucial role in this thesis. Particularly important will be anomalies, i.e. classical symmetries that do not survive at the quantum level, since their cancellation in gauge theories provides a robust consistency condition and also are essential in axion solutions to the strong CP problem.

Symmetries, and in particular, gauge symmetries have led to our understanding of particle dynamics. Indeed, the gauge sector of the SM requires only 3 free parameters of order one, i.e. the interaction couplings, while being highly predictive in terms of number and properties of the particles mediating the interactions (the gauge bosons) and the nature and strength of them. On the other hand, the flavor sector has been built completely *ad hoc* requiring 20 parameters in order to reproduce fermion masses and mixings. The only available method grasp to understand the fermionic matter content of the SM is, again, the gauge principle: complete families are

required by the cancellation of gauge anomalies. This provides consistency conditions on the hypercharges and gauge representations of the SM fermions. These cancellations occur within each generation, though, and hence they fail to explain the origin of the three generations and their Yukawa couplings. In the same way that the distinct structure of the periodic table of elements could be understood in terms of electronic configurations in atomic orbitals, the peculiar pattern of masses and mixings in the fermionic sector calls for an underlying explanation.

Given the success of symmetries in explaining our most fundamental knowledge of nature, it seems very suggestive to try to explain flavor through a symmetry principle. In this direction, the flavor group of the SM, i.e. the global symmetries of the SM in the massless fermion limit, may offer a hint. A ground-breaking possibility is to promote it to a gauge symmetry. This was first attempted in Ref. [7] for the quark sector and we will extend it in Chapter 4 for the lepton sector. Within this framework, the Yukawa couplings are promoted to dynamical fields whose vacuum expectation values (vevs) spontaneously break the flavor group and generate the mass and mixing pattern. The gauging of the lepton flavor group is considered in the Standard Model context and in its extension with three right-handed neutrinos. The gauge anomaly cancellation conditions will be shown to lead to a Seesaw mechanism as underlying dynamics for all leptons, requiring Majorana masses for the neutral sector.

Closely related to the flavor structure of the SM, another problem arises: that of the absence of CP violation in the strong interactions. Measurements of the electric dipole moment of the neutron imply that the strong CP phase $\bar{\theta}$ (containing a phase from the quark mass matrix) is very small $\bar{\theta} < 10^{-10}$, and the lack of an explanation of such small value is the so called strong CP problem. Again symmetries and, in particular, anomalous symmetries could shed some light on this problem, and the solution may lie in the Peccei-Quinn (PQ) mechanism [8,9]. This solution introduces a $U(1)_{PQ}$ symmetry which is anomalous under QCD and allows one to fully reabsorb the $\bar{\theta}$-parameter, making it unphysical and solving the strong CP problem. As a consequence of this mechanism, a new pseudoscalar degree of freedom arises, the axion. The QCD axion is necessarily very light so as to avoid phenomenological constraints with a large decay constant. Although the QCD axion solution was proposed in the 1980's, it is currently a very active topic of research and new ideas both in the theoretical and experimental sides are being proposed. In this context, a change of perspective is spreading. One of the theoretical avenues to allow PQ solutions with low scales consists n relaxing the tight relation between the axion mass and scale by introducing new confining forces that generate a large mass for the axion without spoiling the strong CP solution. In Chapter 5, we will develop a new solution to the strong CP problem via massless fermions and color unification, where a composite axion with large mass arises, due to the extra mass contribution of the small-size instantons of the unified color group. Consequently, the strong CP problem is solved while no axion remains at low scales.

These type of heavy axion models allow one to lower the axion scale, solving one of the issues of QCD axion models: that of the PQ quality. Indeed, QCD axion models typically require the PQ symmetry to be imposed in the Lagrangian, therefore new physics at high scales could induce effective operators that break the PQ symmetry spoiling the Strong CP solution. This constitutes the so-called PQ quality problem. In particular, effective operators stemming from

non-perturbative gravitational corrections have been considered as a possible threat to QCD axion models, when the scale f_a is not very far from the Planck scale. Alternative to lowering the axion scale as in heavy axions, models in which the PQ symmetry arises accidentally can be protected against these operators. Several setups have been proposed in the literature, implementing an accidental PQ symmetry for that purpose. Nonetheless, they typically require extra symmetries either gauge or discrete ones. In Chapter 6 we study a new theoretical proposal in which a minimal composite axion arises from the confinement of a chiral gauge $SU(5)$ with two massless quarks. Gauge anomaly cancellations again guide us in terms of the representations of the exotic fermions under the $SU(5)$ group, $\bar{\mathbf{5}} + \mathbf{10}$ being the simplest anomaly free combination. Within this setup, a PQ symmetry arises automatically as a consequence of gauge symmetry and chirality and presents an inherent protection from quantum gravitational corrections.

Nevertheless, axions are not the only well-motivated scalar extensions of the SM. The discovery of the Higgs boson, probably the first fundamental scalar particle, has finally completed the SM with its last missing piece. At the same time, it has opened new territory, the Higgs particle may not be the only fundamental scalar, and new spin zero particles may be awaiting discovery. Indeed, (pseudo)-scalars appear in plenty of theories that go Beyond the SM (BSM), such as extra dimensions, majorons, flavor models *à la* Froggatt-Nielsen, string theory, etc. They appear commonly in tight connection with hidden symmetries, or spontaneously broken symmetries. These kinds of spin zero particles, when CP odd (i.e. pseudoscalar), are typically called axion-like particles (ALPs). Strikingly, both axions and ALPs represent, in large regions of the parameter space, excellent candidates to explain the nature of Dark Matter (DM), even if motivated by other problems.

Axions and ALPs have been mainly probed through their coupling to photons, fermions and gluons. Nonetheless, in the current context in which new theoretical ideas are being put up such as heavy axion models or photophobic/nucleophobic axions, it is pertinent to also study the putative couplings of axions and ALPs to electroweak (EW) gauge bosons. In Chapter 7, we have studied these axion couplings. Using effective field theories (EFTs), we computed for the first time the model independent contribution to the axion couplings to EW gauge bosons, stemming from the mixing of the axion with the neutral mesons. Furthermore, we perform a two-coupling-at-a-time phenomenological study, where the gluonic coupling together with individual gauge boson couplings are considered.

Regarding the experimental detection of axion and ALPs, flavor physics plays a very important role. Within the SM, Flavor Changing Neutral Currents (FCNCs) are only possible at loop level and are highly suppressed due to the Glashow-Iliopoulos-Maiani (GIM) mechanism, in agreement with the experimental constraints. Flavor observables are so precise that they provide a very powerful tool for the search of New Physics, since effects that correspond to UV complete theories at energies of even 10^5 TeV can compete with the suppressed SM contributions, and therefore be accessible by current experiments. In particular, K- and B-meson decays provide an exceptional tool to probe the axion and ALP parameter space. In Chapter 8, we study the signals of ALPs in FCNC processes, considering the most general effective linear Lagrangian for ALP couplings to

the electroweak bosonic sector, and computing its contribution to FCNC decays up to one-loop order.

In the first part of this thesis – Chapters 1 to 3 – the SM, the strong CP problem and axions and ALPs are reviewed, whereas the original contributions of the thesis are contained in the second part, Chapters 4 to 8.

Part I

Foundations

CHAPTER 1

The Standard Model

The Standard Model of particle physics encompasses our current knowledge of both the matter content of the visible Universe and the three fundamental interactions that have been understood at the quantum level: strong, weak and electromagnetic interactions. It is a particular realization of a Quantum Field Theory (QFT) in which symmetries play a fundamental role. On the one hand, the particles are understood as excitations of more fundamental degrees of freedom, fields that correspond to different representations of the Lorentz symmetry group: scalar (spin-0) for the Higgs, fermionic (spin-1/2) for quarks and leptons, and vectorial (spin-1) for the gauge bosons. On the other hand, interactions among these fields are determined by a local (spacetime dependent) symmetry: the gauge symmetry.

Based on the fundamental principles of locality and causality, and with Lorentz and gauge symmetries at its core, the SM has faced a variety of experimental tests with astonishing success. Its extremely accurate predictions can be beautifully condensed in the following Lagrangian:

$$\begin{aligned}
\mathcal{L}_{SM} = \quad & \mathcal{L}_{\text{gauge}} + \mathcal{L}_{\text{Dirac}} + \mathcal{L}_{\text{Yukawa}} + \mathcal{L}_{\Phi} + \mathcal{L}_{\theta} + \\
= & -\frac{1}{4} G^{\mu\nu}_{A} G^{A}_{\mu\nu} - \frac{1}{4} W^{\mu\nu}_{a} W^{a}_{\mu\nu} - \frac{1}{4} B^{\mu\nu} B_{\mu\nu} \\
& + i\overline{Q}_L \not{D} Q_L + i\overline{U}_R \not{D} U_R + i\overline{D}_R \not{D} D_R + i\bar{\ell}_L \not{D} \ell_L + i\overline{E}_R \not{D} E_R \\
& - \overline{Q}_L Y_u \widetilde{\Phi} U_R - \overline{Q}_L Y_d \Phi D_R - \bar{\ell}_L Y_e \Phi E_R + \text{h.c.} \\
& + \left(D_\mu \Phi\right)^\dagger D^\mu \Phi + \mu^2 \Phi^\dagger \Phi - \lambda \left(\Phi^\dagger \Phi\right)^2 \\
& + \theta \, \frac{\alpha_s}{8\pi} G^{\mu\nu}_{A} \widetilde{G}^{A}_{\mu\nu} \, ,
\end{aligned} \tag{1.0.1}$$

where $G^{\mu\nu}$, $W^{\mu\nu}$ and $B^{\mu\nu}$ stand for the field strengths of the groups $SU(3)_c$, $SU(2)_L$ and $U(1)_Y$, respectively. Φ is the Higgs doublet, Q_L and ℓ_L are the left-handed (LH) quark and leptonic doublets, and U_R, D_R and E_R stand for the right-handed (RH) up, down-type quark singlets and leptonic singlet, respectively.

In the following we will briefly review the key aspects of the SM and then focus on some general aspects of symmetries in QFT.

1.1 The gauge sector

Gauge theories have incredible richness and complexity. They are highly predictive in terms of the number and properties of the particles mediating the forces and nature of the interactions. The SM gauge group is

$$\mathcal{G}_{SM} = SU(3)_c \times SU(2)_L \times U(1)_Y \,, \tag{1.1.1}$$

where each symmetry group is associated with a fundamental force of nature: $SU(3)_c$ corresponds to the strong interactions described by Quantum Chromodynamics (QCD) and $SU(2)_L \times U(1)_Y$ corresponds to the unified electroweak interactions. The number of bosons that mediate a particular interaction corresponds with the number of infinitesimal generators of the group associated to it. Thus, the SM includes 8 massless gluons G^a_μ mediating the strong interactions, and four gauge fields in the electroweak sector W^b_μ, $b = 1, 2, 3$ and B_μ.

$$\begin{aligned} SU(3)_c : &\qquad G^A_\mu, &\qquad A = 1 = 1, ..., 8 \\ SU(2)_L : &\qquad W^a_\mu, &\qquad a = 1 = 1, 2, 3 \\ U(1)_Y : &\qquad B_\mu \,. \end{aligned} \tag{1.1.2}$$

The kinetic terms of the gauge bosons in the Lagrangian of the SM are given by

$$\mathcal{L}_{gauge} = -\frac{1}{4} G^{\mu\nu}_A G^A_{\mu\nu} - \frac{1}{4} W^{\mu\nu}_a W^a_{\mu\nu} - \frac{1}{2} B^{\mu\nu} B_{\mu\nu} \,, \tag{1.1.3}$$

where $G^{\mu\nu}$, $W^{\mu\nu}$, $B^{\mu\nu}$ stand for the field strengths:

$$\begin{aligned} SU(3)_c : &\qquad G^A_{\mu\nu} &= \partial_\mu G^A_\nu - \partial_\nu G^A_\mu + g_s f_{ABC} G^B_\mu G^C_\nu \,, \\ SU(2)_L : &\qquad W^a_{\mu\nu} &= \partial_\mu W^a_\nu - \partial_\nu W^a_\mu + g\, \epsilon_{abc} W^b_\mu W^c_\nu \,, \\ U(1)_Y : &\qquad B_{\mu\nu} &= \partial_\mu B_\nu - \partial_\nu B_\mu \,, \end{aligned} \tag{1.1.4}$$

and g and g_s are the weak and strong coupling constants, and f_{ABC} and ϵ_{abc} are the structure constants of the generators of the non-abelian groups $SU(3)_c$ and $SU(2)_L$, respectively.

This first part of the Lagrangian describes massless mediator bosons and their self-interactions (only present in the non-abelian groups). However, this description is not complete since it does not account for the fact that the short range of the weak interactions indicates that the W and Z bosons are massive. An explicit mass term for the gauge bosons would break gauge invariance so the introduction of an electroweak symmetry breaking sector is needed. Within the SM this problem is explained through the famous Brout-Englert-Higgs mechanism [10–12], that assumes that the Lagrangian remains gauge invariant while the vacuum of the theory (i.e. the ground state) is not. This mechanism introduces a $SU(2)_L$ scalar doublet, the higgs boson Φ, that transforms under the gauge group as shown in the Table 1.1. The most general renormalizable Lagrangian involving the Higgs doublet reads,

$$\mathcal{L}_\Phi = \left(D_\mu \Phi\right)^\dagger D^\mu \Phi + \mu^2 \Phi^\dagger \Phi - \lambda \left(\Phi^\dagger \Phi\right)^2 \,, \tag{1.1.5}$$

where the usual partial derivative $\partial_\mu\Phi$ in the kinteic term has been substituted by the covariant derivative $D_\mu\Phi$ that ensures gauge invariance,

$$D_\mu\Phi = \left(\partial_\mu + ig\frac{\sigma^a}{2}W_\mu^a + ig'\frac{1}{2}B_\mu\right)\Phi\,, \tag{1.1.6}$$

where g' is the coupling constant of the $U(1)_Y$ gauge group and σ^a are the Pauli matrices, i.e. the generators of the $SU(2)_L$ group.

	$SU(3)_c$	$SU(2)_L$	$U(1)_Y$
Φ	1	2	$1/2$

Table 1.1: Transformation properties of the Higgs doublet under the SM gauge group.

The field configuration of Φ that minimizes the potential in Eq. (1.1.5), the ground state for the scalar field, is not invariant under the EW group $SU(2)_L \times U(1)$ for μ^2, $\lambda > 0$. This implies that the minimum of the Higgs potential does not correspond to a vanishing Higgs field. In other words, the Higgs doublet develops a non-zero vacuum expectation value (vev), v,

$$\langle\Phi^\dagger\Phi\rangle = v^2/2 = \mu^2/\lambda\,, \tag{1.1.7}$$

and Electroweak Symmetry Breaking (EWSB) is induced. It should be noted that this breaking is "spontaneous" rather than explicit. Indeed, the interactions in the Lagrangian are exactly invariant under the gauge group and it is only the ground state, the vacuum, that does not explicitly exhibit the symmetry. As a consequence, after expanding around true vacuum, the gauge bosons develop a mass in a gauge invariant way,

$$(D_\mu\Phi)^\dagger(D^\mu\Phi) = \frac{1}{2}\partial_\mu h\partial^\mu h + \frac{(v+h)^2}{4}g^2W_\mu^+W^{-\mu} + \frac{(v+h)^2}{8}(g^2+g'^2)Z_\mu Z^\mu\,, \tag{1.1.8}$$

where h is the physical Higgs boson and the four EW gauge bosons get mixed into the massive weak gauge bosons W^+, W^-, Z^0 and the massless photon A_μ,

$$\begin{aligned} W_\mu^\pm &\equiv \frac{1}{\sqrt{2}}\left(W_\mu^1 \mp iW_\mu^2\right)\,, \\ Z_\mu &\equiv \cos\theta_W\, W_\mu^3 - \sin\theta_W B_\mu\,, \\ A_\mu &\equiv \sin\theta_W\, W_\mu^3 + \cos\theta_W B_\mu\,. \end{aligned} \tag{1.1.9}$$

These combinations are controlled by the weak mixing angle θ_W, which is related to the coupling constants,

$$\tan\theta_W = \frac{g'}{g}\,, \tag{1.1.10}$$

and whose value is fixed from experiments. It follows from Eq. (1.1.8) that the masses of the gauge bosons are given in terms of the EW scale and the gauge couplings,

$$m_W = \frac{gv}{2}\,, \qquad m_Z = \frac{\sqrt{g^2+g'^2}}{2}\,, \qquad v = \frac{1}{\cos\theta_W}m_W\,, \tag{1.1.11}$$

while the photon A_μ remains massless. This is a consequence of the fact that the EW group is not completely broken by the Higgs vev; an abelian subroup of it, $U(1)_{em}$, remains unbroken and corresponds to the electromagnetic interactions, whose coupling constant reads

$$e = g \, \sin\theta_W = g' \cos\theta_W \, . \tag{1.1.12}$$

As a byproduct, this mechanism predicts the existence of a new particle corresponding to the excitations of the scalar field around the minimum of the Higgs potential: the Higgs boson h in Eq. (1.1.8), that was recently discovered in 2012 at CERN [13, 14].

1.2 Matter content

While the particles that mediate the interactions can be predicted given the gauge group, the structure of the matter content is not derived from any fundamental principle within the SM. The basic building blocks of matter are all spin 1/2 fermions, that can be classified into quarks, that feel both the strong and electroweak interactions, and leptons that only interact with the electroweak force.

According to their observed interactions under the electroweak force, each family of quarks is described by three fields, a $SU(2)_L$ doublet Q_L and two singlets U_R and D_R, whereas for leptons two fields suffice, a doublet ℓ_L and a singlet E_R of $SU(2)_L$.

$$\begin{aligned} \ell_L &= \left\{ \begin{pmatrix} \nu_L^e \\ e_L \end{pmatrix}, \begin{pmatrix} \nu_L^\mu \\ \mu_L \end{pmatrix}, \begin{pmatrix} \nu_L^\tau \\ \tau_L \end{pmatrix} \right\}, & E_R &= \{e_R \, , \mu_R, \, \tau_R\} \\ Q_L &= \left\{ \begin{pmatrix} u_L \\ d_L \end{pmatrix}, \begin{pmatrix} c_L \\ s_L \end{pmatrix}, \begin{pmatrix} t_L \\ b_L \end{pmatrix} \right\}, & U_R &= \{u_R, \, c_R, \, t_R\} \\ & & D_R &= \{d_R, \, s_R, \, b_R\} \end{aligned} \tag{1.2.1}$$

The way in which those particles interact with each other determines the transformation properties of the corresponding fields under the gauge group (see Table 1.2). Observations indicate that fermions appear in chiral representations with respect to the EW interactions (LH and RH fermions transform differently), while strong and electromagnetic interactions are vectorial and thus parity invariant. The fermions of the SM come in three different flavors or generations (see Section 1.3), that have exactly the same interactions with the gauge bosons and only differ among each other in their different masses and mixings. These differences and the existence of three replicas define the flavor puzzle.

Given the representation under which the field transforms, the interaction terms can be obtained by substituting the usual derivative by the covariant derivative in the kinetic term, ensuring gauge invariance,

$$\mathcal{L}_{Dirac} = i\overline{Q}_L \not{D} Q_L + i\overline{U}_R \not{D} U_R + i\overline{D}_R \not{D} D_R + i\bar{\ell} \not{D} \ell + i\overline{E}_R \not{D} E_R \, , \tag{1.2.2}$$

	$SU(3)_c$	$SU(2)_L$	$U(1)_Y$
Q_L	3	2	1/6
U_R	3	1	2/3
D_R	3	1	$-1/3$
ℓ_L	1	2	$-1/2$
E_R	1	1	-1

Table 1.2: Transformation properties of the fermionic field under the gauge group $SU(3)_c \times SU(2)_L \times U(1)_Y$.

where $\not{D} = D_\mu \gamma^\mu$ and γ^μ are the gamma matrices (generators of the Clifford algebra) and the sum over the three generations of each field is implicit. The covariant derivative for each field reads:

$$
\begin{aligned}
D_\mu Q_L &= \Big(\partial_\mu + i g_s \frac{\lambda^A}{2} G_\mu^A + i g \frac{\sigma^a}{2} W_\mu^a + i g' \frac{1}{6} B_\mu\Big) Q_L \,, \\
D_\mu U_R &= \Big(\partial_\mu + i g_s \frac{\lambda^A}{2} G_\mu^A + i g' \frac{2}{3} B_\mu\Big) U_R \,, \\
D_\mu D_R &= \Big(\partial_\mu + i g_s \frac{\lambda^A}{2} G_\mu^A - i g' \frac{1}{3} B_\mu\Big) D_R \,, \\
D_\mu \ell_L &= \Big(\partial_\mu + i g \frac{\sigma^a}{2} W_\mu^a + i g' \frac{1}{6} B_\mu\Big) \ell_L \,, \\
D_\mu E_R &= \Big(\partial_\mu - i g' B_\mu\Big) E_R \,.
\end{aligned}
$$

The power of the gauge principle is at play here: not only the number and self interactions of the gauge bosons is predicted, but also the interactions of all the fermions with the gauge mediators, whose universal strength is completely controlled by only three parameters: the gauge couplings g_s, g' and g.

1.2.1 Fermion masses and flavor

In the fermionic sector, explicit masses for the fermions are forbidden by gauge invariance, similar to EW gauge boson masses. Dirac mass terms correspond to the coupling of a left-handed fermion with a right-handed one and, since weak interactions only affect left-handed fields, a doublet scalar field is needed in order to build the needed chirality-flipping interaction. These Yukawa-type terms are included in the most general renormalizable Lagrangian containing fermions and the Higgs,

$$
\mathcal{L}_{\text{Yukawa}} = -\overline{Q}_L Y_u \widetilde{\Phi} U_R - \overline{Q}_L Y_d \Phi D_R - \overline{\ell}_L Y_e \Phi E_R + h.c. \,, \tag{1.2.3}
$$

where $\widetilde{\Phi} = i\sigma^2 \Phi^*$, and Y_u, Y_d and Y_e are 3×3 matrices in flavor space. When the Higgs doublet develops a vev and EWSB is triggered (Eq. (1.1.5)), these Yukawa interactions generate mass

terms for the quarks,

$$\mathcal{L}_{\text{Yukawa}} = -\overline{U}_L M_u U_R - \overline{D}_L M_d D_R - \overline{E}_L M_E E_R + h.c. \tag{1.2.4}$$

In general, the mass matrices M_u, M_d, M_E are not diagonal. By performing an appropriate change of basis,

$$\begin{aligned} U_L &\to V_L^u\, U_L\,, \quad D_L \to V_L^d\, D_L\,, \quad E_L \to V_L^e\, E_L\,, \\ U_R &\to V_R^u\, U_R\,, \quad D_R \to V_R^d\, D_R\,, \quad E_R \to V_R^e\, E_R\,, \end{aligned} \tag{1.2.5}$$

the mass matrices can be diagonalized,

$$\begin{aligned} M_u^{\text{diag}} &= V_L^{u\,\dagger} M_u V_R^u \quad = \text{diag}\,(m_u,\, m_c,\, m_t)\ , \\ M_d^{\text{diag}} &= V_L^{d\,\dagger} M_d V_R^d \quad = \text{diag}\,(m_d,\, m_s,\, m_b)\ , \\ M_e^{\text{diag}} &= V_L^{e\,\dagger} M_e V_R^e \quad = \text{diag}\,\left(m_e,\, m_\mu,\, m_\tau\right)\ , \end{aligned} \tag{1.2.6}$$

where m_i denote the observed quark and charged lepton masses. The set of transformations in Eq. (1.2.5) corresponds to a unitary rotation for each Weyl fermion f, satisfying $V^{f\,\dagger} V^f = \mathbb{1}$. As a consequence, interaction terms of fermions with the photon, the Z boson and gluons that correspond to neutral currents remain invariant under this transformation. However, charged currents in the weak interactions involve simultaneously up-type and down type quarks, and therefore are sensitive to some combination of these mixing matrices,

$$\mathcal{L}_{\text{CC}} = \frac{g}{\sqrt{2}} \left[W_\mu^\dagger \left(\overline{U}_L \gamma^\mu\, V_{\text{CKM}} D_L + \overline{\nu}_L \gamma^\mu E_L \right) + h.c. \right]\ . \tag{1.2.7}$$

In particular, the relevant mixing matrix V_{CKM} corresponds to the Cabibbo-Kobayashi-Maskawa (CKM) matrix, that involves the unitary rotation of left-handed up- and down-type quarks, $V_{CKM} = U_{uL}^\dagger U_{dL}$,

$$V = \begin{pmatrix} V_{ud} & V_{us} & V_{ub} \\ V_{cd} & V_{cs} & V_{cb} \\ V_{td} & V_{ts} & V_{tb} \end{pmatrix}\ . \tag{1.2.8}$$

The elements of this matrix are physical and measurable in the weak interactions, see Eq. (1.2.7). One of the predictions of the SM is the unitarity of the CKM matrix. Indeed, by independently measuring its elements this prediction has been tested and, so far, there has been an excellent agreement with the SM. Consequently, stringent bounds on BSM physics that induce deviations from unitarity have been set.

At this point, there is no mixing in the lepton sector since Eq. (1.2.4) lacks a mass term for neutrinos and therefore any unitary rotation of the charged leptons can be compensated by a neutrino rotation in Eq. (1.2.7). Nevertheless, mixing in the leptonic sector has been measured in the last two decades and, consequently, neutrino mass terms need to be introduced.

1.2.2 Neutrino masses

Neutrinos only interact via the weak force and experiments have established that charged currents only produce left-handed neutrinos (and right-handed antineutrinos) [15, 16]. Consequently, neutrinos can be described by a single LH Weyl fermion ν_L (and its conjugate the RH antineutrino $(\nu_L)^c$), unlike all the other fermions which present a right handed counterpart to each left-handed field . Due to its singular chirality, it is impossible to write a renormalizable mass term for them, so within the SM neutrinos are strictly massless. However, neutrino flavor transitions and oscillations have been experimentally established [17–19], and this phenomenon requires neutrinos to have non-zero masses[1]. According to the latest global fit on neutrino data within the three-flavor oscillation paradigm by the collaboration NuFIT [20], the best fit values for the squared mass differences read[2]

$$\Delta m^2_{21} = (7.39^{+0.21}_{-0.20}) \times 10^{-5}\ \text{eV}^2\ , \qquad \Delta m^2_{32} = \begin{cases} +(2.525^{+0.033}_{-0.031}) \times 10^{-3}\ \text{eV}^2 & \text{NH} \\ -(2.512^{+0.034}_{-0.031}) \times 10^{-3}\ \text{eV}^2 & \text{IH} \end{cases}\ , \tag{1.2.9}$$

where $\Delta m^2_{\nu_{ij}} = m^2_{\nu_j} - m^2_{\nu_i}$.

Nevertheless, oscillation experiments only allow one to measure the difference of squared neutrino masses. This means that the absolute scale neutrino masses remains undetermined. Yet, limits on the sum of neutrino masses can be obtained from cosmological measurements such as the Cosmic Microwave Background (CMB) and Baryon Acoustic Oscillations (BAO). The latest results by the Planck Collaboration set limits which vary in the interval $\sum m_\nu < (0.17 - 0.72)$ eV, depending on the considered dataset [19,21]. This bound should be taken with caution, since it has been derived assuming only three light massive neutrinos and the validity of the ΛCDM model (Λ for the cosmological constant, and CDM for Cold Dark Matter). Deviations from the standard cosmological model that are currently allowed by data could invalidate the bound. For instance, if the neutrino masses are generated dynamically at a relatively late epoch in the evolution of the Universe, this bound would not hold [19,22]. For this reason, experiments trying to directly measure the neutrino absolute mass scale become very relevant, even if they set less stringent bounds. One of the oldest ideas consists of the measurement of the endpoint of the electron spectrum in tritium beta decay. Following this approach, the experiments Troitzk and Mainz [23,24] set bounds of $m_{\overline{\nu}_e} < 2.05$ eV at 95% CL, which are expected to be improved by the upcoming KATRIN experiment, reaching sensitivities of $m_{\overline{\nu}_e} \sim 0.2$ eV [25]. Another type of experiments that could shed light on the neutrino mass scale (if they happen to be Majorana particles) are those looking for neutrinoless double beta decay $0\nu\beta\beta$, that so far has not been measured [26–28].

The observation of neutrino masses constitutes one of the clearest pieces of evidence of the existence of BSM physics that needs to be looked for. So far, the nature of neutrino masses

[1] At least two neutrinos have to be massive since two distinct squared mass differences, Δm^2_{12} and Δm^2_{23} have been measured.

[2] The quoted errors correspond to 1σ, i.e. 68% Confidence Level.

remains unknown, and the scientific community has tried to explain not only their character but also an explanation of their smallness. Indeed, neutrino masses are at least five orders of magnitude smaller than that of the electron and the rest of charged leptons. This suggests that a new mass generation mechanism may be responsible for them. In order to account for these observations, one can either extend the matter content of the SM or abandon the renormalizability of the theory.

Let us first consider one of the simplest realizations of the first avenue and introduce three right-handed neutrinos N_R^i, that are singlets under the full SM gauge group, also called *sterile* neutrinos.[3] These new fermions allow one to write a Yukawa interaction of the leptonic doublet with the Higgs that after EWSB generates a Dirac mass term for the neutrinos, in a similar manner to the rest of the fermions. Furthermore, the RH neutrinos being SM singlets, a Majorana mass term is allowed by the gauge symmetries of the SM,

$$\mathcal{L}^\nu = -\bar{\ell}_L Y_\nu \widetilde{\Phi} N_R - \frac{1}{2}\overline{N_R^c} M_N N_R + \text{h.c.}\,, \tag{1.2.10}$$

where Y_ν is a 3×3 matrix in flavor space containing the Yukawa couplings similar to Eq (1.2.3), M_N is the symmetric 3×3 Majorana matrix and ${N_R}^c \equiv C\,\overline{N_R}^T$ with $C = i\gamma_2\gamma_1$ being the charge conjugation matrix. In the absence of the Majorana term, the Lagrangian possesses a global $U(1)_L$ symmetry called Lepton Number (LN) under which each lepton is charged (see Section 1.3), while the Majorana mass breaks LN by two units. After EWSB, the Dirac mass term is generated, and the mass matrix for the neutrinos reads

$$\mathcal{L}^\nu_{\text{mass}} = -\overline{\nu_L} m_D N_R - \frac{1}{2}\overline{N_R^c} M_N N_R + \text{h.c.} = -\frac{1}{2}\begin{pmatrix} \overline{\nu_L} & \overline{N_R^c} \end{pmatrix}\begin{pmatrix} 0 & m_D \\ m_D^T & M_N \end{pmatrix}\begin{pmatrix} \nu_L \\ N_R \end{pmatrix} + \text{h.c.}\,, \tag{1.2.11}$$

where $m_D = Y_\nu v/\sqrt{2}$. Note that M_N is a free parameter; it is not protected by gauge invariance and, in consequence, it can be arbitrarily large. The limit $M_N \gg m_D$ corresponds to the famous type-I *seesaw* scenario [31–34], in which the smallness of neutrino masses is not generated by tiny Yukawa couplings but by a hierarchy between the two scales. After block diagonalizing the matrix, the neutrino masses yield

$$m_\nu \simeq -m_D^T M_N^{-1} m_D\,, \qquad m_N \simeq M_N\,, \tag{1.2.12}$$

and one obtains an inverse proportionality relation between the heavy and the active neutrinos. Assuming that neutrino Yukawa couplings are close to that of the top quark, $Y_\nu \sim \mathcal{O}(1)$, then Eq. (1.2.12) requires the Majorana scale to lie close to $M_N \sim 10^{14}$ GeV in order to reproduce the observed light neutrino masses.

An alternative avenue to that of adding new matter content to explain neutrino masses is the Effective Field Theory (EFT) approach. By introducing higher dimensional non-renormalizable operators made out of the SM fields and respecting the symmetries, one can describe in a model independent way the low energy effects of a ultraviolet (UV) theory with a characteristic high

[3] For a comprehensive review see [29] and [30].

scale Λ. These operators are suppressed by powers of this large UV scale Λ and can be seen as corrections to the known renormalizable theory. The higher the dimensionality of the effective operator, the larger the power of the scale that suppresses the operator, therefore this framework allows for a consistent perturbative expansion. Strikingly, within the SM matter content and symmetries, there is a single operator at first order in the expansion (dimension 5), often known as Weinberg's Operator [35]. It is precisely this operator that generates Majorana masses for the neutrinos after EWSB,

$$\mathcal{L}^{d=5} = \frac{1}{2}\,\bar{\ell}_{L\,\alpha}\widetilde{\Phi}\frac{C_\nu^{\alpha\beta}}{\Lambda_{LN}}\widetilde{\Phi}^T\ell^c_{L\,\beta} + \text{h.c.} \longrightarrow \frac{v^2}{2\,\Lambda_{LN}}\overline{\nu^c_{L\alpha}}C_\nu^{\alpha\beta}\nu_{L\,\beta} + \text{h.c.} \tag{1.2.13}$$

This operator naturally accommodates the smallness of neutrino masses since one typically expects the new physics scale Λ_{LN} to lie well above the EW scale, and thus the Weinberg operator is strongly suppressed. By taking the EFT approach, a Majorana mass term for light neutrinos has been obtained, like in the type I seesaw considered above. Indeed, these two avenues are not unrelated since it is precisely the Weinberg Operator the one generated after integrating out the heavy RH neutrinos in Eq. (1.2.11). Matching the low energy Wilson coefficient $C_\nu^{\alpha\beta}$ in Eq. (1.2.13) with the parameters of the high energy theory in Eq. (1.2.11), the following relation is obtained

$$\frac{C_\nu^{\alpha\beta}}{\Lambda_{LN}} = \left(Y_\nu M_N^{-1} Y_\nu^T\right)^{\alpha\beta}\,, \tag{1.2.14}$$

that, in the simplified case of the right-handed neutrinos being degenerate and identifying the BSM scale with the Majorana mass scale $\Lambda_{LN} = M_N$, corresponds to

$$C_\nu^{\alpha\beta} = (Y_\nu Y_\nu^T)^{\alpha\beta}\,. \tag{1.2.15}$$

Furthermore, the EFT approach being model independent, it may well also describe other possible scenarios that generate Majorana neutrino masses. In particular, it allows one to investigate systematically what kind on models could generate the Weinberg operator at tree level by adding a single extra representation to the SM matter content. Precisely, there are two other mediators[4] from a UV complete theory that generate the Weinberg operator when integrated out: scalar $SU(2)_L$ triplet in the type II seesaw [36–40] and a fermionic $SU(2)_L$ triplet in the type III seesaw [41–47], as it can be seen in Fig. 1.1.

Regarding the testability of these minimal scenarios, it is important to note that they generically predict new particles with masses close to the Grand Unification Theory (GUT) scales, $\sim 10^{14}$ GeV, and therefore are out of collider reach. Nonetheless, it is possible to naturally lower this scale (e.g. down to the TeV or even GeV) appealing again to symmetries, in particular, an approximate $U(1)_L$ symmetry. These scenarios require an extended matter content like in the inverse seesaw [48, 49] and the linear seesaw models [50] or in scenarios in which the Weinberg operator is generated at loop level [51]. These low scale seesaw scenarios

[4] A scalar singlet, which would also be allowed by gauge invariance, is unable to generate the Weinberg operator since $C_\nu^{\alpha\beta}$ needs to be symmetric.

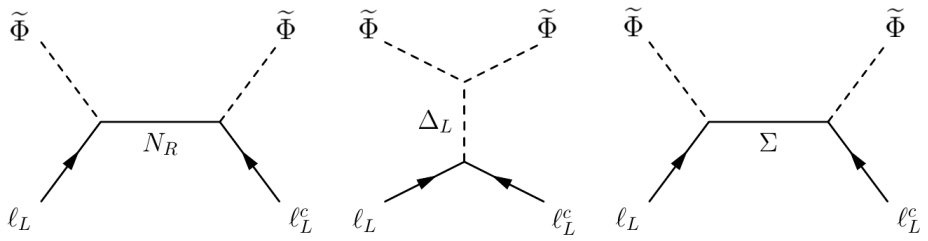

Figure 1.1: The three types of seesaw model for tree level single mediators: type I mediated by a fermionic singlet N_R, type II mediated by a scalar EW triplet Δ_L and type III mediated by a fermionic EW triplet Σ.

are of phenomenological interest since the mediators can be accessible at current experiments and can also leave their imprints indirectly in lepton flavor violating observables. Furthermore, they are theoretically appealing as a Majorana scale $\lesssim$ TeV would avoid a strong contribution to the EW hierarchy problem from the heavy neutrino sector [52–54], see Fig. 1.2.

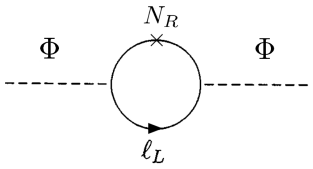

Figure 1.2: Contribution to the hierarchy problem stemming from RH neutrinos.

One of the mysteries of neutrinos is their Majorana or Dirac nature. If the Weinberg operator is responsible for their masses, neutrinos would be Majorana particles, i.e. neutrinos would be their own antiparticle. This would be a ground-breaking discovery since neutrinos would be the only fundamental particles with Majorana character, which would prove that a two-component description of a massive fermion is realized in nature. Also, Majorana neutrinos are one of the best candidates to explain the matter-antimatter asymmetry of the Universe via leptogenesis [55]. But neutrinos may well be Dirac if Lepton Number is not violated. In order to elucidate this issue there are experiments trying to measure LN violating processes such as neutrinoless double beta decay (for a review on $0\nu\beta\beta$ see for example Refs. [56, 57]). So far no experimental evidence for this process has been found, and the character of neutrinos still remains unknown.

Lepton mixing

Once neutrino masses are accounted for by one of the possible mechanisms explained above, a mixing matrix in the lepton sector arises. Analogously to the CKM matrix, the missalignment between the lepton mass eigenstates and the flavor or interaction eigenstates generates the so-

called Pontecorvo-Maki-Nakagawa-Sakata (PMNS) matrix [17, 58],

$$\mathcal{L}_{\rm CC} = \frac{g}{\sqrt{2}} \left[W_\mu^\dagger \left(\overline{\nu_L}\, U_{\rm PMNS}^\dagger \gamma^\mu E_L \right) + h.c. \right] , \tag{1.2.16}$$

that controls flavor-changing processes in the lepton sector and in particular the phenomenon of neutrino oscillations.

1.3 Flavor symmetry

Let us come back for a while to the pure SM. In the limit in which all the Yukawa couplings are set to zero, the only terms in the fermionic Lagrangian are those in Eq. (1.2.2) and the theory presents a large global symmetry: the flavor symmetry [59],

$$\begin{aligned} \mathcal{G}_{\mathcal{F}}^{quarks} &= U(3)_Q \times U(3)_U \times U(3)_D \,, \\ \mathcal{G}_{\mathcal{F}}^{leptons} &= U(3)_\ell \times U(3)_E \,, \end{aligned} \tag{1.3.1}$$

that corresponds to unitary rotations among the different generations or families for each field, see Table 1.3.

	$SU(3)_Q$	$SU(3)_U$	$SU(3)_D$	$SU(3)_\ell$	$SU(3)_E$
Q_L	3	1	1	1	1
U_R	1	3	1	1	1
D_R	1	1	3	1	1
ℓ_L	1	1	1	3	1
E_R	1	1	1	1	3

Table 1.3: Representations of each fermionic field under the non-abelian part of the flavor group

1.3.1 Quark flavor

Once non-zero Yukawa couplings are taken into account, the flavor symmetry of the quark sector is explicitly broken to baryon number,

$$U(3)_Q \times U(3)_U \times U(3)_D \xrightarrow{M_u,\, M_d} U(1)_B \,. \tag{1.3.2}$$

In order to compute the physical degrees of freedom of the flavor sector, it is pertinent to consider the classical symmetries of the Lagrangian that are broken by the Yukawa couplings. Starting with the quark sector, the Yukawa couplings Y_u and Y_d are $n \times n$ complex matrices, therefore each one is determined by $2n^2$ real parameters. Some of those parameters are unphysical since they can be reabsorbed by applying symmetries of the Lagrangian. In particular, to each

symmetry that is solely broken by the Yukawa couplings, one parameter is removed. It follows from Eq. (1.3.2) that there are three unitary symmetries ($3\,n^2$ parameters) among which the combination that corresponds to the unbroken baryon number cannot be employed to reabsorb any parameter, since it leaves the Yukawa couplings unchanged. Therefore the number of physical parameters of the Yukawa couplings in the quark sector is,

$$\text{d.o.f.}(Y_u) + \text{d.o.f.}(Y_d) - \text{d.o.f.}\left(U(n)^3\right) + \text{d.o.f.}(U(1)_B) = 2n^2 + 2n^2 - 3\,n^2 + 1 = n^2 + 1 \quad (1.3.3)$$

In the SM, there are three fermion families. It follows that the number of physical degrees of freedom in the quark flavor sector is ten: the masses of the six different quarks[5],

$$m_u = 2.2\,^{+0.4}_{-0.6}\ \text{MeV}\,, \qquad m_c = 1.28 \pm 0.03\,\text{GeV}\,, \qquad m_t = 173.1 \pm 0.6\,\text{GeV}\,, \quad (1.3.4)$$

$$m_d = 4.7^{+0.5}_{-0.4}\,\text{MeV}\,, \qquad m_s = 96^{+8}_{-4}\,\text{MeV}\,, \qquad m_b = 4.18\,^{+0.04}_{-0.03}\,\text{GeV}\,, \quad (1.3.5)$$

the three mixing angles and the CP violating phase of the CKM matrix. Following the PDG convention [19], these four parameters of the CKM mixing matrix can be parametrized as follows

$$\begin{aligned} V_{\text{CKM}} &= \begin{pmatrix} 1 & 0 & 0 \\ 0 & c_{23} & s_{23} \\ 0 & -s_{23} & c_{23} \end{pmatrix} \begin{pmatrix} c_{13} & 0 & s_{13}e^{-i\delta_{\text{KM}}} \\ 0 & 1 & 0 \\ -s_{13}e^{i\delta_{\text{KM}}} & 0 & c_{13} \end{pmatrix} \begin{pmatrix} c_{12} & s_{12} & 0 \\ -s_{12} & c_{12} & 0 \\ 0 & 0 & 1 \end{pmatrix} \\ &= \begin{pmatrix} c_{12}c_{13} & s_{12}c_{13} & s_{13}e^{-i\delta_{\text{KM}}} \\ -s_{12}c_{23} - c_{12}s_{23}s_{13}e^{i\delta_{\text{KM}}} & c_{12}c_{23} - s_{12}s_{23}s_{13}e^{i\delta_{\text{KM}}} & s_{23}c_{13} \\ s_{12}s_{23} - c_{12}c_{23}s_{13}e^{i\delta_{\text{KM}}} & -c_{12}s_{23} - s_{12}c_{23}s_{13}e^{i\delta_{\text{KM}}} & c_{23}c_{13} \end{pmatrix} \end{aligned} \quad (1.3.6)$$

where $s_{ij} = \sin\theta_{ij}, c_{ij} = \cos\theta_{ij}$. The different elements of the CKM matrix have been measured by a variety of experiments. The global fit obtained by the collaboration CKMfitter [60, 61] gives the following result for the absolute value of the CKM elements:

$$V_{\text{CKM}} = \begin{pmatrix} 0.97434 - 0.00011 & 0.22506 \pm 0.00050 & 0.00357 \pm 0.00015 \\ 0.22492 \pm 0.00050 & 0.97351 \pm 0.00013 & 0.0411 \pm 0.0013 \\ 0.00875^{+0.00032}_{-0.00033} & 0.0403 \pm 0.0013 & 0.99915 \pm 0.00005 \end{pmatrix}. \quad (1.3.7)$$

The value of the CP violating phase according to the latest fit by Ufit is $\delta_{\text{KM}} = 69.2^\circ \pm 2^\circ$ [62]. The CKM matrix is the only source of family changing transitions within the SM and has several distinct properties. First, the fact that the CKM is close to the identity implies that flavor changing processes will be suppressed by the small values of the off-diagonal elements. Note that for these elements not to vanish, the masses for quarks of the same charge need to be non-degenerate, and the mixing angles need to take non-trivial values. Second, Flavor Changing Neutral Currents (FCNC) are absent at tree level. Indeed, the set of transformations in Eq. (1.2.5) leaves neutral currents invariant due to unitarity (photons, Z-bosons and gluons

[5] We report $\overline{\text{MS}}$ quark masses from Ref. [19] at the scale $\mu = 2\text{GeV}$ for light quarks, and at $\mu = m_q$ for $q = c, b, t$.

cannot mediate flavor violation). Therefore, in the SM, FCNC processes only appear at loop level involving W-boson exchange. Furthermore, W-bosons only interact with left-handed fields; chirality flips are thus needed to get a non-zero amplitude, and therefore FCNCs are further suppressed by the Yukawa couplings (either quadratically or logarithmically). These suppressions correspond to the so-called GIM mechanism [63] that was proposed by Glashow, Iliopoulos and Maiani. It successfully explained the suppressed size of flavor transitions and also allowed the prediction of the existence of the charm quark, whose mass was predicted by Gaillard and Lee [64].

The CKM matrix induces CP violation as it contains one phase $\delta_{\rm KM}$, see Eq. (1.3.6). This is just one possible choice of parametrization, hence it is interesting to build a quantity that remains invariant under the flavor transformations and encodes the physical CP violation of the electroweak quark sector. This quantity is the Jarlskog invariant [65, 66],

$$J = \text{Im}\left(V_{ud}V_{cd}^{*}V_{cb}V_{ub}^{*}\right) = c_{12}c_{23}c_{13}^{2}s_{12}s_{23}s_{13}\sin\delta_{\rm KM} \tag{1.3.8}$$

and all CP-violating effects in the electroweak sector of the SM depend on it. Indeed, it is the only basis invariant quantity that can be built with the quark mass matrices and vanishes in the CP-conserving limit,

$$\text{Im}\left(\det\left[M_u M_u^{\dagger}, M_d M_d^{\dagger}\right]\right) = J\left(m_t^2-m_c^2\right)\left(m_t^2-m_u^2\right)\left(m_c^2-m_u^2\right)\left(m_b^2-m_s^2\right)\left(m_s^2-m_d^2\right)\left(m_b^2-m_d^2\right). \tag{1.3.9}$$

The only CP violating phase would become unphysical if any pair of same-charge quarks were degenerate in mass, or any of the mixing angles had a trivial value. Accordingly, the measure of CP violation in Eq. (1.3.9) vanishes in either of this two limits. This allows to understand why CP-violating processes are so suppressed within the SM: even if the CP phase is not small, the product of the mixing angles and the small Yukawa couplings suppresses the CP violating parameter.

This description of the CP phases and number of degrees of freedom in the flavor sector is not complete, though. There is another CP-violating invariant that can be built out of the mass matrices,

$$\text{Arg}\left(\det\left(M_u\, M_d\right)\right). \tag{1.3.10}$$

As it will be further developed in Chapter 2, this combination plays an important role in the Strong CP problem. This extra invariant has remained unnoticed in the counting of physical parameters of Eq. (1.3.3) because one of the symmetries contained in the group $\left[U(3)\right]^3$ of Eq. (1.3.2) is anomalous: the axial symmetry, $U(1)_A$. This symmetry is a valid classical symmetry of the Lagrangian in the massless quark limit, however, it will be later shown that it is anomalous, i.e. explicitly broken at the quantum level by QCD instantons. As a consequence, the $U(1)_A$ cannot reabsorb the parameter in Eq. (1.3.10) since an anomalous term will be generated by the rotation, and the combination

$$\bar{\theta} = \theta_{QCD} + \text{Arg}\left(\det\left(M_u\, M_d\right)\right) \tag{1.3.11}$$

remains physical. This parameter plays no role in the EW sector but would induce CP violation in the strong interactions, see Chapter 2.

1.3.2 Lepton flavor

In the lepton sector, the flavor symmetry is broken by the the charged lepton masses to the product of the three lepton family numbers, i.e. electron L_e, muon L_μ and tau L_τ numbers,

$$U(3)_\ell \times U(3)_E \xrightarrow{M_e} U(1)_e \times U(1)_\mu \times U(1)_\tau \,. \tag{1.3.12}$$

The final fate of the lepton flavor symmetries depends on the neutrino mass mechanism. For illustration, let us consider two cases within the three RH-neutrino paradigm,

$$\mathcal{L}^\nu = -\bar{\ell}_L Y_e \Phi E_R - \bar{\ell}_L Y_\nu \widetilde{\Phi} N_R - \frac{1}{2}\overline{N_R^c} M_N N_R + \text{h.c.} \tag{1.3.13}$$

In the massless limit, this theory has a larger flavor symmetry,

$$U(3)_\ell \times U(3)_E \times U(3)_N \,, \tag{1.3.14}$$

which is broken differently depending on the nature of neutrino masses. It breaks to lepton number if neutrinos are Dirac, while it breaks completely in the case of Majorana neutrinos.

$$U(3)_\ell \times U(3)_E \times U(3)_N \xrightarrow{m_e} U(1)_e \times U(1)_\mu \times U(1)_\tau \xrightarrow{m_\nu} \begin{cases} U(1)_L & \text{Dirac } \nu \text{ masses} \\ \emptyset & \text{Majorana } \nu \text{ masses} \end{cases} . \tag{1.3.15}$$

Let us specify the counting of physical degrees of freedom for the two cases:

- Dirac neutrinos ($M_N = 0$): The counting is analogous to that in the quark sector, since there are two complex matrices Y_e and Y_ν and three $U(n)$ symmetries among which lepton number $U(1)_L$ remains unbroken,

  $$\text{d.o.f.}(Y_e) + \text{d.o.f.}(Y_\nu) - \text{d.o.f.}\left(U(n)^3\right) + \text{d.o.f.}(U(1)_L) = n^2 + 1 \,. \tag{1.3.16}$$

  For three lepton families in the SM, the number of degrees of freedom is again ten: 6 lepton masses, 3 mixing angles and the CP phase of the PMNS matrix.

- Majorana neutrinos ($M_N \neq 0$): The initial parameters consist of two complex matrices Y_e and Y_ν and the complex symmetric matrix M_N that contains $n(n+1)$ parameters. Among those, some parameters can be reabsorbed by the symmetries that are broken by the mass terms: in this case they correspond to the full $\left[U(3)\right]^3$ since LN is also broken,

  $$\text{d.o.f.}(Y_e) + \text{d.o.f.}(Y_\nu) + \text{d.o.f.}(M_N) - \text{d.o.f.}\left(U(n)^3\right) = 2n^2 + n \,. \tag{1.3.17}$$

  These 21 parameters can be parametrized as the 10 parameters discussed in the Dirac case plus two Majorana phases, and the six degrees of freedom of the complex orthogonal matrix R of the Casas-Ibarra parametrization [67]. However not all these 21 parameters will be

accessible with low energy observables. In order to identify them, the same procedure can be applied to the SM extended with the Weinberg operator in Eq. (1.2.13),

$$\text{d.o.f.}(Y_e) + \text{d.o.f.}(C_\nu^{\alpha\beta}) - \text{d.o.f.}\left(U(n)^2\right) = n^2 + n\,. \tag{1.3.18}$$

Thus the number of low-energy parameters of the lepton sector with the d=5 operator is 12, corresponding to the usual ten parameters of the Dirac case plus two Majorana phases, while the remaining six parameters of the Casas-Ibarra matrix R only affect the dynamics of the UV completion and do not leave any low energy imprint.

Analogously to the CKM matrix, the PMNS mixing matrix [17, 58] can be parametrized as,

$$U_{\text{PMNS}} = \begin{pmatrix} c_{12}c_{13} & s_{12}c_{13} & s_{13}e^{-i\delta} \\ -s_{12}c_{23} - c_{12}s_{23}s_{13}e^{i\delta} & c_{12}c_{23} - s_{12}s_{23}s_{13}e^{i\delta} & s_{23}c_{13} \\ s_{12}s_{23} - c_{12}c_{23}s_{13}e^{i\delta} & -c_{12}s_{23} - s_{12}c_{23}s_{13}e^{i\delta} & c_{23}c_{13} \end{pmatrix} \cdot P\,, \tag{1.3.19}$$

where $P = \text{diag}\left(1, e^{i\phi_1}, e^{i\phi_2}\right)$ account for the two possible extra physical CP-phases that are not present in the quark sector if neutrinos are Majorana particles.

Our current knowledge of the physical parameters in the flavor lepton sector can be summarized as:[6]

$$m_e = 0.511 \text{ MeV}\,, \qquad m_\mu = 0.106 \text{ GeV}\,, \qquad m_\tau = 1.78 \text{ GeV}\,, \tag{1.3.20}$$

$$\Delta m^2_{21} = (7.39^{+0.21}_{-0.20}) \times 10^{-5} \text{ eV}^2\,, \qquad \Delta m^2_{32} = \begin{cases} +(2.525^{+0.033}_{-0.031}) \times 10^{-3} \text{ eV}^2 & \text{NH} \\ -(2.512^{+0.034}_{-0.031}) \times 10^{-3} \text{ eV}^2 & \text{IH} \end{cases}, \tag{1.3.21}$$

$$\theta_{12} = \left(33.82^{+0.78}_{-0.76}\right)^\circ\,, \qquad \theta_{23} = \begin{cases} \left(49.7^{+0.9}_{-1.1}\right)^\circ & \text{NH} \\ \left(49.7^{+0.9}_{-1.0}\right)^\circ & \text{IH} \end{cases}, \qquad \theta_{13} = \begin{cases} \left(8.61^{+0.12}_{-0.13}\right)^\circ & \text{NH} \\ \left(8.65^{+0.12}_{-0.13}\right)^\circ & \text{IH} \end{cases},$$

$$\delta_{\text{CP}} = \begin{cases} \left(215^{+40}_{-29}\right)^\circ & \text{NH} \\ \left(284^{+27}_{-29}\right)^\circ & \text{IH} \end{cases}. \tag{1.3.22}$$

Note that within these experimental measurements there are still some incognitos. On the one hand, the absolute mass scale of neutrinos remains undetermined since oscillations are only sensitive to squared mass differences. On the other, the sign of Δm^2_{32} that determines the neutrino mass ordering (whether the lightest neutrino or the second to lightest is mainly

[6] The charged lepton masses are taken from the Particle Data Group [19], and the mixings from global fit performed by the NuFIT 4.0 (2018) collaboration [20] within the three-flavor oscillation paradigm. Note that $\Delta m^2_{31} > 0$ for NO and $\Delta m^2_{32} < 0$ for IO.

composed by electron neutrino) is still unclear, although global fits to current data show some preference to normal hierarchy (NH), over inverted hierarchy (IH). Finally current measurements of the CP-violating phase still have large uncertainties, and the Majorana CP phases remain to be determined.

1.3.3 The SM flavor puzzle

The description above illustrates the striking differences between the flavor and the gauge sector. While gauge interactions are beautifully controlled by only three coupling constants[7] of $\mathcal{O}(1)$, and the gauge sector has been built from fundamental principles, the flavor sector presents a complex structure that requires at least 20 parameters with intricate hierarchies and patterns and whose values are simply imported from observation. Even though the flavor sector has provided predictions that have been confirmed with high accuracy by experiments, this peculiar structure calls for an underlying explanation.

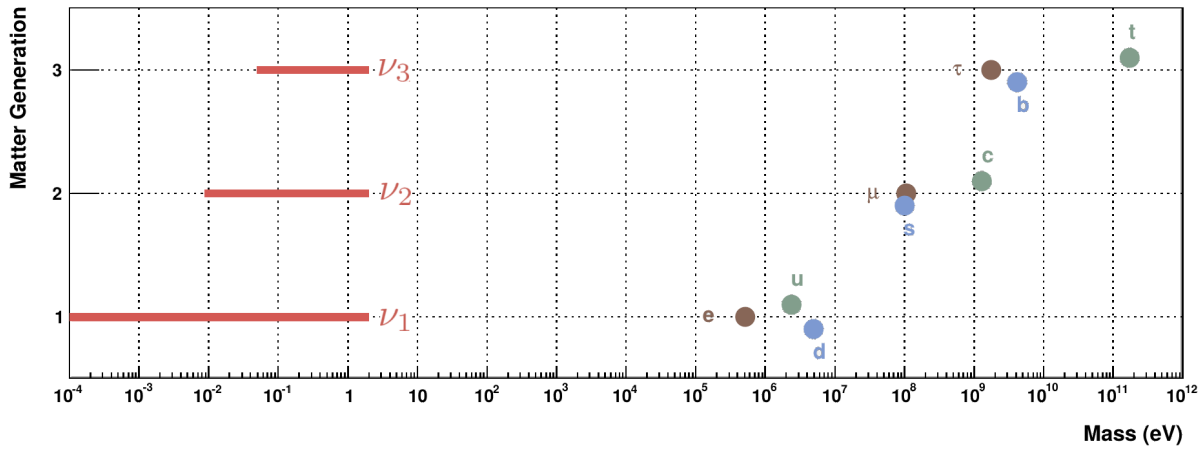

Figure 1.3: Fermion masses in the SM. Figure adapted from Ref. [68].

As is shown in Fig. 1.3, the masses of the charged fermions of the SM span over 6 orders of magnitude or even 12 if we include neutrinos. Not only do the corresponding Yukawa couplings range from order one (for the top quark) to $\mathcal{O}(10^{-6})$ for the electron, or even $\mathcal{O}(10^{-12})$ if neutrinos are Dirac particles, but they also show a strong hierarchy for quarks and charged leptons, while for neutrinos clarification is still needed. Concerning the mixing matrices, while the CKM matrix shows a modest deviation from the identity matrix which corresponds to small mixing among quark families, mixing angles in the lepton sector are large and correspond to matrix elements of the PMNS of the same order of magnitude (see Fig. 1.4).

Why are there three families? What is the *rationale* behind fermion mass hierarchies? Why does the quark sector present small mixings whereas the neutrinos have large mixing angles?

[7] If we include the Higgs sector there are two extra parameters, the Higgs vev v and quartic coupling λ.

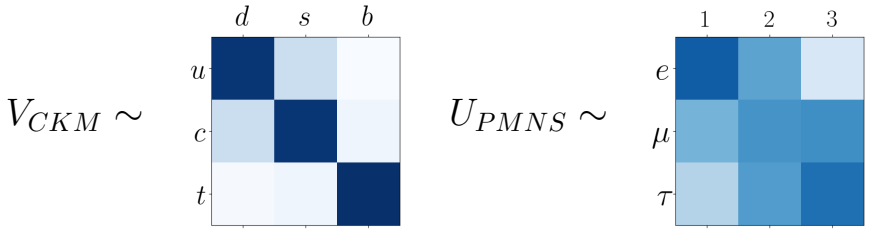

Figure 1.4: Representation of the size of the mixing matrix elements. Lighter colors represent smaller absolute value with respect to darker ones.

These questions constitute the flavor puzzle and have fostered intensive research in trying to understand the possible underlying flavor dynamics behind this complex structure.

New Physics Flavor Puzzle

In spite of the lack of a successful explanation of the origin of flavor, this framework allows one to accommodate in a consistent theory basically all current experimental data. In particular, the fact that FCNC are so suppressed within the SM and the great precision that experiments are achieving in measurements of flavor observables represent a powerful tool for the search of BSM theories. Indeed, generic extensions of the SM need to respect the SM gauge symmetries, but not its global ones. They typically predict thus unacceptable rates for FCNC processes, therefore these observables are able to set stringent bounds on the scale of new physics, well beyond that directly accessible by current experiments. For instance, a striking example is the $K^0 - \overline{K^0}$ system. Measurements of the indirect CP violation parameter ϵ_K and the mass difference Δm_K set bounds on the scale of new physics of the order of $\Lambda \sim 10^5$ TeV [69] for $\mathcal{O}(1)$ Wilson coefficients in the effective operators.

On the other hand, several BSM scenarios motivated by the EW hierarchy problem predict new dynamics not far from the $\sim$ TeV scale. Consequently, in order for them to be compatible with the absence of BSM flavor violation, either the parameters need to be fine-tuned or the energy scale needs to be pushed up to energies several orders of magnitude larger than the TeV scale. This is known as the *new physics flavor puzzle* and suggests that the BSM theories present highly non-trivial flavor structure that resembles that of the SM. For this reason the interest of flavor goes beyond the long-standing dream of explaining the pattern of fermion masses and mixings, and also guides the efforts of constructing any new theory of nature through the stringent constraints it poses.

Flavor beyond the SM

In order to explain the origin of fermion masses and mixings, different BSM constructions have been proposed. Due to the complexity of the flavor pattern it is challenging to find a successful

explanation while agreeing with the precise flavor experimental measurements. Some of these attempts are:

- **Froggat-Nielsen theories**: By imposing the conservation of a global abelian symmetry $U(1)_{FN}$ under which the fermions of different families have different charges, the mass hierarchy can be accommodated [70]. In particular, a scalar "*flavon*" field S with non-vanishing FN charge is introduced and develops a vev, breaking spontaneously the $U(1)_{FN}$. The flavon couples to the fermions with non-renormalizable operators allowed by the abelian symmetry. Accordingly, the different FN-charges of the fermions imply different number of flavon insertions. When the symmetry is spontaneously broken, mass terms for the fermions are generated and the hierarchy is controlled by powers of the small parameter $\epsilon = \langle S \rangle / \Lambda$, where Λ is the scale of flavor dynamics that suppresses the effective operators. This symmetry approach is rather simple but still does not explain the origin of the different charges of each fermion and the full UV complete theory generating those effective operators involves many new fields, complicating the search for an elegant explanation.

- **Discrete symmetries** have also been proposed to be at the origin of the flavor pattern since they avoid the Goldstone bosons that would appear in the case of continuous symmetries that are spontaneously broken. A4 being the most commonly used flavor group [71, 72], the main drawback of this approach is that the discrete symmetry by itself is not sufficient to completely account for the fermion mass hierarchies and mixings in most cases.

- **Grand Unification**: The unification of the strong, weak and electromagnetic interactions [73–75] typically leads to relations among the fermion mass matrices, hence it seems suggestive to try to address both problems simultaneously. Different symmetry groups have been attempted and are still being constructed, the main problem of GUT-based models is the proton stability.

Aside from these specific theoretical frameworks trying to assess the SM flavor pattern, effective approaches have also been constructed in order to explain the New Physics flavor puzzle. Of special relevance for the flavor puzzle is the proposal of Minimal Flavor Violation (MFV) that aims at protecting flavor violation beyond the SM. The MFV hypothesis consists in assuming that the only source of flavor symmetry breaking at low energies are the SM Yukawa couplings themselves, not only in the SM but also in the BSM theories [59, 76–78]. In order to implement MFV, the Yukawa couplings of the SM are promoted to non-dynamical fields, usually called *spurions*, that transform non-trivially under the SM flavor group. Then, the effective field theory is constructed in a way that all effective operators remain invariant under the flavor group by inserting the appropriate spurions.

Minimal Flavor Violation is a way to encode that the low-energy effects of the BSM theory such that they respect the same global symmetries as the SM. In this way, the absence of flavor violation data beyond the SM is justified. However, it is not a theory of flavor since it is unable to explain the complex structure of flavor: neither the hierarchy nor the smallness of

Yukawa couplings are addressed in MFV. In the setup we propose in Chapter 4 that the MFV hypothesis is taken one step ahead by promoting the Yukawa couplings to dynamical fields and the flavor group to a local symmetry, leading to interesting theoretical and phenomenological consequences.

Flavor anomalies

Although the SM beautifully agrees with a large variety of flavor observables, there are currently some intriguing tensions in B-meson physics that may point to New Physics with large lepton-flavor universality violation. In particular, the LHCb Collaboration has reported deviations from the SM in $B \to K^{(*)}\ell^+\ell^-$ decays. In order to reduce the hadronic uncertainties in the theoretical predictions, observables involving ratios of partial widths are particularly useful. Two of those theoretically clean ratios are R_K and R_{K^*} and experimental data from LHCb shows deviations from the SM prediction, which is 1 at leading order, [79, 80]

$$R_K \equiv \frac{\text{BR}\,[B \to K\mu^+\mu^-]}{\text{BR}\,[B \to Ke^+e^-]} = 0.846^{+0.060}_{-0.054}(\text{stat})^{+0.014}_{-0.016}(\text{sys})\,, \tag{1.3.23}$$

$$R_{K^*} \equiv \frac{\text{BR}\,[B \to K^*\mu^+\mu^-]}{\text{BR}\,[B \to K^*e^+e^-]} = 0.69^{+0.11}_{-0.07}(\text{stat})^{+0.05}_{-0.05}(\text{sys})\,, \tag{1.3.24}$$

in the $1.1\text{GeV} < q^2 < 6\text{GeV}$ bin. Each one of these observables presents a deviation from the SM at the 2.5σ level. It is pertinent to note that Belle collaboration measurement [81], that has larger uncertainties is compatible with both the SM prediction and the LHCb result. There are also some discrepancies in other (less theoretically clean) observables, such as $R_{D^{(*)}}$ and in the angular distributions of $B \to K^*\mu^+\mu^-$. Together with these tensions, global fits prefer various BSM scenarios over the SM at the 5σ level [82]. Although the statistical significance of each deviation does not suffice to claim a BSM discovery, data seems to indicate a pattern that deserves to be analyzed with detail. Several models have been proposed to be at the origin of these tensions.

1.4 General considerations on symmetries

Symmetries play a fundamental role in our understanding of the SM and may be the key in the solutions to several of the SM issues. For this reason, it is convenient to review some general considerations of symmetries within QFT, that will be referred to throughout this thesis.

Within the path integral formalism, all the information of a Quantum Field Theory is encoded in the generating functional,

$$\mathcal{Z}[J] = \int [d\phi] e^{i/\hbar\left(S[\phi] + \int d^4x J(x)\phi\right)}\,, \tag{1.4.1}$$

where S corresponds to the action,

$$S[\phi] = \int d^4x \, \mathcal{L}\left(\phi(x), \partial_\mu \phi(x)\right) \,, \tag{1.4.2}$$

and ϕ is a real scalar field chosen as an example. The path integral in Eq. (1.4.1) sums over all possible paths in field space weighted by the exponential of the action, $e^{iS[\phi]/\hbar}$, and allows the computation any time-ordered correlator as,

$$\langle O_1 \dots O_n \rangle := \left\langle 0 \middle| \mathrm{T}\left[\hat{O}_1 \dots \hat{O}_n\right] \middle| 0 \right\rangle = \frac{\int [d\phi]\, O_1[\phi] \dots O_n[\phi] e^{i/\hbar S[\phi]}}{\int [d\phi] e^{i/\hbar S[\phi]}} \,. \tag{1.4.3}$$

This formalism is particularly convenient when evaluating the classical limit. For $\hbar$ much smaller than the relevant action $\hbar \ll S$, the path integral can be evaluated using the stationary phase (or steepest descent) approximation. In this limit, the path integral is dominated by the configurations that correspond to extrema of the action, recovering Hamilton's principle of stationary action that leads to the usual Euler-Lagrange equations of a classical field theory,

$$\partial_\mu \left(\frac{\delta \mathcal{L}}{\delta\left(\partial_\mu \phi\right)} \right) - \frac{\delta \mathcal{L}}{\delta \phi} = 0 \,, \tag{1.4.4}$$

also known as equations of motion (EOM). A symmetry of the action consists in some transformation of the fields that leaves the action invariant,

$$S[\phi + \alpha\, \delta\phi] = S[\phi] \,, \tag{1.4.5}$$

and therefore transforms the Lagrangian in the following way:

$$\mathcal{L} + \delta\mathcal{L} \equiv \mathcal{L}\left(\phi + \beta\, \delta\phi, \partial_\mu \phi + \beta\, \delta \partial_\mu \phi\right) = \mathcal{L}\left(\phi, \partial_\mu \phi\right) + \partial_\mu V^\mu \left(\phi, \partial_\mu \phi, \beta\, \delta\phi\right) \,, \tag{1.4.6}$$

where the boundary term vanishes when integrating over the spacetime, $\int \partial_\mu V^\mu d^4x = 0$. An important feature of theories with continuous symmetries is that they present conserved currents as a consequence of *Noether's Theorem*. It states that to every generator of a continuous symmetry of the theory, there corresponds a conserved current and a time-independent charge. This theorem not only implies the existence of these currents but also allows one to construct them explicitly,

$$J^\mu \equiv -\frac{\delta \mathcal{L}}{\delta \partial_\mu \phi} \delta\phi + V^\mu \,; \qquad \partial_\mu J^\mu = 0 \,. \tag{1.4.7}$$

In addition, as a consequence of the conservation of the current there exists an associated charge that does not change in time,

$$Q(t) \equiv \int d^3x J_0(t,x) \,; \qquad \dot{Q} = \int d^3x \partial_0 J_0 = 0 \,. \tag{1.4.8}$$

It is always possible to write the associated current for any given continuous transformation, even if it does not represent an exact symmetry of the action. In some theories, a symmetry arises when a parameter of the theory is set to zero. If this parameter is small as compared with the relevant parameters of the theory, the transformation is said to be an approximate symmetry. In these cases, Noether's theorem is still useful and states that the associated current is no longer exactly conserved but instead its divergence equals the variation of the Lagrangian,

$$\delta\mathcal{L} = \beta\, \partial_\mu J^\mu \,. \tag{1.4.9}$$

1.4.1 On exact symmetries: Wigner vs Goldstone

There are two possible fates of a continuous exact symmetry in QFT:

- **Wigner-Weyl mode**: The ground state of the theory, the vacuum, is invariant under the symmetry. As a consequence, the corresponding charge (and current) operator annihilates the vacuum, $Q|0\rangle = 0$, $j^\mu|0\rangle = 0$. This implies the existence of degenerate multiplets in the spectrum. In other words, for any state, the symmetry transformation generates another state with the same energy and scattering amplitudes.

- **Nambu-Goldstone mode**: As a consequence of the existence of a continuous family of degenerate minima of the potential, the ground state is not invariant under the symmetry $Q|0\rangle \neq 0$, $j^\mu|0\rangle \neq 0$. The action of the symmetry on a particular vacuum state leads to another degenerate vacuum state. The symmetry is still exact at the Lagrangian level, though. In this case, the symmetry is said to be spontaneously broken and the spectrum of particles does not manifest the symmetry with degenerate multiplets. Instead, the *Goldstone Theorem* implies that there exist as many massless bosonic states as spontaneously broken generators [83–85]. These particles are called Nambu-Goldstone bosons [8] and have a number of interesting properties. First, with respect to the unbroken symmetry, they have the same quantum numbers (or they belong to the same multiplet) as the corresponding broken generator. Second, they are massless particles and their interactions vanish in the limit of the momentum of the Goldstone boson going to zero. In other words, they only present derivative couplings that ensure that the scattering amplitudes are proportional to the GB momentum. It is often the case that the symmetry is not exact but rather approximate. Then, the GB develops a small mass controlled by the parameter that breaks the symmetry, and thus it is called pseudo-Goldstone boson (pGB).

1.4.2 On broken symmetries: Anomalies

So far we have been dealing with symmetries of the action, i.e. classical symmetries. However, the relevant object in a QFT that will determine the values of all observables is the path integral. Thus, for a classical symmetry to survive the process of quantization, the complete path integral has to remain invariant under the transformation, including not only the action but also the functional measure in the path integral (see Eq. (1.4.1)). This is not always the case. There are classical symmetries that are not preserved after the regularization and renormalization procedures. The latter would then provide an explicit breaking. In those cases the symmetry is said to be *anomalous*.

Anomalies have played a central role in our understanding of the SM, from the neutral pion decay to two photons, to the solution of the missing meson problem and the consistency

[8] In the rest of the thesis they will be referred to as Goldstone bosons (GB).

conditions imposed by gauge anomaly cancellation. Indeed, for a QFT to be consistent at the quantum level, its gauge symmetries must be exact both at the classical and at the quantum level. They cannot be anomalous. On the contrary, global symmetries can be anomalous without leading to inconsistencies.

They could also be crucial in some extensions of the SM that search for a solution to the Strong CP problem, such as the Peccei-Quinn solution (see Section 2.3.2). Let us first review the main results of the axial anomaly in a simple theory, and comment next on the general anomaly formula and the main applications.

Axial anomaly

Let us consider a $U(1)$ gauge theory with a charged massive fermion ψ (QED with a massive electron),

$$\begin{aligned}\mathcal{L} &= -\frac{1}{4}F_{\mu\nu}F^{\mu\nu} + \overline{\psi}(i\not{D} - m)\psi \\ &= -\frac{1}{4}F_{\mu\nu}F^{\mu\nu} + \overline{\psi}_L(i\not{\partial} - ie\not{A})\psi_L + \overline{\psi}_R(i\not{\partial} - ie\not{A})\psi_R - m\overline{\psi}_L\psi_R - m\overline{\psi}_R\psi_L\,.\end{aligned} \tag{1.4.10}$$

In the massless limit $m \to 0$, the Lagrangian presents two classical symmetries,

$$\psi \to e^{i\beta_V}\psi, \qquad \psi \to e^{i\beta\gamma_5}\psi \tag{1.4.11}$$

whose corresponding currents can be computed using Noether's formula in Eq. (1.4.7),

$$j_V^\mu = \overline{\psi}\gamma^\mu\psi = \overline{\psi}_R\gamma^\mu\psi_R + \overline{\psi}_L\gamma^\mu\psi_L, \tag{1.4.12}$$

$$j_A^\mu = \overline{\psi}\gamma^\mu\gamma^5\psi = \overline{\psi}_R\gamma^\mu\psi_R - \overline{\psi}_L\gamma^\mu\psi_L\,, \tag{1.4.13}$$

where j_V^μ and j_A^μ denote the vector and the axial currents respectively. Using the EOM, the divergence of the currents can be computed at the classical level, obtaining

$$\partial_\mu j_A^\mu = 2im\overline{\psi}\gamma_5\psi\,, \qquad \partial_\mu j_V^\mu = 0\,. \tag{1.4.14}$$

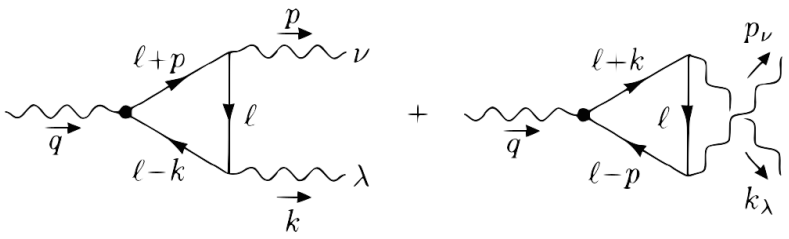

Figure 1.5: Diagrams contributing to the two-photon matrix element of the divergence of the axial vector current. Figure adapted from Ref. [86].

Therefore the vector symmetry is exactly conserved and the axial current is recovered in the massless limit. It is now pertinent to ask whether these symmetries persist once quantum effects are taken into account. The answer was given first by Steinberger [87] and Schwinger [88] in the context of the neutral pion decay $\pi^0 \to \gamma\gamma$, and later on by Adler, Bell and Jackiw [89–91] who found that the axial current is explicitly broken at the quantum level. This constitutes the so-called Adler–Bell–Jackiw (ABJ) anomaly. It can be shown either by computing the transformation of the integral measure, the so-called the Fujikawa method [92], or by computing the triangle diagrams in Fig. 1.5. The result states that in a background of gauge potential fields, the current is no longer conserved, and in the massless fermion limit its divergence reads,

$$\partial_\mu \left\langle J^\mu_A(x) \right\rangle_{A_\mu} = -\frac{e^2}{16\pi^2}\varepsilon^{\mu\nu\alpha\beta}F_{\mu\nu}F_{\alpha\beta} = -\frac{\alpha}{2\pi}F_{\mu\nu}\widetilde{F}_{\alpha\beta}\,, \tag{1.4.15}$$

where $\alpha = e^2/4\pi$ is the electromagnetic fine structure constant, $\widetilde{F}_{\alpha\beta} = \frac{1}{2}\varepsilon^{\mu\nu\alpha\beta}F_{\mu\nu}$ is the dual field strength tensor and $\varepsilon^{\mu\nu\alpha\beta}$ is the fully antisymmetric Levi-Civita symbol with the convention $\varepsilon^{0123} = +1$. A pertinent question is whether this formula receives quantum corrections from higher order diagrams. However, as it was shown by the Adler-Bardeen theorem [93, 94], this result is one-loop exact.

Finally, taking into account the quantum anomaly and fermion masses, the variation of the Lagrangian after performing the axial rotation in Eq. (1.4.11) by an infinitesimal angle β can be obtained using Eq. (1.4.9),

$$\delta\mathcal{L} = \beta\,\partial_\mu J^\mu = 2\beta i m\bar{\psi}\gamma_5\psi - \beta\frac{\alpha}{2\pi}F_{\mu\nu}\widetilde{F}\mu\nu\,. \tag{1.4.16}$$

The ABJ anomaly formula in Eq. (1.4.15) applies to the non-conservation of a global abelian current, the axial current $U(1)_A$, in the presence of a background electromagnetic field, i.e. gauge potential fields of a gauged $U(1)_{em}$ group. Nonetheless the anomaly can also be computed for any generic current,

$$j^\mu_{gen} = \sum \bar{\Psi}_L\gamma^\mu T^a_L\Psi_L + \bar{\Psi}_R\gamma^\mu T^a_R\Psi_R\,, \tag{1.4.17}$$

where T^a_L and T^a_R correspond to the generators of the corresponding fermionic representations under the global symmetry. The **anomaly master formula** for the generic fermionic current in the presence of any gauge group $\mathcal{G}$ reads,

$$\partial_\mu j^\mu_{gen} = \frac{\alpha_X}{8\pi}C^{abc}_{group}\,X_{b\,\mu\nu}\widetilde{X}^{\mu\nu}_c\,, \tag{1.4.18}$$

where $\widetilde{X}^{\mu\nu} = \frac{1}{2}\epsilon^{\mu\nu\sigma\rho}X_{\sigma\rho}$, α_X is the fine structure constant of the corresponding gauge interaction $\alpha_X = g_X^2/4\pi$ and the group theoretical factor C_{group} corresponds to

$$C^{abc}_{group} = \sum Tr\left[T^a_L\{t^b_L, t^c_L\}\right] - \sum Tr\left[T^a_R\{t^b_R, t^c_R\}\right]\,, \tag{1.4.19}$$

where t^b_R and t^b_L are the infinitesimal generators of the representation under the gauge group $\mathcal{G}$ for the fermions Ψ_R and Ψ_L, respectively. The computation of the anomaly for different currents will be relevant at different stages of this thesis. It will allow us to compute the axion anomalous couplings in Chapters 5, 7 and 8, but also to verify the consistency of different theories via gauge anomaly cancellation, or 't Hooft anomaly matching conditions, see Chapters 4 and 6.

Gauge anomalies

When computing the anomaly we have been focusing on the non-conservation of a global current. Interestingly the same analysis can be applied to a gauged or local current. If a gauge symmetry is anomalous, in other words, explicitly broken at the quantum level, the theory becomes non-unitary and therefore inconsistent. The fact that all gauge anomalies have to vanish after summing over all fermion representations puts stringent constraints on the fermionic matter content of chiral gauge theories. Indeed, this is the only theoretical constraint on the SM structure of matter fermionic fields, as the gauge weak interactions are chiral. In particular for the SM, the hypercharges of quarks and leptons are such that all gauge anomalies automatically cancel within each generation.

This consistency condition will be specially relevant in the BSM models that will be developed in Chapters 4 to 6.

't Hooft anomaly matching conditions

In addition to gauge anomaly cancellation, anomalies also provide a consistency condition for the spectrum of confining field theories. In order to state the conditions let us consider a $SU(N)$ confining theory with n flavors of massless quarks ψ^i. At energies above the confinement scale, this theory presents an exact global flavor symmetry G_F, whose associated current reads,

$$j^\mu_{G_F} = \bar{\psi}_L \gamma^\mu T^a_L \psi_L + \bar{\psi}_R \gamma^\mu T^a_R \psi_R \,. \tag{1.4.20}$$

We will consider only exact global symmetries. Thus, their anomalies in the gauge field background of $SU(N)$ need to vanish, $G_F \times [SU(N)]^2$, and the current is exactly conserved,

$$\partial_\mu j^\mu_{G_F} = 0 \,. \tag{1.4.21}$$

After confinement, the spectrum of the theory does not consist of quarks and gauge potentials, but rather singlets of the confining group: hadrons. Then, one can define the current associated with the global symmetry in Eq. (1.4.20) in terms of the massless bound states χ^i,

$$j^\mu_{G_F} = \bar{\psi}_L \gamma^\mu B^a_L \psi_L + \bar{\psi}_R \gamma^\mu B^a_R \psi_R \,. \tag{1.4.22}$$

The 't Hooft consistency condition states that, if the symmetry associated with $j^\mu_{G_F}$ is not spontaneously broken upon confinement, then there exist massless spin 1/2 bound states χ^i, which satisfy the condition,

$$Tr\big[T^a_L\{T^b_L, T^c_L\}\big] - Tr\big[T^a_R\{T^b_R, T^c_R\}\big] = Tr\big[B^a_L\{B^b_L, B^c_L\}\big] - Tr\big[B^a_R\{B^b_R, B^c_R\}\big] \,. \tag{1.4.23}$$

In other words, the *global anomalies* $[G_F]^3$ at high energies in terms of the fundamental quarks, i.e. the left-hand side of Eq. (1.4.23), need to be matched in the low energy theory by massless composite fermions generating the same anomaly. These are called the 't Hooft anomaly matching conditions since they were first proposed by him in Ref. [95], where he

gave the following argument. The symmetry G_F being exact, it can be gauged at the cost of adding massless spectator fermions that only transform under the G_F group and cancel the anomaly $[G_F]^3$. The G_F coupling constant can be made arbitrarily small so that the fermions are effectively unmeasurable. When the $SU(N)$ confines, the spectator fermions are still in the low energy spectrum, and therefore the bound states of $SU(N)$ need to exactly cancel the anomalies generated by the spectators, in order for the gauged G_F to be a consistent theory. Those anomalies are nothing but the original anomaly of the quarks in the high energy theory. This consistency conditions have been also shown in Ref. [96] and by Coleman and Grossman [97] from the basic principles of analyticity and unitarity of the S-matrix.

CHAPTER

2 The strong CP problem

Let us consider the QCD sector of the SM Lagrangian in Eq. (1.1.1) after EWSB,

$$\mathcal{L}_{\rm QCD} = -\frac{1}{4} G^a_{\mu\nu} G^{a\mu\nu} + \theta \frac{\alpha_s}{8\pi} G^a_{\mu\nu} \widetilde{G}^{a\mu\nu} + \overline{Q} \left(i \not{D} - M \right) Q \tag{2.0.1}$$

where Q denotes a vector containing all SM quarks and M is the corresponding mass matrix. This Lagrangian contains two parameters that violate CP invariance, namely the θ-parameter and a global phase in the quark mass matrices. But these two phases are not unrelated.

As we anticipated in Eqs. (1.3.11) and (1.4.15), an axial rotation common to all quarks by a phase β shifts both CP phases,[1]

$$\mathcal{L}_{\not{CP}} = (\theta - 12\beta) \frac{\alpha_s}{8\pi} G^a_{\mu\nu} \widetilde{G}^{a\mu\nu} - \overline{Q} M e^{2i\beta\gamma_5} Q \,, \tag{2.0.2}$$

leaving a single physical CP-violating phase in the strong sector that is invariant under field redefinitions[2],

$$\overline{\theta} \equiv \theta_{\rm QCD} + \ \text{Arg} \left(\det \ M \right) . \tag{2.0.3}$$

The so called $\bar{\theta}$-term,

$$\mathcal{L}_\theta = \bar{\theta} \frac{\alpha_s}{8\pi} G^a_{\mu\nu} \widetilde{G}^{a\mu\nu} \tag{2.0.4}$$

is odd under both parity and time reversal invariance, while it conserves charge conjugation and thus violates CP. As a consequence, CP violating observables such as the electric dipole moment of the neutron (nEDM) are sentitive to the $\bar{\theta}$-parameter and allow one to measure it. So far, experiments designed to detect a nEDM have set stringent bounds, $d_n < 3 \times 10^{-26}$ e·cm (90% c.l.) [98, 99]. Several nEDM projects are expected to improve this bound by 2-3 orders of magnitude in the next 3-5 years [100, 101]. Moreover, the measurement of the EDM of charged particles, such as protons and deuterons, can be performed using storage rings and there are experimental proposals aiming at sensitivities of 10^{-29} e · cm for the proton EDM in the next decade [102].

[1] The shift on the anomalous term can be computed applying the ABJ anomaly formula with the group theory factor corresponding to a rotation of the 6 SM quarks, see Eq. (1.4.19).

[2] In the physical CP phase there is no relative factor since $\text{Arg} \left(\det \left(M e^{2i\beta} \right) \right) = 12\beta$.

The nEDM is still the most constraining observable, though. There are several estimations of the nEDM as a function of $\bar{\theta}$ [103–109] spanning the range $d_n = (0.1 - 2) \times 10^{-15}\bar{\theta}$ e $\cdot$ cm . The bound on the $\bar{\theta}$-parameter which results is, at present,

$$|\bar{\theta}| < (3 - 0.2) \times 10^{-10} \quad (90\% \text{ c.l.}). \tag{2.0.5}$$

The extremely small size of this parameter as compared to an arbitrary $\mathcal{O}(\pi)$ phase constitutes what is called the Strong CP problem. Or in other words, "why does QCD seem not to violate CP?"

It could be tempting to explain the smallness of this parameter by noting that if $\bar{\theta}$ is set to zero, a symmetry emerges, CP, and therefore the parameter is protected by CP invariance. However this is not true since we know for a fact that CP is not a good symmetry of nature. Indeed CP violation in the weak sector is experimentally established and all observations fit within the CKM framework. Therefore the smallness of $\bar{\theta}$ still calls for an explanation. It should be stressed, though, that there is no theoretical inconsistency or actual experimental discrepancy with a vanishing value of $\bar{\theta}$. From this point of view, it is legitimate to argue that the strong CP problem is not actually a real problem but rather a hint, a really interesting hint, that can guide us in the search for a more complete theory of nature.

Although the strong CP problem can be understood in simple terms as we have just reviewed, there are several subtleties and interesting physics behind it. Why does the θ-term have physical implications if it corresponds to a total derivative?[3] What is an instanton and how do we know they exist? How does this relate to the missing meson problem? Why does the θ-parameter describe the QCD vacuum? This chapter will be devoted to clarifying these issues and gain a better understanding of the strong CP problem and the $\bar{\theta}$-parameter.

2.1 The missing meson problem

Let us consider QCD with only two flavors, the up and down quarks. The fermionic Lagrangian reads,

$$\mathcal{L} = \overline{q} i \not{D} q - \overline{q} M_q q = \overline{q}_L i \not{D} q_L + \overline{q}_R i \not{D} q_R - \left(\overline{q}_L \, M_q q_R + \text{h.c.} \right) , \tag{2.1.1}$$

where $q_{L,R} = \left(u_{L,R}, d_{L,R}\right)^T$ and M_q denotes the quark mass matrix for the first generation,

$$M_q = \begin{pmatrix} m_u & 0 \\ 0 & m_d \end{pmatrix} . \tag{2.1.2}$$

Since the up and down quark masses are much smaller than the QCD confinement scale m_u, $m_d \ll \Lambda_{\text{QCD}}$, to a good approximation the second term in Eq. (2.1.1) can be neglected

[3] Bardeen's identity $G^{\alpha}_{\mu\nu}\widetilde{G}^{\mu\nu\alpha} = \partial_\mu K^\mu$.

for the present discussion of the hadronic spectrum. In the massless limit and at the classical level, the Lagrangian remains invariant under the following global transformation,

$$\begin{pmatrix} u_L \\ d_L \end{pmatrix} \to U_L \begin{pmatrix} u_L \\ d_L \end{pmatrix}, \quad \begin{pmatrix} u_R \\ d_R \end{pmatrix} \to U_R \begin{pmatrix} u_R \\ d_R \end{pmatrix}, \tag{2.1.3}$$

where $U_{L,R}$ are general unitary matrices. Therefore it presents a global chiral symmetry $U(2)_L \times U(2)_R = SU(2)_L \times SU(2)_R \times U(1)_L \times U(1)_R$. Their corresponding currents can be arranged into the vectorial R+L (or isospin) and baryon number currents,

$$j_V^\mu = \overline{q}\gamma^\mu q, \qquad j_V^{\mu a} = \overline{q}\gamma^\mu \frac{\sigma^a}{2} q\,, \tag{2.1.4}$$

and the axial R-L currents,

$$j_A^\mu = \overline{q}\gamma^\mu\gamma^5 q, \qquad j_A^{\mu a} = \overline{q}\gamma^\mu\gamma^5 \frac{\sigma^a}{2} q\,, \tag{2.1.5}$$

where σ^a are the Pauli matrices.

As we already commented in Section 1.4.1, there are two possible fates for any symmetry of the interactions: it can be are realized à la Wigner-Weyl or à la Goldstone. The hadronic spectrum shows particles arranged in quasi-degenerate multiplets of the isospin symmetry $U(2)_V = U(2)_{L+R}$, which indicates that the isospin symmetry is realized in the Wigner-Weyl mode. On the other hand, the observed hadrons cannot be arranged in multiplets of the axial transformations; light pseudoscalar particles are observed instead (the three pions), which can be associated with the pseudo-Goldstone bosons of the axial currents $j_A^{\mu a}$ in Eq. (2.1.5). Consequently, the hadronic spectrum can be understood as stemming from the chiral symmetry breaking pattern $SU(2)_L \times SU(2)_R \times U(1)_L \times U(1)_R \longrightarrow SU(2)_V \times U(1)_V$, which is compatible with the chiral condensate taking a non-zero vacuum expectation value $\langle \bar{u}_L u_R + \bar{d}_L d_R \rangle \neq 0$.

However, the current j_A^μ associated to the axial symmetry $U(1)_A$ does not seem to be realized in any of the two possible modes. The Wigner realization would imply the existence of a parity doubled spectrum, in disagreement with experimental observations, while the Goldstone mode would imply the existence of yet another light pseudoscalar in addition to the three pions, a state which is absent in nature.[4] It was Weinberg who pointed out this issue and called it the $U(1)_A$ problem [110], or the missing meson problem.

The solution to this problem was found by 't Hooft [111–113] who realized that the $U(1)_A$ symmetry was indeed badly and explicitly broken in QCD via the ABJ anomaly (see Section 1.4.2),

$$\partial_\mu j_A^\mu = \frac{\alpha}{2\pi} G_{\mu\nu}\widetilde{G}^{\mu\nu}\,. \tag{2.1.6}$$

[4] The lightest pseudoscalar particle with the same quantum numbers as the axial current is the η'-meson, and it has a mass of the order of that of the proton and the rest of QCD bound states $\sim \Lambda_{\rm QCD}$; it cannot thus be associated with the missing pGB.

This is not the end of the story since this anomalous term equals a total derivative due Bardeen's identity [114],

$$G^{\alpha}_{\mu\nu}\widetilde{G}^{\mu\nu\alpha} = \partial_\mu K^\mu \,, \tag{2.1.7}$$

where $K^\mu = 2\epsilon^{\mu\nu\rho\sigma}\,\mathrm{tr}\left(A_\nu\partial_\rho A_\sigma - g_s\frac{2i}{3}A_\nu A_\rho A_\sigma\right)$ is the Chern-Simons current. Usually, when the divergence of a current is non-zero but equals a total derivative, it is possible to redefine the current and construct a new axial current whose divergence vanishes,

$$j'^{\mu}_A = j^\mu_A - K^\mu \quad \Longrightarrow \quad \partial_\mu j'^{\mu}_A = 0\,. \tag{2.1.8}$$

However, even if the anomalous term corresponds to a total derivative, there are field configurations in the QCD vacuum for which the surface integral at infinity does not vanish (see Noether's Theorem in Section 1.4). As a consequeance, the QCD anomaly explicitly breaks the axial symmetry due to instantons, which are configurations generating the non-trivial vacuum structure of QCD, as will be discussed next in more detail. In summary, it became clear that the $U(1)_A$ group is not a good symmetry of QCD to begin with, and therefore, the spectrum does not reflect it neither manifestly nor via Goldstone modes.

With the understanding of the axial anomaly and the role of instantons, the missing meson problem was solved, but another problem emerged: the strong CP problem, since it became clear that the anomalous term cannot be disregarded and deserves full consideration in light of the non-trivial QCD vacuum.

2.2 QCD vacuum

The theory of Quamtum Chrommodynamics becomes strongly coupled at low energies. Therefore the properties of the QCD vacuum cannot be tackled with the usual perturbative expansions, and other methods are required. In the same way that tunneling processes in Quantum Mechanics do not arise at any order in perturbation theory, QCD presents analogous phenomena to barrier penetration that require semi-classical methods. In particular, one of the best methods for computing these kind of properties of QFT is the Euclidean path integral. In this section, we will partially follow the description in the book in Ref. [115] by S. Coleman, supplemented by the lectures of Andrew Cohen in the Invisibles School 2019.

Let us start by refreshing Feynman's path integral formalism in which quantum amplitudes can be expressed as sum over all possible paths interpolating from the intial state $|i\rangle$ to the final state $|f\rangle$,

$$\langle i|e^{-iHt/\hbar}|f\rangle = N\int [d\phi]e^{iS/\hbar}\,. \tag{2.2.1}$$

In this way, the probability of the initial state to time-evolve to the final state can be computed by applying the steepest descent method to compute the path integral.

Let us now consider a completely different matrix element,

$$\mathcal{Z}_{fi}(\tau) = \langle i|e^{-H\tau/\hbar}|f\rangle\,. \tag{2.2.2}$$

Note that this amplitude does not correspond to the time evolution operator due to the absence of the imaginary unit i, and τ is just a parameter and does not correspond to the usual time[5]. This amplitude can be evaluated by inserting a basis of energy eigenstates $|n\rangle$ with corresponding energy eigenvalues E_n,

$$\mathcal{Z}_{fi}(\tau) = \sum_n \langle i|n\rangle\langle n|f\rangle e^{-E_n\tau/\hbar} \xrightarrow{\tau\to\infty} \langle i|\Omega\rangle\langle\Omega|f\rangle e^{-E_0\tau/\hbar}\,. \tag{2.2.3}$$

In the limit $\tau \to \infty$, the matrix element in Eq. (2.2.3) is dominated by the lowest energy eigenstate, i.e. the vacuum or ground state $|\Omega\rangle$ with energy E_0. As a consequence, by computing the matrix element for a given basis, the vacuum of the theory can be fully characterized [115]. The matrix element in Eq. (2.2.2) looks familiar, it seems analogous to that in Eq. (2.2.1). Indeed, if we identify $\tau = it$ we can compute $\mathcal{Z}_{fi}(\tau)$ using the path integral corresponding to a theory with no time but 4 spatial dimensions, i.e. the Euclidean path integral,[6]

$$\lim_{\tau\to\infty} \mathcal{Z}_{fi}(\tau) = \langle i|\Omega\rangle\langle\Omega|f\rangle e^{-E_0\tau/\hbar} = N\int [d\phi] e^{-S_E/\hbar}\,. \tag{2.2.4}$$

To sum up, we have translated the problem of characterizing the non-perturbative vacuum of a QFT in Minkowski spacetime (3 spatial and one temporal dimensions), to computing the path integral for the corresponding theory with 4 spatial dimensions. If the steepest descent method is now applied to the path integral, the result is that the path integral is dominated by the stationary points of S_E, that is the classical solutions of finite action of the Euclidean path integral.

2.2.1 Euclidean Yang-Mills theory

Our goal now is to find all the finite action classical solutions of the Euclidean EOM of a Yang-Mills theory. Let us first briefly review Yang-Mills gauge theories in order to establish notational conventions that will differ from those used in the rest of the thesis.

Yang-Mills theories are based on compact Lie groups that have associated Lie algebras. A representation of this algebra is a set of N hermitian matrices T^a satisfying the following relations,

$$\left[T^a, T^b\right] = if^{abc}T^c\,, \qquad (T^a)^\dagger = T^a\,, \qquad \mathrm{tr}\left(T^aT^b\right) = T(R)\delta^{ab}\,, \tag{2.2.5}$$

where f^{abc} are the fully anti-symmetric structure constants and $T(R)$ is the Dynkin index of the representation R. The common convention for the normalization of the generators of the fundamental representation will be used, $\mathrm{tr}\left(T^aT^b\right)\big|_{\text{fund}} = \frac{1}{2}\delta^{ab}$.

[5] Although sometimes it can be misleading, the parameter τ is often dubbed imaginary time.

[6] Under the change of variables $\tau = it$, the exponent transforms as $iS = i\int dt\mathcal{L} = i\int(-id\tau)(-\mathcal{L}_E) = -\int d\tau\mathcal{L}_E = -S_E$.

Gauge fields. For each element of the algebra a real vector potential is introduced $A^a_\mu(x)$, i.e. the gauge fields, that can be arranged into the following matrix fields,[7]

$$A_\mu(x) \equiv -igA^a_\mu T^a \,, \tag{2.2.6}$$

where g is the gauge coupling constant. Note that this convention differs to that used in Section 1.1, where the coupling constant is not included in the gauge potential (e.g. see Eq. (1.1.4)). The other difference is that throughout this section the metric that contracts the Lorentz indices is the Euclidean metric, with signature $(+,+,+,+)$ and $x_\mu = (\tau, \vec{x})$. The corresponding field strength reads,

$$F_{\mu\nu} = \partial_\mu A_\nu - \partial_\nu A_\mu - i\left[A_\mu, A_\nu\right] \,, \tag{2.2.7}$$

where it is implicit that $F_{\mu\nu} = F^a_{\mu\nu} T^a$.

Gauge transformations. In gauge theories, two field configurations are equivalent if they are related by a gauge transformation, that is a map from space[8] into elements of the Lie Group,

$$g(x) = e^{i\omega^a T^a} \,. \tag{2.2.8}$$

Under a gauge transformation $g(x)$, the gauge potential and the field strength transform as follows,[9]

$$A_\mu \longrightarrow A^{(g)}_\mu = g(x) A_\mu \, g^{-1}(x) + ig(x)\partial_\mu g^{-1}(x) \,, \qquad F_{\mu\nu} \longrightarrow F^{(g)}_{\mu\nu} = g(x) F_{\mu\nu} \, g^{-1}(x) \,. \tag{2.2.9}$$

2.2.2 Instantons

Let us consider the Euclidean action for a pure Yang-Mills theory,

$$S_E = \frac{1}{4g^2} \int d^4x F_{\mu\nu} F^{\mu\nu} \,, \tag{2.2.10}$$

to which corresponds the usual EOM for gauge fields:

$$D_\mu F^{\mu\nu} = 0 \,. \tag{2.2.11}$$

The trivial solution to this equation is $F_{\mu\nu} = 0$, which corresponds to $A_\mu = ig(x)\partial_\mu g^{-1}(x)$. This solution is called "pure gauge" since it corresponds to gauge transformations of $A_\mu = 0$, and the action density vanishes at every point of space. We are interested in finding non-trivial solutions, that is non-zero finite action solutions to Eq. (2.2.11). Before constructing such solutions, let us check if they actually exist and recall the generalization of Derrick's theorem [116] to Yang-Mills theories.

[7] From now on we will refer to the generators of the fundamental representation as T^a whereas the generators of a generic representation R will be $T^a(R)$.

[8] spacetime if we were using the Minkowski metric.

[9] The notation for the coupling constant is g, while the element of the gauge group is $g(x)$.

Theorem. In Euclidean Yang-Mills theories in D spatial dimensions, the only non-singular finite-action classical solutions of the EOM are gauge transformations of $A^\mu = 0$, for $D \neq 4.$, that is, pure gauge configurations.

Proof. Let us assume that the field configuration $\bar{A}_i(x)$ is one of such finite action solutions. From it, one can construct the one-parameter family of field configurations by rescaling lengths,

$$A^\mu_\lambda(x) = \lambda\, \bar{A}^\mu(\lambda x)\,. \tag{2.2.12}$$

Due to Hamilton's principle, any solution of the classical theory has to be a stationary point of the action. As a consequence, it also has to be a stationary point among the family we have just constructed. The action scales as,

$$S_E(\lambda) = S_E[A^\mu_\lambda] = \lambda^{4-D} S_E[\bar{A}^\mu]\,. \tag{2.2.13}$$

For the solution to be stationary we must require that,

$$\left.\frac{dS_E(\lambda)}{d\lambda}\right|_{\lambda=1} = 0 \quad \Longrightarrow \quad 0 = (4-D) S_E[\bar{A}^\mu]\,. \tag{2.2.14}$$

Consequently for $D \neq 4$, the action needs to vanish $S_E[\bar{A}^\mu] = \frac{1}{4g^2}\int d^4x F^2 = 0$. Since the action is the integral of a non-negative function, for the whole integral to vanish the integrand needs to be zero at every point. Therefore the only solution of the classical theory corresponds to the pure gauge $F_{\mu\nu} = 0$. □

Luckily, we live in 3+1 dimensions so we are interested in the 4-dimensional Euclidean Yang-Mills theory for which non-trivial solutions can exist. Let us consider the sphere at infinite radius in Euclidean space, $S^3_\infty \subset \mathbb{R}^4$. For the action to be finite, it is necessary for the integrand in Eq. (2.2.10) to fall for large radius $r = |x| \to \infty$ faster than

$$F_{\mu\nu}F^{\mu\nu} \sim 1/r^{4+\epsilon} \quad \Longrightarrow \quad F_{\mu\nu} \sim 1/r^{2+\epsilon}\,, \tag{2.2.15}$$

for $\epsilon > 0$. One may be tempted to impose that the gauge potential needs to go as $A_\mu \sim 1/r^{1+\epsilon}$, but this would be too restrictive. The general form that A_μ can take is an arbitrary gauge transformation of the previous expression,

$$A_\mu \sim \mathcal{O}\left(\frac{1}{r^{1+\epsilon}}\right) + ig(x)\partial_\mu g(x)^{-1} \xrightarrow{r\to\infty} ig(x)\partial_\mu g^{-1}(x)\,, \tag{2.2.16}$$

where $g(x)$ is a function of the angular variables only. We are then interested in solutions that tend to *a pure gauge configuration at infinity*. Those are fully determined by specifying the element of the gauge group $g(x)$ at every point at infinity, that is a map of the sphere at infinity to the gauge group G,

$$g(x): \quad S^3_\infty \longrightarrow G\,. \tag{2.2.17}$$

A pertinent question now is whether any of those configurations can be gauge transformed to the trivial one. It turns out that these maps fall into disjoint classes that cannot be continuously transformed into one another, i.e. different homotopy classes. The homotopically disconnected

maps from a S^n sphere into some group G are classified by the group $\pi_n(G)$, which in our case of interest is non-trivial,

$$\pi_3\left(SU(n)\right) = \mathbb{Z}\,, \text{ for } n \geq 2\,, \tag{2.2.18}$$

where $\mathbb{Z}$ denotes the set of integer numbers. This means that the connected components of the space of finite-action solutions of Yang-Mills $SU(n)$ theories are in one-to-one correspondence with the homotopy classes of mappings from the 3-sphere to the gauge group, that correspond to $\pi_3\left(SU(n)\right) = \mathbb{Z}$.

The integer that allowsthe classification of these topologically disconnected solutions is the winding number ν, or Pontryagin number for the mathematically oriented. It can be computed for any such map,

$$\nu(g) = \frac{1}{24\pi^2}\int_{\mathbf{S}^3} d\theta_1 d\theta_2 d\theta_3 \epsilon^{ijk}\,\mathrm{tr}\left(g^{-1}\partial_i g g^{-1}\partial_j g g^{-1}\partial_k g\right), \tag{2.2.19}$$

where θ_1, θ_2, θ_3 are three angles parametrizing S^3.[10] The winding number is a topological quantity that only depends on the boundary conditions of the field configuration, in this case on the values of the gauge potential in the sphere S^3 at infinity. It is easy to get an intuitive idea of its meaning in the case of maps of a circle into a circle, $\pi_1(S^1) = \mathbb{Z}$, where the winding number counts the number of times the circle in field space is wrapped around the circle in ordinary space. Gauge transformations transform a given map $g(x)$ into another belonging to the same homotopy class, i.e. same winding number. Thus, the gauge-invariant quantity associated with finite-action solutions is not a map but its homotopy class, given by the winding number. By making use of Eq. (2.2.16) in Eq. (2.2.19), the winding number can be expressed in terms of the tangential components to the 3-sphere of the gauge potential,

$$\nu = -\frac{i}{24\pi^2}\int_{\mathbf{S}^3} d\theta_1 d\theta_2 d\theta_3 \epsilon^{ijk}\,\mathrm{tr}\left(A_i A_j A_k\right) = -\frac{i}{24\pi^2}\int_{\mathbf{S}^3} d^3 S_\mu \epsilon^{\mu\nu\rho\sigma}\,\mathrm{tr}\left(A_\nu A_\rho A_\sigma\right). \tag{2.2.20}$$

This surface integral can be translated into an integral over the volume,

$$\begin{aligned}\nu &= -\frac{i}{24\pi^2}\int_V dx^4 \partial_\mu \epsilon^{\mu\nu\rho\sigma}\,\mathrm{tr}\left(A_\nu A_\rho A_\sigma\right) = \frac{1}{16\pi^2}\int_V dx^4 \partial_\mu \epsilon^{\mu\nu\rho\sigma}\,\mathrm{tr}\left(\frac{-2i}{3}A_\nu A_\rho A_\sigma\right) \\ &= \frac{1}{32\pi^2}\int_V dx^4 \partial_\mu 2\epsilon^{\mu\nu\rho\sigma}\,\mathrm{tr}\left(A_\nu \partial_\rho A_\sigma - \frac{2i}{3}A_\nu A_\rho A_\sigma\right) = \frac{1}{32\pi^2}\int_V dx^4 \partial_\mu K^\mu\,,\end{aligned} \tag{2.2.21}$$

which can be recognized to be the integral of the divergence of the Chern-Simons current K^μ. Therefore, applying Eq. (2.1.7), it follows that the winding number corresponds to the integral over the volume of the anomalous term,[11]

$$\nu = \frac{1}{32\pi^2}\int d^4x F\widetilde{F}\,. \tag{2.2.22}$$

Strikingly, by solving the classical EOM of Yang-Mills theory in Euclidean space, we found that there are non-trivial finite-action solutions, called instantons or pseudoparticles, for which

[10] The choice of angles is irrelevant since the Jacobian of the change of variables cancels that of the ϵ-symbol.

[11] Note the factor of two in $\partial_\mu K^\mu = 2\,\mathrm{tr}(F\widetilde{F}) = F\widetilde{F}$.

the integral of the anomalous term is non-zero, but proportional to a topological charge: the winding number. This indicates that there is no good reason to neglect the $G\widetilde{G}$ term in the QCD Lagrangian even though it corresponds to a total derivative. This will become clearer in Section 2.2.4 were the θ-vacuum is discussed.

The instanton action

In order to construct instanton solutions, the fact that these kind of solutions are stationary points of the action is most useful: they have lower action than any other solutions in the same homotopy class (i.e. same winding number). As a consequence, instantons need to saturate the *Bogomol'nyi bound* [117],

$$S_E = \frac{1}{4g^2}\int d^4x F_{\mu\nu}F^{\mu\nu} = \frac{1}{4g^2}\int d^4x \left[F\widetilde{F} + \frac{1}{2}(F-\widetilde{F})^2\right] = \frac{8\pi^2\nu}{g^2} + \frac{1}{8g^2}\int d^4x (F-\widetilde{F})^2 \,. \tag{2.2.23}$$

Since the last term in Eq. (2.2.23) is positive, the euclidean action of any field configuration with winding number ν has to be larger than the instanton solution with the same winding number,

$$S_E = \left|\frac{1}{4g^2}\int d^4x F_{\mu\nu}F^{\mu\nu}\right| \geq \frac{8\pi^2\nu}{g^2} \,. \tag{2.2.24}$$

The inequality is saturated by the instanton solutions,

$$S_E\big|_{\nu\text{-inst}} = \frac{8\pi^2\nu}{g^2} \,, \tag{2.2.25}$$

for which the the last term of the Eq. (2.2.23) needs to vanish if the winding number is positive and needs to be maximal if ν is negative instead. These two options lead to the self-duality equations,

$$F = \pm\widetilde{F} \,. \tag{2.2.26}$$

Thanks to the Bogomol'nyi argument, it is only necessary to solve the self-duality equations that are first-order differential equations instead of the full EOM,[12] that are of second order. The anti self-dual solutions $F = -\widetilde{F}$ are called anti-instantons and have negative winding number. Once an instanton solution is constructed, it is easy to build the corresponding anti-instanton by making a parity transformation $\vec{x} \to -\vec{x} \implies F\widetilde{F} \to -F\widetilde{F} \implies \nu \to -\nu$.

The BPST instanton

We will now proceed to construct explicitly instanton solutions with $\nu = 1$ for a $SU(2)$ gauge group. We are choosing $SU(2)$ not only because it is the simplest group we can consider (for $U(1)$ every solution is trivial, $\pi_3(U(1)) = 0$) but also because the $SU(2)$ instantons will allow

[12] Any self-dual configuration solves the Yang-Mills EOM $D_\mu F^{\mu\nu} = D_\mu \widetilde{F}^{\mu\nu} = 0$ due to the Bianchi identity.

the construction instantons for any other gauge group containing a $SU(2)$ subgroup. This is a consequence of *Bott's theorem* [118] that states that any mapping from S^3 to a general simple Lie group G can be continuously deformed into a mapping into a $SU(2)$ subgroup of G.

Since the relevant information of an instanton, the winding number, is solely encoded in its gauge configuration in the 3-sphere at infinity, let us start by specifying $A_\mu(|x| \to \infty)$, that needs to correspond to a pure gauge configuration. Thus this configuration at infinity is determined by a map from the S^3 to the gauge group $SU(2)$. For $\nu = 1$, we can define the identity map,

$$g^{(1)} = \frac{\tau + i\vec{x}\cdot\vec{\sigma}}{r}\,. \tag{2.2.27}$$

As Eq. (2.2.8) shows, an element of the gauge group g is determined by the coefficients of the linear combination of the generators in the exponential, ω^a. In the identity map, each point of space is mapped to the gauge group element whose coefficients determining that linear combination coincides with the normalized position vector of that point, $\omega^a = x^a = (\tau, x, y, z)$. The gauge potential at infinity is obtained by plugging the gauge group element of Eq. (2.2.8) in Eq. (2.2.16),

$$A_\mu \xrightarrow{r\to\infty} i\left(\frac{\tau + i\vec{x}\cdot\vec{\sigma}}{r}\right)\partial_\mu\left(\frac{\tau + i\vec{x}\cdot\vec{\sigma}}{r}\right)^{-1}\,. \tag{2.2.28}$$

In order to extend the field configuration to all points in space, one can multiply Eq. (2.2.28) by a function $f(r^2)$ that fulfills two conditions, $f(r^2) \xrightarrow{r\to 0} 0$ to avoid a singularity in the origin, and $f(r^2) \xrightarrow{r\to\infty} 1$ to recover the pure gauge configuration Eq. (2.2.28) at infinity. The self-duality condition can be solved applying these conditions obtaining the Belavin, Polyakov, Schwarz and Tyupkin (BPST) instanton solution [119],

$$A_\mu(x) = if(r^2)\left(\frac{\tau + i\vec{x}\cdot\vec{\sigma}}{r}\right)\partial_\mu\left(\frac{\tau + i\vec{x}\cdot\vec{\sigma}}{r}\right)^{-1}\,, \qquad f(r^2) = \frac{r^2}{r^2+\rho^2}\,, \tag{2.2.29}$$

that can be written in a more compact way by making use of the four dimensional Pauli matrices $\sigma^\mu = (\mathbb{1}, i\vec{\sigma})$ as,

$$A_\mu(x) = i\frac{x_\nu \sigma_{\mu\nu}}{r^2+\rho^2}\,, \tag{2.2.30}$$

where $\sigma^{\mu\nu} = \frac{1}{2}\left(\sigma^\mu\overline{\sigma}^\nu - \sigma^\nu\overline{\sigma}^\mu\right)$ and $\overline{\sigma}^\mu = (I, -i\vec{\sigma})$.

This is not the only possible solution, though. New configurations can be obtained by applying the symmetries of the theory. Via scale transformations, the size of the instanton ρ gets modified. It possible to associate the parameter ρ with the size of the instanton, since for $r \gg \rho$ the gauge potential tends to a pure gauge configuration. Therefore at those points $F_{\mu\nu} \to 0$. For $r \lesssim \rho$ instead, the configuration departs from pure gauge, $F_{\mu\nu} \neq 0$, and provides most of the contribution to the action. That is why it can be said that the instanton is localized in a region with size ρ. In addition, it is possible to perform a translation that would change the position of the instanton to x_0, yielding

$$f(r^2) = \frac{(r-x_0)^2}{(r-x_0)^2+\rho^2}\,, \tag{2.2.31}$$

which adds four parameters to the family of solutions. Finally, the orientation of the instanton in the group space gives 3 more parameters, that can be understood either as the three possible spatial rotations or the three constant (global) gauge transformations [120]. Summing up, the BPST instanton consists in a 8-parameter family of solutions of the Euclidean action, one for the size ρ, four for the position x_0 and three for the orientation in group space.

Finally, it is possible build instantons with larger winding number by following the same procedure but substituting the standard map in Eq. (2.2.27) by the following map:

$$g^{(\nu)} = \left(\frac{\tau + i\vec{x} \cdot \vec{\sigma}}{r} \right)^{\nu} , \tag{2.2.32}$$

which has winding number ν, as it can easily proved noting that the winding number is additive $\nu(g_1 \cdot g_2) = \nu(g_1) + \nu(g_2)$.

Although we have only constructed the $SU(2)$ instantons, Bott's theorem allows one to obtain instantons for any group $G \supset SU(2)$, as already mentioned, by embedding $SU(2)$ instantons into G. Of particular interest is $G = SU(N)$. In this case one possible embedding is given by[13],

$$A_\mu^{SU(N)} = \begin{pmatrix} 0 & 0 \\ 0 & A_\mu^{SU(2)} \end{pmatrix} , \tag{2.2.33}$$

It can be shown [121] that, via constant gauge transformations belonging to the coset space $SU(N)/(SU(N-2) \times U(1))$, new solutions can be constructed, resulting in a family of solutions with $4N - 5$ parameters. Together with the position and size already discussed, this gives a total of $4N$ parameters or collective coordinates for a one instanton solution in $SU(N)$.

2.2.3 Euclidean instantons as tunneling in Minkowski

Once the finite-action classical solutions of Yang-Mills theories have been classified and explicitly constructed, we can go back to our original goal of understanding the QCD vacuum in Minkowski spacetime. As it will be shown next, instanton configurations can be interpreted as paths in Minkowski spacetime producing tunneling between classical vacua. Consequently, the single physical quantum vacuum corresponds to a linear superposition of the classical vacua determined by the tunneling probability [122, 123].

Let us first consider the classical vacua of QCD in Minkowski spacetime. The Hamiltonian density reads

$$\mathcal{H} = \frac{1}{2}\left(\vec{E}^a\right)^2 + \frac{1}{2}\left(\vec{B}^a\right)^2 , \tag{2.2.34}$$

where $E_i^a = G_{0i}^a$, $B_i^a = -\frac{1}{2}\epsilon_{ijk}G_{jk}^a$ denote the chromoelectric and chromomagnetic fields. Classical vacua have vanishing energy density and therefore $\vec{E}^a = \vec{B}^a = 0 \implies F_{\mu\nu} = 0$

[13] Note that Eq. (2.2.33) corresponds to a block matrix. Thus the vanishing blocks, written as 0, actually have dimensions $(N-2) \times (N-2)$, $(N-2) \times 2$ and $2 \times (N-2)$, respectively.

at every point of spacetime or, in other words, they correspond to pure gauge configurations.[14] Quantum effects dramatically change this picture, though. As we have already anticipated, instantons produce tunneling between classical vacua: they will evolve in time.

Let us consider the analytic continuation of the one-instanton solution in Eq. (2.2.29) to the Minkowski spacetime, $A_\mu(\vec{x},t) = A^E_\mu(\vec{x},\tau = it)$, filling the volume delimited by the cylinder depicted in Fig. 2.1. The winding number can still be defined and computed even though we are in Minkowski spacetime, because it is a topological quantity that does not depend on the metric,

$$\nu = \frac{1}{32\pi^2}\int d^4x F\widetilde{F} = -\frac{i}{24\pi^2}\int_{\mathrm{I+II+III}} d^3S_\mu \epsilon^{\mu\nu\rho\sigma}\,\mathrm{tr}\left(A_\nu A_\rho A_\sigma\right)\,. \tag{2.2.35}$$

where I, II and III denote the three surfaces delimiting the cylinder as depicted in Fig. 2.1. Since the instanton has finite action, the field configuration is pure gauge in all the surfaces at infinity. In particular, at initial time $t_1 \to -\infty$ the configuration $A_\mu(\vec{x},t_1)$ describes a classical vacuum,

$$A_\mu(\vec{x},t_1) = ig(\vec{x},t_1)\partial_\mu g^{-1}(\vec{x},t_1)\,, \tag{2.2.36}$$

and analogously, for $t_2 \to \infty$ the configuration describes another classical vacuum,

$$A_\mu(\vec{x},t_2) = ig(\vec{x},t_2)\partial_\mu g^{-1}(\vec{x},t_2)\,. \tag{2.2.37}$$

Finally the remaining boundary is also pure gauge,

$$A_\mu(\vec{x},t) \xrightarrow{|\vec{x}|\to\infty} ig(\vec{x},t)\partial_\mu g^{-1}(\vec{x},t)\,. \tag{2.2.38}$$

In order to simplify the arguments, let us choose the gauge

$$A_0(\vec{x},t) = 0\,, \qquad A_\mu\left(\vec{x},t_1\right) = 0\,, \tag{2.2.39}$$

which corresponds to the temporal gauge (in every point of spacetime) and to setting the gauge potential to zero in the initial vacuum using the residual space-dependent gauge freedom, $g(\vec{x},t_1) = 1$.

With this gauge fixing, the field configuration in the boundary III vanishes. Combining Eqs. (2.2.38) and (2.2.39), it follows that $g(|\vec{x}| \to \infty, t)$ is time-independent and because on the surface I the gauge potential vanishes, $A_\mu\left(\vec{x},t_1\right) = 0$, it must vanish for all t, therefore,

$$A_\mu(\vec{x},t) \xrightarrow{|\vec{x}|\to\infty} 0\,. \tag{2.2.40}$$

This has an interesting consequence in terms of classifying classical vacua in Minkowski. For every spatial slice $t = \mathrm{cte}$, in the limit $|\overrightarrow{x}| \to \infty$ the gauge potential vanishes. Thus these hypersurfaces can be compactified into 3-spheres in which the north pole is associated with all

[14] It can be shown that in three spatial dimensions there are no time-independent non-dissipative finite-energy classical solutions of Yang-Mills, following a similar proof to that in Section 2.2.2. Thus the only time-independent classical solution corresponds to $F_{\mu\nu} = 0$.

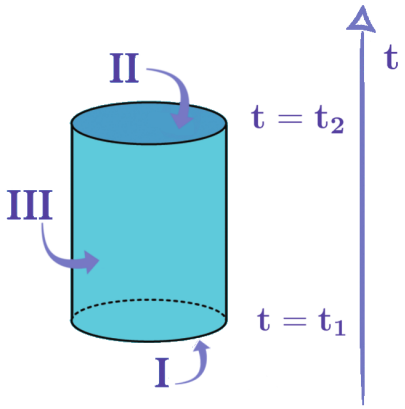

Figure 2.1: Illustration of the chosen boundary of an instanton in Minkowski spacetime.

the points at $|\overrightarrow{x}| \to \infty$. Hence the initial t_1 and final t_2 slices that correspond to classical vacua can be classified by the maps from a 3-sphere into the gauge group, i.e. the winding number,

$$n(t) = -\frac{i}{24\pi^2}\int_{S_t} d^3x^3 \epsilon^{0ijk}\,\mathrm{tr}\left(A_i A_j A_k\right)\,. \tag{2.2.41}$$

This relates the winding number of the instanton with the winding number of the initial and final classical vacua, from Eq. (2.2.35),

$$\nu = -\frac{i}{24\pi^2}\int_{\mathrm{I+II+III}} d^3S_\mu \epsilon^{\mu\nu\rho\sigma}\,\mathrm{tr}\left(A_\nu A_\rho A_\sigma\right) = n(t_2) - n(t_1)\,. \tag{2.2.42}$$

since the integral on the boundary III vanishes.

Several comments are pertinent. The fact that the winding number defined in Eq. (2.2.41) is computed by integrating over an open surface in Minkowski spacetime makes it qualitatively different from the winding number of instantons in Euclidean space. On the one hand, time evolution can smoothly deform a configuration with certain winding number to another one with different winding number. Indeed, the winding number can be computed for any spatial slice $t = \mathrm{cte}$, S_t, by making use of Eq. (2.2.41): $n(t)$ continuously interpolates between the initial and final configurations, $n(t_1) \equiv n_1$ and $n(t_2) \equiv n_2$, taking non-integer values in between where the field configurations are not pure gauge.

On the other hand, so-called large gauge transformations can change the winding number that classifies the classical vacua in Minkowski spacetime.[15] However, if one performs a large gauge transformations and increases the winding number at time t_1 by m units, $n_1 \to n_1 + m$, then the winding number at time t_2 increases by exactly the same amount $n_2 \to n_2 + m$, resulting

[15] This gauge transformations correspond to the space-dependent gauge fixing used to fix the potential in $t = t_1$ in Eq. (2.2.39). They are called *large* because they do not approach the identity at infinity.

in the same total winding number $\nu = n_2 + m - (n_1 + m) = n_2 - n_1$. Consequently, the total winding number is gauge invariant, and corresponds to that of the Euclidean instanton ν.

This can be easily understood by noticing that, while the anomalous term $F\widetilde{F}$ is gauge invariant, the Chern-Simons current K^μ is not. If the winding number is computed by integrating the Chern-Simons current over a closed surface, it can be translated into an integral over the volume of the anomalous term, and therefore the result will be gauge invariant, see Eq. (2.2.21). If the surface over which we integrate is open instead, it cannot be written as a function of gauge invariant operators, and the winding number will be shifted under large gauge transformations.

As we already commented, there are no classical paths that connect two vacua with different winding numbers since the only classical solution corresponds to pure gauge in all points of spacetime. Therefore, this path determined by the instanton solution necessarily involves non-vanishing $F_{\mu\nu}$ and therefore non-vanishing energy density at some intermediate times (otherwise the total winding number vanishes). For this reason these transitions look like tunneling processes between two classical vacua since they are classically forbidden but quantum mechanically allowed via barrier penetration. Indeed it can be shown [124] that *the instanton solution gives rise to the maximal tunneling amplitude in Minkowski space*. This probability is related to the Euclidean action of the corresponding instanton, see Eq. (2.2.3),

$$P \propto e^{-S_E/\hbar} = e^{-\frac{8\pi^2}{g^2\hbar}|\nu|}\,, \tag{2.2.43}$$

where ν is the difference between the winding numbers of the two classical vacua that are connected by this tunneling. The result in Eq. (2.2.43) exhibits the characteristic dependence on the coupling constant of non-perturbative effects $\propto e^{-1/g^2}$, that does not arise at any level in perturbation theory. In fact, instanton techniques can be used to compute barrier penetration amplitudes generically in quantum mechanical problems, obtaining the same semiclassical result that is usually computed using the WKB approximation.

We have showed that an instanton configuration with a given size, position, direction and winding number ν produces tunneling between two classical vacua whose winding numbers differ by the instanton winding number $\nu = n_2 - n_1$. Nevertheless, if we wish to compute the full probability for a transition from a classical vacua $|m\rangle$ to another one, $|n\rangle$, it is necessary to integrate over all possible instanton configurations compatible with that difference in winding number,

$$\left\langle n\middle|e^{-H\tau/\hbar}\middle|m\right\rangle = \int [dA]_{(n-m)} e^{-S_E/\hbar}\,. \tag{2.2.44}$$

In order to evaluate this integral, sometimes it is possible to use the dilute instanton gas approximation (DIGA): assume that all the instanton configurations contributing to the integral are widely separated compared to their size ρ. The matrix element in this approximation reads,

$$\mathcal{Z}_{1,0}(\tau) = \langle 1|e^{-H\tau/\hbar}|0\rangle = CV\tau \int \frac{d\rho}{\rho^5} \left(\frac{8\pi^2}{g^2(1/\rho)\hbar}\right)^{2N} e^{-\frac{8\pi^2}{g^2(1/\rho)\hbar}}\,, \tag{2.2.45}$$

where C is a constant that arises after performing the integration over all the possible the directions in group space of the instantons and depends on the number of colors N for a given

$SU(N)$ theory. $V\tau$ is the Euclidean volume that is obtained after integrating over the instanton positions. It must be noted that this approximation is not valid for small scales (large instanton sizes). Indeed the integral in Eq. (2.2.45) diverges generating what 't Hooft called an *infrared embarrassment*. After all, this divergence should not be a surprise, since the QCD coupling constant becomes large at low energies, where we enter a strongly coupled regime in which the semi-classical approximation that has been assumed does not apply. Although for confining theories the DIGA cannot be applied, and it is not possible to compute the full integral in Eq. (2.2.44), the rest of the discussion holds, and it suffices to characterize the vacuum of the theory.

2.2.4 θ-vacuum

The classical vacua $|n\rangle$ labeled by the winding number n in Minkowski space all have vanishing energy. However, similarly to quantum mechanics, the degeneracy between different classical vacua is lifted if there exists tunneling between them. In order to construct the linear combination of the different states $|n\rangle$ that correspond to the true quantum vacuum, let us impose the condition that it has to be gauge invariant. Large gauge transformations such as,

$$T_1(\vec{x},t) = \frac{i\vec{x}\cdot\vec{\sigma}}{\left(\vec{x}^2+a^2\right)^{1/2}}\,, \tag{2.2.46}$$

increase the winding number of a classical state by one unit, $T_1|n\rangle = |n+1\rangle$. However, the physical quantum vacuum needs to be invariant under such a transformation. In a Hilbert space this amounts to obtaining the same state modulo a phase, $T_1|\text{vac}\rangle = e^{i\theta}|\text{vac}\rangle$. If the quantum vacuum is expressed as a linear combination of the classical states $|n\rangle$, by imposing gauge invariance it follows that,

$$|\text{vac}\rangle = \sum_{n=-\infty}^{\infty} a_n|n\rangle \implies T_1|\text{vac}\rangle = \sum_{n=-\infty}^{\infty} a_n|n+1\rangle = e^{i\theta}|\text{vac}\rangle \tag{2.2.47}$$

$$\implies |\text{vac}\rangle = e^{-i\theta}\sum_{n=-\infty}^{\infty} a_n|n+1\rangle = \sum_{n=-\infty}^{\infty} e^{-i\theta}a_{n-1}|n\rangle = \sum_{n=-\infty}^{\infty} a_n|n\rangle\,, \tag{2.2.48}$$

where a_n are constant coefficients. That is, the coefficients need to follow the recursive relation $a_{n+1} = e^{-i\theta}a_n$. By choosing $a_0 = 1$, which is only a choice of normalization, the true vacuum is unambiguosly found [125]. It can be labeled by the phase θ, $|\text{vac}\rangle \equiv |\theta\rangle$,

$$|\theta\rangle = \sum_{n=-\infty}^{\infty} e^{-in\theta}|n\rangle\,. \tag{2.2.49}$$

This shows that the vacuum of the Yang-Mills theory is characterized by a phase θ that determines the linear superposition of classical vacua which defines the true quantum ground state. A pertinent question is whether states with different values of θ correspond to different

states of the same theory. Let us consider the following matrix element

$$\begin{aligned}\langle\theta'|e^{-iHt/\hbar}|\theta\rangle &= \sum_{m,n} e^{im\theta'}e^{-in\theta}\langle m|e^{-iHt/\hbar}|n\rangle \\ &= \sum_{m,n} e^{im(\theta'-\theta)}e^{i(m-n)\theta}\langle m|e^{-iHt/\hbar}|n\rangle \\ &= \sum_{m,k} e^{im(\theta'-\theta)}e^{ik\theta}\langle k|e^{-iHt/\hbar}|0\rangle = 2\pi\delta(\theta-\theta')\sum_k e^{ik\theta}\langle k|e^{-iHt/\hbar}|0\rangle\,.\end{aligned} \tag{2.2.50}$$

This implies that time evolution does not connect states with different θ's. In fact, it can be shown that the matrix element of any string of local observables $\mathcal{O}_1\ldots\mathcal{O}_k$ vanishes for $\theta'\neq\theta$, $\langle\theta'|\mathcal{O}_1\ldots\mathcal{O}_k|\theta\rangle\propto\delta(\theta-\theta')$. This implies that different values of θ do not label states in a given theory but correspond to different theories.

The next question is whether theories with different values of θ result in different physics. The answer is yes. The energy density of the vacuum depends on θ, as can be shown by computing the matrix element in Eq. (2.2.3) for the vacuum $|\theta\rangle$ and making use of Eq. (2.2.50),

$$\lim_{\tau\to\infty}\mathcal{Z}_{\theta\theta}(\tau) = \langle\theta|\theta\rangle e^{-E_0\tau/\hbar} = e^{-E_0\tau/\hbar} = N\int_\theta [dA]e^{-S_E/\hbar} = \sum_n N\int [dA]_n e^{in\theta}e^{-S_E/\hbar}\,. \tag{2.2.51}$$

Approximating again the integral in the DIGA, it follows that,

$$e^{-E_0\tau/\hbar} = e^{2V\tau K\cos\theta e^{-S_0/\hbar}} \implies \frac{E(\theta)}{V} = \text{cte} - 2K\cos\theta e^{-S_0/\hbar}\,. \tag{2.2.52}$$

Therefore, theories with different values of θ have different vacuum energy. Although the DIGA has been used to obtain this result, the fact that the energy density of the vacuum is θ-dependent holds in any case. In fact, it can be shown in all generality that the minimum energy density of the vacuum corresponds to $\theta=0$ and for any $\theta\neq 0$ the energy density is larger [126]. As a consequence, the value of θ of a given theory has physical impact. Indeed, for a pure Yang-Mills theory several observables would show this physical difference. For example, in Ref. [127] the gluonic two point correlation functions have been computed as a function of the θ-parameter. Also, the mass of the lightest glueball and the full glueball spectrum depend on θ [128].

We are now ready to make the connection of the θ-vacuum with the θ-term appearing in the QCD Lagrangian, see Eq. (2.0.1). The vacuum expectation value of any operator $\mathcal{O}$ can be expressed as,

$$\begin{aligned}\langle\theta|\mathcal{O}|\theta\rangle &= \sum_{m,n} e^{i\theta(m-n)}\langle m|\mathcal{O}|n\rangle = \sum_k e^{i\theta k}\langle k|\mathcal{O}|0\rangle = \sum_k e^{i\theta\int d^4x\frac{1}{32\pi^2}G\tilde{G}}\langle k|\mathcal{O}|0\rangle \\ &= \frac{1}{\mathcal{Z}}\sum_k\int [dA]_k\,\mathcal{O}\,e^{i\int d^4x\left(\mathcal{L}+\frac{\theta}{32\pi^2}G\tilde{G}\right)} = \frac{1}{\mathcal{Z}}\int [dA]\,\mathcal{O}\,e^{i\int d^4x\left(\mathcal{L}+\frac{\theta}{32\pi^2}G\tilde{G}\right)}\,.\end{aligned} \tag{2.2.53}$$

By using the definition of the winding number in terms of the volume integral of the anomalous term, see Eq. (2.2.22), we have found that the result of any observable in a particular vacuum $|\theta\rangle$ amounts to adding to the Lagrangian of the theory the anomalous term

$$\mathcal{L}_\theta = \frac{\theta}{32\pi^2}G^a_{\mu\nu}\widetilde{G}^{a\mu\nu}\,. \tag{2.2.54}$$

Summarizing, by studying the Euclidean Yang-Mills theory we found that the structure of the QCD vacuum cannot be described perturbatively. There exist an infinite number of classically degenerate vacuum states whose coherent superposition labeled by θ defines the true QCD vacuum. The properties of this vacuum can be studied in the semiclassical approximation by constructing the classical solutions of the Euclidean theory that describe tunneling paths between the classical vacua in Minkowski space. Then, it has been shown that the impact on physical observables of a given θ-vacuum can be encoded in the Lagrangian by introducing the corresponding θ-term, see Eqs. (2.2.53) and (2.2.54). As a consequence, QCD interactions are not described by a single dimensionless parameter, the coupling constant g, but by two parameters g and θ.

Furthermore, instantons allow one to solve the missing meson problem which provides experimental evidence for the explicit breaking of the $U(1)_A$ symmetry. Therefore, instantons do have physical consequences, and it becomes clear that the fact that the QCD vacuum is CP-invariant remains to be a puzzle calling for an explanation, a solution to the strong CP problem.

Adding fermions

The instantons and the θ-vacuum for a pure Yang-Mills theory has been have constructed above, but since we are interested in studying QCD, fermions need to be incorporated. One of the immediate consequences of introducing fermions is that it becomes clear why the different classical topological vacua are physically distinguishable: they posses different axial charge. As introduced in Section 1.4.2, the quark axial current is anomalous, that is, in the limit of massless fermions,

$$\partial_\mu j^\mu_A = \frac{\alpha_s}{2\pi} G_{\mu\nu}\widetilde{G}^{\mu\nu}\,, \tag{2.2.55}$$

see Eq. (2.1.6). After integrating over a volume, the difference in axial charge is obtained,

$$\Delta Q_A = Q_A(t=+\infty) - Q_A(t=-\infty) = \int d^4x \partial_\mu j^A_\mu = 2\,\nu\,. \tag{2.2.56}$$

It follows that instantons with winding $\nu = 1$ generate tunneling events in which the axial charge of the vacuum changes by two units: they thus generate fermionic interactions containing one quark and one anti-quark for each flavor. This can also be seen by integrating over the quark fields in the path integral. In the semiclassical approximation the fermionic integration gives rise to the determinant of the Dirac operator in an instanton classical background A_μ,

$$\int \big[d\psi\big]\big[d\bar{\psi}\big] e^{\int d^4x \bar{\psi}(i\not{\partial} - m - \not{A})\psi} = \mathrm{Det}(i\not{\partial} - m - \not{A})\,. \tag{2.2.57}$$

In the limit $m \to 0$, it was shown by 't Hooft that the fermionic zero modes of the Dirac operator make the vacuum to vacuum amplitude vanish [113, 129, 130]. Instead, as we have anticipated studying the chiral charge, the tunneling amplitude is non-zero in the presence of external quarks. In this case, the zero modes of the determinant cancel with the fermionic propagators, resulting

in a non-vanishing amplitude for the fermionic interaction. This corresponds to the so-called 't Hooft determinental interaction.

If the fermions are massive instead, the external legs of this determinental interaction can be closed with the mass terms, generating a non-zero vacuum to vacuum amplitude. [113,130–132] In the DIGA where the determinant factorizes to the product of the determinants for each instanton background, this amounts to multiplying the pure Yang-Mills result by a factor of (ρm_f) for each Weyl fermion[16] with mass m_f.

$$\mathcal{Z} = C_{inst}(N_f, N_c) \int \frac{d\rho}{\rho^5} \prod_f (m_f \rho) \left(\frac{8\pi^2}{g^2(1/\rho)} \right)^{2N_c} e^{-\frac{8\pi^2}{g^2(1/\rho)}} , \tag{2.2.58}$$

where the coefficient C_{inst} for N_f Weyl fermions in a $SU(N_c)$ Yang-Mills theory reads

$$C_{inst}\left(N_f, N_c\right) = \frac{4 \cdot 2^{-2N_c} e^{c_{1/2}\left(-2N_c+2N_f\right)}}{\pi^2 \left(N_c-2\right)! \left(N_c-1\right)!} e^{-c_1+4c_{1/2}} , \tag{2.2.59}$$

where the function $c(x)$ is defined in Ref. [113] and corresponds to $c(1/2) = 0.145873$ and $c(1) = 0.443307$.

2.2.5 Instantons in spontaneously broken theories: constrained instantons

Before reviewing possible solutions to the strong CP problem, let us first comment on instanton solutions in spontaneously broken gauge theories. This will be of special relevance in Chapter 5, where small-size instantons of this type will raise the axion mass.

At first sight, it could seem that the question leads to a dead end, since *exact* instanton solutions do not exist in spontaneously broken theories.

Theorem. In spontaneously broken Euclidean Yang-Mills theories in 4 dimensions with the Lagrangian

$$\mathcal{L} = -\frac{1}{4g^2} F^a_{\mu\nu} F^{\mu\nu}_a + (D_\mu \phi)^\dagger D^\mu \phi - U(\phi) , \tag{2.2.60}$$

where the minimum of the potential $U(\phi)$ corresponds to a non-vanishing value of the scalar field, $\langle \phi \rangle = v \neq 0$, the only non-singular finite-action classical solutions of the EOM are gauge transformations of $A^\mu_a = 0, \phi = v$.

Proof. The action of this theory reads

$$S_E[\phi, A_\mu] = S_G[A_\mu] + S_S[\phi, A_\mu] + S_U[\phi] \tag{2.2.61}$$

[16] This factor $(m_f \rho)$ holds for small instanton sizes $\rho \ll 1/m$. For large instantons $\rho \gg 1/m$ the fermions completely decouple and have no impact on the vacuum to vacuum amplitude.

where the three terms are non-negative and correspond to

$$S_G[A_\mu] = \frac{1}{4g^2}\int d^D x\, F^a_{\mu\nu}F_a^{\mu\nu}\,, \tag{2.2.62}$$

$$S_S[\phi, A_\mu] = \int d^D x\, (D_\mu\phi)^\dagger D^\mu\phi\,, \tag{2.2.63}$$

$$S_U[\phi] = \int d^D x U(\phi)\,. \tag{2.2.64}$$

Analogously to Eq. (2.2.14), let us consider the one-parameter family of field configurations obtained by rescaling lengths in a given solution with finite action $\{\bar{A}^\mu(x), \bar{\phi}(x)\}$,

$$A^\mu_\lambda(x) = \lambda\,\bar{A}^\mu(\lambda x)\,, \qquad \phi_\lambda(x) = \bar{\phi}(\lambda x) \qquad , \tag{2.2.65}$$

whose action reads

$$\begin{aligned} S_E(\lambda) &= S_G[A^\mu_\lambda] + S_S[\phi_\lambda, A^\mu_\lambda] + S_U[\phi_\lambda] \\ &= \lambda^{4-D} S_G[\bar{A}^\mu] + \lambda^{2-D} S_S[\bar{\phi}, \bar{A}^\mu] + \lambda^{-D} S_U[\bar{\phi}]\,. \end{aligned} \tag{2.2.66}$$

For the solution $\bar{A}_i(x)$ to be a stationary point of the action,

$$\left.\frac{dS_E(\lambda)}{d\lambda}\right|_{\lambda=1} = 0 \quad \Longrightarrow \quad 0 = (4-D)S_G[\bar{A}^\mu] + (2-D)S_S[\bar{\phi}, \bar{A}^\mu] - DS_U[\bar{\phi}]\,. \tag{2.2.67}$$

Thus for $D = 4$ spatial dimensions the condition reads

$$0 = -2S_S[\bar{\phi}, \bar{A}^\mu] - 4S_U[\bar{\phi}]\,. \tag{2.2.68}$$

Since both terms are positive both need to be zero independently,

$$S_S[\phi, A_\mu] = \int d^D x\, (D_\mu\phi)^\dagger D^\mu\phi\,, \tag{2.2.69}$$

$$S_U[\phi] = \int d^D x U(\phi)\,. \tag{2.2.70}$$

In both cases the integrand is positive, so it has to identically vanish in every point in order for the full integral to vanish,

$$(D_\mu\phi)^\dagger D_\mu\phi = 0 \quad \forall x\,, \tag{2.2.71}$$

$$U(\phi) = 0 \quad \forall x\,. \tag{2.2.72}$$

The action density of the scalar field therefore vanishes everywhere. However, Eq. (2.2.68) allows for the gauge fields to have finite non-zero action. Nevertheless, we will now show that Eq. (2.2.71) implies that the gauge potential configuration corresponds to a pure gauge in every point of space, and therefore all the solutions of this kind are trivial,

$$|D_\mu\phi|^2 = 0 \implies D_\mu\phi = \left(\partial_\mu + iA_\mu\right)\phi = 0 \implies A_\mu\phi = i\partial_\mu\phi\,. \tag{2.2.73}$$

For the potential $U(\phi)$ to be zero, the scalar field has to be at the minimum in every point of space. Let us us consider one of such zeros of $U(\phi)$, $\phi = v$. Since U is gauge invariant, any gauge transformation of it, $\phi^{(g)} = g\,v$, will also be a zero of the potential. Let us assume that all zeros of the potential are of the kind $g\,v$, excluding any accidental degeneracy or extra global internal symmetry of the Lagrangian. Then the gauge potential reads

$$A_\mu = i\phi^{-1}\partial_\mu\phi = ig^{-1}v^{-1}\partial_\mu g v = ig^{-1}\partial_\mu g\,, \tag{2.2.74}$$

which corresponds to a pure gauge configuration in all points of space time and thus has vanishing action, $S_G[A^\mu_\lambda] = 0$. In consequence, all three terms contributing to the action vanish, and we can conclude that there are no exact classical solutions with non-zero but finite action in spontaneously broken gauge theories in Euclidean space. □

Crucially, in order to be able to infer something about the gauge potential configuration via the condition on Eq. (2.2.73), it is necessary for the theory to be spontaneously broken, that is the scalar needs to develop a non-zero vev. Otherwise if $\langle\phi\rangle = 0$, the condition in Eq. (2.2.73) is automatically satisfied and the usual instantons of Yang-Mills theory are also solutions of the theory with scalars that do not develop a vev.

Constrained instantons

Even if there are *not exact* instanton solutions in spontaneously broken theories, one can construct approximate solutions for instanton sizes smaller than the inverse breaking scale $g\rho v \ll 1$. This is what we call constrained instantons. There are two ways of constructing them. The most rigorous approach was introduced by Affleck in Ref. [133]. It consists in introducing a constraint as a Lagrange multiplier which fixes the instanton size ρ for its exact solution, and then in the integration over this constraint. Alternatively, one can take the approach taken by 't Hooft in Ref. [113] and solve the approximate EOM of the fields for $\rho \ll 1/(gv)$. This approximation consists in neglecting the current induced by the non-vanishing scalar field ϕ in the EOM for the gauge fields, that is,

$$\begin{aligned} D_\mu F_{\mu\nu} &= 0\,, \\ D_\mu D_\mu \phi - U'(\phi) &= 0\,, \end{aligned} \tag{2.2.75}$$

which are solved with the necessary boundary conditions that ensure the finiteness of the action,

$$A_\mu(x) \to ig(x)\partial_\mu g^{-1}(x)\,, \qquad \text{for } r \to \infty\,, \tag{2.2.76}$$

$$\phi(x) \to g(x)v \quad , \qquad \text{for } r \to \infty\,. \tag{2.2.77}$$

In other words, the approximation amounts to considering the instanton solution of pure Yang-Mills theory for small sizes, and then solving the EOM for the scalar in this background. As a result, the action contains the usual Yang-Mills instanton term plus an extra contribution from the scalar field [121, 133–135], yielding

$$S_E = \frac{8\pi^2}{g^2} + 2\pi^2\rho^2 v^2\,. \tag{2.2.78}$$

Although constrained instantons are approximate solutions, they can have important effects and, unlike usual instantons, they can be tackled quantitatively in a reliable way using the DIGA. The breaking scale v provides a natural cut-off for the instanton size and solves the *infrared embarrassment* of the DIGA for confining Yang-Mills theories. In this case of sponteneously broken Yang-Mills theories, the one-instanton contribution to the vacuum functional in the DIGA reads,

$$\mathcal{Z} = C_{inst}(N_f, N_c) \int \frac{d\rho}{\rho^5} \left(\frac{8\pi^2}{g^2(1/\rho)} \right)^{2N_c} e^{-\frac{8\pi^2}{g^2(1/\rho)} - 2\pi^2\rho^2 v^2}, \tag{2.2.79}$$

where C_{inst} is defined in Eq. (2.2.59). The extra contribution of the scalar action to the path integral $e^{-2\pi^2\rho^2 v^2}$ exponentially suppresses large instanton sizes and makes the whole integral convergent. This type of instantons has been considered in the context of B+L violation in the Electroweak sector [112, 113, 129, 134, 136], where the presence of fermions has the same consequences that were discussed in Section 2.2.4 for the confining Yang-Mills theory with fermions.

2.3 Solutions to the strong CP problem

Running of $\bar{\theta}$-parameter

For certain solutions to the strong CP problem, it is important to take into account the running of θ. Although the θ-parameter breaks CP invariance, it is not a technically natural parameter in the 't Hooft sense [95], due to the fact that CP is already explicitly broken within the electroweak sector of the SM. Thus θ is not protected by a symmetry and indeed receives radiative corrections that depend on the complex phase of the CKM matrix, $\delta_{\rm KM}$. In terms of the viability of some solutions to the strong CP problem that set $\bar{\theta} = 0$ at some high scale Λ, it is important to quantify these contributions. This issue was addressed by Ellis and Gaillard in Ref. [137]. They found that the infinite renormalization of θ due to $\delta_{\rm KM}$ vanishes up to 7-loops. As a consequence, even if the "relaxation" scale Λ at which $\bar{\theta}$ is set to zero were to be the Planck scale, this EW contribution is so suppressed, $\Delta\theta \sim 10^{-16}$, that it can be safely neglected when compared with the current and foreseeable experimental precision for the neutron EDM. The rationale behind the tiny value of θ remains open, though.

2.3.1 Nelson-Barr mechanism

One possible solution to the strong CP problem is that of models with spontaneously broken CP symmetry via the Nelson-Barr mechanism [138–140]. If CP were to be an exact symmetry of the interactions, the θ-term would be absent in the Lagrangian. CP violation in the weak sector needs to be accounted for, and within these models it arises through a scalar singlet that develops a complex vev, breaking spontaneously the CP symmetry. The Yukawa and mass terms

are constructed in such a way that at tree level this complex vev only induces a non-zero CKM phase while leaving a vanishing θ.

One of the simplest realizations of this mechanism [141] introduces down-type vector-like quarks $q_{L,R}$ (singlets of $SU(2)_L$) and several complex scalar singlets η_i with the following mass and Yukawa couplings,

$$\mathcal{L} \supset -\mu\, \overline{q}_L q_R - a\, \eta \overline{q}_L D_R - y \Phi \overline{Q}_L D_R \,, \tag{2.3.1}$$

where the flavor indices have been omitted. Note that since CP is an exact symmetry at this level the coulings μ, a and y are real. At some energy scale the scalars η develop complex vevs and break spontaneously CP invariance. After EWSB, the Lagrangian in Eq. (2.3.1) gives rise to the mass matrix

$$M = \begin{pmatrix} \mu & B \\ 0 & m_d \end{pmatrix} , \tag{2.3.2}$$

where $m_d \equiv yv$ is the 3×3 down-type quark mass matrix and $B = a\langle\eta\rangle$. Notice that, since the only complex phases in this mass matrix appear within the submatrix B (both m_d and μ are real), $\mathrm{Arg}\,(\det\, M) = 0$ automatically. It follows that at tree level there are no contributions to the θ-term. On the other hand, the exotic quark gets a large mass since $\mu, a\langle\eta\rangle \gg v$. When it is integrated out of the spectrum it introduces a complex phase in the mass matrix of the SM, giving rise to a non-zero δ_{KM} in the CKM matrix.

Nevertheless, Nelson-Barr models present several problems. First of all, further symmetries are needed in order to enforce the required mass matrix pattern (some allowed renormalizable terms like $\eta \overline{q}_L q_R$ or $\Phi \overline{Q}_L q_R$ need to be forbidden). Furthermore, the vevs of the different complex scalars need to be adjusted to reproduce a large CKM phase, and this introduces a new hierarchy problem. Finally and most importantly, even if no θ-term is present at tree level, loop contributions to θ can be large, requiring sophisticated matter content in order to control them.

Analogous to the Nelson-Barr mechanism, models in which parity is spontaneously broken have also been considered [142–146] . Indeed the θ-term violates both P and CP while conserving C, so by constructing left-right symmetric models where P is spontaneously broken one can also address the strong CP problem. Typically these type of models require new flavor structure that, similar to Nelson-Barr models, induce important contributions to θ at loop level.

2.3.2 Peccei-Quinn mechanism

One of the most elegant and simple solutions to the strong CP problem was proposed by Peccei and Quinn in Ref. [8, 9]. It consists in the introduction of a new global abelian symmetry, the Peccei-Quinn (PQ) symmetry $U(1)_{\mathrm{PQ}}$, that is exactly conserved at the classical level but has a mixed anomaly with QCD,

$$\delta\mathcal{L} = \beta\, \partial_\mu J^\mu = \beta \frac{\alpha}{8\pi} G_{\mu\nu} \widetilde{G}^{\mu\nu} \,, \tag{2.3.3}$$

which explicitly breaks the symmetry at the quantum level. As a consequence, a transformation of the fields that carry PQ charge allows one to reabsorb completely the $\bar{\theta}$ parameter from the

Lagrangian, rendering it unphysical and solving the strong CP problem. In addition, this PQ symmetry is spontaneously broken at a scale f_a giving rise to the existence of a Goldstone boson, the axion a, as was pointed out by Weinberg [147] and Wilczek [148] after the PQ proposal. Due to the explicit PQ breaking by the QCD anomaly, the axion acquires a non-zero mass constituting a pseudo-Goldstone Boson.

One of the most model-independent properties of the axion is that it couples to the QCD anomalous term as a consequence of Eq. (2.3.3),

$$\mathcal{L} = \frac{a}{f_a}\frac{\alpha}{8\pi} G_{\mu\nu}\widetilde{G}^{\mu\nu} \,, \tag{2.3.4}$$

where f_a is the axion scale. This interaction allows for another possible interpretation of the PQ solution in terms of the axion effective Lagrangian. As was shown by Vafa and Witten [126] by considering the Euclidean path integral,

$$e^{-VE(\theta)} = \int \left[dA_\mu\right] \det(\not{D} + M) e^{-\left(1/4g_s^2 \int d^4x\, G_{\mu\nu}G_{\mu\nu}\right)} e^{i\theta/32\pi^2 \int d^4x\, G_{\mu\nu}\widetilde{G}_{\mu\nu}} \,, \tag{2.3.5}$$

the QCD vacuum energy has a minimum for $\theta = 0$. This can be easily shown by taking into account that all the terms in the Euclidean action are real except for the θ-term,[17]

$$e^{-VE(\theta)} \leq \int \left[dA_\mu\right] \left|\det(\not{D} + M) e^{-S_{\text{real}}} e^{i\theta/32\pi^2 \int d^4x\, G_{\mu\nu}\widetilde{G}_{\mu\nu}}\right| \tag{2.3.6}$$

$$= \int \left[dA_\mu\right] \det(\not{D} + M) e^{-S_{\text{real}}} = e^{-VE(0)} \,. \tag{2.3.7}$$

Therefore $E(\theta \neq 0) > E(0)$. This is essential for the viability of axion solutions to the strong CP problem. Effectively, the coupling in Eq. (2.3.4) amounts to promoting the θ-parameter to a dynamical field, the axion, or to substitute $\theta \to \theta + \frac{a}{f_a}$. Since $E(\theta + \frac{a}{f_a}) > E(0)$, the non-perturbative effects of the QCD vacuum will generate a potential whose minimum lies at $\theta + \frac{a}{f_a} = 0$ and therefore forces the vev of the axion to correspond to the CP conserving minimum,

$$\theta_{\text{eff}} = \theta + \left\langle \frac{a}{f_a} \right\rangle = 0 \,. \tag{2.3.8}$$

As consequence, the strong CP problem is solved in any theory which generates the coupling in Eq. (2.3.4) of the anomalous QCD term with a pseudoscalar which possesses a shift symmetry $a \to a + \beta f_a$ only broken by that anomalous term. Chapter 3 is devoted to the review of the properties of the axion.

Massless up-quark solution

The simplest solution to the strong CP problem would be for the up-quark to be massless [112]. In that case, $\text{Arg}\,(\det M)$ would vanish and it would be impossible to have a physical CP

[17] The Euclidean action is real at $\theta = 0$ only if there is no other source of CP violation. Although this is not strictly true in the SM, we have already seen that the effects on θ of the phase of the CKM matrix can be safely neglected.

phase. Ultimately this solution is no different from the PQ mechanism. The axial rotation of the massless up-quark $U(1)_A : u \to e^{i\beta\gamma^5}u$ is a classical symmetry of the massless Lagrangian but explicitly broken by the QCD anomaly, see Eq. (1.4.16) for $m = 0$. Thus this symmetry is a perfectly valid PQ symmetry. Furthermore, this symmetry is also spontaneously broken by the quark condensates upon confinement, giving rise to a pseudo-Goldstone boson. One could then identify the corresponding axion with the η'-meson.[18]

One might wonder how a massless up-quark could be compatible with the observed meson masses. First, Mc Arthur and Georgi [149] showed that instantons can give an effective contribution to the up quark mass $m_u \sim m_d m_s/\lambda_{\rm QCD}$, although the estimate is not reliable since the DIGA cannot be applied in the confining regime. Second, it was shown by Manohar and Kaplan [150] that second order terms in the chiral Lagrangian can generate an effective up quark mass that is also proportional $m_u \propto m_s m_d$ while being compatible with the pseudoscalar meson masses. These two results made the massless up-quark solution very appealing, since it does not require any extension of the SM. Nevertheless, this alternative is now ruled out by lattice QCD results that show that the up quark has non-zero mass [151–155].

2.4 Why is there no Weak CP problem?

Before finishing this chapter about the strong CP problem, it is pertinent to comment on the reason why there is only a strong CP problem but not an electroweak or electromagnetic one. One can also write the topological terms for the electroweak gauge group of the SM $SU(2)_L \times U(1)_Y$,

$$\mathcal{L}_{\not{CP}} = \theta_{\rm QCD}\frac{\alpha_s}{8\pi}G_{\mu\nu}G^{\mu\nu} + \theta_W\frac{\alpha_W}{8\pi}W_{\mu\nu}W^{\mu\nu} + \theta_Y\frac{\alpha_s}{8\pi}B_{\mu\nu}B^{\mu\nu}\,. \tag{2.4.1}$$

All three terms correspond to total derivatives. We showed in the previous sections that in the case of QCD the vacuum contains non-trivial configurations for which the integral in the boundary does not vanish, giving rise to observable effects.

For the case of $U(1)_Y$, the vacuum does not contain such non-trivial configurations since the third homotopy group of the abelian group is trivial $\pi_3(U(1)) = 0$. As a consequence the corresponding θ_Y-term has no physical impact.

For the case of $SU(2)_L$, the situation is a bit more involved. Although non-trivial maps from the sphere at infinity to the gauge group can be constructed as $\pi_3(SU(2)) = \mathbb{Z}$, there are no exact instanton solutions since the theory is spontaneously broken. Still, as we showed in Section 2.2.5 there are approximate solutions of the Euclidean theory called constrained instantons, that could generate a non-trivial vacuum. However, once fermions are taken into account the situation changes. As a consequence of $SU(2)_L$ gauge bosons interacting only with left-handed currents, both the baryon and lepton number current are anomalous,

$$\partial_\mu J^B_\mu = \partial_\mu J^L_\mu = \frac{\alpha_W}{4\pi}W_{\mu\nu}W^{\mu\nu}\,. \tag{2.4.2}$$

[18] Actually, since the anomalous term badly breaks the $U(1)_A$ symmetry, the η' cannot be considered a true pGB. Indeed it is not light and acquires similar mass to that of the rest of hadrons $\sim \Lambda_{QCD}$. However, one can make this analogy by noting that the η' is the lightest meson with the same quantum numbers as the axial current.

Thus via a BN rotation the θ_W can be reabsorbed from the Lagrangian leaving no physical consequence. In other words, baryon (or lepton) number symmetry is the PQ symmetry of the EW topological term since it is classically conserved and explicitly broken solely by the EW anomaly.

CHAPTER 3

Axions and axion-like particles

The QCD axion is a hypothetical pseudoscalar particle ($J^P = 0^-$) that was proposed as the low-energy imprint of the PQ solutions to the strong CP problem [147,156]. In this type of solutions, there is a global $U(1)_{\rm PQ}$ symmetry that is spontaneously broken, implying the existence of an associated pseudo-Goldstone boson, the axion. Since the $U(1)_{\rm PQ}$ is not an exact symmetry of the quantum theory but is explicitly broken by the QCD anomaly instead, the axion is not massless and develops a non-zero mass. Its main properties are reviewed in Section 3.1 and stem from its pGB nature; namely, axions are naturally lighter than the characteristic scale of the UV completion generating them, i.e. the PQ breaking scale f_a, and they interact feebly with the rest of the SM field content via derivative couplings and putatively anomalous couplings.[1] All the axion couplings are inversely proportional to the axion scale.

Furthermore, although axions were proposed as a possible explanation for the absence of significant CP violation in the strong sector, it was later realized that they are excellent Dark Matter candidates. This will be discussed in Section 3.3.

The axion solution is particularly appealing due to its minimality and predictability since it solves two of the problems of the SM with a theory that only involves a single parameter, the axion scale f_a. For QCD axions, this scale determines the strength of the axion couplings to the SM fields and the axion mass,

$$m_a^2 \simeq \frac{f_\pi^2 m_\pi^2}{f_a^2} \frac{m_u m_d}{(m_u + m_d)^2}\,, \tag{3.0.1}$$

where m_π, f_π, m_u, m_d denote the pion mass and coupling constant, and the up and down quark masses, respectively. Note that the axion would remain massless in the limit of vanishing quark

[1] Actually anomalous couplings to the $SU(2)_L \times U(1)$ field strengths can also be seen as derivative couplings since $F\widetilde{F} = \partial_\mu K^\mu$ and the boundary term vanishes due to the trivial vacuum. Axions also couple to the QCD anomalous term but this does not correspond to a derivative coupling due to the θ-vacuum that explicitly breaks $U(1)_{PQ}$.

masses due to the axion mixing with the neutral mesons, as will be derived in Section 3.1. Astrophysical constraints force the axion scale to be large, $f_a \gtrsim 10^8\,\text{GeV}$ (see Section 3.4 for a brief review on experimental searches), and due to Eq. (3.0.1), QCD axions are necessarily light particles $m_a \lesssim 10^{-2}\,\text{eV}$.

However, the motivation to consider pGBs as possible BSM particles goes well beyond the strong CP problem and axions. Indeed, there are a variety of frameworks in which this type of particles arises, such as theories with extra dimensions, Majoron models providing dynamical explanations to neutrino mass generation [157], string theories [158–161], supersymmetric theories [162], DM models [163] and many dynamical flavor theories [156, 164, 165]. These pGB are frequently called axion-like particles (ALPs) due to their shared properties with axions. However, they present an expanded parameter space since the tight relation between the axion scale and mass no longer holds for ALPs. The qualitative effective Lagrangian for ALPs reads

$$\mathcal{L}^{\text{eff}}_{\text{ALP}} \simeq \frac{1}{2}\partial_\mu a \partial^\mu a - \frac{1}{2} m_a^2 a^2 + \frac{\partial_\mu a}{f_a} \times \text{SM}^\mu + \frac{a}{f_a} X^{\mu\nu} \widetilde{X}_{\mu\nu}\,, \tag{3.0.2}$$

where SM^μ denotes a generic SM current and $X^{\mu\nu}$ a generic SM field strength.

Furthermore, new developments in model building have shown that pseudoscalars lying in regions of the parameter space classically associated with ALPs may also solve the strong CP problem and thus deserve to be called axions. On the one hand, some models have been proposed in which the axion coupling to photons is either suppressed [166, 167] or enhanced [168] with respect to the naive expectation of classical models with no cancellations and order one parameters. This leads to photophobic or photophilic axions or even astrophobic axions [169], in which the coupling to nucleons is suppressed avoiding some of the stellar constraints. On the other hand, extensions of the SM involving new confining groups may generate new instanton sources that raise the axion mass. Several of such "heavy axions" have been proposed [4, 170–180] and will be briefly reviewed in Section 3.2.5, and a new setup will be proposed in Chapter 5. Thus the true axion parameter space is opening up and further motivates experimental efforts looking for this type of axions and ALPs.

3.1 Main properties of the QCD axion

Axion low-energy Lagrangian

There are two possible ways of constructing the axion low-energy Lagrangian. In the EFT approach, one writes all the non-renormalizable operators of a given dimension respecting the symmetries of the theory. In this case, in addition to the SM gauge symmetries, the PQ symmetry needs to be preserved by all terms, except the axion coupling to the QCD topological term. A PQ transformation shifts the axion field $a \to a + \alpha f_a$ and thus all axion couplings will be either derivative or anomalous. Below the EWSB scale and considering the first generation

of fermions, the axion effective Lagrangian reads [181, 182],

$$\mathcal{L}_{\rm a}^{\rm eff} = \frac{1}{4} g^0_{agg}\, \hat{a}\, G\tilde{G} + \frac{1}{4} g^0_{a\gamma\gamma}\, \hat{a}\, F\tilde{F} + \frac{c_1^u}{2}\frac{\partial_\mu \hat{a}}{f_a}\left(\bar{u}\,\gamma_\mu\,\gamma_5\,u\right) + \frac{c_1^d}{2}\frac{\partial_\mu \hat{a}}{f_a}\left(\bar{d}\,\gamma_\mu\,\gamma_5\,d\right) + \frac{c_1^e}{2}\frac{\partial_\mu \hat{a}}{f_a}\left(\bar{e}\,\gamma_\mu\,\gamma_5\,e\right) . \tag{3.1.1}$$

Alternatively to the EFT approach, one can obtain the low-energy interactions of the axion for a given model via the PQ current, that in particular contains the axion,[2]

$$j^\mu_{PQ} = \sum_i \chi_i \overline{\psi}_i \gamma^\mu \psi_i + f_{PQ}\partial^\mu a + \dots , \tag{3.1.2}$$

where χ_i denotes the PQ charge of the Weyl fermion ψ_i that may include the SM and/or other exotic fermions, and $f_{\rm PQ}$ is the PQ breking scale. The current of the full theory may also contain other heavy degrees of freedom, such as radial components of scalars, that decouple and do not play a role in the axion low-energy interactions. Due to the anomalous conservation of the PQ current, its divergence reads

$$\partial_\mu j^\mu_{\rm PQ} = -\frac{N}{f_{\rm PQ}}\frac{\alpha_s}{8\pi} G_{\mu\nu}\tilde{G}^{\mu\nu} - \frac{E}{f_{\rm PQ}}\frac{\alpha_{em}}{8\pi} F_{\mu\nu}\tilde{F}^{\mu\nu} , \tag{3.1.3}$$

where the coefficients E and N are the electromagnetic and color anomaly factors, which depend on the charges and representations of the PQ-charged fermions that run in the loop generating the anomaly. They can be computed using Eq. (1.4.19) for the abelian case, yielding[3]

$$E = 2\sum_f \left(\chi^f_L - \chi^f_R\right) q^2_{em} , \qquad N = 2\sum_f \left(\chi^f_L - \chi^f_R\right) T(R_f) , \tag{3.1.4}$$

where q_{em} is the electromagnetic charge, R_f is the representation of the fermion ψ_f under QCD and $T(R_f)$ its corresponding Dynkin index defined as $\mathrm{tr}\left(T^a T^b\right) = T(R)\delta^{ab}$. Inserting Eq. (3.1.2) into Eq. (3.1.3), the axion EOM follows:

$$f_{\rm PQ}\Box\hat{a} + \sum_i \chi_i\, \partial_\mu\left(\overline{\psi}_i\gamma^\mu\psi_i\right) = -\frac{N}{f_{\rm PQ}}\frac{\alpha_s}{8\pi} G_{\mu\nu}\tilde{G}^{\mu\nu} - \frac{E}{f_{\rm PQ}}\frac{\alpha_{em}}{8\pi} F_{\mu\nu}\tilde{F}^{\mu\nu} , \tag{3.1.5}$$

which corresponds to the Euler-Lagrange equation for the axion stemming from the effective Lagrangian,

$$\mathcal{L}_{\rm a}^{\rm eff} = \frac{1}{2}\partial_\mu\hat{a}\partial^\mu\hat{a} - E\,\frac{\alpha_{em}}{8\pi}\frac{\hat{a}}{f_{\rm PQ}} F_{\mu\nu}\tilde{F}^{\mu\nu} - N\,\frac{\alpha_s}{8\pi}\frac{\hat{a}}{f_{\rm PQ}} G_{\mu\nu}\tilde{G}^{\mu\nu} + \frac{\partial_\mu\hat{a}}{f_{\rm PQ}}\sum_i \chi_i\left(\overline{\psi}_i\gamma^\mu\gamma^5\psi_i\right) . \tag{3.1.6}$$

It is customary to define the physical axion scale f_a from the strength of the gluonic coupling,

$$f_a \equiv \frac{f_{\rm PQ}}{N} , \tag{3.1.7}$$

[2] With this definition for the PQ current we are implicitly assigning a unit PQ charge to the scalar that contains the axion.

[3] Note that this definition for E and N differs from that used in Ref. [167] by a factor of 2. In this thesis we will follow the convention dictated by Eq. (3.1.4), that is also widely used in the literature, e.g. [183, 184]

leading to the effective Lagrangian

$$\mathcal{L}_{\rm a}^{\rm eff} = \frac{1}{2}\partial_\mu \hat{a}\partial^\mu \hat{a} - \frac{\alpha_{em}}{8\pi}\frac{E}{N}\frac{\hat{a}}{f_a}F_{\mu\nu}\tilde{F}^{\mu\nu} - \frac{\alpha_s}{8\pi}\frac{\hat{a}}{f_a}G_{a\mu\nu}\tilde{G}_a^{\mu\nu} + \partial_\mu \hat{a}\sum_i \chi_i\left(\overline{\psi}_i\gamma^\mu\psi_i\right), \tag{3.1.8}$$

that can be now matched with the Lagrangian in Eq. (3.1.1),

$$g^0_{agg} = -\frac{\alpha_s}{2\pi f_a}, \qquad g^0_{a\gamma\gamma} = -\frac{\alpha_{\rm em}}{2\pi f_a}\frac{E}{N}, \qquad \frac{c_1^i}{2} = \frac{1}{N}(\chi_L^i - \chi_R^i), \tag{3.1.9}$$

where the index i runs over the first generation fermions, i.e. the up and down quarks and the electron.

QCD axion mass

One of the most robust predictions of classical axion models is the relation between the axion mass and the axion scale. The mass of a pGB is related to the explicit breaking of its corresponding approximate symmetry [185], and for the PQ symmetry it corresponds to the anomalous interactions of axions with gluons $aG\tilde{G}$, that induce a potential for the axion as a consequence of non-perturvative QCD dynamics. Why then is not the QCD axion mass $\sim \Lambda_{\rm QCD}$? The point is that this very same source of breaking is the responsible for the solution to the missing meson problem and therefore will generate a mixing between the PQ and axial currents. That is, there are two pseudoscalars with anomalous couplings to QCD, a and η', and only one source of breaking due to QCD instantons. As a consequence, below the confinement scale the axion will mix with the pseudoscalar meson. It is pertinent to construct the combined mass matrix in order to obtain the axion mass and physical eigenstate.

Let us consider in the two quark approximation the mass Lagrangian for the neutral pion π^0 and η_0 at leading order in the chiral expansion,

$$\mathcal{L}_{\rm a}^{\rm chiral} = B_0 f_\pi^2\left[m_u\cos\left(\frac{\pi_3}{f_\pi}+\frac{\eta_0}{f_\pi}\right) + m_d\cos\left(\frac{\pi_3}{f_\pi}-\frac{\eta_0}{f_\pi}\right)\right] - \frac{1}{2}K\left(2\frac{\eta_0}{f_\pi}+\frac{\hat{a}}{f_a}\right)^2, \tag{3.1.10}$$

where B_0 can be expressed in terms of the QCD quark condensate $\langle\bar{q}q\rangle$ as $B_0 f_\pi^2 = -2\langle\bar{q}q\rangle \sim \Lambda^3_{\rm QCD}$ and the last term encodes the explicit breaking of both $U(1)_{\rm PQ}$ and $U(1)_A$ that creates a potential for both the axion and the η_0 below the confinement scale, $K \sim \Lambda^4_{\rm QCD}$ [186–189].

The resulting mass matrix for the three neutral pseudoscalars is given by

$$M^2_{\{\pi_3,\eta_0,a\}} = \begin{pmatrix} B_0(m_u+m_d) & B_0(m_u-m_d) & 0 \\ B_0(m_u-m_d) & 4K/f_\pi + B_0(m_u+m_d) & 2K/(f_\pi f_a) \\ 0 & 2K/(f_\pi f_a) & K/f_a^2 \end{pmatrix}. \tag{3.1.11}$$

The QCD axion scale is typically large, hence this matrix can be diagonalized in the limit $f_a \gg K^{1/4}, B_0 \gg m_{u,d}$, which results in the axion mass being

$$m_a^2 \simeq \frac{f_\pi^2 m_\pi^2}{f_a^2}\frac{m_u m_d}{(m_u+m_d)^2}. \tag{3.1.12}$$

This relation between the axion mass and scale is a robust prediction of QCD axion models in which the PQ symmetry is only broken by the QCD instantons, as commonly required to successfully implement the PQ solution to the strong CP problem.

Strikingly, the physical axion mass is not proportional to the parameter encoding the PQ breaking due to instantons K, but to the product of quark masses. The reason becomes clear in the chiral limit $m_{u,d} \to 0$. The QCD anomaly is coupled to both the original axion $\hat{a}$ and the η_0, but actually it only generates a mass to a combination of them $2\frac{\eta_0}{f_\pi} + \frac{\hat{a}}{f_a}$ that is identified with the physical η'. The orthogonal combination corresponds to the physical axion and remains massless in the chiral limit. Once quark masses are taken into account the axion develops a mass proportional to them due to its mixing with the η_0-meson and the pion. The axion mass eigenstate corresponds to

$$a \simeq \hat{a} + \theta_{a\pi}\, \pi_3 + \theta_{a\eta'}\, \eta_0 \,, \tag{3.1.13}$$

where the mixing angles read

$$\theta_{a\pi} \simeq -\frac{f_\pi}{2f_a}\frac{m_d - m_u}{m_u + m_d} \,, \qquad\qquad \theta_{a\eta'} \simeq -\frac{f_\pi}{2f_a} \,. \tag{3.1.14}$$

In other words, as was shown in Refs. [190–192], the physical axion is not actually the pGB of the original PQ symmetry but of a modified version of it, the divergenceless PQ,

$$j^\mu_{\mathrm{PQ}'} = j^\mu_{\mathrm{PQ}} - \frac{1}{2}\frac{1}{m_u + m_d}\left(m_d \bar{u}\gamma^\mu\gamma_5 u + m_u \bar{d}\gamma^\mu\gamma_5 d\right) \,, \tag{3.1.15}$$

which is not anomalous under QCD but only broken by the quark mass terms and gives the same physical axion couplings as the diagonalization of Eq. (3.1.13).

Although the mass of the axion has been derived from the Lagrangian in Eq. (3.1.10) which does not include direct couplings of the axion to the SM quarks, it can be shown that it holds in all generality, see Chapter 7 for more details. The axion mass has recently been computed at Next to Leading Order (NLO) in Ref. [183] together with the axion potential [183, 187], that reads

$$V(a) = -m_\pi^2 f_\pi^2 \sqrt{1 - \frac{4m_u m_d}{(m_u + m_d)^2}\sin^2\left(\frac{a}{2f_a}\right)} \,. \tag{3.1.16}$$

Physical axion couplings to photons

Since the physical low-energy axion eigenstate acquires π_3 and η_0 components, it inherits their couplings to photons weighted down by their mixing with the axion. The couplings in Eq. (3.1.9) get modified for the physical axion resulting in,

$$g_{a\gamma\gamma} = g^0_{a\gamma\gamma} + \theta_{a\pi}\, g_{\pi\gamma\gamma} + \theta_{a\eta'}\, g_{\eta'\gamma\gamma} \,, \tag{3.1.17}$$

where the last two terms are the contributions induced by the model-independent axion-pion and axion-η' QCD mixings. It is important to note that this expression is valid below QCD

confinement: at those energies gluons can be integrated out and the anomalous coupling of the axion generates the mixing with the neutral mesons. Substituting the mixings in Eq. (3.1.14), we obtain

$$g_{a\gamma\gamma} = g^0_{a\gamma\gamma} + \frac{\alpha}{2\pi f_a}\left(6\,\frac{q_d^2\,m_u + q_u^2\,m_d}{m_u + m_d}\right) , \tag{3.1.18}$$

where $q_u = 2/3$ and $q_d = -1/3$ are the electric charges of the up and down quarks, resulting in the well-known expression

$$g_{a\gamma\gamma} = \frac{\alpha}{2\pi f_a}\left(\frac{E}{N} - \frac{2}{3}\,\frac{m_u + 4\,m_d}{m_u + m_d}\right) , \tag{3.1.19}$$

which is valid to first order in chiral perturbation theory. The corrections at NLO have been computed in Ref. [183], obtaining

$$g_{a\gamma\gamma} = \frac{1}{2\pi f_a}\alpha_{\rm em}\left(\frac{E}{N} - 1.92(4)\right) . \tag{3.1.20}$$

To sum up, the axion coupling to photons presents two different contributions, the first one is model dependent (it could even vanish for some models, see KSVZ model later on), whereas the second component stems from the axion-meson mixing: this term is model independent and is present for all axion models. The constraints on the axion coupling to photons are shown in Fig. 3.1, where the region of the parameter space $\{m_a, g_{a\gamma\gamma}\}$ that corresponds to KSVZ axion models are depicted as a grey band. More details on this computation and the experimental bounds can be found in Chapter 7, where this known result has been extended for the first time for the axion couplings to EW gauge bosons.

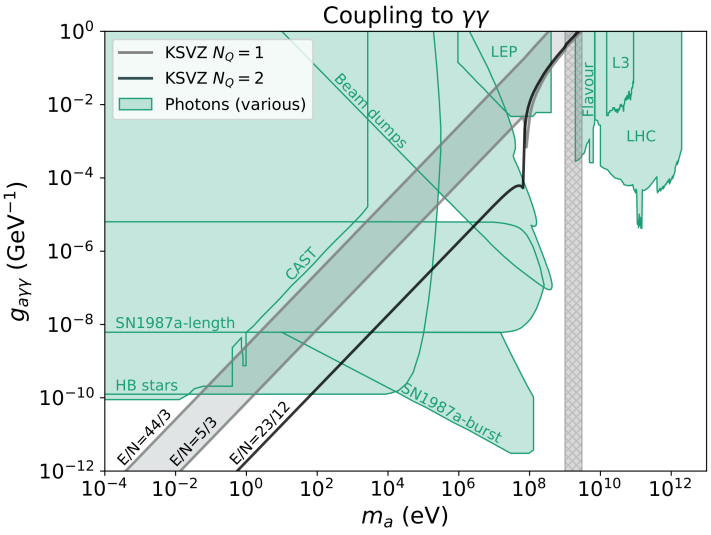

Figure 3.1: Bounds on the axion coupling to photons as a function of the axion mass. The black line and grey band correspond to KSVZ-type QCD axion models for different values of E/N. The description of the experimental limits can be found in Chapter 7.

Physical axion couplings to nucleons

The axion couplings to protons and neutrons can be obtained by formulating the non-relativistic theory for nucleons, whose Wilson coefficients are extracted from the neutron-proton mass splitting and lattice simulations [183]. Similar to the coupling to photons, axion-nucleon couplings present a model independent component stemming from the axion coupling to gluons and another model-dependent component that depends on the PQ charges of the SM quarks. Defining the nucleon coupling analogously to that to quarks,

$$\mathcal{L}_{\rm a}^{\rm eff} \supset c_p \frac{\partial_\mu a}{2f_a}\overline{p}\gamma^\mu\gamma_5 p + c_n \frac{\partial_\mu a}{2f_a}\overline{n}\gamma^\mu\gamma_5 n\,, \tag{3.1.21}$$

where c_p and c_n denote the coupling to protons and neutrons, respectively. The physical axion couplings read

$$\begin{aligned} c_p &= -0.47(3) + 0.88(3)c_1^u - 0.39(2)c_1^d + \delta \\ c_1^n &= -0.02(3) + 0.88(3)c_1^d - 0.39(2)c_1^u + \delta\,, \end{aligned} \tag{3.1.22}$$

where $\delta = -0.038(5)c_1^s - 0.012(5)c_1^c - 0.009(2)c_1^b - 0.0035(4)c_1^t$ includes the small corrections due to the rest of SM quarks.

3.2 QCD axion models

The paradigmatic axion models are reviewed in this section. First, the original PQWW model, in which the axion first appeared, is discussed. Soon after its proposal, this "visible" axion was ruled out by rare meson decay experiments, and the two most famous invisible axions models were proposed: KSVZ and DFSZ. The different implementations of the PQ symmetry in these models is reviewed, together with the case of the composite axion. Finally, we will comment on recent attempts to build heavy axions models in which the axion mass is raised with respect to that of the invisible axions, given in Eq. (3.1.12) due to the existence of new instanton sources.

3.2.1 Visible axion: original PQWW model

The SM does not present any classically exact abelian symmetry, which is only broken by the QCD anomaly. Hence, in order to implement the PQ mechanism, the SM needs to be extended. The first such extension was proposed by Peccei and Quinn [8,9] and consisted on a two Higgs doublet model (2HDM),

$$H_u = \left(\mathbf{1}, \mathbf{2}, \frac{1}{2}\right) \qquad\qquad H_d = \left(\mathbf{1}, \mathbf{2}, \frac{1}{2}\right), \tag{3.2.1}$$

where $\left(\mathbf{1}, \mathbf{2}, \frac{1}{2}\right)$ denotes the representation of each scalar under the SM gauge group, $SU(3)_c \times SU(2)_L \times U(1)_Y$. The leptons can couple to either of the two doublets giving rise to particular

realizations of the type II [193, 194] and flipped 2HDM [195]. For concreteness, only the type II 2HDM will be now discussed, [4] whose Lagrangian reads

$$\mathcal{L}_{\text{Yukawa}} - \overline{Q}_L Y_u \widetilde{H}_u U_R - \overline{Q}_L Y_d H_d D_R - \overline{\ell}_L Y_e H_d E_R + \text{h.c.} \tag{3.2.2}$$

The presence of two scalar doublets with such couplings enlarges the global symmetry of the theory, that now presents a global $U(1)_{\text{PQ}}$ within the abelian symmetries $U(1)_B \times U(1)_L \times U(1)_Y \times U(1)_{\text{PQ}}$. The transformation of a generic combination of these abelian groups reads

$$\begin{aligned} U(1)_{\text{PQ}}: \quad & Q_L \to e^{i\chi_q \alpha} Q_L, \qquad U_R \to e^{i\chi_u \alpha} U_R, \qquad D_R \to e^{i\chi_d \alpha} D_R, \\ & \ell_L \to e^{i\chi_\ell \alpha} \ell_L, \qquad E_R \to e^{i(\chi_\ell - \chi_q + \chi_d)\alpha} E_R\,, \\ & H_u \to e^{i(\chi_u - \chi_q)\alpha} H_u\,, \quad H_d \to e^{i(\chi_q - \chi_d)\alpha} H_d\,, \end{aligned} \tag{3.2.3}$$

where the flavor indices have been omitted and χ_q, χ_u, χ_d and χ_ℓ are the PQ charges of Q_L, U_R, D_R and ℓ_L, respectively. The definition of the PQ symmetry is not unique, though, and will be extracted from the generic transformation in Eq. (3.2.3) by imposing and choosing some conditions. The physical couplings of the axion depend on the axial charges of the fermions so we can fix $\chi_q = \chi_\ell = 0$ via appropriate vectorial transformations, i.e. lepton and baryon number transformations. The symmetry has only two free parameters χ_u, χ_d and corresponds to a combination of $U(1)_{\text{PQ}}$ and $U(1)_Y$, whose current reads

$$\begin{aligned} j^\mu_{\text{PQ}} = & \chi_u\, \overline{U}_R \gamma^\mu U_R + \chi_d\, \overline{D}_R \gamma^\mu D_R + \chi_d\, \overline{E}_R \gamma^\mu E_R \\ & - i\chi_u \big((\partial^\mu H_u^\dagger) H_u - H_u^\dagger (\partial^\mu H_u) \big) + i\chi_d \big((\partial^\mu H_d^\dagger) H_d - H_d^\dagger (\partial^\mu H_d) \big)\,. \end{aligned} \tag{3.2.4}$$

Upon EWSB, the two Higgs doublets develop vacuum expectation values and both the PQ and the EW symmetries are spontaneously broken,

$$\begin{aligned} H_u &= \frac{1}{\sqrt{2}} (v_u + \rho_u)\, e^{i a_u / v_u}\,, \\ H_d &= \frac{1}{\sqrt{2}} (v_d + \rho_d)\, e^{i a_d / v_d}\,, \end{aligned} \tag{3.2.5}$$

where vevs v_u and v_d relate to the EW scale as $v \equiv \sqrt{v_u^2 + v_d^2} = 246\,\text{GeV}$. The CP-odd components of the scalars, a_u and a_d, lead to two different combinations: one corresponds to the axion [147, 148] while the other becomes the longitudinal component of the Z-boson in the unitary gauge. In order to fully specify the PQ charges, the orthogonality condition must be imposed, i.e. the axion must not mix with the Z-boson. One way of obtaining this condition is to perform a $U(1)_Y$ transformation and impose that the axion must remain invariant under it. Let us first identify the linear combination corresponding to the axion by writing the PQ current in Eq. (3.2.4) in terms of the pseudoscalar components of the Higgses, and compare with the generic PQ current in Eq. (3.1.2),

$$j^\mu_{\text{PQ}} = \sum_i \chi_i \overline{\psi}_i \gamma^\mu \psi_i - \chi_u v_u\, \partial^\mu a_u + \chi_d v_d\, \partial^\mu a_d \quad \Longrightarrow \quad f_{\text{PQ}} a = -\chi_u v_u\, a_u + \chi_d v_d\, a_d \tag{3.2.6}$$

[4] In the flipped 2HDM the charged leptons couple to the same Higgs doublet that couples to the up-type quarks and leads to different PQ charge assignments.

where the PQ scale $f_{\rm PQ}$ ensures the proper normalization of the field and corresponds to

$$f_{\rm PQ} = \sqrt{\chi_u^2 v_u^2 + \chi_d^2 v_d^2}\,. \tag{3.2.7}$$

Under a $U(1)_Y$ transformation a_u and a_d get a shift proportional to the hypercharge of the corresponding doublet, and the axion transforms as

$$U(1)_Y: \quad a \longrightarrow \frac{1}{f_{\rm PQ}}\left(-\chi_u v_u\left(a_u + \frac{\beta}{2}v_u\right) + \chi_d v_d\left(a_d + \frac{\beta}{2}v_d\right)\right) \tag{3.2.8}$$

$$= a + \frac{1}{f_{\rm PQ}}\frac{\beta}{2}\left(-\chi_u v_u^2 + \chi_d v_d^2\right). \tag{3.2.9}$$

For the axion to be invariant under $U(1)_Y$, the fermionic PQ charges need to fulfill

$$\frac{\chi_u}{\chi_d} = \frac{v_d^2}{v_u^2}\,. \tag{3.2.10}$$

Defining the ratio of the vevs as $x = v_d/v_u$ and choosing an overall normalization for the charges, we finally get

$$\chi_u = x\,, \qquad \chi_d = \frac{1}{x} \tag{3.2.11}$$

that fully determines the PQ current and allows one to compute the axion couplings, as explained in Section 3.1. In particular we can check that this PQ symmetry is indeed anomalous and therefore the axion couples to the QCD topological term, solving the strong CP problem:

$$\mathcal{L}_{\rm PQWW} \supset N_f\left(1 + \frac{1}{x}\right)\frac{\alpha_s}{8\pi}\frac{a}{f_{\rm PQ}}G_{\mu\nu}\tilde{G}^{\mu\nu}\,, \tag{3.2.12}$$

where $N_f = 3$ is the number of fermion families.

One of the most important features of the PQWW model is that the PQ breaking scale $f_{\rm PQ}$ is of the order of the EW scale and thus the axion has a sizable mass (of the order of $\sim 100\,\text{keV}$), as dictated by Eq. (3.1.12), and sizable couplings to the SM fields, since they are only suppressed by the weak scale. As a consequence and despite solving the Strong CP problem in a minimal way, this *visible* axion model was soon ruled out by different experiments [191, 196–200], the rare meson decays $K^+ \to \pi^+ \text{inv}$ for long-lived axions being especially important.

3.2.2 Invisible axion models

Despite the fact that the first implementation of the PQ mechanism is ruled out, this solution of the Strong CP problem can still be saved. Indeed. it was the identification of the PQ breaking scale with the EW scale in this first attempt that imposed such strong bounds. Therefore by decoupling these two a priori unrelated scales, the PQ mechanism can be safely implemented.

For instance, if there exist a new scalar singlet whose vev breaks the PQ symmetry at a scale that is much larger than that of EW interactions, the axion becomes very light and the

interactions get strongly suppressed $\sim 1/f_a$, evading the experimental bounds. This is the strategy followed by the two paradigmatic invisible axion models, KSVZ and DFSZ axions.

It is also possible, nevertheless, to build invisible axion models without introducing any extra fundamental scalar fields. Although it is sometimes overlooked, this is the case of the composite or dynamical axion [201, 202] where the axion corresponds to a pseudoscalar meson of a new confining force.

DFSZ

A simple extension of the PQWW model was propossed by Zhitnitsky [203] and later by Dine, Fischler and Sredniki [204]. In addition to the two Higgs doublets, a new scalar singlet is introduced, σ, which takes a vev at a high scale. This scalar carries PQ charge due to its couplings to the Higgs doublets in the scalar potential,[5]

$$\begin{aligned} V\big(H_u, H_d, \sigma\big) =& \frac{\lambda_\sigma}{2}|\sigma|^4 + \delta_1\big(H_u^\dagger H_u\big)|\sigma|^2 + \delta_2\big(H_d^\dagger H_d\big)|\sigma|^2 \\ &+ \delta_3\big(H_u^\dagger H_d\big)\sigma^2 + \delta_3\big(H_d^\dagger H_u\big)\sigma^{*2} \end{aligned} \tag{3.2.13}$$

which forces the PQ charge of σ to be,[6]

$$\mathrm{U}(1)_{\mathrm{PQ}}: \quad \sigma \to \mathrm{e}^{\mathrm{i}\beta\chi_\sigma}\sigma\,, \qquad \text{with} \qquad \chi_\sigma = \frac{1}{2}(\chi_u + \chi_d)\,. \tag{3.2.14}$$

The potential in Eq. (3.2.13) generates a non-zero vacuum expectation value for the scalar that breaks spontaneously the PQ symmetry,

$$\sigma = \frac{1}{\sqrt{2}}\,(v_\sigma + \rho_\sigma)\, e^{ia_\sigma/v_\sigma}\,, \tag{3.2.15}$$

and the axion now results from a combination of the CP-odd components of the Higgs doublets in Eq. (3.2.5) together with the new pseudoscalar a_σ,

$$a = \frac{1}{f_{\mathrm{PQ}}}\,(-\chi_u v_u\, a_u + \chi_d v_d\, a_d + \chi_\sigma v_\sigma) \xrightarrow{v_\sigma \gg v_d, v_u} a_\sigma \tag{3.2.16}$$

$$f_{\mathrm{PQ}} = \sqrt{\chi_u^2 v_u^2 + \chi_d^2 v_d^2 + \chi_\sigma^2 v_\sigma^2} \xrightarrow{v_\sigma \gg v_d, v_u} \chi_\sigma v_\sigma\,, \tag{3.2.17}$$

where the case in which v_σ is much larger than the EW scale is shown. Without loss of generality the PQ charge of the scalar can be set $\chi_\sigma = 1/2(\chi_u + \chi_d) = 1$. Due to the large hierarchy among the vevs of the scalars, the axion scale corresponds to the vev of the singlet $f_{PQ} \simeq v_\sigma$, and the PQ pseudo-Goldstone Boson is mostly given by the CP-odd component a_σ.

[5] This potential and PQ charge assignment corresponds to that of the original DFSZ model. There is however another possibility if one substitutes the last two terms of the potential by $H_u^\dagger H_d S$.

[6] Note that $\chi_{u,d}$ denote the PQ charges of the fermions as defined in Eq. (3.2.3). The charges of the doublets read $\chi(H_u) = \chi_u$, $\chi(H_d) = -\chi_d$.

Regarding the axion couplings of the DFSZ axion, they correspond to those of the PQWW model after rescaling the axion scale by a factor $\sim \frac{v}{v_\sigma}$. Since the new scale v_σ is not connected to the EW scale, it can be set to take arbitrarily high values, evading the bounds that ruled out the PQWW model.

The couplings of the DFSZ axion to the SM can be computed using Eqs. (3.1.9), (3.1.20) and (3.1.22). In particular the color and electromagnetic anomalies read,

$$N = 3\,(\chi_u + \chi_d) = 6\,, \qquad E = 16 \quad \Longrightarrow \quad \frac{E}{N} = \frac{8}{3}\,. \tag{3.2.18}$$

KSVZ

Probably the simplest invisible axion model is that propossed by Kim [205] and Shifman, Vainshtein and Zakharov [206] in which only two particles are added to the SM matter content: a vectorial QCD-colored fermion, $\psi_{L,R}$, and a complex scalar singlet, S. The latter plays an analogous role to that of σ in DFSZ, that is, it contains a component of the axion and allows one to set very high axion scales.

The Lagrangian of the theory reads $\mathcal{L} = \mathcal{L}_{\rm SM} + \mathcal{L}_{\rm KSVZ}$,

$$\begin{aligned}\mathcal{L}_{\rm KSVZ} = {} & i\overline{\psi}_L \not{D} \psi_L + i\overline{\psi}_R \not{D} \psi_R + \partial_\mu S^* \partial^\mu S \\ & + y S \overline{\psi}_L \psi_R + \text{h.c.} \\ & + \mu_{\rm S}^2 |S|^2 - \lambda_{\rm S} |S|^4 - \lambda_{\Phi{\rm S}} |\Phi|^2 |{\rm S}|^2\,,\end{aligned} \tag{3.2.19}$$

where y is the Yukawa coupling for the exotic fermions, and $\mu_{\rm S}$, $\lambda_{\rm S}$ and $\lambda_{\Phi{\rm S}}$ are the parameters of the scalar potential. This Lagrangian presents two global abelian symmetries: a vectorial $U(1)_{B'}$ that corresponds to a baryon number for the exotic fermion ψ, and an axial symmetry $U(1)_{\rm PQ}$ under which both the exotic scalar and fermion transform. Note that for this model it is only the exotic degrees of freedom that have non-zero PQ charges, leaving all the SM particles unaffected by a PQ transformation,

$$U(1)_{\rm PQ}: \qquad \psi_L \to e^{i\frac{\alpha}{2}} \psi_L, \quad \psi_R \to e^{-i\frac{\alpha}{2}\alpha} \psi_R, \quad S \to e^{i\alpha} S, \tag{3.2.20}$$

where the choice $\chi_{\psi_L} = 1/2$, $\chi_{\psi_R} = -1/2$ and $\chi_S = 1$ is used, without loss of generality. This symmetry constitutes a valid PQ symmetry, since the QCD charged fermions $\psi_{L,R}$ generate a non-zero anomaly ($N = 1$ if ψ is a color triplet), while being classically exact. The minimum of the scalar potential in Eq. (3.2.19) breaks spontaneously this PQ symmetry $\langle S \rangle = v_S/\sqrt{2}$ giving rise to the axion. In this case, it is straightforward to identify the axion field that simply corresponds to the axial component of the complex scalar S,

$$S = \frac{1}{\sqrt{2}} \left(v_S + \rho_S\right) e^{i\frac{a_s}{v_s}}\,, \tag{3.2.21}$$

and the axion scale corresponds to $f_{\rm PQ} = v_s$, which is assumed to be much larger than the EW scale. The exotic fermion is not observed in the spectrum, and thus it must be very heavy for

the model to be phenomenologically viable. Indeed, it acquires a large mass proportional to the PQ breaking scale, $m_\psi = y\, f_{\rm PQ}$. Similarly the radial component of S also gets decoupled, leaving the axion as the only low energy degree of freedom. Its couplings can be obtained by following the procedure described in Section 3.1. Unlike the DFSZ and PQWW, the KSVZ axion does not have tree-level couplings to SM leptons and quarks, but it can be probed via the model independent component of the coupling to photons or nucleons.

Although in the original KSVZ axion model only one exotic fermion was introduced, a singlet under $SU(2)_L \times U(1)_Y$, it is also possible to add several exotic fermions with non-trivial transformations under the EW gauge group.

In fact, charging the exotic fermions electromagnetically can solve one of the problems of the original model: that of heavy cosmologically stable relics. The problem is that the fermion ψ is cosmologically stable due to the conserved baryon number. After the QCD transition, it hadronizes giving rise to fractionally charged baryons, for which there are strong constraints [207–211]. One possible solution is to assign to the exotic fermion the same hypercharge as one of the SM quarks, allowing for mixing terms of the type $\mathcal{L} \supset \mu \overline{\psi}_L D_R$, that break the exotic baryon number symmetry and open up decay modes for the exotic fermions. As a byproduct, the PQ charged fermions have also electromagnetic charge and therefore contribute to the electromagnetic anomaly. For the simple cases of one fermionic QCD triplet with the same hypercharge as the up- or down-type quarks, the axion coupling to photons is given by Eq. (3.1.20) with,

$$\frac{E}{N} = \frac{8}{3} \text{ for up-type } Y_\psi = \frac{2}{3}\,, \qquad \frac{E}{N} = \frac{2}{3} \text{ for down-type } Y_\psi = -\frac{1}{3}\,. \tag{3.2.22}$$

These two particular cases fall in the grey band of Fig. 3.1. They are called hadronic models and can be generalized introducing several fermions with different transformations under QCD and the EW group. Recently, Refs. [166,167] have studied the possible realizations of the KSVZ model that are compatible with the bounds on cosmological relics, and that do not generate Landau poles below the Planck scale. Given these restrictions in the exotic fermionic matter content, the preferred window for the axion coupling to photons has been refined. Interestingly, the authors show that for certain choices of charges it is possible to build KSVZ models for which the axion coupling to photons vanishes due to a cancellation between the model dependent contribution E/N and the model independent one, see Eq. (3.1.20). Indeed a similar strategy can be applied for the couplings to nucleons, and one can build astrophobic axion models [169] that evade much of the astrophysical constraints due to their suppressed coupling to nucleons. In this context of more sophisticated proposals that can evade certain bounds, it becomes relevant to explore other interactions such as axion couplings to EW gauge bosons, as we will explore in Chapter 7.

Composite axion

Although it has not received as much attention as the KSVZ and DFSZ models, in the same years Kim [201] proposed another invisible axion model in which the axion does not belong to

a fundamental scalar field, but is composite instead. This composite (dynamical) axion model [201, 202] contains a new confining group, the *axicolor* group $SU(N)_a$, whose confinement scale is much larger than that of QCD, $\Lambda_a \gg \Lambda_{\rm QCD}$. Considering that the massless up-quark solution is no longer viable (see Section 2.3.2), the idea is to add exotic massless colored fermions. If these massless quarks are also charged under axicolor they will form bound states whose mass is of the order of the axicolor confinement scale $\sim \Lambda_a$, that can be made arbitrarily large. Nevertheless, if upon confinement chiral symmetries are spontaneously broken, light mesons corresponding to the new Goldstone Bosons of this breaking will arise, one of these composite states being the dynamical axion.

For concreteness, let us consider the massless quark content of the dynamical axion model in Table 3.1.

	$SU(3)_c$	$SU(N)_a$
$\psi_{L,R}$	$\square$	$\square$
$\chi_{L,R}$	1	$\square$

Table 3.1: The massless fermion sector of the dynamical axion model. The fields ψ and χ are Dirac fermions with vectorial transformation properties and $\square$ denotes the fundamental representation.

In this model, two massless quarks are needed because the new confining group, $SU(N)_a$, comes with its new θ-parameter. In order to fully reabsorb both θ paramters from the Lagrangian two independent rotations are needed. In other words, in order to implement the PQ mechanism, the symmetry needs to be explicitly broken by the QCD instantons alone: if we were to add a single massless fermion its axial symmetry would be broken by the instantons of both groups. The Lagrangian for the massless sector reads,

$$\mathcal{L} = i\overline{\psi}_L \not{D} \psi_L + i\overline{\psi}_R \not{D} \psi_R + + i\overline{\chi}_L \not{D} \chi_L + i\overline{\chi}_R \not{D} \chi_R \,. \tag{3.2.23}$$

Since these quarks are massless the theory presents at the classical level a $\left[U(1)\right]^4$ global symmetry: the two vectorial symmetries corresponding to baryon number conservation of the quarks ψ and χ, and the two axial symmetries. These two last symmetries are, however, anomalous under QCD and axicolor. One combination corresponds to the PQ symmetry,

$$j^\mu_{\rm PQ} = \overline{\psi}\gamma^\mu\gamma^5\psi - 3\overline{\chi}\gamma^\mu\gamma^5\chi \,. \tag{3.2.24}$$

It can be easily checked that this symmetry is not anomalous under the axicolor group while presenting a QCD anomaly and, as a consequence, it constitutes a valid PQ symmetry.
Upon chiral symmetry breaking the condensates $\langle\overline{\psi}\psi\rangle = \langle\overline{\chi}\chi\rangle \neq 0$ would form, breaking spontaneously the chiral symmetries,

$$[U(1)]^4 \longrightarrow U(1)_{V,\psi} \times U(1)_{V,\chi} \,, \tag{3.2.25}$$

and giving rise to two Goldstone bosons associated with the two abelian axial symmetries. Nonetheless, analogously to the missing meson problem, one combination of the axial transformations is anomalous under the axicolor group and therefore is not a good symmetry to start with. Consequently the meson with the quantum numbers of that current, is analogous to the η' in the axicolor sector, is not light but has a mass of the order of the confinement scale, as all the rest of the hadrons $m_{\eta'_a} \sim \Lambda_a$. On the other hand, the current in Eq. (3.2.24) is only broken by the QCD anomalies and therefore can be seen as an approximate symmetry whose pGB is the composite axion.

In other words, this theory presents two instanton sources of explicit symmetry breaking: that of the axicolor group and that of QCD. Also, there are two dynamical "axions", one for each classically conserved axial current associated with each massless quark. Taking into account the SM quark sector and thus the SM η', three flavor-singlet pseudoscalars with anomalous couplings result for only two instanton sources of masses. As a consequence, one light axion results. The other two pseudoscalars are the SM η' and a very heavy axion with mass $\sim \Lambda_a$.

Once the PQ mechanism has been implemented, the low energy phenomenology of the invisible axion is recovered, so the composite axion also has the mass in Eq. (3.1.12) and the couplings in Eq. (3.1.8), similar to the original KSVZ, that is with no tree-level couplings to quarks and leptons. The axion scale is related to the confinement scale of the axicolor group $f_{\rm PQ} \sim \Lambda_a/4\pi$. Unfortunately, composite axion models typically have cosmological problems due to the existence of colored stable relics that cannot decay due to the exotic baryon number symmetry, hence the pre-inflationary PQ breaking scenario is usually the only viable possibility in composite axion models, see Section 3.3.

Other invisible axion models

The KSVZ, DFSZ and composite axions constitute the three paradigmatic axion models that are often used as benchmarks. The PQ mechanism, however, can be embedded in a variety of frameworks aiming to solve other problems of the SM. Examples of these attempts of linking several solutions of SM issues are the axion-majoron [212–218], the flaxion or axi-flavon [164,165], the axion in grand unification theories (GUTs) [219–221], the axion in supersymmetric theories [222] and also the model-independent axion arising in string theory [223, 224]. Furthermore, composite axion models have also been constructed aiming to solve one of the issues of invisible axion models: that of the PQ quality problem.

3.2.3 PQ quality problem

Quantum gravity (QG) has been argued to break all global symmetries. The usual argument involves black holes incorporating particles with a global charge and subsequently evaporating via Hawking radiation. Since no information of the global charge is accessible in the evaporation, this process would violate global symmetries [225–233]. These effects can be potentially dangerous for the PQ solution to the strong CP problem.

Invisible axion models typically involve axion scales of the order $f_a \sim 10^8 - 10^{12}$ GeV, which do not lie so far from the Planck scale. One possible way to parametrize the suggested PQ-violating QG effects is via non-renormalizable operators suppressed by powers of the Planck scale. For the KSVZ model, possible effective operators have been considered [225–228] of the following form

$$\mathcal{L}_{\not{P}\not{Q}} = \sum_{n=5} \frac{c_n}{M_{\rm Pl}^{n-4}} S^n + \text{h.c.}\,, \tag{3.2.26}$$

where S is the KSVZ complex scalar, although the same argument applies to KSVZ substituting $S \to \sigma$. The operator in Eq. (3.2.26) would generate a new contribution to the axion potential, that in general will present a relative phase δ with respect to the QCD induced potential.[7] Concentrating on the lowest dimensional (and most dangerous) term, i.e. n=5, the effective potential for the axion reads,

$$\begin{aligned} V(a) &= V_{\rm QCD} + V_{\rm QG}(a) = \\ &- m_\pi^2 f_\pi^2 \sqrt{1 - \frac{4 m_u m_d}{(m_u + m_d)^2} \sin^2\left(\frac{a}{2f_a} + \frac{\bar\theta}{2}\right)} + \frac{|c_5|\, f_a^5 N^5}{8\sqrt{2} M_{\rm Pl}} \cos\left(\frac{1}{N}\frac{a}{f_a} + \bar\theta + \delta\right)\,, \end{aligned} \tag{3.2.27}$$

which no longer has the minimum in the CP conserving point $\langle \frac{a}{f_a} + \bar\theta \rangle = 0$, but gets shifted instead. The displacement from the CP conserving minimum generates an effective $\bar\theta_{\rm eff}$,

$$|\bar\theta_{eff}| = \left\langle \frac{a}{f_a} + \bar\theta \right\rangle = |c_5 \sin(\delta)| \frac{f_a^3 N^4}{8\sqrt{2} m_a M_{\rm Pl}}\,. \tag{3.2.28}$$

For $\mathcal{O}(1)$ values of the coefficient c_5 and $f_a \sim 10^8 - 10^{12}$ GeV, the displacement from the CP conserving minimum spoils the solution to the strong CP problem since it leads to unacceptable values for the nEDM. In other words, assuming that the $d = 5$ operator in Eq. (3.2.26) is present, the nEDM constraint translates into a bound on the coefficient $c_5 \lesssim 10^{-\mathcal{O}(55)}$, representing a fine tuning worse than the strong CP problem itself.

There are several ways out of this problem. While it is commonly accepted that QG violates any global symmetry, it remains controversial whether its effects can be simply parametrized with non-renormalizable operators solely suppressed by powers of $M_{\rm Pl}$. Indeed, a recent study [234] computed the axion potential generated by a minimal coupling of the axion to gravity in a wormhole solution in the decoupling limit for the radial component of the singlet scalar. It was found that the effective operators are further suppressed by the exponential of the gravitational instanton action $\propto e^{-M_{\rm Pl}/f_a}$. These PQ-violating operators are safe from neutron EDM bounds as long as $f_a \lesssim 10^{16}$ GeV.

Other proposals rely on the imposition of gauge discrete symmetries that forbid the operators in Eq. (3.2.26) until a given dimension (from dimension 8 to dimension 11 depending on the axion scale) [235–237], that could arguably stem from spontaneous breaking of gauge symmetries in string theory frameworks [238].

[7] There is no reason for δ to vanish and the operator in Eq. (3.2.26) to be aligned with the θ-parameter of the SM.

Furthermore, these type of operators could be avoided in theories where the PQ symmetry is not imposed on the Lagrangian but rather arises accidentally, due to the gauge symmetries and matter content of the theory [2,227,239–245]. These kinds of solutions are particularly appealing since they provide a rationale for the existence of the symmetry, and allow one to protect against any new physics that could violate the PQ symmetry. In Chapter 6, a minimal composite axion model is built in which the PQ symmetry arises automatically, and it is inherently protected from possibly dangerous QG operators until dimension 9.

Finally, another way of making these operators unimportant is to lower the axion scale f_a. In usual invisible axion models, the axion scale cannot be smaller than $f_a \lesssim 10^8$ GeV due to stellar bounds. However, heavy axion models have been proposed in which the axion is too heavy to be produced in the nuclear stellar medium, and thus its scale can be lowered without being in conflict with those observations.

3.2.4 Domain wall problem

Another important issue is that of the cosmological impact of domain walls (DWs). The non-perturbative axion potential generated by QCD instantons in Eq. (3.1.16) breaks explicitly the PQ symmetry. But this breaking is not complete and there is a residual discrete symmetry due to the periodicity of the potential,

$$S(m) : a \longrightarrow a + \frac{2\pi m}{N} f_{\rm PQ}, \qquad m \in \mathbb{Z}\,. \tag{3.2.29}$$

As a consequence, $U(1)_{\rm PQ} \to \mathbb{Z}_N$ and there exist N distinct degenerate CP conserving minima. In the Early Universe, after the QCD transition this discrete symmetry is spontaneously broken. This means that in different patches of the Universe the axion field falls in different minima. In the boundary that separates two patches that fell in different vacua, the axion field interpolates between the values of the two minima generating a region with non-zero energy density called domain wall. The number of physically distinct minima is called the domain wall number, $N_{\rm DW} = 1$. Although it typically coincides with the color anomaly factor N, for some models this is not the case due to the fact that some of the N minima are connected by gauge transformations and thus are physically equivalent, see for example the model in Chapter 6.

If the number of domain walls is larger that one, $N_{\rm DW} > 1$, the energy density stored in domain walls can soon dominate over that of radiation and matter and lead to an overclosure of the Universe [246, 246–248]. This constitutes the domain wall problem. There are several ways to solve it. First, if the PQ transition occurs before inflation (and it is never restored) our current observable Universe corresponds to a single patch of constant initial misalignment angle, and therefore it will fall to a single minimum with no DW. Another option would be to have models with $N_{\rm DW} = 1$ where there is only one physical vacuum. Finally, DWs could be made unstable by introducing PQ breaking terms, such as those in Eq. (3.2.26) that break the degeneracy and lift some of the minima. In this scenario, after some time the DW would decay before dominating the energy density of the Universe, generating a new production mechanism for axion DM.

3.2.5 Heavy axions

Axions are typically light particles. Indeed, the invisible axion mass formula in Eq. (3.1.12) is a robust prediction of QCD axion models in which QCD instantons are the only source of PQ symmetry breaking, as it is typically required by the strong CP solution.

Nonetheless, the existence of new confining groups or new sources of PQ breaking instantons in a given theory can generate new contributions to the axion mass. The challenge in this case is for the new contributions to be aligned with QCD, in order not to spoil the solution to the strong CP problem.

One possibility to achieve such alignment is to consider the existence of a mirror world that is related with the SM via a $\mathbb{Z}_2$ symmetry [170, 171, 174, 176]. This discrete symmetry is softly broken, so that the mirror Higgs gets a larger vev $\sim 10^{14}$ GeV. Consequently, the mirror quarks get integrated out of the spectrum and thus the mirror QCD runs faster than QCD and confines at a larger scale $\Lambda'_{\rm QCD} \gg \Lambda_{\rm QCD}$. The $\mathbb{Z}_2$ symmetry ensures that the two θ-parameters coincide and therefore a single axion suffices to solve the strong CP problem. But this axion receives mass contributions from the two sectors,

$$m_a^2 f_a^2 \simeq f_\pi^2 m_\pi^2 \frac{m_u m_d}{(m_u + m_d)^2} + \Lambda'^4_{\rm QCD} \,. \tag{3.2.30}$$

Although this framework allows one to raise the axion mass, it requires a large tuning in the scalar potential to achieve such hierarchy between the scales. An alternative to doubling the full SM matter content with a $\mathbb{Z}_2$ symmetry is that of unification. Indeed, unification of the confining sector can be used to naturally identify the θ's of the two sectors and obtain a large axion mass like in Eq. (3.2.30) and solve the strong CP problem [4, 172, 173, 177, 178].

In other recent proposals [4, 179, 180], the QCD gauge group actually corresponds to the diagonal subgroup of the product of two (or more) $SU(3)$ gauge groups, that are spontaneously broken to QCD $SU(3) \times SU(3) \to SU(3)_c$. In these theories, the constrained instantons at the scale of the spontaneous breaking, see Section 2.2.5, that are also called small-size instantons (SSI) constitute a new source of PQ breaking that raises the axion mass [249, 250]. In Chapter 5, we develop the first heavy axion model in which the strong CP problem is solved with color unification and massless quarks.

For heavy axion models $m_a \gtrsim$ GeV, stellar constraints can be avoided (the axion is not kinematically accessible) so the axion scale can be lowered down, and thus the PQ solution is more protected from possibly dangerous QG operators, see Section 3.2.3. Due to the low axion scale, the axion is no longer stable in cosmological timescales and therefore it cannot explain the Dark Matter relic density of the Universe. Heavy axion models, however, typically predict the existence of other stable states that can be good dark matter candidates, e.g. [251].

To sum up, there has been much recent activity in building heavy axion models that show that the PQ mechanism can be implemented without necessarily implying the existence of a light axion in low-energy spectrum. As a consequence, the axion parameter space opens up,

and regions that were classically attributed to ALPs now get populated by axion models that do solve the strong CP problem.

3.3 Axion dark matter

Even if the axion arises as a natural consequence of the PQ solution to the strong CP problem, it constitutes an excellent candidate to solve another pressing problem of the SM: the Dark Matter problem.

QCD axions are naturally stable, weakly interacting and light particles that could be non-thermally produced in the Early Universe and account for the observed DM relic density. The scale at which inflation occurs with respect to the PQ breaking scale strongly impacts the amount of axionic DM that is produced.

In the pre-inflationary scenario, the only axion dark matter production mechanism is the so-called misalignment mechanism. If the PQ transition happens before inflation and it is never restored during reheating, the axion field is constant over the observable Universe, $a(x) = \theta_i f_a$, where θ_i is the initial misalignment angle. This is a consequence of inflation having stretched a small patch of the Universe with constant axionic field to constitute our current observable Universe. Around the QCD epoch, the axion potential is generated and drives the axion field from its initial misalignment towards the CP-conserving minimum. While for low temperatures, the axion potential can be reliably obtained by using chiral Lagrangians, see Eq. (3.1.16), for temperatures close to Λ_{QCD} the perturbative methods fail and the axion potential cannot be accurately computed [183]. Let us assume a cosine-like potential as one would expect from a dilute instanton gas approximation to capture the qualitative behavior,

$$V(a,T) = m_a^2(T) f_a^2 \left(1 - \cos\left(\frac{a}{f_a}\right)\right). \tag{3.3.1}$$

The evolution for the axion field in an expanding Friedman-Robertson-Walker (FRW) Universe can be expressed as[8]

$$\ddot{a} + 3H\dot{a} + m_a^2(T) f_a \sin\left(\frac{a}{f_a}\right) = 0 \tag{3.3.2}$$

where H is the Hubble expansion rate. As the Universe cools down the axion potential becomes more important and the Hubble rate decreases. When the two last terms in Eq. (3.3.2) become comparable, the axion field starts oscillating around the minimum with frequancy m_a. This so-called misalignment mechanism [252–254] produces a coherent state of non-relativistic axions, a Bose-Einstein condensate [255], that behaves as CDM at longer time scales than the period of the oscillations.
The relic axion abundance Ω_a that is generated due to the misalignment mechanism can be

[8] Here it is assumed the axion field is homogeneous, i.e. does not depend on the position, otherwise gradient terms would appear in Eq. (3.3.2).

expressed as a function of the axion decay constant f_a, and the initial misalignment angle $\theta_i = a_i/f_a$. For $|\theta_i| \ll \pi$ it reads [256]

$$\Omega_a\, h^2 = 0.35 \left(\frac{\theta_i}{0.001}\right)^2 \left(\frac{f_a}{3\times 10^{17}\text{GeV}}\right)^{1.17}, \tag{3.3.3}$$

where h is the present Hubble parameter. If axions were to explain the total relic dark matter density, $\Omega_{\text{DM}}\, h^2 \simeq 0.12$ [21], the f_a value required for an initial misalignment angle in the range $\theta_i \in (0.1, 3)$ is

$$f_a \simeq 2\times 10^{10} - 5\times 10^{12}\,\text{GeV}\,. \tag{3.3.4}$$

In the post-inflationary scenario, along with the axion misalignment there exist new production mechanisms such as the decay of topological defects, i.e. strings and domain walls, see Section 3.2.4. On the one hand, if the PQ transition takes place after inflation, the observable Universe is divided in patches with different values of the axion field. As a consequence the initial misalignment angle is no longer a free variable since its statistical average can be computed, $\langle\theta_i^2\rangle = \pi^2/3$, allowing one to estimate the axionic relic density generated by the misalignment mechanism. The situation is much more difficult regarding the decay of topological defects into axions. The string and domain wall network evolution presents highly complex dynamics that need to be tackled with simulations. Although this network was known to approach a scaling solution [257], which allows for extrapolations of the simulations, it has been recently shown [258] that there exist logarithmic violations of the scaling properties of such solutions. As a consequence, the amount of DM axions produced by the decay of strings still remains an open issue. However, since the prediction of the axion relic density in the post-inflationary scenario due to misalignment only depends on the axion scale, by imposing not to overproduce axion DM an upper bound on the axion scale, $f_a \lesssim 4.5\times 10^{11}$ GeV, follows.

3.4 Experimental searches of axions and ALPs

The main motivation for the search of light pseudoscalars with derivative and anomalous couplings is the axion solution to the strong CP problem. That is why the experimental effort for the search pGB has been mainly driven by the invisible axion models. These models are characterized by the tight relation between the axion mass and scale, see Eq. (3.1.12), and not only the mass but also all the axion couplings are inversely proportional to the axion scale. As a consequence, modulo some $\mathcal{O}(1)$ model-dependent coefficients, all the couplings of the axion to the SM are fixed by the axion scale for the paradigmatic invisible axion models, see Eqs. (3.2.18) and (3.2.22). Since all the relevant observables depend on a single parameter, the constraints on invisible axion models can be shown in a unidimensional exclusion plot that spans over several orders of magnitude for f_a, see Fig. 3.2. These constraints arise mostly from the axion couplings to photons, nucleons and electrons and include astrophysical, cosmological and laboratory-based probes. This section does not intend to be an exhaustive review on the experimental searches, for this purpose see [19, 184].

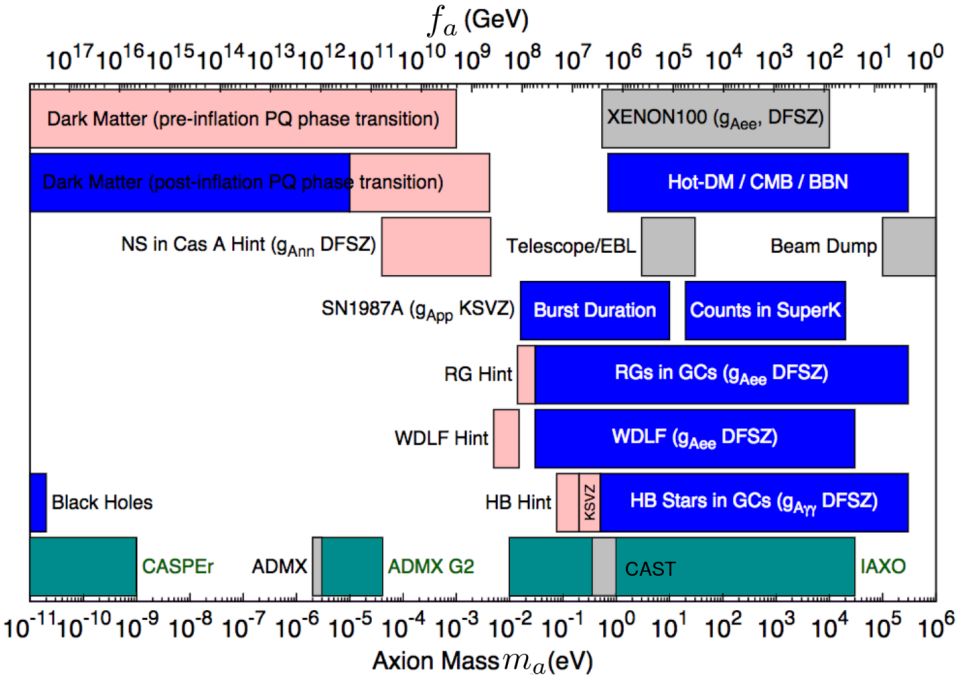

Figure 3.2: Bounds on the axion decay constant and the axion mass. The limits on the axion couplings are translated into limits on f_a and m_a assuming the KSVZ with $E/N = 0$ unless stated otherwise. For DFSZ it has been assumed $x = v_d/v_u = 1$. Prospects of future experiments are indicated in the lower part of the plot. Figure adapted from [19, 259].

Regarding the axion-nucleon interaction, see Eq. (3.1.22), one of the most important bounds comes from the duration of the neutrino burst of the supernova SN1987a [260,261]. The existence of axions coupled to nucleons represents an efficient energy loss mechanism for supernovas, which in the absence of axions, release most of their energy emitting neutrinos. Consequently axions shorten the duration of the neutrino burst. In KSVZ models, the axion-nucleon interactions stem from the $aG\tilde{G}$ coupling and thus the supernova bound automatically translates into a constraint on f_a, whereas in DFSZ models the coupling to nucleons also depends on the quark charges, see Eq. (3.1.22). Despite its constraining power, the supernova bound contains many uncertainties due to the computation of the energy loss [260]. Indeed, a recent work reassessing it has relaxed the SN bound [262] and even some other works [263] are casting doubts on the applicability of such bound.

The axion-photon coupling also has an impact on astrophysical phenomena due to energy losses, and especially relevant is the lifetime of globular clusters in the Horizontal Branch (HB) [264,265]. Moreover, the photon-axion interaction not only allows one to indirectly constrain the axion due to energy losses but also allows one to construct experiments aiming at detecting the axion directly. Those include haloscopes aiming at detecting DM axions via resonant cavities, such as ADMX; helioscopes searching for solar axions, such as CAST [266, 267] or the future experiment IAXO [268, 269], or light shining through wall experiments (LSW) that aim at both

producing and detecting the axion in the laboratory, such as ALPS I [270] and future ALPS II [271]. All these experiments are based on the so-called *Primakoff effect*: in the presence of an external magnetic field, the axion coupling to photons in Eq. (3.1.1) generates axion-photon conversion [272, 273].

The coupling to electrons can also be constrained with astrophysical sources, such as white dwarfs (WD) and red giants (RG), see Fig. 3.2. They set stringent bounds since the axion coupling to electrons leads to an efficient axion production in the stellar nuclear medium: the ABC processes (Axiorecombination, Bremsstrahlung and Compton) [274].

While the energy loss of stars due to axion emission allows to constraint its couplings, it should be noted that there are a number of stellar cooling hints that show some preference for non-zero axion couplings (e.g. that coming from WD cooling prefers at the 3σ level a non-zero electron coupling) [275].

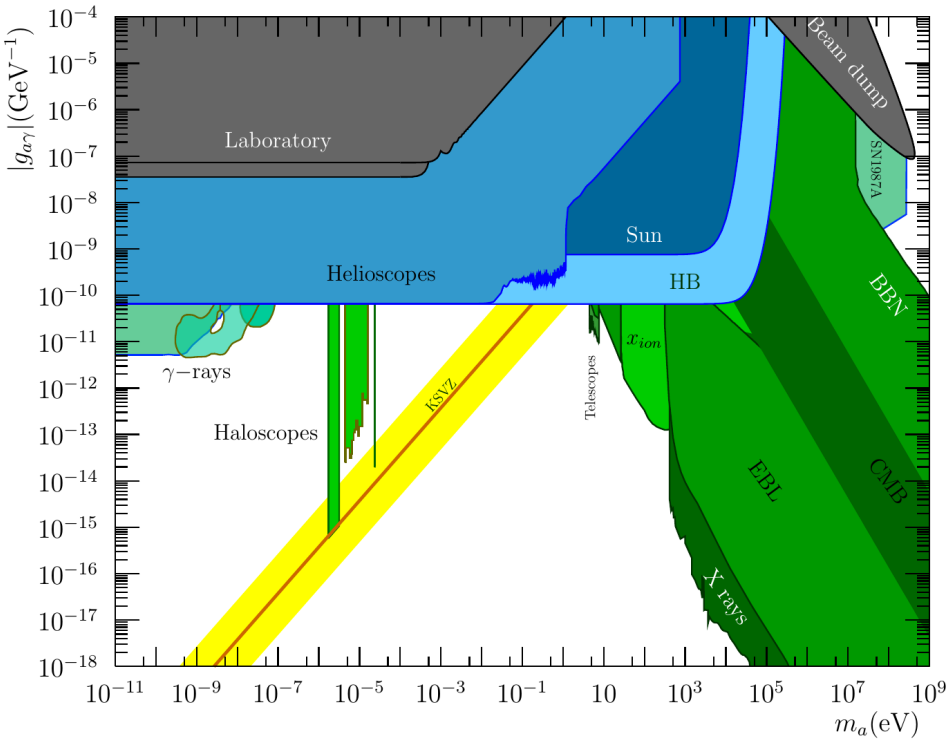

Figure 3.3: Constraints on the axion coupling to photons as a function of the axion mass. In addition to the bounds that are explained in the text, cosmological bounds are also included in green. Figure adapted from [184].

While it is useful to show the invisible axion bounds in the unidimensional plot in Fig. 3.2, it should be noted that it involves several assumptions with respect to the relation between the axion couplings and scale. In particular, for KSVZ models it has been assumed $E/N = 0$ and for DFSZ $x = v_d/v_u = 1$. In order to be model-independent it becomes pertinent to open up the

parameter space and consider the previous constraints in the full $\{m_a, f_a\}$ plane, see Fig. 3.3, where the benchmark KSVZ and DFSZ invisible axion models correspond to the yellow band. However, as we already commented in Section 3.2.2, there are invisible models in which the axion couplings can significantly depart from those values due to cancellations [166, 167, 169]. Moreover in the context of ALPs and heavy axions it becomes pertinent to explore the full parameter space and even consider other ALP couplings that have received less attention such as couplings to the EW gauge bosons, as will be studied in Chapter 7.

In the context of ALPs, but also relevant for heavy axion models, flavor experiments provide valuable constraints. Indeed, the astonishing precision in flavor observables allow one to set stringent bounds on tree-level flavor-violating ALP couplings. Besides, even flavor-conserving ALP couplings are strongly constrained due to ALP mixing with pseudoscalar mesons and loop-induced ALP couplings, which inherit the SM flavor structure. These types of bounds will be analyzed in detail in Chapter 8, where the full ALP electroweak bosonic basis is constructed and the flavor bounds are studied.

The experimental effort in axion and ALP searches in a large range of masses is accelerating with future projects such as Madmax, CASPEr, QUAX, HeXenia, FUNK and electric dipole moment searches (PSI and Co) [276–280]. In the context of flavor, for instance, NA62 [281] is taking data, and new fixed target facilities (e.g. SHIP [282]) are in preparation, with sensitivity to MeV-GeVs ALPs. These experiments present strong complementary potential to tackle ALP couplings to gauge bosons and fermions, as we will study in Chapter 8. Belle-II [283] will also have some sensitivity to this mass range, as well as the LHC with Mathusla, Faser and CodexB [284–286]. Indeed, ALPs may well show up first at colliders [287, 288]. Intense work on ALP signals at the LHC and future colliders is underway [289, 290], and the synergy between collider and low-energy fixed target experiments is increasingly explored [291].

Part II

New dynamics in axions and flavor

CHAPTER

4 Gauged Lepton Flavor

In this Chapter, which is based on the publication in Ref. [5], we explore the posibility of the leptonic flavor symmetry to be gauged and the leptonic Yukawa couplings to become dynamical fields. The vevs of these dynamical Yukawa fields vevs generate the leptonic fermion masses and mixings.

Minimal flavor violation [59, 292], introduced in Section 1.3.3, is a bottom-up approach that describes a class of models that are not afflicted by the new physics flavor problem. Based on the SM global flavor symmetry group, this framework assumes that at low-energies the Yukawa couplings are the only source of flavor in the SM and in whatever the BSM theory of flavor is. Yukawa couplings break the symmetry, and they are then treated as spurions of the flavor group, weighting the possible BSM effective operators so as to make them invariant under the flavor group. As a consequence, MFV predicts the relative rates of flavor changing transitions, and furthermore new effects at or close to the TeV scale are allowed. The MFV ansatz is neither the only flavor ansatz compatible with data nor a theory of flavor, though. There have been attempts to go from the effective approach —where the Yukawas are treated as spurions— to a more fundamental level where the Yukawas are dynamical "flavon" fields, acquiring a non-trivial vacuum expectation value. The potentials for the corresponding scalar fields have been discussed for several possible flavor representations, with interesting consequences [70, 293–302]. Although a dynamical justification for all fermion masses and mixings is still lacking, the potential minima lead, for instance, to no mixing at leading order in the quark sector (in contrast to the lepton sector discussed further below) when each Yukawa coupling is associated with a single flavon, a very encouraging first step.

Nevertheless, unless the continuous symmetry in Eq. (1.3.1) is substituted by a convenient discrete subgroup, a generic consequence of breaking spontaneoulsy the SM global flavor group is unobserved goldstone bosons. Would instead the symmetry be gauged, the goldstone bosons would become the longitudinal degrees of freedom of massive vector bosons. This exploratory effort was launched for the quark sector in Ref. [7] and continued in Refs. [303–308]. In Ref. [7] it was shown that the consistency of the gauge theory via anomaly cancellation conditions requires the addition of fermions with drastic implications for phenomenology.

The masses of the extra fermionic content of those gauged-flavor models are inversely proportional to the masses of the light SM fermions (as it was introduced in Ref. [309]), with the consequence that flavor-changing neutral currents (FCNC) are highly suppressed for light generations and new exotic gauge bosons could be as light as the electroweak scale. This theory, with gauge symmetry at its core, offers a different take on the number of generations; the fields must belong to irreducible representations of the flavor group and thus the number of generations is linked to it, precisely the same sense in which there are three colors in QCD. Although the starting motivation was the phenomenologically successful MFV ansatz, the mechanism for protection against the flavor problem in the gauged-flavor model does not conform to the MFV hypothesis; yet it is still very effective.

Here, the gauging of the lepton flavor group is considered. In contrast to the quark case [7], the unknown nature of neutrino masses opens several possibilities for constructing a consistent model with the lepton flavor symmetry gauged, as evidenced by the various definitions of MFV in the lepton sector [78, 310–313]. The guiding principle followed here will be to consider phenomenologically viable setups with:

- Maximal flavor symmetry group of the Lagrangian for massless SM fermions
- Minimal extension of the spectrum

In a first case, the SM leptonic flavor group is gauged, that is

$$U(3)_\ell \times U(3)_E \,, \tag{4.0.1}$$

see Eq. (1.3.1). The cancellation of gauge anomalies of this pure SM case along the guidelines above will be shown to lead to the introduction of SM fermion singlets and thus to Majorana neutrinos as a very natural consequence.

Secondly, if instead one assumes from the beginning the existence of three right-handed neutrino fields $\mathcal{N}_R$, two symmetry avenues are possible:

- Assuming Dirac neutrinos, the flavor group would be $U(3)_\ell \times U(3)_E \times U(3)_N$, the subscript N referring to the right-handed neutrinos [307].
- Assuming instead Majorana neutrinos, the maximal flavor group is $U(3)_\ell \times U(3)_E \times O(3)_N$, leading naturally to a type I Seesaw [31–34] scenario with degenerate heavy neutrinos.

This last option has been shown [298, 299, 301, 302] to allow a minimum of its scalar potential with one maximal PMNS angle and Majorana phase (and a second angle generically large), at leading order and for minimal flavon content. In contrast, the $U(3)^3$ case tends to disfavor large mixings, consistent with observations in the quark sector but in disagreement with the observed leptonic mixing. The guiding principles chosen above also favor the second option in that the extra field content needed is smaller, and therefore leads to more predictive models: this scenario

will be thus analyzed in detail. Interestingly, both cases –that is with and without right-handed neutrinos– will lead to Majorana masses for the active neutrinos, so that at low energies the Lagrangian responsible for masses and mixings will be, for definiteness:

$$\mathscr{L}_Y = -\bar{\ell}_L \, \Phi \, Y_E \, e_R - \frac{1}{2} \bar{\ell}_L \, \widetilde{\Phi} \frac{C_\nu}{\Lambda_{LN}} \widetilde{\Phi}^T \ell_L^c + h.c. \, , \tag{4.0.2}$$

which corresponds to the usual Yukawa term for charged leptons and the Weinberg operator for light neutrino masses, as introduced in Eq. (1.2.13) and ommitting the flavor indices. The generalized Seesaw pattern obtained below, together with the lightness of the electron as compared to the τ and μ leptons, implies that the least broken subgroups of the flavor symmetry are expected to reside in the $\mu-\tau$ sector. The corresponding approximate symmetries, the spectrum of new particles and the dominant experimental signals will be determined and discussed in the following sections. Furthermore, the differences between the effective low-energy couplings of the gauged-flavor theory and the leptonic MFV ansatz will also be discussed.

The analysis will be restricted to the non-abelian sector of the global flavor symmetry, as the focus is set on flavor-changing effects; some phenomenological differences which result when gauging in addition the two non-anomalous abelian symmetries will be pointed out, though.

4.1 Gauged Lepton Flavor Standard Model: $SU(3)_\ell \times SU(3)_E$

It will be shown in this section how the gauging of the pure SM leptonic flavor group favours a Seesaw pattern and Majorana neutrino masses, and that the leading phenomenological signals are lepton universality violation (LUV), with deviations from the SM predictions which are particularly prominent in the τ sector.

The leptonic global flavor symmetry to be gauged is that exhibited by the SM in the absence of Yukawa couplings, which is that of the kinetic terms,

$$\mathscr{L}_{leptons} = i\bar{\ell}_L \not{D} \ell_L \, + \, i\bar{e}_R \not{D} e_R \, . \tag{4.1.1}$$

Anomaly cancellation of the non-abelian $SU(3)_\ell \times SU(3)_E$ symmetry is accomplished by the addition to the Lagrangian of three extra fermion species, denoted here by $\mathcal{E}_R$, $\mathcal{E}_L$, and $\mathcal{N}_R$. Their quantum numbers are shown in Table 4.1, together with those for the SM fields.

In addition, for all fermion bi-linears invariant under the SM gauge symmetry but not under the flavor symmetry, a scalar is introduced to restore flavor invariance. Only two such scalar *flavon* fields are needed, denoted by $\mathcal{Y}_E$ and $\mathcal{Y}_N$ in Table 4.1, belonging respectively to the bi-fundamental representation of $SU(3)_\ell \times SU(3)_E$ and to the conjugate-symmetric representation of $SU(3)_\ell$. The vevs of these fields are related to the Yukawa matrices but should not be directly identified with them, as functions of the flavon fields may have the same transformation properties under flavor than $\mathcal{Y}_{E,N}$, and they also allow to build flavor invariant Lagrangian terms;[1] this is a property essential to the phenomenological success of the construction. Finally,

[1] For instance $(\mathcal{Y}_E^{-1})^\dagger$ and $\mathcal{Y}_E$ belong to the same flavor representation.

	$SU(2)_L$	$U(1)_Y$	$SU(3)_\ell$	$SU(3)_E$
$\ell_L \equiv (\nu_L\,, e_L)$	2	$-1/2$	3	1
e_R	1	-1	1	3
$\mathcal{E}_R$	1	-1	3	1
$\mathcal{E}_L$	1	-1	1	3
$\mathcal{N}_R$	1	0	3	1
$\mathcal{Y}_E$	1	0	$\bar{3}$	3
$\mathcal{Y}_N$	1	0	$\bar{6}$	1

Table 4.1: Transformation properties of SM fields, of (flavor) mirror fields and of flavons under the EW group and $SU(3)_\ell \times SU(3)_E$.

other scalars charged under the SM gauge group are not considered since they would not respect the condition of minimality of the spectrum, in addition to potentially disrupting the electroweak symmetry breaking (EWSB) mechanism.

Within this framework, the most general renormalizable Lagrangian with $SU(3)_\ell \times SU(3)_E$ gauge symmetry therefore reads:

$$\begin{aligned}\mathscr{L} =& i\sum_\psi \bar{\psi}\not{D}\psi - \frac{1}{2}\sum_I \mathrm{Tr}\left(F^I_{\mu\nu}F_I^{\mu\nu}\right) + \sum_B \mathrm{Tr}\left(D_\mu \mathcal{Y}_B D^\mu \mathcal{Y}_B^\dagger\right) + D_\mu\Phi^\dagger D^\mu\Phi + \\ &+ \mathscr{L}_Y - V(\Phi, \mathcal{Y}_E\,, \mathcal{Y}_N)\,,\end{aligned} \tag{4.1.2}$$

where ψ runs over all lepton species in Table 4.1, $I = \ell, E$ and B identifies flavon indices $B = E, N$. The gauge bosons of $SU(3)_\ell$ and $SU(3)_E$ will be encoded in traceless hermitian matrices in flavor space, A^ℓ_μ with $A^\ell_{\mu,\alpha\beta} = (A^\ell_{\mu,\beta\alpha})^*\,, \Sigma_\alpha A^\ell_{\mu,\alpha\alpha} = 0$, and A^E_μ with $A^E_{\mu,\alpha\beta} = (A^E_{\mu,\beta\alpha})^*\,, \Sigma_\alpha A^E_{\mu,\alpha\alpha} = 0$, which can be alternatively decomposed in terms of generators

$$A^\ell_\mu \equiv \sum_{a=1}^{8} A^{\ell,a}_\mu\, T^a\,, \qquad\qquad A^E_\mu \equiv \sum_{a=1}^{8} A^{E,a}_\mu\, T^a\,, \tag{4.1.3}$$

where T^a are the flavor group generators, with $\mathrm{Tr}(T^aT^b) = \delta^{ab}/2$ and $T^a \equiv \lambda^a_{SU(3)}/2$, and $\lambda^a_{SU(3)}$ denote the Gell-Mann matrices. The gauge couplings of A^ℓ_μ and A^E_μ will be denoted by g_ℓ and g_E, respectively. In Eq. (4.1.2) the field strengths include those for the SM fields and flavor gauge bosons, as do the covariant derivatives, e.g.

$$D_\mu \ell_L = \left(\partial_\mu - i\frac{g'}{2}B_\mu + i\frac{g}{2}\sigma_I W^I_\mu + i g_\ell A^\ell_\mu\right)\ell_L\,, \tag{4.1.4}$$

while

$$\begin{aligned} D_\mu \mathcal{Y}_E &= \partial_\mu \mathcal{Y}_E + i g_E\, A^E_\mu\, \mathcal{Y}_E - i g_\ell\, \mathcal{Y}_E\, A^\ell_\mu\,, \\ D_\mu \mathcal{Y}_N &= \partial_\mu \mathcal{Y}_N - i g_\ell\, (A^\ell_\mu)^T\, \mathcal{Y}_N - i g_\ell\, \mathcal{Y}_N\, A^\ell_\mu\,. \end{aligned} \tag{4.1.5}$$

The Yukawa and mass terms can be written as follows:

$$\begin{aligned}\mathscr{L}_Y = &\lambda_E\, \overline{\ell}_L\, \Phi\, \mathcal{E}_R + \mu_E\, \overline{\mathcal{E}}_L\, e_R + \lambda_{\mathcal{E}}\, \overline{\mathcal{E}}_L\, \mathcal{Y}_E\, \mathcal{E}_R + \text{h.c.} \\ &+ \lambda_\nu\, \overline{\ell}_L\, \tilde{\Phi}\, \mathcal{N}_R + \frac{\lambda_N}{2}\, \overline{\mathcal{N}_R^{\,c}}\, \mathcal{Y}_N\, \mathcal{N}_R + \text{h.c.}\,,\end{aligned} \tag{4.1.6}$$

where ℓ_L, e_R, $\mathcal{E}_L$, $\mathcal{E}_R$ and $\mathcal{N}_R$ are vectors in flavor space. λ_E, $\lambda_{\mathcal{E}}$, λ_ν, λ_N and μ_E are each a single complex parameter, since these couplings must be proportional to the identity to preserve flavor invariance; moreover they can be made real and positive via chiral fermion transformations. In contrast, $\mathcal{Y}_E$ and $\mathcal{Y}_N$ are matrices in flavor space and their nontrivial background values are the only sources of flavor (including CP violation). Notice that μ_E is not the mass of any of the particles in the spectrum, but simply a mass parameter of the Lagrangian. The vev of $\mathcal{Y}_N$ is simultaneously the LN scale and the flavor scale; in the limit $\mathcal{Y}_N = 0$ in which only (diagonal) Dirac mass terms remain, the Lagrangian would acquire a $U(1)_e \times U(1)_\mu \times U(1)_\tau$ symmetry which prevents the appearance of leptonic mixing angles, a setup phenomenologically not viable. For this reason the introduction of $\mathcal{Y}_N$ is necessary and therefore Majorana neutrino masses follow as a natural consequence of gauging flavor in the lepton sector, even when taking as starting point only the SM gauge symmetry.

The above Lagrangian has two accidental $U(1)$ symmetries which are anomaly free under the flavor gauge group. The first is an extension of LN symmetry, under which all fermions transform with the same charge while $\mathcal{Y}_N$ transforms with minus twice that charge. The second accidental symmetry is the abelian $U(1)_E$ acting on right-handed charged leptons, that completes $SU(3)_E$ to a unitary group, and under which e_R, $\mathcal{E}_L$ and $\mathcal{Y}_E$ transform non-trivially. Both $U(1)$'s would be spontaneously broken by the scalar vevs. However, in all generality, the scalar potential contains terms such as $\det(\mathcal{Y}_E)$ and $\det(\mathcal{Y}_N)$ [299], that break explicitly these $U(1)$'s and prevent the appearance of phenomenologically dangerous Goldstone bosons.

In order to yield masses for all fermions, $\mathscr{L}_Y$ in Eq. (4.1.6) must undergo both EWSB and flavor symmetry breaking, so that in the unitary gauge

$$\begin{aligned}\Phi &\equiv (v + h)/\sqrt{2}\,, \\ \mathcal{Y}_E &\equiv \langle \mathcal{Y}_E \rangle + \phi_E/\sqrt{2}\,, \\ \mathcal{Y}_N &\equiv \langle \mathcal{Y}_N \rangle + \phi_N/\sqrt{2}\,,\end{aligned} \tag{4.1.7}$$

where h denotes the physical Higgs particle and ϕ_E and ϕ_N the physical scalar excitations over the flavon vevs $\langle \mathcal{Y}_E \rangle \neq 0$, $\langle \mathcal{Y}_N \rangle \neq 0$ (for simplicity, the Yukawa flavons and their vevs will be denoted with the same symbols in the next sections). The ensuing spectrum contains 6 Dirac electromagnetically charged fermions and 6 Majorana neutral fermions. There are no extra scalars charged under the SM gauge group and EWSB proceeds thus as usual. The dynamics of flavor breaking is encoded in the scalar potential, which has been studied in Refs. [299, 301, 302]. The study of the potential is involved due to the complex flavor structure that it aims to explain, but some general results and approximately conserved symmetries where found in Refs [299, 301, 302]. In particular, a connection between degenerate spectra with large angles and maximal Majorana phases was found for the neutrino sector.

4.1.1 Spectrum

Fermions

The Lagrangian in Eq. (4.1.6) results in leptonic mass matrices for charged and neutral leptons of the form

$$\begin{pmatrix} 0 & \lambda_E v/\sqrt{2} \\ \mu_E & \lambda_{\mathcal{E}}\mathcal{Y}_E \end{pmatrix} + \text{h.c.}\,, \qquad \frac{1}{2}\begin{pmatrix} 0 & \lambda_\nu v/\sqrt{2} \\ \lambda_\nu v/\sqrt{2} & \lambda_N\mathcal{Y}_N \end{pmatrix} + \text{h.c.}\,, \tag{4.1.8}$$

respectively, which suggest immediately a Seesaw-like pattern for both sectors. No additional fermions beyond those in the SM have been detected at experiments and this fact sets strong bounds on the mass of the mirror fermions $\mathcal{E}$ and $\mathcal{N}$ introduced for the sake of flavor anomaly cancellation. This indicates that the mass term for the extra charged leptons, $\lambda_{\mathcal{E}}\mathcal{Y}_E$, should be larger than the other scales of the theory: $\mathcal{Y}_E \gg \mu_E\,, v$, –assuming all dimensionless parameters to be $\mathcal{O}(1)$. This is analogous to the condition for neutrinos $\mathcal{Y}_N \gg v$ in the *canonical* type I Seesaw model on the right-hand side of Eq. (4.1.8), which leads to a mass scale of order $\sim 10^{12}$ GeV for the extra neutral fermions. With these approximations, the Lagrangian in Eq. (4.1.6) yields a Dirac mass for the heavy charged leptons $\mathcal{E}$ and a Majorana mass for the right-handed singlets,

$$\mathcal{M}_{\mathcal{E}} = \lambda_{\mathcal{E}}\mathcal{Y}_E\left(1+\mathcal{O}\left(\frac{v^2}{\mathcal{Y}_E^2}\,,\frac{\mu_E^2}{\mathcal{Y}_E^2}\right)\right)\,, \qquad \mathcal{M}_N = \lambda_N\mathcal{Y}_N\left(1+\mathcal{O}\left(\frac{v^2}{\mathcal{Y}_N^2}\right)\right)\,, \tag{4.1.9}$$

where $\mathcal{M}_{\mathcal{E}}$ and $\mathcal{M}_N$ denote the heavy lepton mass matrices while the mass matrices for the light states obey (see Eq. (4.0.2))

$$\begin{aligned} Y_E &= \frac{m_\ell}{v/\sqrt{2}} = \frac{\lambda_E}{\lambda_{\mathcal{E}}}\left(\frac{\mu_E}{\mathcal{Y}_E}\right)\left(1+\mathcal{O}\left(\frac{v^2}{\mathcal{Y}_E^2}\,,\frac{\mu_E^2}{\mathcal{Y}_E^2}\right)\right)\,, \\ \frac{C_\nu}{\Lambda_{LN}} &= \frac{m_\nu}{v^2/2} = \lambda_\nu\left(\frac{1}{\lambda_N\mathcal{Y}_N}\right)\lambda_\nu\left(1+\mathcal{O}\left(\frac{v^2}{\mathcal{Y}_N^2}\right)\right)\,, \end{aligned} \tag{4.1.10}$$

illustrating that the mirror fermions are proportional to the flavon vevs while SM fermion masses are inversely proportional to them. It follows that

$$m_\ell\mathcal{M}_{\mathcal{E}} \approx \lambda_E\mu_E v/\sqrt{2}\,, \qquad m_\nu\mathcal{M}_N \approx \lambda_\nu^2 v^2/2\,. \tag{4.1.11}$$

The masses of the SM leptons are thus shown to be related to those of the heaviest extra leptons by an inverse proportionality law: a Seesaw mechanism is present both for charged and neutral leptons, similar to the case of quarks in Ref. [7].

All flavor structure being encoded in $\mathcal{Y}_E$ and $\mathcal{Y}_N$, their eigenvalues determine the hierarchy of lepton masses up to common factors:

$$M_{\mathcal{E}} \equiv \left(M_{\hat{e}}\,, M_{\hat{\mu}}\,, M_{\hat{\tau}}\right) \simeq \lambda_E\mu_E\left(3.5\cdot 10^5,\, 1.7\cdot 10^3,\, 10^2\right)\,, \tag{4.1.12}$$

$$M_N \equiv (M_1\,, M_2\,, M_3\,) < |\lambda_\nu|^2\,\frac{v}{\sqrt{2}}\left(\infty,\, 2\cdot 10^{13},\, 3.5\cdot 10^{12}\right)\,, \tag{4.1.13}$$

where $M_{\mathcal{E}}$ (M_N) denotes the diagonal matrix of eigenvalues of the $\mathcal{M}_{\mathcal{E}}$ ($\mathcal{M}_N$) matrix and the hat refers to the individual charged mirror fermions masses.[2]

Figure 4.1: Diagrammatic representation of the generation of SM charged lepton Yukawa couplings (right figure) induced by the exchange of heavy mirror charged leptons (left figure).

The expressions for the SM lepton masses can be also derived diagrammatically by integrating out the heavy states as shown in Fig. 4.1 for charged leptons. It illustrates that all light flavor structure stems from the mass matrix of mirror leptons given by $\mathcal{Y}_E$, as the equivalent of the usual Yukawa couplings, λ_E and $\lambda_{\mathcal{E}}$, as well as μ_E, are overall constants. This resembles the MFV scenario of Ref. [313] that, however, leads to different phenomenology, see Sec. 4.3.

From now on, we will work on a basis in which the charged lepton mass matrix $\mathcal{Y}_E$ is diagonal, and thus $\mathcal{M}_{\mathcal{E}} = M_{\mathcal{E}}$. For later use, it is convenient to explicitly invert the relations in Eq. (4.1.10) to extract the expressions for the flavon vevs,

$$\mathcal{Y}_E = \frac{\lambda_E\,\mu_E}{\sqrt{2}\,\lambda_{\mathcal{E}}}\,\text{diag}\left(\frac{v}{m_e}\,,\frac{v}{m_\mu}\,,\frac{v}{m_\tau}\right)\,,\qquad \mathcal{Y}_N = \frac{\lambda_\nu^2\,v}{2\,\lambda_N}\,U^*\,\text{diag}\left(\frac{v}{m_{\nu_1}}\,,\frac{v}{m_{\nu_2}}\,,\frac{v}{m_{\nu_3}}\right)\,U^\dagger\,, \tag{4.1.14}$$

where U is the PMNS leptonic mixing matrix. Notice that the choice of basis is allowed by the flavor symmetry without loss of generality. The flavon vevs are thus determined by low energy flavor data up to an overall constant.

The spectrum of mirror fermions is illustrated as horizontal lines on the left-hand side of Fig. 4.2 for natural values of the parameters. As anticipated, due to the inverse dependence of mirror lepton masses with respect to their light counterparts the lightest exotic fermion is the τ mirror lepton. The μ mirror lepton appears next, a factor $\sim m_\tau/m_\mu$ higher. The mirror e appears yet a factor m_μ/m_e above. Much higher in mass by a factor $\sim m_e/m_\nu$, the mirror neutrinos 3, 2 and 1 appear (in this illustration normal ordering was assumed for the light neutrinos).

[2]The unknown absolute neutrino mass scale translates in an inequality in contrast with the case of charged leptons, and a bound on M_1 cannot be derived since one neutrino could be massless.

Flavored gauge bosons

Flavor symmetry breaking produces masses for the sixteen flavor gauge bosons encoded in A^{ℓ}_{μ} and A^{E}_{μ}. The relevant part of the Lagrangian, including only terms at most quadratic in the gauge fields, is given by

$$\begin{aligned}\sum_{I=\ell,E} \mathrm{Tr}\left(A^{I}_{\mu}\partial^{2}A^{I,\mu}\right) + \mathrm{Tr}\left\{\left(g_{E}A^{E}_{\mu}\mathcal{Y}_{E} - g_{\ell}\mathcal{Y}_{E}A^{\ell}_{\mu}\right)\left(g_{E}\mathcal{Y}^{\dagger}_{E}A^{E,\mu} - g_{\ell}A^{\ell,\mu}\mathcal{Y}^{\dagger}_{E}\right)\right\} + \\ + g^{2}_{\ell}\mathrm{Tr}\left\{\left(A^{\ell *}_{\mu}\mathcal{Y}_{N} + \mathcal{Y}_{N}A^{\ell}_{\mu}\right)\left(\mathcal{Y}^{\dagger}_{N}\left(A^{\ell,\mu}\right)^{T} + A^{\ell,\mu}\mathcal{Y}^{\dagger}_{N}\right)\right\} - \sum_{I} g_{I}\mathrm{Tr}(A^{I}_{\mu}J^{\mu}_{A^{I}})\,,\end{aligned} \tag{4.1.15}$$

where the currents are hermitian matrices in flavor space:

$$\begin{aligned}\left[J^{\mu}_{A^{\ell}}\right]_{ij} &= \bar{\ell}^{j}_{L}\gamma^{\mu}\ell^{i}_{L} + \overline{\mathcal{E}}^{j}_{R}\gamma^{\mu}\mathcal{E}^{i}_{R} + \overline{\mathcal{N}^{j}_{R}}\gamma^{\mu}\mathcal{N}^{i}_{R}\,,\\ \left[J^{\mu}_{A^{E}}\right]_{ij} &= \bar{e}^{j}_{R}\gamma^{\mu}e^{i}_{R} + \overline{\mathcal{E}}^{j}_{L}\gamma^{\mu}\mathcal{E}^{i}_{L}\,,\end{aligned} \tag{4.1.16}$$

where i, j are flavor indices. The linear equations of motion (EOMs) in matrix form stemming from Eq. (4.1.15) reads

$$\begin{aligned}\partial^{2}A^{\ell}_{\mu} - g_{E}g_{\ell}\mathcal{Y}^{\dagger}_{E}A^{E}_{\mu}\mathcal{Y}_{E} + \frac{g^{2}_{\ell}}{2}\left\{\mathcal{Y}^{\dagger}_{E}\mathcal{Y}_{E} + \mathcal{Y}^{\dagger}_{N}\mathcal{Y}_{N} + \mathcal{Y}^{*}_{N}\mathcal{Y}^{T}_{N},\, A^{\ell}_{\mu}\right\} + \\ + 2g^{2}_{\ell}\mathcal{Y}^{\dagger}_{N}A^{\ell *}_{\mu}\mathcal{Y}_{N} - \frac{g_{\ell}}{2}J^{A^{\ell}}_{\mu} = \frac{1}{n_{g}}\mathrm{Tr}\,(\text{L.H.S.})\,\mathbb{1}\,,\end{aligned} \tag{4.1.17}$$

$$\partial^{2}A^{E}_{\mu} - g_{E}g_{\ell}\mathcal{Y}_{E}A^{\ell}_{\mu}\mathcal{Y}^{\dagger}_{E} + \frac{g^{2}_{E}}{2}\left\{\mathcal{Y}_{E}\mathcal{Y}^{\dagger}_{E},\, A^{E}_{\mu}\right\} - \frac{g_{E}}{2}J^{A^{E}}_{\mu} = \frac{1}{n_{g}}\mathrm{Tr}\,(\text{L.H.S.})\,\mathbb{1}\,, \tag{4.1.18}$$

where $\{\dots\,,\dots\}$ denotes the anti-commutator, $n_{g} = 3$ and L.H.S. stands for left hand side.[3] These equations can be alternatively written as an inhomogeneous linear system for the sixteen gauge fields when the latter are described as an array of sixteen χ^{a}_{μ} fields,

$$\chi_{\mu} \equiv (A^{\ell,1}_{\mu}, \dots, A^{\ell,8}_{\mu}, A^{E,1}_{\mu}, \dots, A^{E,8}_{\mu})\,, \tag{4.1.19}$$

which allows to rewrite the Lagrangian in Eq. (4.1.15) as

$$\mathcal{L}_{gauge} = -\frac{1}{2}\sum_{I=\ell,E}\mathrm{Tr}\left(F^{I}_{\mu\nu}F^{\mu\nu}_{I}\right) + \frac{1}{2}\sum_{a,b=1}^{16}\chi^{a}_{\mu}\left(M^{2}_{A}\right)_{ab}\chi^{b,\mu} - \sum_{I=\ell,E} g_{I}\mathrm{Tr}\left(A^{I}_{\mu}J^{\mu}_{A_{I}}\right)\,, \tag{4.1.20}$$

where the mass matrix M_{A} can be expressed as

$$M^{2}_{A} = \begin{pmatrix} M^{2}_{\ell\ell} & M^{2}_{\ell E} \\ M^{2}_{E\ell} & M^{2}_{EE}\end{pmatrix}\,, \tag{4.1.21}$$

[3] Eq. (4.1.18) displays explicitly the covariant properties of the gauge bosons and the trace removes the singlet component of each term, leaving only the adjoint combination to which the gauge bosons belong.

with

$$\begin{aligned}\left(M^2_{\ell\ell}\right)_{ij} &= g_\ell^2 \Big\{ \mathrm{Tr}\left(\mathcal{Y}_E \left\{T_i, T_j\right\} \mathcal{Y}_E^\dagger\right) + \mathrm{Tr}\left(\mathcal{Y}_N \left\{T_i, T_j\right\} \mathcal{Y}_N^\dagger\right) + \\ &\quad + \mathrm{Tr}\left(\mathcal{Y}_N^\dagger \left\{T_i^T, T_j^T\right\} \mathcal{Y}_N\right) + 2\mathrm{Tr}\left(\mathcal{Y}_N^\dagger T_i^T \mathcal{Y}_N T_j + \mathcal{Y}_N^\dagger T_j^T \mathcal{Y}_N T_i\right) \Big\} , \\ \left(M^2_{\ell E}\right)_{ij} &= \left(M^2_{E\ell}\right)_{ji} = -2 g_\ell g_E \mathrm{Tr}\left(T_i \mathcal{Y}_E^\dagger T_j \mathcal{Y}_E\right) , \\ \left(M^2_{EE}\right)_{ij} &= g_E^2 \mathrm{Tr}\left(\mathcal{Y}_E^\dagger \left\{T_i, T_j\right\} \mathcal{Y}_E\right) ,\end{aligned} \tag{4.1.22}$$

where $i, j = \{1, \ldots, 8\}$, and the linear EOM can be now written in the customary form,

$$(\partial^2 + M_A^2)\chi^\mu = J_A^\mu , \qquad \text{where} \qquad J_\mu^A \equiv (J_{A^\ell}^{\mu,1}, \ldots, J_{A^\ell}^{\mu,8}, J_{A^E}^{\mu,1}, \ldots, J_{A^E}^{\mu,8}) . \tag{4.1.23}$$

Eq. (4.1.22) shows that gauge boson masses are proportional to the scalar fields $\mathcal{Y}_E$ and $\mathcal{Y}_N$ whose structure is in turn given by, and inversely proportional to, light fermion masses and mixings, see Eq. (4.1.14). The spectrum of sixteen mass states is thus determined up to two overall constants, that can be identified with the products $g_E\|\mathcal{Y}_E\|$, $g_\ell\|\mathcal{Y}_N\|$.[4] The hierarchy $\mathcal{Y}_N \gg \mathcal{Y}_E$ that followed from assuming order one dimensionless coefficients and μ_E around the EW scale, implies that:

- The heaviest gauge bosons to good approximation are those of the $SU(3)_\ell$ group, A_μ^ℓ, while the lightest gauge bosons will be those corresponding to the $SU(3)_E$ group, A_μ^E.
- In this regime the mixing between A_μ^E and A_μ^ℓ is small. We will refer to A_μ^E (A_μ^ℓ) as the lightest (heaviest) states.

The spectrum of flavor gauge bosons is shown in Fig. 4.2 next to that for mirror fermions, for natural values of the parameters. Boxes represent flavor gauge bosons and the colored entries in a given box indicate the lepton flavors to which that gauge boson couples. The blue-colored boxes in the upper panel correspond to the A_μ^ℓ gauge bosons, while the red-colored boxes correspond to the A_μ^E gauge bosons; as expected the former are heavier by a factor $\sim m_e/m_\nu$ due to the inverse dependence of their masses with the light neutrino mass.

Lightest gauge bosons

The A_μ^E fields will thus dominate the phenomenology mediated by flavor gauge bosons. Because their mass matrix is to a good approximation proportional to the charged lepton flavon vev $\mathcal{Y}_E$, while the charged lepton mass matrix is instead inversely proportional to it, the hierarchies in

[4] The modulus of a matrix B is defined as $\|B\|^2 \equiv \mathrm{Tr}\left(B^\dagger B\right)$, implying that $\|\mathcal{Y}_E\|$ and $\|\mathcal{Y}_N\|$ are flavor invariant constructions.

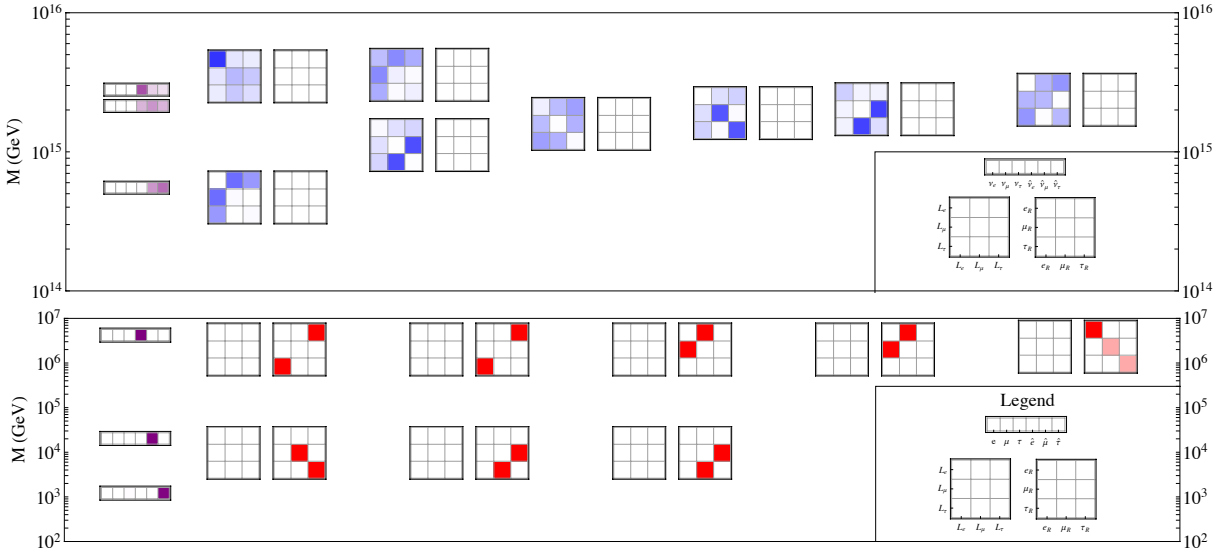

Figure 4.2: Gauge and fermion heavy spectrum for the gauged SM lepton flavor. Boxes composed out of 3×3 squares depict the gauge boson mass eigenstates and rows of squares depict mirror fermions. For the first, the squares are ordered according to the e, μ and τ flavor, from left to right and from top to bottom. The boxes in the upper panel correspond dominantly to the $SU(3)_\ell$ symmetry, with the gauge bosons shown in blue, while the lower panel shows in red the $SU(3)_E$ gauge bosons. In both cases the intensity of the colored cells represents the strength of the coupling between the gauge boson and each lepton bilinear. As for the fermions, the intensity of the cells represents, from left to right, the component of e, μ, τ, $\hat{e}$, $\hat{\mu}$ and $\hat{\tau}$ for the lower panel, and of ν_e, ν_μ, ν_τ, $\nu_{\hat{e}}$, $\nu_{\hat{\mu}}$, and $\nu_{\hat{\tau}}$ in the upper panel. Normal ordering was assumed for neutrinos and the parameter values used are $\theta_{23} = 45°$, $\theta_{12} = 33°$, $\theta_{13} = 8.8°$, Dirac CP phase $\delta = 2\pi/3$, Majorana phases $\alpha_1 = \alpha_2 = 0$, lightest neutrino mass $m_{\nu_1} = 10^{-11}$ GeV; all flavor gauge coupling constants and all λ's are set to 0.1, with $\mu_E = 15$ GeV.

charged lepton masses translate into hierarchies in the gauge boson spectrum: the lightest A^E_μ gauge bosons will be those mediating transitions which involve the heaviest right-handed charged leptons and in particular the τ_R lepton. In fact, because of the zero trace of the generators, at least two different leptons must participate in any coupling, and the overall conclusion is that the lightest flavor gauge bosons will produce deviations in both μ_R and τ_R sectors.

Technically, the A^E_μ mass eigenstates are largely aligned with the $SU(3)$ generators except for the diagonal components given by

$$\hat{T}_3 \equiv (\sqrt{3}T_8 - T_3)/2 = \frac{1}{2}\begin{pmatrix} 0 & 0 & 0 \\ 0 & 1 & 0 \\ 0 & 0 & -1 \end{pmatrix}, \qquad \hat{T}_8 \equiv (\sqrt{3}T_3 + T_8)/2 = \frac{1}{2\sqrt{3}}\begin{pmatrix} 2 & 0 & 0 \\ 0 & -1 & 0 \\ 0 & 0 & -1 \end{pmatrix}. \tag{4.1.24}$$

It follows from Eq. (4.1.22) that their respective masses are given by

$$M^2_{A^{E,a}_\mu} \simeq 2g_E^2 \frac{\left\|\hat{T}_a m_\ell^{-1}\right\|^2}{\left\|\mathcal{Y}_E^{-1}\right\|^2} \sum_{\alpha=e,\mu,\tau} m_\alpha^2, \tag{4.1.25}$$

where $\hat{T}^a = T^a$ for all $a \neq 3, 8$, m_ℓ is the mass matrix of the charged leptons and greek indices stand from now on for charged lepton flavors. The fact that the size of $\mathcal{Y}_E$ ($\mathcal{Y}_E^{-1}$) is dominated by the electron (tau) mass,

$$\|\mathcal{Y}_E\|^2 = \frac{\lambda_E^2 \mu_E^2}{2\lambda_\mathcal{E}^2} \frac{v^2}{m_e^2} \left(1 + \frac{m_e^2}{m_\mu^2} + \frac{m_e^2}{m_\tau^2}\right), \qquad \left\|\mathcal{Y}_E^{-1}\right\|^2 = \frac{2\lambda_\mathcal{E}^2}{\lambda_E^2 \mu_E^2} \frac{m_\tau^2}{v^2} \left(1 + \frac{m_\mu^2}{m_\tau^2} + \frac{m_e^2}{m_\tau^2}\right), \tag{4.1.26}$$

makes all gauge bosons with a right-handed electron entry a factor m_μ/m_e heavier than the rest. Indeed, because $m_e \ll m_\mu, m_\tau$, this can be seen as an approximate $SU(2)$ symmetry in the $\mu-\tau$ sector when $\mathcal{Y}_E$ is taken to be diag$(1/y_e, 0, 0)$, which is the reason why the diagonal generators $\hat{T}_8$, $\hat{T}_3$ are better suited to describe mass states than T_8, T_3. Moreover, under the $U(1)_e \times U(1)_\mu \times U(1)_\tau$ approximate symmetry present for $\mathcal{Y}_N \gg \mathcal{Y}_E$, the off-diagonal gauge bosons transform as $A^E_{\alpha\beta} \to e^{i\theta_\alpha - i\theta_\beta} A^E_{\alpha\beta}$, which requires that both components of each off-diagonal entry have the same mass (so as to combine into a complex gauge boson): this approximate symmetry will suppress charged lepton flavor violation.

In summary, the three A^E_μ gauge bosons corresponding to the approximate $SU(2)$ symmetry in the $\mu-\tau$ sector are found to be the lightest (first layer of the lower panel in Fig. 4.2); a factor m_μ/m_e higher the remaining five $SU(3)_E$ gauge bosons appear (second layer in that figure). In turn, the leading phenomenological signals consists of flavor-conserving leptonic observables and, furthermore, low energy processes mediated by A^E_μ for the lighter leptons are suppressed by heavier mass scales, providing a flavor protection mechanism, as previously described for quarks in Ref. [7].

As for the relative mass of mirror fermions versus flavor gauge bosons, the lightest particle turns out to be the mirror tau lepton $\hat{\tau}$, see Fig. (4.2). Indeed, the lightest gauge boson mass $\sim \left(g_E/\left\|\mathcal{Y}_E^{-1}\right\|\right)(m_\tau/m_\mu)$ is a factor $\sim m_\tau/m_\mu$ larger than the lightest mirror fermion mass $\sim \lambda_\mathcal{E}/\left\|\mathcal{Y}_E^{-1}\right\|$, due to the tracelessness of the generators implying a non-vanishing $\mu\mu$ or $\mu\tau$ entry in the three lightest gauge boson interactions. In contrast, were the full $U(3)_E$ group gauged an associated lighter $(A^E_\mu)_{\tau\tau}$ gauge boson would appear in the spectrum.

Scalars

Flavor symmetry breaking gives rise to $18\,(\mathcal{Y}_E) + 12\,(\mathcal{Y}_N) - 16\,(SU(3)^2) = 14$ physical scalar bosons, corresponding to fluctuations around the 6 mixing parameters, 6 masses and $U(1)_\ell$ and $U(1)_E$ phases. This part of the spectrum will in general contribute to the same observables than

flavor gauge bosons, although without disrupting the flavor structure [7]. The detailed scalar mass spectrum depends however on the scalar potential parameters, as opposed to the gauge bosons and fermions, and it will not be discussed further in this work.

4.1.2 Interactions

The distinction between fermionic mass and interaction eigenstates will be relevant: therefore, for the rest of this section flavor eigenstates will be denoted with a prime[5] and described by

$$\begin{gathered}\begin{pmatrix} e'_L \\ \mathcal{E}'_L \end{pmatrix} = \begin{pmatrix} c_\Theta & s_\Theta \\ -s_{\Theta^\dagger} & c_{\Theta^\dagger} \end{pmatrix} \begin{pmatrix} e_L \\ \mathcal{E}_L \end{pmatrix}, \quad \begin{pmatrix} e'_R \\ \mathcal{E}'_R \end{pmatrix} = \begin{pmatrix} c_{\Theta_R^\dagger} & -s_{\Theta_R^\dagger} \\ -s_{\Theta_R} & -c_{\Theta_R} \end{pmatrix} \begin{pmatrix} e_R \\ \mathcal{E}_R \end{pmatrix}, \\ \begin{pmatrix} \nu_L^{c\prime} \\ \mathcal{N}'_R \end{pmatrix} = \begin{pmatrix} c_{\Theta_\nu^\dagger} & i\, s_{\Theta_\nu^\dagger} \\ -s_{\Theta_\nu} & i\, c_{\Theta_\nu} \end{pmatrix} \begin{pmatrix} \nu_L^c \\ \mathcal{N}_R \end{pmatrix},\end{gathered} \tag{4.1.27}$$

where unprimed fields are here mass eigenstates and the mixing angles are encoded in 3×3 matrices in flavor space Θ, $c_\Theta = (-1)^n/(2n)!(\Theta\Theta^\dagger)^n$, $s_\Theta = (-1)^n\Theta/(2n+1)!(\Theta^\dagger\Theta)^n$ [314]. These unitary rotations diagonalize the mass terms stemming from Eq. (4.1.6) (see also Eqs. (4.1.9) and Eqs. (4.1.10)):

$$\begin{aligned} &- \begin{pmatrix} c_\Theta & -s_\Theta \\ s_{\Theta^\dagger} & c_{\Theta^\dagger} \end{pmatrix} \begin{pmatrix} 0 & \lambda_E v/\sqrt{2} \\ \mu_E & \lambda_\mathcal{E}\mathcal{Y}_E \end{pmatrix} \begin{pmatrix} c_{\Theta_R^\dagger} & -s_{\Theta_R^\dagger} \\ -s_{\Theta_R} & -c_{\Theta_R} \end{pmatrix} = \begin{pmatrix} m_\ell & 0 \\ 0 & M_\mathcal{E} \end{pmatrix}, \\ &- \begin{pmatrix} c_{\Theta_\nu^\dagger} & -s_{\Theta_\nu} \\ i\, s_{\Theta_\nu^\dagger} & i\, c_{\Theta_\nu} \end{pmatrix} \begin{pmatrix} 0 & \lambda_\nu v/\sqrt{2} \\ \lambda_\nu v/\sqrt{2} & \lambda_N\mathcal{Y}_N \end{pmatrix} \begin{pmatrix} c_{\Theta_\nu^\dagger} & i\, s_{\Theta_\nu^\dagger} \\ -s_{\Theta_\nu} & i\, c_{\Theta_\nu} \end{pmatrix} = \begin{pmatrix} m_\nu & 0 \\ 0 & \mathcal{M}_N \end{pmatrix}, \end{aligned} \tag{4.1.28}$$

where $\Theta_\nu^T = \Theta_\nu$ has been used. Although these equations can be solved exactly, as done in Ref. [7] for the quark case, the absence of a large Yukawa like that of the top quark seems to indicate that an expansion in $v/\mathcal{Y}$ is valid. In particular in the charged lepton sector, given Eq. (4.1.14), the mixing terms are diagonal in flavor space ($\Theta_{\alpha\beta} = \delta_{\alpha\beta}\,\Theta_{\alpha\alpha}$ and analogously for Θ_R) :

$$\begin{aligned} \Theta &= \frac{\lambda_E v}{\sqrt{2}\lambda_\mathcal{E}\mathcal{Y}_E} + \mathcal{O}\left(\frac{v^3}{\mathcal{Y}_E^3}\right) \simeq \frac{\lambda_E v}{\sqrt{2}M_{\hat{\tau}}}\frac{m_\ell}{m_\tau}, \\ \Theta_R &= \frac{\mu_E}{\lambda_\mathcal{E}\mathcal{Y}_E} + \mathcal{O}\left(\frac{\mu_E^3}{\mathcal{Y}_E^3}\right) \simeq \frac{m_\ell^2}{m_\tau M_{\hat{\tau}}}\frac{1}{\Theta} = \frac{\mu_E}{M_{\hat{\tau}}}\frac{m_\ell}{m_\tau}, \\ \Theta_\nu &= \frac{\lambda_\nu v}{\sqrt{2}\lambda_N\mathcal{Y}_N} + \mathcal{O}\left(\frac{v^3}{\mathcal{Y}_N^3}\right) \simeq \frac{\lambda_\nu v}{\sqrt{2}\mathcal{M}_N}. \end{aligned} \tag{4.1.29}$$

[5] For instance, all fermions in Table 1 will be considered as primed fields for the sake of this section.

In the case of $\mathcal{O}(1)$ dimensionless parameters considered here, the heavy $\mathcal{N}_R$ neutrino scale suppresses the mixing Θ_ν which turns out to be $\mathcal{O}(10^{-10})$; all the effects associated to Θ_ν will thus be neglected in what follows.

After rotating to the mass basis, the fermion interaction Lagrangian is not diagonal, and in particular heavy-light couplings arise. It can be written as a sum of three terms:

$$\mathscr{L}_{\psi-int} = \mathscr{L}_{\bar\psi\psi A^{SM}} + \mathscr{L}_{\bar\psi\psi A^{FL}} + \mathscr{L}_{\bar\psi\psi\phi}\,. \tag{4.1.30}$$

The couplings to the SM gauge bosons can be casted in the conventional form,

$$\mathscr{L}_{\bar\psi\psi A^{SM}} = -eA_\mu J^\mu_A - \frac{g}{2c_W} Z_\mu J^\mu_Z - \left(\frac{g}{\sqrt{2}} W^+_\mu J^{-\mu}_W + \text{h.c.}\right)\,, \tag{4.1.31}$$

with modified currents defined as

$$\begin{aligned}
J^\mu_\gamma &= -\,\bar e\gamma^\mu e - \bar{\mathcal{E}}\gamma^\mu\mathcal{E}\,,\\
J^{-\mu}_W &= \bar\nu_L\, U^\dagger\gamma^\mu\,(c_\Theta e_L + s_\Theta \mathcal{E}_L)\,,\\
J^\mu_Z &= \bar e\gamma^\mu\left(-(c_{2W} - s_\Theta s_{\Theta^\dagger})P_L + 2s^2_W P_R\right) e - \overline{\mathcal{E}}\gamma^\mu\left(s_{\Theta^\dagger}s_\Theta P_L - 2s^2_W\right)\mathcal{E} +\\
&\quad + \bar\nu_L\gamma^\mu\nu_L - \left(\overline{\mathcal{E}}_L\gamma^\mu s_{\Theta^\dagger}c_\Theta e_L + \text{h.c.}\right)\,,
\end{aligned} \tag{4.1.32}$$

where c_W (c_{2W}) and s_W stand for the cosine and sine of (twice) the Weinberg angle, respectively, and $P_{L,R}$ are the chirality projectors. Notice that the right-handed mixing Θ_R does not appear in the gauge interactions, because the SM quantum numbers of $\mathcal{E}_R$ and e_R are the same. Most relevantly, as Θ is a diagonal matrix in flavor space as given in Eq. (4.1.29), the transitions mediated by SM electroweak gauge bosons differ in the charged τ, μ and e sectors, with relative amplitudes given by $m_\tau/m_\mu/m_e$.

The interactions with flavor gauge bosons can be written as

$$\mathscr{L}_{\bar\psi\psi A^{FL}} = -g_\ell \text{Tr}(A^\ell_\mu J^\mu_{A^\ell}) - g_E \text{Tr}(A^E_\mu J^\mu_{A^E})\,, \tag{4.1.33}$$

where the currents are given in Eq. (4.1.16). Notice that the difference between flavor and mass bases has been neglected in the previous expression, as that difference would only induce subleading effects in the observables of interest.

Finally, the couplings to the radial components of the scalar fields –that is, to the physical scalars– read, in the unitary gauge:

$$\begin{aligned}
\mathscr{L}_{\bar\psi\psi\phi} =& \frac{-1}{\sqrt{2}}\begin{pmatrix}\bar e_L & \overline{\mathcal{E}}_L\end{pmatrix}\begin{pmatrix}(\lambda_E c_\Theta\, h - \lambda_{\mathcal{E}} s_\Theta\,\phi_E)s_{\Theta_R} & (\lambda_E c_\Theta\, h - \lambda_{\mathcal{E}} s_\Theta\,\phi_E)c_{\Theta_R}\\ (\lambda_{\mathcal{E}} c_{\Theta^\dagger}\,\phi_E + \lambda_E s_{\Theta^\dagger}\, h)s_{\Theta_R} & (\lambda_{\mathcal{E}} c_{\Theta^\dagger}\,\phi_E + \lambda_E s_{\Theta^\dagger}\, h)c_{\Theta_R}\end{pmatrix}\begin{pmatrix} e_R\\ \mathcal{E}_R\end{pmatrix} +\\
&- \frac{\lambda_\nu}{\sqrt{2}}\, h\,\bar\nu_L\mathcal{N}_R - \frac{1}{2\sqrt{2}}\overline{\mathcal{N}_R^c}\,\phi_N\mathcal{N}_R + \text{h.c.}\,.
\end{aligned} \tag{4.1.34}$$

The purely bosonic interactions follow from the Lagrangian in Eq. (4.1.2) once the scalar potential is specified. The variables in this potential will determine the scalar mass spectrum

which we do not examine in this work. However the scalar couplings to fermions given above do enjoy the flavor suppression characteristic of this model and will not disturb the flavor structure, as previously stated. Scalar excitation effects will be neglected in the phenomenological analysis that follows.

4.1.3 Phenomenology

The exchange of mirror charged leptons and $SU(3)_E$ gauge bosons provides the dominant signals, as argued above, and it will be shown here that LUV signals are particularly prominent for τ-related observables, while no charged lepton flavor violation (cLFV) is induced due to the preserved $U(1)$ lepton number symmetry for each flavor: all modifications to SM couplings induced are flavor diagonal, as explained earlier. Flavor observables for the leading signals can be written in terms of only three independent parameters, which here are chosen to be

- The mixing parameter Θ.[6]
- The lightest mirror fermion mass $M_{\hat{\tau}}$.
- The norm $\left\|\mathcal{Y}_E^{-1}\right\|$, which is given approximately by its largest eigenvalue proportional to m_τ, see Eq. (4.1.26).

We determine next the bounds on these three parameters.

Bounds on the mixing parameters: The strongest bounds on Θ come from non-universality and non-unitarity of the PMNS matrix that follow from the (flavor diagonal) modifications of the couplings of leptons to Z and W bosons, Eq. (4.1.32). The decay rate of the Z boson to a pair of charged leptons (denoted by l in the following equation) is now given by:

$$\begin{aligned}\Gamma(Z\to l^-l^+) &= \frac{g^2 M_Z}{96\pi c_W^2}\left(c_{2W}^2+4s_W^4-2c_{2W}s_\Theta^2\right)+\mathcal{O}(\Theta^4)\\ &= \Gamma_{SM}\left(Z\to l^-l^+\right)\left(1-\frac{2c_{2W}}{c_{2W}^2+4s_W^4}\Theta_{ll}^2\right)+\mathcal{O}\left(\Theta^4\right),\end{aligned} \tag{4.1.35}$$

where the second line illustrates that the new contribution can only have a destructive interference with the SM one. The ratio of the branching ratios for the decay of Z into $\tau^+\tau^-$ and e^+e^- allows to extract explicitly the dependence on $\Theta_{\tau\tau}$,

$$\frac{\mathrm{Br}\left(Z\to\tau^+\tau^-\right)}{\mathrm{Br}\left(Z\to e^+e^-\right)}-1\simeq -2.14\Theta_{\tau\tau}^2\,. \tag{4.1.36}$$

[6] Given one mixing angle, the other two are obtained from it by scaling.

The experimental bound [315] on the observable on the left hand side of this expression leads to a strong limit on Θ:

$$\frac{\mathrm{Br}\left(Z \to \tau^+\tau^-\right)}{\mathrm{Br}\left(Z \to e^+e^-\right)} - 1 = 0.0019 \pm 0.0032 \quad \Longrightarrow \quad |\Theta_{\tau\tau}| = \frac{\lambda_E v}{\sqrt{2}M_{\hat{\tau}}} \leq 4.5 \times 10^{-2}\,, \tag{4.1.37}$$

where the bound has been rescaled to the 95% CL assuming a gaussian behaviour. In consequence, using Eq. (4.1.29),

$$|\Theta_{\mu\mu}| \leq 2.7 \times 10^{-3}\,, \qquad |\Theta_{ee}| \leq 1.3 \times 10^{-5}\,. \tag{4.1.38}$$

At this point it is pertinent to ask whether the persistent anomalies in the decay of B meson into K and K^* bosons [316, 317] could be induced by the modifications to Z-fermion couplings just discussed, as it is precisely these couplings which tend to diminish the decay rate into μ and τ leptons while the electronic channels are almost uncorrected; this could happen for instance via a Z-penguin loop attached to the quark legs and/or through the equivalent mechanisms when gauging flavor in the quark sector [7]. Nevertheless, the bounds just set on $\Theta_{\mu\mu}$ are too strong compared with the experimental anomaly which, if confirmed, would require $\mathcal{O}(1)$ corrections.

Similar bounds on Θ can be inferred from the analysis of non-unitary contributions to the diagonal elements of the PMNS matrix U, to which other observables contribute. The leptonic mixing matrix is now corrected by

$$\tilde{U} \equiv \cos\Theta U\,, \qquad (\tilde{U}\tilde{U}^\dagger)_{\alpha\beta} - \delta_{\alpha\beta} \simeq -\Theta^2_{\alpha\beta} = -\frac{\lambda_E^2 v^2}{2M_{\hat{\tau}}^2}\delta_{\alpha\beta}\frac{m_\alpha^2}{m_\tau^2}, \tag{4.1.39}$$

and in consequence the most stringent bound stems again from the $\tau\tau$ entry; bounds on the diagonal entries can be derived from a global fit to lepton universality and precision electroweak observables [318], yielding

$$|\Theta_{\tau\tau}| \leq 7.5 \times 10^{-2} \tag{4.1.40}$$

at 95% CL. An alternative bayesian global fit can be found in Ref. [319] resulting in $|\Theta_{\tau\tau}| \leq 7.6 \times 10^{-2}$.

Bounds on $M_{\hat{\tau}}$: The heavy-light fermion mixing is controlled by the Yukawa couplings, see Eq. (4.1.6), and in consequence the lightest fermion of the heavy spectrum —the mirror tau— will decay predominantly to channels involving longitudinal gauge bosons W_L and Z_L and the Higgs particle, provided $\hat{\tau}$ is heavy enough,

$$\Gamma(\hat{\tau} \to Z_L\tau) = \frac{\lambda_E^2 M_{\hat{\tau}}}{64\pi}\,, \qquad \Gamma(\hat{\tau} \to W_L\nu_\tau) = \frac{\lambda_E^2 M_{\hat{\tau}}}{32\pi}\,, \qquad \Gamma(\hat{\tau} \to h\tau) = \frac{\lambda_E^2 M_{\hat{\tau}}}{64\pi}\,. \tag{4.1.41}$$

The $\hat{\tau}$ fermion is electrically charged and it would thus be copiously pair-produced in e^+e^- colliders via photon exchange, if sufficiently light. The lack of evidence for new resonances and for charged heavy leptons in LEP data [320] sets a constraint

$$M_{\hat{\tau}} \gtrsim 100.8 \text{ GeV} \qquad \text{at} \quad 95\%\,\text{CL}, \tag{4.1.42}$$

a bound that does not depend on the mixing parameter Θ. The LHC can provide stronger constraints on the mass of the mirror taus. The most sensitive channel would involve pair production of $\hat{\tau}$ via neutral current or photon exchange and their subsequent decay to $\tau + Z$ with $\sim 25\%$ branching ratio. To the best of our knowledge such a search has not been performed yet. Related searches for SUSY chargino pair production and their decay to W plus missing energy (neutralino) currently constrain chargino masses to be above $\sim$ 620 GeV [321]. The decay of the $\hat{\tau}$ to $W + \nu$ would lead to a similar final state, although with somewhat different kinematics. Thus, similar constraints are expected to hold for the $\hat{\tau}$, however a dedicated search that directly applies to this scenario is still missing and needed.

Bounds on $\left\|\mathcal{Y}_E^{-1}\right\|$: Eq. (4.1.42) can be translated into a limit on the flavon vev, applying Eq. (4.1.9),

$$\left\|\mathcal{Y}_E^{-1}\right\| = \frac{\lambda_{\mathcal{E}}}{M_{\hat{\tau}}}\left(1 + \mathcal{O}(m_\mu^2/m_\tau^2)\right) < 0.01\,\lambda_{\mathcal{E}}\,\text{GeV}^{-1}\,, \qquad \text{at} \quad 95\%\,\text{CL}\,. \tag{4.1.43}$$

Moreover, bounds on $\left\|\mathcal{Y}_E^{-1}\right\|$ independent from $\lambda_{\mathcal{E}}$ can be extracted from the limits on four-lepton interactions induced by the exchange of $SU(3)_E$ gauge bosons among right-handed charged SM leptons. Integrating out those A_μ^E gauge bosons results in effective low-energy couplings of the form

$$-\frac{c_E^{\alpha\beta\kappa\rho}}{2}\left\|\mathcal{Y}_E^{-1}\right\|^2\left(\bar{e}_R^\alpha\gamma_\mu e_R^\beta\right)\left(\bar{e}_R^\kappa\gamma^\mu e_R^\rho\right)\,, \tag{4.1.44}$$

which do not exhibit a dependence on the coupling constant g_E. The coefficient c_E encodes a specific flavor-conserving suppression:

$$c_E^{\alpha\beta\kappa\rho} = \frac{m_\alpha^2 m_\kappa^2}{\sum_\gamma m_\gamma^2}\left[\delta_{\alpha\rho}\delta_{\beta\kappa}\,\frac{1}{m_\alpha^2 + m_\kappa^2} - \delta_{\alpha\beta}\delta_{\kappa\rho}\,\frac{1}{2\sum_\gamma m_\gamma^2}\right]\,, \tag{4.1.45}$$

where the last term would be absent if gauging the full $U(3)_E$. This expression is (tree-level) exact up to $\mathcal{Y}_E/\mathcal{Y}_N$ corrections as opposed to the approximate mass formula in Eq. (4.1.25). Considering specifically a process involving two electrons (denoted here by e_R^1) and two other generic charged leptons e_R^α, Eq. (4.1.44) becomes[7]

$$\left\|\mathcal{Y}_E^{-1}\right\|^2\frac{m_e^2}{m_\tau^2}(1+\delta_{\alpha 1})\left(\frac{2m_\tau^2 m_\alpha^2 - m_\alpha^2(m_e^2+m_\alpha^2)}{2(m_e^2+m_\alpha^2)m_\tau^2}\right)\left(\bar{e}_R^1\gamma^\mu e_R^1\right)\left(\bar{e}_R^\alpha\gamma^\mu e_R^\alpha\right)\,, \tag{4.1.46}$$

where $\sum m_\beta^2 \simeq m_\tau^2$ has been used. These operators are suppressed by an extra $\sim m_e^2/m_\tau^2$ factor with respect to the case where no flavor symmetry is implemented [322]. Equivalently, it can be argued that the effective scale associated to the new physics responsible for these processes can be m_τ/m_e smaller than in the case without flavor symmetry protection, in a pattern reminiscent

[7] In Eqs. (4.1.45) and (4.1.46) $m_1 = m_e$, $m_2 = m_\mu$ and $m_3 = m_\tau$.

of MFV as expected. The bounds stemming from LEP data [323] on four-fermion interactions involving two electrons can thus be translated into 95% CL constraints on $\left\|\mathcal{Y}_E^{-1}\right\|$:

$$\begin{aligned} e^+e^- \to e^+e^- \quad &\Longrightarrow \quad \left\|\mathcal{Y}_E^{-1}\right\| < 0.41(0.44)\ \text{GeV}^{-1}\,, \\ e^+e^- \to \mu^+\mu^- \quad &\Longrightarrow \quad \left\|\mathcal{Y}_E^{-1}\right\| < 0.37(0.30)\ \text{GeV}^{-1}\,, \\ e^+e^- \to \tau^+\tau^- \quad &\Longrightarrow \quad \left\|\mathcal{Y}_E^{-1}\right\| < 0.57(0.57)\ \text{GeV}^{-1}\,, \end{aligned} \tag{4.1.47}$$

where the first (second) value is for destructive (constructive) interference with the SM contributions. These constraints are weak but complementary to that in Eq. (4.1.43) since they are independent from $\lambda_{\mathcal{E}}$.

Stronger bounds on $\left\|\mathcal{Y}_E^{-1}\right\|$ can be inferred from present data on other flavor conserving processes such as magnetic moments, to which the flavor $SU(3)_E$ gauge bosons may contribute. Defining as is customary the muon anomalous magnetic moment, a_μ, as the coefficient of the muon dipole operator in the effective Lagrangian [324]

$$\mathscr{L}_{(g-2)_\mu} \equiv -\frac{a_\mu e}{4m_\mu}\bar{\mu}\,\sigma_{\rho\delta}\,\mu\,F^{\rho\delta} + \text{h.c.}\,, \tag{4.1.48}$$

it is easy to see that penguin diagrams mediated by the $SU(3)_E$ flavor gauge bosons induce a correction of the form

$$\delta a_\mu = -\frac{m_\mu^2}{12\pi^2}\sum \frac{g_E^2}{M_{A_a^E}^2}(\hat{T}^a\cdot\hat{T}^a)_{\mu\mu} \simeq -\frac{3}{4}\frac{m_\mu^4}{6\pi^2 m_\tau^2}\left\|\mathcal{Y}_E^{-1}\right\|^2\,, \tag{4.1.49}$$

where the Casimir factor of 3/4 results from the $SU(2)_{\mu-\tau}$ quasi-degeneracy among the lightest gauge bosons. Note that the sign of the contribution obtained is negative[8], as the SM one, and therefore it does not help to relax the tension between the SM prediction and the experimental determination, $\Delta a_\mu \equiv a_\mu^{Exp} - a_\mu^{SM} = 287(63)(49)\times 10^{-11}$ [315]. However, requiring that the flavor correction does not increase the present tension beyond 5σ, the following bound follows:

$$\left\|\mathcal{Y}_E^{-1}\right\| \leq 0.047\text{GeV}^{-1}\,, \qquad \text{or equivalently} \qquad \|\mathcal{Y}_E\| \geq 7.4\times 10^4\text{GeV}\,. \tag{4.1.50}$$

Note that, unlike for the other constraints discussed in this section, a 95% CL has not been adopted in this bound since the SM prediction itself already presents a stronger disagreement with current data.

It is interesting to translate the bounds on $\|\mathcal{Y}_E\|$ into a limit on the flavor gauge boson mass scale. Eq. (4.1.50) translates into a limit on the mass of the lightest gauge bosons $A^{E,3}$, $A^{E,6}$, $A^{E,7}$ given by

$$M_{A^{E,i}} \gtrsim 2.5\times 10^2\, g_E\,\text{GeV}\,, \tag{4.1.51}$$

[8]The sign of the contribution is negative because the lightest gauge bosons couple only to the right-handed leptons. For a detailed analysis of the role of the chirality of the couplings to leptons in the $g-2$ contributions see, *e.g.,* Ref. [325]

as a function of the gauge flavor coupling g_E. In the case of the illustrative benchmark spectrum considered in Fig. 4.2, the lightest flavor gauge bosons have masses of $\mathcal{O}(10)$ TeV, largely satisfying the bounds obtained in this section assuming a perturbative weak regime for the new gauge sectors.

4.2 Gauged Lepton Flavor Seesaw Model: $SU(3)_\ell \times SU(3)_E \times SO(3)_N$

In the context of the type I Seesaw theory with three degenerate right-handed neutrinos N_R, the maximal flavor symmetry group of the Lagrangian in the limit of vanishing masses for the three known fermion families is $U(3)_\ell \times U(3)_E \times O(3)_N$. The latter is the symmetry exhibited by the kinetic terms plus heavy degenerate right-handed neutrinos,

$$\mathcal{L} = i\bar{\ell}_L \not{D} \ell_L + i\bar{e}_R \not{D} e_R + i\overline{N}_R \not{\partial} N_R + \frac{1}{2}\{\mu_{LN} \overline{N_R^c} N_R + \text{h.c.}\}\,. \tag{4.2.1}$$

As earlier stated, we focus on flavor effects and restrain here to gauging the non-abelian factors $SU(3)_\ell \times SU(3)_E \times SO(3)_N$ only. The field content that needs to be added then in order to cancel gauge anomalies is identical to that in the previous model, since triangle diagrams cancel for $SO(3)_N$ and the N_R fermions are singlets under the SM gauge symmetry. The fermion spectrum is summarized in Tab. 4.2; note that the quantum numbers for $\mathcal{Y}_N$ differ from those in the previous section.

	$SU(2)_L$	$U(1)_Y$	$SU(3)_\ell$	$SU(3)_E$	$SO(3)_N$
$\ell_L \equiv (\nu_L\,, e_L)$	2	$-1/2$	3	1	1
e_R	1	-1	1	3	1
N_R	1	0	1	1	3
$\mathcal{E}_R$	1	-1	3	1	1
$\mathcal{E}_L$	1	-1	1	3	1
$\mathcal{N}_R$	1	0	3	1	1
$\mathcal{Y}_E$	1	0	$\bar{3}$	3	1
$\mathcal{Y}_N$	1	0	$\bar{3}$	1	3

Table 4.2: Transformation properties of SM fields, of (flavor) mirror fields and of flavons under the EW group and $SU(3)_\ell \times SU(3)_E \times SO(3)_N$.

Using again and until further notice unprimed fields to denote flavor eigenstates, the Lagrangian describing the model can be written as that in Eq. (4.1.2), where now $\mathscr{L}_Y$ encodes

both Yukawa interactions and Majorana mass terms,

$$\begin{aligned}\mathcal{L}_Y =& \lambda_E\, \overline{\ell}_L\, \Phi\, \mathcal{E}_R + \mu_E\, \overline{\mathcal{E}}_L\, e_R + \lambda_\mathcal{E}\, \overline{\mathcal{E}}_L\, \mathcal{Y}_E\, \mathcal{E}_R \\ &+ \lambda_\nu\, \overline{\ell}_L\, \tilde{\Phi}\, \mathcal{N}_R + \lambda_N\, \overline{N_R^c}\, \mathcal{Y}_N\, \mathcal{N}_R + \frac{\mu_{LN}}{2}\, \overline{N_R}^c N_R + \text{h.c.},\end{aligned} \tag{4.2.2}$$

where again all overall constants, i.e., λ's and μ's, can be made real via chiral rotations. The only source of CP violation lies then in the non-trivial flavor structure of the vevs of the scalar fields $\mathcal{Y}_E$ and $\mathcal{Y}_N$. The charged lepton mass matrix inferred from this Lagrangian is identical to that in Eq. (4.1.8), and in consequence the particle spectrum and phenomenology of the $SU(3)_E$ sector (gauge bosons and mirror charged leptons) matches the description given in the previous section. In contrast, the particle spectrum and phenomenology of the $SU(3)_\ell$ and $SO(3)_N$ sectors (gauge bosons and heavy neutral fermions) will now depend on three fundamental scales: the vevs of $\mathcal{Y}_E$ and $\mathcal{Y}_N$ and the lepton number parameter μ_{LN}. Note that now the LN and flavor scales are distinct; for instance for $\mu_{LN} = 0$, there will still be be physical leptonic mixing and flavor effects associated to $\mathcal{Y}_N$. The neutral fermions mass matrix in the Lagrangian Eq. (4.2.2) (in the $\{\ell^c, \mathcal{N}_R, N_R\}$ basis),

$$\frac{1}{2}\begin{pmatrix} 0 & \lambda_\nu v/\sqrt{2} & 0 \\ \lambda_\nu v/\sqrt{2} & 0 & \lambda_N \mathcal{Y}_N^T \\ 0 & \lambda_N \mathcal{Y}_N & \mu_{LN} \end{pmatrix} + \text{h.c.}, \tag{4.2.3}$$

is typical of inverse Seesaw scenarios [326–328], in which generically that separation of the two scales holds. Eq. (4.2.3) immediately suggests two interesting limiting regimes for the parameters $\mathcal{Y}_N$ and μ_{LN}:

$\boldsymbol{\mu_{LN} \gg \mathcal{Y}_N}$: In this limit the N_R fields would decouple producing an effective mass term for the $\mathcal{N}_R$ of the form $\mathcal{Y}_N \mathcal{Y}_N^T/\mu_{LN}$. The basic type I Lagrangian of the previous model is recovered, albeit with the $(2,2)$ entry of the neutral mass matrix in Eq. (4.1.8) replaced by that effective mass.

$\boldsymbol{\mathcal{Y}_N \gg \mu_{LN}}$: An approximate $U(1)_{LN}$ symmetry holds in this limit, as often explored within low-scale inverse Seesaw scenarios [54, 329, 330]. ${N_R}^c$ and $\mathcal{N}_R$ would form pseudo-Dirac pairs and the light neutrino masses will be suppressed by a factor $\mu_{LN}/(\lambda_N \mathcal{Y}_N)$ with respect to those for the basic type I Seesaw in Eq. (4.1.8).

The second limit leads to new phenomenology and will be the focus of the rest of the section. The interplay between $\mathcal{Y}_E$ and $\mathcal{Y}_N$ will determine the spectrum and the phenomenology of the flavor gauge bosons and will be discussed next.

4.2.1 Fermion Spectrum and Interactions: $\boldsymbol{\mathcal{Y}_N \gg \mu_{LN}}$ case

It is possible to expect in this model measurable signals of lepton-flavor violation, precisely because the LN parameter (μ_{LN}) and lepton flavor violation scale ($\|\mathcal{Y}_N\|$) are independent and

the latter is not strongly constrained by the tiny value of light neutrino masses. By the same token, the mirror neutral fermions –determined by $\|\mathcal{Y}_N\|$– are now allowed to be much lighter than in the gauged-flavor SM discussed in Section 4.1, see Eq. (4.1.13), and close to those of the charged lepton mirror fermions. Indeed, in the $\mu_{LN} \ll \mathcal{Y}_N$ limit the singlet fermions $\mathcal{N}_R$ and ${N_R}^c$ form Dirac pairs of mass

$$\mathcal{M}_N \simeq \lambda_N \mathcal{Y}_N \,, \tag{4.2.4}$$

where we neglected $\lambda_\nu v$ contributions and the mass splitting in quasi-Dirac fields is given by μ_{LN}, while the three light neutrinos acquire Majorana masses suppressed by the LN scale, which does not carry flavor structure,[9]

$$m_\nu = \frac{v^2}{2}\frac{C_\nu}{\Lambda_{LN}} \simeq \frac{v^2}{2}\frac{{\lambda_\nu}^2}{\lambda_N^2}\frac{1}{\mathcal{Y}_N}\mu_{LN}\frac{1}{\mathcal{Y}_N^T} \,. \tag{4.2.5}$$

The lightness of neutrino masses can be thus attributed to a small μ_{LN} instead of a very large $\|\mathcal{Y}_N\|$ (needed in the previous section): this is a technically natural solution as μ_{LN} is protected by the approximate $U(1)_{LN}$ symmetry. In consequence, $\|\mathcal{Y}_N\|$ can now be of the order of the electroweak scale or even smaller, resulting in putatively observable signals of lepton-flavor violation mediated by flavor gauge bosons of the $SU(3)_\ell \times SO(3)_N$ sector (see further below) independently of the value of light neutrino masses.

Note that, as in the gauged-flavor SM in Section 4.1, the mirror lepton mass matrices are linearly proportional to the flavon vevs $\mathcal{Y}_E$ (Eq. (4.1.9)) and $\mathcal{Y}_N$ (Eq. (4.2.4)), and the mass of the SM charged leptons is inversely proportional to $\mathcal{Y}_E$ (Eq. (4.1.10)); in contrast, the light neutrino masses exhibit now a quadratic inverse dependence on $\mathcal{Y}_N$, Eq. (4.2.5). From this equation a parametrization equivalent to that of Casas-Ibarra [67] can be introduced:

$$\mathcal{Y}_N = \frac{v}{\sqrt{2}}\frac{\lambda_\nu}{\lambda_N}\, R \sqrt{\frac{\mu_{LN}}{m_\nu^{diag}}}\, U^\dagger \,, \tag{4.2.6}$$

where U is the PMNS matrix and m_ν^{diag} is the diagonal matrix of light neutrino masses m_{ν_i},

$$m_\nu^{diag} \equiv (m_{\nu_1}, m_{\nu_2}, m_{\nu_3}) \,, \tag{4.2.7}$$

and R is an orthogonal complex matrix. The latter can be parametrized in general as the exponential of the anti-symmetric Gell-Mann matrices with complex coefficients, although in the case discussed an $SO(3)_N$ transformation allows to remove the imaginary part of these coefficients,

$$R = e^{\eta_i T'^i} \,, \qquad RR^T = \mathbb{1} \,, \qquad R = R^\dagger \,, \tag{4.2.8}$$

where η_i are three real parameters and the matrices T'^i denote the set of three generators $\{T^2, T^5, T^7\}$.

[9] The effective LN scale here is thus $\Lambda_{LN} \sim \|\mathcal{M}_N\|^2 / \mu_{LN}$, as usual in inverse Seesaw constructions, while the scale suppressing flavor effects is $\|\mathcal{M}_N\|$.

In the rest of this section, and in analogy with Eq. (4.1.27), we revert again to the notation in which flavor eigenstates are denoted by primed fields while unprimed ones stand for the mass eigenstates. In the limit of vanishing μ_{LN}, which will be assumed from now on, the mass term for neutrinos coming from Eq. (4.2.2) after symmetry breaking reduces to

$$\left(\lambda_\nu \overline{\nu'_L}\, v/\sqrt{2} + \lambda_N \overline{N'^c_R}\, \mathcal{Y}_N\right) \mathcal{N}'_R + \text{h.c.} = -\overline{N}^c_R \mathcal{M}_N \mathcal{N}_R + \text{h.c.}, \tag{4.2.9}$$

and therefore a unitary rotation among only the ν_L and N_R fields suffices to diagonalize the mass matrix:

$$\begin{pmatrix} \nu'_L \\ N'^{\,c}_R \end{pmatrix} = \begin{pmatrix} c_{\Theta_\nu} & s_{\Theta_\nu} \\ -s_{\Theta^\dagger_\nu} & c_{\Theta^\dagger_\nu} \end{pmatrix} \begin{pmatrix} \nu_L \\ N_R{}^c \end{pmatrix}, \tag{4.2.10}$$

where Θ_ν is as given in Eq. (4.1.29) and we simultaneously define $\mathcal{N}'_R = -\mathcal{N}_R$ in order to recover the usual sign for the Dirac mass term of the heavy states, and in accordance with the definitions in the gauged-flavor SM, Eqs. (4.1.27) and (4.1.34).

Interactions with SM gauge bosons

$\mathcal{Y}_N$ introduces new flavor non-conserving transitions, associated to the extra fermionic states and parameterized by Θ_ν. The flavor changing and light-heavy mixing effects can then be written in the mass basis as in Eq. (4.1.31), where now

$$\begin{aligned}
J^\mu_\gamma =& -\bar{e}\gamma^\mu e - \bar{\mathcal{E}}\gamma^\mu \mathcal{E}\,, \\
J^{-\mu}_W =& \bar{\nu}_L \gamma^\mu U^\dagger c_{\Theta_\nu} \left(c_\Theta e_L + s_\Theta \mathcal{E}_L\right) + \overline{N_R{}^c}\gamma^\mu s^\dagger_{\Theta_\nu} \left(c_\Theta e_L + s_\Theta \mathcal{E}_L\right)\,, \\
J^\mu_Z =& \bar{e}\gamma^\mu \left(-(c_{2W} - s_\Theta s_{\Theta^\dagger})P_L + 2s^2_W P_R\right) e - \overline{\mathcal{E}}\gamma^\mu \left(s_{\Theta^\dagger} s_\Theta P_L - 2s^2_W\right) \mathcal{E} - \left(\overline{\mathcal{E}}_L \gamma^\mu s_{\Theta^\dagger} c_\Theta e_L + \text{h.c.}\right) + \\
&+ \bar{\nu}_L \gamma^\mu c^2_{\Theta_\nu} \nu_L + \overline{N}_R \gamma^\mu s_{\Theta^\dagger_\nu} s_{\Theta_\nu} N_R + (\bar{\nu}_L \gamma^\mu c_{\Theta_\nu} s_{\Theta_\nu} N^c_R + \text{h.c.})\,.
\end{aligned} \tag{4.2.11}$$

Note that the PMNS matrix appearing in W couplings is given by the product $U^\dagger c_{\Theta_\nu} c_\Theta$, with U being its unitary part and Θ_ν and Θ encoding deviations from unitarity. The expressions for the mixing angles equal those in the previous section, Eq. (4.1.29).

Scalar interactions

Using the definitions in Eq. (4.1.7) for the scalar excitations, the generalized Yukawa interactions read for vanishing μ_{LN}:

$$\mathscr{L}_{\bar{\psi}\psi\phi} = \frac{-1}{\sqrt{2}} \begin{pmatrix} \bar{e}_L \\ \overline{\mathcal{E}}_L \end{pmatrix} \begin{pmatrix} (\lambda_E c_\Theta h - \lambda_\mathcal{E} s_\Theta \phi_E) s_{\Theta_R} & (\lambda_E c_\Theta h - \tilde{\lambda}_\mathcal{E} s_\Theta \phi_E) c_{\Theta_R} \\ (\lambda_\mathcal{E} c_{\Theta^\dagger} \phi_E + \lambda_E s_{\Theta^\dagger} h) s_{\Theta_R} & (\lambda_\mathcal{E} c_{\Theta^\dagger} \phi_E + \lambda_E s_{\Theta^\dagger} h) c_{\Theta_R} \end{pmatrix} \begin{pmatrix} e_R \\ \mathcal{E}_R \end{pmatrix} +$$

$$-\frac{\lambda_\nu}{\sqrt{2}}h\left(\bar{\nu}_L\, c_{\Theta_\nu}+\overline{N_R{}^c}\, s_{\Theta_\nu^\dagger}\right)\mathcal{N}_R-\frac{\lambda_N}{\sqrt{2}}\left(\overline{N_R{}^c}\, c_{\Theta_\nu^\dagger}-\bar{\nu}_L\, s_{\Theta_\nu}\right)\phi_N\,\mathcal{N}_R+\text{h.c.}\,. \tag{4.2.12}$$

In this model there are $18+18-19=17$ scalars ϕ_E and ϕ_N,[10] which are fluctuations around the 6 mixing parameters, 6 masses, 3 variables in the orthogonal self-hermitian matrix R and two phases in $U(1)_\ell$ and $U(1)_E$. Their effects are strongly suppressed [7] and will not be further discussed.

Were the extra neutral states N lighter than the Higgs boson, the following decay channel would open:

$$\Gamma(h\to N\nu)=\frac{\lambda_\nu^2}{16\pi}M_h\left(1-\frac{M_N^2}{M_h^2}\right)\,, \tag{4.2.13}$$

where N stands here for the generic mass eigenstates. The N fields will in turn be unstable and decay to lighter charged fermions and neutrinos via the interaction in Eq. (4.2.11), with a pattern that depends strongly on M_N and Θ_ν, potentially leading to new visible Higgs decays, displaced vertices or contributions to the invisible decay. Additional bounds would then apply; we will not further consider this case of heavy neutrinos lighter than the Higgs particle.

Flavor Gauge Boson Spectrum and Interactions

Additional flavor non-conserving effects can be induced by flavor gauge bosons, A_μ^ℓ. Indeed, the theory contains nineteen flavor gauge bosons whose Lagrangian reads

$$\begin{aligned}&\sum_I \text{Tr}\left(A_\mu^I\partial^2 A^{I,\mu}\right)+\text{Tr}\left\{\left(g_E A_\mu^E\mathcal{Y}_E-g_\ell\mathcal{Y}_E A_\mu^\ell\right)\left(g_E\mathcal{Y}_E^\dagger A^{E,\mu}-g_\ell A^{\ell,\mu}\mathcal{Y}_E^\dagger\right)\right\}+\\&+\text{Tr}\left\{\left(g_N A_\mu^N\mathcal{Y}_N-g_\ell\mathcal{Y}_N A_\mu^\ell\right)\left(g_N\mathcal{Y}_N^\dagger A^{N,\mu}-g_\ell A^{\ell,\mu}\mathcal{Y}_N^\dagger\right)\right\}-\sum_I g_I\text{Tr}\left(A_\mu^I J_{A_I}^\mu\right)\,,\end{aligned} \tag{4.2.14}$$

where cubic and quartic gauge boson interactions are not shown as they will play no role in the phenomenological analysis below. In Eq. (4.2.14) the ensemble of fields A_μ^I, $I=\ell,E,N$, is treated as a traceless hermitian matrix and the currents are defined as matrices in flavor space, with the currents $J_{A^\ell}^\mu$ and $J_{A^E}^\mu$ as defined in Eq. (4.1.16) and the $SO(3)_N$ current given by

$$\left[J_{A^N}^\mu\right]_{ij}=\frac{1}{2}\left(\bar{N}_R^j\gamma^\mu N_R^i-\overline{N}{}_R^i\gamma^\mu N_R^j\right)\,. \tag{4.2.15}$$

The EOM resulting from Eq. (4.2.14) for A_μ^E is identical to that in Eq. 4.1.18, while for A_μ^ℓ and A_μ^N they are given by

$$\partial^2 A_\mu^\ell-g_E g_\ell\mathcal{Y}_E^\dagger A_\mu^E\mathcal{Y}_E-g_N g_\ell\mathcal{Y}_\nu^\dagger A_\mu^N\mathcal{Y}_N+\frac{g_\ell^2}{2}\left\{\mathcal{Y}_E^\dagger\mathcal{Y}_E+\mathcal{Y}_N^\dagger\mathcal{Y}_N,\,A_\mu^\ell\right\}-\frac{g_\ell}{2}J_\mu^{A^\ell}=\frac{1}{n_g}\text{Tr}\,(\text{L.H.S.})\,\mathbb{1}\,,$$

[10] Among the 36 real degrees of freedom of the two 3×3 complex matrices $\mathcal{Y}_E$ and $\mathcal{Y}_N$, 19 become the longitudinal components of the 19 flavor gauge bosons of the model.

$$\partial^2 A_\mu^N + \frac{g_N^2}{4}\left\{\mathcal{Y}_N\mathcal{Y}_N^\dagger + \mathcal{Y}_N^*\mathcal{Y}_N^T,\, A_\mu^N\right\} - \frac{g_\ell g_N}{2}\left(\mathcal{Y}_N A_\mu^\ell \mathcal{Y}_N^\dagger - \mathcal{Y}_N^*(A_\mu^\ell)^T\mathcal{Y}_N^T\right) - \frac{g_N}{2}J_\mu^{A^N} = 0\,, \tag{4.2.16}$$

where $n_g = 3$. Eq. (4.2.14) can be alternatively written in a compact matrix notation arranging the flavor gauge bosons in an array $\chi_\mu^a = \left(A_\mu^{\ell,1},\ldots,A_\mu^{\ell,8},A_\mu^{E,1},\ldots,A_\mu^{E,8},A_\mu^{N,1},\ldots,A_\mu^{N,3}\right)$:

$$\mathcal{L}_{gauge} = -\frac{1}{2}\sum_{I=\ell,E,N}\mathrm{Tr}\left(F_{\mu\nu}^I F_I^{\mu\nu}\right) + \frac{1}{2}\sum_{a,b=1}^{19}\chi_\mu^a\left(M_A^2\right)_{ab}\chi^{b,\mu} - \sum_{I=\ell,E,N} g_I\,\mathrm{Tr}\left(A_\mu^I J_{A_I}^\mu\right)\,, \tag{4.2.17}$$

where the mass matrix M_A^2 can be written in blocks as

$$M_A^2 = \begin{pmatrix} M_{\ell\ell}^2 & M_{\ell E}^2 & M_{\ell N}^2 \\ M_{E\ell}^2 & M_{EE}^2 & 0_{8\times 3} \\ M_{N\ell}^2 & 0_{3\times 8} & M_{NN}^2 \end{pmatrix}\,, \tag{4.2.18}$$

with $\left(M_{EE}^2\right)_{ij}$ and $\left(M_{\ell E}^2\right)_{ij} = \left(M_{E\ell}^2\right)_{ji}$ identical to those in Eq. (4.1.22) for the gauged-flavor SM case, while instead

$$\begin{aligned}
\left(M_{\ell\ell}^2\right)_{ij} &= g_\ell^2\left\{\mathrm{Tr}\left(\mathcal{Y}_E\left\{T_i,T_j\right\}\mathcal{Y}_E^\dagger\right) + \mathrm{Tr}\left(\mathcal{Y}_N\left\{T_i,T_j\right\}\mathcal{Y}_N^\dagger\right)\right\}\,,\\
\left(M_{\ell N}^2\right)_{i\hat{j}} &= \left(M_{N\ell}^2\right)_{\hat{j}i} = -2g_\ell g_N\,\mathrm{Tr}\left(T_i\mathcal{Y}_N^\dagger T'_{\hat{j}}\mathcal{Y}_N\right)\,,\\
\left(M_{NN}^2\right)_{\hat{i}\hat{j}} &= g_N^2\,\mathrm{Tr}\left(\mathcal{Y}_N^\dagger\left\{T'_{\hat{i}},T'_{\hat{j}}\right\}\mathcal{Y}_N\right)\,,
\end{aligned} \tag{4.2.19}$$

where $T' \equiv \{T_2,T_5,T_7\}$, $i,j = \{1,\ldots,8\}$ and $\hat{i},\hat{j} = \{1,\ldots,3\}$.

Notice that, contrary to the processes mediated by the exchange of $SU(3)_E$ gauge bosons A_μ^E, those mediated by A_μ^ℓ can indeed lead to observable flavor non-conserving processes given the non-diagonal flavor structure of $\mathcal{Y}_N$ and the related low scales allowed in this gauged-flavor type I Seesaw scenario.

Generally speaking, M_{A^ℓ} will be determined by the largest value between $\|\mathcal{Y}_E\|$ and $\|\mathcal{Y}_N\|$. There are in general too many parameters to make definite predictions, though. The most relevant consequences are briefly discussed next and illustrated in Fig. 4.3 for three relevant limits: $\mathcal{Y}_E > \|\mathcal{Y}_N\|$, $\mathcal{Y}_E \sim \mathcal{Y}_N$ and $\|\mathcal{Y}_E\| < \mathcal{Y}_N$, with the latter two cases being of special phenomenological interest as they lead to putatively observable cLFV in addition to LUV signals.

$\boldsymbol{\mathcal{Y}_E > \|\mathcal{Y}_N\|}$ – Vectorial Flavor-Preserving Gauge Bosons

The heaviest gauge bosons would be those whose mass is dominated by the vev of $\mathcal{Y}_E$. This applies to all $SU(3)_\ell$ and $SU(3)_E$ gauge bosons but two (see below), as $\mathcal{Y}_E$ transforms under

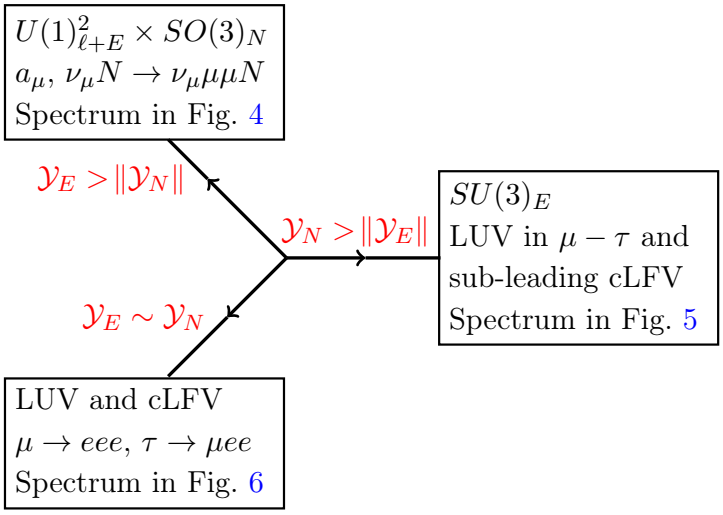

Figure 4.3: Schematic diagram for the relevant phenomenology scenarios. Each box reports the symmetry associated to the relevant gauge bosons and the expected dominant phenomenology.

those two groups. The hierarchical structure of $\mathcal{Y}_E$ —with eigenvalues inversely proportional to the SM charged lepton masses— results in a stratification of those heavier gauge bosons in two layers, as illustrated by the two upper layers of the spectrum in Fig. 4.4: the upper level contains the nine gauge bosons which couple to the electron, while the intermediate level corresponds to those gauge bosons coupling only to muons and taus. The phenomenological impact of the upper level will be neglected in what follows.

The lightest gauge bosons would be those which acquire instead a mass only through the vev of $\mathcal{Y}_N$. There are five such states. Three of them are the $SO(3)_N$ gauge bosons, depicted (in green) in the illustrative case in Fig. 4.4: they carry flavor, mediating transitions only in the N_i realm. Notice that they will only mix for complex $\mathcal{Y}_N$, since the mass cross-term that connects them to the other gauge bosons is $\mathrm{Tr}[T_{3,8}\mathcal{Y}_N^\dagger T_{2,5,7}\mathcal{Y}_N] = -\mathrm{Tr}[T_{3,8}\mathcal{Y}_N^T T_{2,5,7}\mathcal{Y}_N^*]$, see Eq. (4.2.19).

The presence of the other two light eigenstates —the lightest ones in Fig. 4.4— can be understood from the fact that $\mathcal{Y}_E$ can be made diagonal via a rotation in flavor space. This corresponds to the three distinct vectorial and diagonal $U(1)$ symmetries which are preserved: LN which has not been gauged, plus two others which correspond to very light gauge bosons, which acquire a mass only through the vev of $\mathcal{Y}_N$. These states are diagonal in flavor space and traceless —see Fig. 4.4— and given by the linear combination $A_\mu^V = (g_E A_\mu^\ell + g_\ell A_\mu^E)/(g_\ell^2 + g_E^2)^{1/2}$, with mass matrix

$$M_{A_V}^2 \equiv 2g_\ell^2 \begin{pmatrix} \mathrm{Tr}(T_3\mathcal{Y}_N^\dagger\mathcal{Y}_N T_3) & \mathrm{Tr}(T_3\mathcal{Y}_N^\dagger\mathcal{Y}_N T_8) \\ \mathrm{Tr}(T_8\mathcal{Y}_N^\dagger\mathcal{Y}_N T_3) & \mathrm{Tr}(T_8\mathcal{Y}_N^\dagger\mathcal{Y}_N T_8) \end{pmatrix} . \tag{4.2.20}$$

Those two gauge bosons generically couple to all flavors with similar strength, see Eq. (4.2.20),

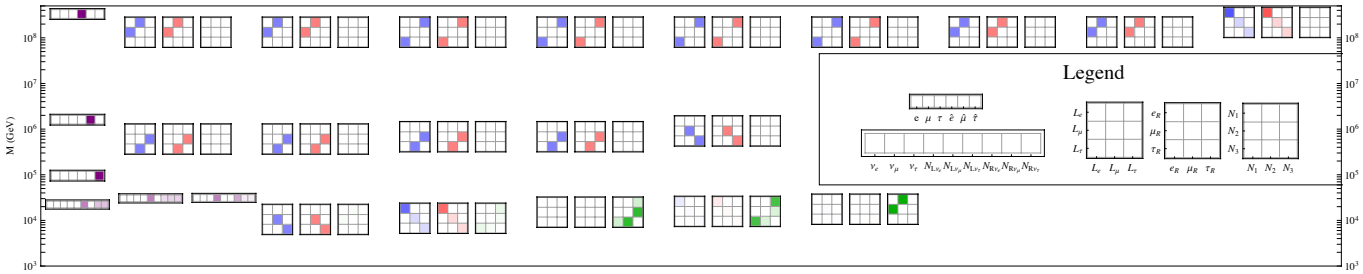

Figure 4.4: Gauge and fermion heavy spectrum for the gauged lepton flavor type I Seesaw model, with $\mathcal{Y}_E \gg \|\mathcal{Y}_N\|$. Boxes correspond to flavor gauge fields and lines to mirror fermions. Neutrino normal ordering was assumed and the parameter values taken are $\theta_{23} = 45°$, $\theta_{12} = 33°$, $\theta_{13} = 8.8°$, Dirac CP phase $\delta = 3\pi/2$, Majorana phases $\alpha_1 = \alpha_2 = 0$, $R = 1$. All g′s and all $\lambda'$$s$ are 0.1 except $\lambda_N = 1$ and $\mu_E = 1$ TeV, $\mu_{LN} = 1$ KeV, while $m_{\nu_1} = 0.03$ eV.

and thus the most stringent bound stems from LEP [331],

$$M_{A_{V_1}} \geq 2.1 \times 10^2 \,\text{GeV}\,, \tag{4.2.21}$$

where A_{V_1} denotes the lightest eigenstate of Eq. (4.2.20). Those two vector bosons also contribute constructively[11] to the muon anomalous magnetic moment:

$$\delta a_\mu = \frac{m_\mu^2}{12\pi^2} \times \frac{g_E^2 g_\ell^2}{g_\ell^2 + g_E^2} \sum_{ij} T_i^{\mu\mu} \left(M_{A_V}^{-2}\right)_{ij} T_j^{\mu\mu}\,. \tag{4.2.22}$$

Although they could potentially explain the existing anomaly, this is excluded by neutrino trident production data, $\nu_\mu \mathcal{N} \to \nu_\mu \mu\mu \mathcal{N}$ with $\mathcal{N}$ denoting here a nucleus. Indeed, the contributions from the flavor gauge bosons to this observable read [332]

$$\frac{\sigma^{(SM+A)}}{\sigma^{(SM)}} = \frac{1 + \left(1 + 4s_W^2 + 2\delta_V\right)^2}{1 + \left(1 + 4s_W^2\right)^2}\,, \qquad \delta_V = v^2 \frac{g_E^2 g_\ell^2}{g_\ell^2 + g_E^2} \sum_{ij} T_i^{\mu\mu} \left(M_{A_V}^{-2}\right)_{ij} T_j^{\mu\mu}, \tag{4.2.23}$$

and are constrained by the CCFR [333] and CHARM-II [334] collaborations, implying the indirect bound $\delta a_\mu < 7.5 \times 10^{-10}$, which precludes an explanation of the muon magnetic moment anomaly via these gauge bosons.

Fig. 4.4 also illustrates that the lightest exotic neutral fermions would be those mirroring the light neutrino sector, as expected since the mirror fermion masses are linearly proportional to the flavon vevs. Therefore, the unitarity deviation Θ_ν induced in the PMNS matrix by the mirror neutrinos dominates over Θ (stemming from the mirror charged leptons), see Eq. (4.2.11). Analyses probing flavor non-conserving processes and electroweak precision data [37, 319, 335–

[11] As opposed to the contribution studied in Eq. (4.1.49), in this case the sign is positive since the coupling of the lightest flavor gauge boson to leptons is vectorial.

358] can then be translated into constrains on the combination $\Theta_\nu\Theta_\nu^\dagger$ [318] as follows:

$$\begin{aligned}
\left(\Theta_\nu\Theta_\nu^\dagger\right)_{ee} &< 2.5\times10^{-3}, & \left(\Theta_\nu\Theta_\nu^\dagger\right)_{e\mu} &< 2.4\times10^{-5},\\
\left(\Theta_\nu\Theta_\nu^\dagger\right)_{\mu\mu} &< 4.0\times10^{-4}, & \left(\Theta_\nu\Theta_\nu^\dagger\right)_{e\tau} &< 2.7\times10^{-3},\\
\left(\Theta_\nu\Theta_\nu^\dagger\right)_{\tau\tau} &< 5.6\times10^{-3}, & \left(\Theta_\nu\Theta_\nu^\dagger\right)_{\mu\tau} &< 1.2\times10^{-3},
\end{aligned} \tag{4.2.24}$$

at 95% CL.

$\mathcal{Y}_N > \|\mathcal{Y}_E\|$ – LUV and subleading cLFV

In this limit, in which all entries of $\mathcal{Y}_N$ are larger than the largest one in $\mathcal{Y}_E$, the lightest gauge bosons correspond to the $SU(3)_E$ symmetry. Therefore, the leading phenomenology described in Section 4.1 when gauging only the SM leptonic flavor group $SU(3)_\ell \times SU(3)_E$ will apply. In particular, as $\|\mathcal{Y}_E\|$ dominates, an effective low-energy $SU(2)_E$ symmetry is at play and mediated by the three lightest gauge bosons, while transitions involving the electron flavor will be additionally suppressed by $(m_e/m_\mu)^2$ with respect to those in the μ–τ sector. The lepton universality violation effects associated to the $\mu-\tau$ sector and dominated by fermionic $\hat{\tau}$ exchanges found in Section 4.1 are also valid for this case.

As for the heavier states, since the leading contribution to the $SU(3)_\ell$ gauge boson masses is given by $\mathcal{Y}_N$ no large hierarchies among the $SU(3)_\ell$ gauge boson masses are expected for a generic R matrix and generic light neutrino mass spectrum. Therefore, the importance of the lepton flavor violating processes mediated by these gauge bosons will not be strongly correlated to the specific flavors involved. This is in contrast to the case for A_μ^E shown in Sec. 4.1.1. However, there are specific limiting cases with approximate symmetries for which hierarchies are introduced and the number of relevant parameters is reduced so that more definite predictions can be made. We briefly consider an example next.

Generic R and degenerate neutrino masses

As expected, the lightest states of the spectrum will be similar to those discussed in Section 4.1, as seen by comparing Fig. 4.2 and Fig. 4.5, while the heavier states can be now much lighter and thus of phenomenological interest, as explained earlier on.

In the limit of degenerate neutrinos, Eqs. (4.2.6) and (4.2.8) lead to

$$\mathcal{Y}_N = \frac{v}{\sqrt{2}}\frac{\lambda_\nu\sqrt{\mu_{LN}}}{\lambda_N\sqrt{m_\nu}}R\,U^\dagger \equiv \frac{v}{\sqrt{2}}\frac{\lambda_\nu\sqrt{\mu_{LN}}}{\lambda_N\sqrt{m_\nu}}e^{\eta_i T'^i}U^\dagger\,. \tag{4.2.25}$$

This expression is invariant under a $U(1)$ subgroup of $SU(3)_\ell \times SO(3)_N$:

$$\mathcal{Y}_N \to e^{i\alpha\,\eta_i T'^i}\,(\mathcal{Y}_N)\,U e^{-i\alpha\,\eta_i T'^i}U^\dagger\,, \tag{4.2.26}$$

where α is the (real) parameter of the transformation. Therefore, the gauge boson associated with this $U(1)$ will only acquire mass through $\mathcal{Y}_E$ and will be lighter than the rest. The generator of this residual $U(1)$ symmetry in the $SU(3)_\ell$ sector is $U\eta_i T'^i U^\dagger$ and therefore the induced cLFV four fermion operator mediated by that state is

$$\frac{g_\ell^2}{M^2_{A_{U(1)}}} \left(\bar{\ell}_L \gamma_\mu U \eta_i T'^i U^\dagger \ell_L\right)^2 . \tag{4.2.27}$$

That lighter state is illustrated by the first gauge boson on the second layer of Fig. 4.5, in

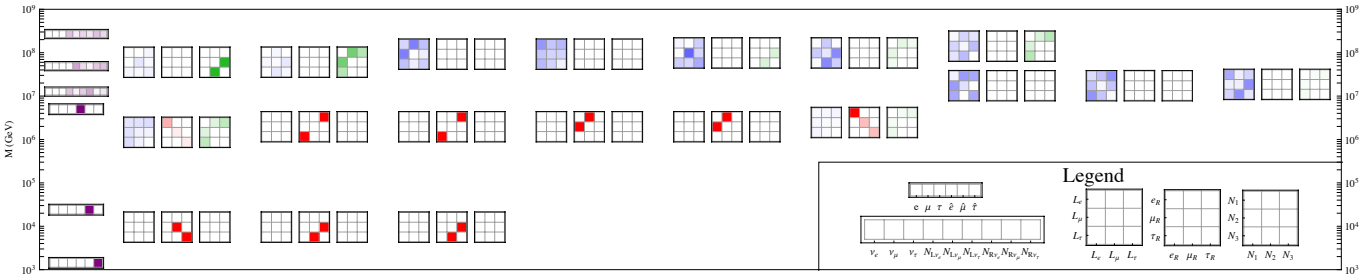

Figure 4.5: Gauge and fermion heavy spectrum for the gauged lepton flavor type I Seesaw model, with $\mathcal{Y}_N > \|\mathcal{Y}_E\|$ and degenerate light neutrinos, CP-odd case. Boxes correspond to flavor gauge fields and lines to mirror fermions. Neutrino normal ordering was assumed for neutrinos and the parameter values taken are $\theta_{23} = 45°$, $\theta_{12} = 33°$, $\theta_{13} = 8.8°$, Dirac CP phase $\delta = 3\pi/2$, Majorana phases $\alpha_{21} = -\pi/2$, $\alpha_{31} = -2\pi/3$, R is a rotation in the 23 sector by angle $-i$ times a 12 rotation by angle i. All g$'$s and all λ's are 1 except $\lambda_N = 2$, $\lambda_\nu = 0.2$, $\mu_E = 15$ GeV, while $\mu_{LN} = 100$ GeV and $m_{\nu_1} = 0.03$ eV.

which generic values of the Dirac CP phase δ and a non-trivial R matrix have been used. In this generic case, the most competitive bound on the operator in Eq. (4.2.27) stems from the $\mu \to eee$ decay.

In the case of a CP conserving PMNS matrix, the antisymmetry of T'^i would imply that the combination $U\eta_i T'^i U^\dagger$ in Eq. (4.2.27) would have vanishing flavor diagonal interactions. The only expected decays would then be $\tau \to \mu ee$ and $\tau \to \mu\mu e$, determined by the specific values of R. Nevertheless, the recent hints [359, 360] of a leptonic CP phase $\delta \sim 270°$ would discard this possibility, if confirmed. In this perspective, we refrain as well from detailing other specific predictions that would follow for scenarios with $\delta = 0$ or π.

$\mathcal{Y}_E \sim \|\mathcal{Y}_N\|$ – LUV and cLFV

This case is involved given the interplay of several scales, although it can be described qualitatively. As $\mathcal{Y}_E$ is intrinsically hierarchical (and determined by the inverse of the charged lepton masses), in the example considered next it is assumed that the norm $\|\mathcal{Y}_N\|$ is heavier than the eigenstates of the approximate $SU(2)_E$ symmetry of the muon-tau sector and lighter than the rest of the $\mathcal{Y}_E$ entries. In consequence, the lightest exotic fermion and gauge boson masses are as in the SM gauged case discussed in Section 4.1, as can be seen by comparing Fig. 4.2 with

the illustrative case in Fig. 4.6. The lightest fields in the spectrum are again the mirror $\hat{\tau}$ lepton and the $SU(2)_E$ gauge bosons, leading to the $\mu - \tau$ phenomenology discussed in Section 4.1.

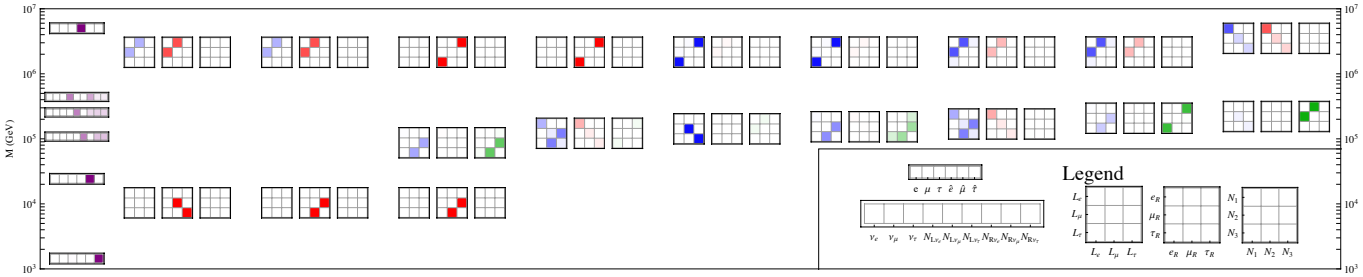

Figure 4.6: Gauge and fermion heavy spectrum for the gauged lepton flavor type I Seesaw model, with $\mathcal{Y}_E \sim \|\mathcal{Y}_N\|$. Boxes correspond to flavor gauge fields and lines to mirror fermions. Neutrino normal ordering was assumed and the parameter values taken are $\theta_{23} = 45°$, $\theta_{12} = 33°$, $\theta_{13} = 8.8°$, Dirac CP phase $\delta = 3\pi/2$, Majorana phases $\alpha_1 = \alpha_2 = 0$, $R = 1$, all λ's and g's are taken to be 0.1 except $\lambda_N = 1$ and $\mu_E = 15$ GeV, $\mu_{LN} = 20$ KeV and $m_{\nu_1} = 0.003$eV.

Additionally, the gauge bosons which take their masses dominantly from $\mathcal{Y}_N$ may now lead to observable cLFV signals, as discussed next. Electron number violation will be suppressed by the largest of the two scales $\|\mathcal{Y}_E\|$ and $\|\mathcal{Y}_N\|$, while muon and tau violation by the largest of $\|\mathcal{Y}_E\|\, m_e/m_\mu$ and $\|\mathcal{Y}_N\|$. Therefore, the generic expectations for flavor violating processes are:

$$\begin{aligned} &\mathrm{Br}_{\mu\to eee}(A_\mu^\ell)\,,\ \mathrm{Br}_{\tau\to\mu e^- e^-}(A_\mu^\ell)\,,\ \mathrm{Br}_{\tau\to\mu\mu e}(A_\mu^\ell) \sim \left(\|\mathcal{Y}_E\|^2 + \|\mathcal{Y}_N\|^2\right)^{-2}\,, \\ &\mathrm{Br}_{\tau\to\mu\mu\mu}(A_\mu^\ell)\,,\ \mathrm{Br}_{\tau\to\mu e^+ e^-}(A_\mu^\ell) \sim \left(\frac{m_e^2}{m_\mu^2}\|\mathcal{Y}_E\|^2 + \|\mathcal{Y}_N\|^2\right)^{-2}\,. \end{aligned} \tag{4.2.28}$$

The experimental bounds in Table 4.3 can then be translated into limits on the combinations

$$\begin{aligned} \sqrt{\|\mathcal{Y}_E\|^2 + \|\mathcal{Y}_N\|^2} &\geq 3.5 \times 10^5 \mathrm{GeV}\,, \qquad \text{from} \quad \mu \to eee\,, \\ \sqrt{\frac{m_e^2}{m_\mu^2}\|\mathcal{Y}_E\|^2 + \|\mathcal{Y}_N\|^2} &\geq 1.9 \times 10^4 \mathrm{GeV}\,, \qquad \text{from} \quad \tau \to \mu e^+ e^-\,. \end{aligned} \tag{4.2.29}$$

$\mathrm{Br}(\mu \to e\gamma) \leq 5.7 \times 10^{-13}$	$\mathrm{Br}(\tau \to \mu\gamma) \leq 4.4 \times 10^{-8}$
$\mathrm{Br}(\tau \to e\gamma) \leq 3.3 \times 10^{-8}$	$\mathrm{Br}(\mu \to eee) \leq 1.0 \times 10^{-12}$
$\mathrm{Br}(\tau \to eee) \leq 2.7 \times 10^{-8}$	$\mathrm{Br}(\tau \to \mu\mu\mu) \leq 2.1 \times 10^{-8}$
$\mathrm{Br}(\tau \to \mu^+\mu^- e) \leq 2.7 \times 10^{-8}$	$\mathrm{Br}(\tau \to \mu\mu^- e^+) \leq 1.7 \times 10^{-8}$
$\mathrm{Br}(\tau \to \mu e^+ e^-) \leq 1.8 \times 10^{-8}$	$\mathrm{Br}(\tau \to \mu^+ e^- e) \leq 1.5 \times 10^{-8}$

Table 4.3: 90% *CL limits on flavor violating decays of a charged lepton into three other charged leptons* [315].

When the two scales $\|\mathcal{Y}_E\|$ and $\|\mathcal{Y}_N\|$ are comparable, $\mu \to eee$ sets a lower bound on each of them of $\sim 2.5 \times 10^5$GeV; when instead $\|\mathcal{Y}_N\| < \|\mathcal{Y}_E\|$, $\tau \to \mu e^+ e^-$ leads to a stronger bound on $\|\mathcal{Y}_E\| \gtrsim 2.9 \times 10^6$GeV. In both cases, flavor observables turn out to be more sensitive to the scale of the flavor gauge bosons than present collider data, as the bounds on $\|\mathcal{Y}_E\|$ are stronger than that extracted from direct searches in Eq. (4.1.50), $\|\mathcal{Y}_E\| \geq 7.4 \times 10^4$GeV.

4.3 Comparison with Minimal Lepton Flavor Violation, for $\mathcal{Y}_N \gg \mathcal{Y}_E$

We have gauged in the preceding sections the maximal non-abelian leptonic global flavor symmetry of the SM and of the type I Seesaw Lagrangian. In doing so, we were inspired by the phenomenological successes of the MFV ansatz in which the Yukawa couplings are treated as scalar spurions. A pertinent question is then whether the resulting low-energy phenomenology described above is compatible with that expected in the original formulation of Minimal Lepton Flavor Violation (MLFV) [78] and subsequent works [310–313].

The low-energy effective Lagrangian of our gauged-flavor models will, by construction, be formally invariant under the spurion analysis of MLFV; the question is whether the analytic dependence on the scalar fields matches that in MLFV. It is shown below that this is not always the case, due mainly to the presence of additional gauge bosons in the gauged-flavor Lagrangians.

For definiteness, we focus here on the specific limit $\mathcal{Y}_N \gg \mathcal{Y}_E$, which applies both to the gauged-flavor SM described in Section 4.1 and to one scenario of the gauged-flavor type I Seesaw model, see Section 4.2.1. Integrating out the flavor gauge bosons and the mirror fermion fields in Eqs. (4.1.2)–(4.1.6), (4.2.1) and (4.2.2), and restricting the expansion to order $\mathcal{Y}^{-2}$ in flavon fields vevs ($\mathcal{Y}_E$ and $\mathcal{Y}_N$), the low-energy Lagrangian reads [12]

$$\begin{aligned}\mathscr{L}^{\text{eff}} = &\left(-\bar{\ell}_L \Phi \frac{\lambda_E \mu_E}{\lambda_{\mathcal{E}} \mathcal{Y}_E} e_R - \ell_L^T \tilde{\Phi} \frac{C_\nu}{\Lambda_{LN}} \tilde{\Phi}^T \ell_L + \text{h.c.}\right) + \\ &+ i\,\bar{e}_R \frac{1}{\lambda_{\mathcal{E}}^2} \frac{\mu_E^2}{\mathcal{Y}_E \mathcal{Y}_E^\dagger} \not{D} e_R + i\,\bar{\ell}_L \Phi \frac{\lambda_E^2}{\lambda_{\mathcal{E}}^2} \frac{1}{\mathcal{Y}_E^\dagger \mathcal{Y}_E} \not{D} \left(\Phi^\dagger \ell_L\right) + i\,\bar{\ell}_L \widetilde{\Phi} \frac{\lambda_\nu^2}{\lambda_N^2} \frac{1}{\mathcal{Y}_N^\dagger \mathcal{Y}_N} \not{D} \left(\widetilde{\Phi}^\dagger \ell_L\right) + \\ &- \frac{c_E}{2} \text{Tr}\left[\frac{1}{\mathcal{Y}_E^\dagger \mathcal{Y}_E}\right] \left(\bar{e}_R \gamma_\mu e_R\right)^2 - \frac{1}{2} \text{Tr}\left[\frac{1}{\mathcal{Y}_N^\dagger \mathcal{Y}_N}\right] \left(\bar{\ell}_L \gamma_\mu \ell_L\right) \left[c_\ell \left(\bar{\ell}_L \gamma_\mu \ell_L\right) + 2\, c_{\ell E} \left(\bar{e}_R \gamma_\mu e_R\right)\right],\end{aligned} \tag{4.3.1}$$

where subleading contributions to the displayed operators have been neglected, e. g. $1/\mathcal{Y}_N^2$ vs $1/\mathcal{Y}_E^2$, given that we assume $\mathcal{Y}_N \gg \mathcal{Y}_E$.

The first line in Eq. (4.3.1) is in fact the general effective Lagrangian in Eq. (4.0.2) which describes the charged lepton and neutrino masses, with the charged lepton Yukawa coupling given by $Y_E = (\lambda_E \mu_E)/(\lambda_{\mathcal{E}} \mathcal{Y}_E)$ in both gauged-flavor models considered, SM and type I Seesaw

[12] Recall that we are working on the convention in which μ_E and all λ_i coefficients are real; otherwise all λ_i^2 should be traded by $|\lambda_i|^2$.

scenario, as already found in Eq. (4.1.10) and Section 4.2. C_ν is linear in $\mathcal{Y}_N^{-1}$ for the former scenario and quadratic for the latter, see respectively Eqs. (4.1.10) and (4.2.5).

The second line in Eq. (4.3.1) displays fermion-bilinear terms which are those resulting from integrating out the mirror fermions, as illustrated in Fig. 4.7. Finally, the last line stems from integrating out the heavy flavor gauge bosons resulting in effective four-fermion operators only; a flavor non-conserving operator resulting from A_μ^ℓ exchange is depicted in Fig. 4.8 as illustration. The coefficient of the first four-fermion operator, c_E, has been given in Eq. (4.1.45), whereas the explicit formulas for c_ℓ and $c_{\ell E}$ depend on the model under consideration; they will be discussed further below for phenomenologically accessible cases.

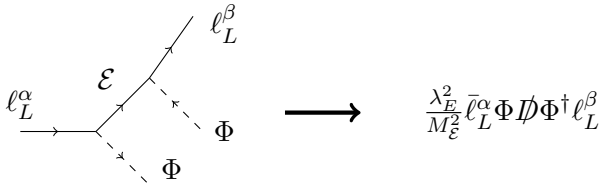

Figure 4.7: Example of effective operator induced via heavy fermion exchange.

Mirror Lepton Exchange

The first term on the second line of Eq. (4.3.1) contributes to the kinetic energy of the right-handed light charged leptons; the field redefinition

$$e_R \to \left(1 - \frac{1}{2\lambda_\mathcal{E}^2}\frac{\mu_E^2}{\mathcal{Y}_E^\dagger \mathcal{Y}_E}\right) e_R\,, \tag{4.3.2}$$

allows to recover canonically normalized kinetic energies and leaves the rest of the Lagrangian unchanged, at the order considered. This confirms the result found in Section 4.1, as the mixing Θ_R among right-handed charged fermions does not affect the gauge interactions.

The second term in that line is a dimension six ($d = 6$) effective operator with a coefficient of order $\mathcal{Y}_E^{-2}$ and therefore quadratic in the charged lepton Yukawa couplings Y_E, see Eq. (4.1.10). Were one to write the $\mathcal{O}(Y_E^2)$ coefficient for such operator with the prescription of MLFV, it would read, in matrix notation,

$$\text{MLFV:} \qquad \frac{i}{\Lambda^2}\bar{\ell}_L \Phi Y_E Y_E^\dagger \not{D}\left(\Phi^\dagger \ell_L\right)\,, \tag{4.3.3}$$

which indeed corresponds to our result in Eq. (4.3.1) provided the associated scale is identified as $\Lambda = \mu_E$, see Eq. (4.1.10). Note that Λ is then not the mass scale of any of the heavy particles in the model and can actually be lower.[13]

[13] If instead the coefficient is written in terms of mass scales, e.g. the mass of the lightest mirror charged lepton, M_τ, it would read $\lambda_E^2/M_\tau^2 \times Y_E Y_E^\dagger / \left\|Y_E^2\right\|$ to order m_μ/m_τ.

The rest of operators produced by fermion exchange can be cast as well in standard MLFV form; in particular the third operator in the second line of Eq. (4.3.1) induces charged flavor violation as was indeed already studied in the context of leptonic MFV in Ref. [312].

A relevant difference between MLFV constructions and the flavor-gauged scenario concerns CP violation. While a priori no symmetry principle prevents from assuming a complex overall phase in non-hermitian MLFV operators, in the lepton gauged-flavor models studied here such extra overall phases are absent. Therefore, the gauging of the lepton flavor symmetries provides a mechanism to protect against CP violation, not present in generic MLFV scenarios. In other words, the only source of CP violation are the scalar vevs and thus the only physical CP-odd phases are those of the PMNS matrix in both gauged-flavor scenarios, plus the usual extra phases of the minimal type I Seesaw model in the gauged-flavor type I Seesaw case.

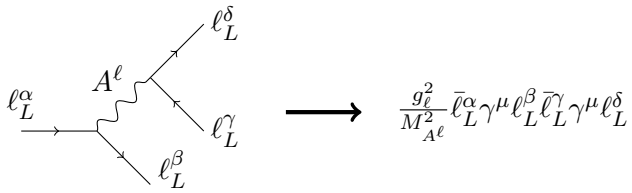

Figure 4.8: Tree-level exchange of a flavor gauge boson resulting in a four-fermion effective operator.

Flavored Gauge Boson Exchange

The effective couplings resulting from the exchange of a heavy flavor gauge boson present a more complicated structure than those mediated by heavy fermions. For instance, the first operator in the third line of Eq. (4.3.1) involves four right-handed charged lepton fields and a coefficient of order $\mathcal{Y}_E^{-2}$. Using Eq. (4.1.45) and Eq. (4.1.10), the dependence on the charged lepton Yukawa coupling Y_E in the gauged-flavor case reads, in matrix notation,

$$-\frac{1}{2}\sum_k (-1)^k\,\overline{e}_R\frac{\gamma_\mu}{\left(Y_E^\dagger Y_E\right)^k}e_R\,\overline{e}_R\gamma_\mu\left(Y_E^\dagger Y_E\right)^{k+1}e_R+\frac{1}{4\mathrm{Tr}\left[Y_E^\dagger Y_E\right]}\left(\overline{e}_R\gamma_\mu Y_E^\dagger Y_E e_R\right)^2\,, \tag{4.3.4}$$

where $1/(1+x)=\sum(-x)^n$ has been used. In contrast, within the MLFV prescription the Lagrangian term would be given by

$$\text{MFV:}\qquad \frac{1}{\Lambda^2}\left(\overline{e}_R\gamma_\mu Y_E^\dagger Y_E e_R\right)\left(\overline{e}_R\gamma_\mu e_R\right)\,, \tag{4.3.5}$$

at leading order. In consequence, the spurion dependences do not match even if formally both are of order Y_E^2. Furthermore, only two leptons are involved in a non-trivial flavor structure in the MLFV case instead of four in the gauged-flavor scenario. In both cases, although this operator induces LUV, it does not induce LFV which is the distinctive feature of MLFV to which we now turn.

The second term in the third line of the Lagrangian Eq. (4.3.1) exhibits a combination of two operators which induce LFV transitions —weighted down by $\mathcal{Y}_N^{-2}$— which can be compared to the operators $O_{4L}^{(1)}$, $O_{4L}^{(2)}$, $O_{4L}^{(3)}$ of Ref. [310]. Those two operators are strongly suppressed in the gauged-flavor SM case as the $\mathcal{Y}_N$ scale is necessarily very high, while they may lead to visible effects in the context of the gauged-flavor type I Seesaw model in Section 4.2.1, as the scale associated to $\mathcal{Y}_N$ can be low enough even if $\mathcal{Y}_N > \|\mathcal{Y}_E\|$. In the following, to allow a fair comparison with MLFV we will focus on flavor non-conserving transitions and consider a CP-even limit of the gauged-flavor type I Seesaw model.

CP Invariance ($R = 1$, $\delta = 0$, $\alpha_{21} = \alpha_{31} = 0$)

In the CP-even limit considered, the combination of two operators appearing in the last term in Eq. (4.3.1),

$$-\frac{1}{2}\mathrm{Tr}\left[\frac{1}{\mathcal{Y}_N^\dagger \mathcal{Y}_N}\right]\left(\bar{\ell}_L^\alpha \gamma_\mu \ell_L^\beta\right)\left[c_\ell^{\alpha\beta\kappa\rho}\left(\bar{\ell}_L^\kappa \gamma^\mu \ell_L^\rho\right) + 2\, c_{\ell E}^{\alpha\beta\kappa\rho}\left(\bar{e}_R^\kappa \gamma^\mu e_R^\rho\right)\right], \tag{4.3.6}$$

is determined by the coefficients given by

$$c_\ell^{\alpha\beta\kappa\rho} = U_{\alpha i}^\dagger U_{j\beta} U_{\kappa r}^\dagger U_{s\rho}\, c_\ell^{ijrs}, \qquad c_{\ell E}^{\alpha\beta\kappa\rho} = U^{\alpha i\dagger} U^{j\beta}\, c_\ell^{ij\kappa\rho}, \tag{4.3.7}$$

with

$$\begin{aligned} c_\ell^{ijrs} =& \frac{1}{\sum_k m_{\nu_k}}\left(\frac{\delta_{is}\delta_{jr} m_{\nu_i} m_{\nu_r}(m_{\nu_i}^2 + m_{\nu_r}^2)}{\left(m_{\nu_i}^2 - m_{\nu_r}^2\right)(m_{\nu_i} - m_{\nu_r}) + \delta_{ir}(2m_{\nu_i})^3} + \right. \\ & \left. - \frac{2\delta_{ir}\delta_{js} m_{\nu_i}^2 m_{\nu_j}^2}{(m_{\nu_i}^2 - m_{\nu_j}^2)(m_{\nu_i} - m_{\nu_j}) - \delta_{ij}(2m_{\nu_i})^3} - \frac{\delta_{ij}\delta_{rs} m_{\nu_i} m_{\nu_r}}{2\sum_k m_{\nu_k}}\right), \end{aligned} \tag{4.3.8}$$

$$\begin{aligned} c_{\ell E}^{ij\kappa\rho} =& \frac{m_\kappa m_\rho}{m_\kappa^2 + m_\rho^2}\frac{1}{\sum_k m_{\nu_k}}\left(\frac{2U_{\kappa j}U_{i\rho}^\dagger m_{\nu_i} m_{\nu_j}(m_{\nu_i}^2 + m_{\nu_j}^2)}{(m_{\nu_i}^2 - m_{\nu_j}^2)(m_{\nu_i} - m_{\nu_j}) + \delta_{ij}(2m_{\nu_i})^3} + \right. \\ & \left. - \frac{4U_{\kappa i}U_{j\rho}^\dagger m_{\nu_i}^2 m_{\nu_j}^2}{(m_{\nu_i}^2 - m_{\nu_j}^2)(m_{\nu_i} - m_{\nu_j}) - \delta_{ij}(2m_{\nu_i})^3} - \frac{\sum_k U_{\kappa\gamma} m_{\nu_k} U_{\gamma\rho}^\dagger\, \delta_{ij} m_{\nu_i}}{\sum_k m_{\nu_k}}\right), \end{aligned} \tag{4.3.9}$$

where the c_ℓ coefficients correspond to transitions between purely left-handed leptons, while $c_{\ell E}$ correspond to left-right mixed terms.[14] Alike to the comparison between the operators in Eqs. (4.3.4) and (4.3.5), the Yukawa dependence of the gauged-flavor model cannot be matched in this case to that in standard approaches to MLFV [78,310]; we will compare here for definiteness with the "extended" model in Ref. [78] for which the MLFV ansatz would suggest a coupling proportional to[15]

$$\bar{\ell}_L \gamma_\mu U\, m_\nu^{diag}\, U^\dagger \ell_L\, \bar{\ell}_L \gamma^\mu \ell_L\,. \tag{4.3.10}$$

[14] The coefficients $c_{\ell E}^{ij\gamma\delta}$ appear suppressed with respect to c_ℓ^{ijkl} by a factor $m_\gamma m_\delta/(m_\gamma^2 + m_\delta^2)$. This implies that left-right $c_{\ell E}$ contributions to transitions between leptons of neighboring flavors (e.g. $\mu \to eee$ and $\tau \to \mu\mu\mu$) are larger than between the third to the first generations (e.g., $\tau \to eee$ or $\tau \to \mu ee$).

[15] In the notation of our gauged-flavor type I Seesaw model in Section 4.2, the coefficient in front of this equation would read $(v^2\, \mu_{LN})^{-1}$, see Footnote 9.

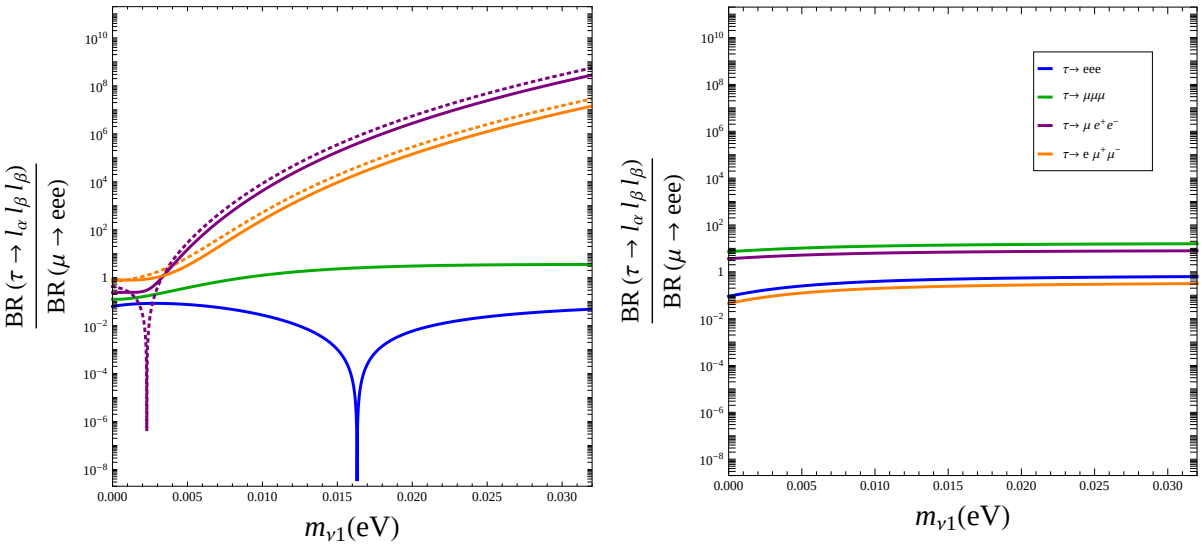

(a) Gauged Flavor, NO **(b)** MLFV, NO

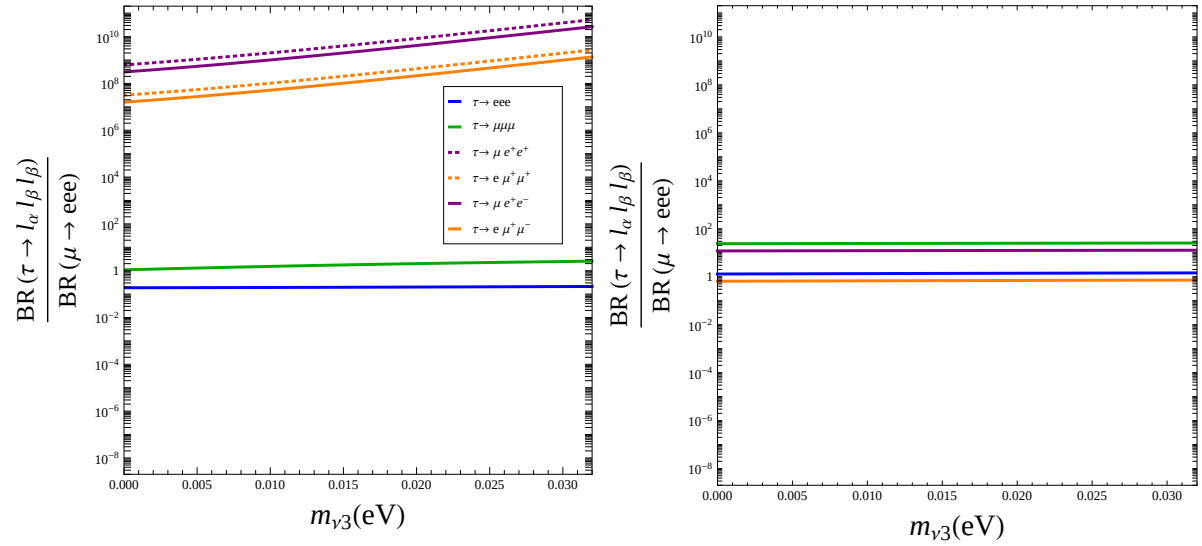

(c) Gauged Flavor, IO **(d)** MLFV, IO

Figure 4.9: Comparison between the gauged-flavor type-I Seesaw scenario and MLFV in a CP-even case: branching ratios for the different lepton rare decays over that for $\mu \to eee$, for neutrino normal ordering (NO) and inverted ordering (IO).

The differences in the operator coefficients in Eqs. (4.3.6)–(4.3.9) versus Eq. (4.3.10) translate into distinctive phenomenological signals; as an illustration, the branching ratios for various $l_\alpha \to l_\beta l_\rho^+ l_\kappa^-$ processes are compared in Fig. 4.9. A first clear difference is the absence of processes that violate lepton flavor by two units in the MLFV case, e.g., $\tau \to \mu e^+ e^+$ and $\tau \to e\mu^+\mu^+$ (the dashed lines in the gauged-flavor case). These processes are suppressed in MLFV by higher-order spurion insertions, while the more intricate dependence on Yukawa couplings of the gauged-flavor case allows them at leading order.

A second prominent feature depicted in Fig. 4.9 is the strong hierarchy between two different type of decays in the gauged-flavor scenario, for inverted neutrino hierarchy and also for normal ordering with large m_{ν_1}: transitions involving only one flavor in the final state are much suppressed, see Figs. 4.9a and 4.9c, unlike in MLFV, Figs. 4.9b and 4.9d. In consequence, the dominant channels for the gauged-flavor scenario are $\tau \to \mu ee$ and $\tau \to e\mu\mu$ (in purple and orange). This hierarchy can be understood in terms of symmetry. If the three light neutrinos are almost degenerate, an approximate $SO(3)_{\ell+N}$ remains unbroken, as already pointed out in Refs. [301, 302]. The three corresponding gauge bosons would therefore be lighter than the rest with masses proportional to the neutrino mass splittings and thus suppressed by a factor $(m_{\nu_i} - m_{\nu_j})/(m_{\nu_i} + m_{\nu_j})$. The lightest of these gauge bosons corresponds to the smallest mass splitting ($\Delta m^2_{sol} \approx 7.50 \times 10^{-5}$ eV^2) between m_{ν_2} and m_{ν_1}, and dominates the contribution for inverted neutrino hierarchy as well as for normal ordering with large m_{ν_1}. Because the couplings of this lightest flavor gauge boson are given by the generator of $SO(2)$ rotations, which is antisymmetric in flavor, a selection rule for the decays follows. This can be seen explicitly in the limit $\Delta m_{sol} \ll \sum m_{\nu_i}$ in which Eqs. (4.3.6)–(4.3.8) simplify to

$$\simeq -\frac{\left\|\mathcal{Y}_N^{-1}\right\|^2}{54}\frac{(\sum_k m_{\nu_k})^2}{\Delta m^2_{sol}}\left(U_{\alpha 1}U^\dagger_{2\beta} - U_{\alpha 2}U^\dagger_{1\beta}\right)\left(U_{\gamma 1}U^\dagger_{2\delta} - U_{\gamma 2}U^\dagger_{1\delta}\right)\bar{\ell}^\alpha_L\gamma_\mu\ell^\beta_L\bar{\ell}^\gamma_L\gamma^\mu\ell^\delta_L\,,$$

from which it follows that whenever two flavors coincide, given the assumption of CP invariance the corresponding operator coefficient vanishes an hence $l \to l'l'l'$ cancels, whereas for more than two flavors involved

$$\frac{\mathrm{Br}\,(\tau \to \mu ee)}{\mathrm{Br}\,(\tau \to \mu\mu e)} = \frac{\sin^2(\theta_{23})}{\sin^2(\theta_{13})} \sim 20\,. \tag{4.3.11}$$

In contrast, in MLFV the $\tau \to \mu\mu\mu$ and $\tau \to eee$ branching ratios are a factor two –due to combinatorics– times those for $\tau \to \mu e^+ e^-$ and $\tau \to e\mu^+\mu^-$, respectively, see Figs. 4.9b and 4.9d.

4.4 Conclusions

We have considered the gauging of leptonic global flavor symmetries that the SM Lagrangian or its fermionic Seesaw extension exhibit in the limit of negligible light lepton masses. A remarkable consequence is that the gauge anomaly cancellation conditions point to a universal underlying Seesaw pattern for both charged and neutral leptons:

- The gauging of the flavor symmetry $SU(3)_\ell \times SU(3)_E$ of the SM Lagrangian (that is, without assuming right-handed neutrinos) leads to the minimal type I Seesaw scenario as the simplest realization in terms of extra fields needed. In other words, without assuming Majorana neutrino masses, the gauging procedure suggests them directly.

- Starting instead from the maximal flavor symmetry of the type I Seesaw Lagrangian, $SU(3)_\ell \times SU(3)_E \times SO(3)_N$, leads to a double Seesaw and in particular an inverse Seesaw pattern.

This study extends previous work on gauging the flavor symmetries of the SM quark sector, which had already shown the existence of a Seesaw-like pattern that protected the model from the customary FCNC issues which tend to be the graveyard of attempts to understand dynamically the flavor puzzle. Interesting signals and correlations have been identified here as a result of gauging the maximal non-abelian flavor symmetries of the SM and of the type I Seesaw Lagrangian. The main leptonic flavor signals expected tend to involve the heavier SM leptons, whose interactions are less constrained by present data.

In the leptonic gauged-flavor SM case, the expected phenomenological signals are flavor-conserving, and include charged-lepton universality violation and non-unitarity of the PMNS matrix that follow from the (flavor diagonal) modifications of the couplings of leptons to Z and W bosons, particularly prominent for τ-related observables. Furthermore, the first particles awaiting discovery would be a tau mirror lepton and $SU(3)_E$ gauge bosons which mediate $\mu_R - \tau_R$ transitions.

Gauging instead the maximal lepton flavor symmetry of type I Seesaw may lead not only to signals of lepton universality violation but also to putatively observable flavor non-conserving transitions among charged leptons. The dominant signals expected depend mainly on the relative hierarchy of the scalar vevs that generate the charged lepton masses $\|\mathcal{Y}_E\|$ versus those that generate the neutrino ones $\|\mathcal{Y}_N\|$ and the LN scale. When all $\mathcal{Y}_E$ vevs are larger than $\|\mathcal{Y}_N\|$, the leading transitions are again flavor-conserving, while the lightest states in the spectrum are mirror neutrinos and gauge bosons whose mass is determined by $\|\mathcal{Y}_N\|$. In the opposite case, that is for $\|\mathcal{Y}_N\| > \|\mathcal{Y}_E\|$, the lowest states are again the mirror tau lepton and the three $SU(3)_E$ gauge bosons which mediate transitions in the $\mu_R - \tau_R$ sector. Of particular interest is the fact that Majorana masses within an approximate $U(1)$ lepton number symmetry setup are allowed, associated to the inverse Seesaw structure that results naturally from the requirement of gauge anomaly cancellation; it is precisely because the lepton scale is then distinct from the lepton number scale, that the latter can be low enough to expect sizeable flavor-changing signals. The precise phenomenology depends much on the CP pattern of the model. For the generic case of CP violation and (almost degenerate) neutrinos, $\mu \to eee$ is at present the most sensitive flavor non-conserving channel.

The results have been also compared with the phenomenological predictions of leptonic minimal flavor violation. We have shown that the presence of additional flavor gauge bosons may provide distinct low-energy transitions among the SM fields. It is also remarkable that the gauging of the lepton flavor symmetries provides a mechanism to protect against extra sources

of CP violation beyond those in the SM (and Seesaw type I), which is absent in generic minimal lepton flavor violation scenarios. In addition, flavor changing transitions among charged leptons involving more than two distinct leptons tend to be stronger than those in which a tau or muon decays into three equal leptons, in contrast again with generic minimal flavor violation. The impact of scalar flavor excitations is model-dependent and remains to be studied in detail, although it is expected to abide by the same flavor protection than the rest of the theory.

The necessary mediation of at least one BSM field is at the basis of the Seesaw mechanism for the generation of light neutrino Majorana masses; it is very suggestive that the mass mechanism for light fermions –quarks and leptons– which results from gauging the flavor symmetries corresponds qualitatively to the same pattern. Interestingly, other theoretical constructions such as "partial compositeness" lead as well to a universal Seesaw-like pattern behind fermion masses; if new flavor signals are indeed observed, an extended and detailed study of many flavor channels will be needed to disentangle a possible flavored-gauge origin. The main drawback of our construction is our ignorance about the absolute value of the scales involved, that could render the predictions of these models out of reach in the foreseeable future. Yet, the quest to identify a dynamical origin to the flavor puzzle is a fundamental and fascinating endeavour plausibly awaiting discovery.

CHAPTER 5

Color Unified Dynamical Axion

In this Chapter, which is based on the publication in Ref. [4], we develop a new solution to the strong CP problem via massless fermions, in which the issue of the different θ parameters that arise in the presence of two or more confining groups is solved via color unification. Color unification with massless quarks is attempted here for the first time. This path is an alternative to the axicolor-type constructions and will lead to different phenomenology. QCD will be unified with another confining sector singlet under the electroweak gauge symmetry. The color unified theory (CUT) breaks spontaneously to QCD and another confining group. The small-size instantons of the unified color group provide an extra source of high masses for the axions of the theory, and it will be shown that typically no axion remains at low scales. The exotic low-energy spectrum is instead fermionic. Furthermore, it will be shown that interesting new phenomenological signals can be explored at colliders. The complete ultraviolet completion of this idea will be developed, implementing two different scenarios: in one of them the two resulting heavy axions are dynamical, while in the other one axion is elementary.

5.1 SU(6) Color Unification

We propose a scenario in which QCD is unified with another confining group into $SU(6)$, and a single, strictly massless $SU(6)$ fermion rotates away simultaneously all θ parameters. The unification path in the context of an extended strong sector to solve the strong CP problem was first proposed by Rubakov long ago [170], in a Grand Unification construction that relied on traditional models *à la* DFSZ [203, 204] with massive exotic fields, and required a Z_2 mirror copy of the complete SM field content. Another recent attempt [177] using unification ideas also relied on massive exotic fermions *à la* DFSZ. Here we instead consider color unification in the presence of massless fermions. The massless $SU(6)$ fermion belongs to the 20 representation of the $SU(6)$ CUT, having a definite chirality (e.g. left-handed) while being a singlet of the SM $SU(2)_L \times U(1)_Y$ gauge symmetry:

	$SU(6)$	$SU(2)_L$	$U(1)$
Ψ_L	20	1	0

Table 5.1: The massless fermion sector of the $SU(6)$ construction above the unification scale.

At a color unification scale $\Lambda_{\rm CUT}$ much higher than the EW one, the $SU(6)$ group breaks into

$$SU(6) \xrightarrow{\Lambda_{\rm CUT}} SU(3)_c \times SU(\tilde{3}) \times U(1)\,. \tag{5.1.1}$$

The parameters θ_c of $SU(3)_c$ and $\tilde{\theta}$ of $SU(\tilde{3})$ are necessarily equal and unphysical down to the unification scale, and will remain so even below the unification scale as long as Ψ remains massless, protected by chiral symmetry. Under spontaneous symmetry breaking of the CUT symmetry, Ψ decomposes as

$$\Psi_L(20) = (1,1)(-3)_L \; + \; (1,1)\,(+3)_L + \; (3,\bar{3})\,(-1)_L + \; (\bar{3},3)(+1)_L\,, \tag{5.1.2}$$

where the charges under the $U(1)$ group in Eq. (5.1.1) are shown in parenthesis for completeness. If the components of the Ψ_L field are to remain massless under the CUT scale, $SU(\tilde{3})$ must confine. The two confining scales $\Lambda_{\rm QCD}$ and $\tilde{\Lambda}$ need to be separated with $\tilde{\Lambda} \gg \Lambda_{\rm QCD}$, as no bound states are observed other than those compatible with QCD. The 20-dimensional representation is thus advantageous because all its components charged under QCD are also charged under $SU(\tilde{3})$, and so will form bound states at the higher scale $\tilde{\Lambda}$. This representation is also pseudo-real, and so the theory is anomaly free. The non-trivial issue of how to separate $\tilde{\Lambda}$ and $\Lambda_{\rm QCD}$ is discussed further below.

	$SU(3)_c$	$SU(\tilde{3})$
ψ_L	$\square$	$\square$
ψ_L^c	$\square$	$\square$
$2 \times \psi_\nu$	1	1

Table 5.2: The massless fermion sector of the $SU(6)$ construction below the unification scale. The notation is such that $\psi_L^c \equiv (\psi^c)_L = (\psi_R)^c$.

The colored-axicolored massless fermions in Eq. (5.1.2) will be denoted $\psi_{L,R}$, see Table 5.2, while ψ_ν will refer to the singlet massless fermions to convey that they act like sterile[1] neutrinos. The ψ_ν fields only connect to the other fields through the unified strong forces, and thus their couplings to the visible universe will be safely suppressed by $\Lambda_{\rm CUT}$, provided the $U(1)$ gauge group in (5.1.1) is also broken near that scale.[2]

[1] By "sterile fermion" is meant any fermion which is not charged under the SM gauge group.
[2] This breaking will become manifest in the next section.

$SU(6)$ color unification is thus a successful path to solve the strong CP problem, and this fact will remain at the heart of the developments in this Chapter. The remaining problem is to obtain a low-energy spectrum which is fully compatible with observations.

The SM fermions

Because of color unification, the SM quarks must belong to $SU(6)$ multiplets. The simplest option is to include them in six-dimensional fundamental representations. For each fermion generation,

$$Q_L(6) \equiv (q\,,\,\tilde{q})_L\,, \qquad U(6) \equiv (u\,,\,\tilde{u})_R\,, \qquad D(6) \equiv (d\,,\,\tilde{d})_R\ , \tag{5.1.3}$$

where q_L, u_R and d_R denote the SM quarks, while their $SU(6)$ partners are signaled by tildes. The $\tilde{q}_L$ fields are necessarily electroweak doublets, and this character turns out to be the major practical issue of this model:

- Leaving the tilde-quark sector massless but confined is unacceptable, as the condensate — assuming chiral symmetry breaking of $SU(\tilde{3})$ — would typically break the SM EW symmetry at the large $\tilde{\Lambda}$ scale.
- Alternatively, giving much larger masses ($\geq \tilde{\Lambda}$) to the tilde quarks is not viable either in this $SU(6)$ setup without spoiling SM quark masses, since they belong to the same multiplet. If a scalar field gave high masses to the tilde quarks [3] by obtaining a high vacuum expectation value (vev), that scalar field would have to be an $SU(2)_L$ doublet. Then its large vev would spontaneously break SM EW symmetry, giving gigantic masses to the W and Z boson.

The main problem of this model is then the unacceptably light tilde-fermion sector. We will develop next an extension whose only purpose is precisely to achieve high masses for the tilde-sector quarks, decoupling them from the low-energy spectrum. By the same token, the necessary separation of $\Lambda_{\rm QCD}$ and a larger confining scale will naturally follow.[4] We will develop in detail two realistic ultraviolet (UV) completions.

5.2 The realistic Color Unified Theory: $SU(6) \times SU(3')$

It is necessary to give large masses to the tilde-quark sector without giving masses to the SM quarks, a challenging enterprise as explained above due to the $SU(6)$ unification. An external mechanism is ideal for this task. The color unified $SU(6)$ group which contains QCD is enlarged via an external non-abelian $SU(3')$ group with additional fermions charged only under the latter.

[3] Through tuned Yukawa couplings of the tilde-quark sector to an extended scalar sector.

[4] If $SU(6)$ sufficed to obtain a realistic spectrum, the $SU(\tilde{3})$ group and $\tilde{\Lambda}$ scale of this section would correspond to those of the axicolor group [202] as described in the introduction. The extension of the CUT group will break this direct correspondence, although two confining groups will still be at play.

	$SU(6)$	$SU(3')$
Q_L	$\square$	1
U_L^c	$\square$	1
D_L^c	$\square$	1
Ψ_L	20	1
q'_L	1	$\square$
u'^c_L	1	$\square$
d'^c_L	1	$\square$
Δ	$\square$	$\square$

	$SU(3)_c$	$SU(3)_{\rm diag}$	$SU(2)_L$	$U(1)_Y$
q_L	$\square$	1	$\square$	$\frac{1}{6}$
$\tilde{\mathbf{q}}_{\mathbf{L}}$	1	$\square$	$\square$	$\frac{1}{6}$
u_L^c	$\square$	1	1	$-\frac{2}{3}$
$\tilde{\mathbf{u}}^{\mathbf{c}}_{\mathbf{L}}$	1	$\square$	1	$-\frac{2}{3}$
d_L^c	$\square$	1	1	$\frac{1}{3}$
$\tilde{\mathbf{d}}^{\mathbf{c}}_{\mathbf{L}}$	1	$\square$	1	$\frac{1}{3}$
ψ_L	$\square$	$\square$	1	0
ψ_L^c	$\square$	$\square$	1	0
$2\times\psi_\nu$	1	1	1	0
$\mathbf{q}'_{\mathbf{L}}$	1	$\square$	$\square$	$-\frac{1}{6}$
$\mathbf{u}'^{\mathbf{c}}_{\mathbf{L}}$	1	$\square$	1	$\frac{2}{3}$
$\mathbf{d}'^{\mathbf{c}}_{\mathbf{L}}$	1	$\square$	1	$-\frac{1}{3}$
–	–	–	1	0

Table 5.3: The matter content. The table on the left describes matter above the CUT scale, while the one on the right gives the transformation properties under the gauge groups remaining after CUT spontaneous breaking. The fermions in bold have masses comparable to $\Lambda_{\rm CUT}$ and are integrated out around the CUT scale. The quantum numbers under the EW gauge group correspond both to the high-energy and low-energy fields.

In fact, all fermions in the theory will be charged under only one of the two groups, $SU(6)$ or $SU(3')$. Ψ_L will be thus taken to be a singlet of $SU(3')$ and the same applies to the multiplets in Eq. (5.1.3) which contain the SM quarks. The two sectors are connected exclusively via a new scalar Δ. QCD remains a subgroup of $SU(6)$, whose θ-parameter is rotated away by the massless Ψ_L fermion in Eq. (5.1.2). This type of auxiliary extension was suggested in Ref. [177] to give high masses to exotic fermions in a different context. The field content of our model is summarized in Table 5.3, in which all fermions except Ψ_L will become massive. It is easy to see that the theory with this matter content is anomaly free. The scalar Δ appearing in the table belongs to the bifundamental of $SU(6)\times SU(3')$, and its vev breaks color unification at a scale $\Lambda_{\rm CUT}$, taken to be much larger than all SM scales,

$$SU(6)\times SU(3') \xrightarrow{\Lambda_{\rm CUT}} SU(3)_c \times SU(3)_{\rm diag}\,. \tag{5.2.1}$$

The fermion quantum numbers under the two resulting groups are also shown in Table 5.3.

A simple CUT-invariant Yukawa Lagrangian which connects the $SU(6)$ and the auxiliary $SU(3')$ extension reads

$$\mathcal{L} \ni \kappa_q\, q'_L \Delta^* Q_L + \kappa_u\, u'^c_L \Delta\, U_L^c + \kappa_d\, d'^c_L \Delta D_L^c \;+\; \text{h.c.}\,. \tag{5.2.2}$$

The CUT symmetry is spontaneously broken upon Δ taking a vev of the order of the CUT breaking scale $\Lambda_{\rm CUT}$

$$\langle \Delta \rangle = \Lambda_{\rm CUT} \begin{pmatrix} 0 & 0 & 0 & 1 & 0 & 0 \\ 0 & 0 & 0 & 0 & 1 & 0 \\ 0 & 0 & 0 & 0 & 0 & 1 \end{pmatrix} . \tag{5.2.3}$$

This breaking generates a large mass for both the tilde- and prime-quark sectors, leaving massless only the SM fermion components of the original fermionic fields:[5]

$$\mathcal{L} \ni \Lambda_{\rm CUT} \left\{ \kappa_q \, q'_L \tilde{q}_L + \kappa_u \, u'^c_L \tilde{u}^c_L + \kappa_d \, d'^c_L \tilde{d}^c_L \right\} + \text{h.c.} . \tag{5.2.4}$$

Unless otherwise stated, we will assume in what follows that all κ_i Yukawa couplings are $\mathcal{O}(1)$, meaning all tilde and prime fermion masses are of order $\Lambda_{\rm CUT}$. Some tuning of the κ_i values could be acceptable, though, as discussed further below.

The SM fermions get their masses through the usual SM Higgs doublet Φ, which in this model is a singlet of $SU(6) \times SU(3')$, [6]

$$\mathcal{L} \ni Y_u^{SM} \, Q_L \Phi U^c_L + Y_d^{SM} \, Q_L \tilde{\Phi} D^c_L \, + \text{h.c.} , \tag{5.2.5}$$

where Y_i^{SM} denote the SM Yukawa couplings. Analogously, the most general Lagrangian compatible with all symmetries discussed above allows us to write Yukawa couplings of the Higgs field to the prime-sector fermions,

$$\mathcal{L} \ni y'_u \, q'_L \Phi u'^c_L + y'_d \, q'_L \tilde{\Phi} d'^c_L \, + \text{h.c.} . \tag{5.2.6}$$

Eqs. (5.2.5) and (5.2.6) induce contributions to the tilde fermion masses which are quantitatively irrelevant in comparison with those from Eq. (5.2.4). In addition, the couplings in Eq. (5.2.6) will be absent for symmetry reasons in one of the models to be developed in this work (Model II in Section 5.2.2).

Both $SU(3)_c$ and $SU(3)_{\rm diag}$ can now remain unbroken and confine at two different scales, $\Lambda_{\rm QCD}$ and $\Lambda_{\rm diag}$, with $\Lambda_{\rm diag} \gg \Lambda_{\rm QCD}$. The task of achieving different values for the two confining scales and getting rid of the tilde sector or any other dangerous exotic sector is thus accomplished.

Note that the Yukawa-type Lagrangian in Eq. (5.2.2) has an inherent global $U(1)$ symmetry under which only the prime fermions and the Δ field would transform – a generalized Baryon number symmetry in the prime sector, with charges

$$BN'\{\Delta, q'_L, u'^c_L, d'^c_L\} = \{+1, +1, -1, -1\} . \tag{5.2.7}$$

[5] Note that we take $\langle \Delta \rangle$ to be real. The phases of the nonvanishing entries in Eq. (5.2.3) can all be made equal by an $SU(6) \times SU(3')$ transformation; the remaining phase can be removed by a transformation under the $U(1)$ defined in Eq. (5.2.7).

[6] In this notation taken from unified models the contraction of the spinor indices is implicit, more precisely the first term would read $Q_L^T C \Phi U^c_L$, where $C = i\gamma_2\gamma_0$ is the charge conjugation matrix.

This symmetry is not chiral, thus not anomalous under $SU(3')$, and irrelevant to the strong CP problem. An associated pGB [7] results after spontaneous breaking, albeit with its couplings safely suppressed by the CUT scale and interacting only with the very heavy prime and tilde sectors.[8]

Finally, the theory below $\Lambda_{\rm CUT}$ contains phenomenologically interesting bound states formed from the massless $\psi_{L,R}$ fermions, to be studied below. The spectrum of free eigenstates below the EW scale contains the usual SM spectrum, plus a harmless pGB and sterile neutrinos.

θ' issue

The extension of the strong sector by the auxiliary external group $SU(3')$ brings a new θ' parameter into the game:

$$\mathcal{L} \supset \theta_6 \frac{\alpha_6}{8\pi} G_6 \tilde{G}_6 + \theta' \frac{\alpha'}{8\pi} G' \tilde{G}' \longrightarrow (\theta_6 + \theta') \frac{\alpha_{\rm diag}}{8\pi} G_{\rm diag} \tilde{G}_{\rm diag} + \theta_6 \frac{\alpha_c}{8\pi} G_c \tilde{G}_c \,, \tag{5.2.8}$$

where G_i denote gauge field strengths with tensorial indices omitted. G_c, G_6, G' and $G_{\rm diag}$ correspond respectively to the SM QCD gauge group, $SU(6)$, $SU(3')$ and $SU(3)_{\rm diag}$. While the rotation of the massless field Ψ was designed to reabsorb θ_6 and ultimately θ_c, θ' may source back a SM strong CP problem through the contamination to the visible sector via the Δ scalar.

Indeed, at low energies the massless quark ψ transforms as a $(3, \bar{3})$, therefore the phase θ_6 cannot be fully reabsorbed in the Lagrangian since the chiral rotation that removes the $SU(3)_c$ θ-term generates a new contribution to the $SU(3)_{\rm diag}$ topological term. Ref. [177] acknowledges this issue (in the context of a different model which does not rely on massless fermions) and leaves it unsolved hoping that some UV completion solves it. In what follows, we will determine and exhaustively analyze two UV solutions, via the simple addition of either

- An extra massless fermion transforming only under $SU(3')$.
- A second bifundamental scalar field, which automatically endows PQ invariance to the above extension procedure.

The first solution is more in line with the spirit of the present work, as *all* θ parameters inducing a strong CP problem are made unphysical via massless fermions, and it is developed next.

[7] This symmetry is broken at loop level by $SU(2)_L$ sphalerons, in the same way that in the SM baryon number current is anomalous. For our purposes this effect is negligible.

[8] As suggested in Ref. [179], this type of pGB could be entirely removed by gauging the U(1) group. There is no real need to implement this procedure in our case, though, given the strongly suppressed couplings of this pGB.

	$SU(6)$	$SU(3)'$	$SU(2)_L$	$U(1)_Y$	$SU(3)_c$	$SU(3)_{\text{diag}}$
χ	1	$\square$	1	0	1	$\square$

Table 5.4: The table shows on the left (right) the quantum numbers above (under) the CUT scale for the massless χ quarks which absorbs θ' in Model I.

5.2.1 Model I: Adding a massless fermion charged under $SU(3')$.

The θ' parameter of the auxiliary $SU(3')$ gauge group can be made unphysical by the addition of a massless fermion field χ that transforms as a fundamental of $SU(3')$ and is an EW and $SU(6)$ singlet. In other words, the field content for this solution is that previously shown in Table 5.3 plus the massless fermion χ with quantum numbers shown in Table 5.4. Additional composite bound states will result from χ, among them composite pseudoscalars with anomalous couplings — dynamical axions — whose masses are discussed further below.

Running of the coupling constants.

The CUT breaking pattern in Eq. (5.2.1) imposes the following relations among the gauge couplings

$$\frac{1}{\alpha_{\text{diag}}(\mu)} = \frac{1}{\alpha_6(\mu)} + \frac{1}{\alpha'(\mu)}\,, \qquad \text{at} \quad \mu = \Lambda_{\text{CUT}}\,, \tag{5.2.9}$$

with the constraint

$$\alpha_c(\Lambda_{\text{CUT}}) = \alpha_6(\Lambda_{\text{CUT}}), \tag{5.2.10}$$

where α_c, α_{diag}, α' and α_6 denote respectively the coupling strength of QCD, $SU(3)_{\text{diag}}$, $SU(3')$ and $SU(6)$. As shown in Fig. 5.1, there is a discontinuity in the running of the coupling constants at the CUT-breaking scale that allows α' to have large values while reproducing the known QCD running at low scales.[9] Those α' values will seed a source of large axion masses, as discussed in Section 5.2.1 further below.

Although the relation in Eq. (5.2.9) imposes $\alpha_{\text{diag}}(\Lambda_{\text{CUT}}) < \alpha_c(\Lambda_{\text{CUT}})$, the presence of the SM q_L, u_R, and d_R quarks at energies well below Λ_{CUT} slows down the running of QCD with respect to that of $SU(3)_{\text{diag}}$. In this regime ψ and χ are the only fields left charged under $SU(3)_{\text{diag}}$ (the $\tilde{q}$ sector generically decouples as their mass scale is set by Λ_{CUT}, see Eq. (5.2.4)). As a consequence, α_{diag} runs faster and thus the $SU(3)_{\text{diag}}$ group confines at a higher scale than Λ_{QCD}, see Fig. 5.1. This mechanism easily achieves the separation of the two confining scales. We computed both the one- and two-loop running and the latter actually reinforces the

[9] Fig. 5.1 assumes a zero χ mass. As will be shown in Sec 5.2.1, χ acquires an effective mass due to small-size instanton effects. Threshold effects near m_χ may alter the running. Even when these effects are large enough to be noticeable, Fig. 5.1 still captures the qualitative behavior of the RG flow.

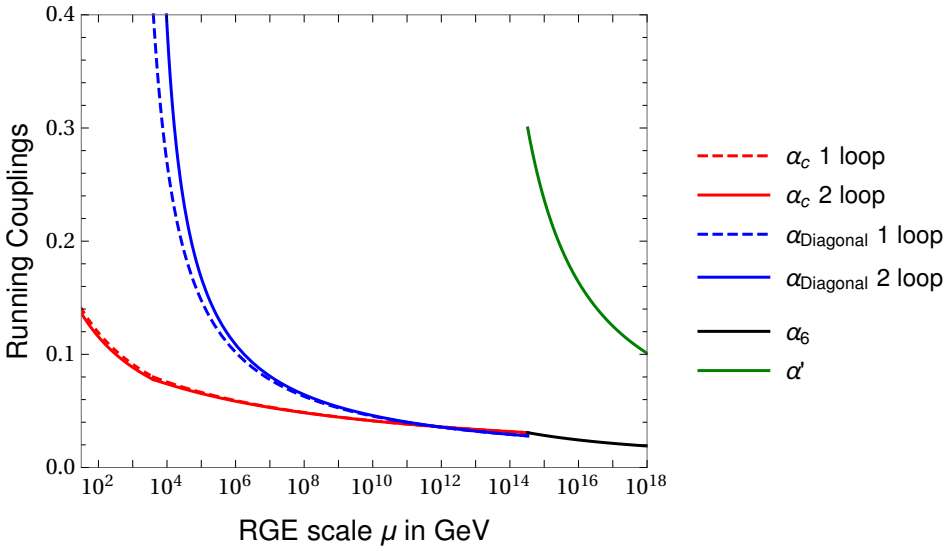

Figure 5.1: Running of $\alpha_{\rm QCD}$, $\alpha_{\rm diag}$, α_6, and α' in the model with the one extra $SU(3')$ fermion of Table 5.4. The full matter content is given by both Tabs. 5.3 and 5.4. The inputs used are $\alpha'(\Lambda_{\rm CUT}) = 0.3$ and $\Lambda_{\rm CUT} = 3.3 \times 10^{14}$ GeV for illustration, which results in $\Lambda_{\rm diag} = 4$ TeV (taken as a benchmark point). The solid (dashed) lines correspond to the two (one) loop results.

pattern, as illustrated in the figure for the choice $\Lambda_{\rm diag} = 4$ TeV. Lower values of $\Lambda_{\rm diag}$ are also phenomenologically acceptable, see Section 5.3.1 below.

Confinement of $SU(3)_{\rm diag}$ and pseudoscalar anomalous couplings to the confining interactions

	$SU(3)_c$	$SU(3)_{\rm diag}$
ψ_L	$\square$	$\square$
ψ_L^c	$\square$	$\square$
χ_L	1	$\square$
χ_L^c	1	$\square$

Table 5.5: The massless quark sector charged under $SU(3)_{\rm diag}$ remaining below the confining scale $\Lambda_{\rm diag}$.

At the scale $\Lambda_{\rm diag}$, $SU(3)_{\rm diag}$ confines and the remaining massless fermions will form massive QCD-colored bound states.

Assuming that both ψ and χ in Table 5.5 remain massless after $SU(3)_{\rm diag}$ confinement, the $SU(3)_{\rm diag}$ Lagrangian exhibits, at the classical level and in the limit in which α_c is switched off, a global flavor symmetry $U(4)_L \times U(4)_R \longrightarrow U(4)_V$. [10] The chiral symmetry is then spontaneously broken by the quark condensates $\langle \bar{\psi}_L \psi_R \rangle$ and $\langle \bar{\chi}_L \chi_R \rangle$. This results in 16 (p)GBs,

$$16 = 8_c + \bar{3}_c + 3_c + 1_c + 1_c \,, \tag{5.2.11}$$

decomposed here in terms of their QCD charges. There is a QCD octet plus a singlet with flavor content $\bar{\psi}\psi$ ($\bar{3}_c \times 3_c = 8_c + 1_c$). The two QCD triplets, 3_c and $\bar{3}_c$, correspond to the combinations $\bar{\psi}\chi$ and $\bar{\chi}\psi$. Finally, a color-singlet composite state is made out of $\bar{\chi}\chi$. The fourteen colored mesons in Eq. (5.2.11) acquire large masses induced by gluon loops that are quadratically divergent and therefore sensitive to the cutoff scale $\Lambda_{\rm diag}$, [11]

$$m^2(8_c) \approx \frac{9\,\alpha_{\rm c}}{4\pi}\Lambda^2_{\rm diag} \,, \qquad\qquad m^2(\bar{3}_c) \approx m^2(3_c) \approx \frac{\alpha_{\rm c}}{\pi}\Lambda^2_{\rm diag} \,. \tag{5.2.12}$$

The remaining two QCD singlets will be denoted here by η'_ψ and η'_χ and are shown next to be dynamical axions. The associated currents are

$$j^\mu_{\psi_A} = \bar{\psi}\gamma^\mu\gamma^5 t^9 \psi \equiv f_{\rm d}\,\partial^\mu \eta'_\psi \,, \qquad t^9 = \frac{1}{\sqrt{6}}\mathbb{1}_{3\times 3} \,, \tag{5.2.13}$$

$$j^\mu_{\chi_A} = \bar{\chi}\gamma^\mu\gamma^5 \chi \equiv f_{\rm d}\,\partial^\mu \eta'_\chi \,, \tag{5.2.14}$$

where $f_{\rm d}$ denotes the $SU(3)_{\rm diag}$ pGB scale, with $\Lambda_{\rm diag} \leq 4\pi f_{\rm d}$. These classically conserved currents are broken at the quantum level by the $SU(6)$ and $SU(3')$ instantons, and so the currents are anomalous. The anomalous terms are

$$\partial_\mu j^\mu_{\psi_A} = -\sqrt{6}\frac{\alpha_6}{8\pi}G_6\tilde{G}_6 \;\longrightarrow -\sqrt{6}\,\frac{\alpha_{\rm diag}}{8\pi}G_{\rm diag}\tilde{G}_{\rm diag} - \sqrt{6}\,\frac{\alpha_c}{8\pi}G_c\tilde{G}_c \,, \tag{5.2.15}$$

$$\partial_\mu j^\mu_{\chi_A} = -2\frac{\alpha'}{8\pi}G'\tilde{G}' \;\longrightarrow -2\,\frac{\alpha_{\rm diag}}{8\pi}G_{\rm diag}\tilde{G}_{\rm diag} \,. \tag{5.2.16}$$

These anomalous terms modify the classical equations of motion of the η'_ψ and η'_χ,

$$f_{\rm d}\,\Box\,\eta'_\psi = -\sqrt{6}\frac{\alpha_6}{8\pi}G_6\tilde{G}_6 \,, \tag{5.2.17}$$

$$f_{\rm d}\,\Box\,\eta'_\chi = -2\frac{\alpha'}{8\pi}G'\tilde{G}' \,, \tag{5.2.18}$$

and give rise to an effective Lagrangian,

$$\mathcal{L} \supset -\frac{\alpha_6}{8\pi}\,\frac{\sqrt{6}\,\eta'_\psi}{f_{\rm d}}\,G_6\tilde{G}_6 - \frac{\alpha'}{8\pi}\,\frac{2\,\eta'_\chi}{f_{\rm d}}G'\tilde{G}' \;\longrightarrow -\frac{\alpha_c}{8\pi}\,\frac{\sqrt{6}\,\eta'_\psi}{f_{\rm d}}\,G_c\tilde{G}_c - \frac{\alpha_{\rm diag}}{8\pi}\left(2\,\frac{\eta'_\chi}{f_{\rm d}} + \sqrt{6}\,\frac{\eta'_\psi}{f_{\rm d}}\right)G_{\rm diag}\tilde{G}_{\rm diag} \,. \tag{5.2.19}$$

[10] $U(4)_V$ remains unbroken and contains as a subgroup the $SU(3)_c$ QCD gauge group.

[11] They contribute to the running of the QCD coupling constant, but given their high masses their impact is unnoticeable.

η'_ψ and η'_χ are thus two dynamical axions. It is to be stressed that the PQ scale in this model is $f_{\rm d} \sim \Lambda_{\rm diag}$ for both axions and not the much larger $\Lambda_{\rm CUT}$ scale. When the SM quarks are taken into account, the $\eta'_{\rm QCD}$ pseudoscalar meson is also present at energies below the QCD confinement scale, and the effective Lagrangian of anomalous couplings reads

$$\mathcal{L} \supset -\frac{\alpha_{\rm diag}}{8\pi}\left(2\,\frac{\eta'_\chi}{f_{\rm d}}+\sqrt{6}\,\frac{\eta'_\psi}{f_{\rm d}}\right)G_{\rm diag}\tilde{G}_{\rm diag}-\frac{\alpha_c}{8\pi}\left(2\,\frac{\eta'_{\rm QCD}}{f_\pi}+\sqrt{6}\,\frac{\eta'_\psi}{f_{\rm d}}\right)G_c\tilde{G}_c\,, \tag{5.2.20}$$

where $\Lambda_{\rm QCD} \leq 4\pi f_\pi$.

$$V_{eff}=\frac{\mathcal{E}^4_{\rm diag}}{2}\left(2\,\frac{\eta'_\chi}{f_{\rm d}}+\sqrt{6}\,\frac{\eta'_\psi}{f_{\rm d}}\right)^2+\frac{\mathcal{E}^4_{\rm QCD}}{2}\left(2\,\frac{\eta'_{\rm QCD}}{f_\pi}+\sqrt{6}\,\frac{\eta'_\psi}{f_{\rm d}}\right)^2. \tag{5.2.21}$$

The scale $\mathcal{E}_{\rm QCD}$ can be expressed in terms of QCD observables from the chiral effective Lagrangian according to the results from Refs. [187, 361, 362] obtained in the large N limit. In the two-quark approximation, $\mathcal{E}_{\rm QCD}$ reads

$$\mathcal{E}^4_{\rm QCD}=\frac{f_\eta^2 m_\eta^2-f_\pi^2 m_\pi^2}{4}\simeq(202\,{\rm MeV})^4\simeq\Lambda^4_{\rm QCD}\,, \tag{5.2.22}$$

and $\mathcal{E}_{\rm diag}$ is obtained by rescaling the previous value

$$\mathcal{E}^4_{\rm diag}=\mathcal{E}^4_{\rm QCD}\left(\frac{\Lambda_{\rm diag}}{\Lambda_{\rm QCD}}\right)^4\simeq\Lambda^4_{\rm diag}\,. \tag{5.2.23}$$

As a consequence, the two instanton-induced scales $\Lambda_{\rm QCD}$ and $\Lambda_{\rm diag}$ provide a contribution to the masses of the pseudoscalars which have anomalous couplings.

It follows that there are only two sources of mass (disregarding corrections from SM quark masses) for three states coupling to anomalous currents: $\eta'_{\rm QCD}$, η'_ψ and η'_χ. In the absence of supplementary mass sources, one axion would get a mass of order $\Lambda_{\rm diag}$ while another one would have remained almost massless, as often happens in models with dynamical axions. The model would be simply an ultraviolet implementation of the invisible axion paradigm.

As we will see next, an additional and important instanton source of mass for the axions is present, though, which lifts the light axion mass. In fact, depending on the model parameters, the χ fermion mass itself may: i) still be lighter than $\Lambda_{\rm diag}$, in which case the above discussed $U(4)$ pattern of global symmetry holds; ii) alternatively, become more massive than $\Lambda_{\rm diag}$ and thus be decoupled from the spectrum above $\Lambda_{\rm diag}$. In the latter case, the approximate global flavor symmetry of the $SU(3)_{\rm diag}$ Lagrangian would instead be $U(3)_L \times U(3)_R \longrightarrow U(3)_V$, suggesting 9 (p)GBs,

$$9 = 8_c + 1_c\,. \tag{5.2.24}$$

The mass of this QCD-colored octet pseudoscalar is as previously given in Eq. (5.2.12) above, while the η'_χ would then disappear from the spectrum at energies above $\Lambda_{\rm diag}$: the presence of η'_χ is to be then disregarded in Eqs. (5.2.14)-(5.2.21).

The impact of small-size instantons on the dynamical axion mass

An additional and putatively large contribution to the axion mass(es) applies in the presence of a spontaneously broken theory: the small-size instantons (SSI) of the theory at the breaking scale, as pointed out long ago in Refs. [249, 250, 363] and very recently in Ref. [179]. SSI can induce a large mass even for perturbative theories if the breaking scale is large enough to overcome the exponential suppression of instanton effects. In our model, the instantons of the color-unified theory in Eq. (5.2.1) near the $\Lambda_{\rm CUT}$ scale provide automatically this third source of axion mass. The $SU(6)$ SSI can be neglected because of the smallness of α_6 at $\Lambda_{\rm CUT}$ (e.g. see Fig. 5.1) and the analysis below will focus on the $SU(3')$ SSI contribution.

At the scales where we will compute the SSI effects, the $SU(3')$ gauge coupling is perturbative. Therefore, for these instantons, the dilute gas approximation [130] gives a reliable estimate of the effective potential for the pseudoscalars. This was not the case for the previous instanton effects which, corresponding to the confinement scales, required the use of the effective chiral Lagrangian to obtain the potential from QCD observables.

It is well known [113, 129, 130, 364] that, in the absence of fermions, the effective Lagrangian that describes instanton configurations for a pure Yang-Mills theory $SU(N_c)$ induces a scale $\Lambda_{\rm inst}$ in the instanton potential given by

$$\Lambda_{\rm inst}^4 = \int \frac{d\rho}{\rho^5} D[\alpha'(1/\rho)] \,, \tag{5.2.25}$$

where ρ is the instanton size, $D[\alpha']$ is the dimensionless instanton density,

$$D[\alpha'(1/\rho)] = C_{inst} \left(\frac{2\pi}{\alpha'(1/\rho)} \right)^{2N_c} e^{-2\pi/\alpha'(1/\rho)} \,. \tag{5.2.26}$$

The constant C_{inst} reads [365, 366]

$$C_{inst}(N_c) = \frac{4}{\pi^2} \frac{2^{-2N_c} e^{-c(1)-2(N_c-2)c(1/2)}}{(N_c-2)!\,(N_c-1)!} \,, \tag{5.2.27}$$

and the function $c(x)$ is defined in Ref. [113] such that $c(1/2) = 0.145873$ and $c(1) = 0.443307$. For the $SU(3')$ instantons of our model $C_{inst} = 0.0015$.[12] In order to compute the integral in Eq. (5.2.25), the running of the coupling constant $\alpha'(\mu)$ must be included. At one loop this reads

$$\frac{2\pi}{\alpha'(\mu)} = b \, \ln\left(\mu/\Lambda_{\rm CUT}\right) + \frac{2\pi}{\alpha'_{\rm CUT}} \,, \tag{5.2.28}$$

where $\alpha'_{\rm CUT} \equiv \alpha'(\Lambda_{\rm CUT})$ and b is the one-loop β-function coefficient. For the spontaneously broken theory, only the SSI instantons with size $\leq 1/\Lambda_{\rm CUT}$ are relevant [367],

$$\Lambda_{\rm SSI}^4 = C_{inst} e^{-2\pi/\alpha'_{\rm CUT}} \int_0^{1/\Lambda_{\rm CUT}} \frac{d\rho}{\rho^5} \left(\rho\Lambda_{\rm CUT}\right)^b \left(-b \, \ln\left(\rho\Lambda_{\rm CUT}\right) + \frac{2\pi}{\alpha'(\Lambda_{\rm CUT})} \right)^6 . \tag{5.2.29}$$

[12] This value differs from that used in Ref. [179] ($C_{inst} = 0.1$) that was taken directly from the original 't Hooft's computation in Ref. [113], for which it was later shown [365] that the factor 2^{-2N_c} was missing. See also Erratum in Ref. [113].

This has the form

$$\Lambda_{\rm SSI}^4 = C_{inst}\, f(\alpha'_{\rm CUT}, b)\, e^{-\frac{2\pi}{\alpha'_{\rm CUT}}}\, \Lambda_{\rm CUT}^4\,, \tag{5.2.30}$$

where $f(\alpha', b)$ is given by

$$f(\alpha', b) = \frac{16}{\alpha'^6 (b-4)^7}\Big(45\alpha'^6 b^6 + 90\pi\alpha'^5 b^5 (b-4) + 90\pi^2\alpha'^4 b^4 (b-4)^2 \\ +60\pi^3\alpha'^3 b^3 (b-4)^3 + 30\pi^4\alpha'^2 b^2 (b-4)^4 + 12\pi^5\alpha' b (b-4)^5 + 4\pi^6 (b-4)^6\Big)\,. \tag{5.2.31}$$

For instance for the benchmark value $\alpha'_{\rm CUT} = 0.3$, the value of $SU(3')$ SSI-induced scale in the absence of fermions (for which $b = 10$) is

$$\Lambda_{\rm SSI}^4 = 3.0 \times 10^{-5}\, \Lambda_{\rm CUT}^4\,. \tag{5.2.32}$$

Nevertheless, the presence of fermions dramatically changes the value of this scale [129]. A suppression factor appears, which results from the interplay of the instantons of the theory and the fermionic spectrum. Moreover, an extra suppression stemming from the Euclidean action of the scalar Δ whose vev $\langle\Delta\rangle = \Lambda_{\rm CUT}$ breaks spontaneously the gauge group, $e^{-2\pi^2\rho^2\Lambda_{\rm CUT}^2}$, needs to be included in the full computation (as it was explained in the context of constrained instantons in Section 2.2.5). For the $SU(3')$ theory under consideration, the prime-fermion Yukawa couplings are relevant.

Small-size instantons with small Yukawa couplings

The massless χ fermions may acquire an effective mass due to the instantons of $SU(3)_{\rm diag}$ and $SU(3')$ SSI, similar to the effective mass in QCD for a hypothetically massless SM up quark. In this section, we assume the y'_i couplings in Eq. (5.2.6) to be small, e.g $\mathcal{O}(0.2)$ for illustration. This is a regime of moderate small-size instanton effects, in which the instanton-induced effective χ mass is smaller than the confinement scale. As a consequence, a composite axion made out of this fermion can be considered to be a pGB.[13]

The impact of the y'_i Yukawa couplings is illustrated by the one-instanton "flower" contribution in the left side of Fig. 5.2. The pure gauge results in Eq. (5.2.25) are now suppressed by three factors: the χ chiral condensate, the scalar contribution to the Euclidean action and the y'_i dependence,

$$\Lambda_{\rm SSI}^4 = -\int \frac{d\rho}{\rho^5}\, D[\alpha'(1/\rho)] \left(\frac{2}{3}\pi^2\rho^3\,\langle\bar\chi\chi\rangle\right) e^{-2\pi^2\rho^2\Lambda_{\rm CUT}^2}\, \frac{1}{(4\pi)^6} \prod_i y'^i_u y'^i_d\,. \tag{5.2.33}$$

$\langle\bar\chi\chi\rangle$ is the order parameter controlling $SU(3)_{\rm diag}$ chiral symmetry breaking and thus expected to be $\langle\bar\chi\chi\rangle \simeq -\Lambda_{\rm diag}^3$. For $\rho \leq 1/\Lambda_{\rm CUT}$, the product $\rho^3\,\langle\bar\chi\chi\rangle \ll 1$ reduces the SSI-induced scale

[13] In Section 5.2.1, we will consider y'_i couplings of $\mathcal{O}(1)$ which corresponds to the regime of large small-size instanton effects, translating to a very heavy χ fermion which decouples from the spectrum well above the confinement regime.

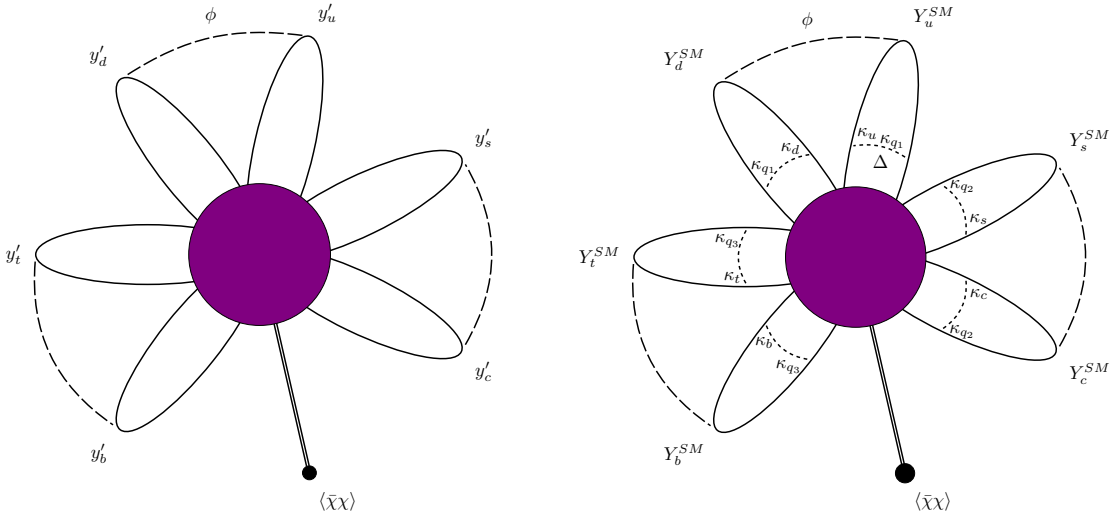

Figure 5.2: Instanton contributions in Model I. The long dashed lines connecting the $y'_i\,\bar{q}'_L\Phi\,u'^c_L$ interactions correspond to ϕ propagators, while the short dashed lines depict propagators of the Δ scalar. For $\mathcal{O}(1)$ Yukawa couplings in the prime sector, the diagram to the left represents the leading order contribution, whereas the one to the right is subdominant since it is further suppressed by the SM Yukawa couplings.

by orders of magnitude, with

$$\Lambda_{\rm SSI}^4 = \frac{2\pi^2}{3}\, C_{inst}\, \Lambda_{\rm CUT}^b\, \Lambda_d^3 e^{-2\pi/\alpha'_{\rm CUT}}\, \frac{1}{(4\pi)^6} \prod_i y'^i_u y'^i_d \times \\ \times \int_0^{1/\Lambda_{\rm CUT}} d\rho\, \rho^{b-2} \left(-b\, \ln\left(\rho\Lambda_{\rm CUT}\right) + \frac{2\pi}{\alpha'_{\rm CUT}}\right)^6 e^{-2\pi^2\rho^2\Lambda^2_{\rm CUT}}, \quad (5.2.34)$$

where, in the presence of N_f Dirac fermions,

$$C_{inst}(N_f, N_c) = \frac{4\cdot 2^{-2N_c} e^{c_{1/2}(-2N_c+2N_f)}}{\pi^2\,(N_c-2)!(N_c-1)!} e^{-c_1+4c_{1/2}}\,. \quad (5.2.35)$$

The integral in Eq. (5.2.34) can be computed exactly, although a good estimation follows from the approximation

$$\left(1 + \frac{-b\,\alpha'_{\rm CUT}}{2\pi}\, \ln\left(\rho\Lambda_{\rm CUT}\right)\right)^6 \simeq 1 + 6\,\frac{-b\,\alpha'_{\rm CUT}}{2\pi}\, \ln\left(\rho\Lambda_{\rm CUT}\right)\,, \quad (5.2.36)$$

which, dropping the scalar contribution, leads to the following parametric dependence on the scales

$$\Lambda_{\rm SSI}^4 \simeq \frac{\pi}{96}\, C_{inst}\, \Lambda_{\rm diag}^3\, \Lambda_{\rm CUT}\, e^{-2\pi/\alpha'_{\rm CUT}}\, \frac{3b\,\alpha'_{\rm CUT} + (b-1)\pi}{\alpha'^6_{\rm CUT}(b-1)^2} \prod_i y'_{u_i} y'_{d_i}\,. \quad (5.2.37)$$

For the benchmark $\alpha'_{\rm CUT} = 0.3$, and substituting $N_f = 7$, $b = 16/3$, $y'_{u_i}, y'_{d_i} = 0.2$, this gives

$$\Lambda^4_{\rm SSI} \simeq 2.9 \times 10^{-14}\, \Lambda^3_{\rm diag}\, \Lambda_{\rm CUT}\,. \tag{5.2.38}$$

The complete computation including fermions can be compared with the one in in Eq. (5.2.32): a strong suppression by a factor of order $(\Lambda_{\rm diag}/\Lambda_{\rm CUT})^3$ is now present.

There is an additional contribution to the SSI scale independent of the the y'_i couplings, but suppressed by the χ chiral condensate, times the product of κ_i Yukawa coupling of the prime-fermion sector in Eq. (5.2.2) *and* the product of SM Yukawa couplings. This contribution is illustrated by the instanton "double flower" in the right side of Fig. 5.2, and given by

$$\delta\Lambda^4_{\rm SSI} = -\int \frac{d\rho}{\rho^5}\, D[\alpha'(1/\rho)] \left(\frac{2}{3}\pi^2\rho^3 \langle\bar\chi\chi\rangle\right) \frac{1}{(4\pi)^{18}}\, e^{-2\pi^2\rho^2\Lambda^2_{\rm CUT}} \prod_i Y^{SM}_{u_i} Y^{SM}_{d_i}\, (\kappa^i_q)^2 \kappa^i_u \kappa^i_d\,, \tag{5.2.39}$$

where the power of the 4π factor results from the 6 SM Yukawa couplings and the 12 κ'_i couplings in the product. For $\rho \le 1/\Lambda_{\rm CUT}$, this contribution is well approximated by

$$\begin{aligned}\delta\Lambda^4_{\rm SSI} = \frac{2}{3}\frac{\pi^2}{(4\pi)^{18}} C_{inst} \Lambda^b_{\rm CUT} e^{-\frac{2\pi}{\alpha'_{\rm CUT}}} \prod_i Y^{SM}_{u_i} Y^{SM}_{d_i}\, {\kappa^i_q}^2 \kappa^i_u \kappa^i_d \times \\ \times \int_0^{1/\Lambda_{\rm CUT}} d\rho\, \rho^{b-2} \left(-b\, \ln(\rho\Lambda_{\rm CUT}) + \frac{2\pi}{\alpha'(\Lambda_{\rm CUT})}\right)^6 e^{-2\pi^2\rho^2\Lambda^2_{\rm CUT}}\,.\end{aligned} \tag{5.2.40}$$

In summary, putting together the two instanton contributions discussed, the SSI scale is given by

$$\begin{aligned}\Lambda^4_{\rm SSI} = -\int \frac{d\rho}{\rho^5}\, D[\alpha'(1/\rho)] \left(\frac{2}{3}\pi^2\rho^3 \langle\bar\chi\chi\rangle\right) e^{-2\pi^2\rho^2\Lambda^2_{\rm CUT}} \times \\ \times \left\{ \frac{1}{(4\pi)^6} \prod_i y'^i_u y'^i_d \;+ \frac{1}{(4\pi)^{18}} \prod_i Y^{SM}_{u_i} Y^{SM}_{d_i}\, (\kappa^i_q)^2 \kappa^i_u \kappa^i_d \right\}.\end{aligned} \tag{5.2.41}$$

Even with $\mathcal{O}(1)$ κ_i Yukawa couplings, the second term is strongly suppressed by the SM Yukawa couplings. Overall, the size of the new scale $\Lambda_{\rm SSI}$ is quite sensitive to the value of the $SU(3')$ coupling constant at the CUT-breaking scale. Fig. 5.3 illustrates the η'_χ axion mass induced by the small size instantons. For the benchmark examples studied, $\Lambda_{\rm SSI}$ significantly affects the properties of the pseudoscalars. It provides an additional contribution to the effective potential in Eq. (5.2.21) of the form

$$\delta V_{eff} = -\Lambda^4_{\rm SSI} \cos\left(2\,\frac{\eta'_\chi}{f_{\rm d}}\right). \tag{5.2.42}$$

A mass is thus generated for the η'_χ axion, given parametrically by

$$m^2_{\eta'_\chi} \sim 1.8 \times 10^{-11}\, \Lambda_{\rm diag}\, \Lambda_{\rm CUT}\,, \tag{5.2.43}$$

where the replacement $\Lambda_{\rm diag} \simeq 4\pi f_{\rm d}$ has been used and the scalar contribution has been drooped. The lighter axion may thus be as light as $\mathcal{O}$(GeV). The other dynamical axion of the theory has been shown to acquire a mass of order $\Lambda_{\rm diag}$, see Eq. (5.2.21). Both dynamical axions have thus acquired masses far above the typical invisible axion regime, as a direct and unavoidable consequence of the instanton potentials inherent to the theory.

How light can the axion that couples to SSI become?

The y_i' values are very relevant for the size of SSI scale. Nevertheless, the mass spectrum and thus the running of coupling constants is basically unaffected by them. Should the y_i' couplings be negligible, $\Lambda_{\rm SSI}$ would be determined by the second term in Eq. (5.2.41). For vanishing y_i' values and generic κ_i couplings of $\mathcal{O}(1)$, the product of $Y_i^{SM}/4\pi$ factors in the second term in Eq. (5.2.41) would suppress the η_χ' axion mass to values of order keV. Such low masses are excluded up to the GeV range [368] for axion scales not far from a TeV, as is the case here. The allowed range is illustrated in Fig. 5.3.[14]

Solution to the strong CP problem

It is pertinent to briefly re-check the status of the strong CP problem after taking into account the impact of the SSI of the spontaneously broken symmetry discussed above. Any new mass term for the axions breaks the PQ symmetry and therefore perturbs the axion potential; it is then important to verify that the vevs of the axions remain in the CP-conserving minimum, solving the strong CP problem. Indeed, this is the case with our color-unified proposal as, according to Eq. (5.2.8), the potential including θ_i dependencies explicitly reads at second order, for the case discussed above in which both dynamical axions are present at the $SU(3)_{\rm diag}$ confinement scale,

$$V_{eff} = \frac{\Lambda_{\rm SSI}^4}{2}\left(-2\,\frac{\eta_\chi'}{f_{\rm d}} + \bar\theta'\right)^2 + \frac{\Lambda_{\rm diag}^4}{2}\left(-2\,\frac{\eta_\chi'}{f_{\rm d}} - \sqrt{6}\,\frac{\eta_\psi'}{f_{\rm d}} + \bar\theta' + \bar\theta_6\right)^2 + \frac{\Lambda_{\rm QCD}^4}{2}\left(-\sqrt{6}\,\frac{\eta_\psi'}{f_{\rm d}} + \bar\theta_6\right)^2 . \tag{5.2.44}$$

For this potential, the minimum is CP-conserving:

$$\left\langle \bar\theta' - 2\,\frac{\eta_\chi'}{f_{\rm d}} \right\rangle = 0\,, \qquad\qquad \left\langle \bar\theta_6 - \sqrt{6}\,\frac{\eta_\psi'}{f_{\rm d}} \right\rangle = 0\,, \tag{5.2.45}$$

since all θ_i dependences cancel. A word of caution is pertinent as the exact dependence of the potential on the phases of the different couplings in the Lagrangian which participate in fermion mass generation (κ_i, Y_i^{SM}, y_i', ...) remains to be computed. Nevertheless, the two massless fermions Ψ and χ guarantee that at energies above CUT the two parameters $\bar\theta_6$ and $\bar\theta'$ are

[14] For higher axion masses there are also collider constraints [368]: dijet searches at the LHC provide bounds on axions with $m_a > 1$ TeV [369]. Thes searches can be extended to axion masses slightly below a TeV by searching for dijet resonances accompanied by hard initial state radiation [370]. These bounds are weak, though, and only apply in a small window of axion masses.

unphysical. Below CUT, the spectrum of the theory is exclusively the SM one plus massless fermions, and the EW SM contributions are known to be negligible [137], even if a mismatch remained in spite of the low-energy presence of the massless quarks. An explicit computation of the threshold effects is elaborate and it is left for future work. Note that without the presence of the second PQ mechanism, that is, without the presence of the η'_χ field and its vev, all θ_i in Eq. (5.2.8) would not have been reabsorbed, while Eq. (5.2.45) demonstrates that its inclusion does ensure a CP-conserving minimum.

It is very positive that in this model there is no contribution to the EW hierarchy problem coming from axion physics. No potential connects the EW and axion scales: the PQ scale f_a [15] is set by $\Lambda_{\rm diag}$ and not $\Lambda_{\rm CUT}$, and all axions are dynamically generated. This is a feature that our Model I shares with the original axicolor model, and in general with models of composite dynamical axion(s). There remains instead the customary fine-tuning in spontaneously broken unified theories, as $\Lambda_{\rm CUT}$ and the EW scale are connected via the scalar potential, but the latter does not communicate to our PQ mechanism.

The demonstrated possibility of lowering the PQ scale towards the electroweak one raises the question of the compatibility of the setup presented here with attempts to solve the EW hierarchy problem, e.g. via compositeness or supersymmetry. This is an interesting question which deserves future work. One could probably build supersymmetric or techincolor version of the models presented here. Nevertheless, the need to strongly separate the $\Lambda_{\rm CUT}$ scale from the EW scale is a non-trivial source of instability in the scalar potential.

Computation of the pseudoscalar mass matrix: η'_χ, η'_ψ, $\eta'_{\rm QCD}$ and light spectrum

After the replacement of the pGBs with anomalous couplings by their physical excitations, $\eta'_\chi \to \langle\eta'_\chi\rangle + \eta'_\chi$, $\eta'_\psi \to \langle\eta'_\psi\rangle + \eta'_\psi$, the effective low-energy potential for the axions and the SM $\eta'_{\rm QCD}$ field is given at second order by (disregarding the effects of SM quark masses)

$$V_{eff} = \frac{\Lambda^4_{\rm SSI}}{2}\left(2\,\frac{\eta'_\chi}{f_{\rm d}}\right)^2 + \frac{\Lambda^4_{\rm diag}}{2}\left(2\,\frac{\eta'_\chi}{f_{\rm d}} + \sqrt{6}\,\frac{\eta'_\psi}{f_{\rm d}}\right)^2 + \frac{\Lambda^4_{\rm QCD}}{2}\left(2\,\frac{\eta'_{\rm QCD}}{f_\pi} + \sqrt{6}\,\frac{\eta'_\psi}{f_{\rm d}}\right)^2 . \quad (5.2.46)$$

Expanding to second order in the fields yields the following mass matrix:

$$M^2_{\eta'_\chi,\eta'_\psi,\eta'_{\rm QCD}} = \begin{pmatrix} 4\frac{\left(\Lambda^4_{\rm SSI}+\Lambda^4_d\right)}{f^2_{\rm d}} & 2\sqrt{6}\,\frac{\Lambda^4_d}{f^2_d} & 0 \\ 2\sqrt{6}\,\frac{\Lambda^4_d}{f^2_d} & 6\,\frac{\left(\Lambda^4_d+\Lambda^4_{\rm QCD}\right)}{f^2_{\rm d}} & 2\sqrt{6}\,\frac{\Lambda^4_{\rm QCD}}{f_\pi f_{\rm d}} \\ 0 & 2\sqrt{6}\,\frac{\Lambda^4_{\rm QCD}}{f_\pi f_{\rm d}} & 4\frac{\Lambda^4_{\rm QCD}}{f^2_\pi} \end{pmatrix} . \quad (5.2.47)$$

[15] The PQ scale (usually denoted by f_{PQ}) and f_a differ by a model-dependent factor stemming from the relative strength of the axion coupling to gluons. Here we disregard the distinction between f_a and f_{PQ}.

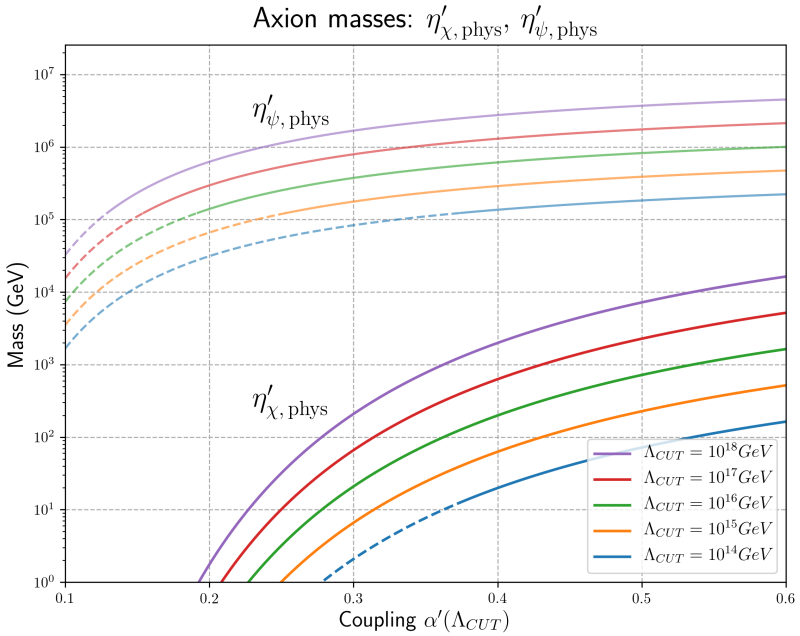

Figure 5.3: Model I with small y'_i Yukawa couplings. The η'_χ axion mass induced by the $SU(3')$ small size instantons at the scale $\Lambda_{\rm CUT}$ is shown together with the smaller mass for the dynamical η'_ψ axion sourced by $\Lambda_{\rm diag}$ instantons. The $\alpha'_{\rm CUT}$ values corresponding to solid lines are allowed, while those for dashed lines correspond to excluded values, for which $SU(3)_{\rm diag}$ would confine below 2.9 TeV, ruled out by searches for scalar octets at LHC [371] (see Sec. 5.3.1).

Assuming the hierarchy of scales $\frac{\Lambda_d^4}{f_{\rm d}^2} \gg \frac{\Lambda_{\rm SSI}^4}{f_{\rm d}^2} \gg \frac{\Lambda_{\rm QCD}^4}{f_\pi^2}$ (valid for certain regions of parameter space, see Fig. 5.3), the three mass eigenvalues[16] are

$$m^2_{\eta'_{\psi,\,phys}} \simeq 6\frac{\Lambda_d^4}{f_{\rm d}^2}\,, \qquad m^2_{\eta'_{\chi,phys}} \simeq 4\frac{\Lambda_{\rm SSI}^4}{f_{\rm d}^2}\,, \qquad m^2_{\eta'_{QCD\,phys}} \simeq 4\frac{\Lambda_{\rm QCD}^4}{f_\pi^2}\,. \tag{5.2.48}$$

As advertised, the usual QCD $\eta'_{QCD\,phys}$ remains as a light eigenstate, while one of the two composite axions acquires a mass in the range GeV to tens of TeV. The other composite axion will have a mass orders of magnitude larger and will be out of collider reach.

Low energy spectrum and observable effects

In addition to the dynamical axion with mass $\mathcal{O}$ (GeV) or larger, under a few TeV the spectrum of the theory contains:

[16] The physical states correspond to the following combinations: $\eta'_{\psi,\,phys} \simeq 1/f_{\rm d}(2\,\eta'_\chi + \sqrt{6}\,\eta'_\psi)$ and $\eta'_{\chi,\,phys} \simeq 1/f_{\rm d}(\sqrt{6}\,\eta'_\chi - 2\eta'_\psi)$.

- The SM pseudoscalar meson $\eta'_{QCD\,phys}$, plus the rest of the SM hadronic spectrum.
- The exotic QCD-colored "pions" — color octets and color triplets — whose masses are given in Eq. (5.2.12) as $m^2 \sim \alpha_c \Lambda^2_{\rm diag}$. With masses naturally lighter than the TeV scale, these QCD-colored pions can be easily produced at the LHC.
- The two sterile fermions stemming from the 20- representation Ψ. They are basically invisible as their interactions with the visible world are suppressed by $\Lambda_{\rm CUT}$, which is much larger than $\Lambda_{\rm diag}$ without any tuning.
- Possibly, a GB associated with generalized baryon number. This GB is harmless as its interactions are suppressed by $\Lambda_{\rm CUT}$. It can also easily be made arbitrarily heavy by gauging that global symmetry.

The very interesting phenomenological bounds and detection prospects for the exotic QCD-colored mesons will be quite similar to those applying to the next model. The ensemble will then be briefly developed in Section 5.3 further below. The same applies to the cosmological consequences of the two color-unified UV completions developed in this work.

Small-size instantons with $\mathcal{O}(1)$ Yukawa couplings

If the Yukawa couplings in the prime sector y'_{u_i}, y'_{d_i} are $\mathcal{O}(1)$, the instanton-induced mass of χ is larger than $\Lambda_{\rm diag}$. The mass of the bound state $\eta_{\chi,\,\rm phys}$ will be then dominated by the χ mass instead of the confinement scale. It is thus relevant to consider the instanton effects on the constituent quarks (i.e. χ), as opposed to the discussion in the previous section in which the instantons contributed directly to the mass of the bound state η'_χ. As a consequence, the relevant diagram (Fig. 5.4) generates an effective mass m_χ for the χ quark induced by SSI instantons:

$$\mathcal{L}_{eff} = -m_\chi \bar{\chi}\chi\,, \tag{5.2.49}$$

which can be computed using the dilute instanton gas approximation:

$$m_\chi = \int \frac{d\rho}{\rho^5}\, D[\alpha'(1/\rho)]\Big(\frac{2}{3}\pi^2\rho^3\Big)\, e^{-2\pi^2\rho^2\Lambda^2_{\rm CUT}} \frac{1}{(4\pi)^6} \prod_i y'^i_u y'^i_d \;\simeq 6.2\times 10^{-12}\Lambda_{\rm CUT}\,. \tag{5.2.50}$$

For the benchmark values used for $\Lambda_{\rm CUT}$ this indicates a mass of tens of TeV or above. As expected, the mass of the χ thus lies well above the confinement scale Λ_d, and therefore the mass of the η'_χ will be dominated by the mass of its constituent fermion: $m_{\eta'_\chi} \sim 2m_\chi$ The two axion masses are represented in the Fig. 5.5, where the mass of the η'_ψ is taken from Eq. (5.2.48) and that of η'_χ from Eq. (5.2.50). Both composite axions have masses typically above the TeV regime and are out of present collider reach.

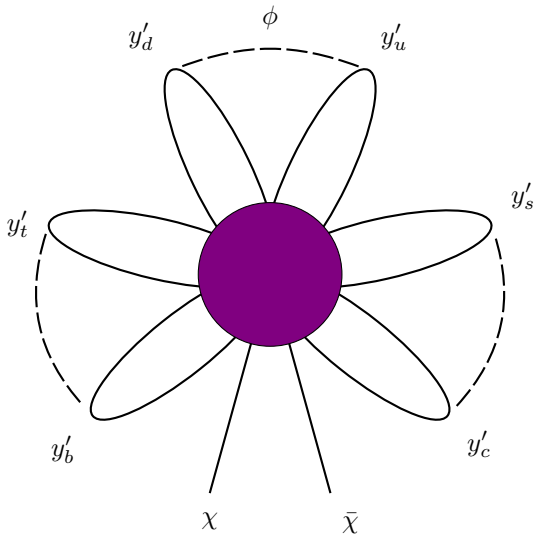

Figure 5.4: Instanton contribution for the second scenario in Model I. It generates an effective mass for the χ.

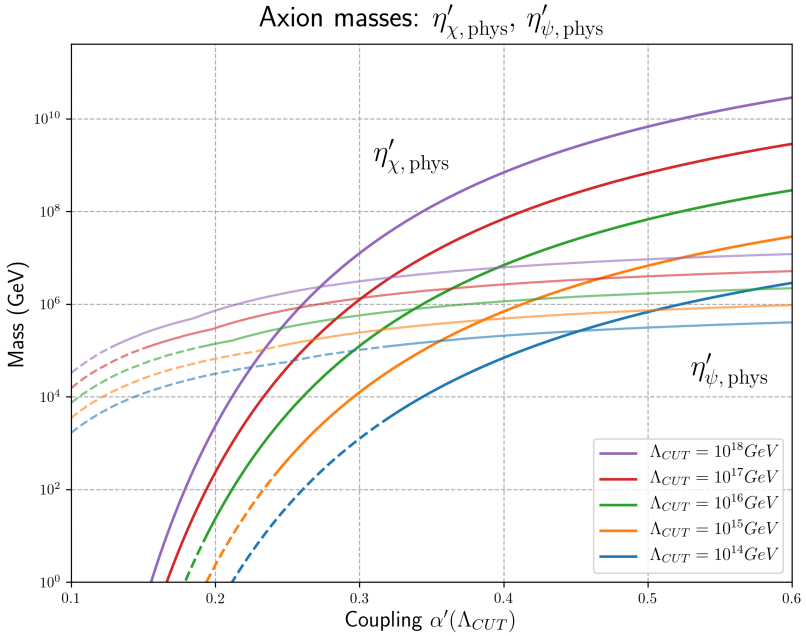

Figure 5.5: Axion masses for Model I, with Yukawa couplings $y'_i \sim \mathcal{O}(1)$. The slight kinks in the η'_ψ curves mark the χ threshold. The η'_χ axion mass, dominated by the instanton effects on the constituent quarks, is shown together with the mass for the dynamical η'_ψ axion sourced by Λ_{diag} instantons. The α'_{CUT} values corresponding to solid lines are allowed, while those for dashed lines correspond to excluded values, for which $SU(3)_{\mathrm{diag}}$ would confine below 2.9 TeV, ruled out by searches for scalar octets at LHC [371] (see Sec. 5.3.1).

Solution to the strong CP problem

Upon $SU(3)_{\rm diag}$ confinement, only one massless fermion remains in the spectrum, ψ. Therefore, the potential contains only one pseudoscalar meson that inherits a shift symmetry: η'_ψ. This does not invalidate the solution to the strong CP problem, since the other phase $\bar{\theta}'$ in Eq. (5.2.44) is reabsorbed when the χ is integrated out of the spectrum. This is a consequence of the mass of the χ being generated by instanton effects: the phase of this mass term will be exactly that of the topological term, and it will be completely removed after integrating out the fermion. After taking all instanton effects into account, the low energy potential for the dynamical axion now reads:

$$V_{eff} = \frac{\Lambda_{\rm diag}^4}{2}\left(-\sqrt{6}\,\frac{\eta'_\psi}{f_{\rm d}} + \bar{\theta}_6\right)^2 + \frac{\Lambda_{\rm QCD}^4}{2}\left(-\sqrt{6}\,\frac{\eta'_\psi}{f_{\rm d}} + \bar{\theta}_6\right)^2 , \tag{5.2.51}$$

and the minimum is CP-conserving:

$$\left\langle \bar{\theta}_6 - \sqrt{6}\,\frac{\eta'_\psi}{f_{\rm d}} \right\rangle = 0\,, \tag{5.2.52}$$

Low energy spectrum and observable effects

For most of the parameter space, the two dynamical axions $\eta'_{\psi,phys}$ and $\eta'_{\chi,phys}$ are typically heavier than the TeV scale and thus very difficult to observe at LHC. Otherwise, under a few TeV the spectrum is the same as that itemized in Section 5.2.1, except that there are no color triplet "axi-pions" because of the χ absence at the relevant energies, see Eq. (5.2.24). Therefore only the color octet "axi-pion" can be searched for at the LHC.

5.2.2 Model II: Addition of a second Δ scalar.

This solution to the θ' problem is an alternative to extending the spectrum by a massless fermion, discussed in the previous subsection. In this second model no extra fermion is added to the $SU(6)\times SU(3')$ Lagrangian, while a second Δ field will be considered instead. The spectrum is that in Table 5.3 albeit with the scalar line duplicated, $\Delta \to \{\Delta_1,\, \Delta_2\}$. This simple extension allows the implementation of a PQ symmetry which reabsorbs the θ' contribution to the strong CP problem. The corresponding PQ symmetry is automatic if the terms in Eq. (5.2.6) are omitted and Eq. (5.2.2) is replaced by

$$\mathcal{L} \ni \kappa_q\, q'_L \Delta_1^* Q_L + \kappa_u\, u'^c_L \Delta_2\, U^c_L + \kappa_d\, d'^c_L \Delta_2 D^c_L \;+ \text{h.c.}\,. \tag{5.2.53}$$

This Lagrangian is invariant under two independent abelian global symmetries; one of them is anomalous with respect to $SU(3')$ and corresponds to the PQ charge assignment [17]

$$PQ\{\Delta_1, \Delta_2, q'_L, u'^c_L, d'^c_L\} = \{+1, -1, +1, +1, +1\}\,. \tag{5.2.54}$$

The vevs of Δ_1 and Δ_2 generalize the CUT spontaneous breaking in Eq. (5.2.3) and at the same time break spontaneously the PQ symmetry; therefore, this PQ scale coincides with the CUT scale. This distinguishes model 2 from model I, as in the latter the PQ scale coincided with $\Lambda_{\rm diag}$. A pGB —an elementary axion— is generated at this stage. The corresponding PQ conserved current is given by

$$j^\mu_{PQ} = \left[\overline{q'_L}\gamma^\mu q'_L + \overline{u'^c_L}\gamma^\mu u'^c_L + \overline{d'^c_L}\gamma^\mu d'^c_L + i(\Delta_1 D^\mu \Delta_1^* - \Delta_2 D^\mu \Delta_2^* - \text{h.c.})\right]\,. \tag{5.2.55}$$

The Δ_i fields are parameterized as

$$\Delta_1 \equiv \frac{1}{\sqrt{2}}(\rho_1 + v_{\Delta_1})e^{ia_1/v_{\Delta_1}}\,, \qquad \Delta_2 \equiv \frac{1}{\sqrt{2}}(\rho_2 + v_{\Delta_2})e^{ia_2/v_{\Delta_2}}\,, \tag{5.2.56}$$

where v_{Δ_1} and v_{Δ_2} denote respectively the Δ_1 and Δ_2 vevs, both of which we take to be real for simplicity. Decoupling the heavy radial modes, the PQ current reads

$$j^\mu_{PQ} \supset v_{\Delta_1}\partial^\mu a_1 - v_{\Delta_2}\partial^\mu a_2 \equiv f_a\,\partial^\mu a\,, \tag{5.2.57}$$

where the elementary axion field $a(x)$ corresponds to the GB combination

$$a(x) = \frac{1}{f_a}(v_{\Delta_1}a_1(x) - v_{\Delta_2}a_2(x))\,, \tag{5.2.58}$$

with

$$f_a = \Lambda_{\rm CUT} = \sqrt{v^2_{\Delta_1} + v^2_{\Delta_2}}\,. \tag{5.2.59}$$

This classically exact PQ symmetry is broken at the quantum level by the $SU(3')$ anomaly, which at lower energies translates into an anomalous current for the $SU(3)_{\rm diag}$ gauge theory.

$$\partial_\mu j^\mu_{PQ} = \frac{\alpha'}{8\pi}N'G'\tilde{G}' \longrightarrow \frac{\alpha_{\rm diag}}{8\pi}N_{\rm diag}G_{\rm diag}\tilde{G}_{\rm diag}\,, \tag{5.2.60}$$

where N' and $N_{\rm diag}$ are the group factors,

$$N' = N_{\rm diag} = \sum_{LH-RH} Tr\left[T^a_{PQ}\{t^b, t^c\}\right] = 12\,, \tag{5.2.61}$$

and where T^a_{PQ} corresponds to the PQ generator and $t^b = \frac{\lambda^b}{2}$ to the Gell-Mann matrices for the $SU(3)$ generators. The anomalous term modifies the classical equations of motion of the axion,

$$f_a\,\Box a + \partial_\mu(\overline{q'_L}\gamma^\mu q'_L) + \partial_\mu(\overline{u'^c_L}\gamma^\mu u'^c_L) + \partial_\mu(\overline{d'^c_L}\gamma^\mu d'^c_L) = \frac{\alpha_{\rm diag}}{8\pi}12\,G_{\rm diag}\tilde{G}_{\rm diag}\,, \tag{5.2.62}$$

[17] The Lagrangian possesses another $U(1)$ symmetry, namely the generalized baryon number symmetry defined in Eq. (5.2.7), which is however non-anomalous under $SU(3')$. See footnotes 7 and 8 on the harmless consequences of the non-anomalous global symmetry.

	$SU(3)_c$	$SU(3)_{\rm diag}$
ψ_L	□	□
${\psi_L}^c$	□	□

Table 5.6: The massless quark sector charged under $SU(3)_{\rm diag}$ below $\Lambda_{\rm CUT}$ in the model with an extra scalar.

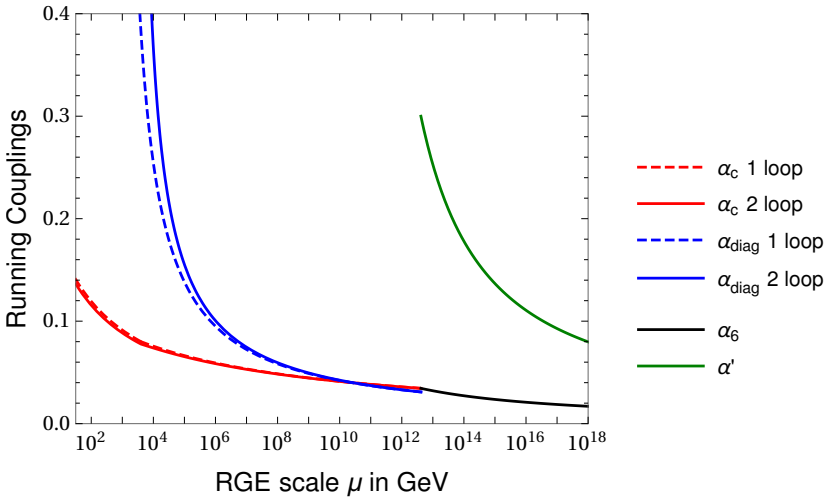

Figure 5.6: Running of $\alpha_{\rm QCD}$, $\alpha_{\rm diagonal}$, α_6, and α' in the model with one extra $SU(6)$ scalar; the only inputs assumed are $\alpha'_{\rm CUT} = 0.3$ and $\Lambda_{\rm CUT} = 4.1 \times 10^{12}$ GeV for illustration, which results in $\Lambda_{\rm diag} = 4$ TeV (taken as a benchmark point). The solid (dashed) lines correspond to the two (one) loop results.

and gives rise to an effective Lagrangian,

$$\mathcal{L} \supset \frac{1}{2}\partial_\mu a \partial^\mu a + \frac{1}{f_a}\partial_\mu a \left(\overline{q'_L}\gamma^\mu q'_L + \overline{u'^c_L}\gamma^\mu u'^c_L + \overline{d'^c_L}\gamma^\mu d'^c_L\right) + \frac{\alpha_{\rm diag}}{8\pi}\frac{12}{f_a}\, a\, G_{\rm diag}\tilde{G}_{\rm diag}\,. \tag{5.2.63}$$

The impact of the SSI of the spontaneously broken theory will again add further contributions, inducing a putatively high mass for the elementary axion as discussed further below.

Running of the coupling constants

The matter content allows $SU(3)_{\rm diag}$ to confine at higher scales than the QCD group $SU(3)_c$ as in Model I. The separation of both scales is made even sharper in the Model II because $\alpha_{\rm diag}$ runs faster. In Model II, only one massless fermion charged under $SU(3)_{\rm diag}$ is ever present under the CUT scale (compare Tabs. 5.5 and 5.6). We have estimated both the one and two-loop running, as illustrated in Fig. 5.6 for $\Lambda_{\rm diag} = 4$ TeV.

Confinement of $SU(3)_{\rm diag}$ and pseudoscalar anomalous couplings to the confining interactions.

At the scale $\Lambda_{\rm diag}$ the QCD coupling constant is small, and the $SU(3)_{\rm diag}$ spectrum with only one massless fermion in Table 5.6 has an approximate classical global symmetry $U(3)_L \times U(3)_R$. Upon chiral symmetry breaking $U(3)_L \times U(3)_R \longrightarrow U(3)_V$ by the quark condensate $\langle \bar{\psi}_L \psi_R \rangle$, nine pGBs appear,

$$9 = 1_c \, + \, 8_c \, . \tag{5.2.64}$$

The gauge QCD group $SU(3)_c$ is again a subgroup of $U(3)_V$ which remains unbroken. The octet of pGBs colored under QCD will acquire large masses due to gluon loops, which at one-loop is given by

$$m^2(8_c) \approx \frac{9\,\alpha_{\rm c}}{4\pi} \Lambda^2_{\rm diag} \, . \tag{5.2.65}$$

The QCD singlet 1_c, denoted η'_ψ, is a dynamical axion. Note that it has the same quark composition as the η'_ψ meson in Model I. The η'_ψ couples to both the $SU(3)_{\rm diag}$ and $SU(3)_c$ anomalies,

$$j^\mu_{\psi_A} = \bar{\psi} \gamma^\mu \gamma^5 t^9 \psi \equiv f_{\rm d} \, \partial^\mu \eta'_\psi \, , \qquad t^9 = \frac{1}{\sqrt{6}} \mathbb{1}_{3\times 3}, , \tag{5.2.66}$$

resulting in a low-energy effective Lagrangian for this axion given by

$$\mathcal{L}_{eff} \subset - \frac{\sqrt{6}\, \eta'_\psi}{f_{\rm d}} \left(\frac{\alpha_s}{8\pi} \, G_c \tilde{G}_c + \frac{\alpha_{\rm diag}}{8\pi} \, G_{\rm diag} \tilde{G}_{\rm diag} \right) \, . \tag{5.2.67}$$

In summary, this solution to the strong CP problem is a hybrid one with two axions: a heavy dynamical axion η'_ψ with mass of order $\Lambda_{\rm diag}$ stemming from a PQ symmetry which reabsorbs the original $\theta_{SU(6)}$ (and thus $\theta_{\rm QCD}$) parameter as in the previous section, and a second elementary axion a resulting from solving the external $SU(3')$ sector *à la* PQWW [8, 147, 148]. Up to now, only two sources of masses have been identified for the ensemble of three pseudoscalars with anomalous couplings ($\eta'_{\rm QCD}$, η'_ψ and a). We analyze next the SSI of this model which provide a large source of axion mass for the elementary axion a.

Impact of small-size instantons on the dynamical axion mass

Small-size instantons of the spontaneously broken CUT

The analysis of SSI for Model II under discussion is simpler than that for Model I developed in the previous subsection. *No* massless fermions charged under $SU(3')$ are present in Model II (in contrast with Model I). Furthermore, PQ symmetry forbids here the y'_i Yukawa couplings which gave the dominant contribution in Model I. In consequence, the terms proportional to κ_i and

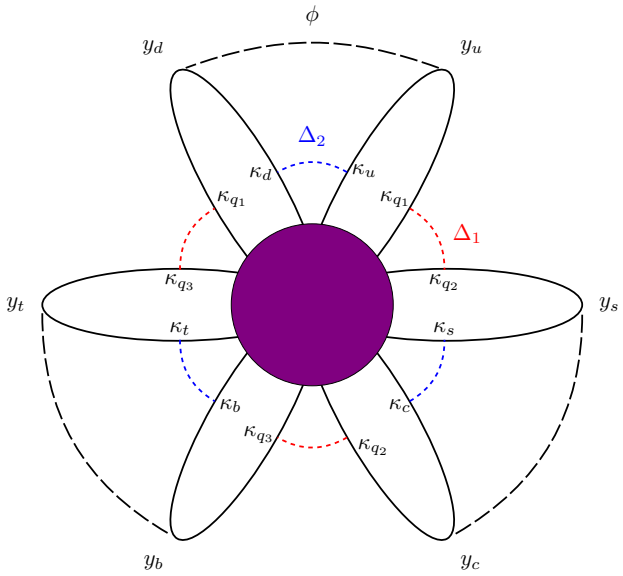

Figure 5.7: Instanton contribution in Model II. The long dashed lines connecting the SM Yukawa interactions correspond to ϕ propagators while the short dashed lines depict Δ_1 or Δ_2 propagators.

mediated by the Δ_1 and Δ_2 scalars and the Higgs field will dominate $\Lambda_{\rm SSI}$. This is illustrated by the instanton "flower" in Fig. 5.7. It results in $\Lambda_{\rm SSI}$ given by

$$\Lambda_{\rm SSI}^4 = -\int \frac{d\rho}{\rho^5}\, D[\alpha'(1/\rho)]\, e^{-2\pi^2\rho^2\Lambda_{\rm CUT}^2} \frac{1}{(4\pi)^{18}} \prod_i Y_{u_i}^{SM} Y_{d_i}^{SM}\, (\kappa_q^i)^2 \kappa_u^i \kappa_d^i\,, \tag{5.2.68}$$

which can be written as

$$\Lambda_{\rm SSI}^4 = C_{inst}\Lambda_{\rm CUT}^b e^{-\frac{2\pi}{\alpha'_{\rm CUT}}} \frac{1}{(4\pi)^{18}} \prod_i Y_{u_i}^{SM} Y_{d_i}^{SM}\, {\kappa_q^i}^2 \kappa_u^i \kappa_d^i \times$$
$$\times \int_0^{1/\Lambda_{\rm CUT}} d\rho\, \rho^{b-5} \left(-b\, \ln(\rho\Lambda_{\rm CUT}) + \frac{2\pi}{\alpha'(\Lambda_{\rm CUT})}\right)^6 e^{-2\pi^2\rho^2\Lambda_{\rm CUT}^2}, \tag{5.2.69}$$

with $b = 5$ in this case. Here the approximation in Eq. (5.2.36) is no longer valid, and the result corresponds to that of the pure Yang-Mills case (Eq. (5.2.30)) with the extra suppression factor of the Yukawa couplings,

$$\Lambda_{\rm SSI}^4 = C_{inst}\, f(\alpha'_{\rm CUT}, b)\, e^{-\frac{2\pi}{\alpha'_{\rm CUT}}} \Lambda_{\rm CUT}^4 \frac{1}{(4\pi)^{18}} \prod_i Y_{u_i}^{SM} Y_{d_i}^{SM}\, {\kappa_q^i}^2 \kappa_u^i \kappa_d^i \tag{5.2.70}$$

where the function $f(\alpha'_{\rm CUT}, b)$ is defined in Eq. (5.2.31) and the scalar action factor can be neglected since the major contribution stems from instanton with sizes smaller than $1/Lambda_{\rm CUT}$.

This result translates into a new contribution to the instanton-induced effective potential of the form

$$\delta V_{eff} = -\Lambda^4_{\rm SSI} \cos\left(12\,\frac{a}{f_a}\right) . \tag{5.2.71}$$

Taking into account that in this model the elementary axion scale coincides with the CUT scale, it follows that for $\alpha'_{\rm CUT} = 0.3$ and with $\mathcal{O}(1)$ κ_i Yukawa couplings,

$$m_a^2 \sim 3.7 \times 10^{-37} \Lambda^2_{\rm CUT} . \tag{5.2.72}$$

For the benchmark values used for $\Lambda_{\rm CUT}$, this implies an elementary axion mass in the range 10^{-5} eV - 10 GeV, see Fig. 5.8 for illustration. In summary, the dynamical axion has a mass of order $\Lambda_{\rm diag}$ and thus of a few TeV or above, while the elementary axion is light although typically heavier than the usual invisible axion.

Solution to the strong CP problem

The minimum of the axion potential can be easily shown to remain CP-conserving after including all contributions to the axion masses. Indeed, the θ_i dependence of the potential can be again read off of Eq. (5.2.8),

$$V_{eff} = \frac{\Lambda'^4_{\rm SSI}}{2}\left(12\,\frac{a}{f_a} + \bar\theta'\right)^2 + \frac{\Lambda^4_{\rm d}}{2}\left(12\,\frac{a}{f_a} - \sqrt{6}\,\frac{\eta'_\psi}{f_{\rm d}} + \bar\theta' + \bar\theta_6\right)^2 + \frac{\Lambda^4_{\rm QCD}}{2}\left(-\sqrt{6}\,\frac{\eta'_\psi}{f_{\rm d}} + \bar\theta_6\right)^2 , \tag{5.2.73}$$

for which the following bosonic vevs lead to a CP-conserving minimum,

$$\left\langle 12\,\frac{a}{f_a} + \bar\theta' \right\rangle = 0 , \qquad \left\langle \bar\theta_6 - \sqrt{6}\,\frac{\eta'_\psi}{f_{\rm d}} \right\rangle = 0 . \tag{5.2.74}$$

After the replacement $a \to \langle a\rangle + a$, $\eta'_\psi \to \langle \eta'_\psi\rangle + \eta'_\psi$ and introducing as well the QCD $\eta'_{\rm QCD}$ field, the effective low-energy potential for the physical mesons which couple to anomalous currents is given at second order by

$$V_{eff} = \frac{\Lambda^4_{\rm SSI}}{2}\left(12\,\frac{a}{f_a}\right)^2 + \frac{\Lambda^4_{\rm d}}{2}\left(12\,\frac{a}{f_a} - \sqrt{6}\,\frac{\eta'_\psi}{f_{\rm d}}\right)^2 + \frac{\Lambda^4_{\rm QCD}}{2}\left(2\,\frac{\eta'_{\rm QCD}}{f_\pi} + \sqrt{6}\,\frac{\eta'_\psi}{f_{\rm d}}\right)^2 . \tag{5.2.75}$$

where all the CP violating phases have been relaxed to zero.

Computation of the pseudoscalar mass matrix: a, η'_ψ, $\eta'_{\rm QCD}$ and light spectrum

Taking into account all contributions except the SM quark masses, the following mass matrix results for the singlet pseudoscalars of the theory which couple to anomalous currents:

$$M^2_{a,\eta'_\psi,\eta'_{\rm QCD}} = \begin{pmatrix} 144\,\frac{\left(\Lambda^4_{\rm SSI}+\Lambda^4_{\rm diag}\right)}{f_a^2} & -12\sqrt{6}\,\frac{\Lambda_d^4}{f_{\rm d} f_a} & 0 \\ -12\sqrt{6}\,\frac{\Lambda_d^4}{f_{\rm d} f_a} & 6\,\frac{\left(\Lambda^4_d+\Lambda^4_{\rm QCD}\right)}{f_{\rm d}^2} & 2\sqrt{6}\,\frac{\Lambda^4_{\rm QCD}}{f_\pi f_{\rm d}} \\ 0 & 2\sqrt{6}\,\frac{\Lambda^4_{\rm QCD}}{f_\pi f_{\rm d}} & 4\frac{\Lambda^4_{\rm QCD}}{f_\pi^2} \end{pmatrix} . \tag{5.2.76}$$

Assuming the hierarchy of scales $\frac{\Lambda_d^4}{f_{\rm d}^2} \gg \frac{\Lambda^4_{\rm QCD}}{f_\pi^2} \gg \frac{\Lambda^4_{\rm SSI}}{f_a^2}$, the resulting mass eigenvalues are

$$m^2_{a_{phys}} \simeq 144\frac{\Lambda^4_{\rm SSI}}{f_a^2}\,, \qquad m^2_{\eta'_{\psi,\,phys}} \simeq 6\frac{\Lambda_d^4}{f_{\rm d}^2}\,, \qquad m^2_{\eta'_{QCD\,phys}} \simeq 4\frac{\Lambda^4_{\rm QCD}}{f_\pi^2}\,. \tag{5.2.77}$$

In this model both the usual QCD η' and the axion a_{phys} remain as light eigenstates, while the other eigenstate $\eta'_{\psi,\,phys}$ will have a mass generically above the TeV scale.

Apart from the axion, the lowest set of exotic states is an octet of exotic "pions" whose masses are $\lesssim$ TeV, see Eq. (5.2.65). A similar colored octet is present in Model I discussed in Sec. 5.2.1, although Model I contains an additional set of color-triplet pseudoscalars in the case of small y'_i Yukawa couplings. In contrast, no color-triplet is ever expected here as the exotic classical flavor symmetry is $U(3)_L \times U(3)_R$, see Eq. (5.2.64), instead of the $U(4)_L \times U(4)_R$ symmetry of Model I.

This Model II with an additional scalar may be less appealing than than Model I with an extra massless fermions for two reasons: a) its axion sector contributes directly to the EW hierarchy problem, as its elementary axion results from a scalar potential which a priori communicates with the Higgs potential; b) it is a hybrid model with both one elementary and one dynamical axion, while Model I is more aligned with the spirit of solving fully the strong CP problem via massless fermions.

5.3 Phenomenological and cosmological limits on the lightest exotic states

A common feature of the ultraviolet complete models constructed above is that the generic spectrum under the EW scale includes, in addition to the SM spectrum, sterile fermions, in contrast with usual axion models. An axion may also be present in this range depending on the model parameters.

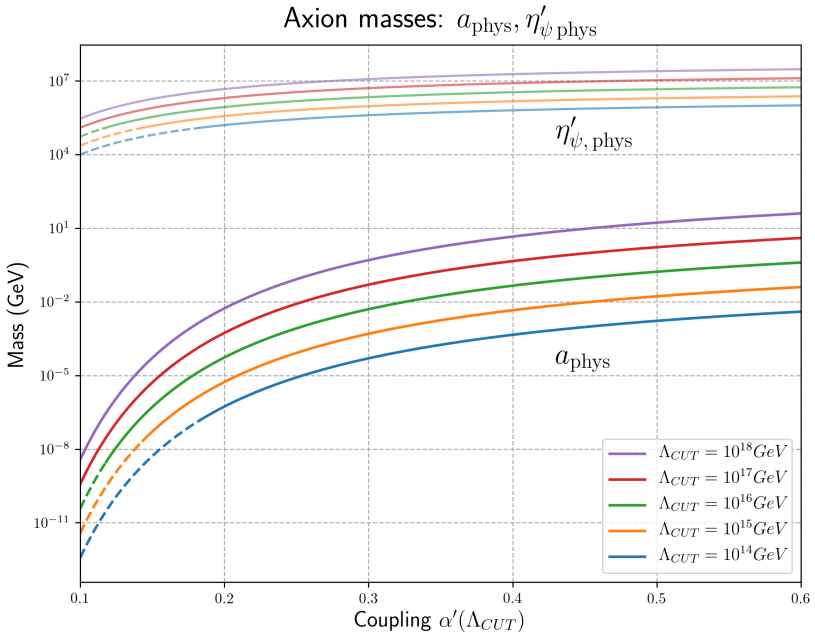

Figure 5.8: Model with a second $SU(6)$ scalar. The a axion mass induced by the $SU(3')$ small size instantons at the scale $\Lambda_{\rm CUT}$ is illustrated, together with the larger mass for the dynamical axion η'_ψ sourced by $SU(3)_{\rm diag}$ instantons. Order one Yukawa couplings in the prime sector have been used in this figure.The $\alpha'_{\rm CUT}$ values allowed correspond to the solid sectors of the lines, while dashed lines correspond to excluded values, for which $SU(3)_{\rm diag}$ would confine below 2.9 TeV, ruled out by searches for scalar octets at LHC [371] (see Sec. 5.3.1).

5.3.1 Collider observable signals

A set of observable exotic states are expected to be the exotic $SU(3)_c$-colored "pions" whose masses may lie under the TeV scale. These resulted from the chiral symmetry breaking of the confining group $SU(3)_{\rm diag}$. All models exhibit as a common characteristic QCD color-octet meson bound states made out of their massless fermions, shown in Table 5.5 and Eq. (5.2.12) for Model I and Table 5.6 and Eq. (5.2.65) for Model II. In addition, QCD color-triplet meson bound states may be observable for Model I with small Yukawa couplings in the primed sector.

In this color-unified axion solution, the exotic fundamental fermions have no SM $SU(2)\times U(1)$ charges. The heavy pions will be produced in colliders only via QCD interactions, e.g. gluon-gluon couplings, through which they also presumably decay before they can hadronize to make color neutral states. As they are colored, they do not mix with ordinary pions or other visible matter.

Color-octet pions from $SU(3)_{\rm diag}$ confinement

The lightest scalar octets in Eqs. (5.2.12) and (5.2.65) are denoted by $\pi_{\rm d} \equiv 8_c$. Their effective coupling to QCD gluons can be written as

$$\mathcal{L} \supset D_\mu \pi_{\rm d} D^\mu \pi_{\rm d} + \frac{3\sqrt{3}\,\alpha_s}{8\pi} \frac{\pi_{\rm d}^a}{f_d} d_{abc} G^b_{\mu\nu} \tilde{G}^{c\mu\nu} \,, \tag{5.3.1}$$

where D_μ denotes the $SU(3)_c$ covariant derivative and d_{abc} is the corresponding symmetric group structure constant. The second term in Eq. (5.3.1) results at one-loop from the triangle diagram with the fermions χ running in the loop. The color-octet exotic pions can thus be either produced in pairs through the gluon-gluon-$\pi_{\rm d}$-$\pi_{\rm d}$ coupling in the kinetic term, or singly produced through their anomalous coupling to gluons. The kinetic term dominates the scalar octet production channels, while the second term allows the $\pi_{\rm d}$ decay, yielding a dijet final state.

Experimental limits on scalar octet pair production via the gluonic interactions in the kinetic term can be inferred by recasting searches of sgluons. A recent search of sgluon pair production by ATLAS using $36.7\,{\rm fb}^{-1}$ of $\sqrt{s} = 13\,{\rm TeV}$ data [371], whose prediction was obtained from the NLO computation in Ref. [372] for $\sqrt{s} = 8$ TeV (rescaled to 13 TeV according to Ref. [373]), sets a bound on the octet scalar exotic pions given by

$$m(\pi_{\rm d}) \gtrsim 770\,{\rm GeV} \,. \tag{5.3.2}$$

From Eqs. (5.2.12) and (5.2.65), this translates into

$$\Lambda_{\rm diag} \gtrsim 2.9\,{\rm TeV} \,. \tag{5.3.3}$$

For Model I and in the particular case of small Yukawa couplings in the primed sector, an alternative bound may be inferred from the limits on color-triplet scalars, which can be produced via their color interactions. In the absence of couplings which mediate their decay (as the second type of coupling in Eq. (5.3.1) is not possible for scalar triplets), they will bind with SM quarks to form stable hadrons. This search is expected to result in a sensitivity similar to the one above [374].

It is very interesting to pursue the experimental search for colored pseudoscalars and stable exotic hadrons. Their detection would be a powerful indication of the dynamical solution to the strong CP problem proposed here.

Dynamical axion and exotic fermions

The dynamical axion denoted above by $\eta'_{\psi,\,phys}$ with instanton-induced mass of order $\Lambda_{\rm diag}$, Eqs. (5.2.48) and (5.2.77), can *a priori* be either pair-produced through the kinetic coupling or singly produced through the dimension five anomalous operator. It would decay dominantly to two back-to-back jets and can be searched for in dijet resonance searches. Its production, however, may be suppressed by its high mass. For instance, for $\Lambda_{\rm diag} \simeq 2.9\,{\rm TeV}$, $m_{\eta'_{\psi,\,phys}} \sim$

90 TeV, which is beyond the reach of present collider searches. The other mesons and baryons resulting from the $SU(3)_{\rm diag}$ confinement have masses in the TeV range and above; they would lead to collider signatures similar to those for the exotic pseudo-goldstone bosons.

The axion coupled to SSI

In Model I, the second axion is also dynamical and it was denoted by $\eta'_{\chi,\,phys}$. Its mass can span a large range, depending on the strength of the Yukawa couplings in the prime sector:

- For y'_i couplings of $\mathcal{O}(1)$, this second axion becomes typically heavier than the TeV scale and is thus out of LHC reach.
- For small y'_i couplings ($\mathcal{O}(0.2)$ have been illustrated), an observable axion with mass in the GeV-tens of TeV regime is realistic. Given the low PQ scale (f_d, close to a TeV) lower masses are excluded.

The second axion in Model II, denoted a and of elementary nature, is expected to be light although heavier than the invisible axion, with a mass in the 10 eV - 10 GeV range for $\mathcal{O}(1)$ Yukawa couplings in the prime-fermion sector. By lowering the values of the latter couplings, it can even become as light as the usual invisible axion and with similar phenomenology, as its associated axion scale is the color-unified scale, $f_a \sim \Lambda_{\rm CUT}$.

5.3.2 Cosmological and Gravitational aspects

We briefly discuss next the cosmological aspects of the models constructed above, as well as the putative instability threat from gravitational non-perturbative effects.

Stable particles and cosmological structures

Stable particles with masses higher than about 10^5 GeV may lead to cosmological problems, dominating the mass density and overclosing the universe [375]. This is often a problem in previous models of composite axions because exotic stable baryons bound by the extra confining force [202, 376] are expected.

However, as pointed out in Refs. [240, 376], if axicolor can be unified with a SM gauge group, then the unified forces could mediate the decay of axihadrons into lighter states, and the model would be cosmologically safe. The color unification of this work automatically employs this mechanism. The heavy exotic hadrons decay to the sterile fermions ψ_ν, which are part of the CUT massless multiplet Ψ in Eq. (5.1.2) and Table 5.2. It remains to be determined whether the lifetime for these CUT-induced decay channels is too large to avoid problems from stable

exotic hadrons. If the decays are made to be fast enough, the resulting sterile fermions may induce in turn other cosmological problems. This analysis is left to a future work.

A similar concern pertains to the domain walls which may arise due to the spontaneous breaking of the discrete shift symmetry in the instanton potential, Eqs. (5.2.46) and (5.2.75). The walls need to disappear before they dominate the matter density of the universe, or else other mechanisms must be applied to solve the domain wall problem [201, 227, 377–379].

In any case, if the universe went through an inflation phase any relic previously present will be wiped out. If the reheating temperature is lower than the PQ scales, meaning lower than $\Lambda_{\rm diag}$ here, neither the heavy stable particles nor any putative domain walls are produced again after inflation, and the problems mentioned above are avoided altogether. We defer to a future work the in-depth study of the cosmological aspects of Model I and Model II, with either high- or low-scale inflation.

The question of gravitational quantum effects

Gravitational quantum corrections have been suggested to be relevant and dangerous for axion models in which the PQ scale is not far from the Planck scale. In Model I, both PQ scales correspond to $\Lambda_{\rm diag}$, which is much lower than the Planck scale, and no instability resulting from gravitational quantum effects is at stake. In Model II instead, while the dynamical PQ scale is analogously low, the second PQ symmetry is realized at the CUT scale and gravitational quantum effects could be relevant.

It has often been argued that all global symmetries may be violated by non-perturbative quantum gravitational effects, see for instance Refs. [225–229]. For instance, a black hole can eat global charges and subsequently evaporate. Similar effects may exist with virtual black holes. Another indication that gravity might not respect global symmetries comes from wormhole physics [230–233]. The natural scale of violation in this case is the wormhole scale, usually thought to be very near (within an order of magnitude or so) the Planck mass $M_{\rm Planck}$.

For axion models with high PQ scales, such as the typical scale of invisible axion models $f_a \sim 10^9 - 10^{12}$ GeV, it has been argued that those non-perturbative quantum gravitational effects could lead to extreme fine-tunings. The authors of Ref. [225–228] concentrated on the simplest (and the most dangerous) hypothetical dimension five effective operator

$$g_5 \frac{|\Phi|^4 (\Phi + \Phi^*)}{M_{\rm Planck}}, \tag{5.3.4}$$

where g_5 is a dimensionless coefficient and Φ would be a field whose vev breaks the PQ invariance. This term threatens the standard invisible axion solutions to the strong CP problem, as it would change the shape of the effective potential. The minimum moves unacceptably away from a CP-conserving solution unless the coefficient is strongly fine-tuned, for instance $g_5 < 10^{-54}$ for $f_a \sim 10^{12}$ GeV. These potentially dangerous terms can be avoided if the global PQ symmetry arises accidentally as a consequence of other gauge groups [239,241]. Nevertheless, the idea that gravity

breaks all global symmetries is indeed an assumption — and sometimes an incorrect one — at least at the Lagrangian level. [18] Furthermore, very recently the impact of non-perturbative effects has been clarified and quantified in Ref. [234]. The effects may be extremely suppressed by an exponential dependence on the gravitational instanton action, and be harmless even with high axion scales. The demonstration relied on assuming that the spontaneous breaking of the PQ symmetry is implemented through the vev of a scalar field, and thus it directly applies to our Model II.[19] In summary, Model I is safe from instabilities induced by gravitational quantum corrections and plausibly this also applies to Model II.

5.4 Conclusions

Color unification with massless quarks has been proposed and developed here for the first time. As a simple implementation of the idea, the SM color group has been embedded in $SU(6)$, which is spontaneously broken to QCD and a second confining and unbroken gauge group. An exactly massless $SU(6)$ fermion multiplet solves the strong CP problem. We have fully developed two ultraviolet completions of the mechanism.

In order to implement this idea successfully, it is necessary to give satisfactorily high masses to the $SU(6)$ partners of the SM quarks to achieve a separation between the QCD scale and that of the second confining group. For this purpose, an auxiliary $SU(3')$ gauge group is introduced under which the aforementioned massless fermion is a singlet. $SU(6) \times SU(3') \to SU(3)_c \times SU(3)_{\text{diag}}$ is a simple and realistic option. Both final groups remain unbroken and confine at two different scales, Λ_{QCD} and Λ_{diag}, with $\Lambda_{\text{diag}} \sim \mathcal{O}(\#\ \text{TeV}) \gg \Lambda_{\text{QCD}}$. The scale Λ_{diag} then gives the order of magnitude of the mass of the dynamical composite axion inherent to the color-unified mechanism. Furthermore, massless (or almost massless) sterile fermions are a low-energy trademark remnant of the massless multiplet that solves the SM strong CP problem.

In order to avoid the $SU(3')$ sector sourcing back an extra contribution to the strong CP problem, a minimal extension of its matter sector suffices. Two examples of ultraviolet complete models have been explored in this work: in Model I an extra $SU(3')$ massless fermion is added, while Model II includes instead a second scalar with the same quantum numbers as the color-unification breaking scalar. From the point of view of the strong CP problem, those two models are very different. Model I features a second dynamical axion with a second PQ scale which is also of order Λ_{diag} and thus low. In Model II, this second PQ scale coincides instead with the much larger color-unification scale, and the associated axion is elementary. We computed the two-loop running of all coupling constants involved, showing that the desired separation of all relevant scales is achieved naturally: a color-unification scale much larger than the two confining

[18] For example, orbifold compactifications of the heterotic string have discrete symmetries that prevent the presence of some higher dimension operators, and this can strongly and safely suppress the dangerous effects under discussion [238].

[19] Although no explicit demonstration was given in that work for the case of dynamical breaking via condensates, plausibly the result would also apply for models with dynamical axions and very high axion scales.

ones, $\Lambda_{\rm diag}$ and $\Lambda_{\rm QCD}$, and the subsequent separation of the last two. This separation of scales is robust and stable over a wide range of parameter values.

We have found that regardless of the details of the ultraviolet implementation, generically there are the three sources of anomalous currents: the instantons of the confining $SU(3)_c$, the instantons of the confining $SU(3)_{\rm diag}$, and finally the small-size instantons of the spontaneously broken color-unified theory. There are thus three diverse sources of mass for the three pseudoscalars in the theory which couple to anomalous currents: the QCD η', the dynamical axion inherent to color unification, and the second axion (either dynamical or elementary) associated to the solution of the θ' problem. These three bosons then acquire masses of order $\Lambda_{\rm QCD}$, $\Lambda_{\rm diag}$ and $\Lambda_{\rm SSI}$, respectively, and no standard invisible axion (coupling anomalously only to QCD instantons) is left in the low-energy spectrum. This is generically a very interesting mechanism from the point of view of solving the strong CP problem with heavy axions and scales around a TeV. The mechanism allows a wide extension beyond the invisible axion range of axion parameter space which solves the strong CP-problem. Typical axion masses are in the TeV regime and above, although strictly speaking one of the axions can become as light as the usual invisible axion.

With axion scales around the TeV, observable signals at colliders are expected, as well as other rich phenomenology. Generically, the lightest exotic bound states are colored pseudoscalars (QCD octets and in some cases also triplets in Model I, and only octets in Model II). We have recast the results from present experimental searches for heavy colored mesons to infer a 2.9 TeV bound on the confinement scale of the second confining group, $SU(3)_{\rm diag}$, which is directly related in Model I to the axion scale.

Overall, Model I may be preferred as: i) it is exclusively based on solving the strong CP problem dynamically via massless quarks; ii) from the point of view of naturalness it does not require any fine-tuning to ensure the hierarchy between the PQ and the electroweak scales, as no PQ field is involved in the scalar potential. In Model II instead, one PQ field participates in the color-unification scalar potential, and furthermore this model is a hybrid dynamical-elementary axion solution to the strong CP problem.

Model I is also unquestionably safe from the point of view of stability of the axion solution with respect to non-perturbative effects of quantum gravity, as its PQ scales are $\Lambda_{\rm diag} \sim$ TeV. Furthermore, recent advances suggest that the quantum gravity threat should not be considered a risk even for Model II. The other issue of the cosmological impact of (quasi) stable heavy exotic hadrons and of the (almost) massless sterile fermion remnants can be simply avoided by introducing an inflation scale and reheating temperature lower than $\Lambda_{\rm diag}$. This last subject deserves future detailed attention in particular in view of the dark matter puzzle.

CHAPTER 6

Automatic Peccei-Quinn symmetry

In this Chapter, which is based on the publication in Ref. [2], the axicolor framework introduced in Section 3.2 is approached in a novel way: to assume that the $SU(\tilde{N})$ exotic confining gauge sector is chiral. In a minimalistic approach, we require a fermion content such that:

- It confines and renders the theory free from gauge anomalies.
- The exotic fermion representations are chiral, so that fermionic mass terms are automatically forbidden.
- Minimality in the specific matter content will be a guideline. Two (or more) different axicolored fermions are present, with at least one of them being QCD colored as well.

In this class of set ups, at least two chiral $U(1)$ symmetries emerge in the dynamical sector and nullify the theta angles of the dynamical sector and the QCD sector. It can be checked that it is not possible to obey the three requirements listed above for $SU(3)$, $SU(6)$ or $SU(7)$, at least not with just two exotic fermions in low-dimensional representations of the chiral confining group. It is possible instead for $SU(4)$; nevertheless, this theory would not render an improvement on the gravitational issue, as argued in App. 6.A, and it will not be further developed.

We focus here on the case of chiral gauge $SU(5)$, implemented via its lowest dimensional fermion representations, $\bar{\mathbf{5}}$ and $\mathbf{10}$, which together fulfill the conditions above. The $SU(5)$ confinement scale will be assumed to be much larger than that of QCD, $\Lambda_5 \gg \Lambda_{\rm QCD}$. It will be shown that a satisfactory $U(1)_{PQ}$ symmetry is an automatic consequence of the chiral realization of the gauge group. Note that some models have been previously built for which PQ invariance is accidental, that is, not imposed by hand [238–245]. Nevertheless, they all required extra symmetries in addition to axicolor, either gauge or discrete ones. In contrast, axicolor $SU(5)$ will be shown to suffice because of its chiral character, rendering a particularly simple framework.

Relevant aspects to be developed include on one side the identification of the exotic fermion condensates, which in dynamical axion models are the only source of spontaneous symmetry breaking, e.g. for exotic flavor and for the PQ symmetries. Another important question is the impact of $SU(5)$ gauge invariance on the possible non-perturbative gravitational couplings of the theory.

The idea will be implemented in two alternative realizations, selected so as to achieve minimal matter content. They will only differ in the QCD charges of the exotic $\bar{\mathbf{5}}$ and **10** fermions present: octets of QCD color in one model, while triplets in a second version.

6.1 The SU(5) chiral confining theory

We consider a chiral version of the axicolor model, with $SU(5)$ as an extra confining group, and one set of massless exotic fermions in its five and ten dimensional representations, $\psi_{\bar{5}}$ and ψ_{10} (the notation $\psi_{\bar{5}} \equiv \bar{\mathbf{5}}$, $\psi_{10} \equiv \mathbf{10}$ will be often used for convenience). Such a set cancels all $SU(5)$ gauge anomalies (as in $SU(5)$ GUT models). The complete gauge group of nature would then be

$$SU(5) \times SU(3)_c \times SU(2)_L \times U(1)\,. \tag{6.1.1}$$

An economic implementation is to assume the usual SM fields to be singlets under $SU(5)$, while the exotic chiral fermions in the $\psi_{\bar{5}}$ and ψ_{10} representations of $SU(5)$ are singlets under the electroweak SM gauge group.

	$SU(5)$	$SU(3)_c$
$\psi_{\bar{5}}$	$\bar{\mathbf{5}}$	**R**
ψ_{10}	**10**	**R**

Table 6.1: Charges of exotic fermions under the confining gauge group $SU(5) \times SU(3)_c$. The left-handed Weyl fermions $\psi_{\bar{5}}$ and ψ_{10} are massless and singlets of the SM electroweak gauge group. **R** denotes a pseudoreal representation.

If the exotic fermions carry also QCD color, this theory solves the strong CP problem. Indeed, the presence of (at least) two massless fermions ensures the existence of two distinct $U(1)$ chiral global symmetries, exact at the classical level but explicitly broken by quantum non-perturbative effects. The θ-parameters corresponding to the two confining gauge groups become thus unphysical via chiral rotations of those fermions. Furthermore, the chiral character of the representations forbids fermionic mass terms and thus guarantees that those symmetries are automatic, instead of imposed on a given Lagrangian as customary. Finally, the requirement of a large confining scale $\Lambda_5 \gg \Lambda_{\rm QCD}$ leads to a realistic model, given the non-observation of a spectrum of bound states composed of those massless exotic fermions.

For simplicity, we will consider that the set $\{\psi_{\bar{5}}, \psi_{10}\}$ belongs to a (pseudo)real representation $\mathbf{R}$ of color QCD, so as automatically cancel $\left[SU(3)_c\right]^3$ anomalies, see Table 1. Later on we will develop in detail two specific choices for $\mathbf{R}$: the case of the fundamental of QCD with reducible representation $\mathbf{R} = \mathbf{3} + \bar{\mathbf{3}}$ in one case, and the adjoint $\mathbf{R} = \mathbf{8}$ in the second case. In all cases, all mixed gauge anomalies in the confining sector vanish by construction as well, because only non-abelian $SU(N)$ groups are present and the exotic fermions are electroweak singlets.

6.1.1 Global symmetries

At the scale Λ_5, $SU(5)$ confines and the massless fermions in Tab. 1 will form massive bound states including QCD-colored ones. In the limit in which the QCD coupling constant α_s is neglected, the $SU(5)$ gauge Lagrangian exhibits at the classical level a global flavor symmetry

$$U(n)_{\bar{5}} \times U(n)_{10} \leftrightarrow SU(n)_{\bar{5}} \times SU(n)_{10} \times U(1)_{\bar{5}} \times U(1)_{10}\,, \tag{6.1.2}$$

where n denotes the dimension of $\mathbf{R}$, which plays the role of number of exotic flavors,

$$n = \dim\{\mathbf{R}\}\,. \tag{6.1.3}$$

The two global $U(1)$ symmetries correspond to independent rotations of the two massless fermion representations. However, they are both broken at the quantum level by anomalous couplings to the $SU(5)$ and QCD field strengths. A generic combination of them will lead to the following anomaly coefficients (see App. 6.B):

$$U(1) \times \left[SU(5)\right]^2 : \qquad n \times \left(Q_{\bar{5}} T(\bar{\mathbf{5}}) + Q_{10} T(\mathbf{10})\right) = \frac{n}{2}\left(Q_{\bar{5}} + 3\,Q_{10}\right)\,, \tag{6.1.4}$$

$$U(1) \times \left[SU(3)_c\right]^2 : \qquad T(\mathbf{R}) \times \left(5\,Q_{\bar{5}} + 10\,Q_{10}\right)\,. \tag{6.1.5}$$

Here, $Q_{\bar{5}}$ and Q_{10} denote arbitrary $U(1)$ charges for $\psi_{\bar{5}}$ and ψ_{10}, respectively, and T's denote the Dynkin indices of the corresponding representations. It follows from Eq. (6.1.4) that the charge assignment

$$Q_{\bar{5}} = -3\,, \qquad Q_{10} = 1\,, \tag{6.1.6}$$

renders a combination of $U(1)$'s that is free from $SU(5)$ anomaly. The $SU(5)$ anomaly-free combination is analogous to the $B - L$ symmetry in usual $SU(5)$ GUT's. It will play the role of the PQ symmetry in our model, since it is a classically exact symmetry that is only broken by the QCD anomaly. A second combination will remain explicitly broken[1] by quantum non-perturbative effects of $SU(5)$, so that the classical global symmetry in Eq. (6.1.2) reduces (for $\alpha_s = 0$) to

$$SU(n)_{\bar{5}} \times SU(n)_{10} \times U(1)_{PQ=B-L}\,. \tag{6.1.7}$$

The corresponding global charges of the exotic fermions are shown in Table 6.2.

[1] This can be for instance, the orthogonal combination corresponding to $\{Q_{\bar{5}} = 1, Q_{10} = 3\}$, although any combination different from that free from anomalous $SU(5)$ couplings can play this role.

	$SU(n)_{\bar{5}}$	$SU(n)_{10}$	$U(1)_{B-L} \equiv U(1)_{PQ}$
$\psi_{\bar{5}}$	$\square$	$\mathbf{1}$	-3
ψ_{10}	$\mathbf{1}$	$\square$	1

Table 6.2: Global chiral properties at the classical level, in the limit of vanishing α_s.

Confinement versus chiral symmetry breaking

A first question is whether the confinement of the $SU(5)$ gauge dynamics is accompanied by the spontaneous breaking of the associated chiral global symmetries. Two alternative realizations are possible:

- The global symmetries can be spontaneously broken via fermion condensates. As a result, (almost) massless (pseudo)Goldstone bosons (pGBs) will be present in the low energy theory.
- Conversely, they could remain unbroken and the spectrum of bound states would explicitly reflect those global symmetries via multiplets of degenerate states. In particular, massless baryons are then needed in order to fulfil the 't Hooft anomaly consistency conditions [95] to match the anomalies of the high and low energy theories.

It can be shown that it is not possible to comply with the 't Hooft consistency conditions for the complete flavor group. That is, it is impossible to match the $\left[SU(n)_{\bar{5}}\right]^3$ and $\left[SU(n)_{10}\right]^3$ anomalies before confinement –and thus in terms of quarks– with the anomalies after confinement in terms of massless "baryons". The demonstration can be found in App. 6.D. The confinement of gauge $SU(5)$ is thus necessarily accompanied by the spontaneous breaking of the chiral global $SU(n)_{\bar{5}} \times SU(n)_{10}$ symmetry, and associated (pseudo)Goldstone bosons (pGBs) will be present in the low-energy spectrum.

In contrast, for $U(1)_{PQ}$ it is possible to fulfil 't Hooft anomaly conditions [380, 381]. At high energies and in terms of quarks, the spectrum in Tab. 6.2 contributes to the global anomalies as

$$\left[U(1)_{PQ}\right]^3 : \qquad n\left(5\,(Q_{\bar{5}})^3 + 10\,(Q_{10})^3\right) = -125\,n\,, \tag{6.1.8}$$

$$U(1)_{PQ} \times \left[SU(3)_c\right]^2 : \qquad N \equiv 2\,(5\,Q_{\bar{5}} T(\mathbf{R}) + 10\,Q_{10} T(\mathbf{R})) = -10\,T(\mathbf{R})\,, \tag{6.1.9}$$

$$U(1)_{PQ} \times [\text{grav}]^2 : \qquad n\,(5\,Q_{\bar{5}} + 10\,Q_{10}) = -5\,n\,. \tag{6.1.10}$$

where N denotes as customary the QCD anomaly factor. The low-energy spectrum admits in turn a massless baryon composed by three fermions,

$$\chi \equiv \mathbf{10}\,\bar{\mathbf{5}}\,\bar{\mathbf{5}}\,, \tag{6.1.11}$$

which has PQ charge $Q_\chi = -5$ and can belong to the $\mathbf{R}$ representation of $SU(3)_c$. Its contribution to the anomaly equations matches the anomalies at the quark level in Eqs. (6.1.8) and (6.1.10):

$$\left[U(1)_{PQ}\right]^3 : \qquad n\,Q_\chi^3 = -125\,n\,, \tag{6.1.12}$$

$$U(1)_{PQ} \times \left[SU(3)_c\right]^2 : \qquad N \equiv 2\,Q_\chi\,T(\mathbf{R}) = -10\,T(\mathbf{R})\,, \tag{6.1.13}$$

$$U(1)_{PQ} \times [\text{grav}]^2 : \qquad n\,Q_\chi = -5\,n\,, \tag{6.1.14}$$

In consequence, the chiral confining $SU(5)$ theory would be *a priori* perfectly consistent even if the $U(1)_{PQ}$ were to remain unbroken after confinement. Nevertheless, this is not phenomenologically viable since (almost) massless QCD colored fermions are not observed in nature (other than the light SM quarks).

To sum up, parts of the global symmetries in Eq. (6.1.7) with the field content in Table 6.2 need to be spontaneously broken by fermion condensates upon $SU(5)$ confinement.

6.1.2 Fermion condensates: chiral-breaking versus PQ-breaking

It will be assumed that Λ_5 settles the overall scale for all dynamical breaking mechanisms in the $SU(5)$ sector, which will take place through fermion condensates.

Chiral condensate

The lowest dimension fermionic condensate which is gauge invariant and breaks the non-abelian chiral symmetries in Eq. (6.1.7) is a dimension six operator:

$$\mathbf{10\,10\,10\,\bar{5}}\,, \tag{6.1.15}$$

with vacuum expectation value (VEV) and breaking pattern expected to obey

$$\langle \mathbf{10\,10\,10\,\bar{5}} \rangle \sim \Lambda_5^6 \quad \Longrightarrow \quad SU(n)_{\bar{5}} \times SU(n)_{10} \longrightarrow G \supset SU(3)_c\,. \tag{6.1.16}$$

On the right-hand side of this expression, it has been assumed that the QCD gauge group is contained in the unbroken subgroup G of $SU(n)_{\bar{5}} \times SU(n)_{10}$. This is possible as the product of four $\mathbf{R}$ representations contains an $SU(3)$ singlet since $\mathbf{R}$ is (pseudo)real. It should be noted that the unbroken subgroup G which contains $SU(3)$ is not necessarily aligned with the one which contains $SU(3)_c$ for $\alpha_s = 0$. Once α_s is turned on, on the other hand, the QCD interaction forces the condensates to preserve color, which implies that only the QCD invariant condensates will form (see also[240]).[2]

[2] In the thermal bath, for example, the QCD breaking vacua have higher energy density than the QCD preserving one due to the thermal potential proportional proportional to $m_{\text{gluon}}^2 T^2$, where m_{gluon} denotes the gluon mass on the QCD breaking vacua.

If $\mathbf{R}$ is an irreducible representation of $SU(3)_c$, then the only part of the non-abelian chiral symmetry in Eq. (6.1.16) that is expected to remain unbroken is $SU(3)_c$. If $\mathbf{R}$ is reducible instead, some $U(1)$'s can remain exact (see Sec. 6.2 where $\mathbf{R} = \mathbf{3} + \bar{\mathbf{3}}$). Therefore, irrespective of G, most generators of $SU(n)_{\bar{5}} \times SU(n)_{10}$ other than those of $SU(3)_c$ would be explicitly broken by QCD interactions,

$$SU(n)_{\bar{5}} \times SU(n)_{10} \xrightarrow{\langle \mathbf{10\,10\,10\,\bar{5}} \rangle} G \xrightarrow{\alpha_s \neq 0} SU(3)_c \,. \tag{6.1.17}$$

In consequence, most of the pGBs associated to the broken generators of the non-abelian chiral symmetry are necessarily colored under QCD. Their masses m are quadratically sensitive to large scales via gluon loops and thus safely large,

$$m^2(\mathbf{R}) \sim \frac{3\,\alpha_s}{4\pi}\, C(\mathbf{R})\, \Lambda_5^2 \,, \tag{6.1.18}$$

where C($\mathbf{R}$) is the quadratic Casimir of the QCD representation $\mathbf{R}$ to which a given pGB belongs, $T_R^a T_R^a = C(\mathbf{R})\, \mathbb{1}$.

The chiral condensate in Eq. (6.1.16) is $U(1)_{PQ}$ invariant, though, since its PQ charge is vanishing. The spontaneous breaking of the PQ symmetry (which is phenomenologically the only viable option as earlier explained) can only be achieved via higher dimensional fermionic condensates.

PQ condensate

The lowest dimensional operator which is gauge invariant but has non-vanishing PQ-charge is

$$\bar{\mathbf{5}}\,\bar{\mathbf{5}}\,\mathbf{10}\,\bar{\mathbf{5}}\,\bar{\mathbf{5}}\,\mathbf{10} \,, \tag{6.1.19}$$

which has mass dimension nine and PQ-charge -10. In order to achieve spontaneous $U(1)_{PQ}$ symmetry breaking, we assume that this operator obtains a non-vanishing VEV,[3]

$$\langle \bar{\mathbf{5}}\,\bar{\mathbf{5}}\,\mathbf{10}\,\bar{\mathbf{5}}\,\bar{\mathbf{5}}\,\mathbf{10} \rangle \sim \Lambda_5^9 \,, \tag{6.1.20}$$

which is associated with the QCD axion as a composite field.

In summary, the combined action of the two condensates in Eqs. (6.1.16) and (6.1.20) induces a breaking pattern of the global symmetries of the exotic $SU(5)$ sector of the form

$$SU(n)_{\bar{5}} \times SU(n)_{10} \times U(1)_{PQ} \xrightarrow{\langle \mathbf{10\,10\,10\,\bar{5}} \rangle} G \times U(1)_{PQ} \xrightarrow{\langle \bar{\mathbf{5}}\,\bar{\mathbf{5}}\,\mathbf{10}\,\bar{\mathbf{5}}\,\bar{\mathbf{5}}\,\mathbf{10} \rangle} G' \xrightarrow{\alpha_s \neq 0} SU(3)_c \,. \tag{6.1.21}$$

For later use, it is convenient to parametrize the field combination in Eq. (6.1.20) as

$$\bar{\mathbf{5}}\,\bar{\mathbf{5}}\,\mathbf{10}\,\bar{\mathbf{5}}\,\bar{\mathbf{5}}\,\mathbf{10} \sim \Lambda_5^9\, e^{-i\,10\,a/f_{\rm PQ}} \,, \tag{6.1.22}$$

[3] Its VEV also breaks the non-abelian chiral symmetry, but this effect should be subdominant with respect to that of the lower dimension operator in Eq. (6.1.16).

where the radial degrees of freedom are left implicit, a denotes the dynamical axion that corresponds to the axial excitation of the operator, and the PQ charge of the condensate resulting from Tab. 6.2 is explicitly shown. The PQ scale f_{PQ} associated to the pGB nature of the axion obeys

$$f_{\rm PQ} \propto \Lambda_5 \,. \tag{6.1.23}$$

It should be noted that the PQ charges of the $SU(5)$ invariant states are multiples of 5, and hence, the PQ symmetry in the broken phase is realized by a shift of the axion given by

$$\frac{5a}{f_{PQ}} \to \frac{5a}{f_{PQ}} + \alpha \,, \quad \alpha = [0, 2\pi) \,, \tag{6.1.24}$$

see also App. 6.C.

6.1.3 The axion Lagrangian

In order to obtain the low-energy effective Lagrangian for the axion, the conservation of the PQ current will be studied next. The current at high energies can be computed in terms of the fundamental fermions by applying Noether's formula:

$$j^\mu_{\rm PQ} = Q_5\, \psi^\dagger_{\bar 5} \bar\sigma^\mu \psi_{\bar 5} + Q_{10}\, \psi^\dagger_{10} \bar\sigma^\mu \psi_{10} = -3\, \psi^\dagger_{\bar 5} \bar\sigma^\mu \psi_{\bar 5} + \psi^\dagger_{10} \bar\sigma^\mu \psi_{10} = f_{\rm PQ} \partial^\mu a \,. \tag{6.1.25}$$

At energies below $SU(5)$ confinement, the current can be expressed in terms of the composite fermions (i.e. the composite baryons that will be generically denoted by χ_i) and the composite scalar (the dynamical axion a),

$$j^\mu_{\rm PQ} = f_{\rm PQ} \partial^\mu a + \sum_i Q_{\chi_i} \left(\chi_i^\dagger\, \bar\sigma^\mu\, \chi_i\right) . \tag{6.1.26}$$

This current is classically conserved but it has a QCD anomaly,

$$\partial_\mu j^\mu_{\rm PQ} = N\, \frac{\alpha_s}{8\pi}\, G\tilde G \,. \tag{6.1.27}$$

This ward identity is reproduced by the following effective Lagrangian:

$$\mathcal{L}_{\rm eff} = \frac{1}{2} \partial^\mu a \partial_\mu a + \frac{\partial_\mu a}{f_{\rm PQ}} \sum_i Q_{\chi_i} \left(\chi_i^\dagger\, \bar\sigma^\mu\, \chi_i\right) + N\, \frac{\alpha_s}{8\pi}\, \frac{a}{f_{\rm PQ}} G\tilde G \,, \tag{6.1.28}$$

where the PQ symmetry is realized by the shift of the axion in Eq. (6.1.24) with χ_i's kept invariant.

Relation between $f_{\rm PQ}$ and Λ_5 in Naïve Dimensional Analysis

The effective Lagrangian obtained above can be rewritten in terms of a complex field satisfying $U\, U^\dagger = 1$,

$$U = e^{i\, 5a/f_{\rm PQ}} \,, \tag{6.1.29}$$

where the factor 5 is introduced to take into account that the physical domain of the axion field is $a/f_{\rm PQ} \in [0, 2\pi/5)$, as shown in App. 6.C. The result is

$$\mathcal{L}_{\rm eff} = \frac{1}{2}\left(\frac{f_{\rm PQ}}{5}\right)^2 \partial^\mu U^* \partial_\mu U - 5\,\frac{\partial_\mu a}{f_{\rm PQ}}\left(\chi^\dagger\,\bar\sigma^\mu\,\chi\right) + \dots \tag{6.1.30}$$

where the kinetic term is canonically normalized. In this equation, the sum over composite baryons only shows explicitly the unique type of baryon made out of three fermions, which happens to be the baryon χ with PQ charge $Q_\chi = -5$ defined in Eq. (6.1.11), albeit now being massive.

Applying Naïve Dimensional Analysis (NDA) [382,382,383] to the Lagrangian in Eq. (6.1.30), it follows that

$$\mathcal{L}_{\rm eff} = \left(\frac{\Lambda_5}{4\pi}\right)^2 \partial^\mu U^* \partial_\mu U + \left(\frac{4\pi}{\Lambda_5}\right)\partial_\mu a\left(\chi^\dagger\,\bar\sigma^\mu\,\chi\right) + \dots \tag{6.1.31}$$

leading to the identification

$$\Lambda_5 \simeq \frac{4\pi\, f_{\rm PQ}}{5}\,. \tag{6.1.32}$$

Customarily, the axion scale f_a is defined reabsorbing in it the QCD anomaly factor N,

$$f_a \equiv \frac{f_{\rm PQ}}{N}\,. \tag{6.1.33}$$

Coupling to gluons and Domain Walls

Because of the periodicity of the instanton potential, the anomalous coupling of the axion to gluons breaks explicitily $U(1)_{PQ}$ to a discrete symmetry $S(m)$,

$$S(m) : a \longrightarrow a + \frac{2\pi m}{N} f_{\rm PQ}, \qquad m \in \mathbb{Z}\,. \tag{6.1.34}$$

Nevertheless, not all $S(m)$ transformations are nontrivial, as some of them are equivalent via gauge transformations (see App. 6.C). The physical discrete symmetry corresponds to the quotient $S_{\rm phys} = S/\mathbb{Z}_5$, where $\mathbb{Z}_5$ is the center of the $SU(5)$ group [220]. This implies that the QCD potential has $\dim[S_{\rm phys}]$ degenerate minima and therefore a number of domain walls $N_{DW} = \dim[S_{\rm phys}]$ will be generated when the axion field takes a VEV, as this breaks spontaneously the discrete symmetry,

$$N_{\rm DW} = \frac{|N|}{5}\,. \tag{6.1.35}$$

Any theory with $N_{\rm DW} > 1$ has a domain wall problem: domain walls could dominate the energy density of the universe and overclose it. It will be seen further below that in our theory indeed $N_{\rm DW} > 1$, and in consequence a pre-inflationary PQ-transition will be assumed to avoid this issue (see e.g. [384] and references therein). Besides, we also assume that the highest temperature after inflation is lower than Λ_5 to avoid the production of massive particles in the dynamical sector, as some of them are stable due to the $\mathbb{Z}_2$ unbroken subgroup of the PQ symmetry, leading to an unacceptably large relic density.

6.1.4 Planck suppressed operators

It has been argued that quantum gravity may violate all global symmetries. In particular, Planck suppressed operators which are not PQ invariant could be dangerous for axion solutions to the strong CP problem, since they can unacceptably displace the minimum of the axion potential from the CP conserving point.

Within our model, because of gauge invariance and chirality, the lowest dimensional operator of this type has mass dimension nine, as previously argued: it is the operator in Eq. (6.1.20), whose VEV breaks PQ spontaneously. This significantly strong Planck suppression suggest that our model can be protected from those gravitational issues. This is to be contrasted with the usual expectation in axion models which allow lower dimension effective operators of gravitational origin, e.g. dimension five couplings as in Eq. (5.3.4).

The prefactors of the effective operator are relevant and they can be settled using NDA [382, 383], resulting in:

$$\mathcal{L}_{\not{PQ}} = c\,\frac{1}{4\pi}\,\frac{1}{M_{\rm Pl}^5}\,\frac{1}{2!\,4!}\,\bar{\mathbf{5}}\,\bar{\mathbf{5}}\,\mathbf{10}\,\bar{\mathbf{5}}\,\bar{\mathbf{5}}\,\mathbf{10}\,, \tag{6.1.36}$$

at around the Planck scale. Here, c would be generically of order one and a combinatorial factor due to the presence of identical fields has been explicitly included in the definition of the operator.[4] In order to quantify its impact on the location of the minimum of the axion potential, it is necessary to express it in terms of the low-energy composite fields. NDA leads to

$$\mathcal{L}_{\not{PQ}} = c\,\frac{(4\pi)^2}{2!\,4!}\left(\frac{N}{5}\right)^9\,\frac{f_a^9}{M_{\rm Pl}^5}e^{-i\frac{10}{N}a/f_a} + \text{h.c.}\,. \tag{6.1.37}$$

The resulting axion potential, including as well the QCD contribution reads [5]

$$V(a) = -m_a^2 f_a^2\cos\left(\frac{a}{f_a}\right) - c\,\frac{(4\pi)^2}{4!}\left(\frac{N}{5}\right)^9\,\frac{f_a^9}{M_{\rm Pl}^5}\cos\left(\frac{10}{N}\frac{a}{f_a}+\delta\right)\,, \tag{6.1.38}$$

where δ is the relative phase between the Planck-suppressed operator in Eq. (6.1.37) and the QCD vacuum parameter. The displacement of the axion VEV with respect to the CP conserving minimum is then given by

$$|\Delta\bar{\theta}_{eff}| = |c\sin(\delta)|\,\frac{2\,(4\pi)^2}{4!}\left(\frac{N}{5}\right)^8\,\frac{f_a^7}{M_{\rm Pl}^5\,m_a^2}\,, \tag{6.1.39}$$

which is strongly constrained by the experimental limit on the neutron electric dipole moment (EDM). For a given implementation of the $SU(5)$ theory, this indicates an upper bound on the f_a value needed to avoid to fine-tune the coefficient of the gravitationally induced effective operator.

[4] Consistently, this would correspond to a combinatorial factor of 1 in the corresponding Feynman rules.

[5] The QCD axion potential is approximated here by a cosine dependence, since we are only interested in the displacement of the minimum where that approximation is perfectly valid. For the correct dependence using chiral Lagrangians at NLO see Ref. [183].

There is a certain degree of uncertainty when using power counting arguments in the present context, though, which may change the prefactors significantly. As illustration, if f_a is taken as the PQ physics scale (instead of saturating it by $\Lambda_5 \sim 4\pi f_{PQ}/5$ as in NDA), the operator in Eq. (6.1.36) would translate into

$$\mathcal{L}_{\not{PQ}} = c\,\frac{1}{2!\,4!}\,\frac{f_a^9}{M_{\rm Pl}^5} e^{-i\frac{10}{N}a/f_a} + \text{h.c.}\,, \tag{6.1.40}$$

instead of Eq. (6.1.37). The displacement induced on the effective QCD vacuum angle would then be significantly smaller, depending on the value of the anomaly factor N in a given realization of the chiral confining SU(5) theory.

We will apply next the analysis above to two examples of the confining chiral $SU(5)$ theory, which differ in the QCD charges of the exotic fermions $\{\psi_{\bar{5}}, \psi_{10}\}$, corresponding respectively to a reducible and irreducible QCD representation $\mathbf{R}$. In the first model $R = 3 + \bar{3}$, while $R = 8$ will be assumed in the second model. While the former requires four exotic fermions (instead of just two for the second option), its matter content is smaller in terms of number of degrees of freedom.

Planck suppressed operators and neutrino masses

In addition to the dimension nine operator in Eq. (6.1.36), other operators with lower dimensionality may be present, e.g.: [6]

$$\mathcal{L}_{\not{PQ}} = c\,\frac{1}{4\pi}\,\frac{1}{M_{\rm Pl}^5}\,\frac{1}{2!}\,\bar{\mathbf{5}}\,\bar{\mathbf{5}}\,\mathbf{10}\,L\Phi \;+\; \frac{c_\nu}{M_{\rm Pl}}(L\Phi)^2, \tag{6.1.41}$$

where L and Φ denote the lepton and Higgs doublets, respectively. The combination of these two operators breaks the PQ symmetry[7], modifying the axion potential and thus displacing $\theta_{\rm eff}$. However, for pseudo-Dirac neutrinos (where the size of the observed neutrino masses is dominated by a Dirac Yukawa coupling), the impact of these operators is a negligible correction to the coefficient of the dimension nine operator discussed above in Eq. (6.1.36). Nevertheless, depending on the mechanism responsible for realistic neutrino masses, the presence of fields beyond the SM ones may or may not allow for additional dangerous operators. For instance, for the seesaw type I mechanism the following terms should be considered

$$\mathcal{L} = \frac{1}{M_{\rm Pl}^3}\left(\bar{\mathbf{5}}\,\bar{\mathbf{5}}\,\mathbf{10}\overline{N}\right) + M\overline{N^c}\,N + y_\nu \overline{N}\,L\Phi\,, \tag{6.1.42}$$

where N denotes a singlet fermion, M is the Majorana scale, and y_ν its Yukawa coupling. The combination of the couplings present in Eq. (6.1.42) generates the dimension nine operator

[6] We thank the referee for pointing out this coupling.

[7] Because any global symmetry is expected to be broken by gravitational effects, B-L may not be an exact low energy symmetry and a Planck suppressed Majorana contribution to neutrino masses may be present, although numerically negligible.

discussed above,

$$\mathcal{L} \propto \frac{1}{M_{\rm Pl}^2}\frac{1}{M_{\rm Pl}^2}\frac{1}{M}\left(\bar{\mathbf{5}}\,\bar{\mathbf{5}}\,\mathbf{10}\,\bar{\mathbf{5}}\,\bar{\mathbf{5}}\,\mathbf{10}\right), \tag{6.1.43}$$

albeit with a milder suppression by a factor $M_{\rm Pl}/M$. In consequence, the gravity-induced operator $\left(\bar{\mathbf{5}}\,\bar{\mathbf{5}}\,\mathbf{10}\overline{N}\right)$ can be dangerous and result in a larger displacement of $\bar{\theta}_{\rm eff}$ than that considered in this work. A simple option to avoid this type of operators would be to gauge B-L in the SM sector with three right-handed neutrinos. In this case, the gauged B-L symmetry would be spontaneously broken the vev of a scalar field, leaving a residual gauge Z_2 (under which N and $L\Phi$ are odd) that forbids the two Planck-suppressed operators considered above, see Eqs. (6.1.41-6.1.42).

6.2 Model I: color-triplet fermions

In the first model, the exotic $\{\psi_{\bar{5}}, \psi_{10}\}$ fermions appear in the fundamental representation of QCD, alike to SM quarks, with

$$\mathbf{R} = \mathbf{3} + \bar{\mathbf{3}}\,, \tag{6.2.1}$$

as shown in Table 6.3. The $\left[SU(3)_c\right]^3$ anomalies are then automatically cancelled due to the the four distinct $SU(5)$ fermions present. The latter being massless, at the classical level this spectrum has four independent $U(1)$ global chiral symmetries. One combination is broken by non-perturbative $SU(5)$ effects, and three would remain unbroken for vanishing α_s, one of them being the PQ symmetry. The dimension of the (pseudo)real representation is then

$$n = 6\,. \tag{6.2.2}$$

As indicated in Eq. (6.1.7), the global chiral symmetries correspond to $SU(6)_{\bar{5}} \times SU(6)_{10} \times U(1)_{PQ}$ for $\alpha_s = 0$, which is explicitly broken by QCD down to

$$SU(6)_{\bar{5}} \times SU(6)_{10} \times U(1)_{PQ} \xrightarrow{\alpha_s \neq 0} SU(3)_c \times U(1)_{V,\bar{5}} \times U(1)_{V,10}\,. \tag{6.2.3}$$

That is, only QCD plus two global $U(1)$ symmetries remain unbroken for $\alpha_s \neq 0$, while $U(1)_{PQ}$ is broken by the non-perturbative QCD effects. The two surviving $U(1)$ symmetries are the left-over of the four classical $U(1)$ symmetries associated to the four independent massless fermions of this model (see Table 6.3), as two were explicitly broken by anomalous couplings at the quantum level: respectively $SU(5)$ and QCD interactions.

The question of whether the QCD group $SU(3)_c$ is indeed the surviving unbroken group after chiral symmetry breaking, as indicated in Eqs. (6.1.16), (6.1.17) and (6.1.21), deserves a specific discussion. To see this, let us note that an $SO(6)$ subgroup of the global symmetry $SU(6)_{\bar{5}} \times SU(6)_{10}$ satisfies the 't Hooft anomaly consistency conditions. Besides, the condensates $\langle \mathbf{10}\,\mathbf{10}\,\mathbf{10}\,\bar{\mathbf{5}}\rangle$ and $\langle \bar{\mathbf{5}}\,\bar{\mathbf{5}}\,\mathbf{10}\,\bar{\mathbf{5}}\,\bar{\mathbf{5}}\,\mathbf{10}\rangle$ can be $SO(6)$ singlets. This means that the unbroken subgroup G of the global symmetry $SU(6)_{\bar{5}} \times SU(6)_{10}$ contains $SO(6)$, i.e. $G \supset SO(6)$.[8] The $SU(3)$

[8] Our arguments do not depend on whether $G = SO(6)$ or $G \supsetneq SO(6)$, although we expect that $G = SO(6)$.

	$SU(5)$	$SU(3)_c$	$U(1)_{PQ}$	$U(1)_{V,\bar{5}}$	$U(1)_{V,10}$
$\psi_{(\bar{5},3)}$	$\bar{\mathbf{5}}$	$\mathbf{3}$	-3	1	0
$\psi_{(\bar{5},\bar{3})}$	$\bar{\mathbf{5}}$	$\bar{\mathbf{3}}$	-3	-1	0
$\psi_{(10,3)}$	$\mathbf{10}$	$\mathbf{3}$	$+1$	0	1
$\psi_{(10,\bar{3})}$	$\mathbf{10}$	$\bar{\mathbf{3}}$	$+1$	0	-1

Table 6.3: Model I: charges of exotic fermions under the confining gauge group $SU(5) \times SU(3)_c$, the PQ symmetry and the spontaneously broken global $U(1)$ symmetries. The left-handed Weyl fermions $\psi_{\bar{5}}$ and ψ_{10} are massless and singlets of the SM electroweak gauge group; their QCD representation has been indicated as an additional subscript.

subgroup of $SO(6)$ is then obtained by identifying the vector representation of $SO(6)$ to be $\mathbf{3}+\bar{\mathbf{3}}$. Therefore, it is clear that an $SU(3)$ global symmetry remains unbroken below the confinement scale.

It should be noted that an $SO(6)$ subgroup of $SU(6)_{\bar{5}} \times SU(6)_{10}$ is not uniquely determined, and hence, the unbroken $SO(6)$ is not in general aligned to the one which contains $SU(3)_c$ for $\alpha_s = 0$. However, it has been argued that, among the possible condensate channels, the minimum of the potential corresponds to the one preserving QCD for $\alpha_s \neq 0$ [240]. Thus, we find that it is most likely that the $SU(5)$ dynamics with the non-vanishing chiral and PQ condensates in Eqs. (6.1.16) and (6.1.20) preserves $SU(3)_c$.

The $U(1)_{V,\bar{5}}$ and $U(1)_{V,10}$ symmetries are generically broken by those condensates. In fact, the chiral condensate in Eq. 6.1.16 breaks spontaneously $U(1)_{\bar{5}} \times U(1)_{10}$ down to a $U(1)$, where the number of positive and negative charges with respect to this $U(1)$ is balanced at the QCD preserving vacuum. The PQ condensate could also break this remaining $U(1)$ if the quarks in the condensates are all either in the $\mathbf{3}$ or in the $\bar{\mathbf{3}}$ representation of QCD. Accordingly, the model predicts one or two additional pGBs which obtain tiny masses from the higher dimensional gravitational operators in Eq. (6.1.36). As those pGBs decouple from the thermal bath at a temperature much higher than the weak scale, the contribution of each pGB to the effective number of relativistic species is suppressed, i.e. $\Delta N_{\rm eff} \simeq 0.03$, and hence the model is consistent with the current constraint $N_{\rm eff} = 2.99^{+0.34}_{-0.33}$ [21].

In this model, the PQ current in Eq. (6.1.25) takes the form

$$j^\mu_{\rm PQ} = -3\psi^\dagger_{(\bar{5},3)}\bar{\sigma}^\mu\psi_{(\bar{5},3)} - 3\psi^\dagger_{(\bar{5},3^*)}\bar{\sigma}^\mu\psi_{(\bar{5},3^*)} \tag{6.2.4}$$

$$+ \psi^\dagger_{(10,3)}\bar{\sigma}^\mu\psi_{(10,3)} + \psi^\dagger_{(10,3^*)}\bar{\sigma}^\mu\psi_{(10,3^*)} = f_{\rm PQ}\partial^\mu a\,. \tag{6.2.5}$$

For fermions in the fundamental of QCD ($T(\bar{\mathbf{3}}) = T(\mathbf{3}) = 1/2$), the QCD anomaly factor and the domain wall number in Eqs. (6.1.10) and (6.1.35) are then, respectively,

$$N = -10\,, \qquad N_{\rm DW} = 2\,. \tag{6.2.6}$$

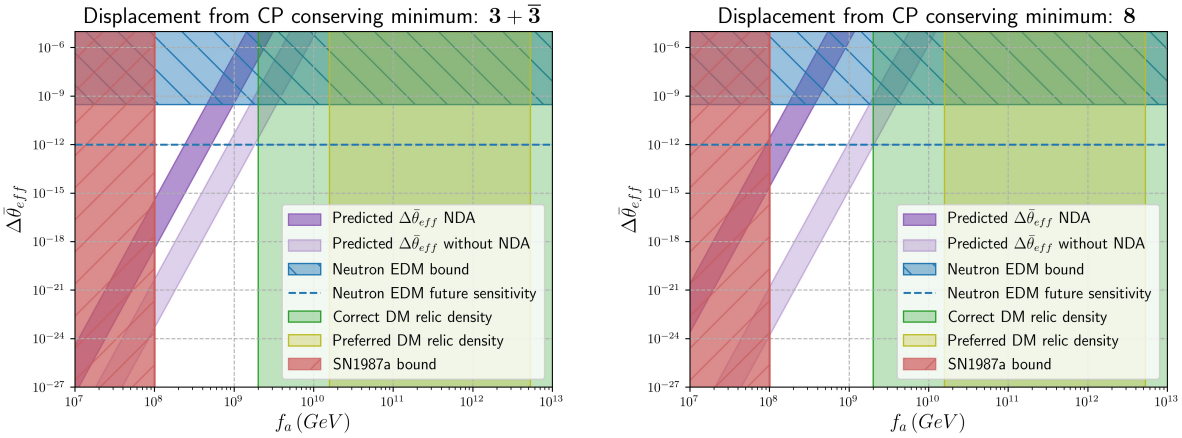

Figure 6.1: Displacement of the CP conserving minimum due to the presence of the Planck suppressed operator, for $|c\sin(\delta)| \in (0.001, 1)$and assuming NDA. The regions excluded by the experimental limits on the neutron EDM are depicted in blue, while future prospects are indicated by a dashed blue line. The red band corresponds to the SN1987a bounds axion-nucleon couplings [262]. The f_a values that suffice to account for the full content of dark matter in the pre-inflationary scenario are depicted in green.

The resulting domain wall problem is avoided here by the assumption of pre-inflationary PQ transition, as earlier explained.

Planck suppressed operators

For the value of N in Eq. (6.2.6), the displacement induced on the QCD $\bar{\theta}$ parameter by the NDA estimation of the Planck suppressed operator in Eq. (6.1.37) is illustrated in Fig. 6.1 (left panel). The figure also depicts the stringent constraint imposed by the experimental bound on the neutron EDM [99], which for the most conservative estimates [385] translates into the requirement

$$\mathbf{3}+\bar{\mathbf{3}}\ \text{Model:} \qquad f_a \lesssim (\,4.5\times 10^8\,,\,1\times 10^9\,)\,\text{GeV}\,, \qquad \text{for}\,|c\sin(\delta)| \in (0.001, 1)\,. \tag{6.2.7}$$

The softer constraint that follows if NDA is disregarded and substituted by the estimation stemming from Eq. (6.1.40) is also depicted.[9] The degree of tuning of the operator coefficient is illustrated in Fig. 6.2 (left panel).

[9]The explicit breaking can be further suppressed if, for example, we assume supersymmetry with R-symmetry. In such cases, f_a in the preferred value for the DM relic density is also allowed, though we do not pursue such possibilities further in this thesis.

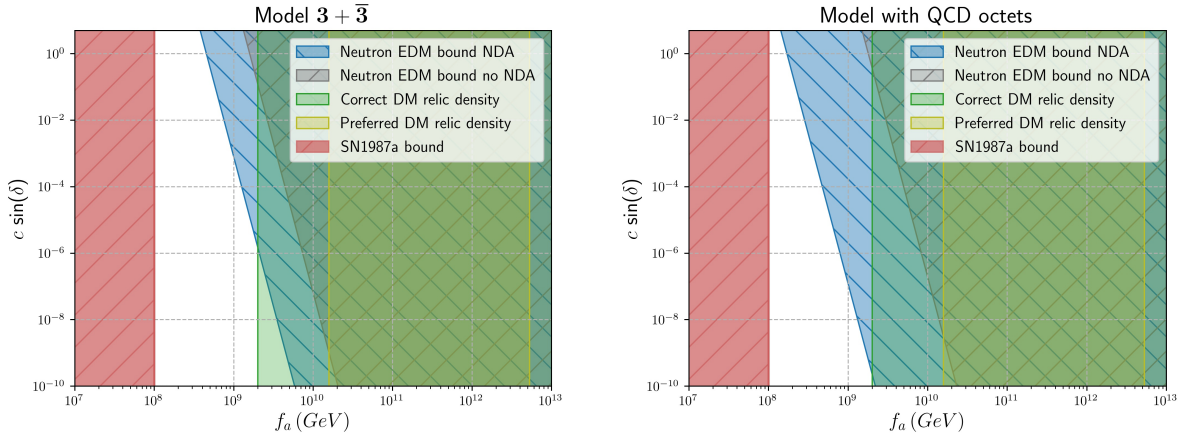

Figure 6.2: Allowed values for the Planck suppressed operator coefficient $|c\sin(\delta)|$, for axion dark matter compatible with neutron EDM and SN1987a bounds.

Axion dark matter

In the misalignment mechanism, the relic axion abundance Ω_a depends then on two variables: the axion decay constant f_a, and the initial misalignment angle $\theta_i = a_i/f_a$. For $|\theta_i| \ll \pi$ it reads [256]

$$\Omega_a\, h^2 = 0.35 \left(\frac{\theta_i}{0.001}\right)^2 \left(\frac{f_a}{3\times 10^{17}\text{GeV}}\right)^{1.17} , \tag{6.2.8}$$

where h is the present Hubble parameter. If axions were to explain the total relic dark matter density $\Omega_{\rm DM}\, h^2 \simeq 0.12$ [21], the f_a value required for an initial misalignment angle in the range $\theta_i \in (0.1, 3)$ is

$$f_a \simeq 2\times 10^{10} - 5\times 10^{12}\,\text{GeV}\,. \tag{6.2.9}$$

However, for values of $\theta_i \sim \pi$, the anharmonicities of the QCD potential are important and f_a can be as low as [19, 256, 386]

$$f_a \sim 2\times 10^{9}\,\text{GeV}\,. \tag{6.2.10}$$

These two estimations of the f_a values that allow axions to constitute all the dark matter of the universe have been depicted in Fig. 6.1 by green bands dubbed, respectively, "preferred" and "correct" densities. The bounds on f_a stemming from measurements of the neutrino burst duration of SN1987a are depicted in red. [10]

The lower f_a value in Eq. (6.2.10) is about a factor of two too large to be compatible with that required in Eq. (6.2.7) by the neutron EDM bounds. This option requires a fine-tuning of the coefficient c of the Planck suppressed operator of $\mathcal{O}(10^{-7})$, to be compared with the typical adjustment by 54 orders of magnitude in axion models with dimension five Planck-suppressed

[10] Assuming the fiducial density profile for the proto-neutron star in Ref. [262], the bound reads $f_a > 10^8$ GeV.

operators. Furthermore, for a misalignment angle close to π and low inflation scales, lower values of f_a are possible and the fine-tuning of c could be avoided altogether, even in this most conservative case of the NDA estimate of the effect. Conversely, would the NDA prefactors be disregarded, $\mathcal{O}(1)$ coefficients for the Planck suppressed operator are seen to be allowed in a large fraction of the parameter space.

6.3 Model II: color-octet fermions

We consider here an alternative realization with only one $\{\psi_{\bar{5}}, \psi_{10}\}$ set of two fermions charged under $SU(5)$ and belonging to the adjoint representation of QCD, see Table 6.4. All gauge anomalies cancel then automatically. This model is less economical than Model I, though, from the point of view of the total number of exotic degrees of freedom.

	$SU(5)$	$SU(3)_c$	$U(1)_{PQ}$
$\psi_{\bar{5}}$	$\bar{\mathbf{5}}$	$\mathbf{8}$	-3
ψ_{10}	$\mathbf{10}$	$\mathbf{8}$	$+1$

Table 6.4: Model II: charges of exotic fermions under the confining gauge group $SU(5) \times SU(3)_c$. Their PQ charges are shown as well. The left-handed Weyl fermions $\psi_{\bar{5}}$ and ψ_{10} are massless and singlets of the SM electroweak gauge group.

In the limit of vanishing α_s the number of flavors of the $SU(5)$ fermionic sector is

$$n = 8\,, \tag{6.3.1}$$

and thus the global chiral symmetries of the $SU(5)$ Lagrangian correspond to

$$SU(8)_{\bar{5}} \times SU(8)_{10} \times U(1)_{PQ} \xrightarrow{\alpha_s \neq 0} SU(3)_c\,. \tag{6.3.2}$$

In consequence, in this model only QCD remains unbroken for $\alpha_s \neq 0$, and hence no light pNGs appear associated with the spontaneous breaking of the non-abelian global symmetries.

To see whether the QCD gauge group remains ultimately unbroken, note that an $SO(8)$ subgroup of the global symmetry $SU(8)_{\bar{5}} \times SU(8)_{10}$ satisfies the 't Hooft anomaly consistency conditions, while the condensates $\langle \mathbf{10\,10\,10\,\bar{5}} \rangle$ and $\langle \bar{\mathbf{5}}\,\bar{\mathbf{5}}\,\mathbf{10}\,\bar{\mathbf{5}}\,\bar{\mathbf{5}}\,\mathbf{10} \rangle$ can be $SO(8)$ singlets. In this case, we find that the unbroken subgroup G contains $SO(8)$, i.e. $G \supset SO(8)$. The $SU(3)$ subgroup of $SO(8)$ is realized as the special maximal embedding where the vector representation of $SO(8)$ is identified with the octet of $SU(3)$ (see e.g. [387]). Thus, it is again clear that an $SU(3)$ global symmetry remains unbroken below the confinement scale, with non-vanishing $\langle \mathbf{10\,10\,10\,\bar{5}} \rangle$ and $\langle \bar{\mathbf{5}}\,\bar{\mathbf{5}}\,\mathbf{10}\,\bar{\mathbf{5}}\,\bar{\mathbf{5}}\,\mathbf{10} \rangle$ condensates. Finally, the $SO(8)$ symmetry is aligned with that

containing $SU(3)_c$ once $\alpha_s \neq 0$ is taken into account. This shows that, also in this model, it is most likely for the $SU(5)$ dynamics to preserve $SU(3)_c$.

For fermions in the adjoint of QCD ($T(\mathbf{R}) = 3$), the QCD anomaly factor and the domain wall number in Eqs. (6.1.10) and (6.1.35) are, respectively,

$$N = -30\,, \qquad N_{\rm DW} = 6\,. \tag{6.3.3}$$

Planck suppressed operators

Fig. 6.1 (right panel) shows the displacement induced by the operator in Eq. (6.1.37) on the QCD vacuum parameter, for the value of N expected from NDA, see Eq. (6.3.3), which implies the requirement

$$\textbf{8}\ \text{Model:} \qquad f_a \lesssim (\,1.7\times 10^8\,,\,3.7\times 10^8\,)\,\text{GeV}\,, \qquad \text{for}\,|c\sin(\delta)| \in (0.001, 1)\,, \tag{6.3.4}$$

to comply with the experimental bound on the neutron EDM. This constraint is stronger than that for Model I for QCD-triplet exotic fermions, Eq. (6.2.7). A softer constraint if NDA was disregarded in the estimation is also illustrated.

Axion dark matter

The comparison between Eq. (6.3.4) and the f_a ranges in Eqs. (6.2.9) and (6.2.10) shows that this model with exotic fermions in the adjoint of QCD is more in tension than model I, if axions are to explain all the dark matter of the universe without recurring to fine tunings. Fig. 6.1 (right panel) illustrates this situation. For the NDA estimation of Planck suppressed couplings, f_a as required by dark matter is a factor of five too large with respect to the neutron EDM constraint; this translates into the requirement of a $\mathcal{O}(10^{-10})$ fine-tuning of the coefficient c of the Planck suppressed operator, as illustrated in Fig. 6.2 (right panel). Alternatively, the present model could explain a subdominant fraction of the dark matter content.

A comparison without NDA power counting estimates is also illustrated: non-fine tuned values of the coefficient c are then compatible with the axion accounting for the ensemble of dark matter, while complying with EDM limits. Overall, the uncertainty on the estimations of non-perturbative gravitational effects, and on the f_a values required to account for dark matter, is large enough to still consider this model as a candidate scenario for purely axionic dark matter.

6.4 Conclusions

We have presented a novel composite axion theory that solves the strong CP problem and has as singular features:

- A gauge confining symmetry which is chiral, unlike usual axicolor models which use vectorial fermions. In consequence, the PQ symmetry is automatic, without any need to invoke extra symmetries.
- Exotic $SU(5)$ fermions in (pseudo)real representations of QCD.
- Inherent protection from dangerous quantum non-perturbative gravitational effects.

The gauge group selected and illustrated here is chiral $SU(5)$ with two massless fermions in its $\bar{\mathbf{5}}$ and $\mathbf{10}$ representations and a confining scale much higher than that of QCD. A new spectrum of composite bound states is expected.

We showed that the 't Hooft anomaly conditions for the global symmetries of the exotic fermionic sector imply that the non-abelian global symmetries must be spontaneously broken. The global abelian symmetries, e.g. the PQ symmetry, must also be spontaneously broken for the theory to be phenomenologically viable, resulting in a dynamical invisible axion. Furthermore, the PQ invariance is the analogous of the $B - L$ symmetry in $SU(5)$ Grand Unified Theory (GUT).

We have determined the fermionic operators with lowest dimension which may condense and induce spontaneous breaking. Because of $SU(5)$ gauge invariance, six is the minimal dimension for the operator whose VEV may break the exotic flavor symmetries. An even higher dimensional condensate is needed in order to break PQ invariance: the VEV of a dimension nine operator. The latter is also the lowest dimensional effective operator which could result from gravitational quantum contributions, breaking explicitly the PQ symmetry, as these effects must respect gauge invariance. Its high dimensionality is at the heart of the inherent protection of this theory with respect to the gravitational issue.

We have developed two complete ultraviolet completions of the chiral confining $SU(5)$ theory, which only differ in the (pseudo)real QCD representations chosen for the exotic fermions: a reducible $\mathbf{3} + \bar{\mathbf{3}}$ representation for Model I, and the irreducible adjoint in model II. The former is more economical in terms of the total number of degrees of freedom. Both models are phenomenological viable and largely protected from quantum gravitational concerns. Remarkably, in the case of exotic fermions in the fundamental of QCD, the f_a range allowed if axions are to explain the full dark matter content of the universe can be compatible with that required to avoid a fine-tuned coefficient for the Planck suppressed operator. For octet-color fermions the compatibility is marginal but still possible.

The basic novel idea of the construction is to use a chiral confining group, which provides an automatic implementation of PQ invariance. The most economic avenue is to implement

it via just two exotic fermions in (pseudo)real representations of QCD. In this perspective, we have briefly explored other confining groups as well. For instance, a chiral and confining gauge $SU(4)$ symmetry would be a viable alternative, although it does not enjoy a sufficient protection from gravitational issues, at least in the case of only two exotic fermions. Even the smaller chiral confining $SU(3)$ symmetry is possible, although the versions with only two exotic fermions require very high-dimensional representations of the confining group and, again, they are less protected from gravitational issues than the $SU(5)$ case (see App. 6.A). Nevertheless, as the estimation of gravitational effects is somehow uncertain, it may be pertinent to dedicate specific studies to these alternative directions.

Appendices

Appendix 6.A Alternative confining groups: $SU(3)$ and $SU(4)$

SU(4) Model

It is also possible to construct a chiral axicolor model that fulfills the requirements explained in the begining of the present Chapter with an $SU(4)$ gauge group.

	$SU(4)$	$SU(3)_c$	$U(1)_{PQ}$
$\psi_{\bar{4}}$	$\bar{\mathbf{4}}$	$\mathbf{8}$	-3
ψ_{10}	$\mathbf{10}$	$\mathbf{1}$	4

Table 6.A.1: Charges of exotic fermions under the confining gauge group $SU(4) \times SU(3)_c$. The left-handed Weyl fermions $\psi_{\bar{4}}$ and ψ_{10} are massless and singlets of the SM electroweak gauge group.

It is easy to check that this theory is free from gauge anomalies [11] and that the global $U(1)_{PQ}$ in Table 6.A.2 is exact at the classical level but explicitly broken by $SU(3)_c$ instantons, solving therefore the strong CP problem à la Peccei-Quinn.

However we will not study this model further since it lacks special protection against PQ-violating gravity operators. Indeed the lowest dimensional non-renormalizable operators that break PQ and could be generated by quantum gravity effects are

$$\mathcal{L}_{Planck} \propto \frac{c}{M_{\rm Pl}^2}\frac{1}{4!}\,\bar{\mathbf{4}}\,\bar{\mathbf{4}}\,\bar{\mathbf{4}}\,\bar{\mathbf{4}} + \frac{c}{M_{\rm Pl}^2}\frac{1}{4!}\,\mathbf{10}\,\mathbf{10}\,\mathbf{10}\,\mathbf{10}\,, \tag{6.A.1}$$

and would lead to unacceptable deviations from the CP-conserving minimum (barring a fine-tuning of c by several tens of orders of magnitude) and thus spoil the solution of the strong CP problem.

Alternative SU(4)

It is possible to implement the confining gauge $SU(4)$ solution in a setup in which two exotic fermions belong to the adjoint of QCD, by considering higher $SU(4)$ representations, e.g. $\bar{\mathbf{35}}$ and $\mathbf{70}$ since $A(\bar{\mathbf{35}}) = -112\,, \quad A(\mathbf{70}) = +112$, see Table 6.A.2.

[11] $\left[SU(4)\right]^3$ anomaly: $8A(\bar{\mathbf{4}}) + A(\mathbf{10}) = 0$, since $A(\bar{\mathbf{4}}) = -1$, and $A(\mathbf{10}) = 8$.

	$SU(4)$	$SU(3)_c$	$U(1)_{PQ}$
$\psi_{\bar{35}}$	$\mathbf{\bar{35}}$	$\mathbf{8}$	-98
ψ_{70}	$\mathbf{70}$	$\mathbf{8}$	56

Table 6.A.2: Charges of exotic fermions under the confining gauge group $SU(4) \times SU(3)_c$. The left-handed Weyl fermions $\psi_{\bar{35}}$ and ψ_{70} are massless and singlets of the SM electroweak gauge group.

SU(3) Model

The idea of using a chiral confining theory as solution to the strong CP problem can also be implemented with a confining $SU(3)$ gauge group, for instance via the fermionic content in Table 6.A.3.

	$SU(3)$	$SU(3)_c$	$U(1)_{PQ}$
$\psi_{\bar{15}'}$	$\mathbf{\bar{15}'}$	$\mathbf{R}$	-119
ψ_{42}	$\mathbf{42}$	$\mathbf{R}$	35

Table 6.A.3: Charges of exotic fermions under the confining gauge group $SU(3) \times SU(3)_c$. The left-handed Weyl fermions $\psi_{\bar{15}'}$ and ψ_{42} are massless and singlets of the SM electroweak gauge group.

This theory is anomaly free since $A(\mathbf{\bar{15}'}) = -A(\mathbf{42}) = 77$ and again the exotic fermions transform as pseudoreal representations $\mathbf{R}$ of the QCD group. However, the theory is not as protected against PQ breaking gravitational effect as the $SU(5)$ case, since the corresponding effective operators can appear at dimension six,

$$\mathcal{L}_{Planck} \propto \frac{c}{M_{\rm Pl}^2} \frac{1}{2!2!} \mathbf{\bar{15}'}\, \mathbf{\bar{15}'}\, \mathbf{42}\, \mathbf{42} \ , \tag{6.A.2}$$

and in consequence we will not further elaborate on this model.

Appendix 6.B Anomaly factors

In this appendix we review the group theoretical factors that are relevant when computing the global or gauge anomalies in our theory. Let us consider a given conserved current j^a_μ that corresponds to the symmetry associated to the generator T^a. In the presence of the gauge field F_b the divergence of the current reads,

$$\partial^\mu j^a_\mu = \frac{\alpha_i}{8\pi} C^{abc}_{group} F_{b\,\mu\nu} \tilde{F}^{\mu\nu}_c \,, \tag{6.B.1}$$

where $\tilde{F}^{\mu\nu} = \frac{1}{2}\epsilon^{\mu\nu\sigma\rho}F_{\sigma\rho}$, the fine structure constant of the corresponding gauge interaction is denoted by $\alpha_i = \frac{g_i^2}{4\pi}$ and the group theoretical factor C_{group} is given by

$$C^{abc}_{group} = \sum Tr\left[T^a\{t^b_R, t^c_R\}\right], \tag{6.B.2}$$

where the sum runs over all fermionic representations $\mathbf{R}$ of the gauge group t^a_R. Thoughout the Chapter the fermionic degrees of freedom are expressed in terms of left-handed Weyl fermions.

This formula is used for three different cases, depending on whether the groups are abelian or non-abelian and whether the anomaly is cubic or mixed.

- Non-abelian cubic anomalies:

$$\left[SU(N)\right]^3: \qquad C^{abc}_{group} = \sum_R Tr\left[t^a_R\{t^b_R, t^c_R\}\right] \equiv d^{abc}\sum_R A(\mathbf{R})\,, \tag{6.B.3}$$

  where $A(\mathbf{R})$ denotes anomaly coefficient or triality of the representation $\mathbf{R}$.

- Abelian cubic anomalies:

$$\left[U(1)\right]^3: \qquad C_{group} = \sum_R Tr\left[Q_R\{Q_R, Q_R\}\right] = 2\sum_R Q^3_R\,, \tag{6.B.4}$$

  where Q_R denotes the $U(1)$ charge of the corresponding fermion.

- Mixed anomalies:

$$\left[SU(N)\right]^2 \times U(1): \qquad C^{bc}_{group} = \sum_R Tr\left[Q_R\{t^b_R, t^c_R\}\right] \equiv \delta^{bc}\sum_R Q_R\, 2T(\mathbf{R})\,, \tag{6.B.5}$$

  where $T(\mathbf{R})$ is the Dynkin index of the representation $\mathbf{R}$.

These group theoretical factors are tabulated [388] and can also be computed with the Mathematica package LieART [389].

Appendix 6.C Axion field domain

Our definition of the PQ symmetry according to the charges in Tab. 1 corresponds to the following transformations:

$$\begin{aligned} \psi_{10} &\longrightarrow e^{i\,\alpha}\,\psi_{10}\,, \\ \psi_{\bar{5}} &\longrightarrow e^{-3\,i\,\alpha}\,\psi_{\bar{5}}\,, \end{aligned} \tag{6.C.1}$$

where α is the rotation angle. However, the domain of α does not correspond to the full range $[0, 2\pi)$ since some of these rotations are equivalent due to gauge transformations. In particular, the center of $SU(5)$ is the discrete symmetry $Z\left[SU(5)\right] = \mathbb{Z}_5$, that corresponds to the following gauge transformations:

$$\begin{aligned} \psi_{10} &\longrightarrow e^{2\pi\,i\,k/5}\,\psi_{10}\,e^{2\pi\,i\,k/5} = e^{4\pi\,i\,k/5}\psi_{10}\,, \\ \psi_{\bar{5}} &\longrightarrow e^{-2\pi\,i\,k/5}\,\psi_{\bar{5}}\,, \end{aligned} \tag{6.C.2}$$

for $k = \{0, 1, 2, 3, 4\}$. It is easy to see now that a PQ transformation with angle $\alpha = 2\pi/5$ is gauge equivalent to $\alpha = 2\pi$ with $k = 2$. As a consequence, the axion transforms under PQ as

$$\frac{a}{f_{\rm PQ}} \longrightarrow \frac{a}{f_{\rm PQ}} + \alpha \tag{6.C.3}$$

and its physical domain is

$$\frac{a}{f_{\rm PQ}} \in [0, 2\pi/5)\,. \tag{6.C.4}$$

Appendix 6.D 't Hooft anomaly matching: is $SU(8)_{\bar{5}} \times SU(8)_{10} \times U(1)_{PQ}$ spontaneously broken?

aaa If the $SU(5)$ group confines without breaking the chiral symmetries in Table 6.D.1, the consistency of the theory implies the existence of massless baryons in the low energy that match the global anomalies of the high-energy theory. However, for some theories these 't Hooft anomaly matching conditions cannot be satisfied as a consequence of the properties of the fermionic representations. It must be then concluded that these theories can only be realized via spontaneous breaking of its chiral symmetries. This will be the case for the $SU(8)_{\bar{5}} \times SU(8)_{10}$ chiral symmetry of our $SU(5)$ model.

	$SU(8)_{\bar{5}}$	$SU(8)_{10}$	$U(1)_{PQ}$
$\psi_{\bar{5}}$	$\square$	$\mathbf{1}$	-3
ψ_{10}	$\mathbf{1}$	$\square$	1

Table 6.D.1: Global chiral properties at the classical level, in the limit of vanishing α_s.

Let us first compute the global anomalies in the high energy theory (in terms of the fundamental quarks $\psi_{\bar{5}}$ and ψ_{10}):

$$\left[SU(8)_{\bar{5}}\right]^3: \quad 5 \times A(\square) = 5\,, \tag{6.D.1}$$

$$\left[SU(8)_{10}\right]^3: \quad 10 \times A(\square) = 10\,, \tag{6.D.2}$$

$$U(1)_{PQ} \times \left[SU(8)_{\bar{5}}\right]^2: \quad 5 \times 2\,T(\square) Q_{\bar{5}} = -15\,, \tag{6.D.3}$$

$$U(1)_{PQ} \times \left[SU(8)_{10}\right]^2: \quad 10 \times 2\,T(\square) Q_{10} = 10\,, \tag{6.D.4}$$

$$\left[U(1)_{PQ}\right]^3: \quad 8\left(5\,(Q_{\bar{5}})^3 + 10\,(Q_{10})^3\right) = -1000\,. \tag{6.D.5}$$

If chiral symmetries remain unbroken these anomalies will match those in the low energy theory in terms of the bound states. The simplest $SU(5)$ singlet that can be formed in this theory consists of three fundamental quarks, $\chi \equiv 10\,\bar{\mathbf{5}}\,\bar{\mathbf{5}}$. Can it match the previous anomalies? The transformation properties of χ under the global symmetries are

$$SU(8)_{\bar{5}}: \quad \mathbf{8} \times \mathbf{8} = \mathbf{28} + \mathbf{36}\,, \tag{6.D.6}$$

$$SU(8)_{10}: \quad \mathbf{8}\,, \tag{6.D.7}$$

$$U(1)_{PQ}: \quad -3-3+1 = -5\,. \tag{6.D.8}$$

In consequence, there are two posible representations for the baryon χ under $SU(8)_{\bar{5}} \times SU(8)_{10} \times U(1)_{PQ}$: $(\mathbf{28}, \mathbf{8}, -5)$ and $(\mathbf{36}, \mathbf{8}, -5)$. If the low energy contains a number n_{28} and n_{36} of baryons transforming under each representation respectively, then the anomalies are given by

$$\left[SU(8)_{\bar{5}}\right]^3: \quad 8\left(n_{28}\,A(\mathbf{28}) + n_{36}\,A(\mathbf{36})\right) = 32(n_{28} + 3n_{36})\,, \tag{6.D.9}$$

$$\left[SU(8)_{10}\right]^3: \quad 28\,n_{28}\,A(\mathbf{8}) + 36\,n_{36}\,A(\mathbf{8}) = 4(7\,n_{28} + 9\,n_{36})\,, \tag{6.D.10}$$

$$U(1)_{PQ} \times \left[SU(8)_{\bar{5}}\right]^2: \quad 8\,Q_\chi\left(n_{28}\,2\,T(\mathbf{28}) + n_{36}\,2\,T(\mathbf{36})\right) = -80(3\,n_{28} + 5n_{36})\,, \tag{6.D.11}$$

$$U(1)_{PQ} \times \left[SU(8)_{10}\right]^2: \quad Q_\chi\left(28\,n_{28}\,2\,T(\mathbf{8}) + 36\,n_{36}\,2\,T(\mathbf{8})\right) = -20(7n_{28} + 9n_{36})\,, \tag{6.D.12}$$

$$\left[U(1)_{PQ}\right]^3: \quad 8\,(28n_{28} + 36n_{36})\,\left(Q_\chi\right)^3 = -4000\,(7n_{28} + 9n_{36})\,. \tag{6.D.13}$$

It is easy to see that there is no way of matching these anomalies with n_{28}, $n_{36} \in \mathbb{N}$. If we would alternatively consider 5-quark bound states, there are two options: $\bar{\mathbf{5}}\,\bar{\mathbf{5}}\,\bar{\mathbf{5}}\,\bar{\mathbf{5}}\,\bar{\mathbf{5}}$ and $\mathbf{10}\,\mathbf{10}\,\mathbf{10}\,\mathbf{10}\,\mathbf{10}$.

For the first one, $\bar{\mathbf{5}}\,\bar{\mathbf{5}}\,\bar{\mathbf{5}}\,\bar{\mathbf{5}}\,\bar{\mathbf{5}}$, the transformation properties are:

$$SU(8)_{\bar{5}}: \quad \mathbf{8}\times\mathbf{8}\times\mathbf{8}\times\mathbf{8}\times\mathbf{8} = \quad (\overline{\mathbf{56}}) + 4\,(\overline{\mathbf{504}}) + (\overline{\mathbf{792}}) + 5\,(\overline{\mathbf{1008}}) + 6\,(\overline{\mathbf{1512}}') \tag{6.D.14}$$

$$+5\,(\overline{\mathbf{1680}}) + 4\,(\overline{\mathbf{1848}})\,, \tag{6.D.15}$$

$$SU(8)_{10}: \quad \mathbf{1}\,, \tag{6.D.16}$$

$$U(1)_{PQ}: \quad 5\,(-3) = -15\,. \tag{6.D.17}$$

For $\mathbf{10}\,\mathbf{10}\,\mathbf{10}\,\mathbf{10}\,\mathbf{10}$ the transformation properties are:

$$SU(8)_{\bar{5}}: \quad \mathbf{1}\,, \tag{6.D.18}$$

$$SU(8)_{10}: \quad \mathbf{8}\times\mathbf{8}\times\mathbf{8}\times\mathbf{8}\times\mathbf{8} = \quad (\overline{\mathbf{56}}) + 4\,(\overline{\mathbf{504}}) + (\overline{\mathbf{792}}) + 5\,(\overline{\mathbf{1008}}) + 6\,(\overline{\mathbf{1512}}') \tag{6.D.19}$$

$$+5\,(\overline{\mathbf{1680}}) + 4\,(\overline{\mathbf{1848}})\,, \tag{6.D.20}$$

$$U(1)_{PQ}: \quad 5\,(+1) = +5\,. \tag{6.D.21}$$

Repeating the analogous exercise to that in Eqs. (6.D.9)-(6.D.13), and using the properties of the representations of the 5-quark bound states in Table 6.D.2, it follows the same conclusion as before: the chiral symmetry must necessarily be spontaneously broken due to the impossibility of satisfying 't Hooft anomaly matching conditions.

R	$2\,T(\mathbf{R})$	$A(\mathbf{R})$
$\overline{\mathbf{56}}$	13	-5
$\overline{\mathbf{504}}$	213	75
$\overline{\mathbf{792}}$	713	1287
$\overline{\mathbf{1008}}$	524	294
$\overline{\mathbf{1680}}$	1088	1066
$\overline{\mathbf{1512}}'$	883	777

Table 6.D.2: Dynkin index $T(\mathbf{R})$ and anomaly factor $A(\mathbf{R})$ of the different representations of $SU(8)_{\bar{5}}$ that are contained in $[\mathbf{8}]^5$.

This does not mean, however, that the full $SU(8)_{\bar{5}} \times SU(8)_{10} \times U(1)_{PQ}$ is completely spontaneously broken. Some subgroup can remain unbroken. In particular, it is shown in

the body of the Chapter that it is possible to leave unbroken the $U(1)_{PQ}$ with the baryon in Eq. (6.1.11) satisfying the anomaly matching conditions. Nevertheless, this possibility is phenomenologically excluded due to the absence of colored massless quarks in nature.

CHAPTER 7

Axion couplings to EW gauge bosons

In this Chapter, which is based on the publication in Ref. [3], the axion couplings to EW gauge bosons are studied in the simultaneous presence of the gluonic coupling.

The main phenomenological constraints for QCD axions are obtained from their couplings to photons, gluons and fermions. Nevertheless, as has been commented in Section 3.2, in specific QCD axion models the coupling to photons may be suppressed [166, 167] and moreover large uncertainties may hover over the purely hadronic constraints [390]. It is thus important to analyze the axion couplings to other electroweak gauge bosons, as they may become the phenomenologically dominant couplings in certain regions of the parameter space for those models. Couplings of axions and also of ALPs to heavy gauge bosons are increasingly explored [287–290, 368, 391, 392] in view of present and future collider data, and also in view of rare meson decay data. For instance, in addition to LHC-related signals, recent works [291, 393] consider the one-loop impact of aWW couplings on rare meson decays.

Here we first determine the model-independent components of the coupling of QCD axions with electroweak gauge bosons, which result from the mixing of the axion with the pseudoscalar mesons of the SM. In other words, we determine the equivalent of the 1.92 factor in the photonic coupling in Eq. (3.1.20) for the couplings of the axion to W and Z gauge bosons. A chiral Lagrangian formulation will be used for this purpose, determining the leading-order effects. The heavy electroweak gauge bosons will be introduced in that Lagrangian as external –classical– sources. Our results should impact the analyses for light axions of theories which solve the strong CP problem. They are novel and relevant in particular whenever the axion is lighter than the QCD confining scale and is on-shell in either low-energy or high-energy experiments. They also impact the comparison between the data taken at experiments at low and high-energy. For instance, a null result in NA62 data for $K \to \pi a$ does not imply the absence of a signal at high energy in an accelerator such as that from off-shell axions at LEP or at a collider. This is because model-independent contributions are present at the low momenta dominant in rare decays (and cancellations may then take place), while at high energies they are absent.

As a second step, we will extend the analysis to heavy axions which solve the strong CP problem. Axions much heavier than Λ_{QCD} and with low axion scales are possible within dynamical solutions to the strong CP problem, at the expense of enlarging the confining sector of the Standard Model (SM) beyond QCD [4, 170–180]. These theories introduce a second and large instanton-induced scale $\Lambda' \gg \Lambda_{QCD}$ to which the axion also exhibits anomalous couplings, resulting in the bulk of its large mass. Precisely because the axion mass typically lies well above the MeV regime, these heavy axions avoid the stringent astrophysical and laboratory constraints and present and future colliders may discover them. The transition between the light and heavy axion regime will be explored for the coupling of the axion to the photon and to the electroweak gauge bosons.

Finally, the phenomenological part of the analysis will be carried out on a "two-coupling-at-a-time" basis: it will take into account the simultaneous presence of a given electroweak coupling and the axion-gluon-gluon anomalous coupling (essential to solve the strong CP problem). For the analysis of data, for the first time the experimentally excluded areas for the EW couplings g_{aWW}, g_{aZZ} and $g_{a\gamma Z}$ will be identified and depicted separately, besides the customary ones for the $g_{a\gamma\gamma}$ coupling. Furthermore, the relations among the exclusion regions stemming from electroweak gauge invariance will be determined and exploited. Model predictions will be illustrated over the experimental parameter space.

Aside from the main focus of the work on true axions, our analysis applies to and calls for a timely extension of the ALP parameter space. Very interesting bounds on ALPs from LEP and LHC [287–290, 368, 391, 392, 394, 395] assume often just one electroweak coupling for the axion, and no gluonic coupling. The path to consider any two (or more) couplings at a time will change the experimental perspective on ALPs.

What is the difference between a heavy axion and an ALP with both anomalous electroweak and gluonic couplings? The key distinction is that the former stems from a solution to the strong CP problem while a "gluonic ALP" may not. Both exhibit anomalous couplings to QCD and in both cases there is an external source of mass besides that induced by QCD instantons and mixing. However, for a true heavy axion that extra source of mass does not induce a shift of the θ parameter outside the CP conserving minimum (and thus the solution to the strong CP problem is preserved), while for a generic gluonic ALP such a shift may be induced. Nevertheless, this important distinction is not directly relevant for this work, as the novel aspects and phenomenological analysis developed below are valid for both true heavy axions which solve the strong CP problem and for gluonic ALPs. To sum up, all results below for heavy axions apply directly to gluonic ALPs as well. In addition, the conclusions based purely on EW gauge invariance have an even larger reach: they hold for all type of axions and for generic ALPs (that is, ALPs with or without gluonic couplings).

7.1 The Lagrangian for the QCD axion

Without loss of generality, the axion couplings can be encoded in a model-independent way in an effective Lagrangian. At leading order in inverse powers of the scale $f_{\rm PQ}$ at which the global PQ symmetry is broken, and at energies above the electroweak (EW) scale, it reads

$$\mathcal{L}_{\rm eff} = \mathcal{L}_{\rm SM} + \frac{1}{2}(\partial_\mu \hat{a})(\partial^\mu \hat{a}) + \delta\mathcal{L}_a \,, \tag{7.1.1}$$

where $\hat{a}$ denotes the axion eigenstate at energies well above the confinement scale and $\mathcal{L}_{\rm SM}$ is the SM Lagrangian, see Eq. (1.1.1).

We will work in the basis in which the only PQ-breaking operators in the Lagrangian, $\delta\mathcal{L}_a^{\not{PQ}}$, are the anomalous couplings of axions to gauge bosons. This choice is allowed by the reparametrization invariance of the effective axion Lagrangian (see Appendix 7.B). The CP-conserving and PQ-violating next-to-leading order (NLO) corrections due to axion physics then read [1]

$$\delta\mathcal{L}_a^{\not{PQ}} = N_0\, \mathbf{O}_{\tilde{G}} + L_0\, \mathbf{O}_{\tilde{W}} + P_0\, \mathbf{O}_{\tilde{B}} \,, \tag{7.1.2}$$

with $\mathbf{O}_{\tilde{G}}$, $\mathbf{O}_{\tilde{W}}$ and $\mathbf{O}_{\tilde{B}}$ denoting the anomalous axion couplings to gluons, $SU(2)_L$ and $U(1)_Y$ gauge bosons, respectively,

$$\mathbf{O}_{\tilde{G}} \equiv -\frac{\alpha_s}{8\pi} G^a_{\mu\nu} \tilde{G}^{a\mu\nu} \frac{\hat{a}}{f_{\rm PQ}} \,, \tag{7.1.3}$$

$$\mathbf{O}_{\tilde{W}} \equiv -\frac{\alpha_W}{8\pi} W^a_{\mu\nu} \tilde{W}^{a\mu\nu} \frac{\hat{a}}{f_{\rm PQ}} \,, \tag{7.1.4}$$

$$\mathbf{O}_{\tilde{B}} \equiv -\frac{\alpha_B}{8\pi} B_{\mu\nu} \tilde{B}^{\mu\nu} \frac{\hat{a}}{f_{\rm PQ}} \,, \tag{7.1.5}$$

where α_s, α_W and α_B denote respectively the fine structure constants for the QCD, $SU(2)_L$ and $U(1)$ gauge interactions, and N_0, P_0 and L_0 are dimensionless operator coefficients. Customarily, the Lagrangian in Eq. (7.1.2) is rewritten as

$$\delta\mathcal{L}_a = \frac{1}{4} g^0_{agg}\, \hat{a}\, G\tilde{G} + \frac{1}{4} g^0_{aWW}\, \hat{a}\, W\tilde{W} + \frac{1}{4} g^0_{aBB}\, \hat{a}\, B\tilde{B} \,, \tag{7.1.6}$$

where the Lorentz indices of the field strengths are implicit from now on and

$$g^0_{agg} \equiv -\frac{1}{2\pi f_{\rm PQ}} \alpha_s\, N_0 \,, \qquad g^0_{aWW} \equiv -\frac{1}{2\pi f_{\rm PQ}} \alpha_W\, L_0 \,, \qquad g^0_{aBB} \equiv -\frac{1}{2\pi f_{\rm PQ}} \alpha_B\, P_0 \,. \tag{7.1.7}$$

The model-dependent group theoretical factors can be generically written in terms of the fermionic PQ charges $\mathcal{X}_i$ as

$$N_0 = \sum_{i=\text{heavy}} 2\, \mathcal{X}_i\, T(R_i^{SU(3)}) \,,$$

[1] The derivative operators also present in the most general basis [186, 289, 396, 397] are PQ invariant and thus not shown.

$$\begin{aligned} L_0 &= \sum_{i=\text{heavy}} 2\,\mathcal{X}_i T(R_i^{SU(2)})\,, \\ P_0 &= \sum_{i=\text{heavy}} 2\,\mathcal{X}_i\, Y_i^2\,, \end{aligned} \tag{7.1.8}$$

where $\mathcal{X}_i$ is the difference between the right-handed and left-handed PQ charges:[2]

$$\mathcal{X}_i = \mathcal{X}_{Li} - \mathcal{X}_{Ri}\,. \tag{7.1.9}$$

In Eq. (7.1.8), $T(R_i^{SU(3)})$ and $T(R_i^{SU(2)})$ are respectively the Dynkin indices of the fermionic representation R_i under QCD and $SU(2)_L$, and Y_i denotes the hypercharge. The sum over "heavy" fermions and the subscript 0 indicate that the contribution to the anomalous couplings from all exotic heavy quarks, and/or heavy SM quarks (s, c, b, and t quarks) if PQ charged, is encoded in the N_0, L_0 and P_0 operator coefficients. That is, the possible contribution of the SM first generation up (u) and down (d) quarks is not included in those coefficients. Indeed, for models in which they have PQ charges an additional PQ-invariant term must be considered, replacing the u and d Yukawa couplings in Eq. (1.2.3) by:

$$\delta\mathcal{L}_a^{PQ} = -\bar{Q}_{1L}\, Y_d\, \Phi\, d_R\, e^{i\,\mathcal{X}_d\,\hat{a}/f_{\rm PQ}} - \bar{Q}_{1L}\, Y_u\, \tilde{\Phi}\, u_R\, e^{i\,\mathcal{X}_u\,\hat{a}/f_{\rm PQ}} + \text{h.c.}\,, \tag{7.1.10}$$

which assumes as convention that the axion transforms under the PQ symmetry as $a \to a + f_{\rm PQ}$. The $\mathcal{X}_{u,d}$ dependence in Eq. (7.1.10) will be shown below to generate extra contributions to the physical anomalous couplings. In this equation Q_1 denotes the first family doublet, and flavor-mixing effects as well as leptonic couplings are omitted from now on for simplicity. In all equations above, color and $SU(2)_L$ indices are implicit and the QCD θ angle has been removed from the Lagrangian via the PQ symmetry.

Among the most general set of purely derivative operators, additional couplings could also be considered, e.g.

$$\delta\mathcal{L}_{a,\text{deriv}}^{PQ} = -\frac{\partial_\mu \hat{a}}{f_{\rm PQ}} \left(\bar{Q}_L\, \gamma_\mu\, c_1^Q\, Q_L \,+\, \bar{U}_R\, \gamma_\mu\, c_1^U\, U_R \,+\, \bar{D}_R\, \gamma_\mu\, c_1^D\, D_R \right)\,, \tag{7.1.11}$$

where c_1^Q, c_1^U and c_1^D are matrices of arbitrary coefficients in flavor space. Nevertheless, the reparametrization invariance of the Lagrangian [398] allows to work in a basis in which these terms (which would seed pseudoscalar kinetic mixing) are absent and their impact is transferred to other axionic couplings.[3] From now on they will be disregarded all through the analysis on pseudoscalar mixing. In summary, the Lagrangian to be analyzed below when considering mixing effects reads

$$\delta\mathcal{L}_a = \delta\mathcal{L}_a^{\not{PQ}} + \delta\mathcal{L}_a^{PQ}\,. \tag{7.1.12}$$

[2] Obviously, only left-handed quarks may contribute to L_0; in any case, it is always possible to work in a convention in which only left-handed quarks are PQ charged.

[3] In App. 7.B it will be explicitly shown that they do not have physical impact on mixing. Note that possible flavor non-diagonal couplings are not considered.

Below EW symmetry breaking and above confinement

After electroweak symmetry breaking but before QCD confinement, the effective Lagrangian in Eq. (7.1.12) results in

$$\begin{aligned}\delta\mathcal{L}_a \;=& -\bar{u}_L\, m_u\, u_R\, e^{i\,\mathcal{X}_u\,\hat{a}/f_{\rm PQ}} \;-\; \bar{d}_L\, m_d\, d_R\, e^{i\,\mathcal{X}_d\,\hat{a}/f_{\rm PQ}} \;+\; \text{h.c.} \\ &+\frac{1}{4}g^0_{agg}\,\hat{a}\,G\tilde{G} + \frac{1}{4}g^0_{a\gamma\gamma}\,\hat{a}\,F\tilde{F} + \frac{1}{4}g^0_{aWW}\,\hat{a}\,W\tilde{W} + \frac{1}{4}g^0_{aZZ}\,\hat{a}\,Z\tilde{Z} + \frac{1}{4}g^0_{a\gamma Z}\,\hat{a}\,F\tilde{Z}\,, \end{aligned} \tag{7.1.13}$$

where

$$g^0_{agg} = -\frac{1}{2\pi f_{\rm PQ}}\,\alpha_s\,N_0 \tag{7.1.14}$$

$$g^0_{a\gamma\gamma} = -\frac{1}{2\pi f_{\rm PQ}}\alpha_{\rm em}\,E_0\,, \tag{7.1.15}$$

$$g^0_{aWW} = -\frac{1}{2\pi f_{\rm PQ}}\,\frac{\alpha_{\rm em}}{s_w^2}\,L_0\,, \tag{7.1.16}$$

$$g^0_{aZZ} = -\frac{1}{2\pi f_{\rm PQ}}\,\frac{\alpha_{\rm em}}{s_w^2 c_w^2}\,Z_0\,, \tag{7.1.17}$$

$$g^0_{a\gamma Z} = -\frac{1}{2\pi f_{\rm PQ}}\,\frac{\alpha_{\rm em}}{s_w c_w}\,2R_0\,, \tag{7.1.18}$$

In these equations s_w and c_w denote the sine and cosine of the Weinberg mixing angle and $\alpha_{em} = \alpha_W c_w^2 = \alpha_B s_w^2$.

For models in which the the first generation of SM quarks are not PQ charged, $\mathcal{X}_{u,d} = 0$. When those quarks are instead charged under PQ, their contribution to the anomalous gauge couplings has to be included in the group theory factors, which are replaced by

$$N = N_0 + N_{u,d}\,, \qquad E = E_0 + E_{u,d}\,, \qquad L = L_0 + L_{u,d}\,, \tag{7.1.19}$$

$$Z = Z_0 + Z_{u,d}\,, \qquad R = R_0 + R_{u,d}\,, \tag{7.1.20}$$

as computed further below. In all cases, only two among the four parameters E, L, Z and R are linearly independent, because of gauge invariance, see Eq. (7.1.2),

$$E \equiv L + P\,, \qquad Z \equiv L c_w^4 + P s_w^4\,, \qquad R \equiv L c_w^2 - P s_w^2\,. \tag{7.1.21}$$

A non-vanishing N is the trademark of axion models which solve the strong CP problem, while the presence of the other couplings is model-dependent. It is customary to define the physical axion scale f_a from the strength of the gluonic coupling:

$$f_a \equiv \frac{f_{PQ}}{N}\,. \tag{7.1.22}$$

7.1.1 The Lagrangian below the QCD confinement scale

Three pseudoscalars mix once quarks are confined: the axion, the SM singlet η_0 and the neutral pion π_3. The π_3-η_0 mixing is due to the quark mass differences which break the global flavor symmetry. At leading order in the chiral expansion and in the two quark approximation, the mass Lagrangian for the pions and η_0 reads

$$\mathcal{L} \supset B_0 \frac{f_\pi^2}{2} \mathrm{Tr}\left(\mathbf{\Sigma}\, \mathrm{M_q^\dagger} + \mathrm{M_q}\, \mathbf{\Sigma}^\dagger\right) , \tag{7.1.23}$$

where B_0 can be expressed in terms of the QCD quark condensate $\langle \bar{q} q \rangle$ as $B_0 f_\pi^2 = -2\langle \bar{q} q \rangle$, and M_q denotes the quark mass matrix,

$$M_q = \begin{pmatrix} m_u & 0 \\ 0 & m_d \end{pmatrix} . \tag{7.1.24}$$

The matrix of pseudoscalar fields can be written as

$$\mathbf{\Sigma}(x) = \exp[\mathrm{i}(2\eta_0/(\mathrm{f}_\pi \sqrt{2})\, \mathbf{1}] \exp[\mathrm{i}\, \mathbf{\Pi}/\mathrm{f}_\pi] , \tag{7.1.25}$$

where the η_0 decay constant has been approximated by f_π and

$$\mathbf{\Pi} \equiv \begin{pmatrix} \pi_3 & \sqrt{2}\pi^+ \\ \sqrt{2}\pi^- & -\pi_3 \end{pmatrix} . \tag{7.1.26}$$

In the presence of the axion, the anomalous QCD current $G\tilde{G}$ couples to both the axion and the η_0 fields and mixes them. The two mixing sources combined result ultimately in an axion-pion mixing. For simplicity, we will first consider the case with $\mathcal{X}_{u,d} = 0$ in Eq. (7.1.10), and afterwards the case $\mathcal{X}_{u,d} \neq 0$.

SM light quarks not charged under PQ ($\mathcal{X}_{u,d} = 0$)

A popular example of this class of models are KSVZ ones, in which only heavy exotic quarks are charged under PQ. For any model in which the u and d SM quarks are singlets of the PQ symmetry, their quark mass matrix in the basis here considered is that in Eq. (7.1.24). In this case $N = N^0$, as all contributions to the anomalous gluonic coupling are already included in N^0. The potential for the three pseudoscalars is, at first order in the pseudoscalar masses,

$$V = -B_0 f_\pi^2 \left[m_u \cos\left(\frac{\pi_3}{f_\pi} + \frac{\eta_0}{f_\pi}\right) + m_d \cos\left(\frac{\pi_3}{f_\pi} - \frac{\eta_0}{f_\pi}\right)\right] + \frac{1}{2} K \left(2\frac{\eta_0}{f_\pi} + \frac{a}{f_a}\right)^2 , \tag{7.1.27}$$

where the last term stems from the instanton potential with $K \sim \Lambda_{QCD}^4$ [187–189]. The resulting mass matrix for the three neutral pseudoscalars is given by

$$M^2_{\{\pi_3,\,\eta_0,a\}} = \begin{pmatrix} B_0\,(m_u+m_d) & B_0\,(m_u-m_d) & 0 \\ B_0\,(m_u-m_d) & 4K/f_\pi + B_0(m_u+m_d) & 2K/(f_\pi f_a) \\ 0 & 2K/(f_\pi f_a) & K/f_a^2 \end{pmatrix} . \tag{7.1.28}$$

The diagonalization leads to the well-known expressions for the pseudoscalar mass terms:

$$m_\pi^2 \simeq B_0\,(m_u+m_d), \quad m_{\eta'}^2 \simeq \frac{4K}{f_\pi^2} + B_0\,(m_u+m_d), \quad m_a^2 \simeq \frac{f_\pi^2 m_\pi^2}{f_a^2}\frac{m_u m_d}{(m_u+m_d)^2} . \tag{7.1.29}$$

It follows from these expressions that K can be expressed in terms of the low-energy physical parameters as

$$K \simeq \frac{1}{4}\,(m_\eta^2 - m_\pi^2)\,f_\pi^2 . \tag{7.1.30}$$

The corresponding mixing matrix is given by

$$\begin{pmatrix} 1 & \frac{f(m_d-m_u)}{2f_a(m_d+m_u)} & \frac{f}{2f_a} \\ -\frac{f(m_d-m_u)}{2f_a(m_d+m_u)} & 1 & -\frac{m_\pi^2}{m_{\eta'}^2}\frac{(m_d-m_u)}{(m_d+m_u)} \\ -\frac{f}{2f_a} & \frac{m_\pi^2}{m_{\eta'}^2}\frac{(m_d-m_u)}{(m_d+m_u)} & 1 \end{pmatrix} , \tag{7.1.31}$$

or, equivalently, the mass eigenstates are given by

$$a \simeq \hat{a} + \theta_{a\pi}\,\pi_3 + \theta_{a\eta'}\,\eta_0 , \tag{7.1.32}$$

$$\pi^0 \simeq \pi_3 + \theta_{\pi\,a}\,a + \theta_{\pi\eta'}\,\eta_0 , \tag{7.1.33}$$

$$\eta' \simeq \eta_0 + \theta_{\eta'\,a}\,a + \theta_{\eta'\,\pi}\,\pi_3 . \tag{7.1.34}$$

Here, all the mixing angles are assumed small and

$$\theta_{a\pi} \simeq -\frac{f_\pi}{2f_a}\frac{m_d-m_u}{m_u+m_d} , \qquad \theta_{a\eta'} \simeq -\frac{f_\pi}{2f_a} , \qquad \theta_{\pi\eta'} \simeq \frac{m_\pi^2}{m_{\eta'}^2}\frac{(m_d-m_u)}{(m_d+m_u)} , \tag{7.1.35}$$

$$\theta_{\pi\,a} \simeq -\theta_{a\pi} , \qquad \theta_{\eta'\,a} \simeq -\theta_{a\eta'} , \qquad \theta_{\eta'\,\pi} \simeq -\theta_{\pi\eta'} . \tag{7.1.36}$$

Only the leading terms for each mixing entry have been kept in Eqs. (7.1.31)-(7.1.36). The impact of the extra terms in $1/f_a$ and in quark masses, that is, $\mathcal{O}(m_\pi^2/m_\eta^2)$, may be comparable to that of next-to-leading operators in the chiral expansion and will thus not be retained here.

The results in Eqs. (7.1.32)-(7.1.36) illustrate that the physical low-energy axion eigenstate acquires π_3 and η_0 components and thus inherits their couplings to *all gauge bosons*, weighted down by their mixing with the axion. These results apply to any physical process in which the axion is on-shell and the axion mass is lighter than the confinement scale.

We are interested in identifying the model-independent contributions in the coupling to the electroweak gauge bosons for light axions and for the SM light pseudoscalars. We will first recover in our basis the customary axion-photon couplings, to set the framework.

Axion-photon coupling

The physical $g_{a\gamma\gamma}$ is given by

$$g_{a\gamma\gamma} = g^0_{a\gamma\gamma} + \theta_{a\pi}\, g_{\pi\gamma\gamma} + \theta_{a\eta'}\, g_{\eta'\gamma\gamma}\,, \tag{7.1.37}$$

where the last two terms are the contributions induced by the model-independent axion-pion and axion-η' QCD mixing. Denoting by q_u and q_d the electric charges of the up and down quarks, respectively, the photonic couplings of the SM light pseudoscalars are given by

$$g_{\pi\gamma\gamma} \equiv -\frac{3\,\alpha}{\pi\, f_\pi}\left(q_u^2 - q_d^2\right), \qquad g_{\eta'\gamma\gamma} \equiv -\frac{3\,\alpha}{\pi\, f_\pi}\left(q_u^2 + q_d^2\right). \tag{7.1.38}$$

For the present case with $\mathcal{X}_{u,d} = 0$, that is $E_0 = E$ and $N_0 = N$, it follows that

$$g_{a\gamma\gamma} = g^0_{a\gamma\gamma} + \frac{\alpha}{2\pi f_a}\left(6\,\frac{q_d^2\, m_u + q_u^2\, m_d}{m_u + m_d}\right), \tag{7.1.39}$$

resulting in the well-known expression

$$g_{a\gamma\gamma} = -\frac{\alpha}{2\pi f_a}\left(\frac{E}{N} - \frac{2}{3}\,\frac{m_u + 4\, m_d}{m_u + m_d}\right), \tag{7.1.40}$$

which is valid to first order in chiral perturbation theory.

SM light quarks charged under PQ ($\mathcal{X}_{u,d} \neq 0$)

The quark mass matrix in Eq. (7.1.23) is to be replaced by

$$M_q = \begin{pmatrix} m_u & 0 \\ 0 & m_d \end{pmatrix}\begin{pmatrix} e^{i\,\mathcal{X}_u\,\hat{a}/f_{\rm PQ}} & 0 \\ 0 & e^{i\,\mathcal{X}_d\,\hat{a}/f_{\rm PQ}} \end{pmatrix}. \tag{7.1.41}$$

The potential in Eq. (7.1.27) is now generalized to

$$V = -B_0 f_\pi^2\left[m_u \cos\left(\frac{\pi_3}{f_\pi} + \frac{\eta_0}{f_\pi} - \mathcal{X}_u\,\frac{\hat{a}}{f_{\rm PQ}}\right) + m_d \cos\left(\frac{\pi_3}{f_\pi} - \frac{\eta_0}{f_\pi} - \mathcal{X}_d\,\frac{\hat{a}}{f_{\rm PQ}}\right)\right] + \frac{1}{2}\,K\left[2\frac{\eta_0}{f_\pi} + N_0\frac{\hat{a}}{f_{\rm PQ}}\right]^2, \tag{7.1.42}$$

resulting in a pseudoscalar squared mass matrix $M^2_{\{\pi_3,\,\eta_0,a\}}$ which takes the form

$$M^2_{\{\pi_3,\,\eta_0,a\}} = \begin{pmatrix} B_0\,(m_u+m_d) & B_0\,(m_u-m_d) & -B_0\,\frac{f_\pi}{f_{\rm PQ}}\left(m_u\,\mathcal{X}_u - m_d\,\mathcal{X}_d\right) \\ B_0\,(m_u-m_d) & \frac{4K}{f_\pi} + B_0(m_u+m_d) & \frac{2\,N_0 K}{f_\pi f_{\rm PQ}} + B_0\,\frac{f_\pi}{f_{\rm PQ}}\left(m_u\,\mathcal{X}_u + m_d\,\mathcal{X}_d\right) \\ -B_0\,\frac{f_\pi}{f_{\rm PQ}}\left(m_u\,\mathcal{X}_u - m_d\,\mathcal{X}_d\right) & \frac{2\,N_0 K}{f_\pi f_{\rm PQ}} + B_0\,\frac{f_\pi}{f_{\rm PQ}}\left(m_u\,\mathcal{X}_u + m_d\,\mathcal{X}_d\right) & \frac{N_0^2\,K}{f_{\rm PQ}^2} + B_0\,\frac{f_\pi^2}{f_{\rm PQ}^2}\left(m_u\,\mathcal{X}_u^2 + m_d\,\mathcal{X}_d^2\right) \end{pmatrix}. \tag{7.1.43}$$

The mixing angles in Eqs. (7.1.35)-(7.1.36) still hold but for the pion-axion mixing which is now given by [4]

$$\theta_{a\pi} \simeq -\frac{f_\pi}{2f_{\rm PQ}}\left(\mathcal{X}_d - \mathcal{X}_u + \left(N_0 + \mathcal{X}_d + \mathcal{X}_u\right)\frac{m_d - m_u}{m_u + m_d}\right) . \tag{7.1.44}$$

The coefficient in front of the mass-dependent term in this equation coincides with the strength of the physical gluonic couplings,[5] given by

$$N = \left(N_0 + \mathcal{X}_d + \mathcal{X}_u\right) , \tag{7.1.45}$$

and in consequence

$$\theta_{a\pi} \simeq -\frac{f_\pi}{2N f_a}\left(\mathcal{X}_d - \mathcal{X}_u + N\frac{m_d - m_u}{m_u + m_d}\right) . \tag{7.1.46}$$

The expressions for the mass of the physical pion, η' and axion are the same than those in Eq. (7.1.29).

Axion-photon coupling

For the case in which the up and down quarks are charged under PQ, $\mathcal{X}_{u,d} \neq 0$, N is given by Eq. (7.1.45) resulting in

$$g_{a\gamma\gamma} = g^0_{a\gamma\gamma} - \frac{\alpha}{2\pi f_a}\left(\frac{E_{u,\,d}}{N} - \frac{2}{3}\frac{m_u + 4\,m_d}{m_u + m_d}\right) , \tag{7.1.47}$$

where

$$E_{u,\,d} \;=\; 6\,\mathcal{X}_u\,q_u^2 \;+\; 6\,\mathcal{X}_d\,q_d^2 . \tag{7.1.48}$$

In consequence

$$g_{a\gamma\gamma} = -\frac{\alpha}{2\pi f_a}\left(\frac{E_0}{N} + \frac{E_{u,\,d}}{N} - \frac{2}{3}\frac{m_u + 4\,m_d}{m_u + m_d}\right) = -\frac{\alpha}{2\pi f_a}\left(\frac{E}{N} - \frac{2}{3}\frac{m_u + 4\,m_d}{m_u + m_d}\right) . \tag{7.1.49}$$

In summary, the most general mass matrix leads to the same expression than for the case $\mathcal{X}_{u,d} = 0$ in Eq. (7.1.54) if taking into account in E also the contribution of the up and down quarks.

[4] This expression for the axion-pion mixing agrees with the result of Ref. [390] for the case where the only PQ charged fermions are the up and down quarks, i.e. $N_0 = 0$.

[5] As expected from the triangle diagram, all fermions (including the up and down quarks) run in the loop and contribute to $N = N_0 + \sum_{u,\,d} 2\,\mathcal{X}\,T(R) = N_0 + \mathcal{X}_d + \mathcal{X}_u$.

7.1.2 Axion couplings to EW gauge bosons

The description in terms of the effective chiral Lagrangian is only appropriate for energies/momenta not higher than the cutoff of the effective theory, $4\pi f_\pi$, that is, the QCD scale as set by the nucleon mass. In this context, the W and Z bosons can be considered as external currents that couple to a QCD axion whose energy/momentum is not higher than Λ_{QCD}, for instance a light enough on-shell QCD axion. In other words, the W and Z bosons enter the effective chiral Lagrangian as classical sources, alike to the treatment of baryons in the effective chiral Lagrangian.

We extend here the results of the previous section to the interactions of axions with SM heavy gauge bosons. Eq. (7.1.54) is thus generalized for any pair of electroweak gauge bosons X, Y,

$$g_{aXY} = g^0_{aXY} + \theta_{a\pi}\, g_{\pi XY} + \theta_{a\eta'}\, g_{\eta' XY}\,. \tag{7.1.50}$$

Indeed, all axion couplings to EW bosons receive a model-independent component due to the pion-η'-axion mixings, in the regime in which the involved energy/momenta are smaller or comparable to the confinement scale. A relevant point when computing the couplings of the QCD axion to heavy EW bosons is the fact that, after confinement, a new type of $SU(2)_L$-breaking effective interaction of the form

$$\hat{a}\, W^3_{\mu\nu}\tilde{B}^{\mu\nu}\,, \tag{7.1.51}$$

is present in addition to those in Eqs. (7.1.3)-(7.1.5). It stems via axion-pion coupling from the $\pi_a W^a_{\mu\nu}\tilde{B}^{\mu\nu}$ effective interaction. The details of the computation can be found in App. 7.A. In terms of the physical photon, Z and W, the interaction Lagrangian for the QCD axion is then given by

$$\delta\mathcal{L}_a^{gauge} = \frac{1}{4} g_{agg}\, a\, G\tilde{G} + \frac{1}{4} g_{aWW}\, a\, W\tilde{W} + \frac{1}{4} g_{aZZ}\, a\, Z\tilde{Z} + \frac{1}{4} g_{a\gamma\gamma}\, a\, F\tilde{F} + \frac{1}{4} g_{a\gamma Z}\, a\, F\tilde{Z}\,, \tag{7.1.52}$$

where

$$g_{agg} = -\frac{1}{2\pi f_a}\alpha_s\,, \tag{7.1.53}$$

$$g_{a\gamma\gamma} = -\frac{1}{2\pi f_a}\alpha_{\rm em}\left(\frac{E}{N} - \frac{2}{3}\frac{m_u + 4m_d}{m_u + m_d}\right)\,, \tag{7.1.54}$$

$$g_{aWW} = -\frac{1}{2\pi f_a}\frac{\alpha_{\rm em}}{s_w^2}\left(\frac{L}{N} - \frac{3}{4}\right)\,, \tag{7.1.55}$$

$$g_{aZZ} = -\frac{1}{2\pi f_a}\frac{\alpha_{\rm em}}{s_w^2 c_w^2}\left(\frac{Z}{N} - \frac{11 s_w^4 + 9 c_w^4}{12} - \frac{s_w^2(s_w^2 - c_w^2)}{2}\frac{m_d - m_u}{m_u + m_d}\right)\,, \tag{7.1.56}$$

$$g_{a\gamma Z} = -\frac{1}{2\pi f_a}\frac{\alpha_{\rm em}}{s_w c_w}\left(\frac{2R}{N} - \frac{9c_w^2 - 11 s_w^2}{6} - \frac{1}{2}(c_w^2 - 3 s_w^2)\frac{m_d - m_u}{m_u + m_d}\right)\,. \tag{7.1.57}$$

Eq. (7.1.54) is the known leading-order result [182,183] for the photonic couplings of the QCD axion, which holds in all generality for on-shell axions lighter than the QCD confinement scale.

The contributions in Eqs. (7.1.55)-(7.1.57) are new and extend that result to the couplings of heavy gauge bosons in the appropriate energy range. Indeed, the last term in the parenthesis for each of these couplings encodes the impact of the mixing of the axion with the pion and η', see Eqs. (7.1.14)-(7.1.18) for comparison with the unmixed case. These are model-independent contributions, valid for any QCD axion, i.e., for any model in which the SM strong gauge group is the only confining force and thus the only source of an instanton potential for the axion. In other words, they are valid for any axion whose mass and scale are related by Eq. (7.1.29). Note that those corrections hold precisely because the axion mass is smaller than the confining scale of QCD, which is the regime in which the SM pseudoscalars lighter than the QCD scale are the physical eigenstates of the spectrum and the mixing effects are meaningful.

Numerically, at leading order in the chiral expansion it follows that

$$g_{a\gamma\gamma} = -\frac{1}{2\pi f_a}\alpha_{\rm em}\left(\frac{E}{N} - 2.03\right) , \tag{7.1.58}$$

$$g_{aWW} = -\frac{1}{2\pi f_a}\frac{\alpha_{\rm em}}{s_w^2}\left(\frac{L}{N} - 0.75\right) , \tag{7.1.59}$$

$$g_{aZZ} = -\frac{1}{2\pi f_a}\frac{\alpha_{\rm em}}{s_w^2 c_w^2}\left(\frac{Z}{N} - 0.52\right) , \tag{7.1.60}$$

$$g_{a\gamma Z} = -\frac{1}{2\pi f_a}\frac{\alpha_{\rm em}}{s_w c_w}\left(\frac{2R}{N} - 0.74\right) . \tag{7.1.61}$$

The numerical value of the model-independent term in Eq. (7.1.58) differs from the usual one [183] of 1.92 in Eq. (3.1.20), as the latter includes higher order chiral corrections, a refinement out of the scope of this thesis and left for future work.

The model-independent results obtained here for the coupling of light QCD axions to the SM electroweak bosons may impact axion signals in rare decays in which they participate. For instance, in low-energy processes the axion could be be photophobic at low energies [166] (or more generally, EW-phobic), in models in which the terms in parenthesis cancel approximately, unlike at higher energies at which the model-independent component disappears and only the model-dependence (encoded in E/N, M/N, Z/N and R/N) is at play.

Gauge invariance

As it was already enforced in Eq. (7.1.21), the couplings of the axion to the EW gauge bosons are not independent as a consequence of gauge invariance. Indeed, all four couplings stem from the two independent effective operators in Eqs. (7.1.4) and (7.1.5), plus that in Eq. (7.1.51) for a light QCD axion ($m_a \ll \Lambda_{QCD}$). In consequence, three physical couplings can be independent among the set $\{g_{a\gamma\gamma}\,, g_{aWW}\,, g_{aZZ}\,, g_{a\gamma Z}\}$, and the following relation must hold:

$$g_{aZZ} = -\left(c_w^2 + \frac{s_w^4}{c_w^2}\right) g_{aWW} + \frac{c_w^3}{s_w} g_{a\gamma\gamma} + \left(1 + c_w^2 + \frac{s_w^4}{c_w^2}\right) g_{a\gamma Z}\,. \tag{7.1.62}$$

Note that this result does not depend on the details of any particular axion model; it is independent of the presence or absence of gluonic couplings and it thus applies in all generality for a light pseudoscalar with only anomalous electroweak couplings. That is, it is also valid for generic ALPs which only have EW interactions. Furthermore, it suggests that it may be inconsistent to assume only one EW coupling: the minimum number of physical EW couplings for an axion or ALP is two. The relation in Eq. (7.1.62) sets an avenue to oversconstrain the parameter space which is promising. It allows to use the better constrained EW couplings to bound the fourth one.

7.2 Beyond the QCD axion

We discuss in this section the case of a "heavy axion": an axion whose mass is not given by the QCD axion expression in Eq. (3.1.12)) but receives instead extra contributions. We have in mind a true axion which solves the strong CP problem, for which the source of this extra mass does not spoil the alignment of the CP conserving minimum. This is the case for instance of models in which the confining sector of the SM is enlarged involving a new force with a confining scale much larger than the QCD one [4, 170–180]. This avenue is of particular interest as it allows to consider heavy axions and low axion scales (e.g. $\mathcal{O}$(TeV)), and still solve the SM strong CP problem. The axion mass can then expand a very large range of values. It can become much larger than the EW scale or, conversely, be in the GeV range or lower. For the purpose of this work, the latter range is to be kept in mind as a general guideline, so as to remain in the range of validity of the effective Lagragian with confined hadrons. The procedure will also serve as a template to show how the mixing effects disappear from the axion-gauge couplings as the axion mass is raised.

In practice, the analysis below applies identically to a true heavy axion which solves the strong CP problem and to a gluonic ALP, that is, any ALP which has both electroweak and gluonic anomalous couplings, even if not related to a solution to the strong CP problem. For the sake of generality, consider the addition of an extra mass term to the effective Lagrangian obtained after EW symmetry breaking but above confinement in Eq. (7.1.13),

$$\delta\mathcal{L}_a = \frac{1}{2}\, M^2 \hat{a}^2. \tag{7.2.1}$$

For simplicity, from now on we focus on the case in which the first generation of SM quarks carry no PQ charge, as it is straightforward to enlarge the analysis beyond this hypothesis, as shown in the previous section. After confinement, the pseudoscalar mass matrix in Eq. (7.1.28) is then replaced by

$$M^2_{\{\pi_3,\,\eta_0,a\}} = \begin{pmatrix} B_0\,(m_u+m_d) & B_0\,(m_u-m_d) & 0 \\ B_0\,(m_u-m_d) & 4K/f_\pi + B_0(m_u+m_d) & 2K/(f_\pi f_a) \\ 0 & 2K/(f_\pi f_a) & K/f_a^2 + M^2 \end{pmatrix}. \tag{7.2.2}$$

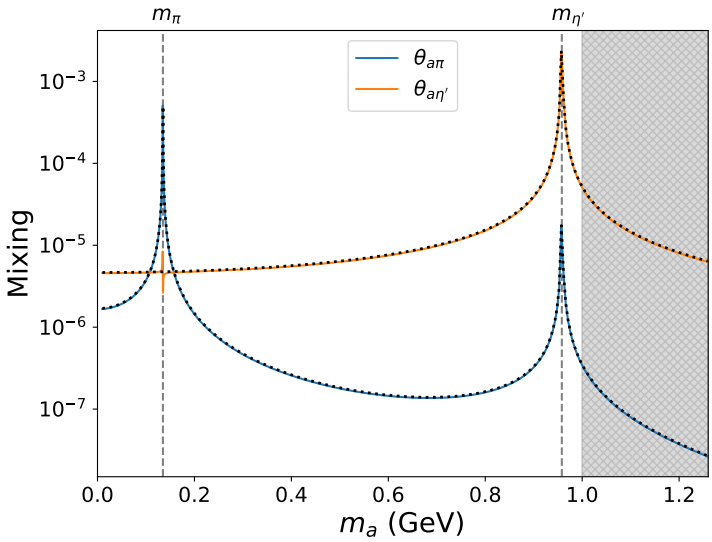

Figure 1: *Mixing angles as a function of the (heavy) axion mass m_a, for a value of $f_a = 10$ TeV. The grey area indicates the range where the validity of the chiral expansion breaks down. The figure also applies to gluonic ALPs.*

In the limit $f_a \gg K^{1/4}$ (i.e. $f_a \gg \Lambda_{QCD}$) the expressions for the π, η' and a mass eigenvalues become

$$m_\pi^2 \simeq B_0\,(m_u + m_d), \quad m_{\eta'}^2 \simeq \frac{4K}{f_\pi^2} + B_0\,(m_u + m_d), \quad m_a^2 \simeq M^2 + \frac{f_\pi^2 m_\pi^2}{f_a^2}\frac{m_u m_d}{(m_u + m_d)^2}\,. \tag{7.2.3}$$

The corresponding axion-pion and axion-η' mixing angles take a very simple form in the limit $M \gg m_\pi$,

$$\theta_{a\pi} \simeq -\frac{f_\pi}{2f_a}\frac{m_d - m_u}{m_u + m_d}\frac{1}{1 - \frac{M^2}{m_\pi^2}}\frac{1}{1 - \frac{M^2}{m_{\eta'}^2}}\,, \qquad \theta_{a\eta'} \simeq -\frac{f_\pi}{2f_a}\frac{1}{1 - \frac{M^2}{m_{\eta'}^2}}\,, \tag{7.2.4}$$

where again only the leading term on each entry of the mixing matrix has been retained. In fact, it can be checked that these equations hold even for small values of M, as long as M is non-degenerate with the pion or η' mass. The comparison with Eq. (7.1.35) ilustrates that the M-dependent corrections may be important for axion masses near the pion mass or the η' mass. The divergences in Eq. (7.2.4) for an axion degenerate in mass with the pion or the η' are an artifact of the approximations which in practice correspond to large mixing values, as expected in those ranges. The numerical results do not rely on that approximation and are illustrated in Fig. 1: the spikes correspond to an axion degenerate with either the pion or the η'.

7.2.1 Heavy axion couplings to EW gauge bosons

The couplings of the heavy axion to the electroweak gauge bosons reflect the dependence of the mixing parameters on the extra source of mass M, as follows:

$$g_{aWW} = -\frac{1}{2\pi f_a}\frac{\alpha_{\rm em}}{s_w^2}\left(\frac{L}{N} - \frac{3}{4}\frac{1}{1-\left(\frac{M}{m_{\eta'}}\right)^2}\right), \tag{7.2.5}$$

$$g_{a\gamma\gamma} = -\frac{1}{2\pi f_a}\alpha_{\rm em}\left[\frac{E}{N} - \frac{1}{1-\left(\frac{M}{m_{\eta'}}\right)^2}\left(\frac{5}{3} + \frac{m_d - m_u}{m_u + m_d}\frac{1}{1-\left(\frac{M}{m_\pi}\right)^2}\right)\right], \tag{7.2.6}$$

$$g_{aZZ} = -\frac{1}{2\pi f_a}\frac{\alpha_{\rm em}}{s_w^2 c_w^2}\left[\frac{Z}{N} - \frac{1}{1-\left(\frac{M}{m_{\eta'}}\right)^2}\left(\frac{11s_w^4 + 9c_w^4}{12} - \frac{s_w^2(s_w^2 - c_w^2)}{2}\frac{m_d - m_u}{m_u + m_d}\frac{1}{1-\left(\frac{M}{m_\pi}\right)^2}\right)\right], \tag{7.2.7}$$

$$g_{a\gamma Z} = -\frac{1}{2\pi f_a}\frac{\alpha_{\rm em}}{s_w c_w}\left[\frac{2K}{N} - \frac{1}{1-\left(\frac{M}{m_{\eta'}}\right)^2}\left(\frac{9c_w^2 - 11s_w^2}{6} - \frac{1}{2}(c_w^2 - 3s_w^2)\frac{m_d - m_u}{m_u + m_d}\frac{1}{1-\left(\frac{M}{m_\pi}\right)^2}\right)\right]. \tag{7.2.8}$$

The M-dependent corrections in these couplings can be relevant for heavy axions which solve the strong CP problem as well as for gluonic ALPs, as long as their mass parametrized by Eq. (7.2.3) is sensibly larger than that for the QCD (i.e. invisible) axion, $M^2 > m_\pi^2 f_\pi^2/f_a^2$. These expressions hold as long as chiral perturbation theory is valid, that is $M \lesssim 1\,\text{GeV}$.

For values of M noticeably larger than the η' mass the model prediction depicted is only indicative, as the effective Lagrangian in terms of pions and η' is not really adequate and the description should the be done in terms of the couplings to quarks. At those energies ($m_a \gg m_{\eta'}$) QCD is perturbative and it would be pertinent to compute the two-loop contribution of the gluonic coupling to the EW gauge boson couplings. For the case of photons, a qualitative estimation has been performed in Ref. [290] with the result:

$$\delta g_{a\gamma\gamma} = -\frac{3\,\alpha_{\rm em}\,\alpha_s(m_a^2)}{\pi^2}\,g_{agg}\sum_f q_f^2 B_1(\tau_f)\log\left(\frac{f_{\rm PQ}^2}{m_f^2}\right), \tag{7.2.9}$$

leading to a photonic axion coupling given by

$$g_{a\gamma\gamma} = -\frac{1}{2\pi f_a}\alpha_{\rm em}\left(\frac{E}{N} - \frac{3\,\alpha_s^2}{2\pi^2}\sum_f q_f^2 B_1(\tau_f)\log\left(\frac{f_{\rm PQ}^2}{m_f^2}\right)\right). \tag{7.2.10}$$

The loop function $B_1(\tau)$ will be defined later in Eq. 7.3.6. The derivation of the equivalent formula for the coupling of axions to heavy EW gauge boson couplings is left for future work. Nevertheless, the analysis presented here conveys the qualitative behaviour expected for the transition between the low and high axion mass regimes.

Gauge invariance

For high axion masses (i.e. $M \gg \Lambda_{QCD}$ in Eq. (7.2.3)), the mixing of the axion with the SM pseudoscalars becomes negligible. For those scales, QCD enters the perturbative regime and

Eq. (7.2.9) illustrates how the model-independent contributions to the EW couplings diminish. As the latter become negligible, the axion coupling to EW gauge bosons is parametrized by just the two effective interactions in Eqs. (7.1.4) and (7.1.5). In other words, the heavy axion EW couplings span a parameter space with two degrees of freedom (instead of three for light axions with $m_a \ll \Lambda_{QCD}$, see Section 7.1.2). Two independent constraints follow for heavy axions:

$$g_{aWW} = g_{a\gamma\gamma} + \frac{c_w}{2\, s_w} g_{a\gamma Z}\,, \tag{7.2.11}$$

$$g_{aZZ} = g_{a\gamma\gamma} + \frac{c_w^2 - s_w^2}{2\, s_w c_w} g_{a\gamma Z}\,, \tag{7.2.12}$$

where we have chosen to express the couplings g_{aWW}, g_{aZZ} in terms of the overall better constrained ones $g_{a\gamma\gamma}$ and $g_{a\gamma Z}$.[6] These powerful relations will be exploited in the next section to further constrain uncharted regions of the experimental parameter space.

Alike to the discussion after Eq. (7.1.62), the relations in Eqs. (7.2.11) and (7.2.12) apply not only to heavy axions and heavy gluonic ALPs, but also to generic ALPs which only exhibit EW interactions and are much heavier than nucleons. The corollary that at least two EW couplings –if any– must exist for any axion or ALP holds as well.

7.3 Phenomenological analysis

The impact of the results obtained above on present and future axion searches will be illustrated in this section. Both tree-level and loop-level effects will be taken into account. Indeed the latter are relevant when confronting data on photons, electrons and nucleons, as the experimental constraints on these channels are so strong that they often dominate the bounds on EW axion couplings.

7.3.1 Loop-induced couplings

The tree-level coupling of the axion to photons can be suppressed in some situations [166, 167] (photophobic ALPs are also possible [392]). Additionally, many models have no tree-level couplings to leptons or suppressed couplings to nucleons [169]. However, all possible effective couplings will mix at the loop level. This affects the renormalization group (RG) evolution, via which all couplings allowed by symmetry will be generated even when assuming only a subset of couplings at some scale.

Before proceeding with the phenomenological analysis, we discuss in this subsection the loop-induced effective interactions arising from the direct coupling to electroweak gauge bosons. Because the experimental and observational limits are usually strongest for photons, electrons,

[6] Obviously, the milder constrain in Eq. (7.1.62) also applies here.

and nucleons, the loop-induced contributions to these channels can give stronger constraints than those stemming from the tree-level impact on other channels.

Denoting the effective axion-fermion Lagrangian by

$$\delta\mathcal{L}_{a\,\text{eff}} \supset \sum_f c_{1\,\text{eff}}^f \frac{\partial_\mu \hat{a}}{f_{\text{PQ}}} \left(\bar{f}\,\gamma_\mu\,\gamma_5\,f \right) , \tag{7.3.1}$$

it has been shown [290] that the coefficient $c_{1\,\text{eff}}^f$ receives one loop-induced corrections from electroweak couplings,

$$\begin{aligned}
\frac{c_{1\,\text{eff}}^f}{f_a} &= \frac{3}{4}\left(\frac{\alpha_{\text{em}}}{4\pi\, s_w^2} \frac{3}{4} g_{aWW} + \frac{\alpha_{\text{em}}}{4\pi\, c_w^2} \left(Y_{f_L}^2 + Y_{f_R}^2 \right) g_{aBB} \right) \log \frac{f_{\text{PQ}}^2}{m_W^2} \;+\; \frac{3}{2} \frac{\alpha_{\text{em}}}{4\pi} Q_f^2 g_{a\gamma\gamma} \log \frac{m_W^2}{m_f^2} \\
&= \frac{9}{16} \frac{\alpha_{\text{em}}}{4\pi\, s_w^2} g_{aWW} \log \frac{f_{\text{PQ}}^2}{m_W^2} \;+\; \frac{3}{4} \frac{\alpha_{\text{em}}}{4\pi\, s_w^2 c_w^2} \left(\frac{3}{4} c_W^4 + \left(Y_{f_L}^2 + Y_{f_R}^2 \right) s_W^4 \right) g_{aZZ} \log \frac{f_{\text{PQ}}^2}{m_W^2} \\
&+ \frac{3}{4} \frac{\alpha_{\text{em}}}{4\pi\, s_w c_w} \left(\frac{3}{4} c_W^2 - \left(Y_{f_L}^2 + Y_{f_R}^2 \right) s_W^2 \right) g_{a\gamma Z} \log \frac{f_{\text{PQ}}^2}{m_W^2} \;+\; \frac{3}{2} \frac{\alpha_{\text{em}}}{4\pi} Q_f^2 g_{a\gamma\gamma} \log \frac{f_{\text{PQ}}^2}{m_f^2} \,.
\end{aligned} \tag{7.3.2}$$

To obtain this result, the ultraviolet scale inside the loop diagrams has been identified with the axion scale f_{PQ}, which is the cutoff of the effective theory. Note that the one-loop induced contributions to the fermion couplings are independent of the axion mass (other than a negligible dependence through the axion-gauge couplings such as $g_{a\gamma\gamma}$, see below). They are generically of order $\alpha/4\pi$ as expected, that is, over two orders of magnitude smaller than the original effective gauge coupling. Nevertheless, the experimental constraints are so strong that they will often provide the leading bounds on gauge-axion couplings.

The most relevant fermionic limits are those on the coupling to electrons and light quarks. While Eq. (7.3.2) is directly applicable to leptons and heavy quarks, at low energies light quarks form hadrons: the loop-induced coupling to nucleons have highest impact. Following Refs. [169, 183], the relation between nucleon and light quark couplings can be written as

$$\begin{aligned}
c_p + c_n &= 0.50(5) \left(c_1^u + c_1^d - 1 \right) - 2\delta \,, \\
c_p - c_n &= 1.273(2) \left(c_1^u - c_1^d - \frac{1-z}{1+z} \right) ,
\end{aligned} \tag{7.3.3}$$

where $z = m_u/m_d = 0.48(3)$ and c_1^u and c_1^d are defined in terms of the coefficients in Eq. (7.1.11) as

$$c_1^u = \frac{c_1^U - c_1^Q}{2} \,, \qquad c_1^d = \frac{c_1^D - c_1^Q}{2} \,. \tag{7.3.4}$$

In Eq. (7.3.3), δ is a combination of the heavy SM quark coeficients analogous to those in Eq. (7.3.4), $\delta = 0.038(5) c_1^s + 0.012(5) c_1^c + 0.009(2) c_1^b + 0.0035(4) c_1^t$.

The combination of Eqs. (7.3.2) and (7.3.3) allows to derive the coupling to nucleons induced by the coupling to electroweak bosons.

The axion-photon coupling also receives one-loop corrections in the presence of couplings of the axion to fermions or gauge bosons. For energies or masses in the loops higher than $\Lambda_{\rm QCD}$, quarks are the appropiate propagating degrees of freedom,[7] and the one-loop contributions for an on-shell axion can be expressed as [290]

$$g^{\rm eff}_{a\gamma\gamma} = g^0_{a\gamma\gamma} + \sum_f N_C^f Q_f^2 \frac{\alpha_{em}}{\pi}\frac{2c_1^f}{f_a} B_1(\tau_f) + 2\frac{\alpha_{em}}{\pi} g_{aWW} B_2(\tau_W), \tag{7.3.5}$$

where the subscript f runs over leptons and heavy quarks. Here, $\tau_i = 4m_i^2/m_a^2$ and

$$\begin{aligned} B_1(\tau) &= 1 - \tau f^2(\tau) \\ B_2(\tau) &= 1 - (\tau-1) f^2(\tau) \end{aligned} \quad , \qquad f(\tau) = \begin{cases} \arcsin \frac{1}{\sqrt{\tau}} & , \quad \tau \geq 1 \\ \frac{\pi}{2} + \frac{i}{2}\log\frac{1+\sqrt{1-\tau}}{1-\sqrt{1-\tau}} & , \quad \tau < 1 \end{cases} . \tag{7.3.6}$$

Asymptotically, $B_1 \to 1$ in the limit $m_a \gg m_f$ and $B_1 \to -m_a^2/(12m_f^2)$ when $m_a \ll m_f$. This means that the contribution of fermions heavier than the axion is strongly suppressed. Similarly, $B_2 \to 1 + \pi^2/4 - \log^2 m_a/m_W$ when $m_a \gg m_W$, whereas $B_2 \to m_a^2/(6m_W^2)$ in the $m_a \ll m_W$ limit.

It is worth noting that chaining the two previous one-loop contributions gives an approximate estimation of the two-loop contribution of a given heavy gauge boson coupling to the axion-photon coupling. As an example, consider g_{aWW} in Eq. (7.3.2): it results in an effective fermion coupling $c^f_{1\,\rm eff}$ which, when subsequently inserted in the second term in Eq. (7.3.5), results in an effective axion-photon coupling. This can be compared with the third term which gives directly a one-loop contribution of g_{aWW} to $g_{a\gamma\gamma}$: for $m_a \ll m_W$, the second term in Eq. (7.3.5) may actually be numerically larger than the third term, that is, the two-loop contribution via fermionic couplings may dominate over the one-loop gauge one, as it was pointed out in Refs. [290,392]. Indeed, this two-loop contribution may be phenomenologically the most relevant one to constrain the axion couplings to heavy electroweak gauge bosons. A caveat is that only a true two-loop computation may settle the dominant pattern, but the analysis discussed is expected to provide an order of magnitude estimate.

7.3.2 Axion decay channels and lifetime

The plethora of couplings discussed, contributing either at tree or loop level, produces a rich variety of production and decay channels of the axion, depending on its mass and on the relative strength of the couplings. A quantitative evaluation of the lifetime and branching ratios is essential for assessing what experiments or searches are more adequate to test different regions of parameter space.

[7] For energies below the QCD scale, radiative corrections involving light quarks have to be evaluated using chiral Lagrangian methods. This was achieved in Ref.[290], the conclusion being that the results remain qualitatively right once the quarks masses are substituted by an appropriate hadronic scale, m_π for u and d and m_η for s. However, in the presence of gluonic couplings this contribution is subdominant to the one computed in the previous sections and will thus not be considered here.

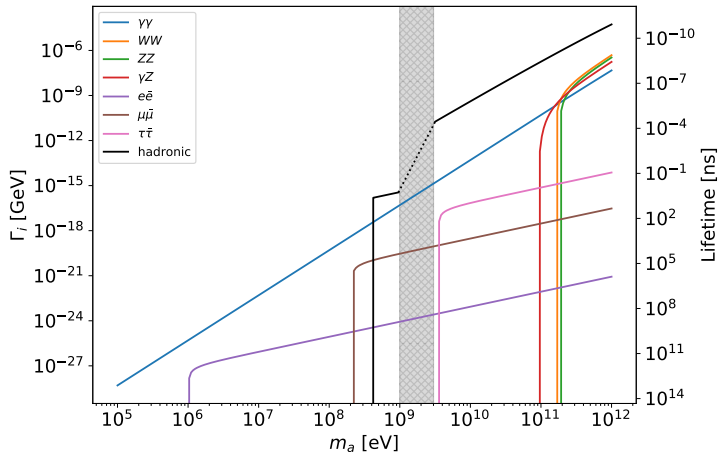

Figure 2: Illustration of the axion (or ALP) decay widths, as a function of the axion mass for a benchmark value of $g_{a\gamma\gamma} = 10^{-7}$ GeV^{-1} and the rest of gauge boson couplings as in Eq. (7.3.8). The grey hatched region signals the 1-3 GeV "no human's land" for hadronic decays in between the chiral and the perturbative regimes, where the dots indicate that no reliable prediction is possible.

In order to determine the detection capabilities of a given final state channel, an important element is whether the axion can decay into it within the detector, or escapes and contributes to an "invisible" channel. For purely illustrative purposes, Fig. 2 compares the axion decay widths into different final states for a particular choice of the model-dependent parameters.[8] This figure serves to indicate the mass threshold for the different channels and is also a good indicator of the relative width of each decay channel. The determination of the areas experimentally excluded –to be developed in Sec. 7.3.3– will not depend on the value of the effective couplings assumed in this figure, though.[9]

In the low mass region $m_a < 3m_\pi$, only decays to pairs of electrons, muons or photons are possible. The axion typically becomes long lived enough so as to be stable at collider and flavor experiments. Note that this region is particularly sensitive to a possible cancellation/suppression of the photonic coupling $g_{a\gamma\gamma}$ (this happens for instance in models of axions in which the model-dependent parameter E/N partially cancels the model-independent contribution, see Eqs. (7.1.54) and (7.2.6)). This would suppress the decay width to photons and thus enhance the branching fraction to fermions, especially close to the respective mass thresholds.

The hadronic channel plays a central role as soon as it opens. It then dominates the decay of the axion due to the large gluonic coupling. The lightest possible hadronic final state is three neutral pions. At around the GeV scale many other final states become viable, but in this region chiral perturbation theory starts to break down and we refrain from making any quantitative

[8] The value for $g_{a\gamma\gamma}$ used in this figure corresponds approximately to $f_a = 10$ TeV and $E = 1$ in axion models. Rescaling for other values of the couplings can be achieved by taking into account that $\Gamma_i \propto g^2_{aXY}$.

[9] The widths used in determining the colored regions in Figs. 4 induced at tree-level derive directly from the effective g_{aXY} value for each point of the parameter space.

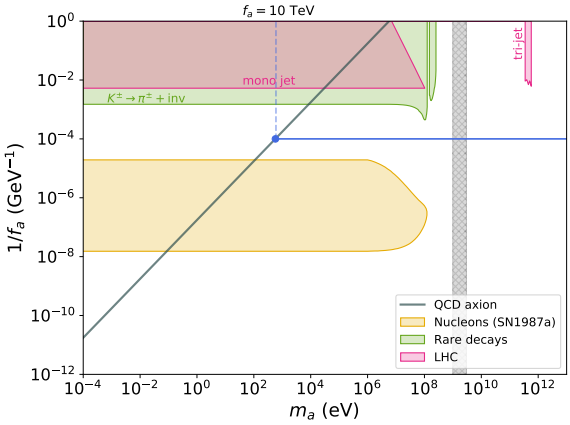

Figure 3: Coupling to gluons. The excluded areas rely on considering exclusively the coupling g_{agg} by itself. The SN1987a limit was computed in Ref. [262], while the rare decays and LHC exclusions are obtained using the results of Ref. [400] and Refs. [288, 369], respectively. Particular models are represented by the overlaid lines, the black one corresponding to the QCD axion and the blue one to heavy axion models (here for a benchmark choice of $f_a = 10\,\text{TeV}$). See Sec. 7.3.4 for more details. We provide exclusion plots without superimposed lines as auxiliary files.

predictions.[10] At high axion masses above 3 GeV the inclusive decay to hadrons can be safely estimated within perturbative QCD.[11]

At much higher energies, tree-level decays to pairs of EW gauge bosons become possible and, though subdominant with respect to the hadronic one, will play a relevant role in collider searches.

7.3.3 Experimental constraints on the (heavy) axion parameter space

We have reinterpreted a number of axion searches into our framework. Far from an in-depth review, this study primarily intends to point out the relative strength of the different observables in probing different flavors and parameter regions of axion and ALP models. Interestingly and contrary to common lore, we find that some regions of parameter space can be better tested through the axion couplings to heavy gauge bosons rather than to photons.

The colored areas in Fig. 3 show the regions experimentally excluded if taking into account *exclusively* the axion-gluon coupling g_{agg} (which in axion models fixes the axion scale f_a). Although this work focuses on the case where also EW gauge boson couplings are present, this parameter space is also shown for reference.

[10] After this work was completed, Ref. [399] appeared which discusses the hadronic decays of axions in this region $1\,\text{GeV} < m_a < 3\,\text{GeV}$.

[11] Note that heavy-flavor tagging can allow to distinguish final states involving heavy quarks, but this separation will not be taken into account here.

The couplings of axions to EW gauge bosons ($g_{a\gamma\gamma}$ g_{aWW}, g_{aZZ} and $g_{a\gamma Z}$) will be instead explored within a two-operator framework: *the axion-gluon coupling g_{agg} and one electroweak gauge coupling are to be simultaneously considered*. In other words, for each EW axion coupling g_{aXY}, the regions experimentally excluded will be determined assuming the Lagrangian [12]

$$\delta\mathcal{L}_a = \frac{1}{4} g_{agg}\, a\, G\tilde{G} + \frac{1}{4} g_{aXY}\, a\, X\tilde{Y} + \frac{1}{2}\, M^2 a^2 \,. \tag{7.3.7}$$

This choice is mainly motivated by the focus on solving the strong CP problem, or alternatively as an ALP analysis which goes beyond the traditional consideration of only one operator at a time. The regions experimentally excluded for axion-EW gauge boson couplings are then depicted in Fig. 4 as colored areas. Note that we don't discuss any cosmological bounds. The reason for this is that models of heavy axions, typically containing an extended confining sector, are expected to significantly alter the standard cosmological picture that is usually assumed to obtain such exclusions. The study of heavy axion cosmology thus requires a full self-consistent study which is left for future work.

The resulting greenish regions in Fig. 4a match well-known exclusion regions for $g_{a\gamma\gamma}$, although the overlap is not complete because the latter typically only take into account the effective axion-photon coupling; the additional presence in our analysis of the axion-gluon coupling g_{agg} has a particularly relevant impact in the heavy axion region (see below).

Figs. 4b, 4c and 4d respectively for g_{WW}, g_{ZZ} and $g_{\gamma Z}$ are novel. The possibility of measuring four distinct EW observables offers a multiple window approach and a superb cross-check if a signal is detected, given the fact that for axion masses much smaller (larger) than Λ_{QCD} only three (two) couplings are independent among the set $\{g_{a\gamma\gamma}\ g_{aWW}, g_{aZZ}, g_{a\gamma Z}\}$, see Eq. (7.1.62) (Eqs. (7.2.11) and (7.2.12)).

For the majority of the regions excluded in Fig. 4, the experiment directly constraints certain regions of the parameter space $\{g_{aXY}, m_a\}$ and no further assumptions are required; those constraints apply then also to ALPs which have no gluonic couplings. However, for some collider searches the interplay between the particular EW coupling g_{aXY} under analysis and the coupling to gluons plays a relevant role, and it is necessary to assume their relative strength. This will be taken as given by

$$\frac{g_{agg}}{g_{aXY}} = \frac{\alpha_s}{\alpha_{XY}} \,. \tag{7.3.8}$$

This is well motivated by pseudo Nambu-Goldstone bosons with anomalous couplings generated by the triangle diagram with $\mathcal{O}(1)$ group theory factors. In any case, the results are largely insensitive to this assumption, since in the best limits stemming from LHC searches the production cross section times branching ratio scales as

$$\sigma(pp \to a) \times \mathrm{BR}(a \to XY) \propto \frac{g_{agg}^2\, g_{aXY}^2}{8 g_{agg}^2 + g_{aXY}^2} \xrightarrow{g_{agg} \gg g_{aXY}} \frac{g_{aXY}^2}{8} \,. \tag{7.3.9}$$

[12] The axion mass m_a is a combination of M and the instanton contribution related to the first term, as previously explained (see Eq. 7.2.3).

It is then enough to adopt the reasonable assumption that the coupling to gluons is larger than that to EW gauge bosons $g_{agg} \gtrsim g_{aXY}$. This assumption has been adopted exclusively for LHC searches in the axion mass region where the hadronic decay channels are open, i.e. $m_a > 3\, m_\pi$.

In addition, the bounds obtained via loop contributions have a logarithmic dependence on the cut-off scale f_a. A relation between f_a and g_{aXY} needs to be assumed in order to translate the bounds on fermionic or photonic couplings into bounds on EW gauge boson couplings. In these cases, Eq. (7.3.8) will be used again, which for axion models translates into

$$f_a = \frac{\alpha_{XY}}{2\pi\, g_{aXY}}\,, \tag{7.3.10}$$

where Eq. (7.1.53) has been used. In any case, as the cutoff dependence in loops is logarithmic this assumption has a minor impact on the exclusion plots.

To sum up, for each EW-axion coupling the experimentally excluded regions in Fig. 4 are depicted on the parameter space $\{g_{aXY}, m_a\}$ without any assumption, except:

A For LHC searches and $m_a > 3\, m_\pi$, Eqs. (7.3.8) and (7.3.9) were used, which for most cases is equivalent to assume $g_{agg} \gg g_{aXY}$.

B For the regions labelled as "photons", "electrons" and "nucleons" in Figs. 4b , 4c and 4d, the loop-induced bounds have a very mild dependence on the assumption in Eq. (7.3.10).

After having presented the general strategy that we use for the reinterpretation of constraints into our setup, we proceed to describe the origin of each of the exclusion regions colored in Fig. 4.

Coupling to photons

The combination of astrophysical and terrestrial probes makes this search a particularly powerful tool to test the axion paradigm, especially for low mass axions. Even in the case of relatively large axion masses and/or situations where the coupling to photons can be suppressed, photons still place strong constraints both at tree-level and through loop-induced effects.

The experimental limits on $g_{a\gamma\gamma}$ are compiled in Fig. 4a. At the lowest axion masses considered here, $m_a \lesssim 10$ meV, the most competitive bounds come from the CAST helioscope [401], and will improve in the future with the upgrade to the IAXO experiment [269] . At slightly larger masses up to $m_a \sim 1\,\text{keV}$, $g_{a\gamma\gamma}$ is constrained by an energy-loss argument applied to Horizontal Branch (HB) stars [260]. A similar argument applies to the supernova SN1987a and constrains larger masses up to the 100 MeV range, both using extra cooling arguments [402] and by the lack of observation of a photon burst coming from decaying emitted axions [403]. In the same mass range, larger couplings can be constrained using beam dump experiments, with these exclusions led at present by the NuCal [404] experiment together with the 137 [405] and 141 [406]

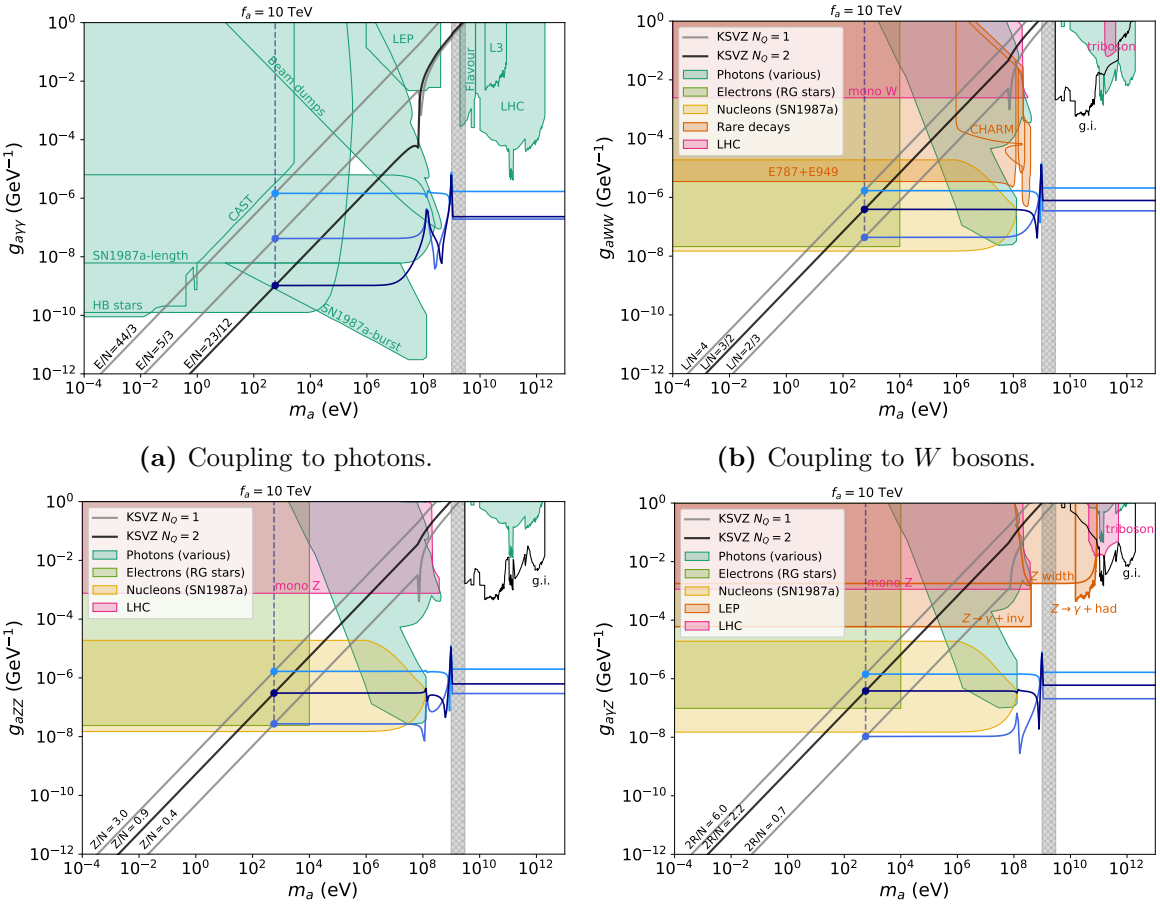

(a) Coupling to photons. **(b)** Coupling to W bosons.

(c) Coupling to Z bosons. **(d)** Coupling to a photon and a Z boson.

Figure 4: Coupling to EW gauge bosons. A two-operator framework is used: each panel assumes the existence of the corresponding electroweak coupling plus the axion-gluon coupling. The colored regions are experimentally excluded. In panels b, c and d, the loop-induced constraints labelled as "photons", "electrons" and "nucleons" depend mildly on f_a (see text). The label "g.i." illustrates the exclusion power of EW gauge invariance. The superimposed lines correspond to KSVZ-type QCD axion models (black line and grey band) and to one benchmark heavy axion model with $f_a = 10\,\text{TeV}$ (blue lines). The parameter space for heavy axions corresponds to moving up and down that set of blue lines, see Sec. 7.3.4. The results apply as well to gluonic ALPs (we provide exclusion plots without superimposed lines as auxiliary files).

experiments at SLAC. We adapt here the constraints compiled in Ref. [407], noting that these bounds rely solely on the photon coupling.

For yet higher axion masses, where colliders provide the best limits, the gluon coupling plays a relevant role. As long as no hadronic decay channel is open, the LEP constraints based on $Z \to \gamma\gamma$ and $Z \to \gamma\gamma\gamma$ searches obtained in [287, 288] for ALPs without gluonic couplings are also applicable to heavy axions. However, for masses above $3m_\pi$, hadronic final states start

to dominate and we refrain from claiming any exclusion, as a new dedicated analysis would be required to use these channels. This explains the white gap just left of the grey hatched "no human's land" region, which should be at least partially covered when the forementioned analysis is performed. It is nevertheless possible to exploit some collider searches, if a relation between the gluonic and the EW couplings is assumed. Assumption A is adopted here. Our reinterpretation of the analysis in Ref. [408], in which the $L3$ collaboration looked for hadronic final states accompanied by a hard photon, yields the limit labelled "L3" in Fig. 4a, though it is ultimately superseded by LHC exclusions. The region labelled "Flavor" is excluded by data from Babar [409] and LHCb [410], as computed in Ref. [395]. For high axion masses near the TeV scale, the limits from LHC are much stronger than those from LEP, because of the enhanced axion production via gluon-gluon fusion. We have included the limits obtained in this context in Refs. [411, 412] using run 1 data. These limits are extremely strong and should improve with the addition of run 2 data, especially at higher energies.

Finally, the bounds on $g_{a\gamma\gamma}$ described above have been translated –using assumption B– into competitive bounds for the other EW axion couplings, by means of their loop-mediated impact.

Coupling to fermions

Flavor blind observables involving fermions can be used to constrain gauge boson couplings via the impact of the latter at loop level, see Eq. (7.3.2). In order to fix the mild logarithmic dependence on the cutoff scale, assumption B will be adopted.

The most relevant constraints on flavor-blind axion-fermion interactions are of astrophysical origin and come from either electrons or nucleons. Firstly, a coupling of the axion to electrons allows for efficient extra cooling of some stars, which allows to place a bound on the axion-electron coupling g_{aee} via the observation of Red Giants (RG) [260]. Secondly, and in a manner similar to the discussion above for photons, a too strong coupling of the axion to nucleons would have shortened the duration of the neutrino burst of the supernova SN1987a. We use the most recent evaluation of this bound calculated in Ref. [262]. These two observations (RG and SN1987a) give the strongest limits on the coupling of axions to gauge bosons for axion masses respectively below 10 keV and 10 MeV, as can be seen in Fig. 4.

In addition, the one-loop induced fermion couplings also play a role in many of the observables considered here. In particular, they open potential axion decay channels into pairs of fermions.

Rare decays

For axion masses in the MeV-GeV range, g_{aWW} is best tested by its one-loop impact on rare meson decay experiments, where axions can be produced in flavor-changing neutral current (FCNC) processes. This search was first proposed in Ref. [291] (where ALPs either stable or decaying to photons were considered). Recently, these bounds have been recomputed in Ref. [392] in the context of photophobic ALPs, considering as well the potential decays of the

axion to a pair of fermions due to the one-loop induced coupling in Eq. (7.3.2). We reinterpret these searches, taking into account in addition the effects of the gluonic axion coupling under the assumptions A and B. The main consequence is that, for axion masses $m_a > 3m_\pi$, the sensitivity is drastically reduced because of the opening of hadronic axion decay channels.

At low axion masses below $2m_\mu$, the axion is long-lived enough so that it can be considered stable for experimental purposes. This means that in these regions the axion has to be looked for in invisible searches. The most stringent limits were placed by the E787 and E949 experiments testing the $K^+ \to \pi^+ X$ channel, with X invisible [400]. Following Ref. [291], we reinterpret this search in terms of axions coupled to W bosons, which yields the constraint shown in Fig. 4b. These bounds will be improved in the near future by the NA62 experiment.

Axions can also be produced from rare meson decays in proton beam dump experiments, where they can be looked for in searches for long-lived particles. The current best limits are set by the CHARM experiment [413], where the axion can be produced in Kaon and B meson decays and subsequently decays to a pair of electrons or muons. The framework developed in Ref. [414] has been recast to obtain the limit on g_{aWW} shown in Fig. 4b.[13]

Direct couplings to heavy gauge bosons

LEP provides the best environment to directly test the $g_{a\gamma Z}$ coupling for axion masses below m_Z, as shown in Fig. 4d. The first constraint set assuming only the $g_{a\gamma Z}$ coupling was placed in Ref. [289] exploiting the limit on the uncertainty of the total Z width [416], $\Gamma(Z \to \text{BSM}) \lesssim 2\,\text{MeV}$ at 95% C.L., which allows to set a conservative bound on the process $Z \to a\gamma$. Stronger limits can be placed by more specific searches, as studied in Ref. [392]. The best limit at axion masses low enough for the axion to be long-lived stem from the $Z \to \gamma +$ inv. search. For higher axion masses, the large hadronic branching fraction makes the $Z \to \gamma +$ had. search the more fruitful one to look for axions. Under assumption A for the relative strength of the gluonic and EW couplings, we exploit the results of the search performed by the L3 collaboration as presented in Ref. [408] to obtain strong limits for m_a in the range from 10 GeV up to the Z mass. Note that, even if the search is the same than that used to constrain the photonic axion coupling, the exclusion for $g_{a\gamma Z}$ has a larger reach due to the fact that the process is mediated by an on-shell Z boson, instead of a very virtual photon.

LHC allows to look for a plethora of processes sensitive to axions. In particular, for heavy axions it provides the best limits on the coupling to heavy EW gauge bosons. The drawback of restricting the analysis to processes that separately involve only one of the EW gauge boson couplings plus the gluon coupling is the reduced number of available searches. Nevertheless, the advantage is that it provides robust and model-independent constraints.

[13] After this work was completed, Ref. [415] appeared which revisits the CHARM exclusion contour and provides projections of the expected NA62 and SHiP sensitivities.

The authors of Ref. [289] studied the LHC phenomenology of axions that are stable on collider lengths and thus would manifest themselves as missing energy. In particular, mono-W and mono-Z final states where an axion is radiated as missing energy/momentum can set constraints on the three couplings g_{aWW}, g_{aZZ} and $g_{a\gamma Z}$, as shown in Fig. 4. For large axion masses $m_a > m_Z$, the authors of Ref. [392] suggested that triboson final states place the strongest bounds on ALPs coupling to massive gauge bosons, though the sensitivity of this search is hindered for axions because of the large hadronic branching ratio that we take into account. Adapting their constraints –with assumption A– leads to the exclusion of regions in parameter space near the TeV range, as shown in Figs. 4b and 4d for g_{aWW} and $g_{a\gamma Z}$, respectively. Note that significant exclusions can also be placed through the loop-induced coupling to photons. However, the most promising LHC search is one that –to the best of our knowledge– has not been performed yet. We advocate [417] the use of $pp \to a \to VV'$ processes, which benefit from the large production cross section through the gluonic coupling together with the clean final states that the decay to EW gauge bosons produce. We foresee that this search will have a sensitivity to the couplings of axions to heavy EW gauge bosons similar to the photonic case presented in Fig. 4a. Though potentially very interesting, the detailed analysis that this study requires is beyond the scope of this work and is left for the future [418].

7.3.4 Impact on (heavy) axion models and gluonic ALPs

The black oblique line in Fig. 3 corresponds to the linear relation between $1/f_a$ and m_a for the QCD axion, Eq. (3.1.12). The horizontal blue branch is one example of how that relation changes after Eq. (7.2.3) for an illustrative example of a true heavy axion.

The black, grey and blue lines in Fig. 4 illustrate possible $\{m_a, f_a\}$ values for axions which have a gluonic coupling g_{agg} (and thus may solve the strong CP problem) in addition to at least one coupling to heavy gauge bosons. Those model-dependent lines are superimposed[14] on the colored/white regions excluded/allowed by experiments for each one of the couplings in the set $\{g_{a\gamma\gamma},\ g_{a\gamma Z},\ g_{aZZ}, g_{aWW}\}$, as determined above. The examples chosen corresponds to KSVZ-type axions: either a standard QCD axion or a heavy axion as in theories with an enlarged confining gauge sector.

In each panel, for a given value of the model-dependent coupling:

- The expectation for the pure QCD axion is depicted by grey and black lines. The bands in Fig. 4 delimited by grey lines correspond to just one exotic KSVZ fermion representation. The values of the model-dependent parameters delimiting these benchmark bands [166] are summarized in Table 1. The black line is instead an illustrative case with two fermion representations such that the coupling to photons $g_{a\gamma\gamma}$ cancels up to theoretical uncertainties [166]. The upward bending of the lines obeys the expected change of the

[14] For the reader interested in generic gluonic ALPs rather than heavy axions, we provide the exclusion plots without any superimposed lines as auxiliary files.

	$SU(3)_c \times SU(2)_L \times U(1)_Y$
$(E/N)_{\rm max} = 44/3$	$(3, 3, -4/3)$
$(E/N)_{\rm min} = 5/3$	$(3, 2, +1/6)$
$(L/N)_{\rm max} = 4$	$(3, 3, Y)$
$(L/N)_{\rm min} = 2/3$	$(8, 2, -1/2)$
$(Z/N)_{\rm max} = 2.9$	$(3, 3, -4/3)$
$(Z/N)_{\rm min} = 0.4$	$(8, 2, -1/2)$
$(2R/N)_{\rm max} = 5.9$	$(3, 3, -1/3)$
$(2R/N)_{\rm min} = 0.7$	$(8, 2, -1/2)$

Table 1: Maximum and minimum values of the model-dependent coefficients for the benchmark KSVZ models with only one exotic fermion representation depicted in Fig. 4.

prediction for axion masses larger than the η' mass, a regime in which the last term in the parentheses in Eqs.(7.1.54)-(7.1.57) is absent.

- The expectations for heavy axions are illustrated with blue lines. The big dots which fall on the QCD axion lines correspond to $M = 0$ in Eqs. (7.2.1)-(7.2.3). The heavy axion trajectories start on those points and the prediction moves on each blue line towards the right as M grows. As the value of the axion mass gets near the pion and the η' masses, the prediction reflects the "resonances" found in the pseudoscalar mixing angles and the physical couplings to gauge bosons. For larger values of M the mixing effects progressively vanish, as physically expected and reflected in Eqs. (7.2.5)-(7.2.8), and the predictions stabilize again. The asymptotic value of the couplings is then induced only by the model-dependent parameters (E, L, Z, R), and it is often higher than for heavy axions lighter than the pion, for which the partial cancellation between the model-dependent and model-independent mixing effects may operate.

The figures illustrate that the M-dependent corrections may be relevant even for not very large M values. For instance, two close values of the model-dependent photon couplings E/N may give a very close $g_{a\gamma\gamma}$ prediction for M values above the η' mass, while that prediction can widely differ for M values smaller than the QCD scale. This is clearly reflected by the lines corresponding to the smaller values of E/N in Fig. 4a.

The parameter space for heavy axion models spans in fact most of the region to the right of the oblique band for the QCD axion: parallel sets of horizontal lines above and below the blue ones depicted are possible and expected for other values of the heavy axion parameters. For a given f_a, varying M (that is, varying m_a) is tantamount to move right or left on a horizontal blue line, while varying f_a displaces up or down the set of horizontal blue lines. Finally, all these considerations for heavy axion models apply as well to gluonic ALPs, as argued earlier.

Gauge invariance

For heavy axions or any type of ALP with masses $m_a \gg \Lambda_{QCD}$, couplings to EW gauge bosons are directly tested and gauge invariance imposes the two relations in Eqs. (7.2.11) and (7.2.12). Therefore, the combination of the experimental constrains on two of the operators in the set $\{g_{a\gamma\gamma}, g_{aWW}, g_{aZZ}, g_{a\gamma Z}\}$ translates in model independent bounds on the other two couplings. For light masses $m_a \leq \Lambda_{QCD}$, only Eq. (7.1.62) applies instead. These bounds based solely on EW gauge invariance have been depicted by black curves on the upper right corner of Figs. 4b, 4c and 4d. They susbtantially reduce the latter parameter space, especially in the cases of g_{aWW} and g_{aZZ}, whose current direct constraints are less powerful. They are to be taken with caution, though, since in each of the exclusion plots only one EW coupling was taken into account, while the relations deduced from gauge invariance involve several non-vanishing EW couplings. Furthermore, in a future multiparameter analysis where tree-level axion-fermion couplings are included, those relations could be corrected via one-loop effects.

7.3.5 Implications for heavy axion models

In existing models that solve the strong CP problem with heavy axions, often either

$$M^2 \sim \Lambda'^4/f_a^2\,, \qquad \text{or} \qquad M^2 \sim m_{\pi'}^2 f_{\pi'}^2/f_a^2 \tag{7.3.11}$$

where $\Lambda' \gg \Lambda_{QCD}$ is a new strong confining scale, and the primed fields denote exotic "pions" corresponding to the exotic fermions charged under the extra confining force. Let us assume the first option as an example. In this case,[15]

$$\Lambda'^4 \sim (m_a^2 f_a^2 - m_\pi^2 f_\pi^2)\,. \tag{7.3.12}$$

Assume that an experiment detects an axion-photon signal and a certain value for the axion mass which correspond to a point in the white region of Fig. 4a and located to the right of the QCD band. For instance, let us consider a point located on one of the flat sections of the blue lines depicted. The interpretation in terms of a heavy axion depends on whether the axion is heavier or lighter than the pion and η', respectively:

- $m_a \gg m'_\eta$. The model-independent effects due to the mixings with SM pseudoscalars have become negligible, and $g_{a\gamma\gamma}$ is a direct measure of the product $(1/f_a)E/N$.
- $m_a \ll m_\pi$. In this case the measured $g_{a\gamma\gamma}$ value is undistinguishable from that for the QCD axion, with the E/N and f_a dependence given by Eq. (7.1.54). In other words, it would indicate either a heavy axion or a QCD axion with some degree of photophobia, as in that region they become undistinguishable. This is so at least for the lowest axion masses and/or without the help of other measurements involving heavy EW gauge bosons.

[15] The $m_u m_d/(m_u + m_d)^2$ factor in the QCD contribution is not shown for simplicity.

In both cases, in the framework of a KSVZ model, an additional measurement of the axion coupling to heavy gauge bosons would be enough to disentangle the values of f_a and M, that is, to determine the high scale Λ'. The model-independent corrections determined in Eqs. (7.2.5)-(7.2.8) can be essential when exploiting low-energy processes (e.g. rare decays), specially when they lead to the cancellation of a given coupling. Such cancellation in a channel in general will not apply to the couplings of the axion to other gauge bosons. Overall, the fact that only two or three axion-EW couplings are independent, while four channels can be explored, will allow to overconstrain the system.

7.4 Conclusions

Among the novel results of this work, we have first determined at leading order in the chiral expansion the model-independent components of the coupling of the QCD axion to heavy EW gauge bosons: $g_{a\gamma Z}$, g_{aZZ} and g_{aWW}. They stem from the axion-η'-pion mixing induced by the anomalous QCD couplings of the axion and η'. Our results extend to heavy EW gauge bosons the well known result for the photonic coupling of the axion $g_{a\gamma\gamma}$. They must be taken into account whenever an axion lighter than Λ_{QCD} is on-shell and/or the energy and momenta involved in a physical process are of the order of the QCD confining scale or lower. As a previous step, we re-derived pedagogically the leading contributions to $g_{a\gamma\gamma}$ for the case of the most general axion couplings (App. 7.B), and then proceeded to the determination of the couplings to the SM heavy gauge bosons.

This analysis of the EW couplings of the QCD axion may have rich consequences when comparing the presence/absence of signals at two different energy regimes. For instance, the axion could be photophobic at low energies [166] or even EW-phobic (e.g. in rare meson decays) because of cancellations between the model-independent and model-dependent components, while an axion signal may appear at accelerators or other experiments at higher energies at which the model-independent component disappears.

We have next extended those results to the case of heavy axions which solve the strong CP problem. This has allowed to explore how the mixing of the axion with the pion and η' evolves with rising axion mass, and in consequence how the model-independent contributions to all four EW axion couplings vanish as the axion mass increases above the QCD confinement scale. We have determined the modified expression for $g_{a\gamma\gamma}$ relevant for heavy axions, which may have rich consequences: an hypothetical measurement of that coupling outside the QCD axion band could point to either a heavy axion or a photophobic QCD axion. The analogous expressions for $g_{a\gamma Z}$, g_{aZZ} and g_{aWW} have been also worked out.

On the purely phenomenological analysis, we developed a "two simultaneous coupling" approach in order to determine the regions experimentally excluded by present data for $g_{a\gamma\gamma}$, $g_{a\gamma Z}$, g_{aZZ} and g_{aWW} versus the axion mass. Each EW coupling has been considered simultaneously with the anomalous gluonic coupling essential to solve the strong CP problem. The allowed/excluded experimental areas have been depicted for each of those couplings as a

function of the axion mass. This is the first such reinterpretation for $g_{a\gamma Z}$, g_{aZZ} and g_{aWW}. Even for $g_{a\gamma\gamma}$, the results of previous studies often did not apply and must be reanalysed: for instance the present bounds extracted from LEP and LHC data tend to focus on ALPs which would not have gluonic couplings, with very few exceptions [288,395,411,412]. Furthermore, we have included an estimation of the one-loop induced bounds for each EW axion coupling, which leads to supplementary constraints.

The expectations from KSVZ-type of theories have been then projected and illustrated over the obtained experimental regions, both for the QCD axion and for heavy axions. The compatibility of hypothetical *a priori* contradictory signals in high and low energy experiments in terms of a given axion has been pointed out. Furthermore, we discussed how to interpret an eventual signal (or null result) outside the QCD axion band in terms of the value of the new high confining scale generically present in heavy axion theories.

A simple point with far reaching consequences results from EW gauge invariance. In all generality, not all couplings of axions to EW gauge bosons are independent among the four physical ones in the set $\{g_{a\gamma\gamma}\ g_{a\gamma Z}$, g_{aZZ} and $g_{aWW}\}$. In particular, the relations obtained imply that at least two EW gauge couplings –if any– must be non-vanishing for any axion or ALP. These facts have been used to project the exclusion limits for the presently best constrained couplings onto the parameter space for the less constrained ones. In particular, for axions/ALPs much heavier than Λ_{QCD}, those relations have been projected on the parameter space for g_{aWW}, g_{aZZ} and $g_{a\gamma Z}$, reinforcing their constraints. A future multiparameter analysis may correct them via loop corrections. Nevertheless, the results obtained here clear up the uncharted experimental regions and may be of use in setting a search strategy. More in general, the existence of four physical axion couplings to EW bosons at experimental reach constitutes a phenomenal tool to over-constrain the axion parameter space and to check the origin of an eventual axion signal.

Finally, all results obtained for heavy axions apply as well to ALPs which have both EW and gluonic anomalous couplings. The constraints stemming from EW gauge invariance extend even to generic ALPs which do not couple to gluons. In consequence, this work also extends automatically the usual parameter space for ALPs that do not intend to solve the strong CP problem, adding to the incipient efforts to go towards a multi-parameter strategy.

Appendices

Appendix 7.A Anomalous couplings of the pseudoscalar mesons to the EW gauge bosons

In addition to the axion couplings in Eqs. (7.1.3)-(7.1.5), new couplings involving gauge bosons are expected as soon as the extra pseudoscalar mesons appear in the spectrum below the confinement scale. In particular, for the η_0 and the pions, the following interactions with EW gauge bosons (considered as external currents) are possible below the QCD confinement scale:

$$W^a_{\mu\nu}\tilde{W}^{a\mu\nu}\frac{\eta_0}{f_\pi}\,, \qquad B_{\mu\nu}\tilde{B}^{\mu\nu}\frac{\eta_0}{f_\pi}\,, \qquad B_{\mu\nu}\tilde{B}^{\mu\nu}\frac{\pi_3}{f_\pi}\,, \qquad W^a_{\mu\nu}\tilde{B}^{\mu\nu}\frac{\pi_a}{f_\pi}\,. \tag{7.A.1}$$

The lightness of pseudoscalar mesons in QCD appears as a natural consequence of the spontaneous breaking of the chiral symmetry $U(2)_L \times U(2)_R \longrightarrow U(2)_V$. The pions and eta mesons can be identified as the pseudo Nambu-Goldstone bosons of the broken symmetry. However, the chiral symmetry is only approximate. It is explicitly broken not only by the quark masses, but also by the electroweak gauge interactions. This fact famously explains the difference between charged and neutral pion masses but also allows the computation of the coupling of pseudoscalar mesons to the EW bosons through the anomaly,

$$\partial^\mu j^a_\mu = \frac{\alpha_i}{8\pi} C^{abc}_{group} F_{b\,\mu\nu}\tilde{F}^{\mu\nu}_c\,, \tag{7.A.2}$$

where $\tilde{F}^{\mu\nu} = \frac{1}{2}\epsilon^{\mu\nu\sigma\rho}F_{\sigma\rho}$, the fine structure constant of the corresponding gauge interaction is denoted by $\alpha_i = \frac{g_i^2}{4\pi}$ and the group theoretical factor C_{group} is given by

$$C^{abc}_{group} = \sum_{LH-RH} Tr\left[T^a\{t^b, t^c\}\right]. \tag{7.A.3}$$

Here, T^a is the generator associated to the conserved current (i.e. to the global symmetry) and t^a are the generators of the representation of the gauge group under which each fermion transforms.

Applying these formulas, the anomalous couplings of the neutral pseudoscalar mesons π^3 and η' to the EW gauge bosons can be computed. For the pion,

$$\mathcal{L} \supset \frac{1}{4}g_{\pi BB}\,\pi_3 B\tilde{B} + \frac{1}{4}g_{\pi BW}\,\pi_3 B\tilde{W^3} \longrightarrow \frac{1}{4}g_{\pi ZZ}\,\pi_3 Z\tilde{Z} + \frac{1}{4}g_{\pi\gamma\gamma}\,\pi_3 F\tilde{F} + \frac{1}{4}g_{\pi\gamma Z}\,\pi_3 F\tilde{Z}, \tag{7.A.4}$$

with

$$g_{\pi BB} \equiv -\frac{\alpha}{2\pi\, f_\pi}\left(\frac{1}{c_w^2}\right), \qquad g_{\pi ZZ} \equiv -\frac{\alpha}{2\pi\, f_\pi}\left(\frac{s_w^2}{c_w^2} - 1\right),$$
$$g_{\pi BW} \equiv -\frac{\alpha}{2\pi\, f_\pi}\left(\frac{1}{c_w\, s_w}\right), \qquad g_{\pi\gamma\gamma} \equiv -\frac{\alpha}{\pi}\frac{1}{f_\pi},$$

$$g_{\pi\gamma Z} \equiv -\frac{\alpha}{2\pi\, f_\pi}\left(\frac{c_w^2 - 3s_w^2}{c_w\, s_w}\right).$$

Equivalently for the η meson,

$$\mathcal{L} \supset \frac{1}{4} g_{\eta' WW}\, \eta_0\, W\tilde{W} + \frac{1}{4} g_{\eta' BB}\, \eta_0\, B\tilde{B} \longrightarrow \frac{1}{4} g_{\eta' ZZ}\, \eta_0\, Z\tilde{Z} + \frac{1}{4} g_{\eta'\gamma\gamma}\, \eta_0\, F\tilde{F} + \frac{1}{4} g_{\eta'\gamma Z}\, \eta_0\, F\tilde{Z}, \tag{7.A.5}$$

with

$$\begin{aligned} g_{\eta' WW} &\equiv -\frac{\alpha}{2\pi\, f_\pi}\left(\frac{3}{2}\frac{1}{s_w^2}\right), & g_{\eta' WW} &\equiv -\frac{\alpha}{2\pi\, f_\pi}\left(\frac{3}{2}\frac{1}{s_w^2}\right), \\ g_{\eta' BB} &\equiv -\frac{\alpha}{2\pi\, f_\pi}\left(\frac{11}{6}\frac{1}{c_w^2}\right), & g_{\eta' ZZ} &\equiv -\frac{\alpha}{2\pi\, f_\pi}\left(\frac{11\, s_w^4 + 9\, c_w^4}{6\, s_w^2 c_w^2}\right), \\ & & g_{\eta'\gamma\gamma} &\equiv -\frac{\alpha}{2\pi\, f_\pi}\left(\frac{10}{3}\right), \\ & & g_{\eta'\gamma Z} &\equiv -\frac{\alpha}{2\pi\, f_\pi}\left(\frac{9\, c_w^4 - 11\, s_w^4}{3\, s_w^2 c_w^2}\right). \end{aligned} \tag{7.A.6}$$

The mixing of the axion with the η' and the neutral pion will result in additional contributions to the coefficients of the interactions in Eqs. (7.1.4) and (7.1.5), via the first three operators in Eq. 7.A.1. The fourth one results in a neutral pion-W^3B coupling, which in turn induces a $SU(2)_L$-breaking coupling of the physical axion to W^3B . In other words, below $\Lambda_{\rm QCD}$ the operator space of axion electroweak couplings spans three degrees of freedom, instead of the two above the QCD confinement scale, with

$$\delta\mathcal{L}_a^{gauge} = \frac{\alpha_s}{8\pi}\frac{a}{f_a} G\tilde{G} + \frac{1}{4} g_{aWW}\, a\, W\tilde{W} + \frac{1}{4} g_{aBB}\, a\, B\tilde{B} + \frac{1}{4} g_{aBW}\, a\, B\tilde{W}\,, \tag{7.A.7}$$

where

$$\begin{aligned} g_{aWW} &= -\frac{1}{2\pi f_a}\frac{\alpha_{\rm em}}{s_w^2}\left(\frac{L}{N} - \frac{3}{4}\right), \\ g_{aBB} &= -\frac{1}{2\pi f_a}\frac{\alpha_{\rm em}}{c_w^2}\left(\frac{P}{N} - \frac{5m_u + 17m_d}{12(m_u + m_d)}\right), \\ g_{aBW} &= \frac{1}{2\pi f_a}\frac{\alpha_{\rm em}}{s_w c_w}\left(\frac{1}{2}\frac{m_d - m_u}{m_u + m_d}\right) \end{aligned} \tag{7.A.8}$$

are obtained using the result for the mass mixing of the axion with the pseudoscalar mesons given in Eq. (7.1.32).

Similarly for the heavy axion case,

$$
\begin{aligned}
g_{aWW} &= -\frac{1}{2\pi f_a}\frac{\alpha_{\rm em}}{s_w^2}\left(\frac{L}{N}-\frac{3}{4}\frac{1}{1-\left(\frac{M}{m_{\eta'}}\right)^2}\right),\\
g_{aBB} &= -\frac{1}{2\pi f_a}\frac{\alpha_{\rm em}}{c_w^2}\left[\frac{P}{N}-\frac{1}{1-\left(\frac{M}{m_{\eta'}}\right)^2}\left(\frac{11}{6}+\frac{1}{2}\frac{m_d-m_u}{m_u+m_d}\frac{1}{1-\left(\frac{M}{m_\pi}\right)^2}\right)\right], \qquad (7.A.9)\\
g_{aBW} &= \frac{1}{2\pi f_a}\frac{\alpha_{\rm em}}{s_w c_w}\left(\frac{1}{2}\frac{m_d-m_u}{m_u+m_d}\frac{1}{1-\left(\frac{M}{m_\pi}\right)^2}\frac{1}{1-\left(\frac{M}{m_{\eta'}}\right)^2}\right).
\end{aligned}
$$

Appendix 7.B How general is the mass matrix in Eq. (7.1.28)?

Let us start with the most general Lagrangian above the QCD confinement scale that is relevant for the mass and mixings of the axion:

$$\begin{aligned}\delta\mathcal{L}_a =& \frac{1}{2}\,\partial^\mu\hat{a}\,\partial_\mu\hat{a} \;+\; c_1^u\,\frac{\partial_\mu\hat{a}}{f_{\rm PQ}}\left(\bar{u}\,\gamma_\mu\,\gamma_5\,u\right) \;+\; c_1^d\,\frac{\partial_\mu\hat{a}}{f_{\rm PQ}}\left(\bar{d}\,\gamma_\mu\,\gamma_5\,d\right)\\ &-\bar{u}_L\,m_u\,u_R\,e^{i\,c_2^u\,\hat{a}/f_{\rm PQ}} \;-\; \bar{d}_L\,m_d\,d_R\,e^{i\,c_2^d\,\hat{a}/f_{\rm PQ}} \;+\; \text{h.c.}\\ &+c_3\,\frac{\alpha_s}{8\pi}\,\frac{\hat{a}}{f_{\rm PQ}}G\tilde{G}+\frac{1}{4}g^0_{a\gamma\gamma}\,\hat{a}\,F\tilde{F}\,.\end{aligned} \tag{7.B.1}$$

For simplicity, here we focus on the coupling to photons but the discussion is of course applicable to the other EW gauge bosons. The relation of the $c_1^{u,d}$ couplings with the corresponding ones c_1^Q, c_1^U and c_1^D in the $SU(2)\times U(1)$ gauge invariant formulation in Eq. (7.1.11) are given by Eq. (7.3.4), while $c_3 = N_0$ in that equation. Without loss of generality, PQ invariance can be imposed on all operators in the Lagrangian but the anomalous couplings. As a consequence, the couplings $c_2^{u,\,d}$ are related to the PQ charges of the up and down quarks in in Eq. (7.1.11) in the following way, $\mathcal{X}_{u,d} = c_2^{u,\,d}\,\mathcal{X}_a$ (where the charge of the axion can be set to $\mathcal{X}_a = 1$).

This Lagrangian has a reparametrization invariance [398],[16] that corresponds to making the usual axion dependent quark field rotations,

$$\begin{aligned} c_1^{u,d} &\to c_1^{u,d} + \alpha_{u,d}\,,\\ c_2^{u,d} &\to c_2^{u,d} - 2\,\alpha_{u,d}\,,\\ c_3 &\to c_3 + 2\,\alpha_u + 2\,\alpha_d\,,\\ g_{a\gamma\gamma} &\to g_{a\gamma\gamma} - \frac{\alpha}{2\pi f_{\rm PQ}}\left(12\alpha_u\,q_u^2 + 12\alpha_d\,q_d^2\right)\,. \end{aligned} \tag{7.B.2}$$

In the body of the Chapter we are considering $c_1^{u,d} = 0$, when computing the axion mass and mixings. This is general due to the reparametrization invariance.

When QCD confines and the chiral symmetry is broken by the quark condensate, the couplings in Eq. (7.B.1) translate into effective operators involving mesons. Defining the π and η_0-fields in terms of the currents:

$$\begin{aligned} j_3^\mu &= \frac{1}{2}\,\left(\bar{u}\,\gamma_\mu\,\gamma_5\,u \;-\; \bar{d}\,\gamma_\mu\,\gamma_5\,d\right) \equiv f_\pi D_\mu\pi_3\,,\\ j_0^\mu &= \frac{1}{2}\,\left(\bar{u}\,\gamma_\mu\,\gamma_5\,u \;+\; \bar{d}\,\gamma_\mu\,\gamma_5\,d\right) \equiv f_\pi D_\mu\eta_0\,. \end{aligned} \tag{7.B.3}$$

The low energy chiral Lagrangian can be decomposed in three terms:

$$\delta\mathcal{L}_a = \delta\mathcal{L}_{a,\,\rm kin} + \delta\mathcal{L}_{a,\,\rm mass} + \delta\mathcal{L}_{a,\,\rm anom}\,. \tag{7.B.4}$$

[16] Note that this reparametrization invariance differs from that in Ref. [398].

- The derivative couplings $c_1^{u,d}$ generate kinetic mixing between the axion and the mesons,

$$\delta\mathcal{L}_{a,\,\mathrm{kin}} = \frac{1}{2}\,D_\mu\hat{a}\,D^\mu\hat{a} + \frac{1}{2}\,D_\mu\pi_3\,D^\mu\pi_3 + \frac{1}{2}\,D_\mu\eta_0\,D^\mu\eta_0 + \left(c_1^u - c_1^d\right)\frac{f_\pi}{f_{\mathrm{PQ}}}\,D_\mu\hat{a}\,D^\mu\pi_3 + \left(c_1^u + c_1^d\right)\frac{f_\pi}{f_{\mathrm{PQ}}}\,D_\mu\hat{a}\,D^\mu\eta_0\,. \quad (7.\mathrm{B}.5)$$

- The Yukawa couplings $c_2^{u,d}$ produce mass mixing. In the chiral formulation the effects of these operators can be encoded in an axion-dependent mass matrix,

$$M_a = \begin{pmatrix} m_u & 0 \\ 0 & m_d \end{pmatrix}\begin{pmatrix} e^{i\,c_2^u\,\hat{a}/f_{\mathrm{PQ}}} & 0 \\ 0 & e^{i\,c_2^d\,\hat{a}/f_{\mathrm{PQ}}} \end{pmatrix}. \quad (7.\mathrm{B}.6)$$

  So that the chiral Lagrangian induced at low energies contains the term

$$\begin{aligned}\delta\mathcal{L}_{a,\,\mathrm{mass}} &= B_0\frac{f_\pi^2}{2}\,\mathrm{Tr}\left(\Sigma\mathrm{M}_{\mathrm{a}}^\dagger + \mathrm{M}_{\mathrm{a}}\Sigma^\dagger\right)\\ &= B_0 f_\pi^2\left[m_u\cos\left(\frac{\pi_3}{f_\pi} + \frac{\eta_0}{f_\pi} - c_2^u\,\frac{\hat{a}}{f_{\mathrm{PQ}}}\right) + m_d\cos\left(\frac{\pi_3}{f_\pi} - \frac{\eta_0}{f_\pi} - c_2^d\,\frac{\hat{a}}{f_{\mathrm{PQ}}}\right)\right].\end{aligned} \quad (7.\mathrm{B}.7)$$

- The coupling to gluons generates an effective potential that is responsible for the bulk of the mass of the η' and can be parametrized at low energies as,

$$\delta\mathcal{L}_{a,\,\mathrm{anom}} = -\frac{\alpha_s}{8\,\pi}\left(2\frac{\eta_0}{f_\pi} + c_3\,\frac{\hat{a}}{f_a}\right)G\tilde{G} \longrightarrow -\frac{1}{2}\,K\,\left(2\frac{\eta_0}{f_\pi} + c_3\,\frac{\hat{a}}{f_a}\right)^2. \quad (7.\mathrm{B}.8)$$

Altogether, the relevant chiral Lagrangian reads,

$$\begin{aligned}\delta\mathcal{L}_a &= \frac{1}{2}\,D_\mu\hat{a}\,D^\mu\hat{a} + \frac{1}{2}\,D_\mu\pi_3\,D^\mu\pi_3 + \frac{1}{2}\,D_\mu\eta_0\,D^\mu\eta_0 + \alpha_\pi\,D_\mu\hat{a}\,D^\mu\pi_3 + \alpha_\eta\,D_\mu\hat{a}\,D^\mu\eta_0\\ &+ B_0 f_\pi^2\left[m_u\cos\left(\frac{\pi_3}{f_\pi} + \frac{\eta_0}{f_\pi} - c_2^u\,\frac{\hat{a}}{f_{\mathrm{PQ}}}\right) + m_d\cos\left(\frac{\pi_3}{f_\pi} - \frac{\eta_0}{f_\pi} - c_2^d\,\frac{\hat{a}}{f_{\mathrm{PQ}}}\right)\right]\\ &- \frac{1}{2}\,K\,\left(2\frac{\eta_0}{f_\pi} + c_3\,\frac{\hat{a}}{f_a}\right)^2.\end{aligned} \quad (7.\mathrm{B}.9)$$

The coefficients α_π, α_η parametrizing the kinetic mixing are

$$\alpha_\pi = \left(c_1^u - c_1^d\right)\frac{f_\pi}{f_{\mathrm{PQ}}}; \qquad \alpha_\eta = \left(c_1^u + c_1^d\right)\frac{f_\pi}{f_{\mathrm{PQ}}}. \quad (7.\mathrm{B}.10)$$

In order to obtain the mass matrix and ultimately the mass eigenvalues and mixings, the kinetic terms have to be diagonalized first. This can be done by the following transformations:

$$\hat{a} \;\to\; \frac{\hat{a}}{\sqrt{1-\alpha_\pi^2-\alpha_{\eta'}^2}} \simeq \hat{a}\,,$$

$$\pi_3 \;\to\; \pi_3 - \frac{\alpha_\pi\,\hat{a}}{\sqrt{1-\alpha_\pi^2-\alpha_{\eta'}^2}} \simeq \pi_3 - \left(c_1^u - c_1^d\right)\frac{f_\pi}{f_{\rm PQ}}\,\hat{a}\,,$$
$$\eta_0 \;\to\; \eta_0 - \frac{\alpha_\eta\,\hat{a}}{\sqrt{1-\alpha_\pi^2-\alpha_{\eta'}^2}} \simeq \eta_0 - \left(c_1^u + c_1^d\right)\frac{f_\pi}{f_{\rm PQ}}\,\hat{a}\,. \tag{7.B.11}$$

The Lagrangian Eq. (7.B.9) becomes[17] ,

$$\begin{aligned}\delta\mathcal{L}_a \;=\; &\frac{1}{2}\,D_\mu\hat{a}\,D^\mu\hat{a} \;+\; \frac{1}{2}\,D_\mu\pi_3\,D^\mu\pi_3 \;+\; \frac{1}{2}\,D_\mu\eta_0\,D^\mu\eta_0 \\ &+\; B_0 f_\pi^2\left[m_u\cos\left(\frac{\pi_3}{f_\pi}+\frac{\eta_0}{f_\pi}-\bar{c}_2^u\,\frac{\hat{a}}{f_{\rm PQ}}\right)+m_d\cos\left(\frac{\pi_3}{f_\pi}-\frac{\eta_0}{f_\pi}-\bar{c}_2^d\,\frac{\hat{a}}{f_{\rm PQ}}\right)\right] \\ &-\;\frac{1}{2}\,K\left(2\frac{\eta_0}{f_\pi}+\bar{c}_3\,\frac{\hat{a}}{f_{\rm PQ}}\right)^2\,,\end{aligned} \tag{7.B.12}$$

where $\bar{c}_2^u$, $\bar{c}_2^d$ and $\bar{c}_3$ are given by

$$\begin{aligned}\bar{c}_2^u &= 2\,c_1^u + \;c_2^u\,,\\ \bar{c}_2^d &= 2\,c_1^d + \;c_2^d\,,\\ \bar{c}_3 &= c_3 - 2\,c_1^u - \;2\,c_1^d\,.\end{aligned} \tag{7.B.13}$$

As expected, these coefficients are invariant under the reparametrization invariance in Eq.(7.B.2). Therefore, the squared mass matrix coming from Eq. (7.B.12) is completely general,

$$M^2_{\{\pi_3,\,\eta_0,a\}} = \begin{pmatrix} B_0\,(m_u+m_d) & B_0\,(m_u-m_d) & -B_0\,\frac{f_\pi}{f_{\rm PQ}}\left(m_u\,\bar{c}_2^u - m_d\,\bar{c}_2^d\right) \\ B_0\,(m_u-m_d) & \frac{4K}{f_\pi}+B_0(m_u+m_d) & \frac{2\,\bar{c}_3 K}{f_\pi f_{\rm PQ}}+B_0\,\frac{f_\pi}{f_{\rm PQ}}\left(m_u\,\bar{c}_2^u + m_d\,\bar{c}_2^d\right) \\ -B_0\,\frac{f_\pi}{f_{\rm PQ}}\left(m_u\,\bar{c}_2^u - m_d\,\bar{c}_2^d\right) & \frac{2\,\bar{c}_3 K}{f_\pi f_{\rm PQ}}+B_0\,\frac{f_\pi}{f_{\rm PQ}}\left(m_u\,\bar{c}_2^u + m_d\,\bar{c}_2^d\right) & \bar{c}_3^2\,\frac{K}{f_{\rm PQ}^2}+B_0\,\frac{f_\pi^2}{f_{\rm PQ}^2}\left(m_u\,(\bar{c}_2^u)^2 + m_d\,(\bar{c}_2^d)^2\right) \end{pmatrix}. \tag{7.B.14}$$

This matrix can be diagonalized analytically in the limit $f_{\rm PQ} \gg B_0,\, m_{u,d},\, f_\pi$. We find that the physical axion corresponds to the combination:

$$a \simeq \hat{a} + \theta_{a\pi}\,\pi_3 + \theta_{a\eta'}\,\eta_0\,, \tag{7.B.15}$$

where all mixing angles are assumed small and

$$\theta_{a\pi} \simeq -\frac{f_\pi}{2f_{\rm PQ}}\,\frac{\left(\bar{c}_3+2\bar{c}_2^d\right)m_d - \left(\bar{c}_3+2\bar{c}_2^u\right)m_u}{m_u+m_d}\,, \qquad \theta_{a\eta'} \simeq -\frac{f_\pi}{2f_{\rm PQ}}\,\bar{c}_3. \tag{7.B.16}$$

[17] The same Lagrangian can be obtained by making use of the reparametrization invariance in Eq. (7.B.2) and choosing $\alpha_u = c_1^u$ and $\alpha_d = c_1^d$.

Note that this gives the physical axion in terms of the fields whose kinetic terms are already diagonalized. In order to express it in terms of the *flavor* meson fields (as defined in Eq. (7.B.3)), the transformation in Eq. (7.B.11) needs to be taken into account. The final mixings read,

$$\theta_{a\pi} \simeq -\frac{f_\pi}{2f_{\rm PQ}}\left(c_2^d - c_2^u + \left(c_3 + c_2^u + c_2^d\right)\frac{m_d - m_u}{m_u + m_d}\right), \qquad \theta_{a\eta'} \simeq -\frac{f_\pi}{2f_{\rm PQ}}\, c_3\,, \tag{7.B.17}$$

expressed in terms of the couplings of the starting Lagrangian in Eq. (7.B.1). It is worth noting that the physical mixing parameters do not depend on the coefficient $c_1^{u,\,d}$ of the derivative operator, since it is PQ invariant and therefore it has no impact on the masses and the mixings.

Now we are ready to study the effect of these two diagonalizations in the coupling of the axion to photons,

$$g_{a\gamma\gamma} = g^0_{a\gamma\gamma} + \theta_{a\pi}\, g_{\pi\gamma\gamma} + \theta_{a\eta'}\, g_{\eta'\gamma\gamma}\,. \tag{7.B.18}$$

Taking into account that the coupling of the mesons to photons are given by

$$g_{\pi\gamma\gamma} \equiv -\frac{3\,\alpha}{\pi\, f_\pi}\left(q_u^2 - q_d^2\right), \qquad g_{\eta'\gamma\gamma} \equiv -\frac{3\,\alpha}{\pi\, f_\pi}\left(q_u^2 + q_d^2\right), \tag{7.B.19}$$

where q_u and q_d are the electromagnetic charges of the up and down quarks, we find,

$$g_{a\gamma\gamma} = g^0_{a\gamma\gamma} + \frac{\alpha}{2\pi f_{\rm PQ}}\left(-6\, c_2^u\, q_u^2 - 6\, c_2^d\, q_d^2 - 6\left(c_3 + c_2^u + c_2^d\right)\frac{q_d^2\, m_u - q_u^2\, m_d}{m_u + m_d}\right). \tag{7.B.20}$$

Recalling that the coefficients $c_2^{u,\,d}$ correspond to the PQ charges, the combinations that appear in the above equation can be identified as the electromagnetic and QCD anomaly coefficients for the up and down quarks,

$$E_{u,\,d} = \sum_{\psi = u,\,d} 2\,\mathcal{X}_\psi\, q_\psi^2 = -6\, c_2^u\, q_u^2 - 6\, c_2^d\, q_d^2\,, \qquad N = c_3 + c_2^u + c_2^d\,. \tag{7.B.21}$$

Redefining the axion decay constant as usual $f_a = f_{\rm PQ}/N$, we can express

$$g_{a\gamma\gamma} = g^0_{a\gamma\gamma} + \frac{\alpha}{2\pi f_a}\left(\frac{E_{u,\,d}}{N} - \frac{2}{3}\frac{m_u + 4\, m_d}{m_u + m_d}\right). \tag{7.B.22}$$

To sum up, from the most general mass matrix we have obtained the same result of Eq. (7.1.54) taking into account that in the E/N we have to sum over all fermions transforming under the PQ symmetry, that means including the up and down quarks $E = E_{\rm heavy} + E_{u,\,d}$,

$$g_{a\gamma\gamma} = \frac{\alpha}{2\pi f_a}\left(\frac{E_{\rm heavy}}{N} + \frac{E_{u,\,d}}{N} - \frac{2}{3}\frac{m_u + 4\, m_d}{m_u + m_d}\right). \tag{7.B.23}$$

CHAPTER 8

Flavor constraints on electroweak ALP couplings

In this Chapter, which is based on the publication in Ref. [1], we explore ALP contributions to flavor changing neutral current (FCNC) processes, formulating them in a model-independent approach via the linear realization of the ALP effective Lagrangian. The complete basis of bosonic and CP-even ALP couplings to the electroweak sector is considered. That is, the set of gauge invariant and independent leading-order couplings to the W, Z, photon and Higgs doublet is discussed. Given that these operators are flavor blind, they may impact flavor-changing data only at loop level. The couplings of ALPs to heavy SM bosons had been largely disregarded until recently, even if *a priori* they are all expected to be on equal footing with the pure photonic ones because of electroweak gauge invariance. In addition to novel collider signatures [289, 290], rare hadron decays provide a superb handle on the ALP couplings to massive vector bosons [3] for ALP masses below 5 GeV. The one-loop impact on FCNC processes of the anomalous ALP-W-W coupling was first considered in Ref. [291]: it was shown to induce flavor-changing rare meson decays via W exchange, with the ALP radiated from the W boson [291, 393, 419]. The axion can then either decay in some visible channel or escape the detector unnoticed, and novel bounds were derived in both cases. Given the level of accuracy provided by present flavor experiments, it is most pertinent to take into account the competing contribution of other electroweak ALP couplings leading to the same final states. In other words, the ensemble of the linearly independent ALP-electroweak couplings should be considered simultaneously in order to delimitate the parameter space. Putative anomalous couplings of ALPs to gluons could also contribute to flavor-blind decays into visible channels, but not to FCNC processes other than via pseudoscalar (e.g. ALP-η' and ALP-pion) mixing in SM flavor-changing decays, and they are not considered in this Chapter.

The analysis of two (or more) couplings simultaneously has the potential to change the experimental perspective on ALPs. Our theoretical analysis is confronted with the prospects for ALP detection in present and upcoming fixed-target experiments and B-physics experiments. After the theoretical analysis, the structure of this Chapter reflects successively the two alternative scenarios mentioned above, in which the ALP produced in FCNC meson decays

can then either decay into visible channels within the detector, or it can be invisible by escaping the detector (or decaying to a hidden sector). For both cases, the comparison with data considers first each coupling separately and then the ensemble in combination, and the resulting interference patterns are worked out in detail.

8.1 Bosonic ALP lagrangian

The most general effective Lagrangian describing ALP couplings contains – at leading order in the linear expansion – only three independent operators involving electroweak gauge bosons [186, 289, 396, 397],

$$\delta\mathcal{L}_{\rm eff} = \frac{1}{2}\partial_\mu a\,\partial^\mu a - \frac{1}{2}m_a^2\,a^2 + c_{a\Phi}\,\mathcal{O}_{a\Phi} + c_B\,\mathcal{O}_B + c_W\,\mathcal{O}_W\,, \tag{8.1.1}$$

with

$$\begin{aligned}
\mathcal{O}_{a\Phi} &\equiv i\frac{\partial^\mu a}{f_a}\,\Phi^\dagger \overleftrightarrow{D}_\mu \Phi\,,\\
\mathcal{O}_B &\equiv -\frac{a}{f_a}B_{\mu\nu}\widetilde{B}^{\mu\nu}\,,\\
\mathcal{O}_W &\equiv -\frac{a}{f_a}W^a_{\mu\nu}\widetilde{W}^{\mu\nu}_a\,,
\end{aligned} \tag{8.1.2}$$

where c_i are real operator coefficients and $\Phi \overleftrightarrow{D}_\mu \Phi \equiv \Phi^\dagger\big(D_\mu\Phi\big) - \big(D_\mu\Phi\big)^\dagger\Phi$. Note that the notation here for the anomalous effective operators for the axion differs to that in Chapter 7, the relation among them being $\mathbf{O}_{\tilde{X}} = \frac{\alpha_X}{8\pi}\,\mathcal{O}_X$.

Upon electroweak symmetry breaking, $\mathcal{O}_{a\Phi}$ induces a mixing between a and the would-be Goldstone boson eaten by the Z. Its physical impact is best illustrated via an ALP-dependent rotation of the Higgs field, namely $\Phi \to \Phi\, e^{ic_{a\Phi}a/f_a}$ [396], which trades $\mathcal{O}_{a\Phi}$ for the following fermionic couplings:

$$\mathcal{O}_{a\Phi} \to i\,\frac{a}{f_a}\Big[\overline{Q}\,Y_u\widetilde{\Phi}\,u_R - \overline{Q}\,Y_d\Phi\,d_R - \overline{L}\,Y_\ell\Phi\,\ell_R\Big] + \text{h.c.}\,, \tag{8.1.3}$$

where $Y_{u,d,\ell}$ denote the SM Yukawa matrices, flavor indices are omitted, and neutrino masses are disregarded. The ALP-electroweak operators in Eq. (8.1.2) are flavor blind, but $\mathcal{O}_{a\Phi}$ and $\mathcal{O}_W$ can participate in FCNC processes at one loop via $W^\pm$ gauge boson exchange. At this order, the parameter space of ALP-electroweak couplings in FCNC processes is thus reduced to two dimensions spanned by the coefficients

$$\{c_W\,, c_{a\Phi}\}\,. \tag{8.1.4}$$

They may contribute to rare decays as illustrated in the left ($c_{a\Phi}$) and right (c_W) panels of Fig. 2. While c_W has been discussed separately in Ref. [3, 291], and the effective ALP-fermionic interactions have also been considered by themselves before [290, 368, 393, 419–421], the interplay between c_W and $c_{a\Phi}$ will be shown below to lead to interesting new features.

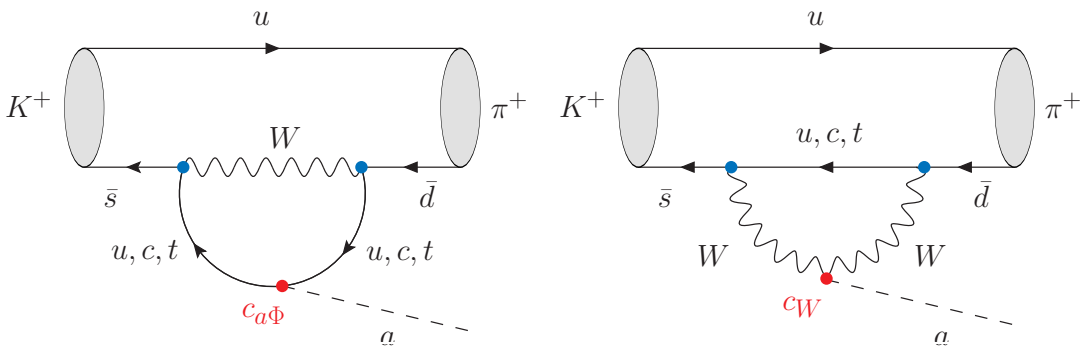

Figure 1: Illustration of diagrams giving one-loop contributions to the process $K^+ \to \pi^+ a$ via the interactions defined in Eq. (8.1.3).

8.2 FCNC ALP interactions

The effective interaction between a pGB and left-handed fermions can be expressed in all generality as

$$\mathcal{L}_{\text{eff}}^{d_i \to d_j} = -g_{ij}^a \left(\partial_\mu a\right) \bar{d}_j \gamma^\mu P_L d_i + \text{h.c.}\,, \tag{8.2.1}$$

where latin indices i, j denote flavor and g_{ij}^a is an effective coupling.

The impact of $\mathcal{O}_{a\Phi}$ and $\mathcal{O}_W$ on $d_i \to d_j a$ (with $i \neq j$) transitions via one-loop $W^\pm$ exchange induces a left-handed current of the form in Eq. (8.2.1), and thus a contribution to rare meson decays. The corresponding Feynman diagrams at the quark level are those contained in the illustration in Fig. 1, as well as the corresponding self-energy diagrams with the ALP operator inserted on the quark lines external to the W loop. At the quark level, those one-loop W exchanges result in a contribution to g_{ij}^a, for $i \neq j$, given by

$$g_{ij}^a = g^2 \sum_{q=u,c,t} \frac{V_{qi} V_{qj}^*}{16\pi^2} \left[\frac{3 c_W}{f_a} g(x_q) - \frac{c_{a\Phi}}{4 f_a} x_q \log\left(\frac{f_a^2}{m_q^2}\right) \right], \tag{8.2.2}$$

where g is the electroweak gauge coupling, and V_{qi} are the CKM matrix elements. In this equation, m_q denotes the mass of a given up-type quark q that runs in the loop, the approximation $m_{d_j}, m_{d_i} \ll m_W$ has been used, $x_q = m_q^2/m_W^2$, and the loop function is given by

$$g(x) = \frac{x\left[1 + x(\log x - 1)\right]}{(1-x)^2}\,. \tag{8.2.3}$$

It follows that the decay rate for the process $K^+ \to \pi^+ a$ can be expressed as

$$\Gamma(K^+ \to \pi^+ a) = \frac{m_K^3 |g_{sd}^a|^2}{64\pi} f_0(m_a^2)^2 \lambda_{\pi a}^{1/2} \left(1 - \frac{m_\pi^2}{m_K^2}\right)^2,$$

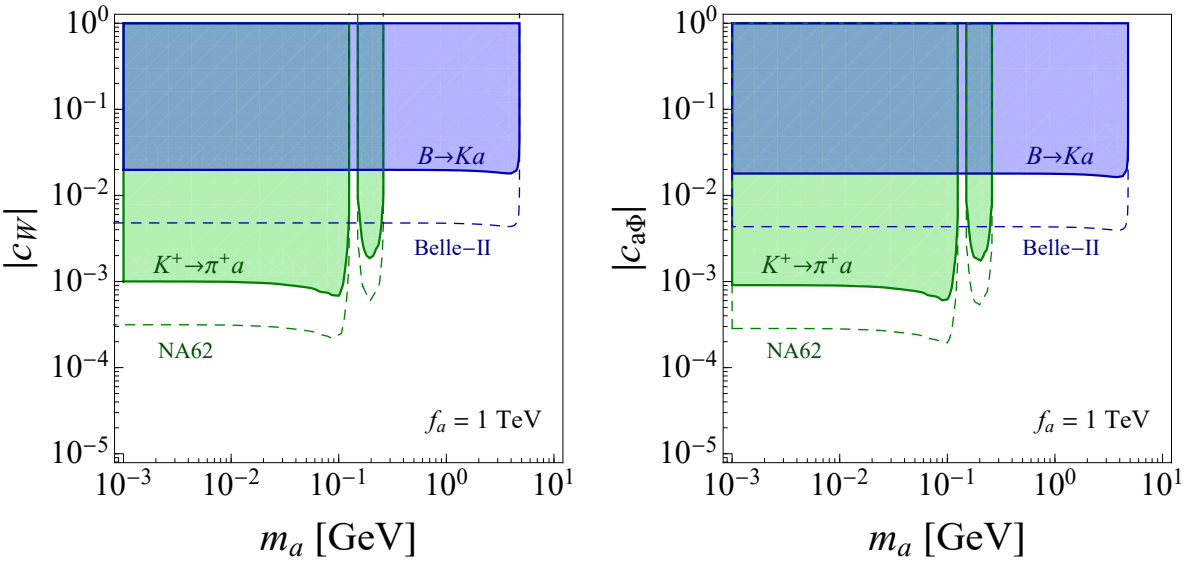

Figure 2: Invisible ALP: constraints on the absolute value of c_W (left panel) and $c_{a\Phi}$ (right panel) as a function of the ALP mass, considering each of these couplings separately. The exclusion contours have been derived from the experimental limits on $\mathcal{B}(K^+ \to \pi^+ + \text{inv})$ [422] (green) and $\mathcal{B}(B \to K + \text{inv})$ [423] (blue) by fixing $f_a = 1$ TeV and by setting the other couplings to zero. Projections for NA62 [291] and Belle-II [424] experiments are illustrated by dashed lines.

with $\lambda_{\pi a} = \left[1 - \frac{(m_a+m_\pi)^2}{m_K^2}\right]\left[1 - \frac{(m_a-m_\pi)^2}{{m_K}^2}\right]$. In this expression, f_0 denotes the $K \to \pi$ scalar form factor, which has been computed in lattice QCD in Ref. [425]. An analogous expression can be obtained *mutatis mutandis* for the decay $B \to Ka$, in which case the relevant form factors can be found in Refs. [426, 427].

In Eq. (8.2.2), the contribution proportional to c_W is finite due to the Glashow–Iliopoulos–Maiani (GIM) mechanism, in agreement with the results of Ref. [291]. The $c_{a\Phi}$ term is instead logarithmically sensitive to the ultraviolet scale of the theory f_a, and its contribution is thus approximated by the leading log model-independent component. Furthermore, because $g(x) \sim x + \mathcal{O}(x^2)$ for small x, the contributions from the up and charm quarks are sub-leading in both terms with respect to that of the top quark. Also, note that the logarithmic enhancement of the $c_{a\Phi}$ term ($\propto \log\left(f_a/m_t\right)$) should be particularly relevant for large values of f_a. This logarithmic divergence is a consequence of the operator $\mathcal{O}_{a\Phi}$ being non-renormalizable [393, 420, 421], in contrast with renormalizable scenarios such as two-Higgs doublet models [199, 393, 428, 429].

The interplay between $c_{a\Phi}$ and c_W presents interesting features which depend on their relative sign. Their contributions to ALP production in rare decays can interfere destructively if and only if $c_{a\Phi}/c_W > 0$. Such a cancellation would leave a region in parameter space which cannot be probed by relying only on FCNC decays such as $K \to \pi a$ and $B \to Ka$. An alternative to

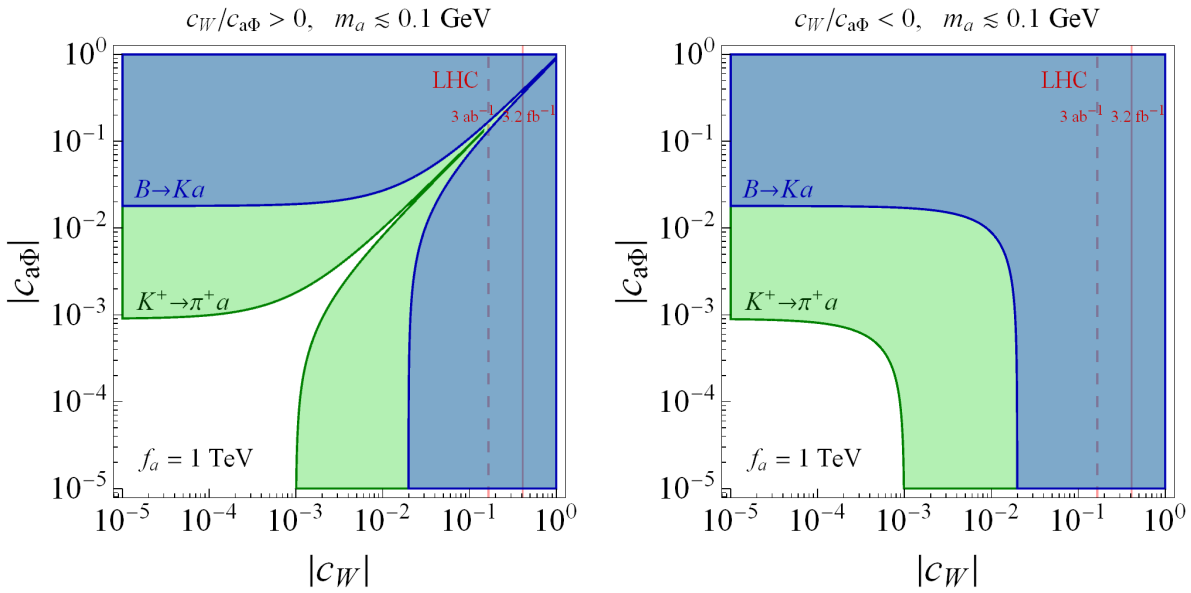

Figure 3: Allowed $\{c_W, c_{a\Phi}\}$ parameter space for the invisible ALP when those two couplings are simultaneously present. The superposition of the constraints from $K^+ \to \pi^+ + \text{inv}$ (green) and $B^+ \to K^+ + \text{inv}$ (blue) data is shown for an illustrative case with $f_a = 1$ TeV and $m_a \lesssim 100$ MeV. The left (right) panel shows the destructive (constructive) interference of the two couplings for $c_W/c_{a\Phi} > 0$ ($c_W/c_{a\Phi} < 0$). The red solid (dashed) lines correspond to the current (projected) limits from mono-W searches at the LHC with 3.2 fb^{-1} (3 ab^{-1}) of data [289].

lift this degeneracy using LHC constraints will be discussed further below, after deriving the constraints that follow from rare meson decays.

In order to determine the detection possibilities for a given final state channel, an important element is whether the ALP can decay into visible particles within the detector, or whether it escapes and contributes to an "invisible" channel. We discuss next both cases.

8.3 The invisible ALP

Let us consider first the scenario of an ALP that does not decay into visible particles in the detector, which we shall refer to as the "invisible ALP". This situation can arise if a is sufficiently light, making a long-lived, or if there are large couplings of a to a dark sector, making $\mathcal{B}(a \to \text{inv})$ sufficiently large. The analysis performed below is general and applies to both cases.

The experimental constraints relevant for different m_a ranges are listed next:

- $m_a \in (0, m_K - m_\pi)$:
  Searches for the decay $K \to \pi\nu\bar{\nu}$ have been performed at the E787 and E949 experiments. The

bounds obtained can be directly reinterpreted to limit the parameter space of new undetected particles. E787 and E949 experiments take measurements in two regions of pion momentum, namely $p_\pi \in (140, 199)$ MeV and $p_\pi \in (211, 229)$ MeV, which can be translated into the ALP mass ranges 150 MeV $\lesssim m_a \lesssim$ 260 MeV and $m_a \lesssim 115$ MeV, respectively. The limits reported in these searches are $\mathcal{B}(K^+ \to \pi^+ \nu\bar{\nu})^{\text{exp}} = \left(1.73^{+1.15}_{-1.05}\right) \times 10^{-10}$ [422] and $\mathcal{B}(K^+ \to \pi^+ \nu\bar{\nu})^{\text{exp}} < 2.2 \times 10^{-9}$ [423], which lie slightly above the SM prediction, $\mathcal{B}(K^+ \to \pi^+ \nu\bar{\nu})^{SM} = (9.11 \pm 0.72) \times 10^{-11}$ [430]. Similar searches have been performed at the NA62 experiment, which aims at attaining the SM rates in the very near future [431]. In our analysis, we consider the E787 and E949 constraints, as summarized in Ref. [422].

- $m_a \in (0, m_B - m_K)$:

  The most constraining experimental limits on $\mathcal{B}(B \to K^{(*)} + \text{inv})$ were obtained by the Belle collaboration. These are $\mathcal{B}(B \to K\nu\bar{\nu}) < 1.6 \times 10^{-5}$ and $\mathcal{B}(B \to K^*\nu\bar{\nu}) < 2.7 \times 10^{-5}$ (90% C.L.) [432], which lie respectively a factor of 3.9 and 2.7 above the SM predictions [433]. In the near future, Belle-II aims at measuring the SM value with a $\mathcal{O}(10\%)$ precision [424]. For the new physics scenario considered here, the strongest constraint arises from the $B \to K\nu\bar{\nu}$ result.

We have explicitly checked that $\Delta F = 2$ constraints on the effective couplings g^a_{ij} are less stringent than the ones presented above for most of the ALP parameter space considered here. Nevertheless, those constraints should provide the best bounds on $c_{a\Phi}$ and c_W for masses larger than ~ 5 GeV, which are out of reach of rare decays, see Fig. 2. Those observables are not included in our analysis, though, since the consistent assessment of the corresponding limits would require a complete two-loop computation, as well as the additional consideration of higher dimension ALP operators, which goes beyond the scope of this thesis.

The constraints set on ALP-electroweak coefficients by data will be analyzed in two steps: first within a *one coupling at a time* approach, where either only c_W *or* $c_{a\Phi}$ are switched on; next, the $\{c_{a\Phi}, c_W\}$ parameter space spanned by the *simultaneous presence of both couplings* will be considered.

Fig. 2 depicts the allowed values of c_W (left panel) and $c_{a\Phi}$ (right panel) as a function of the ALP mass, when only one of these two couplings is added to the SM. The constraints obtained on the $\{m_a, c_W\}$ plane (left panel) coincide with those derived in Ref. [291]. The constraints on the parameter space for $\{m_a, c_{a\Phi}\}$ (right panel) are a novel contribution of this work. The case illustrated corresponds to $f_a = 1$ TeV. The quantitative similarity of the exclusion limits on the two couplings depicted in Fig. 2 is fortuitous; it is easy to check that the constraints on $c_{a\Phi}$ become stronger than those for c_W for larger values of f_a, as expected from the logarithmic dependence of its contribution, see Eq. (8.2.2).

These plots also indicate that kaon constraints are typically one order of magnitude stronger than those derived from B-meson decays, although limited to a more restricted m_a range. Future prospects from NA62 and Belle-II are also illustrated in Fig. 2 with dashed lines.

When both $c_{a\Phi}$ and c_W are simultaneously considered, an interesting pattern of destructive interference can take place, as anticipated in Sec. 8.2. Fig. 3 depicts the result of combining the different experimental constraints for fixed values of f_a and $m_a \lesssim 0.1$ GeV. This shows indeed that when the relative sign of both couplings is positive, a blind direction in parameter space appears. This unconstrained direction is exactly aligned for kaon and B-meson decays. For this reason, additional experimental information is then needed to lift the degeneracy. One possibility is to consider the decays $D \to \pi(a \to \text{inv})$, which are sensitive to a different combination of $c_{a\Phi}$ and c_W, since the up- and down-type quark contributions to the term proportional to $c_{a\Phi}$ have opposite signs, see Eq. 8.1.3. These decays, however, suffer from a heavy GIM suppression, and no such experimental searches have been performed to our knowledge. A more promising possibility is to consider LHC constraints that are sensitive to a specific ALP coupling. For example, LHC searches for mono-W final states are only sensitive to c_W[1]. In Ref. [289] the authors derived the current (projected) bounds

$$\frac{|c_W|}{f_a} \lesssim 0.41\ (0.16)\ \text{TeV}^{-1}\,, \tag{8.3.1}$$

from 3.2 fb^{-1} (3 ab^{-1}) of LHC data: these have been superimposed in Fig. 3. Similarly, a reinterpretation of $pp \to t\bar{t} + \text{MET}$ at the LHC would constrain only $c_{a\Phi}$, but such analysis goes beyond the scope of this letter. Typically, LHC constraints are weaker than flavor bounds, except in the region of parameter space where the flavor signal is suppressed due to a cancellation between two contributions. In this case, the complementarity of low and high-energy constraints becomes an important handle on new physics.

8.4 The visible ALP

We analyze next the case of ALPs produced at loop level via rare meson decays, but decaying into visible states via the same set of bosonic interactions introduced in Eq. (8.1.2). For the m_a range considered in this work, the kinematically accessible decays are $a \to \gamma\gamma$, $a \to$ hadrons and $a \to \ell\ell$, with $\ell = e, \mu, \tau$. Both tree-level and loop-level contributions to the decays are to be taken into account. Indeed, experimental limits on ALP couplings to photons, electrons, and nucleons are so stringent that (indirect) loop-induced observables can give stronger constraints than (direct) tree-level ones [3, 290].

At tree level, c_W and $c_{a\Phi}$ contribute respectively to ALP decays into photons and into fermions. Nevertheless, the coupling c_B may also enter the game for these decays: at tree level for the photonic channel and at loop level for the fermionic channel. That is, while the parameter space for the production of an ALP via rare meson decays is still the two-dimensional one in Eq. (8.1.4), the whole set of ALP electroweak couplings $\{c_{a\Phi}, c_W, c_B\}$ is relevant for the analysis of visible decay channels. For consistency, all one-loop contributions induced by these three couplings are to be taken into account.

[1] Bounds stemming from mono-Z signals are slightly better, but this final state can also be generated by another coupling (c_B), which complicates slightly the reinterpretation in terms of c_W and $c_{a\Phi}$.

For instance, the partial width for ALP decay into leptons, including one-loop corrections, reads

$$\Gamma(a \to \ell^+\ell^-) = |c_{\ell\ell}|^2 \frac{m_a m_\ell^2}{8\pi f_a^2} \sqrt{1 - \frac{4m_\ell^2}{m_a^2}} \tag{8.4.1}$$

where $\alpha_{\rm em}$ is the fine structure constant and $c_{\ell\ell}$ is given at one-loop order by

$$\begin{aligned} c_{\ell\ell} = c_{a\Phi} &+ \frac{3\,\alpha_{\rm em}}{4\pi}\left(\frac{3\,c_W}{s_w^2} + \frac{5\,c_B}{c_w^2}\right)\log\frac{f_a}{m_W} \\ &+ \frac{6\,\alpha_{\rm em}}{\pi}\left(c_B\,c_w^2 + c_W\,s_w^2\right)\log\frac{m_W}{m_\ell}\,, \end{aligned} \tag{8.4.2}$$

where $s_w = \sin\theta_w$, $c_w = \cos\theta_w$ and θ_W denotes the weak mixing angle. For the $a \to \gamma\gamma$ decay, the partial width reads

$$\Gamma(a \to \gamma\gamma) = |c_{a\gamma\gamma}|^2 \frac{m_a^3}{4\pi f_a^2}\,, \tag{8.4.3}$$

where the $c_{a\gamma\gamma}$ coupling is defined at tree level, as

$$c_{a\gamma\gamma}\Big|_{\rm tree} \equiv c_B\,c_w^2 + c_W\,s_w^2\,. \tag{8.4.4}$$

Furthermore, bosonic loops give corrections to $c_{a\gamma\gamma}$ proportional to c_W. Fermionic loops may also induce nonzero values of $c_{a\gamma\gamma}$ at the scale $\mu = f_a$, even if the ALP has no tree-level couplings to gauge bosons, i.e. $c_W = c_B = 0$ [290]. To sum up, both c_W and $c_{a\Phi}$ induce one-loop corrections to the photonic width. Specifically, for $m_a \ll \Lambda_{\rm QCD}$,

$$\begin{aligned} c_{a\gamma\gamma}\Big|_{1-\rm loop} =& c_W\left[s_w^2 + \frac{2\,\alpha_{\rm em}}{\pi}B_2(\tau_W)\right] + c_B\,c_w^2 \\ &- c_{a\Phi}\,\frac{\alpha_{\rm em}}{4\pi}\left(B_0 + \frac{m_a^2}{m_\pi^2 - m_a^2}\right), \end{aligned} \tag{8.4.5}$$

where B_0 and $B_2(\tau_f)$ are loop functions, which are detailed in Appendix 8.A. For $m_a \gg \Lambda_{\rm QCD}$, the second term in the last line of the above equation is absent, since it stems from π-a mixing which becomes negligible in this mass range.

For hadronic decays, it is pertinent to consider two separate m_a regions: (i) between $3\,m_\pi$ and 1 GeV, and (ii) above 3 GeV. In the former region, the dominant hadronic decay is $a \to 3\pi$ which can be computed by employing chiral pertubation theory [290]. In the region above 3 GeV, the dominant decays are $a \to c\bar{c}$ and $a \to b\bar{b}$, which are well described by a perturbative expression analogous to Eq. (8.4.1) multiplied by the color factor $N_c = 3$.[2] In this work we remain agnostic about the intermediate region $m_a \in (1, 3)$ GeV, since several hadronic channels, which are particularly difficult to estimate reliably, open up for these masses.[3] In this region,

[2] Note that the decay $a \to gg$ is not induced at one-loop level in our setup, since the up- and down-type quark contributions cancel due to the different signs in Eq. (8.1.3).

[3] A first attempt to compute these rates by using a data-driven approach in this particular m_a interval has been proposed in Ref. [399] for the $G\widetilde{G}\,a$ couplings.

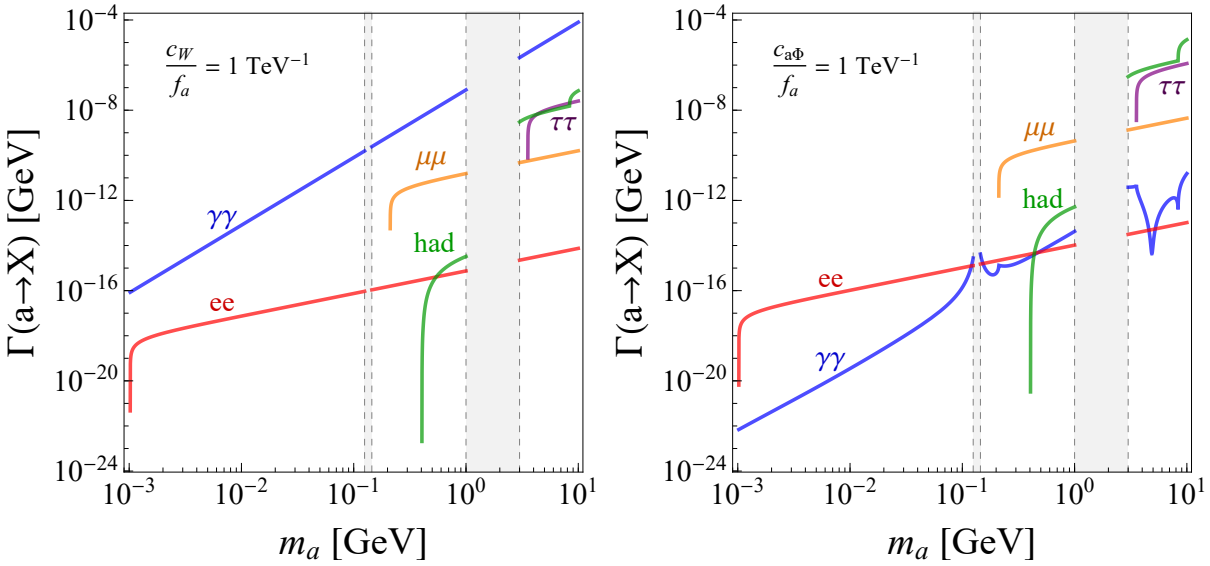

Figure 4: ALP partial decay widths to various two-particle channels as a function of m_a, in presence of either c_W (left panel) or $c_{a\Phi}$ (right panel), for $c_W/f_a = 1$ TeV^{-1} and $c_{a\Phi}/f_a = 1$ TeV^{-1}, respectively. The grey shaded areas correspond: i) to the pion mass region, which is experimentally excluded due to the large π^0-a mixing; ii) the interval $(1, 3)$ GeV, in which the hadronic width cannot be fully assessed either with chiral estimates or perturbatively.

the total hadronic width Γ_a will be replaced by its value at the range frontier at $m_a = 3$ GeV. Note that this is the most conservative choice, since the hadronic width is a continuous and strictly increasing function of m_a.

Fig. 4 illustrates the ALP partial widths as a function of m_a, when either only c_W (left panel) or $c_{a\Phi}$ (right panel) are present, for the benchmark values $c_W/f_a = 1$ TeV^{-1} and $c_{a\Phi}/f_a = 1$ TeV^{-1}. The mass thresholds for each of the fermionic channels are clearly delineated.

In order to analyze the impact of an intermediate on-shell ALP on rare meson decays to visible channels, ALP production via the couplings in Eq. (8.1.2) needs to be convoluted with ALP decay into SM particles via that same set of couplings. When $c_{a\Phi}$ and c_W are simultaneously present, a very interesting pattern of constructive/destructive interference is expected. We will assume for simplicity $c_B = c_W$ to illustrate the effect. While a positive sign for $c_W/c_{a\Phi}$ leads to destructive interference in ALP production (see Eq. (8.2.2) and Fig. 3), the opposite can occur in the subsequent ALP decay into visible channels. Indeed, the decay into leptons shows destructive interference for negative $c_{a\Phi}/c_W$, see Eq. (8.4.1). The expectation for the photonic channel is more involved and depends on the ALP mass: for $m_a < m_\pi$ the terms in the last parenthesis in Eq. (8.4.5) are both real and positive and the interference pattern is thus analogous to that for ALP production, while for larger masses it may differ. Table 1 summarizes the interference pattern expected.

$c_W/c_{a\phi}$	Production	$a \to \ell^+\ell^-$	$a \to \gamma\gamma$
> 0	Destructive	Constructive	Destructive
< 0	Constructive	Destructive	Constructive

Table 1: *ALP-mediated rare meson decays: interference pattern between $c_{a\Phi}$ and c_W in ALP production and decay as a function of $c_W/c_{a\phi}$ sign, by assuming $c_B = c_W$. The $a \to \gamma\gamma$ column assumes $m_a < m_\pi$, see text for details.*

Three sets of experimental data that will be considered in order to constrain the $\{m_a, c_{a\Phi}, c_W\}$ parameter space for a visible ALP: 1) displaced vertices; 2) semileptonic and photonic meson decays; 3) leptonic meson decays.

1. *Displaced vertices.* Of particular interest are searches for long-lived scalars, which would result in displaced vertices. Two m_a ranges are pertinent:

   (a) $m_a \in (2m_\mu, m_B - m_K)$

   The LHCb collaboration perfomed searches for long-lived (pseudo)scalar particles in the decays $B \to K^{(*)}a$, with $a \to \mu\mu$ [435, 436]. Limits on $\mathcal{B}(B \to K^{(*)}a) \cdot \mathcal{B}(a \to \mu\mu)$ which vary between 10^{-10} and 10^{-7} are reported as a function of m_a and the proper lifetime, τ_a. For $\tau_a < 1$ ps, the limit derived is independent of τ_a since the ALP would decay promptly. The best constraints are those for values of τ_a between 1 ps and 100 ps, for which the dimuon vertex would be displaced from the interaction vertex. See also Ref. [415] for a recent reinterpretation of these limits.

   (b) $m_a \in (2m_\mu, m_K - m_\pi)$

   Similar searches have also been performed by the NA48/2 Collaboration for the decay $K^+ \to \pi^+ a$, followed by $a \to \mu\mu$ [434]. The limits reported on $\mathcal{B}(K^+ \to \pi^+ a) \cdot \mathcal{B}(a \to \mu\mu)$ decrease with ALP lifetime until $\tau_a = 10$ ps, becoming constant for smaller values of τ_a. The best experimental limits are $\mathcal{O}(10^{-10})$ and obtained for $\tau_a \leq 10$ ps.

2. *Semileptonic and photonic meson decays.* Relevant constraints on ALPs can be inferred from their indirect contributions to low-energy meson decays. In particular:

   (a) *Kaon decays.* The measured kaon branching fractions $\mathcal{B}(K^+ \to \pi^+ ee)^{\text{exp}} = (3.00 \pm 0.09) \times 10^{-7}$, $\mathcal{B}(K^+ \to \pi^+ \mu\mu)^{\text{exp}} = (9.4 \pm 0.6) \times 10^{-8}$ [19], and $\mathcal{B}(K^+ \to \pi^+ \gamma\gamma)^{\text{exp}} = (1.01 \pm 0.06) \times 10^{-7}$ [439] will be taken into account. In order to avoid the uncertainty related to the unknown SM long-distance contributions, it will be required that the ALP contribution alone does not saturate the 2σ experimental bounds.

   (b) *B-meson decays.* Recently, LHCb observed several deviations from the expected values in ratios of $B \to K^{(*)}\mu\mu$ and $B \to K^{(*)}ee$ decays in different bins of dilepton squared

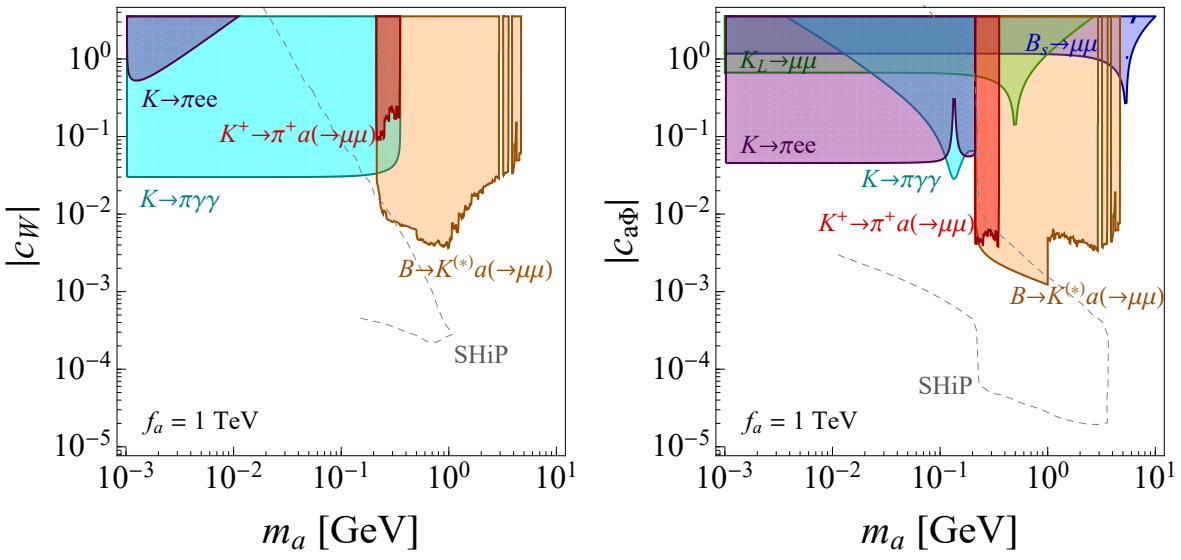

Figure 5: Visible ALP: constraints on the absolute value of c_W (left panel) and $c_{a\Phi}$ (right panel) when these couplings are considered separately, as a function of the ALP mass and for $f_a = 1$ TeV. The exclusion contours follow from the experimental limits on $K^+ \to \pi^+ a(\to \mu\mu)$ (red) [434], $B \to K^{(*)} a(\to \mu\mu)$ (orange) [435, 436], $\mathcal{B}(K_L \to \mu\mu)$ (green) [19], $\mathcal{B}(B_s \to \mu\mu)$ (blue) [437, 438], $\mathcal{B}(K \to \pi ee)$ (purple) [19] and $\mathcal{B}(K \to \pi\gamma\gamma)$ (cyan) [439]. The grey dashed lines are projections for the SHiP experiment [282]. The unconstrained regions in the range of the LHCb bounds correspond to the masses of several hadronic resonances which are vetoed in their analysis.

mass [80, 317]. If these anomalies turn out to imply new physics, ALP couplings would not explain them. More precisely, pseudoscalar effective operators induced by a heavy mediator cannot reproduce current deviations due to the constraints derived from $\mathcal{B}(B_s \to \mu^+\mu^-)^{\rm exp}$ [437]. On the other hand, a light ALP with $m_a \lesssim m_B - m_K$ would face stringent limits from LHCb searches for long-lived (pseudo)scalar particles in $B \to K^{(*)}a(\to \mu\mu)$, as mentioned above [435, 436]. For these reasons, we leave out of our analysis the constraints that would stem from the comparison of exclusive $B \to K^{(*)}\mu\mu$ measurements with the SM expectation until further clarification is provided by the B-physics experiments.

3. *Leptonic B_s and K_L decays*:

   While the constraints in 1) and 2) above correspond to on-shell ALPs, off-shell contributions are relevant in leptonic meson decays. LHCb measured $\mathcal{B}(B_s \to \mu\mu)^{\rm exp} = (3.0 \pm 0.6^{+0.3}_{-0.2}) \times 10^{-9}$ [437], which agrees with the SM prediction, $\mathcal{B}(B_s \to \mu\mu)^{\rm SM} = (3.65 \pm 0.23) \times 10^{-9}$ [438]. The ALP contribution to this observable can be computed by a straightforward modification of the expressions provided in Ref. [429]. Similarly, we consider the kaon decay $\mathcal{B}(K_L \to \mu\mu)^{\rm exp} = (6.84 \pm 0.11) \times 10^{-9}$ [19]. In the latter case, we impose once again the conservative requirement that the ALP (short-distance) contribution does not saturate the 2σ experimental values. When the complete set of electroweak couplings in Eq. (8.1.2) will be simultaneously

considered for an off-shell ALP, the interference pattern in the amplitudes can be understood analogously to the separate discussion on production and decay for on-shell ALPs.

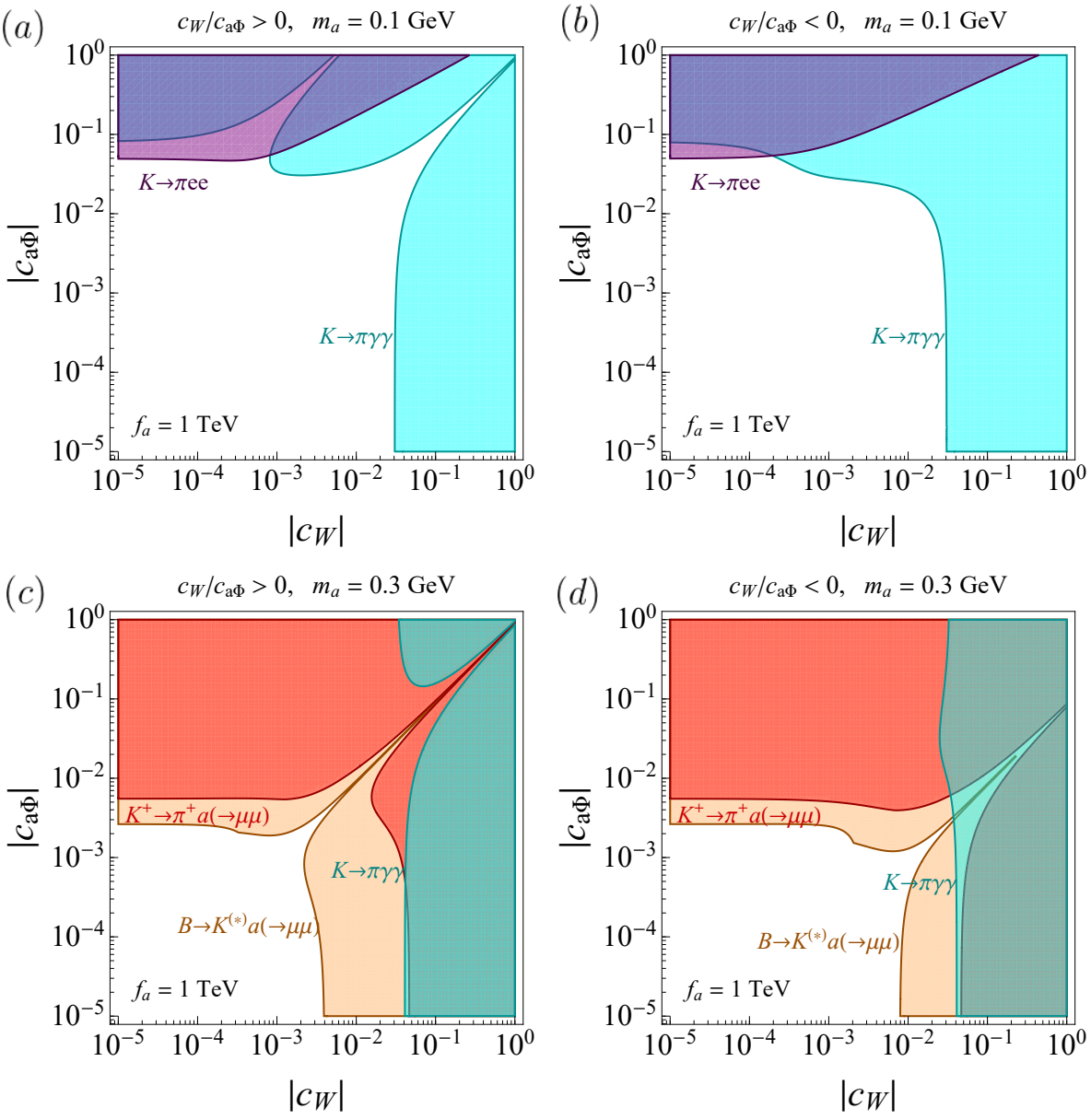

Figure 6: Visible ALP: Allowed parameter space when the couplings $\{c_{aW}, c_{a\Phi}\}$ are simultaneously present, for $f_a = 1$ TeV and $m_a = 0.1$ GeV (upper plots) or $m_a = 0.3$ GeV (lower plots). The different flat directions observed in the figures correspond to the destructive interferences of both couplings in ALP production and/or the various ALP channel decays, which depend on the sign of $c_W/c_{a\Phi}$. See text for details.

In analogy with the case of the invisible ALP in the previous section, all of these data will be analyzed first within a *one coupling at a time* approach, where either only c_W *or* $c_{a\Phi}$ are switched on (as c_B by itself cannot mediate FCNC processes). In a second step, the *simultaneous presence of* $\{c_{a\Phi}, c_W, c_B\}$ will be taken into account. We assume $c_B = c_W$ in the figures because c_B has only a modulating role, and this choice does not preclude or fine-tune any particular decay channel.

Fig. 5 illustrates the allowed values of $|c_W|$ (left panel) and $|c_{a\Phi}|$ (right panel) in the one-coupling-at-a-time analysis, as a function of the ALP mass and for $f_a = 1$ TeV. Constraints from $\mathcal{B}(K \to \pi\mu\mu)$ [19] are not displayed, since they are superseded by NA48/2 constraints on long-lived particles in $K^+ \to \pi^+ a(\to \mu\mu)$ decays. The grey dashed lines are projections for the SHiP experiment [282]. The figure reflects the stringent constraints from LHCb searches for displaced vertices in the dimuon channel [415, 435, 436] for the large mass range $m_a \in (2\mu, m_B - m_K)$, see point 1.(a) above. These limits are more constraining than the analogous searches performed in the kaon sector [434]. Remarkably, this is in contrast to the invisible scenario discussed in Sec. 8.3, for which kaon constraints are considerably stronger than those derived from B-meson decays if $K^+ \to \pi^+ a$ is kinematically allowed. These results, which take into account only one coupling at a time, could be of special interest in specific new physics scenarios. For instance, the case of a non-vanishing $c_{a\Phi}$ with c_B and c_W disregarded (right panel) is motivated by perturbative models producing $c_{a\Phi}$ at tree level but $\{c_B, c_W\}$ only at loop level (e.g. $c_B \sim c_W \simeq g^2/(16\pi^2)\, c_{a\Phi}$). Nevertheless, in all generality and for a rigorous approach, the simultaneous presence of all couplings in the electroweak bosonic basis in Eq. (8.1.2) must be considered. This may essentially modify the bounds inferred, as discussed above and illustrated next.

Fig. 6 depicts the bounds resulting when $c_{a\Phi}$, c_W and c_B are simultaneously considered. Once again, in the ALP mass region in which B-physics data on displaced vertices apply, they are seen to be more constraining than the bounds inferred from the kaon sector, see Figs. 6c and 6d. Furthermore, the four panels in the figure clearly illustrate – for two values of m_a and $c_W = c_B$ – the remarkable pattern of constructive/destructive interference expected from the analysis in Sec. 8.4 and Table 1. For instance, the two flat directions in the photonic channel in Fig. 6a result from destructive interference in both production and decay for positive $c_W/c_{a\Phi}$ and $m_a < m_\pi$. The rest of the figures can be analogously understood. Once again, the various flat directions in different channels call for complementarity with collider data and other experimental projects. In particular, the degeneracy in parameter space which induces the flat direction in Fig. 6a and Fig. 6c, common to all rare decay channels discussed in this work, could be resolved by LHC data. Some of the flat directions appearing in ALP decays (cf. e.g. Fig. 6d) could also be probed by proposed beam-dump experiments such as SHiP, since they can measure ALP decays into both photons and muons, and because $\mathcal{B}(a \to \mu\mu)$ and $\mathcal{B}(a \to \gamma\gamma)$ do not simultaneously vanish. This is also true for various LHC searches, and so both experiments could be good handles on removing flat directions, though a full analysis is beyond the scope of this work.

8.5 Conclusions

The field of axions and ALPs is blooming, with an escalation of efforts both in theory and experiment. Theoretically, the fact that no new physics has shown up yet at colliders or elsewhere positions the SM fine-tuning issues as the most pressing ones and leads to further implications for our perspective of dark matter. The silence of data is calling for a rerouting guided by fundamental issues such as the strong CP problem and an open-minded approach to hunt for the generic tell-tale of global hidden symmetries: derivative couplings as given by axions (light or heavy) and ALPs. Experimentally, the worldwide program to hunt specifically for axions and ALPs is growing fast. At the same time, other experimental programs are realizing their potential to tackle the axion and ALP parameter space, e.g. the LHC and beam dump experiments.

In the absence of data supporting any concrete model of physics beyond the SM, effective Lagrangians provide a model-independent tool based on the SM gauge symmetries. Very often the effective analyses rely on considering one effective coupling at a time, though, instead of the complete basis of independent couplings. The time is ripe for further steps in the direction of a multi-parameter analysis of the ALP effective field theory, and this is the path taken by this work.

We have considered the impact on FCNC processes of the complete basis of bosonic electroweak ALP effective operators at leading order (dimension 5), taking into account the simultaneous action of those couplings. As this basis is flavor-blind, its impact on flavor-changing transitions (e.g. $d_i \to d_j a$, with $i \neq j$) starts at loop level. Indeed, the experimental accuracy achieved on rare-decay physics, as well as on limits of ALP couplings to photons, electrons, and nucleons, is so stringent that loop-induced contributions may provide the best bounds in a large fraction of the parameter space.

We first revisited previous results in the literature, which had been derived considering just one operator at a time. We studied next the simultaneous action of the various electroweak couplings. An interesting pattern of constructive/destructive interference has been uncovered, which depends on the relative sign of the couplings and on the channel and mass range considered. In this way, the previous very stringent bounds stemming from kaon and B-decay data are alleviated. Furthermore, LHC searches for light pseudoscalar particles have been highlighted as more important in regions where deconstructive interference weakens flavor bounds. While they are generally considerably less sensitive than flavor observables, LHC searches are shown to provide complementary information to low-energy probes, exploring otherwise inaccessible directions in the ALP parameter space. We have also explicitly illustrated how they can overcome some of the blind directions on rare meson decays identified here.

We have derived the most up-to-date constraints on the effective electroweak ALP parameter space for two well-motivated scenarios: (i) an ALP decaying into channels invisible at the detector; (ii) an ALP decaying into $\gamma\gamma$, ee and/or $\mu\mu$. The conclusion is that searches for $K \to \pi\nu\bar{\nu}$ decays provide the most stringent constraints in the first case. In contrast, for the second scenario, the strongest constraints arise from searches at LHCb for long-lived (pseudo)scalars

(displaced vertices) in the decays $B \to K^{(*)}a(\to \mu\mu)$. This illustrates beautifully the potential of flavor-physics observables to constrain new physics scenarios. These searches will be improved in the years to come thanks to the experimental effort at NA62, KOTO, LHCb and Belle-II, providing tantalizing oportunites to discover new physics, complementary to the direct searches performed at the LHC.

Much remains to be done to fully encompass the ALP parameter space. For instance, the anomalous ALP gluonic coupling has not been considered in this work. Even if it cannot mediate FCNC processes, it may impact our results for the visible ALP via the quantitative modification of the branching ratios. In fact, recent ALP analyses of FCNC decays [3] take into account the simultaneous presence of the gluonic coupling and just one electroweak ALP coupling, but no work considers all ALP bosonic couplings together, let alone the complete basis of operators including the most general fermionic ones. This effort is very involved and will be the object of future work. In a different realm, note that the type of effective operators considered above assumes a linear realization of electroweak symmetry breaking; the alternative of analyzing ALP FCNC processes via the non-linear effective SM Lagrangian is pertinent and also left for future consideration.

Appendices

Appendix 8.A Loop factors

The loop contributions to the ALP decay into photons and fermions have been computed in Ref. [290]. The loop functions in Eq. (8.4.5) read

$$B_0 = \left(\sum_{f=u,c,t} N_c Q_f^2 \, B_1(\tau_f) - \sum_{f=d,c,b,\ell_\alpha^-} N_c Q_f^2 \, B_1(\tau_f) \right) \tag{8.A.1}$$

where

$$\begin{aligned} B_1(\tau) &= 1 - \tau \, f^2(\tau) \,, \\ B_2(\tau) &= 1 - (\tau - 1) \, f^2(\tau) \,, \end{aligned} \tag{8.A.2}$$

with

$$f(\tau) = \begin{cases} \arcsin \frac{1}{\sqrt{\tau}} \,; & \tau \geq 1 \,, \\ \frac{\pi}{2} + \frac{i}{2} \ln \frac{1+\sqrt{1-\tau}}{1-\sqrt{1-\tau}} \,; & \tau < 1 \,. \end{cases} \tag{8.A.3}$$

where $\tau_f \equiv 4m_f^2/m_a^2$, Q_f denotes the electric charge of the fermion f and N_c^f is the color multiplicity (3 for quarks and 1 for leptons.

Part III

Conclusions

Summary and conclusions

This thesis is devoted to explore *new dynamical solutions* to two central puzzles of the SM, the strong CP problem and the flavor puzzle, and to study the phenomenological consequences of such solutions. Complementarily, the model-independent techniques of effective field theories are applied to the physics of axions and ALPs, in order to charter new territory on their parameter space.

New dynamical theories

In the first part of the thesis, we have explored new theoretical setups which invoke additional symmetries and promote couplings to dynamical fields. In the first work, the leptonic Yukawa couplings are promoted to dynamical fields, looking for an explanation to the fermionic mass and mixing pattern. In a different realm, two composite (dynamical) axion solutions to the strong CP problem are proposed to tackle the PQ quality problem with two completely different strategies: raising the axion mass in the color unified dynamical axion model and, alternatively, making the Peccei-Quinn symmetry accidental in the automatic PQ symmetry model.

In the flavor territory, the *gauging of the leptonic flavor symmetries* has been considered here for the first time. As a remarkable consequence of gauge anomaly cancellation, a universal underlying Seesaw mechanism for both charged and neutral leptons arises. A characteristic inverse proportionality relation between each lepton mass and that of its mirror partner results, and thus the leading flavor signals tend to involve the heavier SM leptons, whose interactions are less constrained by present data. Two main cases were studied: that of the SM Lagrangian, and that of its Seesaw type I extension.

- The gauging the SM flavor symmetry $SU(3)_\ell \times SU(3)_E$ leads to the minimal type I Seesaw scenario. That is, starting from the pure SM, the anomaly cancellation suggests a Majorana character for neutrinos as the most economic option. The expected phenomenological signals are flavor-conserving, and include charged-lepton universality violation (in Z decays for instance) and non-unitarity of the PMNS matrix. The first particles accessible in the energy frontier would be a tau mirror lepton and $SU(3)_E$ gauge bosons which mediate $\mu_R - \tau_R$ transitions.

- Gauging instead the flavor symmetries of the type I Seesaw mechanism, assuming the maximal flavor symmetry for the latter in the massless limit for SM leptons, $SU(3)_\ell \times SU(3)_E \times SO(3)_N$, leads to an inverse Seesaw pattern. Besides the discussed new signals of the previous case, this scenario may also lead to charged lepton flavor non-conserving

transitions. Although the leading signal depends on the hierarchy among the scalar vevs and the lepton number violating scale, one of the leading flavor non-conserving signals is $\mu \to eee$, for almost degenerate light neutrinos.

The phenomenological consequences obtained in the gauged lepton flavor framework have been compared with those of the effective approach of lepton minimal flavor violation (MFV). We have found that, while the effective operators generated by integrating out the exotic mirror leptons resemble those of MFV, the flavor gauge bosons generate distinctive signals at low-energies, lepton flavor violating decays such as $\tau \to \mu e^+ e^+$ being particularly important to disentangle both approaches.

Promoting couplings to dynamical fields may provide not only an explanation for the origin of the flavor pattern but also an elegant solution to a very different issue, that of the strong CP problem via the axion solution. One possible UV completion of the invisible axion model is that of composite axions, an approach based on postulating the existence of QCD-colored exotic massless quarks. These massless fermions are confined into bound states due to an additional strong sector: one of such bound states is the composite or *dynamical axion*.

We have implemented here for the first time *color unification within a composite axion model*. The confining sector is embedded in a larger group which is spontaneously broken to QCD and an additional strong group. The studied breaking pattern is $SU(6) \times SU(3') \to SU(3)_c \times SU(3)_{\rm diag}$. Both unbroken groups confine at two different scales, $\Lambda_{\rm QCD}$ and $\Lambda_{\rm diag}$, respectively, with $\Lambda_{\rm diag} \sim \mathcal{O}(\text{ TeV}) \gg \Lambda_{\rm QCD}$. The existence of two independent θ-parameters (one for each high energy group) requires the presence of two anomalous symmetries to solve the strong CP problem. One of them is implemented via a massless fermion in the 20 representation of $SU(6)$. Regarding the implementation of the second anomalous symmetry, two alternative ultraviolet complete models have been explored: in Model I an extra $SU(3')$ massless fermion is added, while Model II includes instead a second scalar with the same quantum numbers as the color-unification breaking scalar. Model I features a composite axion with a PQ scale which is of order $\Lambda_{\rm diag}$ and thus low. In Model II, the PQ scale coincides instead with the much larger color-unification scale, and the associated axion is elementary. We computed the two-loop running of all gauge couplings involved, showing that the desired separation of all relevant scales is achieved naturally: a color-unification scale much larger than the two confining ones, $\Lambda_{\rm diag}$ and $\Lambda_{\rm QCD}$, and a robust separation of the last two due to the SM fields that slow the running of QCD with respect to that of the extra confining sector.

Strikingly, no standard invisible axion is left in the low-energy spectrum, since the constrained small-size instantons around the spontaneous breaking scale raise the axion mass, typically at about the TeV range. This mechanism successfully solves the strong CP problem *à la* PQ without a light axion. The novel ultraviolet complete models developed here are *proofs of concept* of the feasibility of this type of scenario. This extends the parameter space for an axion which solves the strong CP problem well beyond the traditional QCD axion band, and drastically changes the associated phenomenology. With axion scales around the TeV, observable signals at colliders are expected, in particular pair production of the lightest exotic bound states that correspond to colored pseudoscalars (QCD octets). Furthermore, massless (or almost massless) sterile fermions are a low-energy trademark remnant of the massless multiplet that solves the

SM strong CP problem. Model I may be preferred as it is exclusively based on solving the strong CP problem dynamically via massless quarks and thus no additional scalars worsen the EW hierarchy problem. Moreover, Model I is safe regarding the stability of the axion solution with respect to non-perturbative effects of quantum gravity, as its PQ scales are $\Lambda_{\rm diag} \sim$ TeV.

An alternative way to that of lowering the axion scale in order to solve the PQ quality problem is to build models in which the PQ symmetry arises accidentally, rather than being imposed in the Lagrangian. In this direction, we have proposed a novel composite axion theory where the extra confining symmetry is chiral, unlike usual composite axion models which use vectorial fermions. In consequence, the *PQ symmetry is automatic*, without any need to invoke extra symmetries. This setup has been illustrated with a minimal $SU(5)$ confining group with two massless fermions in its $\bar{\mathbf{5}}$ and $\mathbf{10}$ representations, in which the automatic PQ invariance is the analogous of the $B-L$ symmetry in $SU(5)$ Grand Unified Theory (GUT).

In order to explore whether the global chiral symmetries are spontaneously broken upon $SU(5)$ confinement, the 't Hooft anomaly conditions have been studied for this theory. We have shown that, while the non-abelian global symmetries must be spontaneously broken for the theory to be consistent, for the $U(1)_{\rm PQ}$ both alternatives lead to well-defined theories. The only phenomenologically viable option, though, is that of spontaneously broken PQ symmetry that results in a composite axion.

Within this framework, due to gauge invariance and chirality, the PQ solution is largely protected by construction from quantum gravitational corrections stemming from operators with mass dimension lower than nine. Remarkably, even assuming $\mathcal{O}(1)$ coefficient for the putative leading operator of dimension nine, there are viable values of f_a compatible with neutron EDM bounds, which allow one to explain the full dark matter content of the universe in terms of axions.

Effective field theories and phenomenology

In the second part of the thesis, the effective field theory framework is applied in order to study the phenomenological consequences of axions and ALPs. Effective field theories constitute an exceptional tool to study the low-energy effects of axions. Due to its Goldstone boson nature, there is a natural separation between the characteristic axion scale and the axion mass. A consistent description in terms of non-renormalizable effective operators can be thus performed. Furthermore, the EFT approach is model-independent: it allows one to study not only axions but more generically ALPs, which arise in a plethora of BSM theories.

In this context, we have studied the axion and ALP couplings to EW gauge bosons in the presence of gluonic couplings. We have first determined, at leading order in the chiral expansion, the model-independent components of the coupling of the QCD axion to heavy EW gauge bosons: $g_{a\gamma Z}$, g_{aZZ} and g_{aWW}. This contribution stems from the mixing of the axion with the neutral mesons, π^0, η', induced by the anomalous QCD couplings of the axion. It is relevant whenever the axion mass and/or the characteristic energy of the physical process at work is smaller than the QCD scale. We have then extended these results to the case in which there is an extra source for the axion mass, i.e. heavy axions and ALPs. In this case the axion mixing with the neutral mesons diminishes with rising axion mass, and thus the model-independent contribution to all four EW axion couplings vanishes as the axion mass increases above the QCD scale.

We have also performed a phenomenological analysis, with a *two-coupling-at-a-time* approach in order to determine the regions experimentally excluded by present data for $g_{a\gamma\gamma}$, $g_{a\gamma Z}$, g_{aZZ} and g_{aWW} versus the axion mass. Each EW coupling has been considered simultaneously with the anomalous gluonic coupling needed to solve the strong CP problem. We found that certain bounds from previous studies often do not apply in the presence of the gluonic coupling. Furthermore, we have included an estimation of the one-loop induced bounds for each EW axion coupling, which leads to supplementary constraints. Finally, it has been shown how gauge invariance relates the different elements in the set of EW gauge boson couplings to axions/ALPs. This leads to very interesting consequences in terms of over-constraining the axion parameter space.

In another work, the case of ALPs with no gluonic couplings has been considered. Following the path of going beyond the *one-coupling-at-a-time* analysis we have considered the complete basis of bosonic electroweak ALP effective operators at leading order. The phenomenological impact on flavor observables, taking into account the simultaneous action of those couplings, has been studied. Although its impact on flavor-changing transitions appears first at loop level, rare-decay experiments are achieving such precise measurements that loop-induced contributions provide the best bounds in large regions of the parameter space. An interesting pattern of constructive/destructive interference has been identified. Consequently, previous very stringent bounds stemming from kaon and B-meson decays are alleviated in some regions of parameter space. As a result, although LHC searches for light pseudoscalar particles are considerably less sensitive than flavor observables, they can give complementary information in regions where destructive interference weakens flavor bounds.

We have then derived the most up-to-date constraints on the effective electroweak ALP parameter space for two well-motivated scenarios: (i) a long-lived ALP or an ALP decaying into invisible channels; (ii) an ALP decaying into $\gamma\gamma$, ee and/or $\mu\mu$. Searches for $K \to \pi +$ inv decays provide the most stringent constraints in the first case; whereas, for the second scenario, the strongest constraints arise from searches at LHCb for long-lived pseudoscalars that generate displaced vertices in the decays $B \to K^{(*)}a(\to \mu\mu)$. These searches are expected to be improved by the upcoming experimental results by NA62, KOTO, LHCb and Belle-II, providing tantalizing opportunities to discover new physics, complementary to the direct searches performed at the LHC.

The fact that no new physics has shown up yet at colliders or elsewhere positions the SM fine-tuning issues as the most pressing. The situation calls for an open-minded approach to alternative solutions to them. Within this thesis we have proposed some dynamical scenarios addressing the flavor and the strong CP puzzles. Theoretical developments, though, need to come along with phenomenological studies and, in the absence of BSM signals, the EFT provides an exceptional tool to explore a more complete theory of nature. Indeed, much remains to be done to fully encompass the axion and ALP parameter space. A multiparameter analysis taking into account simultaneously the effects of the operators in the full basis is pertinent. This must include one-loop effects, since they have been shown to have a strong impact on the constraints. The quest to identify a dynamical origin to the flavor and strong CP puzzles remains open. This is a fundamental and fascinating endeavor plausibly awaiting major discoveries.

Resumen y conclusiones

Esta tesis está dedicada a explorar *nuevas soluciones dinámicas* a dos enigmas centrales del Modelo Estándar (ME): el problema CP fuerte y el puzzle del sabor, así como a estudiar las consecuencias fenomenológicas de tales soluciones. Complementariamente, se han aplicado las técnicas de teorías efectivas de campos (TEC), que no dependen del modelo concreto, a la física de axiones y de partículas de tipo axión (PPTA), con el fin de explorar nuevos territorios en su espacio de parámetros.

Nuevas teorías dinámicas

En la primera parte de la tesis, hemos explorado nuevas propuestas teóricas que hacen uso de simetrías adicionales y en las que ciertos acoplos son considerados como campos dinámicos. En el primer trabajo, los acoplos de Yukawa leptónicos son ascendidos a campos dinámicos, buscando una explicación a la estructura de masas y de parámetros de mezcla de los fermiones. En un ámbito diferente, se han propuesto dos soluciones de axión compuesto (dinámico) al problema CP fuerte que abordan el problema de la calidad de la simetría Peccei-Quinn (PQ) con dos estrategias completamente diferentes: elevando la masa del axión en el modelo de axión dinámico con unificación del color y, alternativamente, obteniendo la simetría de PQ de forma accidental en el modelo de simetría de PQ automática.

En el territorio del sabor, se ha considerado por primera vez que las simetrías de sabor leptónicas sean simetrías *gauge*. Como consecuencia de la cancelación de las anomalías *gauge*, surge un mecanismo de *seesaw* universal para los todos los leptones, tanto cargados como neutros. Como parte de este mecanismo surge de forma característica una relación de proporcionalidad inversa entre la masa de cada leptón y la de su pareja y, por lo tanto, las principales señales de sabor tienden a involucrar a los leptones ME más pesados, cuyas interacciones están menos restringidas por los datos actuales. Se han estudiado dos casos principales: el del Lagrangiano del ME y el de su extensión con el *seesaw* de tipo I.

– Convertir la simetría de sabor ME, $SU(3)_\ell \times SU(3)_E$, en una simetría *gauge* conduce al escenario mínimo de *seesaw* tipo I. Es decir, partiendo del ME puro, la cancelación de las anomalías sugiere un carácter Majorana para los neutrinos como opción más económica. Las señales fenomenológicas esperadas conservan el sabor e incluyen violación de la universalidad de los leptones cargados (en desintegraciones del bosón Z , por ejemplo) y la no unitariedad de la matriz PMNS. Las primeras partículas accesibles serían la pareja del leptón tau y bosones *gauge* del grupo $SU(3)_E$, que median transiciones $\mu_R - \tau_R$.

– En cambio, convertir las simetrías de sabor del escenario *seesaw* tipo I en simetrías *gauge* conduce a un modelo *seesaw* inverso, asumiendo la máxima simetría de sabor en el límite en el que los leptones del ME no tienen masa, es decir, $SU(3)_\ell \times SU(3)_E \times SO(3)_N$. Además de las nuevas señales discutidas en el caso anterior, este escenario también puede conducir a transiciones que no conservan el sabor en leptones cargados. Aunque la señal dominante de este escenario depende de la jerarquía entre los valores esperados en el vacío de los escalares y la escala de violación del número leptónico, una de las señales características que violan el sabor en este modelo es $\mu \to eee$, para neutrinos ligeros casi degenerados.

Las consecuencias fenomenológicas obtenidas para las teorías en las que las simetrías leptónicas de sabor son de tipo *gauge* se han comparado con las del enfoque efectivo de violación mínima del sabor (VMS). Hemos descubierto que, si bien los operadores efectivos generados al desacoplar los leptones exóticos coinciden con los de VMS, los bosones *gauge* de sabor generan señales distintivas a bajas energías, siendo particularmente relevantes a la hora de distinguir ambos enfoques las desintegraciones leptónicas que violan el sabor, como $\tau \to \mu e^+ e^+$.

La promoción de los acoplos a campos dinámicos puede proporcionar no sólo una explicación al origen de sabor, sino también una solución elegante a un problema muy diferente, el problema CP fuerte, gracias a la solución de tipo axion. Un posible modelo que completa en el ultravioleta el modelo de axión invisible es el axión compuesto, un enfoque basado en postular la existencia de quarks exóticos sin masa con carga de color bajo QCD. Estos fermiones sin masa están confinados en estados ligados debido a un sector fuerte adicional: uno de estos estados ligados es el *axión dinámico* o *compuesto*.

Hemos implementado por primera vez la *unificación del color en un modelo de axión compuesto*. El sector confinante está incluido dentro de un grupo más grande que se rompe espontáneamente en QCD y un grupo fuerte adicional. El patrón de ruptura considerado es $SU(6) \times SU(3') \to SU(3)_c \times SU(3)_{\text{diag}}$. Los dos grupos exactos confinan en dos escalas diferentes, Λ_{QCD} y Λ_{diag}, respectivamente, con $\Lambda_{\text{diag}} \sim \mathcal{O}(\text{ TeV }) \gg \Lambda_{\text{QCD}}$. La existencia de dos parámetros independientes θ (uno para cada grupo a altas energías) requiere de la presencia de dos simetrías anómalas para resolver el problema CP fuerte. Una de ellas se implementa a través de un fermión sin masa en la representación de 20 de $SU(6)$. Con respecto a la implementación de la segunda simetría anómala, se han explorado dos modelos completos alternativos: en el Modelo I se introduce otro fermión sin masa transformando bajo $SU(3')$, mientras que el Modelo II incluye un segundo escalar con los mismos números cuánticos que el escalar que rompe el grupo unificado de color. El modelo I presenta un axión compuesto con una escala PQ del orden de Λ_{diag} y, por lo tanto, baja. En el Modelo II, la escala PQ coincide la escala de unificación de color que es mucho más grande, y el axión asociado es elemental. Hemos calculado la dependencia con la energía de las constantes de acoplo involucradas hasta dos *loops*, mostrando que la separación deseada de todas las escalas relevantes se logra forma natural: la escala de unificación de color es mucho más grande que las dos escalas de confinamiento, Λ_{diag} y Λ_{QCD}, y además estas dos últimas también aparecen naturalmente separadas debido a que los campos ME suavizan la dependencia con la energía del acoplo de QCD con respecto al del sector de confinamiento adicional.

Sorprendentemente, no queda ningún axión invisible al uso en el espectro de baja energía, ya que los instantones de pequeño tamaño alrededor de la escala de ruptura espontánea

aumentan la masa del axión, típicamente hasta escalas del orden del TeV. Este mecanismo permite resolver con éxito el problema CP fuerte *à la* PQ sin un axión ligero. Estos nuevos modelos completos son *pruebas de concepto* de la viabilidad de este tipo de escenario. Esto extiende el espacio de parámetros para un axión que resuelve el problema CP fuerte mucho más allá de la banda de axiones de QCD tradicionales, y cambia drásticamente la fenomenología asociada. Con escalas del axión alrededor del TeV, se esperan señales observables en los colisionadores, en particular la producción por pares de los estados ligados exóticos más ligeros, que corresponden a pseudoescalares de color (octetes de QCD). Además, fermiones estériles sin masa (o prácticamente sin masa) son un remanente característico a bajas energías del multiplete sin masa que resuelve el problema CP fuerte. El Modelo I resulta más atractivo ya que se basa exclusivamente en quarks sin masa para resolver el problema CP fuerte dinámicamente y, por lo tanto, ningún escalar adicional empeora el problema de la jerarquía electrodébil (ED). Además, el Modelo I es seguro en relación a la estabilidad de la solución de tipo axión con respecto a posibles efectos no perturbativos provenientes de correcciones de gravedad cuántica, ya que sus escalas de PQ son $\Lambda_{\rm diag} \sim$ TeV.

Una forma alternativa a reducir la escala del axión para resolver el problema de la calidad de la simetría PQ consiste en construir modelos en los que la simetría PQ surge accidentalmente, en lugar de imponerse en el Lagrangiano. En esta dirección, hemos propuesto una nueva teoría de axiones compuestos donde la simetría de confinamiento adicional es quiral, a diferencia de los modelos de axiones compuestos habituales que usan fermiones vectoriales. En consecuencia, la *simetría PQ es automática*, sin necesidad de recurrir a simetrías adicionales. Esta idea se ha ilustrado con un grupo de confinamiento mínimo $SU(5)$ con dos fermiones sin masa en representaciones $\bar{\mathbf{5}}$ y $\mathbf{10}$. Con este contenido de materia, la invariancia PQ surge de forma automática y es análoga a la simetría $B - L$ en Teorías de Gran Unificación $SU(5)$.

Para explorar si las simetrías quirales globales están espontáneamente rotas tras el confinamiento del grupo $SU(5)$, se han estudiado las condiciones de *matching* de las anomalías de 't Hooft. Hemos demostrado que, si bien las simetrías globales no abelianas deben romperse espontáneamente para que la teoría sea consistente, para la simetría $U(1)_{\rm PQ}$ ambas alternativas conducen a teorías bien definidas. Sin embargo, la única opción fenomenológicamente viable es que la simetría de PQ se rompa espontáneamente, dando como resultado un axión compuesto.

Dentro de este marco, debido a la invariancia *gauge* y la quiralidad, la solución PQ está ampliamente protegida por construcción de correcciones gravitacionales cuánticas derivadas de operadores con dimensión menor que nueve. Sorprendentemente, incluso suponiendo que el coeficiente del posible operador dominante de dimensión nueve es $\mathcal{O}(1)$, existen valores viables de f_a compatibles con los límites del momento dipolar eléctrico del neutrón que permiten explicar el total del contenido de materia oscura del universo en términos de axiones.

Teorías y fenomenología de un campo efectivo

En la segunda parte de la tesis, se ha aplicado el marco de las teorías efectivas de campos para estudiar las consecuencias fenomenológicas de axiones y partículas tipo axión. Las teorías de campo efectivas constituyen una herramienta excelente para estudiar los efectos a bajas energías de los axiones. Debido a su naturaleza de bosón de Goldstone, existe una separación natural entre la escala característica del axión y su masa. Por tanto, se puede realizar una descripción

consistente en términos de operadores efectivos no renormalizables. Además, el enfoque de TEC es independiente del modelo: permite estudiar no solo axiones, sino más genéricamente PPTA, que surgen en una gran cantidad de teorías más allá del ME. En este contexto, hemos estudiado los acoplos de axiones y PPTA con los bosones *gauge* electrodébiles en presencia de acoplos gluónicos. En primer lugar, hemos determinado, a primer orden en la expansión quiral, la contribución al acoplo del axión a los bosones *gauge* ED pesados ($g_{a\gamma Z}$, g_{aZZ} y g_{aWW}) que no depende del modelo concreto. Esta contribución proviene de la mezcla del axión con los mesones neutros, π^0, y η', inducida por el acoplo del axión a la anomalía de QCD. Dicha contribución es relevante siempre que la masa del axión y/o la energía característica del proceso físico sea menor que la escala de QCD. Posteriormente hemos extendido estos resultados al caso en el que hay una fuente adicional para la masa del axión, es decir, axiones pesados y PPTA. En este caso, la mezcla del axión con los mesones neutros disminuye al aumentar la masa del axión y, por lo tanto, la contribución que no depende del modelo a los cuatro acoplos ED del axión desaparece a medida que la masa del axión aumenta por encima de la escala de confinamiento QCD.

También hemos realizado un análisis fenomenológico, teniendo en cuenta los efectos de dos acoplos del axión de forma simultánea para determinar las regiones excluidas experimentalmente por los datos actuales para $g_{a\gamma\gamma}$, $g_{a\gamma Z}$, g_{aZZ} y g_{aWW}, frente a la masa del axión. Cada acoplo ED se ha considerado simultáneamente con el acoplo gluónico anómalo necesario para resolver el problema CP fuerte. Hemos descubierto que ciertos límites de estudios previos a menudo no se aplican en presencia del acoplo gluónico. Además, hemos incluido una estimación de los límites inducidos a un *loop* para cada acoplo ED del axión, lo que conduce a cotas adicionales. Finalmente, se ha demostrado cómo la invariancia *gauge* relaciona los diferentes acoplos de bosones gauge ED con axiones/PPTA. Esto lleva a consecuencias muy interesantes en términos de acotar espacio de parámetros del axión con múltiples estrategias complementarias.

En otro trabajo, se ha considerado la fenomenología de las PPTA sin acoplos gluónicos. Siguiendo el camino de ir más allá del análisis en el que sólo un acoplo es considerado a la vez, hemos construido la base completa de operadores efectivos de bosones electrodébiles acoplados a PPTA a primer orden. Hemos estudiado el impacto fenomenológico en los observables de sabor, teniendo en cuenta la acción simultánea de esos acoplos. Aunque su impacto en las transiciones de tipo *FCNC* aparece a nivel de *loop*, los experimentos de desintegraciones de mesones con cambio de sabor están logrando medidas tan precisas que las contribuciones inducidas a un *loop* proporcionan los límites más restrictivos en grandes regiones del espacio de parámetros. Hemos identificado un patrón interesante de interferencia constructiva/destructiva. Como consecuencia, límites previos muy estrictos derivados de las desintegraciones de kaones y mesones B se ven aliviados en algunas regiones del espacio de parámetros. Por ello, aunque las búsquedas de pseudoescalares ligeros en el LHC sean considerablemente menos sensibles que los observables de sabor, estas pueden proporcionar información complementaria en regiones donde la interferencia destructiva debilita los límites de sabor.

Hemos derivado las cotas más actualizadas sobre el espacio de parámetros de la PPTA con acoplos electrodébiles para dos escenarios bien motivados: (i) una PTA de larga vida media, o que se desintegra en canales invisibles; (ii) una PTA que se desintegra en $\gamma\gamma$, ee y/o $\mu\mu$. Las búsquedas de desintegraciones $K \to \pi +$ inv proporcionan las cotas más restrictivas en el primer caso; mientras que, para el segundo escenario, las cotas más fuertes surgen de las

búsquedas de pseudoescalares con larga vida media en LHCb que generan vértices desplazados en las desintegraciones $B \to K^{(*)}a(\to \mu\mu)$. Se espera que los resultados de estas búsquedas mejoren gracias a los próximos resultados experimentales de NA62, KOTO, LHCb y Belle-II, que brindarán oportunidades únicas para descubrir nueva física, de forma complementaria a las búsquedas directas realizadas en el LHC.

El hecho de que todavía no se haya descubierto nueva física en colisionadores ni en otros experimentos nos hace volver la vista hacia los enigmas teóricos o problemas de ajuste fino del ME. Esta situación requiere que exploremos con la mente abierta soluciones alternativas. En esta tesis, hemos propuesto escenarios dinámicos que solucionan el problema del sabor y el problema CP fuerte. No obstante, los desarrollos teóricos deben venir acompañados de estudios fenomenológicos y, en ausencia de señales más allá del ME, la TEC proporciona una herramienta excepcional para explorar una teoría de la naturaleza más completa. De hecho, queda mucho por hacer para abarcar completamente el espacio de parámetros del axión y de la PTA. Es pertinente un análisis multiparamétrico que tenga en cuenta simultáneamente los efectos de todos los operadores. Además, este futuro análisis debe incluir efectos de un loop, ya que se ha demostrado que tienen un fuerte impacto en las cotas experimentales. La búsqueda para identificar un origen dinámico para el sabor y el problema CP fuerte permanece abierta. Se trata de un proyecto fundamental y fascinante, que posiblemente llevará a grandes descubrimientos.

Bibliography

[1] M. B. Gavela, R. Houtz, P. Quilez, R. Del Rey, and O. Sumensari, "Flavor constraints on electroweak ALP couplings," *Eur. Phys. J.* **C79** no. 5, (2019) 369, arXiv:1901.02031 [hep-ph]. i, 217

[2] M. B. Gavela, M. Ibe, P. Quilez, and T. T. Yanagida, "Automatic Peccei–Quinn symmetry," *Eur. Phys. J.* **C79** no. 6, (2019) 542, arXiv:1812.08174 [hep-ph]. i, 78, 155

[3] G. Alonso-Álvarez, M. B. Gavela, and P. Quilez, "Axion couplings to electroweak gauge bosons," *Eur. Phys. J.* **C79** no. 3, (2019) 223, arXiv:1811.05466 [hep-ph]. i, 181, 217, 218, 223, 231

[4] M. K. Gaillard, M. B. Gavela, R. Houtz, P. Quilez, and R. Del Rey, "Color unified dynamical axion," *Eur. Phys. J.* **C78** no. 11, (2018) 972, arXiv:1805.06465 [hep-ph]. i, 64, 79, 123, 182, 192

[5] R. Alonso, E. Fernandez Martinez, M. B. Gavela, B. Grinstein, L. Merlo, and P. Quilez, "Gauged Lepton Flavour," *JHEP* **12** (2016) 119, arXiv:1609.05902 [hep-ph]. i, 87

[6] P. Quilez Lasanta, "Gauging Lepton Flavour," in *Proceedings, 52nd Rencontres de Moriond on Electroweak Interactions and Unified Theories: La Thuile, Italy, March 18-25, 2017*, pp. 417–420. 2017. arXiv:1705.06094 [hep-ph]. i

[7] B. Grinstein, M. Redi, and G. Villadoro, "Low Scale Flavor Gauge Symmetries," *JHEP* **1011** (2010) 067, arXiv:1009.2049 [hep-ph]. 5, 87, 88, 92, 97, 98, 101, 108

[8] R. D. Peccei and H. R. Quinn, "CP Conservation in the Presence of Instantons," *Phys. Rev. Lett.* **38** (1977) 1440–1443. [,328(1977)]. 5, 58, 69, 145

[9] R. D. Peccei and H. R. Quinn, "Constraints Imposed by CP Conservation in the Presence of Instantons," *Phys. Rev.* **D16** (1977) 1791–1797. 5, 58, 69

[10] F. Englert and R. Brout, "Broken Symmetry and the Mass of Gauge Vector Mesons," *Phys. Rev. Lett.* **13** (1964) 321–323. [,157(1964)]. 12

[11] P. W. Higgs, "Broken Symmetries and the Masses of Gauge Bosons," *Phys. Rev. Lett.* **13** (1964) 508–509. [,160(1964)]. 12

[12] G. S. Guralnik, C. R. Hagen, and T. W. B. Kibble, "Global Conservation Laws and Massless Particles," *Phys. Rev. Lett.* **13** (1964) 585–587. [,162(1964)]. 12

[13] **CMS** Collaboration, S. Chatrchyan *et al.*, "Observation of a new boson at a mass of 125 GeV with the CMS experiment at the LHC," *Phys. Lett.* **B716** (2012) 30–61, arXiv:1207.7235 [hep-ex]. 14

[14] **ATLAS** Collaboration, G. Aad *et al.*, "Observation of a new particle in the search for the Standard Model Higgs boson with the ATLAS detector at the LHC," *Phys. Lett.* **B716** (2012) 1–29, arXiv:1207.7214 [hep-ex]. 14

[15] C. S. Wu, E. Ambler, R. W. Hayward, D. D. Hoppes, and R. P. Hudson, "Experimental Test of Parity Conservation in Beta Decay," *Phys. Rev.* **105** (1957) 1413–1414. 17

[16] M. Goldhaber, L. Grodzins, and A. W. Sunyar, "Helicity of Neutrinos," *Phys. Rev.* **109** (1958) 1015–1017. 17

[17] B. Pontecorvo, "Neutrino Experiments and the Problem of Conservation of Leptonic Charge," *Sov. Phys. JETP* **26** (1968) 984–988. [Zh. Eksp. Teor. Fiz.53,1717(1967)]. 17, 21, 25

[18] V. N. Gribov and B. Pontecorvo, "Neutrino astronomy and lepton charge," *Phys. Lett.* **28B** (1969) 493. 17

[19] **Particle Data Group** Collaboration, M. Tanabashi *et al.*, "Review of Particle Physics," *Phys. Rev.* **D98** no. 3, (2018) 030001. 17, 22, 25, 81, 82, 168, 226, 227, 229

[20] I. Esteban, M. C. Gonzalez-Garcia, A. Hernandez-Cabezudo, M. Maltoni, and T. Schwetz, "Global analysis of three-flavour neutrino oscillations: synergies and tensions in the determination of $\theta_2 3, \delta_C P$, and the mass ordering," *JHEP* **01** (2019) 106, arXiv:1811.05487 [hep-ph]. 17, 25

[21] **Planck** Collaboration, N. Aghanim *et al.*, "Planck 2018 results. VI. Cosmological parameters," arXiv:1807.06209 [astro-ph.CO]. 17, 81, 166, 168

[22] R. Fardon, A. E. Nelson, and N. Weiner, "Dark energy from mass varying neutrinos," *JCAP* **0410** (2004) 005, arXiv:astro-ph/0309800 [astro-ph]. 17

[23] **Troitsk** Collaboration, V. N. Aseev *et al.*, "An upper limit on electron antineutrino mass from Troitsk experiment," *Phys. Rev.* **D84** (2011) 112003, arXiv:1108.5034 [hep-ex]. 17

[24] C. Kraus *et al.*, "Final results from phase II of the Mainz neutrino mass search in tritium beta decay," *Eur. Phys. J.* **C40** (2005) 447–468, arXiv:hep-ex/0412056 [hep-ex]. 17

[25] **KATRIN** Collaboration, J. Angrik *et al.*, "KATRIN design report 2004,". 17

[26] M. Agostini *et al.*, "Background-free search for neutrinoless double-β decay of ^{76}Ge with GERDA," arXiv:1703.00570 [nucl-ex]. [Nature544,47(2017)]. 17

[27] **CUORE** Collaboration, C. Alduino *et al.*, "Measurement of the two-neutrino double-beta decay half-life of^{130} Te with the CUORE-0 experiment," *Eur. Phys. J.* **C77** no. 1, (2017) 13, arXiv:1609.01666 [nucl-ex]. 17

[28] B. Schwingenheuer, "Status and prospects of searches for neutrinoless double beta decay," *Annalen Phys.* **525** (2013) 269–280, arXiv:1210.7432 [hep-ex]. 17

[29] C. Giunti and C. W. Kim, *Fundamentals of Neutrino Physics and Astrophysics*. 2007. 18

[30] M. C. Gonzalez-Garcia and M. Maltoni, "Phenomenology with Massive Neutrinos," *Phys. Rept.* **460** (2008) 1–129, arXiv:0704.1800 [hep-ph]. 18

[31] P. Minkowski, "mu → e gamma at a Rate of One Out of 1-Billion Muon Decays?," *Phys. Lett.* **B67** (1977) 421. 18, 88

[32] R. N. Mohapatra and G. Senjanovic, "Neutrino Mass and Spontaneous Parity Nonconservation," *Phys. Rev. Lett.* **44** (1980) 912. [,231(1979)]. 18, 88

[33] T. Yanagida, "Horizontal gauge symmetry and masses of neutrinos," *Conf. Proc.* **C7902131** (1979) 95–99. 18, 88

[34] M. Gell-Mann, P. Ramond, and R. Slansky, "Complex Spinors and Unified Theories," *Conf. Proc.* **C790927** (1979) 315–321, arXiv:1306.4669 [hep-th]. 18, 88

[35] S. Weinberg, "Baryon and Lepton Nonconserving Processes," *Phys. Rev. Lett.* **43** (1979) 1566–1570. 19

[36] M. Magg and C. Wetterich, "Neutrino Mass Problem and Gauge Hierarchy," *Phys. Lett.* **94B** (1980) 61–64. 19

[37] J. Schechter and J. W. F. Valle, "Neutrino Masses in SU(2) x U(1) Theories," *Phys. Rev.* **D22** (1980) 2227. 19, 111

[38] C. Wetterich, "Neutrino Masses and the Scale of B-L Violation," *Nucl. Phys.* **B187** (1981) 343–375. 19

[39] G. Lazarides, Q. Shafi, and C. Wetterich, "Proton Lifetime and Fermion Masses in an SO(10) Model," *Nucl. Phys.* **B181** (1981) 287–300. 19

[40] R. N. Mohapatra and G. Senjanovic, "Neutrino Masses and Mixings in Gauge Models with Spontaneous Parity Violation," *Phys. Rev.* **D23** (1981) 165. 19

[41] R. Foot, H. Lew, X. G. He, and G. C. Joshi, "Seesaw Neutrino Masses Induced by a Triplet of Leptons," *Z. Phys.* **C44** (1989) 441. 19

[42] E. Ma, "Pathways to naturally small neutrino masses," *Phys. Rev. Lett.* **81** (1998) 1171–1174, arXiv:hep-ph/9805219 [hep-ph]. 19

[43] E. Ma and D. P. Roy, "Heavy triplet leptons and new gauge boson," *Nucl. Phys.* **B644** (2002) 290–302, arXiv:hep-ph/0206150 [hep-ph]. 19

[44] T. Hambye, Y. Lin, A. Notari, M. Papucci, and A. Strumia, "Constraints on neutrino masses from leptogenesis models," *Nucl. Phys.* **B695** (2004) 169–191, arXiv:hep-ph/0312203 [hep-ph]. 19

[45] B. Bajc, M. Nemevsek, and G. Senjanovic, "Probing seesaw at LHC," *Phys. Rev.* **D76** (2007) 055011, arXiv:hep-ph/0703080 [hep-ph]. 19

[46] I. Dorsner and P. Fileviez Perez, "Upper Bound on the Mass of the Type III Seesaw Triplet in an SU(5) Model," *JHEP* **06** (2007) 029, arXiv:hep-ph/0612216 [hep-ph]. 19

[47] P. Fileviez Perez, "Supersymmetric Adjoint SU(5)," *Phys. Rev.* **D76** (2007) 071701, arXiv:0705.3589 [hep-ph]. 19

[48] R. N. Mohapatra and J. W. F. Valle, "Neutrino Mass and Baryon Number Nonconservation in Superstring Models," *Phys. Rev.* **D34** (1986) 1642. [,235(1986)]. 19

[49] J. Bernabeu, A. Santamaria, J. Vidal, A. Mendez, and J. W. F. Valle, "Lepton Flavor Nonconservation at High-Energies in a Superstring Inspired Standard Model," *Phys. Lett.* **B187** (1987) 303–308. 19

[50] M. Malinsky, J. C. Romao, and J. W. F. Valle, "Novel supersymmetric SO(10) seesaw mechanism," *Phys. Rev. Lett.* **95** (2005) 161801, arXiv:hep-ph/0506296 [hep-ph]. 19

[51] E. Ma, "Neutrino Mass: Mechanisms and Models," arXiv:0905.0221 [hep-ph]. 19

[52] F. Vissani, "Do experiments suggest a hierarchy problem?," *Phys. Rev.* **D57** (1998) 7027–7030, arXiv:hep-ph/9709409 [hep-ph]. 20

[53] J. A. Casas, J. R. Espinosa, and I. Hidalgo, "Implications for new physics from fine-tuning arguments. 1. Application to SUSY and seesaw cases," *JHEP* **11** (2004) 057, arXiv:hep-ph/0410298 [hep-ph]. 20

[54] A. Abada, C. Biggio, F. Bonnet, M. B. Gavela, and T. Hambye, "Low energy effects of neutrino masses," *JHEP* **12** (2007) 061, arXiv:0707.4058 [hep-ph]. 20, 105

[55] M. Fukugita and T. Yanagida, "Baryogenesis Without Grand Unification," *Phys. Lett.* **B174** (1986) 45–47. 20

[56] S. Dell'Oro, S. Marcocci, M. Viel, and F. Vissani, "Neutrinoless double beta decay: 2015 review," *Adv. High Energy Phys.* **2016** (2016) 2162659, arXiv:1601.07512 [hep-ph]. 20

[57] J. D. Vergados, H. Ejiri, and F. Simkovic, "Theory of Neutrinoless Double Beta Decay," *Rept. Prog. Phys.* **75** (2012) 106301, arXiv:1205.0649 [hep-ph]. 20

[58] Z. Maki, M. Nakagawa, and S. Sakata, "Remarks on the unified model of elementary particles," *Prog. Theor. Phys.* **28** (1962) 870–880. [,34(1962)]. 21, 25

[59] R. S. Chivukula and H. Georgi, "Composite Technicolor Standard Model," *Phys.Lett.* **B188** (1987) 99. 21, 28, 87

[60] A. Hocker, H. Lacker, S. Laplace, and F. Le Diberder, "A New approach to a global fit of the CKM matrix," *Eur. Phys. J.* **C21** (2001) 225–259, arXiv:hep-ph/0104062 [hep-ph]. 22

[61] **CKMfitter Group** Collaboration, J. Charles, A. Hocker, H. Lacker, S. Laplace, F. R. Le Diberder, J. Malcles, J. Ocariz, M. Pivk, and L. Roos, "CP violation and the CKM matrix: Assessing the impact of the asymmetric B factories," *Eur. Phys. J.* **C41** no. 1, (2005) 1–131, arXiv:hep-ph/0406184 [hep-ph]. 22

[62] **UTfit** Collaboration, M. Bona *et al.*, "The Unitarity Triangle Fit in the Standard Model and Hadronic Parameters from Lattice QCD: A Reappraisal after the Measurements of Delta m(s) and BR(B —¿ tau nu(tau))," *JHEP* **10** (2006) 081, arXiv:hep-ph/0606167 [hep-ph]. 22

[63] S. L. Glashow, J. Iliopoulos, and L. Maiani, "Weak Interactions with Lepton-Hadron Symmetry," *Phys. Rev.* **D2** (1970) 1285–1292. 23

[64] M. K. Gaillard and B. W. Lee, "Rare Decay Modes of the K-Mesons in Gauge Theories," *Phys. Rev.* **D10** (1974) 897. 23

[65] C. Jarlskog, "A Basis Independent Formulation of the Connection Between Quark Mass Matrices, CP Violation and Experiment," *Z. Phys.* **C29** (1985) 491–497. 23

[66] C. Jarlskog, "Commutator of the Quark Mass Matrices in the Standard Electroweak Model and a Measure of Maximal CP Violation," *Phys. Rev. Lett.* **55** (1985) 1039. 23

[67] J. Casas and A. Ibarra, "Oscillating neutrinos and muon —¿ e, gamma," *Nucl.Phys.* **B618** (2001) 171–204, arXiv:hep-ph/0103065 [hep-ph]. 24, 106

[68] J. J. Gomez-Cadenas, J. Martin-Albo, M. Mezzetto, F. Monrabal, and M. Sorel, "The Search for neutrinoless double beta decay," *Riv. Nuovo Cim.* **35** (2012) 29–98, arXiv:1109.5515 [hep-ex]. 26

[69] G. Isidori, Y. Nir, and G. Perez, "Flavor Physics Constraints for Physics Beyond the Standard Model," *Ann. Rev. Nucl. Part. Sci.* **60** (2010) 355, arXiv:1002.0900 [hep-ph]. 27

[70] C. D. Froggatt and H. B. Nielsen, "Hierarchy of Quark Masses, Cabibbo Angles and CP Violation," *Nucl. Phys.* **B147** (1979) 277. 28, 87

[71] G. Altarelli and F. Feruglio, "Tri-bimaximal neutrino mixing from discrete symmetry in extra dimensions," *Nucl. Phys.* **B720** (2005) 64–88, arXiv:hep-ph/0504165 [hep-ph]. 28

[72] G. Altarelli and F. Feruglio, "Tri-bimaximal neutrino mixing, A(4) and the modular symmetry," *Nucl. Phys.* **B741** (2006) 215–235, arXiv:hep-ph/0512103 [hep-ph]. 28

[73] J. C. Pati and A. Salam, "Unified Lepton-Hadron Symmetry and a Gauge Theory of the Basic Interactions," *Phys. Rev.* **D8** (1973) 1240–1251. 28

[74] H. Georgi and S. L. Glashow, "Unity of All Elementary Particle Forces," *Phys. Rev. Lett.* **32** (1974) 438–441. 28

[75] J. R. Ellis, M. K. Gaillard, and D. V. Nanopoulos, "Baryon Number Generation in Grand Unified Theories," *Phys. Lett.* **80B** (1979) 360. [Erratum: Phys. Lett.82B,464(1979)]. 28

[76] G. D'Ambrosio, G. F. Giudice, G. Isidori, and A. Strumia, "Minimal flavor violation: An Effective field theory approach," *Nucl. Phys.* **B645** (2002) 155–187, arXiv:hep-ph/0207036 [hep-ph]. 28

[77] A. J. Buras, P. Gambino, M. Gorbahn, S. Jager, and L. Silvestrini, "Universal unitarity triangle and physics beyond the standard model," *Phys. Lett.* **B500** (2001) 161–167, arXiv:hep-ph/0007085 [hep-ph]. 28

[78] V. Cirigliano, B. Grinstein, G. Isidori, and M. B. Wise, "Minimal flavor violation in the lepton sector," *Nucl.Phys.* **B728** (2005) 121–134, arXiv:hep-ph/0507001 [hep-ph]. 28, 88, 115, 118

[79] **LHCb** Collaboration, R. Aaij *et al.*, "Search for lepton-universality violation in $B^+ \to K^+\ell^+\ell^-$ decays," *Phys. Rev. Lett.* **122** no. 19, (2019) 191801, arXiv:1903.09252 [hep-ex]. 29

[80] **LHCb** Collaboration, R. Aaij *et al.*, "Test of lepton universality with $B^0 \to K^{*0}\ell^+\ell^-$ decays," *JHEP* **08** (2017) 055, arXiv:1705.05802 [hep-ex]. 29, 227

[81] **Belle** Collaboration, A. Abdesselam *et al.*, "Test of lepton flavor universality in $B \to K^*\ell^+\ell^-$ decays at Belle," arXiv:1904.02440 [hep-ex]. 29

[82] M. Algueró, B. Capdevila, A. Crivellin, S. Descotes-Genon, P. Masjuan, J. Matias, and J. Virto, "Emerging patterns of New Physics with and without Lepton Flavour Universal contributions," arXiv:1903.09578 [hep-ph]. 29

[83] J. Goldstone, "Field Theories with Superconductor Solutions," *Nuovo Cim.* **19** (1961) 154–164. 31

[84] J. Goldstone, A. Salam, and S. Weinberg, "Broken Symmetries," *Phys. Rev.* **127** (1962) 965–970. 31

[85] Y. Nambu, "Axial vector current conservation in weak interactions," *Phys. Rev. Lett.* **4** (1960) 380–382. [,107(1960)]. 31

[86] M. E. Peskin and D. V. Schroeder, *An Introduction to quantum field theory*. Addison-Wesley, Reading, USA, 1995. http://www.slac.stanford.edu/~mpeskin/QFT.html. 32

[87] J. Steinberger, "On the Use of subtraction fields and the lifetimes of some types of meson decay," *Phys. Rev.* **76** (1949) 1180–1186. 33

[88] J. S. Schwinger, "On gauge invariance and vacuum polarization," *Phys. Rev.* **82** (1951) 664–679. [,116(1951)]. 33

[89] S. L. Adler, "Axial vector vertex in spinor electrodynamics," *Phys. Rev.* **177** (1969) 2426–2438. [,241(1969)]. 33

[90] J. S. Bell and R. Jackiw, "A PCAC puzzle: $\pi^0 \to \gamma\gamma$ in the σ model," *Nuovo Cim.* **A60** (1969) 47–61. 33

[91] W. A. Bardeen, "Anomalous Ward identities in spinor field theories," *Phys. Rev.* **184** (1969) 1848–1857. 33

[92] K. Fujikawa, "Path Integral Measure for Gauge Invariant Fermion Theories," *Phys. Rev. Lett.* **42** (1979) 1195–1198. 33

[93] S. L. Adler and W. A. Bardeen, "Absence of higher order corrections in the anomalous axial vector divergence equation," *Phys. Rev.* **182** (1969) 1517–1536. [,268(1969)]. 33

[94] S. L. Adler, "Anomalies to all orders," in *50 years of Yang-Mills theory*, G. 't Hooft, ed., pp. 187–228. 2005. arXiv:hep-th/0405040 [hep-th]. 33

[95] G. 't Hooft, "Naturalness, chiral symmetry, and spontaneous chiral symmetry breaking," *NATO Sci. Ser. B* **59** (1980) 135–157. 34, 57, 158

[96] Y. Frishman, A. Schwimmer, T. Banks, and S. Yankielowicz, "The Axial Anomaly and the Bound State Spectrum in Confining Theories," *Nucl. Phys.* **B177** (1981) 157–171. 35

[97] S. R. Coleman and B. Grossman, "'t Hooft's Consistency Condition as a Consequence of Analyticity and Unitarity," *Nucl. Phys.* **B203** (1982) 205–220. 35

[98] J. M. Pendlebury *et al.*, "Revised experimental upper limit on the electric dipole moment of the neutron," *Phys. Rev.* **D92** no. 9, (2015) 092003, arXiv:1509.04411 [hep-ex]. 37

[99] C. A. Baker *et al.*, "An Improved experimental limit on the electric dipole moment of the neutron," *Phys. Rev. Lett.* **97** (2006) 131801, arXiv:hep-ex/0602020 [hep-ex]. 37, 167

[100] **nEDM** Collaboration, E. P. Tsentalovich, "The nEDM experiment at the SNS," *Phys. Part. Nucl.* **45** (2014) 249–250. 37

[101] A. P. Serebrov *et al.*, "New search for the neutron electric dipole moment with ultracold neutrons at ILL," *Phys. Rev.* **C92** no. 5, (2015) 055501. 37

[102] F. Rathmann and N. N. Nikolaev, "Electric dipole moment searches using storage rings," in *23rd International Symposium on Spin Physics (SPIN 2018) Ferrara, Italy, September 10-14, 2018*. 2019. arXiv:1904.13166 [nucl-ex]. 37

[103] V. Baluni, "CP Violating Effects in QCD," *Phys. Rev.* **D19** (1979) 2227–2230. 38

[104] R. J. Crewther, P. Di Vecchia, G. Veneziano, and E. Witten, "Chiral Estimate of the Electric Dipole Moment of the Neutron in Quantum Chromodynamics," *Phys. Lett.* **88B** (1979) 123. [Erratum: Phys. Lett.91B,487(1980)]. 38

[105] K. Kanaya and M. Kobayashi, "Strong CP Violation in the Chiral σ Model," *Prog. Theor. Phys.* **66** (1981) 2173. 38

[106] H. J. Schnitzer, "The Soft Pion Skyrmion Lagrangian and Strong CP Violation," *Phys. Lett.* **139B** (1984) 217–222. 38

[107] P. Cea and G. Nardulli, "A Realistic Calculation of the Electric Dipole Moment of the Neutron Induced by Strong CP Violation," *Phys. Lett.* **144B** (1984) 115–118. 38

[108] M. M. Musakhanov and Z. Z. Israilov, "THE ELECTRIC DIPOLE MOMENT OF THE NEUTRON IN THE CHIRAL BAG MODEL," *Phys. Lett.* **137B** (1984) 419–421. 38

[109] M. A. Morgan and G. A. Miller, "The Neutron Electric Dipole Moment in the Cloudy Bag Model," *Phys. Lett.* **B179** (1986) 379–384. 38

[110] S. Weinberg, "The U(1) Problem," *Phys. Rev.* **D11** (1975) 3583–3593. 39

[111] G. 't Hooft, "How Instantons Solve the U(1) Problem," *Phys. Rept.* **142** (1986) 357–387. 39

[112] G. 't Hooft, "Symmetry Breaking Through Bell-Jackiw Anomalies," *Phys. Rev. Lett.* **37** (1976) 8–11. [,226(1976)]. 39, 57, 59

[113] G. 't Hooft, "Computation of the Quantum Effects Due to a Four-Dimensional Pseudoparticle," *Phys. Rev.* **D14** (1976) 3432–3450. [,70(1976)]. 39, 53, 54, 56, 57, 133

[114] W. A. Bardeen, "Anomalous Currents in Gauge Field Theories," *Nucl. Phys.* **B75** (1974) 246–258. 40

[115] S. Coleman, *Aspects of Symmetry*. Cambridge University Press, Cambridge, U.K., 1985. 40, 41

[116] G. H. Derrick, "Comments on nonlinear wave equations as models for elementary particles," *J. Math. Phys.* **5** (1964) 1252–1254. 42

[117] E. B. Bogomolny, "Stability of Classical Solutions," *Sov. J. Nucl. Phys.* **24** (1976) 449. [Yad. Fiz.24,861(1976)]. 45

[118] R. Bott, "An Application of Morse theory to the topology of Lie groups," *Bull. Soc. Math. Fr.* **84** (1956) 251–281. 46

[119] A. A. Belavin, A. M. Polyakov, A. S. Schwartz, and Yu. S. Tyupkin, "Pseudoparticle Solutions of the Yang-Mills Equations," *Phys. Lett.* **B59** (1975) 85–87. [,350(1975)]. 46

[120] R. Jackiw, C. Nohl, and C. Rebbi, "Conformal Properties of Pseudoparticle Configurations," *Phys. Rev.* **D15** (1977) 1642. [,128(1976)]. 47

[121] S. Vandoren and P. van Nieuwenhuizen, "Lectures on instantons," arXiv:0802.1862 [hep-th]. 47, 56

[122] J.-L. Gervais and B. Sakita, "WKB Wave Function for Systems with Many Degrees of Freedom: A Unified View of Solitons and Instantons," *Phys. Rev.* **D16** (1977) 3507. [,226(1977)]. 47

[123] S. R. Coleman, "The Fate of the False Vacuum. 1. Semiclassical Theory," *Phys. Rev.* **D15** (1977) 2929–2936. [Erratum: Phys. Rev.D16,1248(1977)]. 47

[124] K. M. Bitar and S.-J. Chang, "Vacuum Tunneling of Gauge Theory in Minkowski Space," *Phys. Rev.* **D17** (1978) 486. 50

[125] R. Jackiw and C. Rebbi, "Vacuum Periodicity in a Yang-Mills Quantum Theory," *Phys. Rev. Lett.* **37** (1976) 172–175. [,353(1976)]. 51

[126] C. Vafa and E. Witten, "Restrictions on Symmetry Breaking in Vector-Like Gauge Theories," *Nucl. Phys.* **B234** (1984) 173–188. 52, 59

[127] S. Mori, J. Frison, R. Kitano, H. Matsufuru, and N. Yamada, "Instanton effects on CP-violating gluonic correlators," *EPJ Web Conf.* **175** (2018) 12009. 52

[128] A. Athenodorou and M. Teper, "SU(N) gauge theories in 2+1 dimensions: glueball spectra and k-string tensions," *JHEP* **02** (2017) 015, arXiv:1609.03873 [hep-lat]. 52

[129] M. A. Shifman, A. I. Vainshtein, and V. I. Zakharov, "Instanton Density in a Theory with Massless Quarks," *Nucl. Phys.* **B163** (1980) 46–56. 53, 57, 133, 134

[130] C. G. Callan, Jr., R. F. Dashen, and D. J. Gross, "Toward a Theory of the Strong Interactions," *Phys. Rev.* **D17** (1978) 2717. [,36(1977)]. 53, 54, 133

[131] N. Andrei and D. J. Gross, "The Effect of Instantons on the Short Distance Structure of Hadronic Currents," *Phys. Rev.* **D18** (1978) 468. 54

[132] L. Baulieu, J. R. Ellis, M. K. Gaillard, and W. J. Zakrzewski, "NONPERTURBATIVE QCD EFFECTS AT LARGE MOMENTUM TRANSFERS," *Phys. Lett.* **77B** (1978) 290–294. 54

[133] I. Affleck, "On Constrained Instantons," *Nucl. Phys.* **B191** (1981) 429. [,247(1980)]. 56

[134] O. Espinosa, "High-Energy Behavior of Baryon and Lepton Number Violating Scattering Amplitudes and Breakdown of Unitarity in the Standard Model," *Nucl. Phys.* **B343** (1990) 310–340. 56, 57

[135] C. Csaki and H. Murayama, "Instantons in partially broken gauge groups," *Nucl. Phys.* **B532** (1998) 498–526, arXiv:hep-th/9804061 [hep-th]. 56

[136] A. Ringwald, "High-Energy Breakdown of Perturbation Theory in the Electroweak Instanton Sector," *Nucl. Phys.* **B330** (1990) 1–18. 57

[137] J. R. Ellis and M. K. Gaillard, "Strong and Weak CP Violation," *Nucl. Phys.* **B150** (1979) 141–162. 57, 138

[138] A. E. Nelson, "Naturally Weak CP Violation," *Phys. Lett.* **136B** (1984) 387–391. 57

[139] S. M. Barr, "Solving the Strong CP Problem Without the Peccei-Quinn Symmetry," *Phys. Rev. Lett.* **53** (1984) 329. 57

[140] S. M. Barr, "A Natural Class of Nonpeccei-quinn Models," *Phys. Rev.* **D30** (1984) 1805. 57

[141] L. Bento, G. C. Branco, and P. A. Parada, "A Minimal model with natural suppression of strong CP violation," *Phys. Lett.* **B267** (1991) 95–99. 58

[142] K. S. Babu and R. N. Mohapatra, "A Solution to the Strong CP Problem Without an Axion," *Phys. Rev.* **D41** (1990) 1286. 58

[143] S. M. Barr, D. Chang, and G. Senjanovic, "Strong CP problem and parity," *Phys. Rev. Lett.* **67** (1991) 2765–2768. 58

[144] R. N. Mohapatra and A. Rasin, "Simple supersymmetric solution to the strong CP problem," *Phys. Rev. Lett.* **76** (1996) 3490–3493, arXiv:hep-ph/9511391 [hep-ph]. 58

[145] R. Kuchimanchi, "Solution to the strong CP problem: Supersymmetry with parity," *Phys. Rev. Lett.* **76** (1996) 3486–3489, arXiv:hep-ph/9511376 [hep-ph]. 58

[146] R. N. Mohapatra and A. Rasin, "A Supersymmetric solution to CP problems," *Phys. Rev.* **D54** (1996) 5835–5844, arXiv:hep-ph/9604445 [hep-ph]. 58

[147] S. Weinberg, "A New Light Boson?," *Phys. Rev. Lett.* **40** (1978) 223–226. 59, 63, 70, 145

[148] F. Wilczek, "Problem of Strong p and t Invariance in the Presence of Instantons," *Phys. Rev. Lett.* **40** (1978) 279–282. 59, 70, 145

[149] H. Georgi and I. N. McArthur, "INSTANTONS AND THE mu QUARK MASS,". http://inspirehep.net/record/164546. 60

[150] D. B. Kaplan and A. V. Manohar, "Current Mass Ratios of the Light Quarks," *Phys. Rev. Lett.* **56** (1986) 2004. 60

[151] J. Gasser and H. Leutwyler, "Quark Masses," *Phys. Rept.* **87** (1982) 77–169. 60

[152] D. R. Nelson, G. T. Fleming, and G. W. Kilcup, "Is strong CP due to a massless up quark?," *Phys. Rev. Lett.* **90** (2003) 021601, arXiv:hep-lat/0112029 [hep-lat]. 60

[153] S. Aoki *et al.*, "Review of lattice results concerning low-energy particle physics," *Eur. Phys. J.* **C77** no. 2, (2017) 112, arXiv:1607.00299 [hep-lat]. 60

[154] J. Frison, R. Kitano, and N. Yamada, "Topological susceptibility with a single light quark flavour," *EPJ Web Conf.* **175** (2018) 14017, arXiv:1710.06643 [hep-lat]. 60

[155] J. Frison, R. Kitano, and N. Yamada, "$N_f = 1 + 2$ mass dependence of the topological susceptibility," *PoS* **LATTICE2016** (2016) 323, arXiv:1611.07150 [hep-lat]. 60

[156] F. Wilczek, "Axions and Family Symmetry Breaking," *Phys. Rev. Lett.* **49** (1982) 1549–1552. 63, 64

[157] G. B. Gelmini and M. Roncadelli, "Left-Handed Neutrino Mass Scale and Spontaneously Broken Lepton Number," *Phys. Lett.* **99B** (1981) 411–415. 64

[158] A. A. Anselm and N. G. Uraltsev, "A SECOND MASSLESS AXION?," *Phys. Lett.* **114B** (1982) 39–41. 64

[159] A. Arvanitaki, S. Dimopoulos, S. Dubovsky, N. Kaloper, and J. March-Russell, "String Axiverse," *Phys. Rev.* **D81** (2010) 123530, arXiv:0905.4720 [hep-th]. 64

[160] M. Cicoli, M. Goodsell, and A. Ringwald, "The type IIB string axiverse and its low-energy phenomenology," *JHEP* **10** (2012) 146, arXiv:1206.0819 [hep-th].

[161] M. Cicoli, "Axion-like Particles from String Compactifications," in *Proceedings, 9th Patras Workshop on Axions, WIMPs and WISPs (AXION-WIMP 2013): Mainz, Germany, June 24-28, 2013*, pp. 235–242. 2013. arXiv:1309.6988 [hep-th]. 64

[162] B. Bellazzini, A. Mariotti, D. Redigolo, F. Sala, and J. Serra, "R-axion at colliders," *Phys. Rev. Lett.* **119** no. 14, (2017) 141804, arXiv:1702.02152 [hep-ph]. 64

[163] W. Hu, R. Barkana, and A. Gruzinov, "Cold and fuzzy dark matter," *Phys. Rev. Lett.* **85** (2000) 1158–1161, arXiv:astro-ph/0003365 [astro-ph]. 64

[164] Y. Ema, K. Hamaguchi, T. Moroi, and K. Nakayama, "Flaxion: a minimal extension to solve puzzles in the standard model," *JHEP* **01** (2017) 096, arXiv:1612.05492 [hep-ph]. 64, 76

[165] L. Calibbi, F. Goertz, D. Redigolo, R. Ziegler, and J. Zupan, "Minimal axion model from flavor," *Phys. Rev.* **D95** no. 9, (2017) 095009, arXiv:1612.08040 [hep-ph]. 64, 76

[166] L. D. Luzio, F. Mescia, and E. Nardi, "Window for preferred axion models," *Phys. Rev.* **D96** no. 7, (2017) 075003, 1705.05370. 64, 74, 84, 181, 191, 195, 205, 208

[167] L. Di Luzio, F. Mescia, and E. Nardi, "Redefining the Axion Window," *Phys. Rev. Lett.* **118** no. 3, (2017) 031801, arXiv:1610.07593 [hep-ph]. 64, 65, 74, 84, 181, 195

[168] M. Farina, D. Pappadopulo, F. Rompineve, and A. Tesi, "The photo-philic QCD axion," *JHEP* **01** (2017) 095, arXiv:1611.09855 [hep-ph]. 64

[169] L. Di Luzio, F. Mescia, E. Nardi, P. Panci, and R. Ziegler, "Astrophobic Axions," *Phys. Rev. Lett.* **120** no. 26, (2018) 261803, arXiv:1712.04940 [hep-ph]. 64, 74, 84, 195, 196

[170] V. A. Rubakov, "Grand unification and heavy axion," *JETP Lett.* **65** (1997) 621–624, arXiv:hep-ph/9703409 [hep-ph]. 64, 79, 123, 182, 192

[171] H. Fukuda, K. Harigaya, M. Ibe, and T. T. Yanagida, "Model of visible QCD axion," *Phys. Rev.* **D92** no. 1, (2015) 015021, arXiv:1504.06084 [hep-ph]. 64, 79, 182, 192

[172] Z. Berezhiani, L. Gianfagna, and M. Giannotti, "Strong CP problem and mirror world: The Weinberg-Wilczek axion revisited," *Phys. Lett.* **B500** (2001) 286–296, arXiv:hep-ph/0009290 [hep-ph]. 64, 79, 182, 192

[173] S. D. H. Hsu and F. Sannino, "New solutions to the strong CP problem," *Phys. Lett.* **B605** (2005) 369–375, arXiv:hep-ph/0408319 [hep-ph]. 64, 79, 182, 192

[174] A. Hook, "Anomalous solutions to the strong CP problem," *Phys. Rev. Lett.* **114** no. 14, (2015) 141801, arXiv:1411.3325 [hep-ph]. 64, 79, 182, 192

[175] C.-W. Chiang, H. Fukuda, M. Ibe, and T. T. Yanagida, "750 GeV diphoton resonance in a visible heavy QCD axion model," *Phys. Rev.* **D93** no. 9, (2016) 095016, arXiv:1602.07909 [hep-ph]. 64, 182, 192

[176] S. Dimopoulos, A. Hook, J. Huang, and G. Marques-Tavares, "A Collider Observable QCD Axion," *JHEP* **11** (2016) 052, arXiv:1606.03097 [hep-ph]. 64, 79, 182, 192

[177] T. Gherghetta, N. Nagata, and M. Shifman, "A Visible QCD Axion from an Enlarged Color Group," *Phys. Rev.* **D93** no. 11, (2016) 115010, arXiv:1604.01127 [hep-ph]. 64, 79, 123, 126, 128, 182, 192

[178] A. Kobakhidze, "Heavy axion in asymptotically safe QCD," arXiv:1607.06552 [hep-ph]. 64, 79, 182, 192

[179] P. Agrawal and K. Howe, "Factoring the Strong CP Problem," *JHEP* **12** (2018) 029, arXiv:1710.04213 [hep-ph]. 64, 79, 128, 133, 182, 192

[180] P. Agrawal and K. Howe, "A Flavorful Factoring of the Strong CP Problem," *JHEP* **12** (2018) 035, arXiv:1712.05803 [hep-ph]. 64, 79, 182, 192

[181] M. Srednicki, "Axion couplings to matter: (i). cp-conserving parts," *Nuclear Physics B* **260** no. 3, (1985) 689 – 700. http://www.sciencedirect.com/science/article/pii/0550321385900549. 65

[182] D. B. Kaplan, "Opening the axion window," *Nucl. Phys. B* **260** no. 1, (1985) 215 – 226. http://www.sciencedirect.com/science/article/pii/0550321385903190. 65, 190

[183] G. Grilli di Cortona, E. Hardy, J. Pardo Vega, and G. Villadoro, "The QCD axion, precisely," *JHEP* **01** (2016) 034, arXiv:1511.02867 [hep-ph]. 65, 67, 68, 69, 80, 163, 190, 191, 196

[184] I. G. Irastorza and J. Redondo, "New experimental approaches in the search for axion-like particles," *Prog. Part. Nucl. Phys.* **102** (2018) 89–159, arXiv:1801.08127 [hep-ph]. 65, 81, 83

[185] R. F. Dashen, "Chiral SU(3) x SU(3) as a symmetry of the strong interactions," *Phys. Rev.* **183** (1969) 1245–1260. 66

[186] K. Choi, K. Kang, and J. E. Kim, "Effects of η' in Low-energy Axion Physics," *Phys. Lett.* **B181** (1986) 145–149. 66, 183, 218

[187] P. Di Vecchia and G. Veneziano, "Chiral Dynamics in the Large n Limit," *Nucl. Phys.* **B171** (1980) 253–272. 66, 67, 132, 187

[188] P. Di Vecchia, G. Rossi, G. Veneziano, and S. Yankielowicz, "Spontaneous CP breaking in QCD and the axion potential: an effective Lagrangian approach," *JHEP* **12** (2017) 104, arXiv:1709.00731 [hep-th]. 66, 187

[189] P. Di Vecchia and F. Sannino, "The physics of the θ-angle for composite extensions of the standard model," *The European Physical Journal Plus* **129** no. 12, (Dec, 2014) 262. https://doi.org/10.1140/epjp/i2014-14262-4. 66, 187

[190] W. A. Bardeen and S. H. H. Tye, "Current Algebra Applied to Properties of the Light Higgs Boson," *Phys. Lett.* **74B** (1978) 229–232. 67

[191] W. A. Bardeen, R. D. Peccei, and T. Yanagida, "Constraints on Variant Axion Models," *Nucl. Phys.* **B279** (1987) 401–428. 67, 71

[192] J. E. Kim, "Light Pseudoscalars, Particle Physics and Cosmology," *Phys. Rept.* **150** (1987) 1–177. 67

[193] J. F. Donoghue and L. F. Li, "Properties of Charged Higgs Bosons," *Phys. Rev.* **D19** (1979) 945. 70

[194] H. E. Haber, G. L. Kane, and T. Sterling, "The Fermion Mass Scale and Possible Effects of Higgs Bosons on Experimental Observables," *Nucl. Phys.* **B161** (1979) 493–532. 70

[195] V. D. Barger, J. L. Hewett, and R. J. N. Phillips, "New Constraints on the Charged Higgs Sector in Two Higgs Doublet Models," *Phys. Rev.* **D41** (1990) 3421–3441. 70

[196] T. W. Donnelly, S. J. Freedman, R. S. Lytel, R. D. Peccei, and M. Schwartz, "Do Axions Exist?," *Phys. Rev.* **D18** (1978) 1607. 71

[197] A. Zehnder, "Axion Search in a Monochromatic γ Transition: A New Lower Limit for the Axion Mass," *Phys. Lett.* **104B** (1981) 494–498. [,184(1981)]. 71

[198] Y. Asano, E. Kikutani, S. Kurokawa, T. Miyachi, M. Miyajima, Y. Nagashima, T. Shinkawa, S. Sugimoto, and Y. Yoshimura, "Search for a Rare Decay Mode K+ —¿ pi+ Neutrino anti-neutrino and Axion," *Phys. Lett.* **107B** (1981) 159. [,411(1981)]. 71

[199] J. M. Frere, J. A. M. Vermaseren, and M. B. Gavela, "The Elusive Axion," *Phys. Lett.* **103B** (1981) 129–133. 71, 220

[200] R. D. Peccei, "The Strong CP Problem," *Adv. Ser. Direct. High Energy Phys.* **3** (1989) 503–551. 71

[201] J. E. Kim, "A COMPOSITE INVISIBLE AXION," *Phys. Rev.* **D31** (1985) 1733. 72, 74, 75, 152

[202] K. Choi and J. E. Kim, "Dynamical Axion," *Phys. Rev.* **D32** (1985) 1828. 72, 75, 125, 151

[203] A. R. Zhitnitsky, "On Possible Suppression of the Axion Hadron Interactions. (In Russian)," *Sov. J. Nucl. Phys.* **31** (1980) 260. [Yad. Fiz.31,497(1980)]. 72, 123

[204] M. Dine, W. Fischler, and M. Srednicki, "A Simple Solution to the Strong CP Problem with a Harmless Axion," *Phys. Lett.* **B104** (1981) 199–202. 72, 123

[205] J. E. Kim, "Weak Interaction Singlet and Strong CP Invariance," *Phys. Rev. Lett.* **43** (1979) 103. 73

[206] M. A. Shifman, A. I. Vainshtein, and V. I. Zakharov, "Can Confinement Ensure Natural CP Invariance of Strong Interactions?," *Nucl. Phys.* **B166** (1980) 493–506. 73

[207] E. Nardi and E. Roulet, "Are exotic stable quarks cosmologically allowed?," *Phys. Lett.* **B245** (1990) 105–110. 74

[208] M. L. Perl, P. C. Kim, V. Halyo, E. R. Lee, I. T. Lee, D. Loomba, and K. S. Lackner, "The Search for stable, massive, elementary particles," *Int. J. Mod. Phys.* **A16** (2001) 2137–2164, arXiv:hep-ex/0102033 [hep-ex]. 74

[209] M. L. Perl, E. R. Lee, and D. Loomba, "A Brief review of the search for isolatable fractional charge elementary particles," *Mod. Phys. Lett.* **A19** (2004) 2595–2610. 74

[210] L. Chuzhoy and E. W. Kolb, "Reopening the window on charged dark matter," *JCAP* **0907** (2009) 014, arXiv:0809.0436 [astro-ph]. 74

[211] M. L. Perl, E. R. Lee, and D. Loomba, "Searches for fractionally charged particles," *Ann. Rev. Nucl. Part. Sci.* **59** (2009) 47–65. 74

[212] A. G. Dias, A. C. B. Machado, C. C. Nishi, A. Ringwald, and P. Vaudrevange, "The Quest for an Intermediate-Scale Accidental Axion and Further ALPs," *JHEP* **06** (2014) 037, arXiv:1403.5760 [hep-ph]. 76

[213] J. E. Kim, "Reason for SU(6) Grand Unification," *Phys. Lett.* **107B** (1981) 69–72. 76

[214] P. Langacker, R. D. Peccei, and T. Yanagida, "Invisible Axions and Light Neutrinos: Are They Connected?," *Mod. Phys. Lett.* **A1** (1986) 541. 76

[215] M. Shin, "Light Neutrino Masses and Strong CP Problem," *Phys. Rev. Lett.* **59** (1987) 2515. [Erratum: Phys. Rev. Lett.60,383(1988)]. 76

[216] G. Ballesteros, J. Redondo, A. Ringwald, and C. Tamarit, "Unifying inflation with the axion, dark matter, baryogenesis and the seesaw mechanism," *Phys. Rev. Lett.* **118** no. 7, (2017) 071802, arXiv:1608.05414 [hep-ph]. 76

[217] G. Ballesteros, J. Redondo, A. Ringwald, and C. Tamarit, "Standard Model—axion—seesaw—Higgs portal inflation. Five problems of particle physics and cosmology solved in one stroke," *JCAP* **1708** no. 08, (2017) 001, arXiv:1610.01639 [hep-ph]. 76

[218] E. Ma, T. Ohata, and K. Tsumura, "Majoron as the QCD axion in a radiative seesaw model," *Phys. Rev.* **D96** no. 7, (2017) 075039, arXiv:1708.03076 [hep-ph]. 76

[219] M. B. Wise, H. Georgi, and S. L. Glashow, "SU(5) and the Invisible Axion," *Phys. Rev. Lett.* **47** (1981) 402. 76

[220] A. Ernst, A. Ringwald, and C. Tamarit, "Axion Predictions in $SO(10) \times U(1)_{\rm PQ}$ Models," *JHEP* **02** (2018) 103, arXiv:1801.04906 [hep-ph]. 76, 162

[221] A. Ernst, L. Di Luzio, A. Ringwald, and C. Tamarit, "Axion properties in GUTs," in *Corfu2018: 18th Hellenic School and Workshops on Elementary Particle Physics and Gravity (Corfu2018) Corfu, Corfu, Greece, August 31-September 28, 2018*. 2018. arXiv:1811.11860 [hep-ph]. 76

[222] H. P. Nilles and S. Raby, "Supersymmetry and the strong CP problem," *Nucl. Phys.* **B198** (1982) 102–112. 76

[223] E. Witten, "Some Properties of O(32) Superstrings," *Phys. Lett.* **149B** (1984) 351–356. 76

[224] J. P. Conlon, "The QCD axion and moduli stabilisation," *JHEP* **05** (2006) 078, arXiv:hep-th/0602233 [hep-th]. 76

[225] R. Holman, S. D. H. Hsu, T. W. Kephart, E. W. Kolb, R. Watkins, and L. M. Widrow, "Solutions to the Strong CP Problem in a World with Gravity," *Phys. Lett.* **B282** (1992) 132–136, arXiv:hep-ph/9203206 [hep-ph]. 76, 77, 152

[226] M. Kamionkowski and J. March-Russell, "Planck Scale Physics and the Peccei-Quinn Mechanism," *Phys. Lett.* **B282** (1992) 137–141, arXiv:hep-th/9202003 [hep-th]. 76, 77, 152

[227] S. M. Barr and D. Seckel, "Planck Scale Corrections to Axion Models," *Phys. Rev.* **D46** (1992) 539–549. 76, 77, 78, 152

[228] S. Ghigna, M. Lusignoli, and M. Roncadelli, "Instability of the Invisible Axion," *Phys. Lett.* **B283** (1992) 278–281. 76, 77, 152

[229] H. M. Georgi, L. J. Hall, and M. B. Wise, "Grand Unified Models with an Automatic Peccei-Quinn Symmetry," *Nucl. Phys.* **B192** (1981) 409–416. 76, 152

[230] S. B. Giddings and A. Strominger, "Loss of Incoherence and Determination of Coupling Constants in Quantum Gravity," *Nucl. Phys.* **B307** (1988) 854–866. 76, 152

[231] S. R. Coleman, "Why There is Nothing Rather Than Something: a Theory of the Cosmological Constant," *Nucl. Phys.* **B310** (1988) 643–668. 76, 152

[232] G. Gilbert, "Wormhole Induced Proton Decay," *Nucl. Phys.* **B328** (1989) 159–170. 76, 152

[233] S.-J. Rey, "The Axion Dynamics in Wormhole Background," *Phys. Rev.* **D39** (1989) 3185. 76, 152

[234] R. Alonso and A. Urbano, "Wormholes and masses for Goldstone bosons," arXiv:1706.07415 [hep-ph]. 77, 153

[235] T. Banks and M. Dine, "Note on discrete gauge anomalies," *Phys. Rev.* **D45** (1992) 1424–1427, arXiv:hep-th/9109045 [hep-th]. 77

[236] K. S. Babu, I. Gogoladze, and K. Wang, "Stabilizing the axion by discrete gauge symmetries," *Phys. Lett.* **B560** (2003) 214–222, arXiv:hep-ph/0212339 [hep-ph]. 77

[237] A. G. Dias, V. Pleitez, and M. D. Tonasse, "Naturally light invisible axion in models with large local discrete symmetries," *Phys. Rev.* **D67** (2003) 095008, arXiv:hep-ph/0211107 [hep-ph]. 77

[238] D. Butter and M. K. Gaillard, "The Axion mass in modular invariant supergravity," *Phys. Lett.* **B612** (2005) 304–310, arXiv:hep-th/0502100 [hep-th]. 77, 153, 155

[239] L. Randall, "Composite axion models and Planck scale physics," *Phys. Lett.* **B284** (1992) 77–80. 78, 152, 155

[240] B. A. Dobrescu, "The Strong CP Problem Versus Planck Scale Physics," *Phys. Rev.* **D55** (1997) 5826–5833, arXiv:hep-ph/9609221 [hep-ph]. 78, 151, 155, 159, 166

[241] M. Redi and R. Sato, "Composite Accidental Axions," *JHEP* **05** (2016) 104, arXiv:1602.05427 [hep-ph]. 78, 152, 155

[242] H. Fukuda, M. Ibe, M. Suzuki, and T. T. Yanagida, "A "gauged" $U(1)$ Peccei–Quinn symmetry," *Phys. Lett.* **B771** (2017) 327–331, arXiv:1703.01112 [hep-ph]. 78, 155

[243] H. Fukuda, M. Ibe, M. Suzuki, and T. T. Yanagida, "Gauged Peccei-Quinn symmetry – A case of simultaneous breaking of SUSY and PQ symmetry," *JHEP* **07** (2018) 128, arXiv:1803.00759 [hep-ph]. 78, 155

[244] M. Ibe, M. Suzuki, and T. T. Yanagida, "$B - L$ as a Gauged Peccei-Quinn Symmetry," *JHEP* **08** (2018) 049, arXiv:1805.10029 [hep-ph]. 78, 155

[245] B. Lillard and T. M. P. Tait, "A High Quality Composite Axion," arXiv:1811.03089 [hep-ph]. 78, 155

[246] P. Sikivie, "Of Axions, Domain Walls and the Early Universe," *Phys. Rev. Lett.* **48** (1982) 1156–1159. 78

[247] Ya. B. Zeldovich, I. Yu. Kobzarev, and L. B. Okun, "Cosmological Consequences of the Spontaneous Breakdown of Discrete Symmetry," *Zh. Eksp. Teor. Fiz.* **67** (1974) 3–11. [Sov. Phys. JETP40,1(1974)]. 78

[248] A. Vilenkin, "Cosmic Strings and Domain Walls," *Phys. Rept.* **121** (1985) 263–315. 78

[249] B. Holdom and M. E. Peskin, "Raising the Axion Mass," *Nucl. Phys.* **B208** (1982) 397–412. 79, 133

[250] M. Dine and N. Seiberg, "String Theory and the Strong CP Problem," *Nucl. Phys.* **B273** (1986) 109–124. 79, 133

[251] H. Fukuda, M. Ibe, and T. T. Yanagida, "Dark Matter Candidates in a Visible Heavy QCD Axion Model," *Phys. Rev.* **D95** no. 9, (2017) 095017, arXiv:1702.00227 [hep-ph]. 79

[252] J. Preskill, M. B. Wise, and F. Wilczek, "Cosmology of the Invisible Axion," *Phys. Lett.* **B120** (1983) 127–132. [,URL(1982)]. 80

[253] L. F. Abbott and P. Sikivie, "A Cosmological Bound on the Invisible Axion," *Phys. Lett.* **B120** (1983) 133–136. [,URL(1982)]. 80

[254] M. Dine and W. Fischler, "The Not So Harmless Axion," *Phys. Lett.* **B120** (1983) 137–141. [,URL(1982)]. 80

[255] P. Sikivie and Q. Yang, "Bose-Einstein Condensation of Dark Matter Axions," *Phys. Rev. Lett.* **103** (2009) 111301, arXiv:0901.1106 [hep-ph]. 80

[256] K. Saikawa, "Axion as a non-WIMP dark matter candidate," *PoS* **EPS - HEP2017** (2017) 083, 1709.07091. 81, 168

[257] D. P. Bennett and F. R. Bouchet, "Evidence for a Scaling Solution in Cosmic String Evolution," *Phys. Rev. Lett.* **60** (1988) 257. 81

[258] M. Gorghetto, E. Hardy, and G. Villadoro, "Axions from Strings: the Attractive Solution," *JHEP* **07** (2018) 151, arXiv:1806.04677 [hep-ph]. 81

[259] R. del Rey Bajo, *Spin zero windows to new physics*. PhD thesis, Madrid, Autonoma U., 2018. http://hdl.handle.net/10486/682694. 82

[260] G. G. Raffelt, "Astrophysical axion bounds," *Lect. Notes Phys.* **741** (2008) 51–71, arXiv:hep-ph/0611350 [hep-ph]. [,51(2006)]. 82, 201, 203

[261] W. Keil, H.-T. Janka, D. N. Schramm, G. Sigl, M. S. Turner, and J. R. Ellis, "A Fresh look at axions and SN-1987A," *Phys. Rev.* **D56** (1997) 2419–2432, arXiv:astro-ph/9612222 [astro-ph]. 82

[262] J. H. Chang, R. Essig, and S. D. McDermott, "Supernova 1987A Constraints on Sub-GeV Dark Sectors, Millicharged Particles, the QCD Axion, and an Axion-like Particle," *JHEP* **09** (2018) 051, arXiv:1803.00993 [hep-ph]. 82, 167, 168, 199, 203

[263] N. Bar, K. Blum, and G. D'Amico, "Is there a supernova bound on axions?," arXiv:1907.05020 [hep-ph]. 82

[264] A. Ayala, I. Domínguez, M. Giannotti, A. Mirizzi, and O. Straniero, "Revisiting the bound on axion-photon coupling from Globular Clusters," *Phys. Rev. Lett.* **113** no. 19, (2014) 191302, arXiv:1406.6053 [astro-ph.SR]. 82

[265] O. Straniero, A. Ayala, M. Giannotti, A. Mirizzi, and I. Dominguez, "Axion-Photon Coupling: Astrophysical Constraints," in *Proceedings, 11th Patras Workshop on Axions, WIMPs and WISPs (Axion-WIMP 2015): Zaragoza, Spain, June 22-26, 2015*, pp. 77–81. 2015. 82

[266] K. Zioutas *et al.*, "A Decommissioned LHC model magnet as an axion telescope," *Nucl. Instrum. Meth.* **A425** (1999) 480–489, arXiv:astro-ph/9801176 [astro-ph]. 82

[267] **CAST** Collaboration, M. Arik *et al.*, "Search for Solar Axions by the CERN Axion Solar Telescope with ^{3}He Buffer Gas: Closing the Hot Dark Matter Gap," *Phys. Rev. Lett.* **112** no. 9, (2014) 091302, arXiv:1307.1985 [hep-ex]. 82

[268] I. G. Irastorza *et al.*, "Towards a new generation axion helioscope," *JCAP* **1106** (2011) 013, arXiv:1103.5334 [hep-ex]. 82

[269] E. Armengaud *et al.*, "Conceptual Design of the International Axion Observatory (IAXO)," *JINST* **9** (2014) T05002, arXiv:1401.3233 [physics.ins-det]. 82, 201

[270] K. Ehret *et al.*, "New ALPS Results on Hidden-Sector Lightweights," *Phys. Lett.* **B689** (2010) 149–155, arXiv:1004.1313 [hep-ex]. 83

[271] R. Bähre *et al.*, "Any light particle search II —Technical Design Report," *JINST* **8** (2013) T09001, arXiv:1302.5647 [physics.ins-det]. 83

[272] D. A. Dicus, E. W. Kolb, V. L. Teplitz, and R. V. Wagoner, "Astrophysical Bounds on the Masses of Axions and Higgs Particles," *Phys. Rev.* **D18** (1978) 1829. 83

[273] G. Raffelt and L. Stodolsky, "Mixing of the Photon with Low Mass Particles," *Phys. Rev.* **D37** (1988) 1237. 83

[274] J. Redondo, "Solar axion flux from the axion-electron coupling," *JCAP* **1312** (2013) 008, arXiv:1310.0823 [hep-ph]. 83

[275] M. Giannotti, I. G. Irastorza, J. Redondo, A. Ringwald, and K. Saikawa, "Stellar Recipes for Axion Hunters," *JCAP* **1710** no. 10, (2017) 010, arXiv:1708.02111 [hep-ph]. 83

[276] **MADMAX interest Group** Collaboration, B. Majorovits *et al.*, "MADMAX: A new road to axion dark matter detection," in *15th International Conference on Topics in Astroparticle and Underground Physics (TAUP 2017) Sudbury, Ontario, Canada, July 24-28, 2017*. 2017. arXiv:1712.01062 [physics.ins-det]. 84

[277] D. Budker, P. W. Graham, M. Ledbetter, S. Rajendran, and A. Sushkov, "Proposal for a Cosmic Axion Spin Precession Experiment (CASPEr)," *Phys. Rev.* **X4** no. 2, (2014) 021030, arXiv:1306.6089 [hep-ph]. 84

[278] G. Ruoso, A. Lombardi, A. Ortolan, R. Pengo, C. Braggio, G. Carugno, C. S. Gallo, and C. C. Speake, "The QUAX proposal: a search of galactic axion with magnetic materials," *J. Phys. Conf. Ser.* **718** no. 4, (2016) 042051, arXiv:1511.09461 [hep-ph]. 84

[279] **FUNK Experiment** Collaboration, D. Veberič *et al.*, "Search for hidden-photon dark matter with the FUNK experiment," *PoS* **ICRC2017** (2018) 880, arXiv:1711.02958 [hep-ex]. 84

[280] **nEDM** Collaboration, J. Zenner, "The nEDM experiment at the Paul Scherrer Institute, Switzerland," *AIP Conf. Proc.* **1560** no. 1, (2013) 254–256. 84

[281] **NA62** Collaboration, E. Cortina Gil *et al.*, "The Beam and detector of the NA62 experiment at CERN," *JINST* **12** no. 05, (2017) P05025, arXiv:1703.08501 [physics.ins-det]. 84

[282] S. Alekhin *et al.*, "A facility to Search for Hidden Particles at the CERN SPS: the SHiP physics case," *Rept. Prog. Phys.* **79** no. 12, (2016) 124201, arXiv:1504.04855 [hep-ph]. 84, 227, 229

[283] **Belle-II** Collaboration, G. De Pietro, "First data at Belle II and Dark Sector physics," *PoS* **BEAUTY2018** (2018) 034, arXiv:1808.00776 [hep-ex]. 84

[284] **MATHUSLA** Collaboration, C. Alpigiani *et al.*, "A Letter of Intent for MATHUSLA: A Dedicated Displaced Vertex Detector above ATLAS or CMS.," arXiv:1811.00927 [physics.ins-det]. 84

[285] J. L. Feng, I. Galon, F. Kling, and S. Trojanowski, "Axionlike particles at FASER: The LHC as a photon beam dump," *Phys. Rev.* **D98** no. 5, (2018) 055021, arXiv:1806.02348 [hep-ph]. 84

[286] V. V. Gligorov, S. Knapen, M. Papucci, and D. J. Robinson, "Searching for Long-lived Particles: A Compact Detector for Exotics at LHCb," *Phys. Rev.* **D97** no. 1, (2018) 015023, arXiv:1708.09395 [hep-ph]. 84

[287] J. Jaeckel and M. Spannowsky, "Probing MeV to 90 GeV axion-like particles with LEP and LHC," *Phys. Lett.* **B753** (2016) 482–487, arXiv:1509.00476 [hep-ph]. 84, 181, 182, 202

[288] K. Mimasu and V. Sanz, "ALPs at Colliders," *JHEP* **06** (2015) 173, arXiv:1409.4792 [hep-ph]. 84, 181, 182, 199, 202, 209

[289] I. Brivio, M. B. Gavela, L. Merlo, K. Mimasu, J. M. No, R. del Rey, and V. Sanz, "ALPs Effective Field Theory and Collider Signatures," *Eur. Phys. J.* **C77** no. 8, (2017) 572, arXiv:1701.05379 [hep-ph]. 84, 181, 182, 183, 204, 205, 217, 218, 221, 223

[290] M. Bauer, M. Neubert, and A. Thamm, "Collider Probes of Axion-Like Particles," *JHEP* **12** (2017) 044, arXiv:1708.00443 [hep-ph]. 84, 181, 182, 194, 196, 197, 217, 218, 223, 224, 231

[291] E. Izaguirre, T. Lin, and B. Shuve, "Searching for Axionlike Particles in Flavor-Changing Neutral Current Processes," *Phys. Rev. Lett.* **118** no. 11, (2017) 111802, arXiv:1611.09355 [hep-ph]. 84, 181, 203, 204, 217, 218, 220, 222

[292] G. D'Ambrosio, G. Giudice, G. Isidori, and A. Strumia, "Minimal flavor violation: An Effective field theory approach," *Nucl.Phys.* **B645** (2002) 155–187, arXiv:hep-ph/0207036 [hep-ph]. 87

[293] A. Anselm and Z. Berezhiani, "Weak mixing angles as dynamical degrees of freedom," *Nucl. Phys.* **B484** (1997) 97–123, arXiv:hep-ph/9605400 [hep-ph]. 87

[294] R. Barbieri, L. J. Hall, G. L. Kane, and G. G. Ross, "Nearly degenerate neutrinos and broken flavor symmetry," arXiv:hep-ph/9901228 [hep-ph]. 87

[295] Z. Berezhiani and A. Rossi, "Flavor structure, flavor symmetry and supersymmetry," *Nucl. Phys. Proc. Suppl.* **101** (2001) 410–420, arXiv:hep-ph/0107054 [hep-ph]. [,410(2001)]. 87

[296] P. F. Harrison and W. G. Scott, "Covariant extremisation of flavor-symmetric Jarlskog invariants and the neutrino mixing matrix," *Phys. Lett.* **B628** (2005) 93, arXiv:hep-ph/0508012 [hep-ph]. 87

[297] T. Feldmann, M. Jung, and T. Mannel, "Sequential Flavour Symmetry Breaking," *Phys.Rev.* **D80** (2009) 033003, arXiv:0906.1523 [hep-ph]. 87

[298] R. Alonso, M. Gavela, L. Merlo, and S. Rigolin, "On the scalar potential of minimal flavour violation," *JHEP* **1107** (2011) 012, arXiv:1103.2915 [hep-ph]. 87, 88

[299] R. Alonso, M. Gavela, D. Hernandez, and L. Merlo, "On the Potential of Leptonic Minimal Flavour Violation," *Phys.Lett.* **B715** (2012) 194–198, arXiv:1206.3167 [hep-ph]. 87, 88, 91

[300] J. R. Espinosa, C. S. Fong, and E. Nardi, "Yukawa hierarchies from spontaneous breaking of the $SU(3)_L \times SU(3)_R$ flavour symmetry?," *JHEP* **02** (2013) 137, arXiv:1211.6428 [hep-ph]. 87

[301] R. Alonso, M. B. Gavela, D. Hernández, L. Merlo, and S. Rigolin, "Leptonic Dynamical Yukawa Couplings," *JHEP* **08** (2013) 069, arXiv:1306.5922 [hep-ph]. 87, 88, 91, 120

[302] R. Alonso, M. Gavela, G. Isidori, and L. Maiani, "Neutrino Mixing and Masses from a Minimum Principle," *JHEP* **1311** (2013) 187, arXiv:1306.5927 [hep-ph]. 87, 88, 91, 120

[303] T. Feldmann, "See-Saw Masses for Quarks and Leptons in SU(5)," *JHEP* **1104** (2011) 043, arXiv:1010.2116 [hep-ph]. 87

[304] D. Guadagnoli, R. N. Mohapatra, and I. Sung, "Gauged Flavor Group with Left-Right Symmetry," *JHEP* **04** (2011) 093, arXiv:1103.4170 [hep-ph]. 87

[305] A. J. Buras, L. Merlo, and E. Stamou, "The Impact of Flavour Changing Neutral Gauge Bosons on $\bar{B} \to X_S\gamma$," *JHEP* **08** (2011) 124, arXiv:1105.5146 [hep-ph]. 87

[306] A. J. Buras, M. V. Carlucci, L. Merlo, and E. Stamou, "Phenomenology of a Gauged $SU(3)^3$ Flavour Model," *JHEP* **1203** (2012) 088, arXiv:1112.4477 [hep-ph]. 87

[307] B. Fornal, *Baryon number violation beyond the standard model*. PhD thesis, Caltech, 2014. http://resolver.caltech.edu/CaltechTHESIS:04082014-225653991. 87, 88

[308] T. Feldmann, C. Luhn, and P. Moch, "Lepton-Flavour Violation in a Pati-Salam Model with Gauged Flavour Symmetry," arXiv:1608.04124 [hep-ph]. 87

[309] Z. G. Berezhiani and M. Yu. Khlopov, "The Theory of broken gauge symmetry of families. (In Russian)," *Sov. J. Nucl. Phys.* **51** (1990) 739–746. [Yad. Fiz.51,1157(1990)]. 88

[310] V. Cirigliano and B. Grinstein, "Phenomenology of Minimal Lepton Flavor Violation," *Nucl. Phys.* **B752** (2006) 18–39, arXiv:hep-ph/0601111 [hep-ph]. 88, 115, 118

[311] S. Davidson and F. Palorini, "Various definitions of Minimal Flavour Violation for Leptons," *Phys.Lett.* **B642** (2006) 72–80, arXiv:hep-ph/0607329 [hep-ph]. 88, 115

[312] M. Gavela, T. Hambye, D. Hernandez, and P. Hernandez, "Minimal Flavour Seesaw Models," *JHEP* **0909** (2009) 038, arXiv:0906.1461 [hep-ph]. 88, 115, 117

[313] R. Alonso, G. Isidori, L. Merlo, L. A. Munoz, and E. Nardi, "Minimal flavour violation extensions of the seesaw," *JHEP* **1106** (2011) 037, arXiv:1103.5461 [hep-ph]. 88, 93, 115

[314] M. Blennow and E. Fernandez-Martinez, "Parametrization of Seesaw Models and Light Sterile Neutrinos," *Phys. Lett.* **B704** (2014) 223–229, arXiv:1107.3992 [hep-ph]. 98

[315] **Particle Data Group** Collaboration, K. A. Olive *et al.*, "Review of Particle Physics," *Chin. Phys.* **C38** (2014) 090001. 101, 103, 114

[316] **LHCb** Collaboration, R. Aaij *et al.*, "Measurement of Form-Factor-Independent Observables in the Decay $B^0 \to K^{*0}\mu^+\mu^-$," *Phys. Rev. Lett.* **111** (2013) 191801, arXiv:1308.1707 [hep-ex]. 101

[317] **LHCb** Collaboration, R. Aaij *et al.*, "Test of lepton universality using $B^+ \to K^+\ell^+\ell^-$ decays," *Phys. Rev. Lett.* **113** (2014) 151601, arXiv:1406.6482 [hep-ex]. 101, 227

[318] E. Fernandez-Martinez, J. Hernandez-Garcia, and J. Lopez-Pavon, "Global constraints on heavy neutrino mixing," *JHEP* **08** (2016) 033, arXiv:1605.08774 [hep-ph]. 101, 112

[319] S. Antusch and O. Fischer, "Non-unitarity of the leptonic mixing matrix: Present bounds and future sensitivities," *JHEP* **10** (2014) 094, arXiv:1407.6607 [hep-ph]. 101, 111

[320] **L3** Collaboration, P. Achard *et al.*, "Search for heavy neutral and charged leptons in e^+e^- annihilation at LEP," *Phys. Lett.* **B517** (2001) 75–85, arXiv:hep-ex/0107015 [hep-ex]. 101

[321] **ATLAS** Collaboration, T. A. collaboration, "Search for supersymmetry with two and three leptons and missing transverse momentum in the final state at $\sqrt{s} = 13$ TeV with the ATLAS detector,". 102

[322] E. Eichten, K. D. Lane, and M. E. Peskin, "New Tests for Quark and Lepton Substructure," *Phys. Rev. Lett.* **50** (1983) 811–814. [,369(1983)]. 102

[323] **DELPHI, OPAL, LEP Electroweak, ALEPH, L3** Collaboration, S. Schael *et al.*, "Electroweak Measurements in Electron-Positron Collisions at W-Boson-Pair Energies at LEP," *Phys. Rept.* **532** (2013) 119–244, arXiv:1302.3415 [hep-ex]. 103

[324] R. Jackiw and S. Weinberg, "Weak interaction corrections to the muon magnetic moment and to muonic atom energy levels," *Phys. Rev.* **D5** (1972) 2396–2398. 103

[325] F. S. Queiroz and W. Shepherd, "New Physics Contributions to the Muon Anomalous Magnetic Moment: A Numerical Code," *Phys. Rev.* **D89** no. 9, (2014) 095024, arXiv:1403.2309 [hep-ph]. 103

[326] R. N. Mohapatra, "Mechanism for understanding small neutrino mass in superstring theories," *Phys. Rev. Lett.* **56** (Feb, 1986) 561–563. http://link.aps.org/doi/10.1103/PhysRevLett.56.561. 105

[327] R. N. Mohapatra and J. W. F. Valle, "Neutrino mass and baryon-number nonconservation in superstring models," *Phys. Rev. D* **34** (Sep, 1986) 1642–1645. http://link.aps.org/doi/10.1103/PhysRevD.34.1642. 105

[328] J. Bernabéu, A. Santamaria, J. Vidal, A. Mendez, and J. Valle, "Lepton flavour non-conservation at high energies in a superstring inspired standard model," *Physics Letters B* **187** no. 3, (1987) 303 – 308. http://www.sciencedirect.com/science/article/pii/0370269387911002. 105

[329] G. C. Branco, W. Grimus, and L. Lavoura, "THE SEESAW MECHANISM IN THE PRESENCE OF A CONSERVED LEPTON NUMBER," *Nucl. Phys.* **B312** (1989) 492. 105

[330] J. Kersten and A. Yu. Smirnov, "Right-Handed Neutrinos at CERN LHC and the Mechanism of Neutrino Mass Generation," *Phys. Rev.* **D76** (2007) 073005, arXiv:0705.3221 [hep-ph]. 105

[331] **Particle Data Group** Collaboration, J. Beringer *et al.*, "Review of Particle Physics (Rpp)," *Phys. Rev.* **D86** (2012) 010001. 111

[332] W. Altmannshofer, S. Gori, M. Pospelov, and I. Yavin, "Neutrino Trident Production: A Powerful Probe of New Physics with Neutrino Beams," *Phys. Rev. Lett.* **113** (2014) 091801, arXiv:1406.2332 [hep-ph]. 111

[333] **CCFR** Collaboration, S. R. Mishra *et al.*, "Neutrino tridents and W Z interference," *Phys. Rev. Lett.* **66** (1991) 3117–3120. 111

[334] **CHARM-II** Collaboration, D. Geiregat *et al.*, "First observation of neutrino trident production," *Phys. Lett.* **B245** (1990) 271–275. 111

[335] R. E. Shrock, "New Tests For, and Bounds On, Neutrino Masses and Lepton Mixing," *Phys. Lett.* **B96** (1980) 159–164. 111

[336] R. E. Shrock, "General Theory of Weak Leptonic and Semileptonic Decays. 1. Leptonic Pseudoscalar Meson Decays, with Associated Tests For, and Bounds on, Neutrino Masses and Lepton Mixing," *Phys. Rev.* **D24** (1981) 1232. 111

[337] R. E. Shrock, "General Theory of Weak Processes Involving Neutrinos. 2. Pure Leptonic Decays," *Phys. Rev.* **D24** (1981) 1275. 111

[338] P. Langacker and D. London, "Mixing Between Ordinary and Exotic Fermions," *Phys.Rev.* **D38** (1988) 886. 111

[339] S. M. Bilenky and C. Giunti, "Seesaw type mixing and muon-neutrino —¿ tau-neutrino oscillations," *Phys.Lett.* **B300** (1993) 137–140, arXiv:hep-ph/9211269 [hep-ph]. 111

[340] E. Nardi, E. Roulet, and D. Tommasini, "Limits on neutrino mixing with new heavy particles," *Phys.Lett.* **B327** (1994) 319–326, arXiv:hep-ph/9402224 [hep-ph]. 111

[341] D. Tommasini, G. Barenboim, J. Bernabeu, and C. Jarlskog, "Nondecoupling of heavy neutrinos and lepton flavor violation," *Nucl.Phys.* **B444** (1995) 451–467, arXiv:hep-ph/9503228 [hep-ph]. 111

[342] S. Bergmann and A. Kagan, "Z - induced FCNCs and their effects on neutrino oscillations," *Nucl.Phys.* **B538** (1999) 368–386, arXiv:hep-ph/9803305 [hep-ph]. 111

[343] W. Loinaz, N. Okamura, T. Takeuchi, and L. Wijewardhana, "The NuTeV anomaly, neutrino mixing, and a heavy Higgs boson," *Phys.Rev.* **D67** (2003) 073012, arXiv:hep-ph/0210193 [hep-ph]. 111

[344] W. Loinaz, N. Okamura, S. Rayyan, T. Takeuchi, and L. Wijewardhana, "Quark lepton unification and lepton flavor nonconservation from a TeV scale seesaw neutrino mass texture," *Phys.Rev.* **D68** (2003) 073001, arXiv:hep-ph/0304004 [hep-ph]. 111

[345] W. Loinaz, N. Okamura, S. Rayyan, T. Takeuchi, and L. Wijewardhana, "The NuTeV anomaly, lepton universality, and nonuniversal neutrino gauge couplings," *Phys.Rev.* **D70** (2004) 113004, arXiv:hep-ph/0403306 [hep-ph]. 111

[346] S. Antusch, C. Biggio, E. Fernandez-Martinez, M. Gavela, and J. Lopez-Pavon, "Unitarity of the Leptonic Mixing Matrix," *JHEP* **0610** (2006) 084, arXiv:hep-ph/0607020 [hep-ph]. 111

[347] S. Antusch, J. P. Baumann, and E. Fernandez-Martinez, "Non-Standard Neutrino Interactions with Matter from Physics Beyond the Standard Model," *Nucl.Phys.* **B810** (2009) 369–388, arXiv:0807.1003 [hep-ph]. 111

[348] C. Biggio, "The Contribution of fermionic seesaws to the anomalous magnetic moment of leptons," *Phys. Lett.* **B668** (2008) 378–384, arXiv:0806.2558 [hep-ph]. 111

[349] R. Alonso, M. Dhen, M. Gavela, and T. Hambye, "Muon conversion to electron in nuclei in type-I seesaw models," *JHEP* **1301** (2013) 118, arXiv:1209.2679 [hep-ph]. 111

[350] A. Abada, D. Das, A. Teixeira, A. Vicente, and C. Weiland, "Tree-level lepton universality violation in the presence of sterile neutrinos: impact for R_K and R_π," *JHEP* **1302** (2013) 048, arXiv:1211.3052 [hep-ph]. 111

[351] E. Akhmedov, A. Kartavtsev, M. Lindner, L. Michaels, and J. Smirnov, "Improving Electro-Weak Fits with TeV-scale Sterile Neutrinos," *JHEP* **1305** (2013) 081, arXiv:1302.1872 [hep-ph]. 111

[352] L. Basso, O. Fischer, and J. J. van der Bij, "Precision tests of unitarity in leptonic mixing," *Europhys.Lett.* **105** no. 1, (2014) 11001, arXiv:1310.2057 [hep-ph]. 111

[353] A. Abada, A. Teixeira, A. Vicente, and C. Weiland, "Sterile neutrinos in leptonic and semileptonic decays," *JHEP* **1402** (2014) 091, arXiv:1311.2830 [hep-ph]. 111

[354] S. Antusch and O. Fischer, "Testing sterile neutrino extensions of the Standard Model at future lepton colliders," *JHEP* **05** (2015) 053, arXiv:1502.05915 [hep-ph]. 111

[355] A. Abada, V. De Romeri, and A. M. Teixeira, "Impact of sterile neutrinos on nuclear-assisted cLFV processes," *JHEP* **02** (2016) 083, arXiv:1510.06657 [hep-ph]. 111

[356] E. Fernandez-Martinez, J. Hernandez-Garcia, J. Lopez-Pavon, and M. Lucente, "Loop level constraints on Seesaw neutrino mixing," *JHEP* **10** (2015) 130, arXiv:1508.03051 [hep-ph]. 111

[357] A. Abada and T. Toma, "Electric Dipole Moments of Charged Leptons with Sterile Fermions," *JHEP* **02** (2016) 174, arXiv:1511.03265 [hep-ph]. 111

[358] A. Abada and T. Toma, "Electron electric dipole moment in Inverse Seesaw models," arXiv:1605.07643 [hep-ph]. 111

[359] **T2K** Collaboration, K. Abe *et al.*, "Measurements of neutrino oscillation in appearance and disappearance channels by the T2K experiment with 6.6x10^{20} protons on target," *Phys. Rev.* **D91** no. 7, (2015) 072010, arXiv:1502.01550 [hep-ex]. 113

[360] **NOvA** Collaboration, P. Adamson *et al.*, "First measurement of electron neutrino appearance in NOvA," *Phys. Rev. Lett.* **116** no. 15, (2016) 151806, arXiv:1601.05022 [hep-ex]. 113

[361] E. Witten, "Current Algebra Theorems for the U(1) Goldstone Boson," *Nucl. Phys.* **B156** (1979) 269–283. 132

[362] G. Veneziano, "U(1) Without Instantons," *Nucl. Phys.* **B159** (1979) 213–224. 132

[363] J. M. Flynn and L. Randall, "A Computation of the Small Instanton Contribution to the Axion Potential," *Nucl. Phys.* **B293** (1987) 731–739. 133

[364] M. A. Shifman, *Instantons in Gauge Theories*. 1994. 133

[365] C. W. Bernard, "Gauge Zero Modes, Instanton Determinants, and QCD Calculations," *Phys. Rev.* **D19** (1979) 3013. [,109(1979)]. 133

[366] F. Sannino and V. Skrinjar, "Safe and Free Instantons," arXiv:1802.10372 [hep-th]. 133

[367] A. Ringwald, "Electroweak instantons / sphalerons at VLHC?," *Phys. Lett.* **B555** (2003) 227–237, arXiv:hep-ph/0212099 [hep-ph]. 133

[368] M. Bauer, M. Heiles, M. Neubert, and A. Thamm, "Axion-Like Particles at Future Colliders," *Eur. Phys. J.* **C79** no. 1, (2019) 74, arXiv:1808.10323 [hep-ph]. 137, 181, 182, 218

[369] **ATLAS** Collaboration, T. A. collaboration, "Search for new light resonances decaying to jet pairs and produced in association with a photon or a jet in proton-proton collisions at $\sqrt{s} = 13$ TeV with the ATLAS detector,". 137, 199

[370] A. Belyaev, G. Cacciapaglia, H. Cai, G. Ferretti, T. Flacke, A. Parolini, and H. Serodio, "Di-boson signatures as Standard Candles for Partial Compositeness," *JHEP* **01** (2017) 094, arXiv:1610.06591 [hep-ph]. [Erratum: JHEP12,088(2017)]. 137

[371] **ATLAS** Collaboration, M. Aaboud *et al.*, "A search for pair-produced resonances in four-jet final states at $\sqrt{s} = 13$ TeV with the ATLAS detector," *Eur. Phys. J.* **C78** no. 3, (2018) 250, arXiv:1710.07171 [hep-ex]. 139, 141, 149, 150

[372] D. Goncalves-Netto, D. Lopez-Val, K. Mawatari, T. Plehn, and I. Wigmore, "Sgluon Pair Production to Next-To-Leading Order," *Phys. Rev.* **D85** (2012) 114024, arXiv:1203.6358 [hep-ph]. 150

[373] C. Degrande, B. Fuks, V. Hirschi, J. Proudom, and H.-S. Shao, "Automated Next-To-Leading Order Predictions for New Physics at the Lhc: the Case of Colored Scalar Pair Production," *Phys. Rev.* **D91** no. 9, (2015) 094005, arXiv:1412.5589 [hep-ph]. 150

[374] **ATLAS** Collaboration, M. Aaboud *et al.*, "Search for heavy long-lived charged R-hadrons with the ATLAS detector in 3.2 fb^{-1} of proton–proton collision data at $\sqrt{s} = 13$ TeV," *Phys. Lett.* **B760** (2016) 647–665, arXiv:1606.05129 [hep-ex]. 150

[375] E. W. Kolb and M. S. Turner, "The Early Universe," *Front. Phys.* **69** (1990) 1–547. 151

[376] K. Choi, K. Kang, and J. E. Kim, "COSMOLOGICAL CONSTRAINTS ON HEAVY UNSTABLE PARTICLES," *Phys. Rev.* **D32** (1985) 2822. 151

[377] H.-Y. Cheng, "The Strong CP Problem Revisited," *Phys. Rept.* **158** (1988) 1. 152

[378] J. Preskill, S. P. Trivedi, F. Wilczek, and M. B. Wise, "Cosmology and broken discrete symmetry," *Nucl. Phys.* **B363** (1991) 207–220. 152

[379] G. R. Dvali and G. Senjanovic, "Is there a domain wall problem?," *Phys. Rev. Lett.* **74** (1995) 5178–5181, arXiv:hep-ph/9501387 [hep-ph]. 152

[380] S. Dimopoulos, S. Raby, and L. Susskind, "Light Composite Fermions," *Nucl. Phys.* **B173** (1980) 208–228. 158

[381] N. Arkani-Hamed and Y. Grossman, "Light active and sterile neutrinos from compositeness," *Phys. Lett.* **B459** (1999) 179–182, arXiv:hep-ph/9806223 [hep-ph]. 158

[382] A. G. Cohen, D. B. Kaplan, and A. E. Nelson, "Counting 4 pis in strongly coupled supersymmetry," *Phys. Lett.* **B412** (1997) 301 – 308, hep-ph/9706275. 162, 163

[383] B. M. Gavela, E. E. Jenkins, A. V. Manohar, and L. Merlo, "Analysis of General Power Counting Rules in Effective Field Theory," *Eur. Phys. J.* **C76** no. 9, (2016) 485, 1601.07551. 162, 163

[384] M. Kawasaki and K. Nakayama, "Axions: Theory and Cosmological Role," *Ann. Rev. Nucl. Part. Sci.* **63** (2013) 69–95, arXiv:1301.1123 [hep-ph]. 162

[385] J. Engel, M. J. Ramsey-Musolf, and U. van Kolck, "Electric Dipole Moments of Nucleons, Nuclei, and Atoms: The Standard Model and Beyond," *Prog. Part. Nucl. Phys.* **71** (2013) 21–74, arXiv:1303.2371 [nucl-th]. 167

[386] L. Visinelli and P. Gondolo, "Dark Matter Axions Revisited," *Phys. Rev.* **D80** (2009) 035024, arXiv:0903.4377 [astro-ph.CO]. 168

[387] P. Ramond, *Group theory: A physicist's survey*. 2010. http://www.cambridge.org/de/knowledge/isbn/item2710157. 169

[388] R. Slansky, "Group Theory for Unified Model Building," *Phys. Rept.* **79** (1981) 1–128. 175

[389] R. Feger and T. W. Kephart, "LieART—A Mathematica application for Lie algebras and representation theory," *Comput. Phys. Commun.* **192** (2015) 166–195, arXiv:1206.6379 [math-ph]. 175

[390] D. S. M. Alves and N. Weiner, "A viable QCD axion in the MeV mass range," *JHEP* **07** (2018) 092, arXiv:1710.03764 [hep-ph]. 181, 189

[391] C. Frugiuele, E. Fuchs, G. Perez, and M. Schlaffer, "Relaxion and light (pseudo)scalars at the HL-LHC and lepton colliders," *JHEP* **10** (2018) 151, arXiv:1807.10842 [hep-ph]. 181, 182

[392] N. Craig, A. Hook, and S. Kasko, "The Photophobic ALP," *JHEP* **09** (2018) 028, arXiv:1805.06538 [hep-ph]. 181, 182, 195, 197, 203, 204, 205

[393] M. Freytsis, Z. Ligeti, and J. Thaler, "Constraining the Axion Portal with $B \to K l^+ l^-$," *Phys. Rev.* **D81** (2010) 034001, arXiv:0911.5355 [hep-ph]. 181, 217, 218, 220

[394] S. Knapen, T. Lin, H. K. Lou, and T. Melia, "Searching for Axionlike Particles with Ultraperipheral Heavy-Ion Collisions," *Phys. Rev. Lett.* **118** no. 17, (2017) 171801, arXiv:1607.06083 [hep-ph]. 182

[395] X. Cid Vidal, A. Mariotti, D. Redigolo, F. Sala, and K. Tobioka, "New Axion Searches at Flavor Factories," arXiv:1810.09452 [hep-ph]. 182, 203, 209

[396] H. Georgi, D. B. Kaplan, and L. Randall, "Manifesting the Invisible Axion at Low-energies," *Phys. Lett.* **169B** (1986) 73–78. 183, 218

[397] A. Salvio, A. Strumia, and W. Xue, "Thermal axion production," *JCAP* **1401** (2014) 011, arXiv:1310.6982 [hep-ph]. 183, 218

[398] J. E. Kim and G. Carosi, "Axions and the Strong CP Problem," *Rev. Mod. Phys.* **82** (2010) 557 – 602, 0807.3125. 184, 213

[399] D. Aloni, Y. Soreq, and M. Williams, "Coupling QCD-scale axion-like particles to gluons," arXiv:1811.03474 [hep-ph]. 199, 224

[400] **BNL-E949** Collaboration, A. V. Artamonov *et al.*, "Study of the decay $K^+ \to \pi^+ \nu\bar{\nu}$ in the momentum region $140 < P_\pi < 199$ MeV/c," *Phys. Rev.* **D79** (2009) 092004, arXiv:0903.0030 [hep-ex]. 199, 204

[401] **CAST** Collaboration, V. Anastassopoulos *et al.*, "New CAST Limit on the Axion-Photon Interaction," *Nature Phys.* **13** (2017) 584–590, arXiv:1705.02290 [hep-ex]. 201

[402] A. Payez, C. Evoli, T. Fischer, M. Giannotti, A. Mirizzi, and A. Ringwald, "Revisiting the SN1987A gamma-ray limit on ultralight axion-like particles," *JCAP* **1502** no. 02, (2015) 006, arXiv:1410.3747 [astro-ph.HE]. 201

[403] J. Jaeckel, P. C. Malta, and J. Redondo, "Decay photons from the axionlike particles burst of type II supernovae," *Phys. Rev.* **D98** no. 5, (2018) 055032, arXiv:1702.02964 [hep-ph]. 201

[404] J. Blumlein and J. Brunner, "New Exclusion Limits on Dark Gauge Forces from Proton Bremsstrahlung in Beam-Dump Data," *Phys. Lett.* **B731** (2014) 320–326, arXiv:1311.3870 [hep-ph]. 201

[405] J. D. Bjorken, S. Ecklund, W. R. Nelson, A. Abashian, C. Church, B. Lu, L. W. Mo, T. A. Nunamaker, and P. Rassmann, "Search for Neutral Metastable Penetrating Particles Produced in the SLAC Beam Dump," *Phys. Rev.* **D38** (1988) 3375. 201

[406] E. M. Riordan *et al.*, "A Search for Short Lived Axions in an Electron Beam Dump Experiment," *Phys. Rev. Lett.* **59** (1987) 755. 201

[407] B. Döbrich, J. Jaeckel, F. Kahlhoefer, A. Ringwald, and K. Schmidt-Hoberg, "ALPtraum: ALP production in proton beam dump experiments," *JHEP* **02** (2016) 018, arXiv:1512.03069 [hep-ph]. [JHEP02,018(2016)]. 202

[408] **L3** Collaboration, O. Adriani *et al.*, "Isolated hard photon emission in hadronic Z0 decays," *Phys. Lett.* **B292** (1992) 472–484. 203, 204

[409] **BaBar** Collaboration, J. P. Lees *et al.*, "Search for hadronic decays of a light Higgs boson in the radiative decay $\Upsilon \to \gamma A^0$," *Phys. Rev. Lett.* **107** (2011) 221803, arXiv:1108.3549 [hep-ex]. 203

[410] S. Benson and A. Puig Navarro, "Triggering $B_s^0 \to \gamma\gamma$ at LHCb," Tech. Rep. LHCb-PUB-2018-006. CERN-LHCb-PUB-2018-006, CERN, Geneva, Apr, 2018. https://cds.cern.ch/record/2314368. 203

[411] J. Jaeckel, M. Jankowiak, and M. Spannowsky, "LHC probes the hidden sector," *Phys. Dark Univ.* **2** (2013) 111–117, arXiv:1212.3620 [hep-ph]. 203, 209

[412] A. Mariotti, D. Redigolo, F. Sala, and K. Tobioka, "New LHC bound on low-mass diphoton resonances," *Phys. Lett.* **B783** (2018) 13–18, arXiv:1710.01743 [hep-ph]. 203, 209

[413] **CHARM** Collaboration, F. Bergsma *et al.*, "Search for Axion Like Particle Production in 400-GeV Proton - Copper Interactions," *Phys. Lett.* **157B** (1985) 458–462. 204

[414] J. D. Clarke, R. Foot, and R. R. Volkas, "Phenomenology of a very light scalar (100 MeV ¡ m_h ¡ 10 GeV) mixing with the SM Higgs," *JHEP* **02** (2014) 123, arXiv:1310.8042 [hep-ph]. 204

[415] B. Döbrich, F. Ertas, F. Kahlhoefer, and T. Spadaro, "Model-independent bounds on light pseudoscalars from rare B-meson decays," *Phys. Lett.* **B790** (2019) 537–544, arXiv:1810.11336 [hep-ph]. 204, 226, 229

[416] **SLD Electroweak Group, DELPHI, ALEPH, SLD, SLD Heavy Flavour Group, OPAL, LEP Electroweak Working Group, L3** Collaboration, S. Schael *et al.*, "Precision electroweak measurements on the Z resonance," *Phys. Rept.* **427** (2006) 257–454, arXiv:hep-ex/0509008 [hep-ex]. 204

[417] M. B. Gavela, J. M. No, V. Sanz, and J. F. de Trocóniz, "Non-Resonant Searches for Axion-Like Particles at the LHC," arXiv:1905.12953 [hep-ph]. 205

[418] J. F. de Troconiz et al. work in progress. 205

[419] G. Hiller, "B physics signals of the lightest CP odd Higgs in the NMSSM at large tan beta," *Phys. Rev.* **D70** (2004) 034018, arXiv:hep-ph/0404220 [hep-ph]. 217, 218

[420] M. J. Dolan, F. Kahlhoefer, C. McCabe, and K. Schmidt-Hoberg, "A taste of dark matter: Flavour constraints on pseudoscalar mediators," *JHEP* **03** (2015) 171, arXiv:1412.5174 [hep-ph]. [Erratum: JHEP07,103(2015)]. 218, 220

[421] B. Batell, M. Pospelov, and A. Ritz, "Multi-lepton Signatures of a Hidden Sector in Rare B Decays," *Phys. Rev.* **D83** (2011) 054005, arXiv:0911.4938 [hep-ph]. 218, 220

[422] **E949** Collaboration, A. V. Artamonov *et al.*, "New measurement of the $K^+ \to \pi^+ \nu\bar{\nu}$ branching ratio," *Phys. Rev. Lett.* **101** (2008) 191802, arXiv:0808.2459 [hep-ex]. 220, 222

[423] **E787** Collaboration, S. Adler *et al.*, "Further search for the decay K+ —¿ pi+ nu anti-nu in the momentum region P ¡ 195-MeV/c," *Phys. Rev.* **D70** (2004) 037102, arXiv:hep-ex/0403034 [hep-ex]. 220, 222

[424] **Belle-II** Collaboration, W. Altmannshofer *et al.*, "The Belle II Physics Book," arXiv:1808.10567 [hep-ex]. 220, 222

[425] N. Carrasco, P. Lami, V. Lubicz, L. Riggio, S. Simula, and C. Tarantino, "$K \to \pi$ semileptonic form factors with $N_f = 2 + 1 + 1$ twisted mass fermions," *Phys. Rev.* **D93** no. 11, (2016) 114512, arXiv:1602.04113 [hep-lat]. 220

[426] P. Ball and R. Zwicky, "New results on $B \to \pi, K, \eta$ decay formfactors from light-cone sum rules," *Phys. Rev.* **D71** (2005) 014015, arXiv:hep-ph/0406232 [hep-ph]. 220

[427] A. Bharucha, D. M. Straub, and R. Zwicky, "$B \to V\ell^+\ell^-$ in the Standard Model from light-cone sum rules," *JHEP* **08** (2016) 098, arXiv:1503.05534 [hep-ph]. 220

[428] X.-Q. Li, J. Lu, and A. Pich, "$B^0_{s,d} \to \ell^+\ell^-$ Decays in the Aligned Two-Higgs-Doublet Model," *JHEP* **06** (2014) 022, arXiv:1404.5865 [hep-ph]. 220

[429] P. Arnan, D. Bečirević, F. Mescia, and O. Sumensari, "Two Higgs doublet models and $b \to s$ exclusive decays," *Eur. Phys. J.* **C77** no. 11, (2017) 796, arXiv:1703.03426 [hep-ph]. 220, 227

[430] A. J. Buras, D. Buttazzo, J. Girrbach-Noe, and R. Knegjens, "$K^+ \to \pi^+ \nu\bar{\nu}$ and $K_L \to \pi^0 \nu\bar{\nu}$ in the Standard Model: status and perspectives," *JHEP* **11** (2015) 033, arXiv:1503.02693 [hep-ph]. 222

[431] **NA62** Collaboration, E. Cortina Gil *et al.*, "First search for $K^+ \to \pi^+ \nu\bar{\nu}$ using the decay-in-flight technique," *Phys. Lett.* **B791** (2019) 156–166, arXiv:1811.08508 [hep-ex]. 222

[432] **Belle** Collaboration, J. Grygier *et al.*, "Search for $B \to h\nu\bar{\nu}$ decays with semileptonic tagging at Belle," *Phys. Rev.* **D96** no. 9, (2017) 091101, arXiv:1702.03224 [hep-ex]. [Addendum: Phys. Rev.D97,no.9,099902(2018)]. 222

[433] A. J. Buras, J. Girrbach-Noe, C. Niehoff, and D. M. Straub, "$B \to K^{(*)}\nu\bar{\nu}$ decays in the Standard Model and beyond," *JHEP* **02** (2015) 184, arXiv:1409.4557 [hep-ph]. 222

[434] **NA48/2** Collaboration, J. R. Batley *et al.*, "Searches for lepton number violation and resonances in $K^{\pm} \to \pi\mu\mu$ decays," *Phys. Lett.* **B769** (2017) 67–76, arXiv:1612.04723 [hep-ex]. 226, 227, 229

[435] **LHCb** Collaboration, R. Aaij *et al.*, "Search for hidden-sector bosons in $B^0 \to K^{*0}\mu^+\mu^-$ decays," *Phys. Rev. Lett.* **115** no. 16, (2015) 161802, arXiv:1508.04094 [hep-ex]. 226, 227, 229

[436] **LHCb** Collaboration, R. Aaij *et al.*, "Search for long-lived scalar particles in $B^+ \to K^+\chi(\mu^+\mu^-)$ decays," *Phys. Rev.* **D95** no. 7, (2017) 071101, arXiv:1612.07818 [hep-ex]. 226, 227, 229

[437] **LHCb** Collaboration, R. Aaij *et al.*, "Measurement of the $B_s^0 \to \mu^+\mu^-$ branching fraction and effective lifetime and search for $B^0 \to \mu^+\mu^-$ decays," *Phys. Rev. Lett.* **118** no. 19, (2017) 191801, arXiv:1703.05747 [hep-ex]. 227

[438] C. Bobeth, M. Gorbahn, T. Hermann, M. Misiak, E. Stamou, and M. Steinhauser, "$B_{s,d} \to l^+l^-$ in the Standard Model with Reduced Theoretical Uncertainty," *Phys. Rev. Lett.* **112** (2014) 101801, arXiv:1311.0903 [hep-ph]. 227

[439] **E949** Collaboration, A. V. Artamonov *et al.*, "Search for the decay K+ to pi+ gamma gamma in the pi+ momentum region P ¿ 213 MeV/c," *Phys. Lett.* **B623** (2005) 192–199, arXiv:hep-ex/0505069 [hep-ex]. 226, 227